Performance of Flexible Pavement Systems
Containing Geosynthetic Separators

Dr. Richard Coffman
Ashique Ali Raffique Boga

MBTC DOT 3020
March 2012

Prepared for
Mack-Blackwell Rural Transportation Center
University of Arkansas
The National Transportation Security Center of Excellence:
A Department of Homeland Security
Science and Technology Center of Excellence

ACKNOWLEDGEMENT
This material is based upon work supported by the U.S. Department of Transportation under Grant Award Number DTRT07-G-0021. The work was conducted through the Mack-Blackwell Rural Transportation Center at the University of Arkansas.

REPORT DOCUMENTATION PAGE

Form Approved
OMB No. 0704-0188

1. AGENCY USE ONLY *(Leave Blank)*	2. REPORT DATE	3. REPORT TYPE AND DATES COVERED
	Submitted to MBTC on March 13, 2012	Technical 7/1/2010 – 12/31/2011

4. TITLE AND SUBTITLE

Performance of Flexible Pavement Systems Containing Geosynthetic Separators

5. FUNDING NUMBERS

6. AUTHOR(S)
Dr. Richard Coffman, Ashique Ali Raffique Boga

7. PERFORMING ORGANIZATION NAME(S) AND ADDRESS(ES)
Mack-Blackwell Rural Transportation Center
4190 Bell Engineering Center
University of Arkansas
Fayetteville, AR 72701

8. PERFORMING ORGANIZATION REPORT NUMBER

MBTC DOT 3020

9. SPONSORING/MONITORING AGENCY NAME(S) AND ADDRESS(ES)
US Department of Transportation
Research and Special Programs Administration
400 7th Street, S.W.
Washington, DC 20590-0001

10. SPONSORING/ MONITORING AGENCY REPORT NUMBER

11. SUPPLEMENTARY NOTES

Supported by a grant from the U.S. Department of Transportation University Transportation Centers program

12a. DISTRIBUTION/AVAILABILITY STATEMENT

12b. DISTRIBUTION CODE

N/A

13. ABSTRACT (MAXIMUM 200 WORDS)

Base course drainage, strength, and modulus are important parameters that must be considered in the design of a roadway system. Pavement service life is maintained if the base course is permeable, strong, and rigid. Two recent MBTC projects have focused primarily on the rigidity of pavement systems. MBTC Project 2027 focused on the strength, permeability, and rigidity of quarry obtained, preplaced, Class 7 base course using laboratory tests; while MBTC Project 3013 is investigating the effects of geosynthetic separators, geosynthetic reinforcement, and base course thickness on pavement system rigidity. To tie both projects together, the base course at the Marked Tree test site will be analyzed (permeability, strength, grain size, Atterberg limits) to determine if geosynthetic separators have prevented plastic "clayey" fines from migrating into the base layer from the prepared subsoil. The in-situ fines content at the Marked Tree site will also be compared with the preplaced quarry obtained fines content to determine if additional fines are created during transportation, placement, and use of the roadway base.

14. SUBJECT TERMS

15. NUMBER OF PAGES
370

16. PRICE CODE
N/A

17. SECURITY CLASSIFICATION OF REPORT	18. SECURITY CLASSIFICATION OF THIS PAGE	19. SECURITY CLASSIFICATION OF ABSTRACT	20. LIMITATION OF ABSTRACT
none	none	none	N/A

Standard Form 298

1. Report Number	2. Government Access No.	3. Recipient's Catalog No.
MBTC DOT 3020		

4. Title and Subtitle	5. Report Date
Performance of Flexible Pavement Systems Containing Geosynthetic Separators	Submitted to MBTC on March 13, 2012
	6. Performance Organization Code

7. Author(s)	8. Performing Organization Report No.
Dr. Richard Coffman, Ashique Ali Raffique Boga	

9. Performing Organization Name and Address	10. Work Unit No. (TRAIS)
Mack-Blackwell Rural Transportation Center 4190 Bell Engineering Center University of Arkansas Fayetteville, AR 72701	11. Contract or Grant No.
	13. Type of Report and Period Covered Technical 7/1/2010 – 12/31/2011
12. Sponsoring Agency Name and Address US Department of Transportation Research and Special Programs Administration 400 7th Street, S.W. Washington, DC 20590-0001	14. Sponsoring Agency Code

15. Supplementary Notes

Supported by a grant from the U.S. Department of Transportation University Transportation Centers program

16. Abstract

Base course drainage, strength, and modulus are important parameters that must be considered in the design of a roadway system. Pavement service life is maintained if the base course is permeable, strong, and rigid. Two recent MBTC projects have focused primarily on the rigidity of pavement systems. MBTC Project 2027 focused on the strength, permeability, and rigidity of quarry obtained, preplaced, Class 7 base course using laboratory tests; while MBTC Project 3013 is investigating the effects of geosynthetic separators, geosynthetic reinforcement, and base course thickness on pavement system rigidity. To tie both projects together, the base course at the Marked Tree test site will be analyzed (permeability, strength, grain size, Atterberg limits) to determine if geosynthetic separators have prevented plastic "clayey" fines from migrating into the base layer from the prepared subsoil. The in-situ fines content at the Marked Tree site will also be compared with the preplaced quarry obtained fines content to determine if additional fines are created during transportation, placement, and use of the roadway base.

17. Key Words	18. Distribution Statement
Permeability, geosynthetics, triaxial shear tests, grain size analysis	No restrictions. This document is available from the National Technical Information Service, Springfield, VA 22161

19. Security Classif. (of this report)	20. Security Cassif. (of this page)	21. No. of Pages	22. Price
unclassified	unclassified	370	N/A

Table of Contents

List of Tables

List of Figures

List of Equations

Chapter 1. Introduction

1.1. Background

Since the 1920's geosynthetics have been placed between the subgrade and base course layers in pavement systems to serve as reinforcement, layer separation, drainage, and moisture barriers (Al-Qadi et al., 1999). Geosynthetics (specifically geotextiles) have been shown to prevent fines migration from the subgrade to base course when used as a filter and to prevent intrusion of base course materials into the subgrade layer when used as a layer separator.

According to Tingle and Jersey (1989), geosynthetics have been used to improve the performance of roadways, especially for low volume roads, by increasing service life or by reducing the quantity of base course as indicated by an improved ability to manage vehicle traffic with a reduced aggregate thickness. Comparable performance between unreinforced and reinforced road sections has also been observed (Tingle and Jersey, 1989).

Coffman (2010) states that base course drainage, strength, and rigidity are important parameters to be considered for roadway design and performance. More specifically, Coffman (2010) states that geosynthetics may be used to improve the drainage, strength, and rigidity of the pavement system. The objective of the research associated with the AHTD Transportation Research Center (TRC) Project 0406 was to determine the extent of improvement and mechanism responsible for improvement in low volume roadways reinforced with geosynthetics. The test sections installed as part of AHTD TRC Project 0406 were utilized in the research project described in this report.

Two recent projects sponsored by the MBTC and the AHTD have focused on the strength and rigidity of pavement systems. Researchers working on MBTC Project 2027 focused on the effects of fines content (by weight) on the strength and hydraulic conductivity of Class 7 base

course while researchers working on AHTD TRC Project 0903 were studying the effects of geosynthetic separators/reinforcement and base course thickness on pavement system rigidity (Coffman, 2010).

The research documented in this report and conducted as a part of MBTC Project 3020 will contribute to the above mentioned projects by analyzing the performance of the geotextile products installed in the pavement sections at the Marked Tree, Arkansas, test site.

1.2. Hypothesis and Objectives

Geotextiles used as geosynthetic filters and geosynthetic separators prevent fines migration from the subgrade into the base course and prevent base course penetration into the subgrade, respectively, enhancing the ability of the base course to drain and improving roadway performance. This hypothesis will be verified by performing field observations and field and laboratory tests. The following will be obtained from these observations and tests:

- observations during exhumation of base course, geosynthetics, and subgrade materials,
- identification and characterization [I&C] of base course and subgrade materials at the Marked Tree, Arkansas site,
- field hydraulic conductivity [FHP] values of in-situ base course,
- lab hydraulic conductivity [LHP] values of recompacted base course,
- permittivity and transmissivity [P&T] values of geosynthetic separators.

1.3. Need for Research

In roadways constructed on clayey subgrades, fines may be transferred into the base course and the base course may penetrate into the subgrade as a result of vehicle loading. This transfer of fines and penetration of base course may cause ponding or distress, leading to alligator cracking, rutting and premature roadway failure. Geotextiles are considered a cost effective technique (implemented in place of additional base course thickness) to improve roadway performance by filtering subgrade particles and separating the base course and subgrade. The research described in this report is aimed at justifying the potential benefits of

geotextiles as a filtration and separation medium. Past research has not provided satisfactory results (results which can be implemented in design) for highly plastic, clayey subgrade (the subgrade conditions associated with the Marked Tree site). Therefore, a need to conduct additional research was observed leading to the formation of this research project.

1.4. Report Overview

The research conducted to investigate the need for geotextiles to be used as geosynthetic filters to prevent fines migration from the subgrade into the base course and as geosynthetic separators to prevent penetration of the base course into the subgrade is documented in this report. The manuscript is divided into five chapters. An introduction to the research, hypothesis, objectives, need for the research, and overview of this report are contained in this chapter. More specifically, this chapter is a brief summary of this report and a guideline for readers.

A classification of geosynthetics, with details about geotextiles and a review of existing literature about field and laboratory studies conducted utilizing geotextiles as a separator and filtration medium between base course and subgrade interface are presented in Chapter 2. The field studies presented in Chapter 2 include: Howard (2006), Al-Qadi et al. (1999), Blanco (2003), Freeman et al. (2000), and Tabor (2007). The laboratory studies presented in Chapter 2 include: Lawrence (2006), Koerner (1994) and Benson (2010).

The social, demographic, and weather information for Marked Tree, AR along with site location and site selection are also presented in Chapter 2. The subgrade, base course, and geosynthetic sample acquisition processes and descriptions of testing procedures (field and laboratory) are presented in Chapter 3.

In Chapter 4, results obtained from the field and laboratory testing is presented. Specifically, the results from four types of laboratory testing (wash sieving, hydrometers,

Atterberg limits, and specific gravity) performed on the exhumed subgrade samples, six types of laboratory testing (dry sieving, wet sieving, hydrometers, specific gravity, modified proctor, and hydraulic conductivity) performed on the exhumed base course samples, two types of laboratory testing (transmissivity and permittivity) performed on the exhumed geotextile samples and in-situ hydraulic conductivity testing conducted on base course samples are presented in Chapter 4. Comparisons between the index properties obtained from the Marked Tree site as a part of this research and the index properties obtained from the Marked Tree site as a part of past research, and the measured hydraulic conductivity values for the base course and empirically obtained hydraulic conductivity values for the base course are presented in Chapter 4. A review of the design of geotextiles (for filtration and separation) for the geotextiles installed at the Marked Tree site, the pavement profile, the pavement distress survey (modified from Goldman, 2011) and the site observations from field visits are also presented in Chapter 4.

Conclusions derived from this research and recommendations for additional research are presented in Chapter 5. Detailed results obtained from laboratory testing performed on base course, subgrade, and geotextile samples are presented in Appendix A for completeness. Detailed results obtained from field testing are presented in Appendix B for completeness.

Chapter 2. Literature Review

2.1. Introduction

The American Society for Testing and Materials defines geosynthetics as:

"A planar product manufactured from polymeric material used with soil, rock, earth, or other geotechnical engineering related material as an integral part of a man-made project, structure, or system"(ASTM D4439, 2005).

This definition is expanded upon in Sections 2.2 and 2.3 when the classifications of geosynthetics are discussed. Previous field studies and laboratory studies relating to the use of geosynthetics are presented in Sections 2.4 and 2.5, respectively. The Marked Tree test site, from which all samples for this investigation were obtained, is discussed in Section 2.6.

2.2. Classifications of Geosynthetics

Geosynthetic products can be divided into eight different categories:

- Geotextile (GT),
- Geogrid (GG),
- Geonet (GN),
- Geomembrane(GM),
- Geosynthetic Clay Liner (GCL),
- Geopipe (GP),
- Geofoam (GF) and
- Geocomposite.

Although there are eight categories, the three most common types of geosynthetics for roadway applications (the focus of this research) are geogrids, geotextiles, and geocomposites (Holtz et al., 1998). The classifications for each geosynthetic type along with the primary function(s) of individual geosynthetics are presented in Table 2.1.

Geosynthetics can be manufactured using natural or synthetic products (Holtz et al., 1998). The manufacturing process of a geosynthetic product is largely dependent on the geosynthetics application. A classification of common types, and common uses of geosynthetics based on material and manufacturing process is presented in Figure 2.1. Although all of the

geosynthetic types are displayed in Table 2.1and Figure 2.1, the focus of this research is geotextiles, wich are discussed in further detail in Section 2.3.

Table 2.1. Primary function and description of geosynthetics (Holtz, 1998 and Koerner, 2005).

Type of Geosynthetic (GS)	Description	Primary Function				
		Separation	Reinforcement	Filtration	Drainage	Containment
Geotextile (GT)	Permeable synthetic fibers woven together to form a porous, flexible fabric	X	X	X	X	
Geogrid (GG)	High-density polypropylene or polyethylene with an open mesh structure which allows interlocking with the surrounding materials		X			
Geonet (GN)	Continuous extrusion of parallel sets of polymeric ribs at acute angles into a net like configuration				X	
Geomembrane (GM)	Impervious, very soft, thin sheets of rubber or plastic materials.					X
Geosynthetic Clay Liner (GCL)	Thin layers of bentonite clay sandwiched between two geotextiles or bonded to a geomembrane					X
Geopipe (GP)	Typically used as leachate collection pipes under high compressive loads				X	
Geofoam (GF)	Polymeric expansion process resulting in "foam" that consists of gas filled cells	X				
Geocomposite (GC)	Multi-purpose system consisting of two or more types of geosynthetics to achieve more than one function	X	X	X	X	X

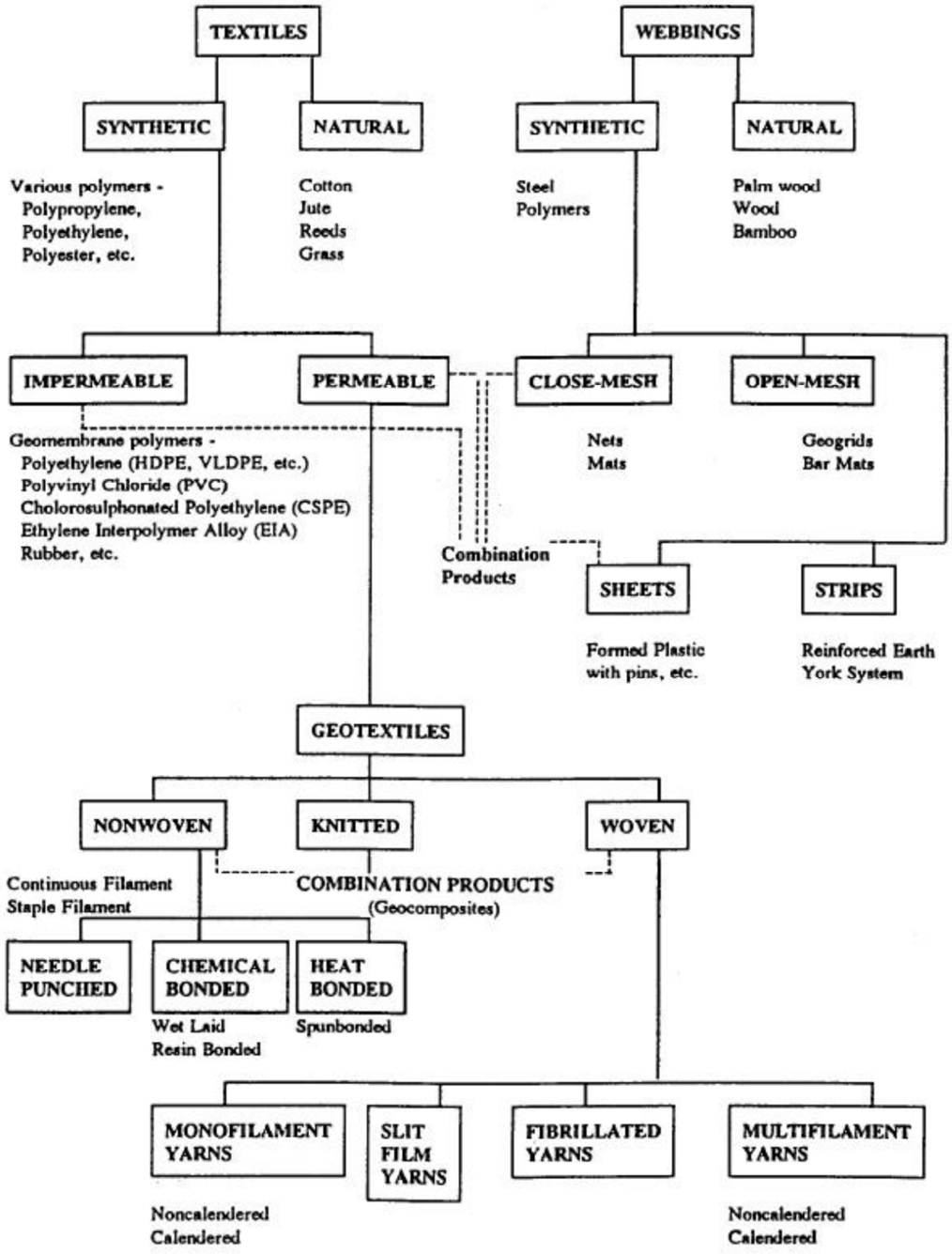

Figure 2.1. Classification of geosynthetics (from Holtz et al., 1998).

2.3. Geotextiles

As shown previously in Figure 2.1, geotextiles are classified as non-woven or woven depending on the method of production. Geotextiles can be used for separation, reinforcement, filtration, and/or drainage as presented previously in Table 2.1. According to Appea, 1997 geotextiles are commonly used as a filtration medium and hence are referred to as filter fabric. The typical placement of a geotextile product is at the interface between the subgrade and base course (Appea, 1997). This is usually performed to achieve separation and filtration between the subgrade and base course materials in roadway applications.

In the late 1960's, Rhone-Poulenc Textiles, France (Appea, 1997) initiated research on, and production of, non-woven fabrics for different applications. The company was interested in utilizing the non-woven fabrics to reinforce unpaved roads, railroad ballast, and embankments (Appea, 1997). In addition to reinforcement capabilities, geotextiles have gained popularity in the recent past as a tool to improve base course hydraulic conductivity by preventing fines migration into the base course.

2.4. Previous Field Studies

Discussion of previous research projects in which the use of geotextiles were used for separation and studied are presented in this section. These projects are well documented in the literature and provide real-world performance data for geotextiles. The projects discussed in this section include:

- Section 2.4.1- full-scale field studies and finite element modeling of flexible pavement systems containing geosynthetics (Marked Tree, Arkansas) as presented in Howard, 2006.
- Section 2.4.2-evaluation of geosynthetics used as separators (Bedford County, Virginia) as presented in Al-Qadi et al., 1999.
- Section 2.4.3-characterization of permeability of pavement bases in the Missouri Department of Transportation roadway system (Missouri) as presented in Blanco, 2003.

- Section 2.4.4-geotextile separators for hike and bike trails (Columbia, Missouri) as presented in Freeman, 2000.
- Section 2.4.5-geotextile separators for equestrian trails (Missouri) as presented in Tabor, 2007.

The results observed in these research projects and recommendations derived from these studies are also presented in this section.

2.4.1. Full-Scale Field Study and Finite Element Modeling of a Flexible Pavement Containing Geosynthetics (Marked Tree, Arkansas) as presented in Howard, 2006

An 850-foot long flexible pavement secondary road was instrumented and constructed in 2005 in Marked Tree, Arkansas. Sixteen test sections, and an additional transition section, were installed in a newly constructed frontage road as displayed in Figure 2.2. Section 7 was created as a transition section, transitioning the thickness of base course material from ten-inches thick to six-inches thick (Howard, 2006).

As presented in Figure 2.2a, these test sections contained control sections and various geosynthetic configurations including geotextile, geogrid, or geogrid on top of geotextile. These sections were heavily instrumented with asphalt strain gauge, earth pressure cells, geotextile strain gauges, geogrid strain gauges, moisture content probes, piezometers, and thermocouples (Figure 2.2b). The effects of including geosynthetics within the pavements of low volume roads constructed on poor subgrade soils encompassing different base course thicknesses and utilizing different types of geosynthetics was the focus of this research (Howard, 2006).

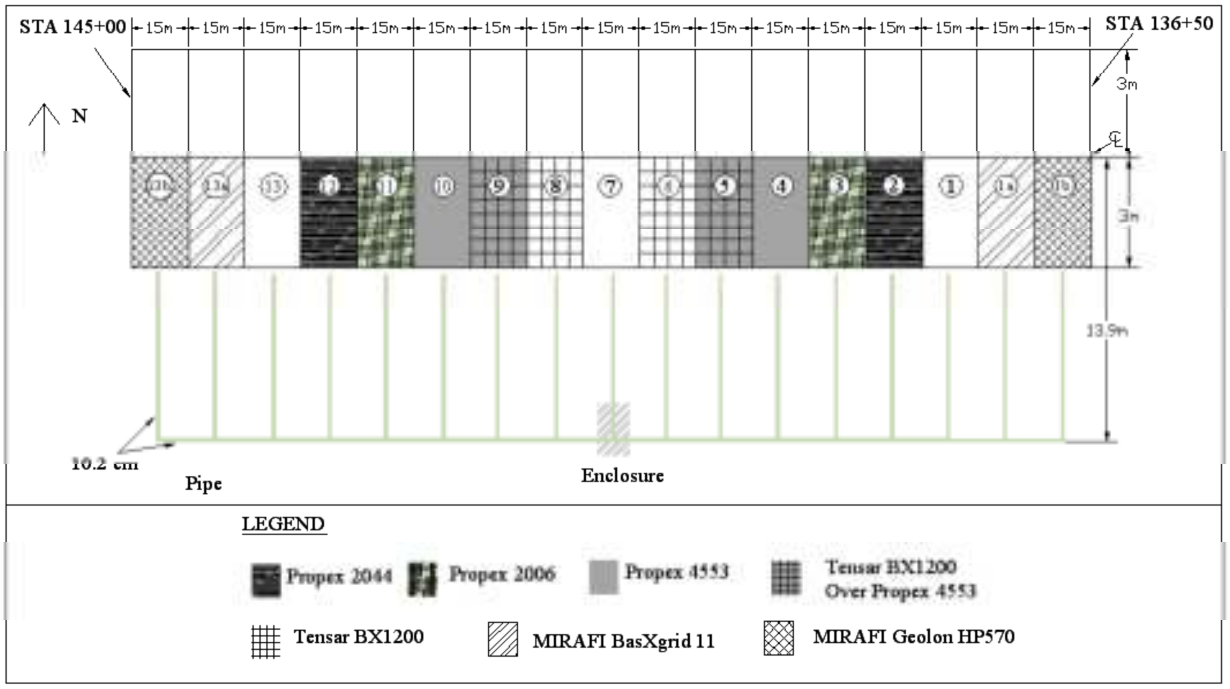

(a)

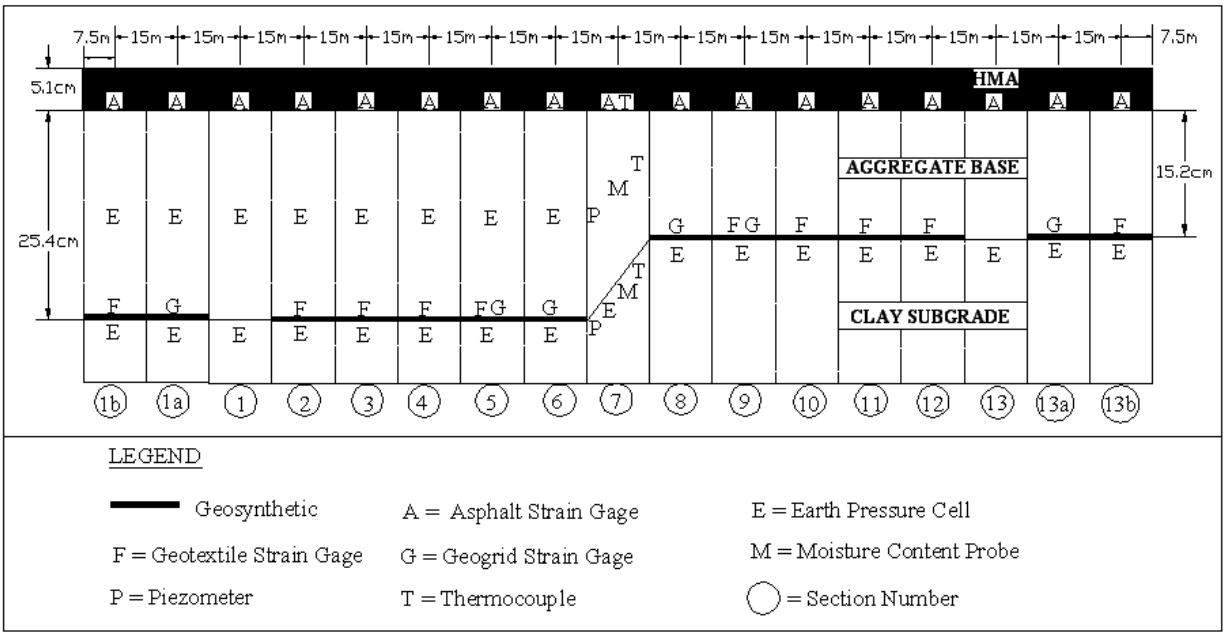

(b)

Figure 2.2. a) Plan (a) and profile (b) view of test sections, Marked Tree, Arkansas (from Howard, 2006).

According to Howard (2006), the full-scale, instrumented roadway was reinforced with multiple types of geosynthetics and constructed over a period of three months. A total of 129

sensors were installed which required approximately 16,400 feet of sensor cable and 1,210 feet of protective conduit. Immediately following completion of the pavement system, a fully loaded, single axle dump truck drove over the test section over 2,000 times (Howard, 2006). During a six month period (September 2005 to February 2006) over 500 falling weight deflectometer (FWD) drops were placed on the pavement (Howard, 2006). Some rutting and minimal to no fatigue cracking (less than 3.5 percent) was observed for all sections except Section 9 (11.7 percent) (Howard, 2006). Typical rut depths ranged from 0.13 to 0.25 inches and compared favorably with the values that were calculated using the Asphalt Institute (Asphalt Institute, 1982) transfer functions (Howard, 2006).

The moisture content varied from 3.4 percent to 7.1 percent from construction initiation to the end of testing (Howard, 2006). The optimum moisture content for the subgrade sections as determined by AHTD and the roadway contractor ranged from 16.8 to 20.4 percent (Howard, 2006). According to Howard (2006) it was concluded that the compacted subgrade moisture content had minor variations from optimum conditions.

According to Howard (2006) the advantages of the geosynthetic materials were not recognized in this investigation because of the dry climatic conditions and reduced testing intervals (Howard, 2006).

2.4.2. Evaluation of Geosynthetics Used as Separators (Bedford County, Virginia) as presented in Al-Qadi et al., 1999

In 1994, a 150 meter long flexible pavement secondary road was constructed and instrumented in Bedford County, Virginia. According to Bhutta (1998), the site was located 62 miles (100 km) from the Virginia Tech campus at the intersection of State Route 757 and State Route 616 in Bedford County, VA (Figure 2.3). The test site contained a total of nine test

sections as presented in Figure 2.4. A summary of base course thicknesses and geosynthetics installed is presented in Table 2.2.

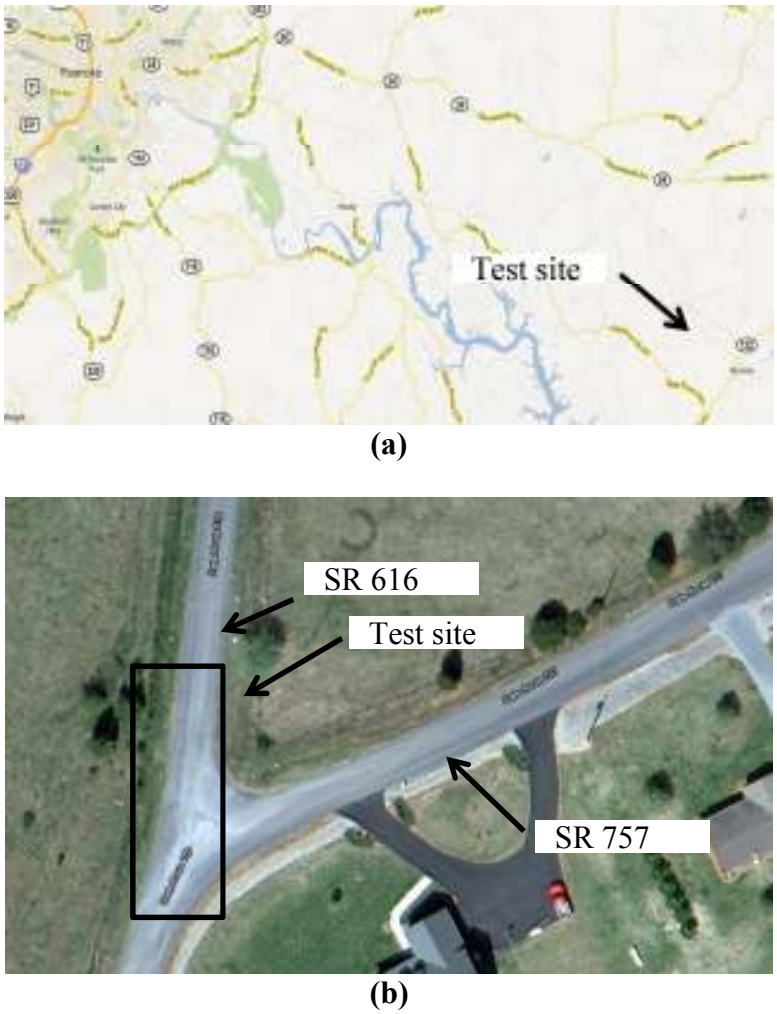

Figure 2.3. Google Maps images a) zoomed out and b) zoomed in satellite image of test site located on State Route 757 and State Route 616, Bedford County, VA (modified from Google Maps, 2011).

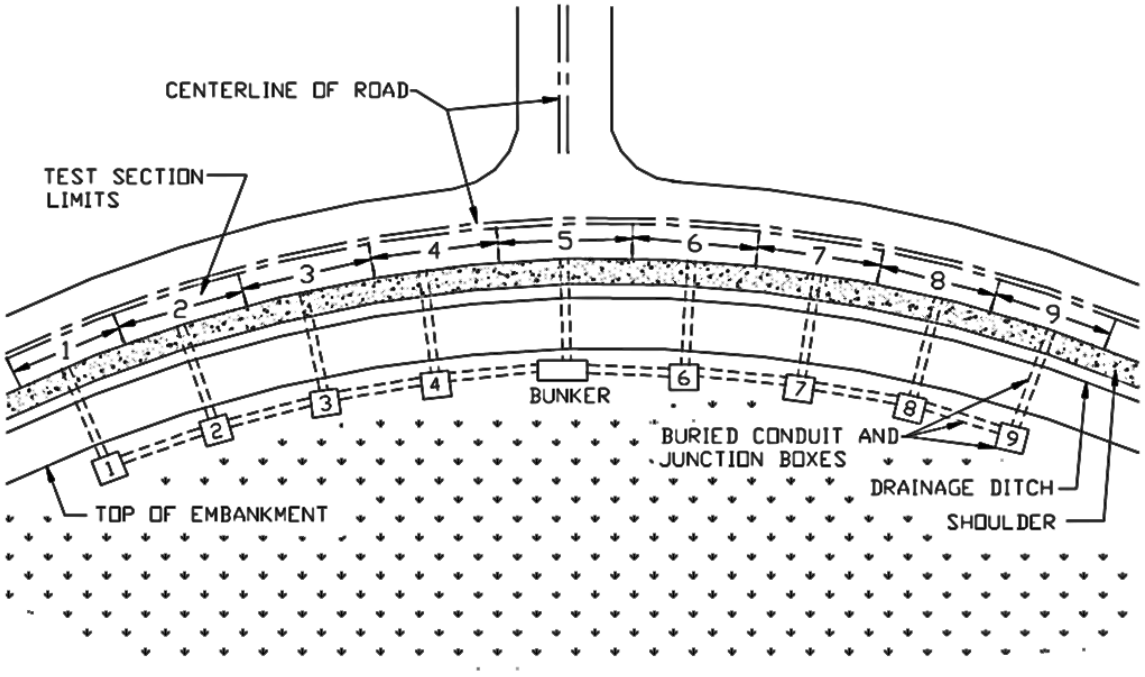

Figure 2.4. Layout of test sections installed for the research project (from Bhutta, 1998).

Table 2.2. Summary of base course thickness and geosynthetic installed (from Bhutta, 1998).

Section No.	Description	Base Course Thickness (mm)
1	Control	100
2	Woven Geotextile	100
3	Geogrid	100
4	Control	150
5	Woven Geotextile	150
6	Geogrid	150
7	Control	200
8	Woven Geotextile	200
9	Geogrid	200

As presented in Table 2.2, the sections were divided into three groups based on base course thickness. For the first group, the base course thickness was 100 mm thick; for the second group the base course thickness was 150 mm thick; for the third group a base course thickness was 200 mm thick (Al-Qadi et al., 1999). According to Al-Qadi et al., (1999) one section in each

group was stabilized with an Amoco 2002 woven geotextile (GT), one section in each group was stabilized with a Tensar BX 1200 geogrid (GG), and one section in each group was a control section (i.e. contained no geosynthetic). All geosynthetics were placed at the base course/subgrade interface.

The Average Daily Traffic (ADT) was approximately 500 vehicles (in summer) with eight to ten percent truck traffic (Al-Qadi et al., 1999). The pavement was instrumented with pressure cells, strain gauges, thermocouples, moisture sensors, and piezoelectric sensors. Periodic rut measurements and ground-penetrating radar (GPR) surveys were performed at the test sections (Al-Qadi et al., 1999).

Based on periodic GPR surveys conducted over the three years of pavement service life, contamination (fines migration from subgrade to base course) had occurred in the control sections; while no contamination was observed in the sections stabilized with geosynthetics (Al-Qadi et al., 1999). The initial fines content of the base course was reported as 5.5 percent by Al-Qadi et al., 1999. A summary of results obtained from testing conducted on the exhumed base course and the exhumed subgrade soil are presented in Tables 2.3 and 2.4, respectively.

Table 2.3.Test results for base course samples at the test site in Bedford County, VA (from Bhutta, 1998).

Base Course Classification	GW
Coefficient of Uniformity (C_u) [unitless]	16
Coefficient of Uniformity (C_c) [unitless]	1.5
Specific Gravity [unitless]	2.78
Max. Dry Density (kN/m^3) [Modified proctor]	22.4
Optimum Water Content (percent) [Modified proctor]	6.1
Fines content in control sections [percent]	16.1
Fines content in geogrid sections [percent]	15.0
Fines content in geotextile sections [percent]	12.4

Table 2.4. Test results for the subgrade soil at the test site in Bedford County, VA (from Bhutta, 1998).

Soil Classification	CH	ML
Section	1 to 3, 6 to 9	4 and 5
Finer than #200 [percent]	76	73
Liquid Limit (LL) [percent]	56 to 68	approximately 41
Plasticity Index (PI) [percent]	28 to 37	4 to 6
Specific Gravity	2.77	2.74
Max. Dry Density [kN/m^3] Standard Energy	15.8	17.1
Optimum Water Content [percent] Standard Energy	24.4	17

The maximum dry density for the base course obtained using modified proctor energy was 22.4 kN/m^3 at optimum water content (dry weight basis) of 6.1 percent. Based on the results from wash sieve analysis tests conducted on the exhumed base course samples, after the roadway was in service for three years, the control sections contained 16.1 percent fines, the geogrid sections contained 15 percent fines, and the geotextile sections contained 12.4 percent fines. The presence of subgrade fines in base course was attributed to pumping from the subgrade transferring to beneath the pavement under vehicle loading. Strength and elongation results of the exhumed geotextile and geogrid material before installation and after three years of service life are presented in Table 2.5.

Table 2.5. Characteristics and properties of the geosynthetics before installation and after exhumation (from Al-Qadi et al., 1999).

Material	Direction	Before Installation (July 1994)		After exhumation (October 1997)	
		Ultimate Strength	Ultimate Elongation	Ultimate Strength	Ultimate Elongation
		(kN/m)	(percent)	(kN/m)	(percent)
Geotextile	Warp	27	14.8	18	23.6
	Fill	25	9.9	25	12.5
Geogrid	Machine	19	8.9	19	12.4
	Cross Machine	33	9.3	32	14.1

It was observed that the ultimate strength of the geotextile in the warp direction was reduced by 33 percent, whereas in the fill direction the geotextile strength after the service life was the same as the geotextile strength prior to installation. The ultimate strength of the geogrid after the service life was compliable to the initial ultimate strength (Al-Qadi et al., 1999). Strain development in the exhumed geotextile was 59 percent in the warp direction and 26 percent in the fill direction. The geogrid developed 39 percent strain in the machine direction and a 52 percent strain in the cross-machine direction (Al-Qadi et al., 1999).

At terminal rutting criteria of 20 mm along with linear rutting progression equations obtained from measurements of rutting were used to calculate service life of the pavement systems containing the geogrid, the geotextile, and no geosynthetic (control sections). Inclusion of geosynthetics increased the service life of the pavement based on the rutting progression equations. The geogrid stabilized sections carried 82 percent more Equivalent Single Axle Load (ESALs) before failure (20 mm of rutting) than the control section, while the geotextile stabilized sections carried 134 percent more ESALs before failure than the control sections (Al-Qadi et al., 1999). Therefore, the use of geosynthetics, specifically the use of geotextiles improved the pavement performance of this secondary road (Al-Qadi et al., 1999).

2.4.3. Characterization of Hydraulic Conductivity of Pavement Bases in the Missouri Department of Transportation Roadway System as discussed in Blanco, 2003

According to Blanco (2003), a research project was conducted for the Missouri Department of Transportation (MODOT) to ensure that hydraulic conductivity of Type 5 base course was adequate to drain the pavement system. Type 5 base course is predominantly used in roadway projects in the State of Missouri (Blanco, 2003). The Type 5 base course material used in this research was classified as silty sands or silty, clayey sands as per the Unified Soil Classification System (USCS). The Type 5 base course material was also classified as A-1-a and A-1-b as per the AASHTO classification method (Blanco, 2003). Samples from supplier quarries, on-site stock piles, and from compacted in-place roadway bases around the state of Missouri were obtained in bulk quantities (Blanco, 2003). A summary of the acquired samples is presented in Table 2.6.

Table 2.6. Summary of sample acquisition (from Blanco, 2003).

Location	Dates	Source	Sampling location	Type
Route 71, McDonald Co.	September 2001	Lanagan Quarry	Quarry, field	Type 5
Route 13, St. Clair Co.	September 2001	Ash Groove Quarry	Quarry, field	Type 5
Route 63, Rudolph Co.	September 2001	Riggs Quarry	Stockpile at site	Type 5
Route 71, Nodaway Co.	September 2001	Idecker Quarry	Stockpile at site, field	Type 5
Taney Co.	December 2001	Journegan Quarry	Stockpile at site	Rockfill
Crawford Co.	December 2001	from site	Stockpile at site	Rockfill

The “Rockfill” alternate material includes individual particle sizes as large as 12 inches filled with a mixture of coarse and fines aggregates (Blanco, 2003). The actual rockfill is crushed rock with sand added to maintain the plasticity index (less than six) of material passing No. 40 (Blanco, 2003). Index properties, fines content, and soil classification of the Type 5 base and Rockfill alternate as obtained from Blanco, (2003) are presented in Table 2.7. The material used in the MODOT research is called Type 5 base (Blanco, 2003) as it meets the gradation requirement based on dry sieving as presented in Table 2.8 (MODOT, 2011).

Table 2.7. Soil classification, index properties and, fines content for Type 5 base and alternate rockfill (from Blanco, 2003).

Source	D_{60}	D_{30}	D_{15}	D_{10}	C_u	C_z	[1]P_{200}	γ_{dmax}	[2]OMC	[3]e	Soil Classification
	(mm)	(mm)	(mm)	(mm)	(unitless)		(%)	(pcf)	(%)	(unitless)	USCS
Ash Grove Quarry	5.3	1.0	0.20	**0.05**	106.0	3.8	12	136.5	7.0	0.21	GP-GM
Ash Grove Field	3.8	0.5	**0.10**	**0.02**	190.0	3.3	17	136.5	7.0	0.21	SM
Idecker Quarry	9.1	2.7	0.25	**0.02**	455.0	40.1	13	125.0	10.0	0.32	GM-GC
Idecker Field	8.0	1.3	**0.03**	**0.01**	800.0	21.1	18	125.0	10.0	0.32	GM/GM-GC
Lanagan Quarry	4.0	0.8	0.10	**0.04**	100.0	4.0	13	141.0	6.5	0.17	SM
Riggs Quarry	4.8	0.4	**0.04**	**0.02**	237.5	1.7	19	137.0	8.0	0.21	SM
Crawford Co.	5.1	0.5	0.10	**0.05**	102.0	1.0	14	138.7	8.0	0.19	SM
Taney Co.	4.8	1.0	0.08	**0.02**	237.5	10.5	15	138.9	7.7	0.19	SM

Bold values represent extrapolated values from grain size distribution based on wet sieving.

[1]Percent passing No. 200 sieve

[2]OMC is optimum moisture content

[3]Void Ratio

Table 2.8. Gradation requirement for Type 5 base course as per Missouri Department of Transportation (from MODOT, 2011).

Sieve	Percent passing by weight
1 inch	100
1/2 inch	60-90
No. 4	35-60
No. 30	10-35
No. 200	0-15

The values of hydraulic conductivity as measured in laboratory, field, and estimated (using different techniques) are presented in Table 2.9. The hydraulic conductivity values were obtained in the laboratory using a constant head permeameter (CHP) and a flexible wall permeameter (FWP). The sample size for the laboratory hydraulic conductivity testing was six-inches in diameter and 4.5 or 4.75 inches tall. According to Blanco (2003) the infiltration values were obtained in the field using a double-ring infiltrometer (DRI), and the hydraulic conductivity was calculated following the procedures outlined in ASTM D3385 (2008). The values obtained in the laboratory and fields are presented in Figure 2.5. The field measured hydraulic

conductivity values ranged from 1.9E-05 cm/s to 1.9E-03 cm/s while the laboratory obtained hydraulic conductivity values ranged from 3.0E-07 cm/s to 8.8E-02 cm/s (Blanco, 2003). The measured laboratory hydraulic conductivity values obtained in the laboratory were usually higher than the measured hydraulic conductivity values obtained in the field except for samples obtained from Ash Groove Field, Idecker Field, and Crawford Co.

Table 2.9. Estimated, laboratory, field hydraulic conductivity values for Type 5 base (from Blanco, 2003).

Source	Properties			Predicted Hydraulic Conductivity			Measured Hydraulic Conductivity	
	γ_d	w	[1]e	Hazen (k)	Sherard (k)	Moulton (k)	Lab k*	Field k
	(lb/ft^3)	(%)	(unitless)	(cm/s)	(cm/s)	(cm/s)	(cm/s)	(cm/s)
Ash Grove Quarry	131.0	8.0	0.21	2.5E-03	1.4E-02	5.4E-06	2.8E-03	1.9E-03
Ash Grove Field	134.6	8.0	0.21	4.0E-04	3.5E-03	1.1E-06	**3.0E-06**	1.9E-03
Idecker Quarry	119.3	9.0	0.32	4.0E-04	2.2E-02	1.2E-05	8.8E-02	4.6E-05
Idecker Field	138.7	9.0	0.32	1.0E-04	3.2E-04	3.6E-06	**3.0E-07**	4.6E-05
Lanagan Quarry	133.6	4.0	0.17	1.6E-03	3.5E-03	1.2E-06	5.4E-03	9.7E-05
Riggs Quarry	137.7	9.0	0.21	4.0E-04	5.6E-04	9.4E-07	5.2E-03	3.7E-05
Crawford Co.	136.3	8.8	0.19	2.5E-03	3.5E-03	2.9E-06	**4.5E-06**	9.1E-05
Taney Co.	144.4	7.9	0.19	4.0E-04	2.0E-03	6.8E-07	3.0E-04	1.9E-05

***Bold** values represent flexible wall permeameter test and remaining are constant head permeameter test

[1]Void Ratio

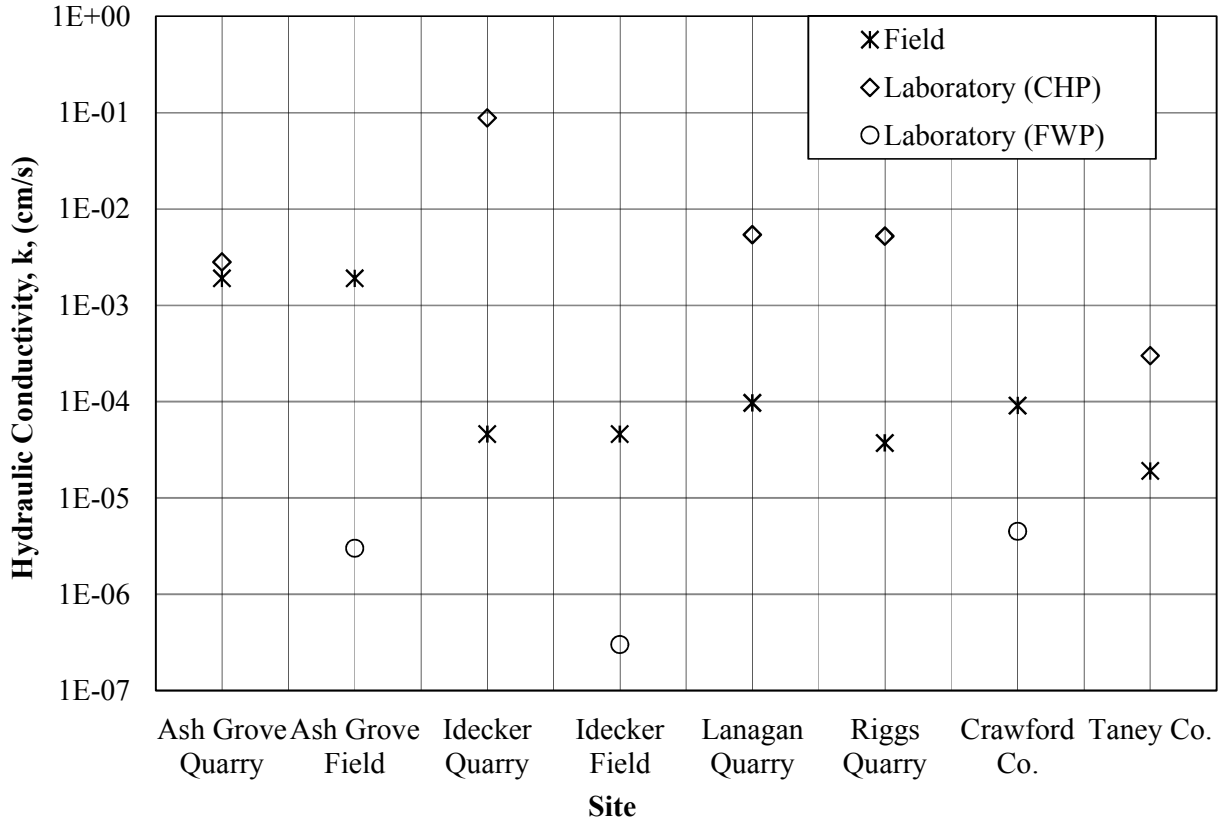

Figure 2.5. Field and laboratory measured hydraulic conductivities (modified from Blanco, 2003).

The hydraulic conductivity of base course was also predicted using the empirical relationships presented by Hazen (1930), Moulton (1980), and Sherard et al., (1984). The Hazen (1930) and Sherard et al., (1984) methods utilize values obtained from grain size distribution (D_{10} or D_{15}, respectively) while the Moulton (1980) method utilizes both values obtained from the grain size distribution (D_{10} and P_{200}) and also the porosity (n) of the soil. The Hazen (1930) equation is provided in Equation 2.1, the Sherard et al., (1984) equation is provided in Equation 2.2, and the Moulton (1980) equation is provided in Equation 2.3.

$$k = CD_{10}^{2} \qquad \text{(Hazen, 1930)} \qquad \textbf{Equation 2.1}$$

Where
k is hydraulic conductivity (cm/s);

D_{10} is size opening through which 10 percent by weight of dry sample will pass (mm);
C is empirical coefficient (for this study 1.0).

$$k = 0.35\, D_{15}^{2} \qquad \text{(Sherard et al., 1984)} \qquad \textbf{Equation 2.2}$$

Where
k is hydraulic conductivity (cm/s);
D_{15} is size opening through which 15 percent by weight of dry sample will pass (mm).

$$k = \frac{6.214 * 10^{5}\, D_{10}^{1.478}\, n^{6.654}}{P_{200}^{0.597}} \qquad \text{(Moulton, 1980) and (Blanco, 2003)} \qquad \textbf{Equation 2.3}$$

Where
k is hydraulic conductivity (ft/day);
D_{10} is size opening through which 10 percent by weight of dry sample will pass (mm);
n is porosity of the material (unitless);
P_{200} is percent of material finer than the No. 200 sieve (75 μm).

A comparison between the measured laboratory hydraulic conductivity values and the measured field hydraulic conductivity values and the estimated hydraulic conductivity values obtained using the Hazen (1930), Sherard et al., (1984) and Moulton (1980) equations is presented in Figure 2.6. The predicted hydraulic conductivity values based on the Hazen (1930) and Sherard et al., (1984) methods range from 10^{-2} cm/s to 10^{-4} cm/s (Blanco, 2003). These predictions are one to two orders of magnitude higher than the hydraulic conductivity values measured in laboratory using the CHP and the hydraulic conductivity values measured in field using the DRI. The hydraulic conductivity values obtained using the Moulton (1980) equation ranged from 10^{-5} cm/s to 10^{-7} cm/s (Blanco, 2003) which are within the range of values measured using the FWP but underestimate the field hydraulic conductivity values measured using the DRI (by one to two orders of magnitude); these empirically predicted values are also several orders of magnitude lower than the hydraulic conductivity measured using CHP.

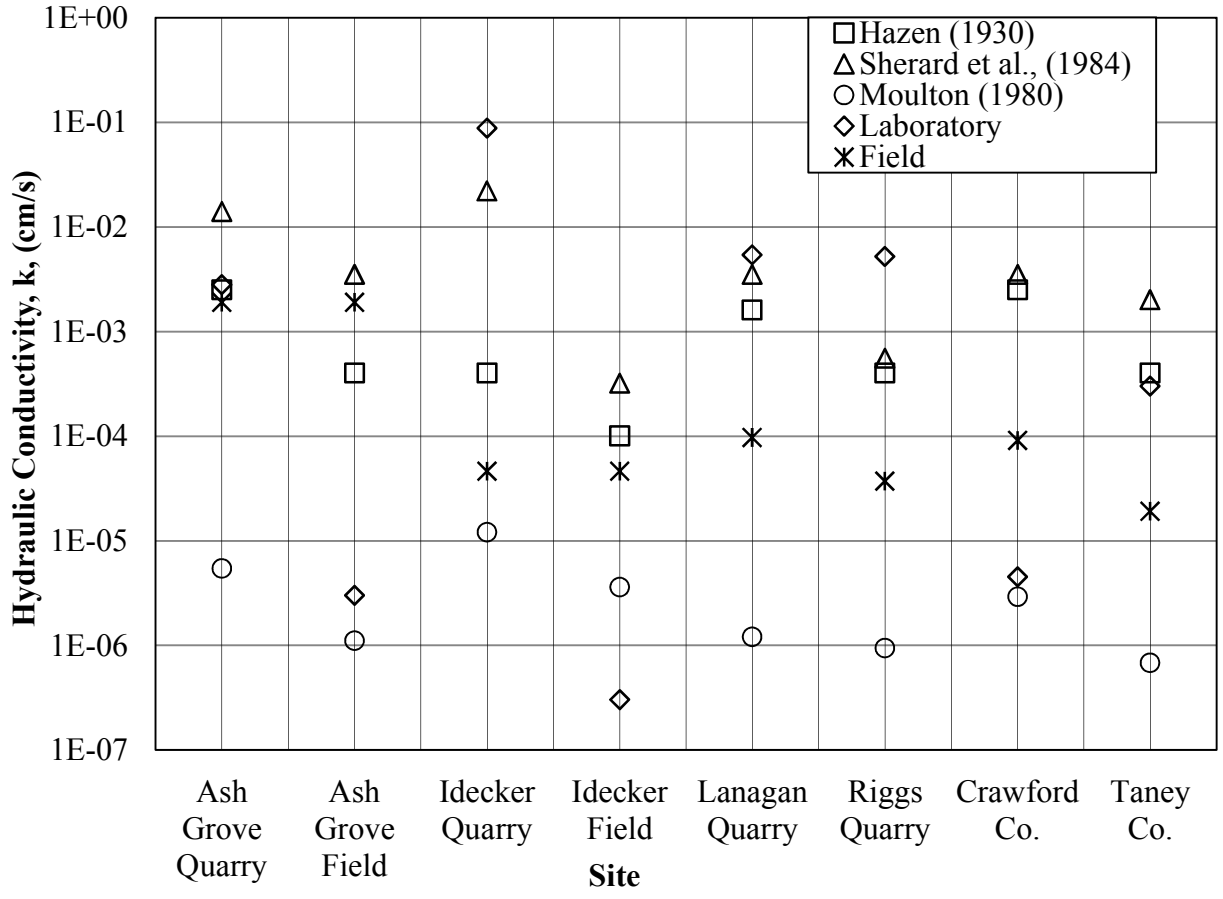

Figure 2.6. Laboratory measured, field measured and estimated hydraulic conductivities of base course samples obtained from various sources (modified from Blanco, 2003).

The in-situ hydraulic conductivity was regarded as the most relevant in this study. The hydraulic conductivity values as measured in laboratory and in field (ranging from 10^{-3} to 10^{-5} cm/s) do not meet the 1 cm/s permeable base drainage criteria but did meet the gradation requirements (Blanco, 2003). The study proved that materials tested that are in compliance with the gradation specification for base materials, as used in roadway construction in Missouri, are not drainable.

2.4.4. Geotextile Separators for Hike and Bike Trail (Missouri, Columbia) as presented in Freeman et al., 2000

A 4.7 mile hike and bike trail is maintained by the City of Columbia, Missouri Parks and Recreation Department and constructed on the former Missouri-Kansas-Texas (MKT) railroad line (Freeman et al., 2000). The MKT trail is currently designated as a blue route by City of Columbia (Figure 2.7). The blue route is defined by the City of Columbia (2011) as, "mostly soft-surfaced pathways, open only to non-motorized traffic, and shared with pedestrian traffic".

Figure 2.7. MKT trail on City of Columbia, Missouri bike map (City of Columbia, 2011)

According to Freeman et al., (2000), the sub-surface of the trail consists of railroad ballast, outcrop rocks, and clayey soils. The wearing surface consisted of five to ten centimeters of crushed limestone as presented in Figure 2.8. Intrusion of the wearing surface aggregate into the subgrade soil and excessive rutting within the wearing surface and subgrade in the frequently used paths caused locations of water ponding and muddy spots (Freeman et al., 2000). Because of the intrusion of the wearing surface aggregate into the subgrade, approximately $17,000 was spent each year towards maintenance of the trail.

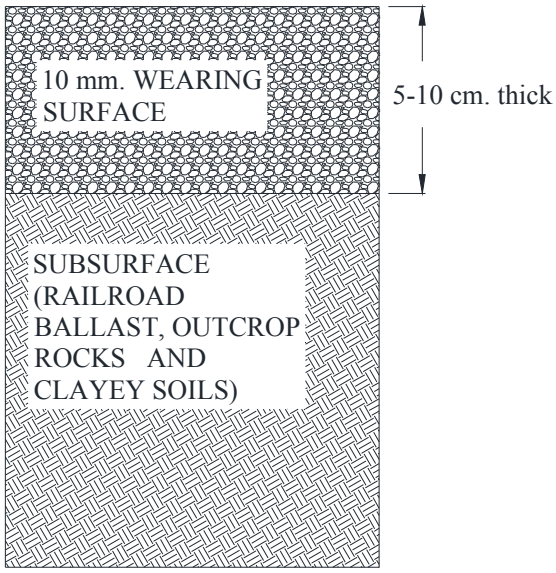

Figure 2.8. Sub-surface profile of the hike and bike trail (Freeman et al., 2000).

To mitigate the intrusion of the wearing surface aggregate into the subgrade, three test sites (Figure 2.9) were selected in June of 1998. The sites are labeled as Section 1, Section 2, and Section 3 in Figure 2.9. According to Freeman et al., (2000), the sites were selected based on the following selection criteria:

- Past record of intrusion of the wearing surface aggregate into the subgrade
- Water ponding on the surface
- Excessive rutting

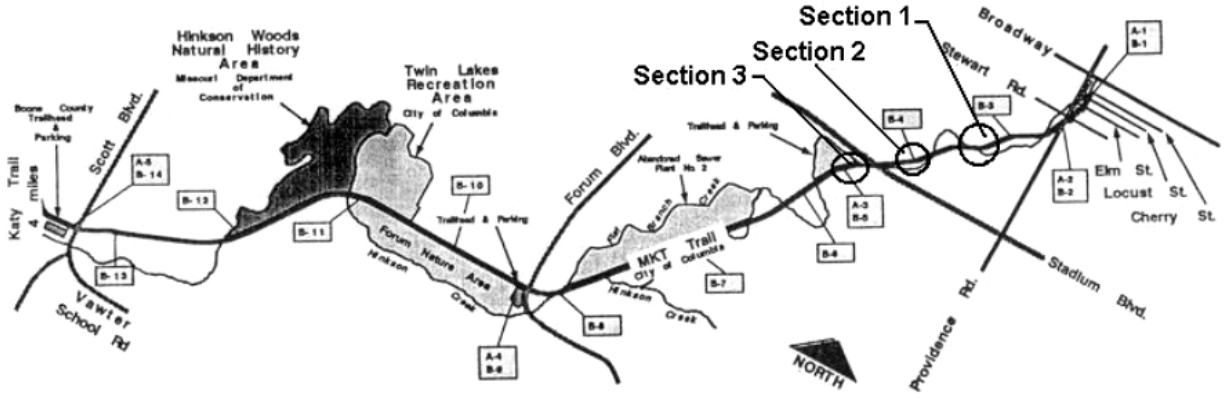

Figure 2.9. The 4.7 mile hike and bike trail maintained by City of Columbia Missouri Parks and Recreation Department (from Freeman et al., 2000).

Geotextile separators were investigated as a plausible solution to mitigate the aggregate intrusion into the subgrade by installing a geotextile between the wearing surface and the subgrade as presented in Figure 2.10.

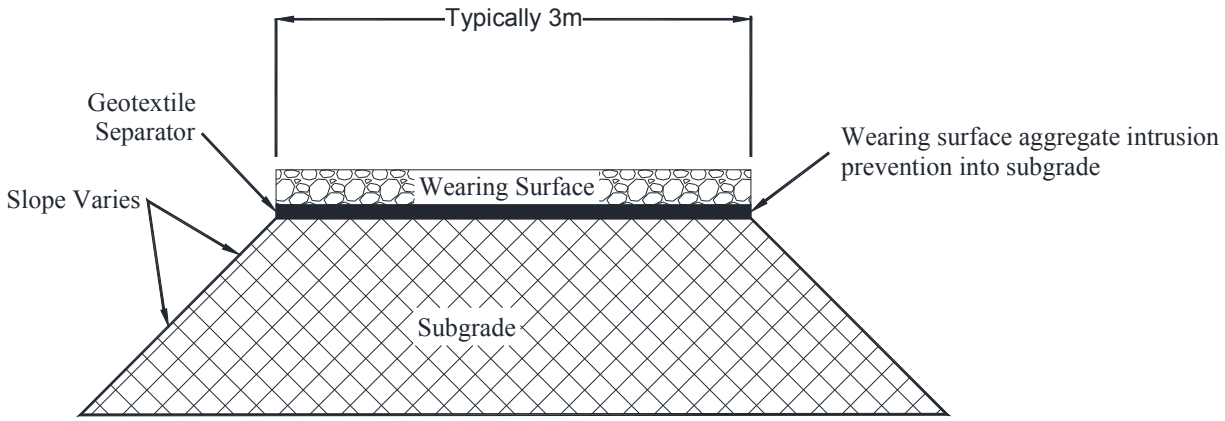

Figure 2.10. Typical cross section of Columbia, Missouri hike and bike trail as stabilized using geotextiles (modified from Freeman et. al., 2000).

Each site contained one test section, measuring thirty meters long by three meters wide. The top five to ten cm of wearing surface aggregate and subgrade soil was removed using a box scraper. The section was then inspected for debris that might puncture the newly installed geotextile (Freeman et.al. 2000). The geotextile was then directly placed over the exposed subgrade.

A non-woven needle-punched geotextile was installed in Sections 1 and 2 and a non-woven spun bonded geotextile was installed in Section 3 (Freeman et al., 2000). After placement of the geotextile, the surface of the geotextile was ensured (by visual inspection) to be wrinkle free. The surface aggregate (as obtained from Boone Quarry in Columbia, Missouri) was then placed on top of the geotextile using a ten ton dump truck. While explicitly not described, the unstabilized sections adjacent to the stabilized sections were the control section. Index tests were

performed on the aggregates used for the hike and bike trail before installation of the geotextile (Table 2.10).

Table 2.10. Results of tests performed on the wearing surface aggregate type used for the hike and bike trail in Columbia, Missouri before installation of geotextile (from Freeman et al., 2000).

Test Description	Results
Atterberg Limits	Aggregate fines were classified as Non-Plastic
Passing No. 200 sieve	Eleven percent passing No. 200 sieve
Rigid Wall Permeameter	The fines migrate through the geotextile in the flow direction. The non woven needle-punched geotextile collected more fines within the geotextile as compared to the nonwoven spunbonded

The wearing surface aggregate contained eleven percent of non-plastic fines. The non-woven needle-punched geotextile collected more fines as compared to non-woven spun bonded geotextile in the rigid wall permeameter testing (Freeman et al., 2000). A summary of test results from samples collected one year after the placement of the geotextile are presented in Table 2.11.

Table 2.11. Results of tests performed on the exhumed samples as obtained one year after installation of geotextile specimens in Columbia, Missouri field site test sections (from Freeman et al., 2000).

Site	Geotextile	[1]Δ	[2]Mass	[3]w	[4]w	[5]ψ	[6]ψ
		(cm)	(g)	(%)	(%)	(s^{-1})	(s^{-1})
1B	Nonwoven needle punched	0.40	0.189	5	9.1	1.083	0.815
2A		-2.27	0.194	3.3	6.5	1.083	1.026
2B		-1.98	0.360	4.3	7.4	1.083	0.833
2C		-1.98	0.379	3.6	7.6	1.083	0.835
3A	Nonwoven Spunbonded	1.95	0.091	4	5.8	0.362	-
3B		1.28	0.282	5	4.7	0.362	0.295
3C		0.72	0.189	3.8	6.2	0.362	0.520

[1]Change in base course thickness after one year

[2]Mass of soil in exhumed geotextile samples

[3]Exhumed base course water content

[4]Exhumed subgrade water content

[5]New geotextile permittivity

[6]Exhumed geotextile permittivity

Based on visual observation, rutting, ponding, and aggregate intrusion decreased in the sections stabilized with geotextiles as observed monthly for a one year period. Rutting was prevalent during the observations of Section 2 (a section containing the non-woven needle-punched geotextile) and averaged about 2.1 cm. The exhumed non-woven needle-punched geotextile had more fines (by weight) as compared to non-woven spun bonded geotextile. The reduction in permittivity values for non-woven needle-punched geotextile was greater than the reduction in permittivity values of non-woven spun bonded geotextile, except for Section 3C which increased in permittivity.

According to Freeman et al., (2010) the findings of the study suggest that the sections stabilized using geotextiles were successful in functioning as a filtration and separation barrier for the hike and bike trail. Furthermore, rutting and ponding was reduced in the sections containing geotextiles as compared with sections without geotextiles.

2.4.5. Geotextile Separators for Equestrian Trails (Missouri) as presented in Tabor, 2007

According to Tabor (2007), the 370 miles of equestrian trails under the control of the Missouri Department of Conservation (MDC) were in poor condition due to a lack of design guidelines and maintenance protocol. A research study was conducted to develop a stabilization technique that would reduce maintenance costs and achieve sustainable trails. Stabilization techniques employed include the addition of surface aggregate and the addition of aggregate with geosynthetics (geotextile and geonets).

According to Tabor (2007) the trail segments (constructed between February and July of 2006) were selected based on the following criteria:

- location,
- ease and feasibility of construction,
- implementation of a particular stabilization technique and,

- and feasibility of retro-fitting the existing trail or re-routing trails which could not be retro-fitted.

The three trail segments selected include:

- the Rudolph Bennitt Conservation Area,
- the Forest 44 Conservation Area,
- and the Angeline Conservation Area.

The stabilization techniques utilized, and the post construction observations obtained from the investigations at the Forest 44 Conservation Area, the Angeline Conservation Area, and the Rudolph Bennitt Conservation Area are presented in Tables 2.12, 2.13, and 2.14, respectively. According to Tabor (2007), the successful stabilization performed for the Forest 44 Conservation Area utilized the following geosynthetics: wrap geotextiles, non-wrap geotextiles, and geocells. In the geosynthetics stabilized segments, no sagging was observed, during the post construction observation period of one year. Muddy spots were observed after a rainfall event in segments without geosynthetic stabilization.

Table 2.12. Stabilization techniques implemented and post construction observations in Forest 44 Conservation Area (as reported by Tabor, 2007).

Section	Description of Section	Segment	Existing Conditions of Segment(s)	Stabilization Technique	Post Construction Observation
1	Locally know as "Grey Trail" at Forest 44 which was located on a back slope and travelled parallel to the topographic contours (avg. width three feet)	1 to 4, 9, 11,12	Four to twelve inch deep ruts observed on steep sections while ponding and muddiness on gentle slopes.	Surface aggregate without geosynthetic for trail surface	One to two feet wide depressed path located parallel to the trail corridor on the lower side of outsloped surface.
		5,7,8,10, 13,14		Geosynthetic waterbars	Sag observed in the first two months
		16 to 19	Steep slope (15-17 %), four inch deep and four feet wide ruts. Muddy surface and widened corridor (ten feet)	Two geotextile segments (wrap and non-wrap) and two segments with four inch geocell.	No sagging observed during the first twelve months post construction. Significant amount of fines observed along with 1/4 inch deep foot print in January 2007.
		6 and 20	Crossed two ephemeral drainages	Grade dips with four inch geocells were installed to provide a stable surface and avoid ponding	No segment specific information provided.
2	Located in a valley along the Yellow Trail, 12 feet wide over 800 feet long & stream crossing. Muddiness observed for long periods imitating ephemeral drainage after rain event.	1	Natural soil	No stabilization performed	Muddy after rain events, two inch deep loose dust observed during dry periods.
		2,4	Crowned trail surface	Geotextile wrap	Crowned trail surface, two feet wide path and no depression observed during the twelve month observation period. Smooth surface more fines and one inch particles missing in January 2007.
		3	Stream crossing	Eight inch geocell	Smooth surface, more fines and one inch particles missing in January 2007.
3	300 feet section of the Brown Trail, steep slope, wet and muddy consisting clay	1	Steepest segment (slope 18%)	Four inch geocell, surface crowned and waterbars installed	No depression observed on the crowned surface. Smooth surface and more fines in January 2007.
		2,3	No segment specific information provided.	Geotextile wraps, surface crowned and waterbars installed	Two feet wide travel path observed.
		4	No segment specific information provided.	Non-wrap geotextile, surface crowned and waterbars installed	

The stabilization performed for Angeline Conservation Area utilized non-wrap geotextile, surface aggregate with geosynthetics, and an eight inch thick base course layer in which the top two inches were clean aggregate (Tabor, 2007). Water diversion from uphill to downhill was

unsuccessful after a rainstorm event as evidenced by six-inch deep ruts. Muddiness and ponding were observed along with base course intrusion into subgrade. No benefits from the various stabilization techniques at the Angeline Conservation Area were determined.

As per Tabor (2007), the stabilization performed for Rudolph Bennitt Conservation Area utilized water bars, rerouting of trails, geocells, wrap geotextile and non-wrap geotextile. Muddy surfaces, clogging, and ponding were the major issues observed following implementation. Re-routing of a trail segment also proved ineffective. The geocell was the only stabilization technique that provided satisfactory results.

Table 2.13. Stabilization techniques implemented and post construction observations in Angeline Conservation Area (as reported by Tabor, 2007).

Section	Description of Section	Segment	Existing Conditions of Segment(s)	Stabilization Technique	Post Construction Observation
1	• No drainage, • Rutting on steep slopes, • Surface particles were rock fragments and cobbles (three to five inches), • Surface was saturated clay underlain by dolomite rock, • Constant muddiness and saturation, • Topography was stair stepped/benched and, • No natural soil surface included in this section	1 to 3, 18,19	No segment specific information provided	Surface aggregate without geosynthetic	Rainstorm occurred the night before initial visit and so running water was observed on segments 9,10, 20 to 22. No rutting observed in segments 1 to 21 due to horses. Water diversion was unsuccessful from uphill to downhill and six inch deep ruts observed after the intense thunderstorm in September 2006.
		4 to 11, 13 to 17	Flat bench near Segment 13, Segment 9 and 10 are located within 36 inches of bedrock above a benched topography	Non-wrap geotextile	
		12	Flat bench topography	Wrap geotextile	
		20	Slope 20 percent, located within 36 inches of bedrock	Surface aggregate without geosynthetic	
		21	Slope greater than 40 percent, located within 36 inches of bedrock directly above a footslope		No rutting due to horses but four to six inch deep ruts observed due to wheeled vehicles. Muddiness and ponding also observed. Intermixing of surface aggregate with underlying clay observed
		22	Weak soil near stream crossing, located within 36 inches of bedrock directly above a footslope	Eight inch thick layer consisting two inch clean aggregate and remaining was surface aggregate	

Table 2.14. Stabilization techniques implemented and post construction observations in Rudolph Bennitt Conservation Area (as reported by Tabor, 2007).

Section	Description of Section	Segment	Existing Conditions of Segment(s)	Stabilization Technique	Post Construction Observation
1	Over 3000 feet in length following the ridge top and then travels downhill to the stream crossing.	1 to 21	• Along the ridge top the trail follows an old road bed (ten feet wide and six to twelve inches below the surface), • High plasticity clay and,	Ridge top was rerouted and water barriers* were built along the old trail.	Muddy surface with deep hoof prints observed after rain. Water barriers proved effective except: • Few water bars had geotextile ripped due to aggregate removal and, • Infiltration bars without aggregate were filled with sediments
		22 to 34	• Muddy section with no drainage	Re-routed trail, switchbacks used to lengthen trail and minimize slope & in-situ soil was used as trail surface	Almost always muddy trail with four to six inches deep hoof prints
		35		Four inch geocell	A rut was observed perpendicular to the trail
		36		Geotextile wrap	Surface aggregate was observed to be stable
		37		60 feet of eight inch thick geocell	No segment specific information provided
2	Over 750 feet in length which consisted a new path across the earthen dam for Rudolph Bennitt Lake.	1, 3 and 11	Presence of earthen dam across the trail path	Geocells were installed. Segments 1 and 3 are on the slopes (>10 percent) across the spillway	No ruts observed over a ten month observation period
		2, 4 to10		Wrap and non-wrap geotextiles	
3	1000 feet in length that went up and down the hill (with slopes ranging 10-20 percent).	1 to 18	Poor drainage, muddy trail and unstable path.	Re-routed to follow topographic contours with final length over 1400 feet. Existing drainage crossings were filled with rip-rap and covered with one inch clean aggregate.	• Severe muddiness (March 2007), • Six inch deep hoof print filled with water, • Ponding and clogging of two out of four drainage crossings

**Water barriers consist of water bars, infiltration bars, and grade dips.*

2.5. Previous Laboratory Studies

Discussion of previous research projects in which filtration of geosynthetics was studied using laboratory testing is presented in this section. These projects are well documented in the literature and provide real-world performance data for base course and geotextiles. The previous projects included in this section include:

- Section 2.5.1-investigation of the effects of fines on base course performance (Arkansas) as presented in Lawrence, 2006.
- Section 2.5.2- long-term performance of geosynthetics in drainage applications (nationwide) as presented in Koerner, 1994.
- Section 2.5.3- properties of geosynthetics exhumed from a final cover at a solid waste landfill (Wisconsin) as presented in Benson et al., 2010.

The results of these studies and recommendations proposed by the studies are also presented in this section.

2.5.1. Investigation of the Effect of Fines on Base Course Performance (Arkansas) as presented in Lawrence, 2006

Lawrence (2006) investigated the effects of high base course fines content on the performance of the base course material for roadway applications in Arkansas. Material samples were obtained from five different quarries to represent the effects of fines on various geological materials. A "model" gradation blend was developed based on historical data and the relevant AHTD specifications. According to Lawrence (2006), the model gradation was developed utilizing samples created containing six percent, eight percent, ten percent, twelve percent, fourteen percent, and sixteen percent fines.

As per AHTD specifications, the acceptable range of fines for Class 7 base is between three percent and ten percent. The ability to control the quantity of fines content in Class 7 base is difficult and costly for aggregate suppliers utilizing a rock crusher (Lawrence, 2006). The material specification for Class 7 base (as reported by Lawrence, 2006) is presented in Table

2.15. The quarries as characterized by source rock type, geological formation, and location are presented in Table 2.16.

Table 2.15. AHTD Class 7 material specifications (AHTD 1996 as reported by Lawrence, 2006).

Sieve	Percent Passing	Particle Size Breakpoint
1.5 inch	100	1.5 inch
1 inch	60-100	-
3/4 inch	50-90	3/4 inch
No. 4	25-55	No. 4
No. 40	10-30	No. 40
No. 200	3-10	No. 200
Maximum Liquid Limit (minus No. 40 material)	25	-
Maximum Plasticity Index (minus No. 40 material)	6	-
Minimum crusher-run material	90	-
Maximum percent wear by the Los Angeles Test	45	-

Table 2.16. Characterization of base course materials (as reported by Lawrence, 2006).

Quarry	Location (County)	Aggregate Type	Geological Formation
Sharps	Benton	Limestone	Boone
Preston	Crawford	Sandstone	Hartshorne
Black Rock	Lawrence	Dolomite	Powell
Glen Rose	Hot Springs	Noviculite	Arkansas Noviculite
Granite Mountain	Pulaski	Syenite	Cretaceous

Lawrence (2006) reported that samples were obtained from the working faces of produced Class 7 quarry stockpiles utilizing heavy duty front end loaders. The samples were then transported to the University of Arkansas Engineering Research Center (ERC). Approximately 3,000 to 5,000 pounds of Class 7 material was obtained from each quarry. Fractioning of aggregate was performed using the AHTD gradation acceptance criteria as previously presented in Table 2.15 (Lawrence, 2006).

According to Lawrence (2006), the model gradation was created to characterize

the upper boundary of the historical and the “as received” gradation. This was based on the hypothesis that material properties for the finer grained blends represent the worst case for hydraulic conductivity. The “as received’ and model blends are presented in Figure 2.11.

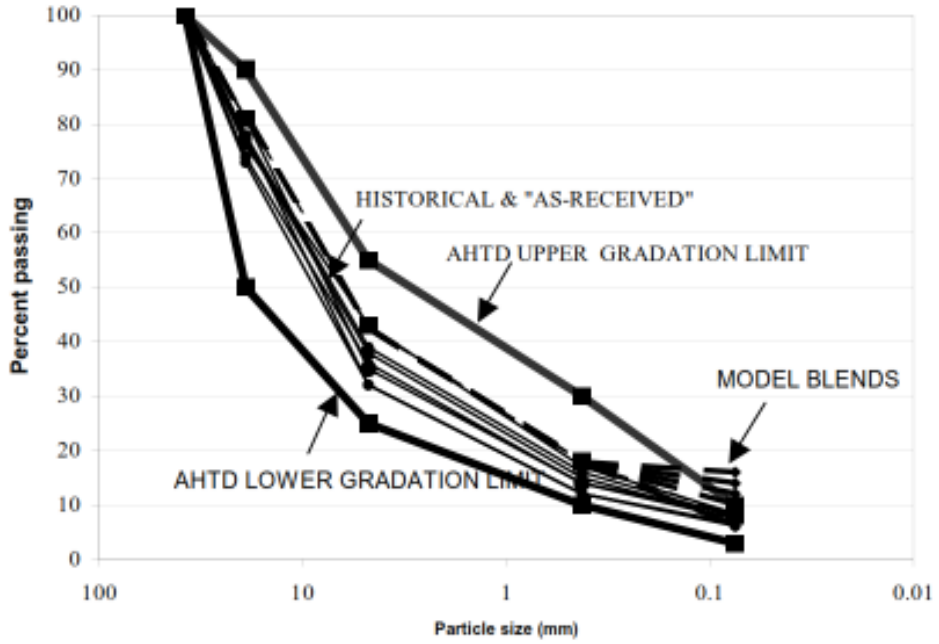

Figure 2.11. Grain size distribution curves for AHTD lower gradation limits, model blends, and historical and “as-received” (from Lawrence, 2006).

The fines content of the model blends ranged from six percent to sixteen percent in two percent increments. The model gradation (not the boundary blends) was expected to imitate crusher production so the fines content was varied on the model gradation.

The classification and index testing results for “as-received” Class 7 base course for the five quarries utilized in the study are presented in Table 2.17 (Lawrence, 2006). A summary of average laboratory hydraulic conductivities for the Class 7 base course utilized for the model gradations from the five quarries are presented in Table 2.18 (Lawrence, 2006).

Table 2.17. Classification and index testing results for "as-received" Class 7 base course for the five quarries utilized in the study (modified from Lawrence, 2006).

Quarry	γ_{dmax}	w_{OMC}	[1]SG	[2]SG	Atterberg Limits						D_{10}	D_{30}	D_{60}	C_u	C_c	[3]P_{200}	Classification
					Wet Method			Dry Method									
					LL	PL	PI	LL	PL	PI							
	(lb/ft^3)	(%)	(unitless)		(%)	(%)	(%)	(%)	(%)	(%)	(mm)	(mm)	(mm)	(unitless)		(%)	[4]USCS
Sharps	141	5.5	2.68	2.51	16	12	4	NP	NP	NA	0.10	1.70	13.00	136.84	2.34	7.50	GW-GM
Preston	132	7.5	2.63	2.51	NP	NP	NP	NP	NP	NA	0.10	2.40	11.00	115.79	5.51	6.00	GP-GM
Black Rock	144	6.5	2.83	2.75	16	13	3	NP	NP	NA	0.11	2.50	13.00	118.18	4.37	9.30	GP-GM
Glen Rose	135	6.0	2.61	2.57	16	11	5	16	11	5	0.16	1.10	9.20	57.50	0.82	8.00	GP-GM
Granite Mountain	134	7.5	2.64	2.62	28	21	8	26	22	4	0.10	1.50	9.00	90.00	2.50	4.10	GW-GM

[1] Apparent Specific Gravity

[2] Bulk Specific Gravity (Historical)

[3] Percent passing No. 200 sieve

[4] Classification based on Atterberg limits from dry method

Table 2.18. Summary of average hydraulic conductivity for the Class 7 base course utilized for the model gradations from the five quarries (from Lawrence, 2006).

Fines content (%)	Testing	Average Hydraulic Conductivity (cm/s)				
		Sharps	Preston	Black Rock	Glen Rose	Granite Mountain
6	CHP[1]	3.97E-03	2.91E-03	5.80E-03	3.88E-03	2.74E-03
8	CHP	1.89E-03	1.60E-03	7.92E-03	3.83E-03	1.21E-04
10	FWP[2]	2.60E-05	9.40E-06	3.84E-05	5.75E-04	1.72E-06
12	FWP	1.14E-05	3.55E-06	5.48E-05	1.11E-04	6.55E-07
14	FWP	1.06E-05	2.96E-06	8.53E-06	1.25E-04	9.36E-07
16	FWP	5.05E-06	3.74E-06	7.12E-06	5.65E-06	9.78E-07

[1] Constant Head Permeameter

[2] Flexible Wall Permemameter

The higher hydraulic conductivity of Glen Rose quarry sample at 16 percent fines content was attributed to river run fines which are more rounded particles. The author postulated that more rounded particles create larger void spaces and result in higher hydraulic conductivity values. No explanation was provided for the increased hydraulic conductivity values for Granite Mountain quarry and Preston quarry samples.

As reported by Lawrence (2006), for every one percent increase in fines content (between six and ten percent) the hydraulic conductivity was reduced by one order of magnitude. However above ten percent (until sixteen percent) the decrease in hydraulic conductivity is less than one order of magnitude for one percent change in fines content. Therefore, it was postulated by Lawrence (2006) that the decrease in hydraulic conductivity for fines content greater than ten percent is relatively unimportant; even though, as per Lawrence (2006), the hydraulic conductivity of granular base course decreases with an increase of fines content.

2.5.2. Long-term performance of geosynthetics in drainage applications (nationwide) as presented in Koerner, 1994.

A research study was conducted to predict drainage systems behavior utilized in transportation applications (Koerner, 1994). As part of a national research program (sponsored by AASHTO), geosynthetic samples were exhumed from pavements at 91 sites in 17 states and tested in laboratory (Koerner, 1994).

According to Koerner (1994) site selection was based on survey responses provided by geotechnical and materials engineers from the Department of Transportation (DOT) offices for the 50 states. The site selection was categorized as sites facing problems, functioning as intended, or observed behavior was uncertain (Koerner, 1994). A summary of the geosynthetic performance of the exhumed specimens along with a definition of acceptable and non-acceptable performance are presented in Table 2.19.

Table 2.19. Summary of results for 91 exhumed geosynthetic performance and classification of acceptable and non-acceptable performance (from Koerner, 1994).

Drainage system	Number of sites	Acceptable performance (A,B, or C)[1]	Non-acceptable performance (D or F)[2]	Non-acceptable performance due to[3]		
				Construction/ Maintenance	Drainage	Geotextile
Prefabricated geocomposite edge drain (PGED)	41	27	14	4	4	10
Geotextile wrapped underdrain (GWUD)	25	16	9	6	1	2
Perforated pipe underdrain (PPUD)	6	5	1	1	1	0
Geotextile socked perforated pipe (GSPP)	12	9	3	2	0	1
Geotextile wall drain filter (GWDF)	3	3	0	0	0	0
Geotextile erosion control filter (GECF)	4	3	1	1	0	1
Total	91	63	28	14	6	14

[1]
A: all three components (system, drain, and filter) performing as intended

B: one component performing less than ideal

C: more than one component performing less than ideal

[2]

D: one component performing poorly

F: more than one component performing poorly or failure of one component

[3]Multiple non acceptable performance on some sites caused the total to be greater than non acceptable performance

Non-acceptable performance due to the geotextile, based on the results previously presented in Table 2.19, became the focus of the investigation (Koerner, 1994). According to Koerner (1994) lack of initial contact between the geotextile and base course caused non-acceptable performance of the geosynthetics based on visual inspection. The testing conducted on geotextile samples includes long term flow test (LTFT), fine fraction filtration test (F^3), and dynamic fine fraction filtration test (DF^3). The criteria utilized to analyze the three testing methods are presented in Table 2.20.

Table 2.20. Criteria to analyze laboratory results conducting on exhumed geotextile samples (from Koerner, 1994).

Number	Criteria
1	Flow can decrease over time until the system is non-functional, which generally signifies excessive clogging of geotextile.
2	Flow can increase over time, which generally signifies the lack of soil retention, hence excessive soil loss through the geotextile.
3	Flow can gradually decrease and then reach an equilibrium value, which should be the allowable flow rate for the system, or in some cases the lower bound of allowable flow rate.

2.5.2.1 Long term flow test (LTFT) testing

According to Koerner (1994) the LTFT is a constant head test in which geosynthetic samples are permeated over long periods of time to show the flow rate through the soil/geotextile system to observe the equilibrated flow rate, excessive clogging, or soil piping. Koerner (1994) further states that the LTFT testing was conducted on four types of geotextile with four different soil types. The soils were artificially made by blending Ottawa sands (100 percent to 5 percent) and loess-type cohesion less silts (0 to 95 percent). The test was conducted using clear and turbid de-aired water. The turbid de-aired water was produced by mixing three grams of cohesion less silt in one liter of water. Summaries containing a list of the geotextiles and soils utilized in this study along with their properties are presented in Tables 2.21 and 2.22, respectively.

Table 2.21. Properties of geotextiles used in LTFT testing (from Koerner, 1994).

Type of geotextile	Permittivity (s^{-1})	AOS O_{95} (U.S. std. sieve)
Non-woven needle-punched polyester	1.8	0.125 (No. 120)
Non-woven heat bonded polypropylene	2.5	0.090 (No. 170)
Woven monofilament polypropylene	0.6	0.212 (No. 70)
Non-woven needle-punched polypropylene	2.9	0.125 (No. 120)

Table 2.22. Gradation properties of soils used in LTFT testing (from Koerner, 1994).

Soil type	D_{85} (mm)	D_{60} (mm)	D_{50} (mm)	D_{15} (mm)	D_{10} (mm)	C_u (unitless)
Ottawa sand (100%)	1.00	0.80	0.75	0.65	0.62	1.3
5%-95% silty sand	1.00	0.69	0.62	0.45	0.40	1.7
25%-75% sandy silt	1.00	0.54	0.46	0.04	0.02	24.5
Silt (100%)	0.05	0.04	0.03	0.02	0.01	3.2

According to Koerner (1994) for the clear water flow, the decrease in flow rates was directly proportional to the quantity of silt blended in the soil. The clear water system was a stable filtration system for all of the soil-geotextile combinations tested. The limit of detectability of the system was observed in the system containing 100 percent silt (Koerner, 1994). In the turbid water flow, silt passage through the soil-geotextile interface achieved steady state at 1,000 hours for all the geotextiles (Koerner, 1994). The geotextiles allowed passage of silt at low percentages ($\leq$ 5 percent) but at higher silt percentages ($\leq$ 25 percent) flow rate was decreased significantly (Koerner, 1994). The LTFT testing was successful in predicting drainage system behavior.

2.5.2.2 Fine fraction filtration (F^3) testing

According to Koerner (1994) the F^3 test is based on a hypothesis "the fine fraction of the soil upstream of a filter poses a major challenge to its long term behavior". Hence, soil samples

with particles that are finer than the apparent opening size (AOS) of the geotextiles were used to conduct testing.

The soil types used were Ottawa sands, fly ash, and well-graded sandy silt locally known as Le Bow soil. The same types of geotextiles, as presented previously in Table 2.21, were used in conjunction with the same type of soils. Ottawa sand built up a layer on the various geotextiles causing equilibrium flow rates (Koerner, 1994). The fly ash completely passed through the geotextiles due to the AOS of the geotextile being greater than the fly ash which implied excessive soil loss. Flow rates through the geotextile were reduced for Le Bow soil due to the gradual built up of the Le Bow soil on the geotextile (Koerner, 1994). These reduced flow rates were obtained for sites with acceptable and non-acceptable performance. No differentiation in flow characteristics were observed between sites classified as "A" or sites classified as "F", as previously presented in Table 2.19, by conducting the F^3 testing.

2.5.2.3 Dynamic fine fraction filtration (DF^3) testing

According to Koerner (1994) the DF^3 testing is required under specialized conditions such as dynamic loading of railroads, erosion control filters for coastal waterways, and etc. The DF^3 is a fine filtration test which utilizes dynamic pulsing of the hydraulic system (Koerner, 1994). The soil types used for the DF^3 testing were fly ash, well graded sand, and Le Bow soil.

The fly ash passed through the non-woven needle-punched geotextile due to the AOS of geotextile being greater than the size of the fine particles. The well graded soil initially decreased the flow through the non-woven needle-punched geotextile and finally equilibrated. The Le Bow soil reduced the flow of the system until the lower system limit (0.01 sec^{-1}) was reached (Koerner, 1994). Similar to the F^3 testing no differentiation in flow characteristics were observed

by conducting the DF^3 testing for sites previously denoted as "A through F" in Table 2.19 (Koerner, 1994).

2.5.3. Properties of geosynthetics exhumed from a final cover at a solid waste landfill as presented in Benson et al, 2010.

A laboratory study was conducted to investigate the performance of exhumed geosynthetic samples in June 2007 from a final cover at a solid waste landfill in Wisconsin (Benson et al., 2010). While the final cover of a landfill is not the same application for the use of geosynthetics as a roadway application, the testing conducted on the samples was similar to the testing conducted as a part of the research discussed in this report. The exhumed geosynthetic samples were geocomposites drains (GCD), geomembrane (GM), and geosynthetic clay liner (GCL). The details of geosynthetic exhumed samples are presented in Table 2.23. The profile of Test Pits 1 to 4 is presented in Figure 2.12.

Table 2.23. Summary of geosynthetics exhumed in June 2007 from a final cover at a solid waste landfill facility in Wisconsin (from Benson et al., 2010).

Test Pit	1	2	3	4
Location	Lower Side Slope (4:1)	Upper Side Slope (4:1)	Top Deck (3%)	Top Deck (3%)
Installation Date	08/2001	08/2001, 9/2002	09/2002	09/2002
Sampling Date	06/2007	06/2007	06/2007	06/2007
Service life (in years)	5.8	4.7, 5.8	4.7	4.7
Surface layer thickness (mm)	915	1145	915	1220
Geocomposite drain (GCD)	GSE HyperNet 5.1 mm HDPE drainage net with 227g nonwoven, polypropylene geotextile heat-bonded both sides.		GSE HyperNet 5.1 mm HDPE drainage net with 170g nonwoven, polypropylene geotextile heat-bonded both sides.	
Geomembrane	GSE 1mm textured LLDPE			
Geosynthetic clay liner (GCL)	CETCO Bentomat ST with 5.1±0.3 kg/m^2 granular bentonite	CETCO Bentomat ST with 5.1±0.3 kg/m^2 granular bentonite, Bentonite NSL 4.7±0.4 kg/m^2 granular bentonite	Bentonite NSL 4.7+0.4 kg/m^2 granular bentonite	

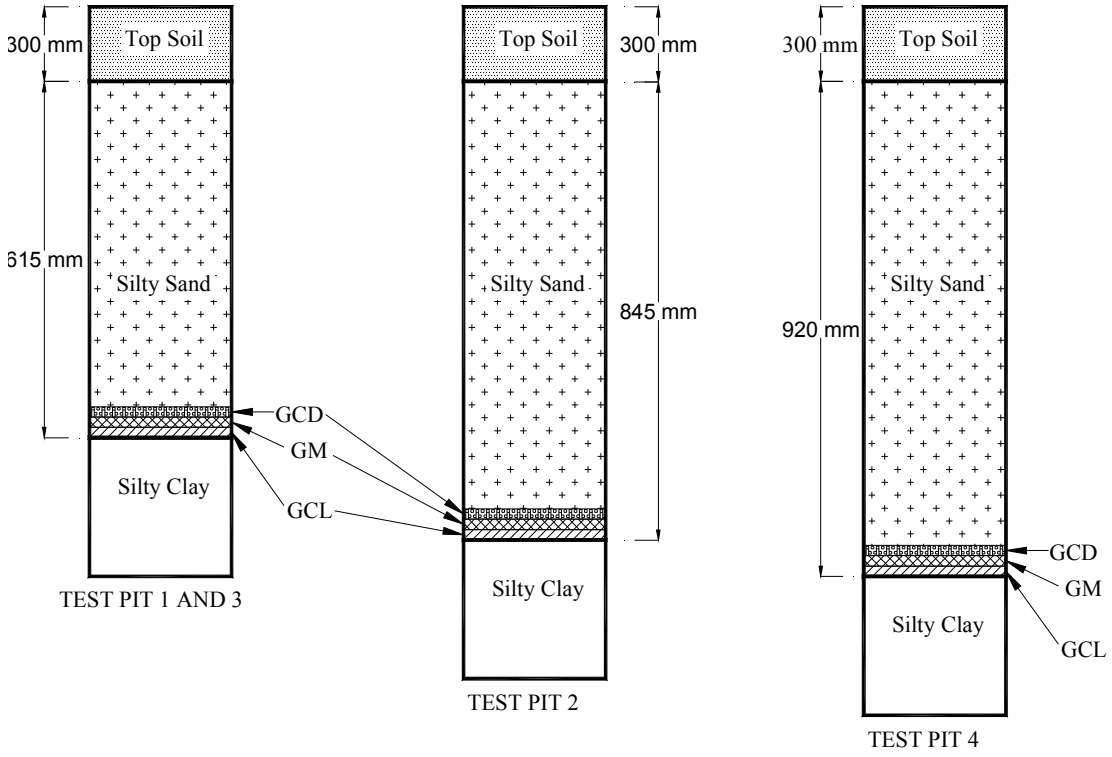

Figure 2.12. Profile of test pits 1 to 4 (from Benson et al., 2010).

According to Benson et al., (2010), no visible defect of exhumed geosynthetics was observed. The overlapped areas of the geotextile had no soil intrusion and hence the geotextile was effective in retaining overlying soil. Fines were observed on the geonet ribs but did not cause excessive clogging. No movement of the GCL had occurred based on the fact that the alignment coordinated with match points (Benson et al., 2010). The exhumed subgrade soil properties are presented in Table 2.24.

Table 2.24. Properties of exhumed subgrade soil (from Benson et al., 2010).

Test Pit	Water Content (%)	Fines content (%)	USCS Designation
Test Pit 1	15.1	79	CL-ML
Test Pit 2	14.5	85	CL-ML
Test Pit 3	15.8	83	CL-ML
Test Pit 4	16.2	76	CL-ML

According to Benson et al. (2010), the water content of the subgrade soil in direct contact of the GCL ranged from 14.5 percent to 15.2 percent and the fines content of the subgrade soil ranged from 76 percent to 83 percent.

According to Benson et al.,(2010), constant head testing was conducted on the GCD with values of head of 10 mm (imitating in-situ conditions) and 50 mm (to compare with the measured permittivity during construction) to measure the permittivity of the exhumed GCD (50 mm diameter specimen). Transmissivity of the exhumed GCD (305 mm by 356 mm specimen) was also measured in the machine direction utilizing a hydraulic gradient of 1.0 and normal stresses of 24kPa (imitating in-situ conditions) and 480 kPa (to compare with manufacture data from Benson et al., 2010). The permittivity and transmissivity values obtained by laboratory testing are presented in Table 2.25.

Table 2.25. Permittivity and transmissivity values obtained by laboratory testing for GCD (from Benson et al., 2010).

Test Pit	Sample	Permittivity (s^{-1})		Transmissivity (m^2/s)	
		Head (10 mm)	Head (50 mm)	σ* (24 kPa)	σ* (480 kPa)
Test Pit 1	1	0.30	0.20	4.4E-4	2.0E-4
	2	0.39	0.31	5.4E-4	2.3E-4
	3	0.61	0.51	3.4E-4	1.4E-4
Test Pit 2	1	0.59	0.42	2.8E-4	1.1E-4
	2	0.68	0.55	6.1E-4	1.7E-4
	3	0.30	0.26	4.0E-4	1.5E-4
Test Pit 3	1	0.35	0.27	3.0E-4	1.2E-4
	2	0.69	0.49	7.2E-4	1.4E-4
	3	0.59	0.46	3.6E-4	1.3E-4
	4	0.45	0.26	5.7E-4	1.5E-4
Test Pit 4	1	0.79	0.60	3.4E-4	1.2E-4
	2	0.81	0.51	5.7E-4	1.2E-4
	3	0.88	0.53	5.6E-4	1.0E-4
	4	0.61	0.38	2.7E-4	1.3E-4

*Normal Stress

According to Benson et al. (2010), consistent permittivity values were obtained by laboratory testing for the head of 10 mm and 50 mm. The permittivity values obtained by laboratory testing for the exhumed GCD at 50 mm head (0.2 s^{-1} to 0.6 s^{-1}) were lower than the permittivity values obtained prior to construction (1.51 s^{-1} to 1.72 s^{-1}). Furthermore, the low permittivity values of the exhumed samples were attributed to soil intrusion. The permittivity was still adequate (at least ten times higher than required) to permit one unit gradient flow from the overlying silty sand (Benson et al., 2010).

According to Benson et al. (2010), consistent transmissivity values were also obtained by laboratory testing at normal stress of 24 kPa and 480 kPa. A summary of the comparison between the transmissivity values of the exhumed samples and the transmissivity values reported by the manufacturer are presented in Table 2.26. The transmissivity values obtained by laboratory testing at a hydraulic gradient of 1.0 and normal stress of 480 kPa for the exhumed GCD samples were higher than the transmissivity values published by the manufacture (Benson et al., 2010). No explanation in increase in the transmissivity values were provided except that the satisfactory filtration was provided and the aperture opening size (AOS) met the common filter criteria (Benson et al., 2010).

Table 2.26. Comparison of GCD transmissivity values obtained in the laboratory for exhumed samples and the manufacture published data for the new samples (from Benson et al., 2010).

Test Pit	Transmissivity at σ^* = 480 kPa	
	Exhumed	Manufacturer
	(m^2/s)	(m^2/s)
Test Pit 1	1.1E-4 to 2.3E-4	4.0E-05
Test Pit 2		
Test Pit 3	1.0E-4 to 1.5E-4	6.0E-05
Test Pit 4		

*Normal Stress

2.6. Arkansas Test Section Site

Social, demographic and weather information about the Marked Tree, Arkansas are presented in Section 2.6.1. The site location and the process used for site selection for the current research project are presented in Section 2.6.2 and 2.6.3, respectively. This information is included for completeness.

2.6.1. Social, Demographic and Weather Information about Marked Tree, Arkansas.

The Arkansas test section site was constructed in Marked Tree, Arkansas, and has been in service since 2006. The elevation of the City of Marked Tree is 224 feet above mean sea level (Marked Tree, AR, 2011). The population of Marked Tree is 3,100 people (Marked Tree, AR, 2011). Mean daily temperatures ranges from 52°F to 72°F (Marked Tree, AR, 2011). The average yearly total precipitation based on 100 years of historical data in Poinsett County is 49.40 inches (National Oceanic and Atmospheric Administration, 2010) as presented in Figure 2.13.

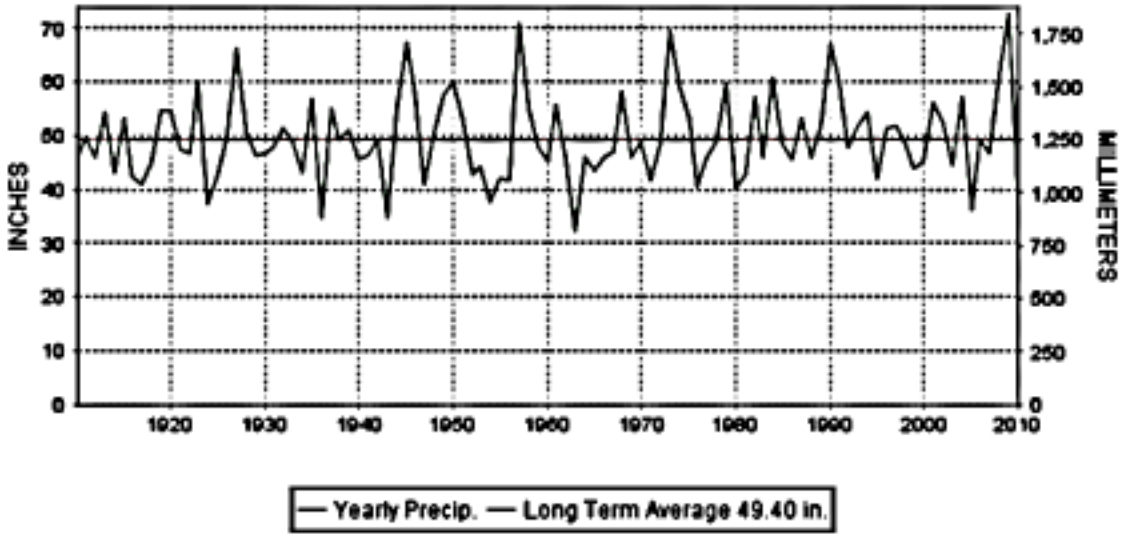

Figure 2.13. Historical precipitation for Poinsett County (modified from NOAA, 2010).

2.6.2. Site Location

The Arkansas Test Section Site is located on Frontage Road 3 in Marked Tree, Arkansas. As discussed in Section 2.5.1, Marked Tree is a small town located in northeast Arkansas. Frontage Road 3 runs parallel to U.S. Highway 63 and connects to Arkansas Highway 75 (Figure 2.14). Major cities in the vicinity of Marked Tree are Jonesboro, Arkansas, located 33 miles to the Northwest, and Memphis, Tennessee, located 39 miles to the Southeast.

Figure 2.14. Google Map satellite image of test site located on Frontage Road 3, Marked Tree, AR (modified from Google Maps, 2010).

2.6.3. Site Selection

Research was conducted at the Marked Tree, AR test section during previous research projects. Specifically, the site was constructed as part of AHTD TRC Project 0406 and the site was investigated as part of AHTD TRC Project 0903. The scope of the AHTD TRC 0406 and AHTD TRC 0903 research projects are listed below for reference.

- As discussed previously in Section 2.4.1, the AHTD TRC 0406 research project was a full scale field study that included finite element modeling to study the effects of geosynthetics on flexible pavement (Hall et al., 2007).

- Researchers associated with AHTD TRC Project 0903 research project evaluated the basal reinforcement of flexible pavement with geosynthetics (Goldman, 2011). The object of the AHTD TRC 0903 research project was to evaluate the mechanisms of basal reinforcement of pavements and to evaluate different field tests to infer the contribution of reinforcement geosynthetics in using pavement performance. The current performance of the pavement sections at the Marked Tree site were evaluated, with the goal of comparing the effects of the different geosynthetics types and base course depths.

The Marked Tree, AR site, as originally constructed, consisted of sixteen flexible pavement sections in the East-bound lane of Frontage Road 3. As shown in Figure 2.15, each section is 50 feet long, and the sections are located between STATION 136+50 and STATION 145+00. Each section contains a unique type of geosynthetic, however the control section do not include any type of geosynthetic. Geosynthetics were placed at the base course/subgrade interface installed under either six-inches or ten-inches of base course thickness. A transition in base course thickness from ten-inches thick to six-inches thick occurs in Section 7. The test sections were constructed with a research focus to study the effects of geosynthetics on pavement performance.

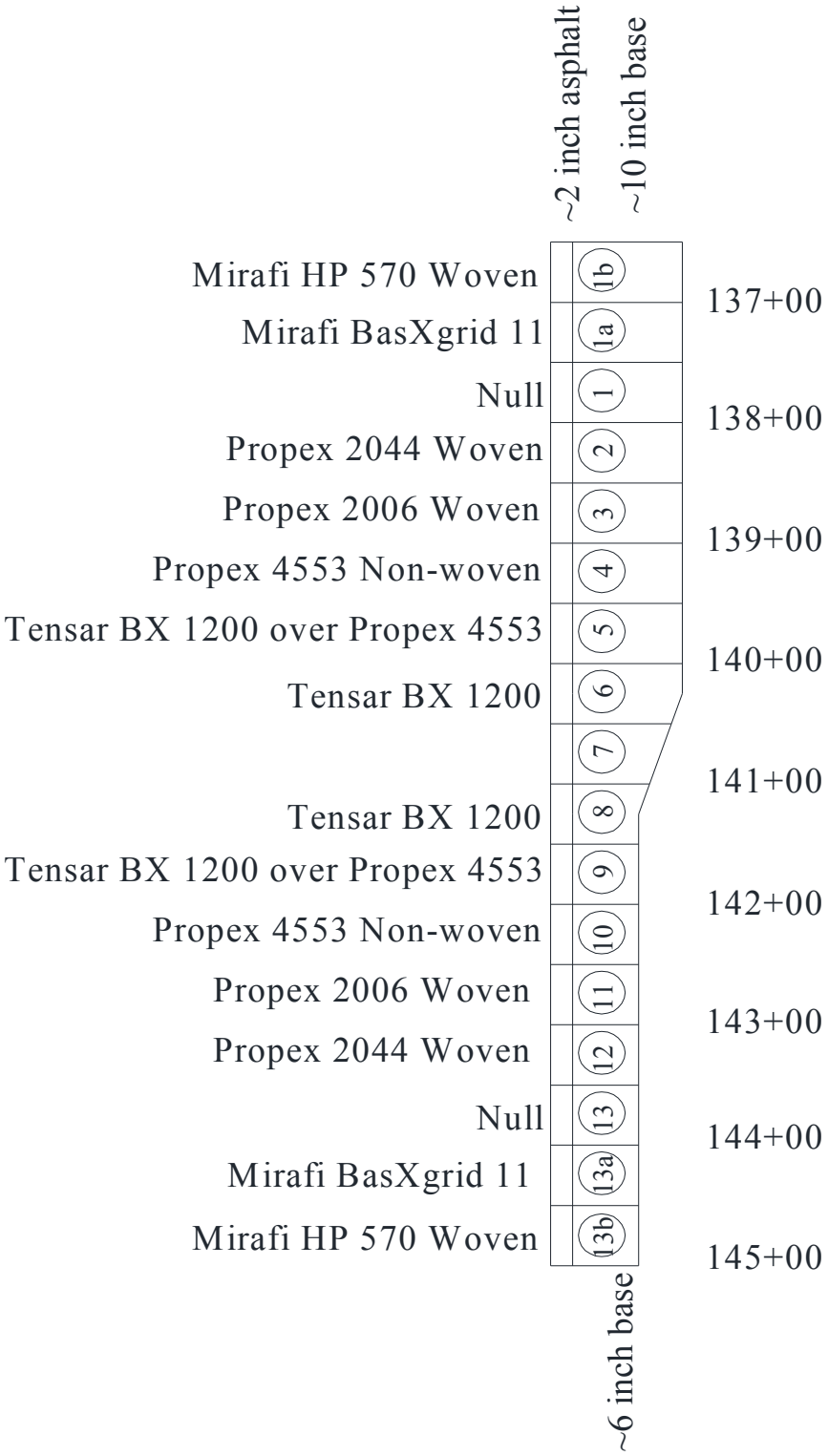

Figure 2.15. Profile view of sections showing various geosynthetics installed at the Marked Tree, AR (from Coffman, 2010).

2.7. Conclusion

The definition, classification, and function of geosynthetics were discussed in this chapter. The functions of geosynthetics include separation, reinforcement, filtration, drainage, and containment. Specifically, as applied to the research discussed in this report, geotextiles are a type of geosynthetic utilized for separation, reinforcement, and filtration.

Past field studies utilizing geotextiles to stabilize roadways, equestrian trails, and hike and bike trails were also presented in this chapter. The site location for these research projects were Arkansas, Virginia, and Missouri. The field studies were conducted to quantify the benefits of utilizing geotextiles as an effective filtration and separation medium in different applications, and to present hydraulic conductivity values for base course in roadway applications for State of Missouri.

Past laboratory studies investigating the filtration and separation aspect of geotextiles were also presented in this chapter. Specifically, different laboratory testing techniques and performance of geotextiles in landfill application were presented. The laboratory techniques explored were long term flow testing, fine fraction filtration testing, dynamic fine filtration testing, permittivity testing, and transmissivity testing. The dynamic fine filtration and fine fraction filtration testing were used to successfully differentiate the in-situ problem but not the site performance. The long term flow testing was successfully used to identify the problem and predict site performance. The major disadvantage of the long term flow testing was lengthy testing period. The permittivity and transmissivity of geocomposite drains was also measured before and after installation to determine the viability of the use of the geocomposite drains. After exhumation, the drains appeared to be in working order based on the results of the permittivity and transmissivity testing.

Site details for the current research project were also presented in this chapter. This site was constructed as part of a research project that investigated the performance of the pavement system using in-situ sensors. The site was also used for previous research projects that attempted to quantify benefits of geotextile using deflection based tests.

Chapter 3. Methods and Procedures

3.1. Introduction

Field sample collection, field testing, field measurements, and laboratory testing performed on the samples which were collected in the field are discussed in this chapter. Base course, subgrade, and geosynthetic samples were exhumed and collected from 18 test sections during a field visit to the Arkansas Test Section site conducted from October 25th to 29th, 2010. The sample collection procedures utilized during this visit are presented in Section 3.2. The procedures used to conduct field hydraulic conductivity testing of the base course are presented in Section 3.3. The laboratory testing schedule and procedures used to conduct the laboratory testing for the base course, subgrade, and geosynthetic samples are presented in Section 3.4. Field measurement techniques, utilized to comprehend the pavement conditions, including: roadway alignment, asphalt and base course thickness, and pavement performance (rutting, alligator cracking, longitudinal cracking, and transverse cracking) are presented in Section 3.5.

The laboratory testing was performed to identify and characterize base course and subgrade materials, to measure the hydraulic conductivity of recompacted base course (for comparison with 1) the hydraulic conductivity values measured in the field, and 2) estimated using the equations presented previously in Section 2.4.3), and to measure the permittivity and transmissivity of geosynthetic separators. The laboratory testing techniques performed on exhumed subgrade samples include: wash sieve, hydrometers, Atterberg limits, and specific gravity. The laboratory testing procedures performed on exhumed base course samples include: dry sieve, wet sieve, hydrometers, specific gravity, modified proctor, and hydraulic conductivity. The laboratory testing procedures performed on exhumed geotextile samples include transmissivity and permittivity.

3.2. Sample Collection

Asphalt cutting and removal and field testing (including dynamic cone penetration testing and California bearing ratio testing) conducted outside of the scope of this project by Goldman (2011) but conducted in conjunction with this research project are described in Section 3.2.1. Base course, geosynthetic, and subgrade samples were collected as described in Sections 3.2.2 and 3.2.3. A flowchart providing a summary of the sample collection and field testing procedures as performed in the field (conducted as a part of this research and conducted as a part of Goldman, 2011) is presented in Figure 3.1. A schematic displaying the plan view of the Marked Tree test containing information about the various geosynthetic types installed in, and exhumed from, the sections is presented in Figure 3.2.

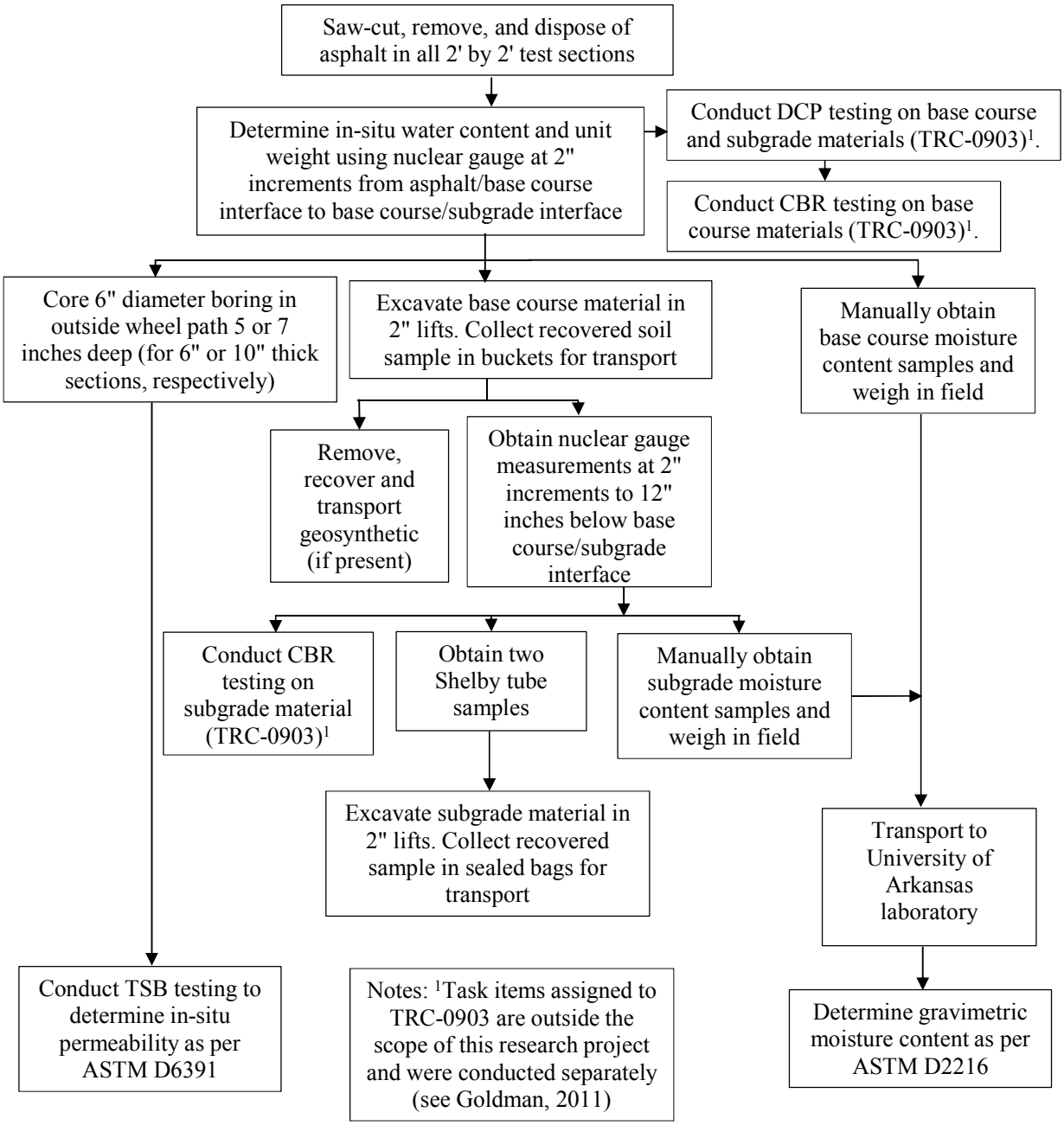

Figure 3.1. Flow chart of sample collection and field testing within each section as conducted in October 2010.

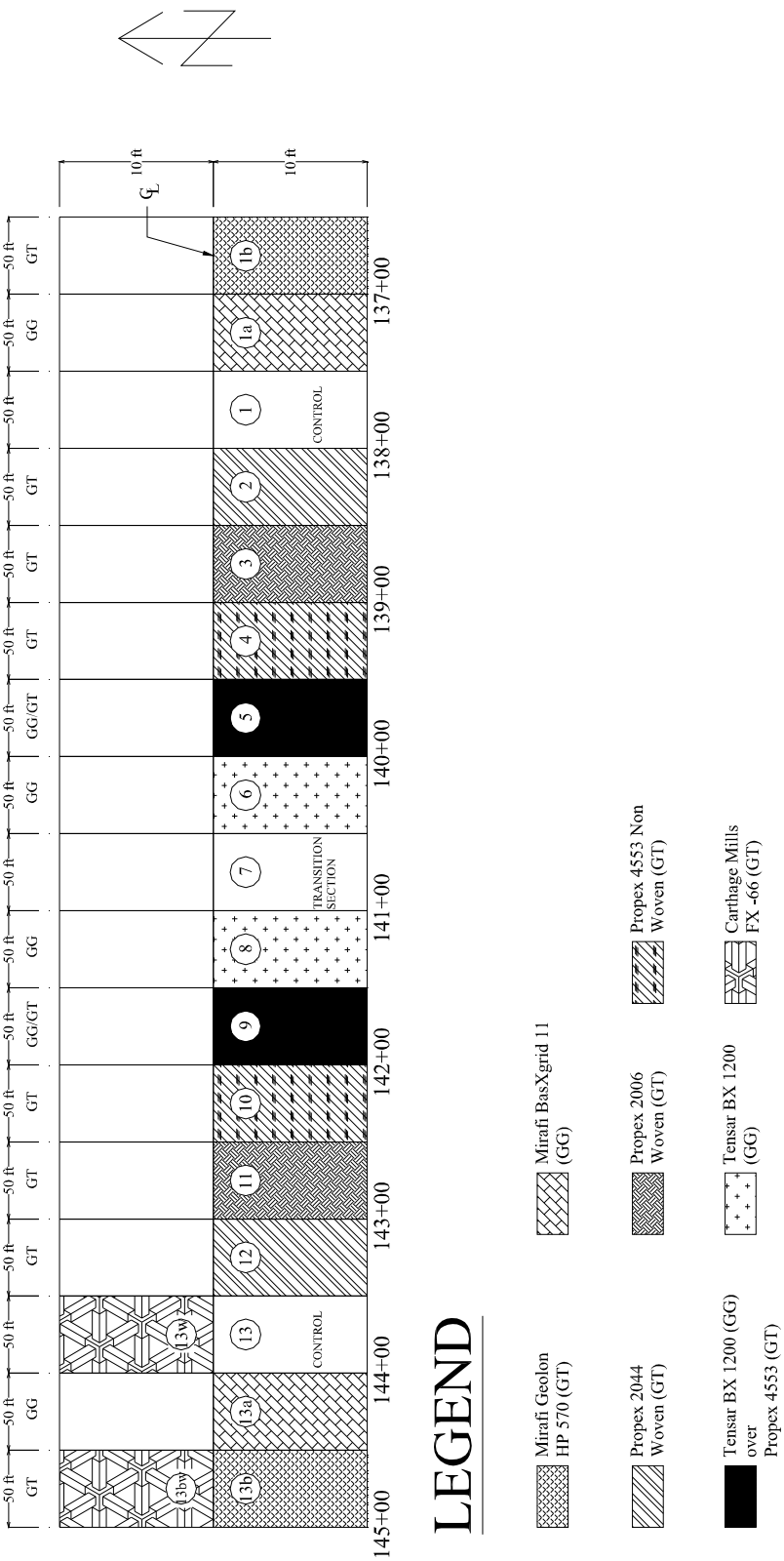

Figure 3.2. Plan view of sections showing various geosynthetics installed at the Marked Tree, AR (modified from Howard, 2007).

3.2.1. Asphalt Cutting and Removal, Dynamic Cone Penetrometer, and California Bearing Ratio Testing

A two foot by two foot test area was clearly marked using spray paint in the outside wheel path of each of the roadway sections (as shown previously in Figure 3.2). The outline of the test areas was then cut by AHTD personnel using a wet circular saw as presented in Figure 3.3. Water introduced during asphalt cutting by the wet saw was removed using a portable vacuum to avoid changing the in-situ moisture content of the base course and subgrade below the asphalt, as presented in Figure 3.4. The asphalt was manually removed using a crowbar, if feasible; otherwise a hammer drill was used to aid in removal of the asphalt (Figure 3.5). A typical section, after removal of the asphalt is presented in Figure 3.6.

(a) **(b)**

Figure 3.3. Two foot by two foot test sections cut by Arkansas State Highway and Transportation Department (AHTD) personnel using a wet concrete saw a) Section 13W and b) Section 8.

(a) (b)

Figure 3.4. Water introduced by cutting the asphalt removed by a portable vacuum a) within the test section and b) around the test section.

(a) (b)

Figure 3.5. Removal of asphalt using a) crowbar (Section 13W) and b) hammer drill (Section 13BW).

Figure 3.6. Two foot by two foot test area after asphalt removal (Section 3).

After the asphalt was removed, one Dynamic Cone Penetrometer (DCP) test was performed in the Southeast corner of each of the test areas (Figure 3.7). Although the DCP testing was conducted during the site visit, this testing was associated with AHTD TRC Project 0903. The full testing procedures and the results obtained from this testing are presented in Goldman (2011). For completeness, a simplified version of the testing procedure is discussed herein.

The cone was driven from the asphalt/base course interface to a depth of 600mm (~24 inch) below the asphalt/base course interface. The DCP rod and cone traveled through the base course, through the geosynthetic (if present), and into the subgrade where the test was completed. The verticality of the DCP rod was difficult to maintain at a depth of ~600mm and hence the test was terminated at this depth. Measurements of the movement of the drive anvil, caused by the impact of the hammer, were recorded after every blow; the movement of the anvil was referenced from the asphalt/base course interface. Since measurements were taken to a depth of 24 inches below the asphalt/base course interface an opening (with the same diameter as the cone) was created in the geosynthetic (if present) by the cone.

Figure 3.7. Dynamic Cone Penetrometer (DCP) testing in progress.

After DCP testing was completed within each section, one California Bearing Ratio (CBR) test was performed in the center of each test area (Figure 3.8). Although the CBR testing was conducted during the site visit, this testing was associated with AHTD TRC Project 0903.The full testing procedures and results associated with this testing are presented in Goldman (2011). For completeness, a simplified version of the testing procedure is discussed herein.

Following the nuclear density testing (as described later in Sections 3.2.2 and 3.2.3) that was conducted on the base course and on the subgrade, a CBR test was conducted within each section at the asphalt/base course interface, and the base course/subgrade interface, respectively. A surcharge load plate was placed on top of the base course layer and loading was applied through a piston ram with the aid of the University of Arkansas vibroseis truck. To achieve a penetration rate of 0.05 in/min, one revolution per every 12 seconds was required. Two LVDTs (one mounted on the truck and another underneath the load cell) were used to measure the piston movement (Goldman, 2011). The deformation of the piston was considered as the difference in movement recorded by the two LVDTs.

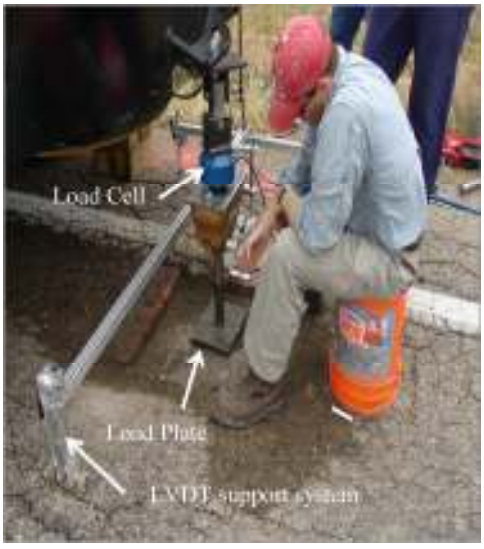

Figure 3.8. California Bearing Ratio (CBR) testing in progress.

3.2.2. Base Course Density Testing (ASTM D6938) and Sampling

After removing the asphalt, in-situ total unit weight and water content readings were obtained using a Troxler® nuclear density gauge (model 3450) following the procedures described in ASTM D6938 (2005). In the Northwest corner of each of the two foot by two foot testing areas a hole was created by driving a pre-hole driver rod through a rod guide. The rod was driven into the base course to a depth of either eight inches or twelve inches for the six-inch thick sections and ten-inch thick sections, respectively (Figure 3.9a). Density and moisture content measurements were obtained at two inch increments by lowering the source rod deeper into each pre-drilled hole within each section (Figure 3.9b). A schematic showing the various source rod positions for ten-inch thick and six-inch thick sections are presented in Figures 3.10a and 3.10b, respectively.

(a) **(b)**

Figure 3.9. a) Pre-hole driver rod driven through the rod guide and b) nuclear gauge positioned at the asphalt base course interface to obtain base course density and water content readings for the base course.

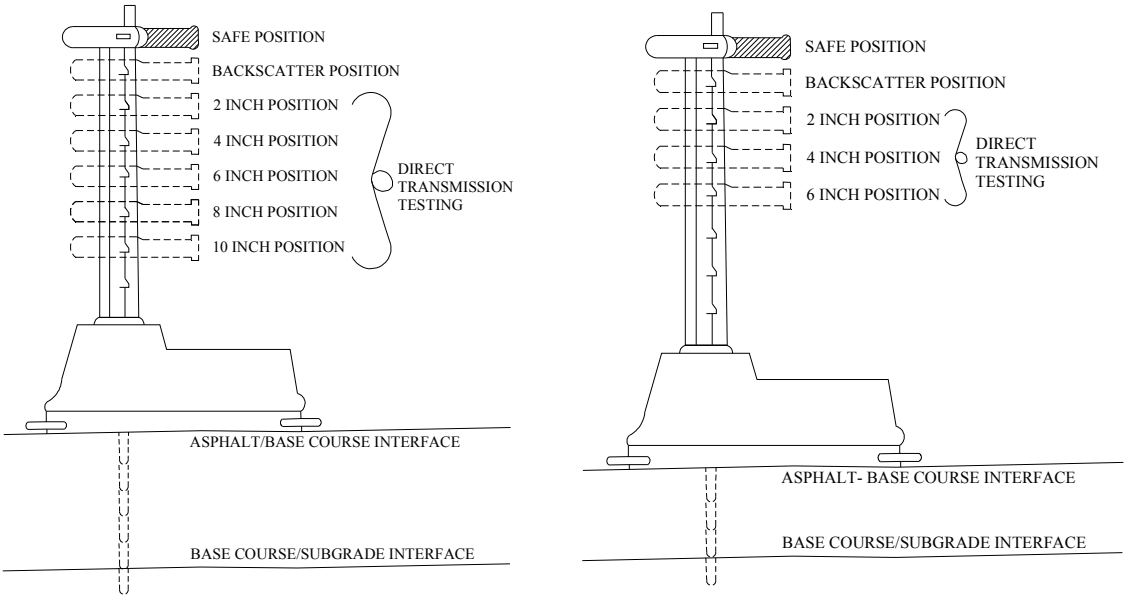

Figure 3.10. Schematic of nuclear gauge (direct transmission testing) for a) ten-inch thick section and b) six-inch thick section (modified from INDOT, 2011).

The in-situ total unit weight determined using the nuclear density gauge is used in conjunction with the gravimetric moisture contents (as described later in this section) to obtain the in-situ dry unit weight because the nuclear density gauge was only placed at the asphalt/base course interface to obtain the density and moisture content of the base course. This procedure of obtaining the moisture content and dry unit weight at one location instead of at every two inch thick lift interface led to incorrect measurements of the in-situ moisture content. Therefore, the gravimetric moisture content was averaged over the corresponding depth that the source rod was inserted to obtain the corrected dry unit weight (Equation 3.1).

$$\gamma_{dry} = \frac{\gamma_{tng}}{1 + \omega_{avg}} \qquad \textbf{Equation 3.1}$$

Where
γ_{dry} is the corrected in-situ dry unit weight (lb/ft^3);
γ_{tng} is the average in-situ total unit weight over the depth that the source rod penetrated below the asphalt/base course interface as obtained using a nuclear gauge (lb/ft^3);

ω_{avg} is the average in-situ gravimetric moisture content over the depth that the source rod penetrated below the asphalt/base course interface as obtained from laboratory measurements (percent).

Every two inches, approximately 50 pounds of sample was obtained by dislodging the base course using a hammer drill and then shoveling the base course into a bucket (Figure 3.11a). A garden trowel was used to obtain the 50 pound sample when in the vicinity of the geosynthetic interface to prevent damage to the geosynthetic (Figure 3.11b). A small portion (approximately 400 grams) of the base course sample obtained from each two inch lift was placed in moisture content tins, and weighed in the field to determine the initial moist weight of the sample (Figure 3.12). The weight of each moist sample, and the corresponding moisture content tin, was measured immediately on site before the samples were transported back to the University of Arkansas laboratory (hereafter referred to as the UofA laboratory) to prevent moisture loss from affecting the moisture content measurements. The dry weight of the samples in the moisture content tins was determined by drying the samples in the oven at the UofA laboratory after the samples were received in the laboratory (as previously depicted in Figure 3.1). Geosynthetic samples were exhumed using a box cutter and placed in pre-labeled bags for testing in the UofA laboratory (Figure 3.13).

(a) **(b)**

Figure 3.11. a) Shoveling and b) hand scooping base course samples into buckets.

Figure 3.12. Base course moisture content sample.

(a) **(b)**

Figure 3.13. Geosynthetic sample a) removal using a box cutter and b) pre-labeled bag ready for placement.

Photographs of a typical geotextile and geogrid located at the base course/subgrade interface are presented in Figure 3.14a and 3.14b, respectively. The base course (stored in buckets) and geotextile (stored in bags) were safely transported to the UofA laboratory.

(a) **(b)**

Figure 3.14. a) Typical geotextile/subgrade interface (Section 4) and b) typical geogrid/subgrade interface (Section 5).

3.2.3. Subgrade Density Testing (ASTM D6938) and Sampling

After removing the base course and geosynthetic, in-situ total unit weight and water content readings were obtained before excavation of the subgrade materials using a Troxler® nuclear density gauge (model 3450) as presented in Figure 3.15. In the Northwest corner of the two foot by two foot test area, a hole was created by driving a pre-hole driver through a rod guide from the base course/subgrade interface to a depth of 14 inches below the base course/subgrade interface (Figure 3.16). Density and moisture content measurements were obtained at two inches by lowering the source rod deeper into each pre-drilled hole until a depth of 12 inches below the base course/subgrade interface was reached within each section. Because the nuclear gauge was not lowered to each two inch thick lift interface, the dry density of the first six-inches of subgrade at each two inch interval, for each section, was computed using Equation 3.1. The dry density of the second six-inches, at each two inch interval, was obtained directly from the nuclear gauge (and are incorrect) because subgrade moisture content samples were not obtained for this depth (as discussed later in this section). No trench correction was applied to the gauge.

Figure 3.15. Nuclear gauge positioned to obtain subgrade density and water content readings (Section13BW).

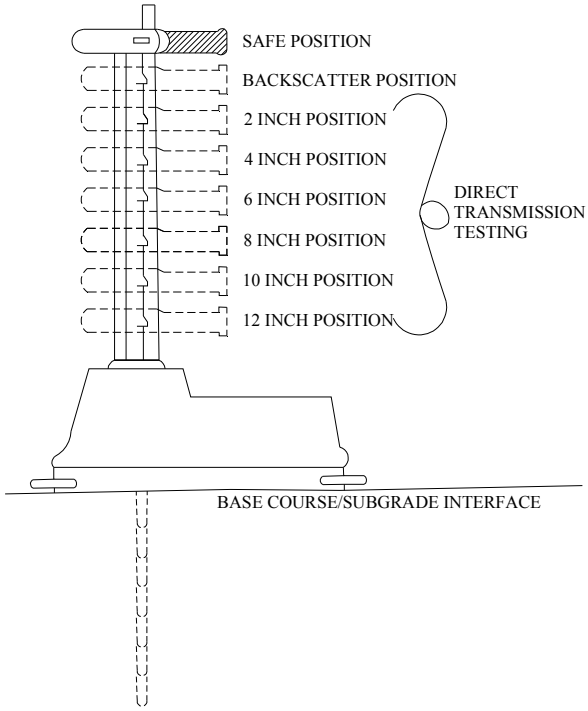

Figure 3.16. Schematic of nuclear gauge (direct transmission testing) placed at the base course/subgrade interface to obtain subgrade density and water content readings at two inch increment by lowering source rod (modified from INDOT, 2011).

Two 30 inch long, three inch diameter Shelby tubes were pushed by Arkansas State Highway and Transportation Department (AHTD) personnel starting at the base course/subgrade interface to a depth of 24 inches below the base course/subgrade interface. Within each section,

one tube was pushed in the Northeast corner of the excavation while the other tube was pushed in the Southwest corner of the excavation for each section (Figure 3.17). Each Shelby tube sample was collected in accordance with ASTM D1587. The ends of each Shelby tube were sealed with O-ring gaskets and melted wax was placed over the gasket to prevent moisture loss.

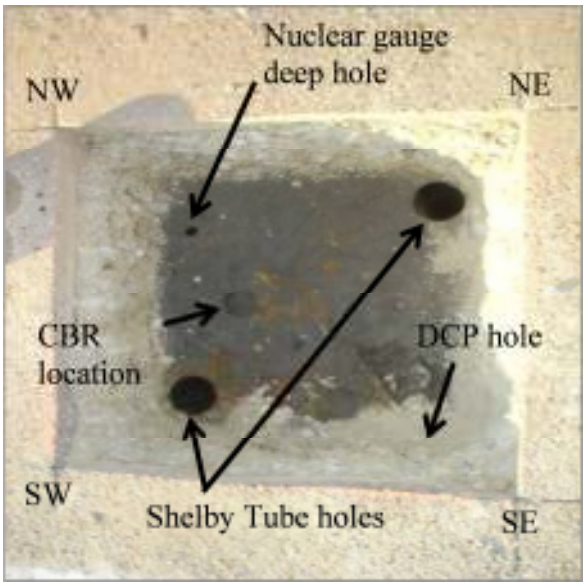

Figure 3.17. Typical location of DCP hole, deep hole (for nuclear gauge readings), and two holes created by obtaining Shelby tubes (Section).

Following collection of the two Shelby tube samples from each section, bag samples of subgrade material were obtained from the center of the excavation using a trowel. Samples were collected in two inch lifts beginning at the base course/subgrade interface and continuing to a depth of six-inches below the subgrade/base course interface. Following collection, the bag samples were transported to the UofA laboratory for further testing. A portion of each two inch thick subgrade sample was retained in the field to determine the in-situ gravimetric moisture content (Figure 3.18). The weight of each moist sample, and the corresponding moisture content tin, was measured immediately on site before the samples were transported back to the UofA laboratory to prevent moisture loss from affecting the moisture content measurements. Subgrade samples (bags, moisture content tins, and Shelby tubes) were safely transported to the laboratory.

The dry weight of the samples in the moisture content tins was determined by drying the samples in the oven at the UofA laboratory after the samples were received in the laboratory (as previously depicted in Figure 3.1).

Figure 3.18. Subgrade moisture content sample.

3.3. Field hydraulic conductivity of base course (ASTM D6391)

Two Stage Borehole (TSB) tests were performed in the field in accordance with ASTM D6391 to determine the in-situ hydraulic conductivity of base course material. Only one stage (the first stage with a flat bottom) of the test was performed. Five tests were completed for each base course thickness. The test was performed on four sections containing geotextiles and one control section. A total of 20 tests were performed, of which ten tests (five tests per base course thickness) were performed in October 2010 in conjunction with sample collection and ten tests (five tests per base course thickness) were performed in May 2011.

The location of each of the TSB tests was marked using spray paint. The asphalt and base course were cored by Arkansas State Highway and Transportation Department (AHTD) personnel using a six-inch diameter core barrel (Figure 3.19). AHTD personnel cored to a depth of five inches and seven inches below the top of the asphalt surface for the six-inch thick

sections and ten-inch thick sections, respectively. The base of the borehole was leveled by placing clean sand in the bottom of the borehole.

Figure 3.19. Coring by Arkansas State Highway and Transportation Department (AHTD) personnel for installation of two stage borehole test casing.

Schedule 40 PVC pipe with a four inch inside diameter, 1/4 inch wall thickness, and eight inch length (for the six-inch thick sections) or ten-inch length (for the ten-inch thick sections) was placed in the borehole. The 3/4 inch wide annulus space between the outside of the PVC pipe and the edge of the borehole was filled with WyoBen No.8 bentonite. The bentonite was placed by layering the dry granular bentonite in 1/2 inch thick lifts. Water was added to each lift, the bentonite was allowed to absorb the water, and the bentonite was compacted using a 1/4 inch diameter wooden dowl.

The bentonite was allowed to hydrate for approximately four hours. The leveling sand was then removed from the inside of the casing using a vacuum, the casing was filled with a sock containing pea gravel (to re-simulate the overburden stress which was removed), and then filled with water. The standpipe and top cap were placed on the device, the standpipe was filled with water, and testing was initiated. The time required for the water level within the standpipe to

drop from 120 mm to 20 mm was recorded. The standpipe was repeatedly refilled, and the time required for the predetermined drop was repeatedly measured. The TSB setup and observation of water infiltration with time are presented in Figures 3.20a and 3.20b, respectively.

(a) **(b)**

Figure 3.20. a) Two stage borehole setup prior to testing and b) ongoing two stage borehole test.

A plan and profile view of a typical test location for the TSB, Shelby tubes, previously installed instrumentation, and locations of previous testing are presented in Figures 3.21 and 3.22 for the six-inch thick sections and for the ten-inch thick sections, respectively. A graphical representation of the sample collection process (previously described in Sections 3.2.2 and 3.2.3) for the six-inch thick sections and the ten-inch thick sections is also presented in Figures 3.21 and 3.22, respectively. The laboratory testing procedures conducted on the samples collected, using the procedures described in this section, are described in Section 3.4. A summary of TSB results for the hydraulic conductivity of the base course is presented in Section 4.8. The in-situ hydraulic conductivity results for the base course are presented in the Appendix, in Section B.4, for completeness.

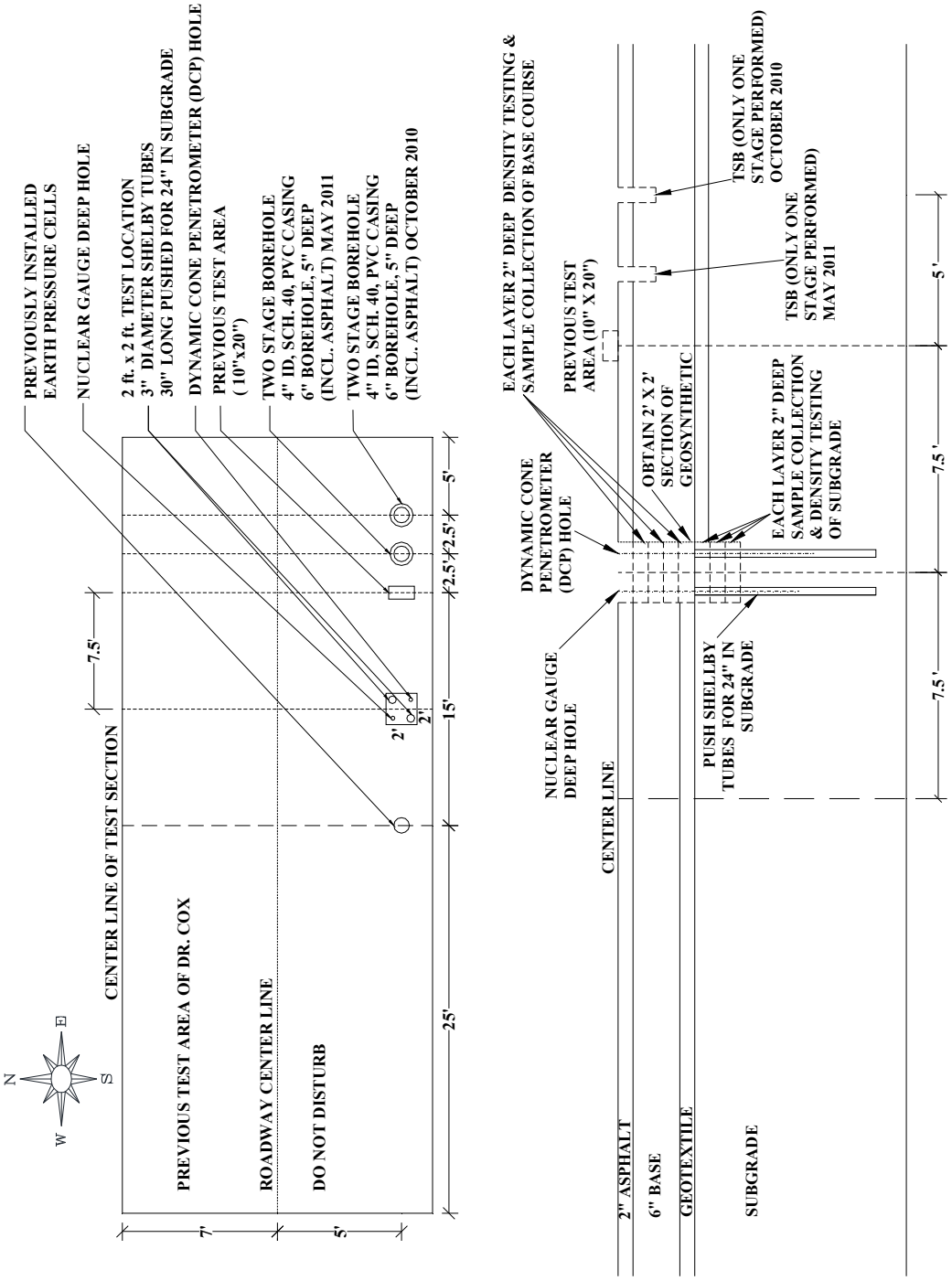

Figure 3.21.Plan and profile view of typical test locations for Shelby tubes, two stage borehole, previously installed earth pressure cells, two foot by two foot test area, and previous test area for the six-inch thick base course sections.

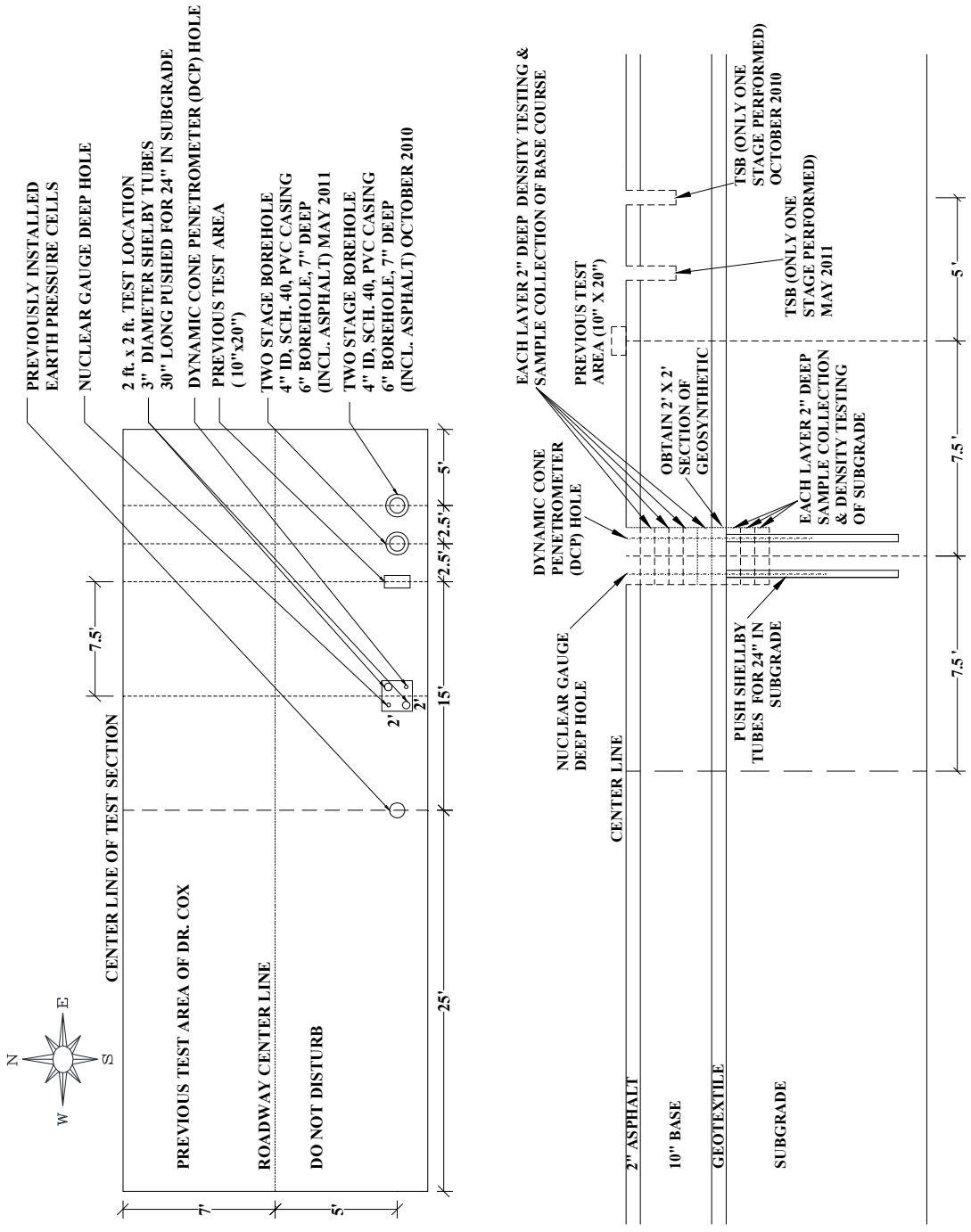

Figure 3.22. Plan and profile view of typical test locations for Shelby tubes, two stage borehole, previously installed earth pressure cells, two foot by two foot test area, and previous test area for the ten-inch thick base course sections.

3.4. Laboratory Testing

The laboratory testing schedule for base course samples obtained from the ten-inch thick sections are presented in Tables 3.1 and 3.2 and for the six-inch thick sections is presented in Table 3.3. The laboratory testing schedule for the subgrade samples obtained from the ten-inch thick sections and the six-inch thick sections are presented in Tables 3.4 and 3.5, respectively. A checkmark in Table 3.1 through 3.5 indicates that the test was conducted as a part of the laboratory testing program.

Table 3.1. Laboratory testing schedule for the exhumed base course samples for the ten-inch thick sections (for Sections 1B to 2).

Location	Depth*	Laboratory testing conducted on exhumed base course samples								
		Dry Sieving			Wash Sieving	Hydrometers	Modified Proctor	Specific Gravity	k	
	(inch)	DS[1]	DS[2]	DS[3]					MB[4]	FWP[5]
Section 1B	0-2	✓			✓	✓		✓		
Section 1B	2-4	✓			✓	✓		✓		
Section 1B	4-6	✓			✓	✓		✓		
Section 1B	6-8	✓			✓	✓		✓		
Section 1B	**8-10**	✓	✓	✓	✓	✓	✓	✓	✓	
Section 1A	0-2	✓			✓	✓		✓		
Section 1A	2-4	✓			✓	✓		✓		
Section 1A	4-6	✓			✓	✓		✓		
Section 1A	6-8	✓			✓	✓		✓		
Section 1A	**8-10**	✓	✓	✓	✓	✓	✓	✓		✓
Section 1	0-2	✓			✓	✓		✓		
Section 1	2-4	✓			✓	✓		✓		
Section 1	4-6	✓			✓	✓		✓		
Section 1	6-8	✓			✓	✓		✓		
Section 1	**8-10**	✓	✓	✓	✓	✓	✓	✓	✓	
Section 2	0-2	✓			✓	✓		✓		
Section 2	2-4	✓			✓	✓		✓		
Section 2	4-6	✓			✓	✓		✓		
Section 2	6-8	✓			✓	✓		✓		
Section 2	**8-10**	✓	✓	✓	✓	✓	✓	✓	✓	

*Depth below asphalt/base course interface

Bold represents the base course samples obtained at the base course/subgrade interface

[1]Dry sieving conducted on 3,000 gram oven dried sample in November 2010

[2]Dry sieving conducted before proctor testing in July 2011

[3]Dry sieving conducted after permeability testing in October 2011

[4]Constant head test performed to measure hydraulic conductivity using a Mariotte Bottle (MB)

[5]Falling head test performed to measure hydraulic conductivity using a Flexible Wall Permeameter (FWP)

Table 3.2. Laboratory testing schedule for the exhumed base course samples for the ten-inch thick sections (for Sections 3 to 6).

Location	Depth*	Laboratory testing conducted on exhumed base course samples								
		Dry Sieving			Wash Sieving	Hydrometers	Modified Proctor	Specific Gravity	k	
	(inch)	DS[1]	DS[2]	DS[3]					MB[4]	FWP[5]
Section 3	0-2	✓			✓	✓		✓		
Section 3	2-4	✓			✓	✓		✓		
Section 3	4-6	✓			✓	✓		✓		
Section 3	6-8	✓			✓	✓		✓		
Section 3	**8-10**	✓	✓	✓	✓	✓	✓	✓	✓	
Section 4	0-2	✓			✓	✓		✓		
Section 4	2-4	✓			✓	✓		✓		
Section 4	4-6	✓			✓	✓		✓		
Section 4	6-8	✓			✓	✓		✓		
Section 4	**8-10**	✓	✓	✓	✓	✓	✓	✓	✓	
Section 5	0-2	✓			✓	✓		✓		
Section 5	2-4	✓			✓	✓		✓		
Section 5	4-6	✓			✓	✓		✓		
Section 5	6-8	✓			✓	✓		✓		
Section 5	**8-10**	✓	✓	✓	✓	✓	✓	✓	✓	
Section 6	0-2	✓			✓	✓		✓		
Section 6	2-4	✓			✓	✓		✓		
Section 6	4-6	✓			✓	✓		✓		
Section 6	6-8	✓			✓	✓		✓		
Section 6	**8-10**	✓	✓	✓	✓	✓	✓	✓	✓	

*Depth below asphalt/base course interface

Bold represents the base course samples obtained at the base course/subgrade interface

[1]Dry sieving conducted on 3,000 gram oven dried sample in November 2010

[2]Dry sieving conducted before proctor testing in July 2011

[3]Dry sieving conducted after permeability testing in October 2011

[4]Constant head test performed to measure hydraulic conductivity using a Mariotte Bottle (MB)

[5]Falling head test performed to measure hydraulic conductivity using a Flexible Wall Permeameter (FWP)

Table 3.3. Laboratory testing schedule for the exhumed base course samples for the six-inch thick sections.

Location	Depth*	Laboratory testing conducted on exhumed base course samples								
		Dry Sieving			Wash Sieving	Hydrometers	Modified Proctor	Specific Gravity	k	
	(inch)	DS[1]	DS[2]	DS[3]					MB[4]	FWP[5]
Section 8	0-2	✓			✓	✓		✓		
Section 8	2-4	✓			✓	✓		✓		
Section 8	**4-6**	✓	✓	✓	✓	✓	✓	✓	✓	
Section 9	0-2	✓			✓	✓		✓		
Section 9	2-4	✓			✓	✓		✓		
Section 9	**4-6**	✓	✓	✓	✓	✓	✓	✓	✓	
Section 10	0-2	✓			✓	✓		✓		
Section 10	2-4	✓			✓	✓		✓		
Section 10	**4-6**	✓	✓	✓	✓	✓	✓	✓	✓	
Section 11	0-2	✓			✓	✓		✓		
Section 11	2-4	✓			✓	✓		✓		
Section 11	**4-6**	✓	✓	✓	✓	✓	✓	✓	✓	
Section 12	0-2	✓			✓	✓		✓		
Section 12	2-4	✓			✓	✓		✓		
Section 12	**4-6**	✓	✓	✓	✓	✓	✓	✓	✓	
Section 13	0-2	✓			✓	✓		✓		
Section 13	2-4	✓			✓	✓		✓		
Section 13	**4-6**	✓	✓	✓	✓	✓	✓	✓	✓	
Section 13W	0-2	✓			✓	✓		✓		
Section 13W	2-4	✓			✓	✓		✓		
Section 13W	**4-6**	✓	✓	✓	✓	✓	✓	✓		✓
Section 13A	0-2	✓			✓	✓		✓		
Section 13A	2-4	✓			✓	✓		✓		
Section 13A	**4-6**	✓	✓	✓	✓	✓	✓	✓	✓	
Section 13B	0-2	✓			✓	✓		✓		
Section 13B	2-4	✓			✓	✓		✓		
Section 13B	**4-6**	✓	✓	✓	✓	✓	✓	✓	✓	
Section 13BW	0-2	✓			✓	✓		✓		
Section 13BW	2-4	✓			✓	✓		✓		
Section 13BW	**4-6**	✓	✓	✓	✓	✓	✓	✓	✓	

*Depth below asphalt/base course interface

Bold represents the base course samples obtained at the base course/subgrade interface

[1]Dry sieving conducted on 3,000 gram oven dried sample in November 2010

[2]Dry sieving conducted before proctor testing in July 2011

[3]Dry sieving conducted after permeability testing in October 2011

[4]Constant head test performed to measure hydraulic conductivity using a Mariotte Bottle (MB)

[5]Falling head test performed to measure hydraulic conductivity using a Flexible Wall Permeameter (FWP)

Table 3.4. Laboratory testing schedule for the exhumed subgrade samples for the ten-inch thick sections.

Location	Depth*	Laboratory testing on exhumed subgrade samples			
	(in)	Wash Sieving	Hydrometers	Atterberg Limits	Specific Gravity
Section 1B	0-2	✓	✓	✓	✓
Section 1B	2-4	✓	✓	✓	✓
Section 1B	4-6	✓	✓	✓	✓
Section 1A	0-2	✓	✓	✓	✓
Section 1A	2-4	✓	✓	✓	✓
Section 1A	4-6	✓	✓	✓	✓
Section 1	0-2	✓	✓	✓	✓
Section 1	2-4	✓	✓	✓	✓
Section 1	4-6	✓	✓	✓	✓
Section 2	0-2	✓	✓	✓	✓
Section 2	2-4	✓	✓	✓	✓
Section 2	4-6	✓	✓	✓	✓
Section 3	0-2	✓	✓	✓	✓
Section 3	2-4	✓	✓	✓	✓
Section 3	4-6	✓	✓	✓	✓
Section 4	0-2	✓	✓	✓	✓
Section 4	2-4	✓	✓	✓	✓
Section 4	4-6	✓	✓	✓	✓
Section 5	0-2	✓	✓	✓	✓
Section 5	2-4	✓	✓	✓	✓
Section 5	4-6	✓	✓	✓	✓
Section 6	0-2	✓	✓	✓	✓
Section 6	2-4	✓	✓	✓	✓
Section 6	4-6	✓	✓	✓	✓

*Depth below base course/subgrade interface

Table 3.5. Laboratory testing schedule for the exhumed subgrade samples for six-inch thick sections.

Location	Depth*	Laboratory testing on exhumed subgrade samples			
	(in)	Wash Sieving	Hydrometers	Atterberg Limits	Specific Gravity
Section 8	0-2	✓	✓	✓	✓
Section 8	2-4	✓	✓	✓	✓
Section 8	4-6	✓	✓	✓	✓
Section 9	0-2	✓	✓	✓	✓
Section 9	2-4	✓	✓	✓	✓
Section 9	4-6	✓	✓	✓	✓
Section 10	0-2	✓	✓	✓	✓
Section 10	2-4	✓	✓	✓	✓
Section 10	4-6	✓	✓	✓	✓
Section 11	0-2	✓	✓	✓	✓
Section 11	2-4	✓	✓	✓	✓
Section 11	4-6	✓	✓	✓	✓
Section 12	0-2	✓	✓	✓	✓
Section 12	2-4	✓	✓	✓	✓
Section 12	4-6	✓	✓	✓	✓
Section 13	0-2	✓	✓	✓	✓
Section 13	2-4	✓	✓	✓	✓
Section 13	4-6	✓	✓	✓	✓
Section 13W	0-2	✓	✓	✓	✓
Section 13W	2-4	✓	✓	✓	✓
Section 13W	4-6	✓	✓	✓	✓
Section 13A	0-2	✓	✓	✓	✓
Section 13A	2-4	✓	✓	✓	✓
Section 13A	4-6	✓	✓	✓	✓
Section 13B	0-2	✓	✓	✓	✓
Section 13B	2-4	✓	✓	✓	✓
Section 13B	4-6	✓	✓	✓	✓
Section 13BW	0-2	✓	✓	✓	✓
Section 13BW	2-4	✓	✓	✓	✓
Section 13BW	4-6	✓	✓	✓	✓

*Depth below base course/subgrade interface

The laboratory testing procedures utilized for this research are identified in Table 3.6 and described in detail in this section. The objective of the testing sequence was to identify and characterize base course and subgrade materials, measure the hydraulic conductivity of recompacted base course samples, and measure the permittivity and transmissivity of geotextile samples.

Table 3.6. Test procedures used in this research project.

ASTM Number	Test Description	Purpose	Number of tests
ASTM C136 (2005)	Standard Test Method for Sieve Analysis of Fine and Coarse Aggregates	I&C[1]	70
ASTM D422 (2005)	Standard Test Method for Particle-Size Analysis of Soils (Hydrometers)	I&C	124
ASTM D854 (2005)	Standard Test Methods for Specific Gravity of Soil Solids by Water Pycnometer (Method B)	I&C	124
ASTM D1140 (2005)	Standard Test Methods for Amount of Material in Soils Finer than No. 200 (75-µm) Sieve (Wash Sieve)	I&C	124
ASTM D1557 (2005)	Standard Test Methods for Laboratory Compaction Characteristics of Soil Using Modified Effort (56,000 ft-lbf/ft^3 (2,700 kN-m/m^3))	I&C	72
ASTM D1587 (2005)	Standard Practice for Thin-Walled Tube Sampling of Soils for Geotechnical Purposes (Shelby Tubes)	I&C	36
ASTM D2216 (2005)	Standard Test Methods for Laboratory Determination of Water (Moisture) Content of Soil and Rock by Mass	I&C	466
ASTM D4318 (2005)	Standard Test Method for Liquid Limit, Plastic Limit, and Plasticity Index of Soils (Atterberg Limits)	I&C	54
ASTM D4491 (2005)	Standard Test Methods for Water Permeability of Geotextiles by Permittivity	P&T[2]	15
ASTM D5084 (2005)	Standard Test Methods for Measurement of Hydraulic Conductivity of Saturated Porous Materials Using a Flexible Wall Permeameter (Method C)	LHC[3]	2
ASTM D6391 (2005)	Standard Test Method for Field Measurement of Hydraulic Conductivity Limits of Porous Materials Using Two Stages Infiltration from a Borehole (TSB) [First Stage Only]	FHC[4]	20
ASTM D6574 (2005)	Standard Test Method for Determining the (In-Plane) Hydraulic Transmissivity of a Geosynthetic by Radial Flow	P&T[2]	15
ASTM D6938 (2005)	Standard Test Method for In-Place Density and Water Content of Soil and Soil-Aggregate by Nuclear Methods (Shallow Depth)	I&C	36
No ASTM	Test Method for Laboratory Measurement of Hydraulic Conductivity using a Mariotte Bottle	LHC[3]	16

[1]Identification and Characterization of base course and subgrade material

[2]Permittivity and Transmissivity of geosynthetic separators

[3]Laboratory hydraulic conductivity of recompacted base course

[4]Field hydraulic conductivity of base course

3.4.1. Identification and Characterization [I&C] of Base Course and Subgrade Materials

A series of tests were performed to identify and characterize the base course and subgrade material. The identification and characterization tests performed for the research project include: grain size distribution (sieve analysis and hydrometers), wash sieve, specific gravity, modified proctor, Atterberg limits, laboratory hydraulic conductivity and moisture content. Each of these testing techniques is discussed in the subsequent subsections (Sections 3.4.1.1 to 3.4.1.7). Empirical predictions of hydraulic conductivity as based on soil properties (porosity and/or grain size) are presented in Section 3.4.1.8.

3.4.1.1 Sieve Analysis (ASTM C136)

Seventy (70) dry sieve analysis tests were conducted in accordance with ASTM C136 (2005) on 3,000 gram oven-dried sub-samples from 70 exhumed base course samples (one test per sample). These sieve analyses were conducted in November 2010 after the samples had been transported from the field to the UofA laboratory. In July 2011, dry sieve analyses were also performed on the base course samples remaining in the buckets for each of the eighteen sections at the base course/subgrade interface layer to ensure the initial 3,000 gram base course sample was a representative sample, and to segregate the material for proctor testing. These sieve analyses were performed to determine the difference in gradation between the initial gradation after sampling (November, 2010) and the remaining bucket sample (July, 2011). The samples ranged in weight from 10,335 grams (Section 4) to 19,636 grams (Section 6) for the ten-inch thick sections and ranged in weight from 7,974 grams (Section 8) to 15,849 grams (Section 13A) for six-inch thick sections.

Dry sieve analyses were also performed in October, 2011 on the 18 recompacted base course samples obtained from the base course/subgrade interface after laboratory hydraulic conductivity testing was conducted. These sieve analyses were performed to determine if a gain

or loss in fines had occurred during proctor testing and hydraulic conductivity testing. The sieve sizes used for dry sieve analyses are presented in Figure 3.23. The results for the sieve analyses are presented in Section 4.2.1, and all of the grain size distribution plots obtained from the sieve analysis testing is presented in the Appendix in Section A.1, for completeness.

Sieve Size	Opening Size (mm)
1.5 inch	38.1
1 inch	25.4
3/4 inch	19.05
3/8 inch	9.525
Number 4	4.75
Number 10	2
Number 40	0.425
Number 200	0.075
Pan	0

(a)

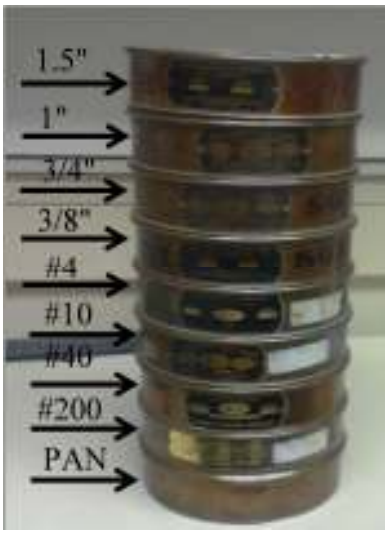

(b)

Figure 3.23. Sieve sizes used for dry sieving as per AHTD (2010) specifications a) opening sizes for each sieve (in mm.) and b) picture of sieves.

For the initial dry sieve analysis tests was performed on the 3,000 gram oven dried base course samples, a representative sample was obtained from the bucket by shaking the bucket prior to collecting the sample to be used for each test. Each test was conducted following ASTM C316 (2005). A Rainhart® model 637 mechanical sieve shaker (Figure 3.24) was used to shake the samples for 7.5 minutes (this reduction in time constitutes a deviation from the ASTM). The sieve sizes utilized for testing were determined using Section 303 of the AHTD specifications for aggregate base course grading requirements (AHTD, 2010).

(a) **(b)**

Figure 3.24. a) sieve set placed in the Rainhart® model 637 mechanical sieve shaker, b) sieve set placed in the RO-TAP® model RX-29 mechanical sieve shaker.

Wash sieving was performed in accordance with ASTM D1140 (2005) on 54 subgrade samples in March 2011 (as previously identified in Tables 3.4 to 3.5 on pages 77 to 78, respectively). Fifty grams of oven dried sample were used for each test. Ceramic bowls were used to assist in particle separation (Figure 3.25). A U.S. No. 200 standard sieve with an apparent opening size of 75μm (herein after referred to as a No. 200 sieve) was used to conduct the test (Figure 3.26). The percent passing the No. 200 sieve, using the wet washing method, was determined using Equation 3.2.

Figure 3.25. Subgrade sample being soaked in water prior to wash sieving.

$$A = [(B - C) / B] \times 100 \qquad \text{(ASTM D1140, 2005)} \qquad \textbf{Equation 3.2}$$

Where
A is the percentage of material finer than the 75 µm sieve by washing (percent);
B is the original dry mass of the sample (g), [50 grams for this research project];
C is the dry mass of the specimen retained on the 75 µm sieve including the amount retained on any upper sieve after washing (g).

Figure 3.26. Wash sieving of subgrade sample using a standard No. 200 sieve.

In a similar procedure to the wash sieving of the subgrade samples, wash sieving was performed for the base course samples following ASTM D1140 (2005). The base course samples were oven dried (1,500 grams following drying) then allowed to soak in water to assist in

particle separation. The base course sample were then transferred to a sieve set containing a No. 40 sieve stacked on top of a eight inch deep No. 200 wash sieve (Figure 3.27a) to prevent damage to No. 200 sieve. The sieve set was then placed under a sink faucet and the faucet was turned on. Gentle stirring of sample was performed by hand without any downward pressure to ensure discharge of particles passing the No. 40 sieve without forcing particles through the screen. When the No. 200 eight inch deep sieve was approximately two thirds full of water and soil the faucet was turned off and the No. 40 sieve was removed (Figure 3.27b).

The No. 200 sieve was then placed in the sink and gently stirred by hand without any downward pressure to ensure discharge of particles passing the No. 200 sieve without forcing particles through the screen. The No. 200 eight inch deep sieve was then placed under the faucet and water was turned on. The test was completed when the water passing the sieve was clear (Figure 3.27b). The entire soil sample retained on the No. 40 and No. 200 sieves were combined into a pan and oven dried at 105°C for 24 hours. The dry weight of the sample was measured and recorded, and the percent passing was determined using Equation 3.2.

(a) **(b)**

Figure 3.27. Wash sieving of base course sample using a) No. 40 sieve stacked on top of eight inch deep No. 200 sieve and b) eight inch deep No. 200 sieve.

3.4.1.2 Hydrometer (ASTM D422)

Hydrometer tests were performed on 70 base course and 54 subgrade samples (as previously identified in Tables 3.1 to 3.5 on pages 74 to 78, respectively). The testing procedure followed ASTM D422 with minor deviations. Six hydrometers tests (each containing a unique sample) were conducted simultaneously, using a common hydrometer control, temperature control, and cleaning bath. By conducting six tests at a time, the process of testing the 124 samples was expedited.

To prepare the salt solution, a one liter glass sedimentation cylinder was filled with deionized, de-aired water until the one liter mark was reached with the bottom of the meniscus. The cylinder was then placed on a digital stirring plate (Figure 3.28.a) and magnetic stirrer was used to agitate the sample in the cylinder. The rate of stirring was adjusted to keep the magnetic stirrer in continuous motion at the center of the sedimentation cylinder.

An antistatic polystyrene white weigh boat (VWR International, 2011) (hereafter referred to as a weigh boat) was tared on a scale and 40 grams of sodium hexametaphosphate (salt) was added to the weighing boat. The salt from the weigh boat was gradually transferred to the sedimentation cylinder (still on the stirring plate) at such a rate such that all crystals were suspended in the solution and did not reach the bottom of the sedimentation cylinder (Figure 3.28b). The stirring was stopped when no visible salt particles were observed in the sedimentation cylinder. In each of the awaiting eight 250 mL capacity beakers, 125 grams of the prepared brine solution was poured.

(a)

(b)

Figure 3.28. a) Digital stirring plate, b) Sodium Hexametaphosphate solution preparation.

Fifty-five (55) grams of air dried base course or air dried subgrade (passing the No. 200 sieve) were required for each test. The required 55 grams of base course material passing the No. 200 sieve were obtained by manual sieving. The required 55 grams of subgrade material passing the No. 200 sieve were obtained by pulverizing the subgrade sample using a mortar and rubber tipped pestle. The six samples (each from a different depth in various sections) were then placed in metal moisture content tins, weighed and oven dried at 105°C for 24 hours. After the six samples were oven dried, 50.00 grams of samples were utilized for each hydrometer test. Each

sample solution (containing 125mL of sodium hexametaphosphate solution mixed with 50 grams of soil sample) was then stirred manually in a 250 mL beaker using a glass stirring rod for two minutes. Each solution was then transferred to a dispersion cup (Figure 3.29a), and the mixture was then mechanically dispersed for five minutes using a dispersion machine (Figure 3.29b).

(a) **(b)**

Figure 3.29. a) Dispersion cup and b) dispersion machine.

Each dispersed solutions was then transferred to an empty one liter sedimentation cylinder. Each cylinder was then filled with deionized water until the one liter mark was reached with the bottom of meniscus for all six samples.

The hydrometer control and temperature control sedimentation cylinders contained the same sodium hexametaphosphate solution and were prepared in the same manner as the soil samples but did not contain 50 grams of soil. Each of the cylinders were sealed using a rubber stopper, one of which contained an opening to insert the thermometer. A third sedimentation cylinder, filled with tap water, was used as a bath to clean the hydrometer between readings.

Following sample preparation, each of the cylinders containing the soil sample solutions, the hydrometer control solution, and the temperature control solution were mixed for one minute

by repeatedly turning the cylinder upside down and right side up. After one minute of mixing, the cylinders were placed on the table and not disturbed until the test was completed (24 hours later). An example of hydrometer testing in progress (six samples) is presented in Figure 3.30.

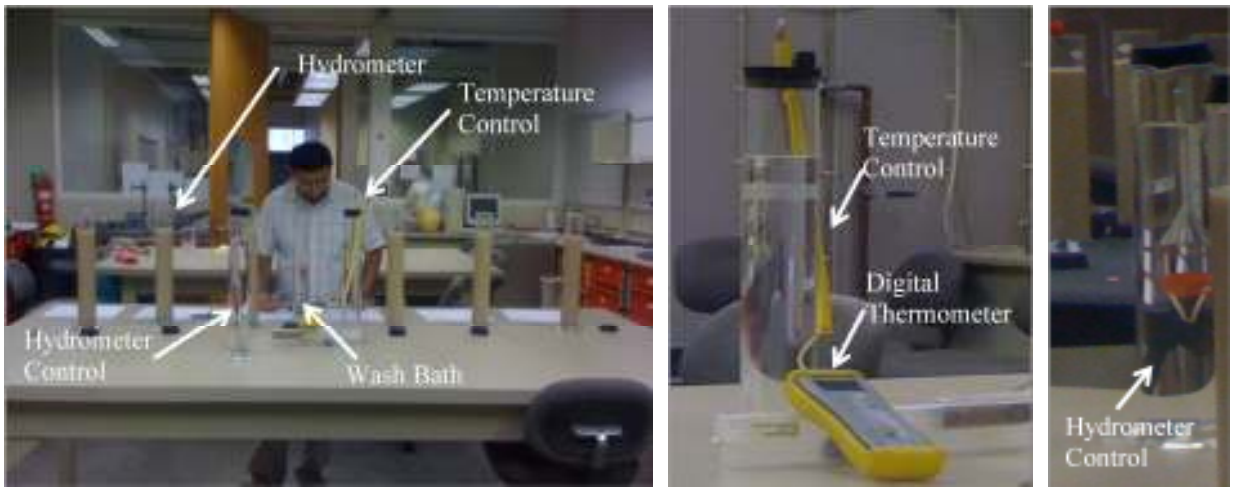

(a) **(b)** **(c)**

Figure 3.30. a) Hydrometer testing in progress, b) temperature control, and c) hydrometer control.

A stopwatch was used to determine the elapsed time from the start of the test. Only one stop watch was used for all the six hydrometers. The stop watch was started when the first cylinder was placed on the table after mixing (by the researcher); simultaneously the second cylinder was picked up (by laboratory assistant) and mixed. Similarly the third cylinder was picked up (by the researcher) concurrently at the time of the placement of the second cylinder (by the laboratory assistant). The two minutes reading for the first cylinder was recorded (by the laboratory assistant) while the third cylinder was being placed on the table (by the researcher). Hence all the readings of the third cylinder were one minute after the readings of the second cylinder which was one minute after the readings of the first cylinder. A similar technique was used for the fourth, fifth and sixth cylinder. At the fifteen minute reading for the third cylinder (recorded by the researcher) the fourth cylinder was picked (by the laboratory assistant) and

mixed for one minute. Therefore, the difference in reading time between the first and fourth cylinder was eighteen minutes. No conflict of readings occurred by implementing this technique.

For each sample, measurements were taken at two (2), five (5), fifteen (15), thirty (30), sixty (60), ninety (90), two hundred and fifty (250), and one thousand four hundred and forty (1440) minutes elapsed time. Each reading was performed as follows (Figure 3.31):

- the hydrometer was lowered into the sedimentation cylinder 15 seconds before the reading,
- care was taken to avoid large movements of the hydrometer in the solution,
- the readings (hydrometer control, temperature control, soil sample) were taken at each specified time,
- and the values observed for the hydrometer control, temperature control, and soil sample were recorded simultaneously.

Figure 3.31. Typical hydrometer test reading recorded.

The results for the hydrometers for base course and subgrade samples are presented in Sections 4.2.2 and 4.2.3, respectively. Plots of the hydrometer results for all of the 70 base course samples (percentages based on the weight of the fine particles, and percentages based on the weight of the entire sample), and the hydrometer results for the 54 subgrade samples are presented in the Appendix, in Sections A.4, A.5, and A.6, respectively, for completeness.

3.4.1.3 Atterberg Limits (ASTM D4318)

The Atterberg limits (plastic limit and liquid limit) were determined for 54 subgrade samples in accordance with ASTM D4318 (2005). For each of the 54 samples, a 200 gram air-dried subgrade sample was added to the dispersion cup. Exactly 100 grams of deionized water was added to the dispersion cup containing each of the 200 gram air dried of subgrade samples. For each test preparation, the dispersion cup was then inserted in the dispersion machine (as previously shown in Figure 3.29b) and the sample was mechanically dispersed. The sample in the dispersion cup was checked periodically for lumps using a metal spatula. The mixing of sample was determined to be completed when the entire sample was free of lumps and at consistent water content throughout the sample. The sample from each of the dispersion cups was then transferred to a coffee filter located within a ceramic bowl. Each sample remained within the coffee filter in the bowl and allowed to air dry for 24 hours.

Each previously prepared sample was then transferred from the filter paper into a small ceramic bowl. Each sample was thoroughly mixed using a metal spatula. If the sample appeared to be dry, water was added to the sample. After a consistent mix was achieved, the sample was spread evenly in the bottom half of the calibrated cup (Figure 3.32).

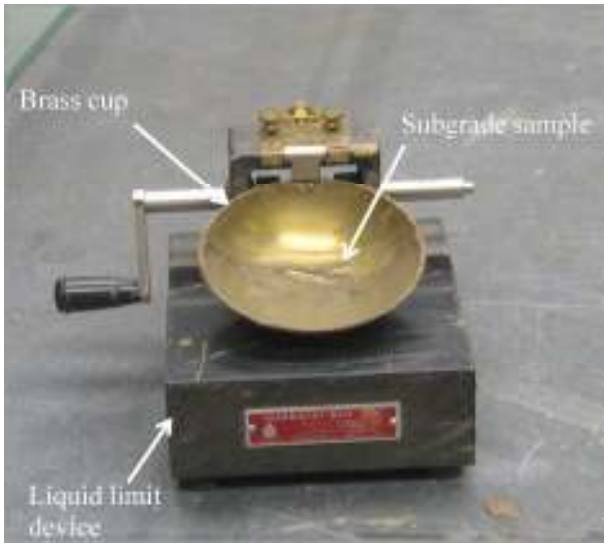

Figure 3.32. Liquid limit test conducted on subgrade sample.

The number of drops that were needed to close a 0.5 inch long portion of the groove was recorded. The test was successful if the grove closed at least 0.5 inch using a minimum of 15 blows or a maximum of 35 blows. A sample was obtained from each test by moving the spatula perpendicular to the groove from one end to another. The sample was placed in a water content tin with pre-determined weight and oven dried at 105°C for 24 hours. The weight of the dry sample and can was measured and recorded. The wet and dry weights of each corresponding sample were used to determine the moisture content of the sample. Because a multi-point liquid limit test was selected, three iterations of the test were performed for each sample at different moisture contents using portions of the same sample. The number of blows required for the three successive points ranged between 15-25, 20-30, and 25-35 blows. If the sample was too dry to achieve the desired number of blows, water was added, and if the sample was wet to achieve the desired number of blows, the sample was dried using an electric hair dryer.

The moisture content obtained for the three trials were plotted against their respective number of blows (Figure 3.33). A best fit logarithmic trend line was plotted through the data points. The point corresponding to 25 blows was the liquid limit (LL) for the sample.

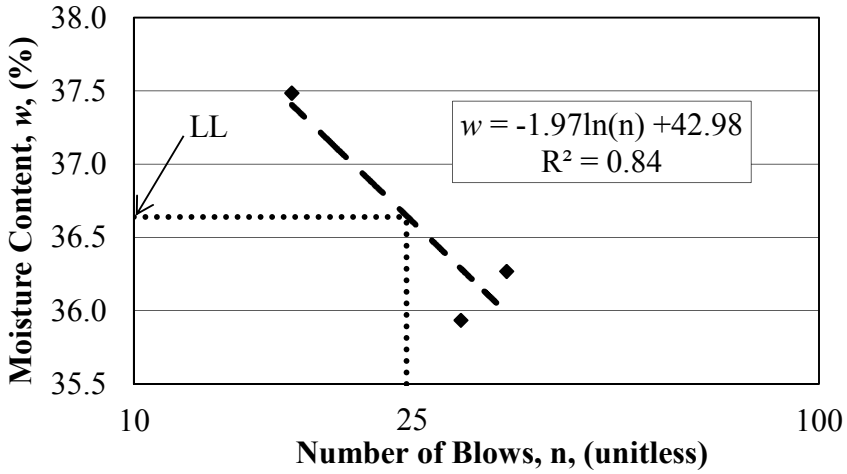

Figure 3.33. Subgrade liquid limit plot for sample obtained from Section 1B at a depth of 0-2 inches below the base course/subgrade interface.

For each sample, one-third of the previously prepared sample was spread on a glass plate which was twelve inches long by twelve inches wide by 0.5 inch thick. The samples were dried until it was feasible to roll the sample without the sample sticking to the glass plate. Sufficient pressure was applied to roll a uniform diameter thread which was approximately 1/8 inch thick. The roll was successful if the resulting thread broke by itself at diameter equal to 1/8 inch. This thread was transferred to a can (with pre-determined weight) and was covered by another can to avoid moisture loss while the additional sample was collected. For each section and depth, a cumulative sample of approximately twelve grams was placed in the two cans and their weights were measured and recorded. Each of the samples was dried at 105°C for 24 hours. The dry weight was measured and recorded. The moisture content (plastic limit) was determined using the wet and dry weights and averaging the results from the two containers. Summarized subgrade Atterberg limits results are presented in Section 4.3 and all of the subgrade Atterberg limits plots for the subgrade samples are presented in the Appendix, in Section A.7, for completeness.

3.4.1.4 Specific Gravity (ASTM D854)

Specific gravity testing was performed on 70 base course and 54 subgrade samples (as previously identified in Tables 3.1 to 3.5 on pages 74 to 78, respectively). The specific gravity tests were conducted in accordance with ASTM D854 (2005), with deviations as discussed later in this section. Because specific gravity testing was only conducted on the portion of the samples passing the No. 200 sieve, 250 mL pycnometers were used. Each pycnometer was calibrated using the procedures specified in ASTM D854 (2005). Specifically, the exact volume of each of the pycnometer was obtained using Equation 3.3:

$$V_p = \frac{(M_{pw,c} - M_p)}{\rho_{w,c}} \qquad \text{(ASTM D854, 2005)} \qquad \textbf{Equation 3.3}$$

where
V_p is the calculated volume of the pycnometer (mL),
$M_{pw,c}$ is the mass of the pycnometer and water at the calibration temperature (g),
M_p is the average mass of the dry pycnometer at calibration (g),
$\rho_{w,c}$ is the mass density of water at the calibration temperature (g/mL).

Exactly 50.00 grams of oven dried base course and subgrade material passing the No. 200 sieve was used to perform each test. As with the hydrometer testing discussed in the previous section, the base course material passing No. 200 sieve was obtained by manual sieving. While the samples of subgrade material passing the No. 200 sieve were obtained by pulverizing the subgrade sample using a mortar and rubber tipped pestle.

During testing, the 50 grams soil sample was added to the pycnometer and the pycnometer was then filled with de-aired water until the bulb was half full. The pycnometer was connected to a vacuum pump via a hose and stopper and continually agitated for five minutes to de-air the sample. The elapsed time was measured using a stop watch. The sample remained in suspension while the solution was in constant motion. The pycnometer was then disconnected from the vacuum pump and the pycnometer was filled with deionized, de-aired water to the 250

mL mark. The pycnometer was again connected to the vacuum pump for five minutes. This ten minute vacuum application was a deviation from ASTM D854 as the ASTM requires the pycnometer (with sample and deionized, de-aired water) to be continually agitated under vacuum for two hours.

The weight of the pycnometer (with sample and deionized, de-aired water) after the de-airing process was measured using a scale. The temperature of the solution was measured using a digital thermometer (Figure 3.34). The weight and temperature were duly recorded.

Figure 3.34. Temperature measured of soil sample de-aired water solution in pycnometer as measured using a digital thermometer.

The corrected specific gravity values at 20°C were calculated using Equations 3.4 to 3.7 (obtained from ASTM D854, 2005). A summary of results for the specific gravity for the fines particles within the base course and subgrade samples is presented in Section 4.4, and all of the specific gravity results for base course and subgrade samples are presented in the Appendix, in Section A.8, for completeness.

$$K = \frac{\rho_w}{0.9982063} \qquad \textbf{Equation 3.4}$$

$$\rho_w = 1.00034038 - (7.77 \times 10^{-6}) \times T - (4.95 \times 10^{-6}) \times T^2 \qquad \textbf{Equation 3.5}$$

$$G_s = \frac{M_s}{(M_{pw,t} - (M_{pws,t} - M_s)} \quad \textbf{Equation 3.6}$$

$$G_{20^\circ C} = K . G_s \quad \textbf{Equation 3.7}$$

Where
K is the temperature correction factor;
ρ_w is the density of water (g/mL);
T is the test temperature (°C);
G_s is the specific gravity
M_s is the mass of the oven dried soil solids (g);
$M_{pw,t}$ is the mass of the pycnometer and water at test temperature (g);
$M_{pws,t}$ is the mass of the pycnometer, water and soil solids at test temperature (g).

3.4.1.5 Modified Proctor (ASTM D1557)

Modified Proctor testing was performed on the 18 base course samples obtained from the base course/subgrade interface in accordance with ASTM D1557 (2005). Four proctor points were conducted per section (i.e. 72 base course samples were tested). Each proctor test was performed at the same gradation, for the base course/subgrade interface sample from the respective sections, as determined by dry sieving of the 3,000 gram sample conducted in November, 2010. A 5.5 kg sample was required per Proctor point to perform the modified proctor test. Due to lack of material in the interface base course sample, the interface samples were supplemented with portions of gradations from other samples within the same section at different depths. For example, the six-inch sections base course/subgrade interface layers located at a depth of four to six-inches below the asphalt/base course interface were supplemented with soil, from required portions of the gradation, within the layers located at a depth of zero to two inches and two to four inches below the asphalt/base course interface, from the same section. Similarly the ten-inch sections base course/subgrade interface layers located at nominal depths of eight to ten-inches below the asphalt/base course interface were supplemented with soil from

required portions of the gradation, from depths of six to eight inches and four to six-inches below the asphalt/base course interface, from the same section. Target moisture contents of three, five, seven, and nine percent were established for the four points based on in-situ conditions and a prior knowledge of the optimum water content for this material. The soil was compacted in five layers using 56 blows per layer. Sieving was performed on all of the oven dry interface samples and supplement samples (in accordance to Section 3.4.1.1). After sieving, the sample retained on each sieve was placed in metal pans (Figure 3.35). The weight of pan was recorded before and after the addition of samples.

Figure 3.35. Individual grain sizes are placed in separate metal pans after sieving.

Certain quantities of individual size particles matching the gradation of the interface sample, as obtained from the sieve analyses conducted in November, 2010 and discussed in Section 3.4.1.1 were placed in three feet by three feet metal pans (Figure 3.36).

Figure 3.36. Piles of individual particle sizes matching the gradation of interface samples obtained in November 2010, and placed in three foot by three foot metal pans.

Each soil samples that had been separated into select gradations and placed in the aforementioned three foot by three foot metal pans was mixed using a trowel. The weight of a plastic spray bottle filled with tap water was measured and recorded. During sample preparations, water was sprayed onto each sample using the spray bottle as the sample was mixed together. The amount of water added to the soil was based on the target water content. The spray bottle was weighed periodically to ensure that an adequate amount of water was added to achieve the target moisture content. Mixing of the sample was concluded when the sample was observed to have uniform amount of water. After an adequate amount of water was added to each sample, the final weight of the spray bottle with water was recorded.

For each sample, the first layer was placed in the mold assembly and the height from the top of the sample to the top of the mold assembly was measured. The sample was placed in the mold in approximate one inch thick layer. As per ASTM D1557 (2005), a manual rammer, 18 inches tall, with a free fall drop height of 18 inches, and weighing 10 pounds was utilized. The mold used was 4.58 inches tall and six-inch diameter. The rammer was positioned perpendicular to the sample surface by holding the guide sleeve. Blows were delivered to the soil by holding

the guide sleeve vertically with one hand and raising the hammer with the other hand and allowing the hammer to fall freely. The first four blows were delivered to the four corners of the mold then the remaining blows were delivered in a circular pattern around the outside of the mold. A total of 56 blows per layer were delivered to the soil sample. After delivering 56 blows, the height from the top of the sample surface to the top of the mold assembly was measured using a ruler. On completion of compaction of the fifth layer, the collar was removed by loosening the screws. Each sample was then trimmed/leveled using a metal straight edge. Any holes in the top surface of the sample were filed with trimmed soil with a maximum hole size of 1/8 inch. Any sample on the base plate or outside the mold was wiped away using a clean cloth towel. The weight of mold with sample (including base plate) was measured on a scale and recorded for each respective sample (Figure 3.37). The weight of the base course sample was calculated by subtracting the individual weights of base and mold from the combined weight of base, mold, and the sample. The unit weight was then determined by dividing the weight of the base course by the volume of the calibrated mold.

Figure 3.37. Weight measurement of base and mold containing compacted base course sample.

For each of the 18 base course samples, an empty metal pan weight was measured and recorded following completion of each proctor test. The mold was then removed from the base plate and placed on the empty metal pan. A hammer was used to manually extrude each sample from the mold. Approximately one half of the sample from each mold was transferred into each pan. The weight of each pan and wet sample was measured using a scale and recorded. Each pan was then placed in an oven and dried at 105°C for 24 hours. The dry weight of each of the pans containing soil was measured on the scale and recorded.

The dry and wet weights for each sample were used to calculate the moisture content of the recompacted base course samples. The wet density, dry density and moisture content of base course sample were calculated using Equations 3.8, 3.9, and 3.10, respectively. The results for the modified proctor testing on base course samples are presented in Section 4.5 and all the modified proctor plots obtained from the modified proctor testing for the base course samples are presented in the Appendix, in Section A.9, for completeness.

$$\rho_w = \frac{M_{sbm} - M_{bm}}{V} \qquad \text{(ASTM D1557, 2005)} \qquad \textbf{Equation 3.8}$$

$$\rho_d = K \times \frac{\rho_w}{1 + w} \qquad \text{(ASTM D1557, 2005)} \qquad \textbf{Equation 3.9}$$

$$w = \frac{M_{wsp} - M_{dsp}}{M_{dsp} - M_p} \times 100 \qquad \text{(ASTM D1557, 2005)} \qquad \textbf{Equation 3.10}$$

Where
ρ_w is the wet base course density (g/cm^3);
M_{sbm} is the mass of soil, base plate, and cylindrical mold (g);
M_{bm} is the mass of base plate and cylindrical mold (g);
V is the volume of the mold (cm^3);
ρ_d is the dry base course density (lb/ft^3);
K is the conversion factor from g/cm^3 to pcf which is 62.43;
w is the moisture content of the sample (percent);
M_{wsp} is the mass of the wet sample and pan (g);
M_{dsp} is the mass of the dry sample and pan (g);
M_p is the mass of the pan (g).

3.4.1.6 Lab Hydraulic Conductivity [LHC] of recompacted base course

One of the laboratory testing techniques utilized to measure the hydraulic conductivity of recompacted base course material was using a Mariotte Bottle (MB) device. No ASTM is available for this testing method. One proctor point from each section was used to determine the laboratory hydraulic conductivity of the corresponding base course sample. As discussed in Section 3.4.1.5, the modified proctor test was performed in accordance with ASTM D1557 to create the recompacted soil.

The sample tested from Section 13W was first placed in the device but no flow was observed over a three day period using the maximum possible hydraulic gradient (i) value of 4.5. The sample was then removed from the MB and transferred to the Flexible Wall Permeameter (FWP) device. Section 1B was initially placed in the FWP but the observed flow was in excess of the flow capacity of the FWP device (i.e. the flow was the same as the flow in FWP with no sample) and the sample was then transferred to the MB. The head in the MB was set at 6.2 cm, 12.1 cm, and 23.8 cm to achieve i values of 0.5, 1.0, and 2.1, respectively. For Sections 10 and 12 no flow was observed at i values of 0.5, 1.0, and 2.1. Therefore, heads of 35.6 cm, 41.4 cm, and 49.6 cm were utilized which resulted in i values of 3.1, 3.6, and 4.3, respectively. Results from constant head tests, using the MB, were obtained for 16 recompacted base course samples. For the MB testing procedure, the proctor mold was used as a rigid wall to encompass the soil during the test. The testing procedure was divided into individual steps, including equipment assembly, testing, and test completion.

The first step in the testing process was equipment assembly. For each test, the base of the MB was placed on a table. A circular expanded metal mesh measuring six-inch in diameter with 1/16 inch circular openings along with synthetic fabric filter, also measuring six-inches in diameter, was then placed on top of the MB base. It was ensured, by visual inspection, that the

synthetic filter fabric was placed in contact with the sample. A black rubber sleeve (with two pipe clamps on the outside of the sleeve and measuring approximately six-inches in diameter) was then fitted on the base of the MB. It was visually ensured that approximately half height of the rubber sleeve was beyond the top of the base of the MB. The mold with the recompacted base course sample was then placed onto the filters (located in the rubber sleeve on the base of the bottle) and set flush with the help of the rubber sleeve. The clamps on the rubber sleeve were tightened using a nut driver. One clamp was used to tighten the sleeve on the base of the MB while the other clamp was used to tighten the sleeve on the mold. Another black rubber sleeve (with two pipe clamps on the outside of the sleeve) was placed on top of the mold. The sleeve was pushed downward so that one half of its height was on the mold. Companion circular expanded metal mesh and synthetic fabric filter were placed on top of the mold. It was ensured, by visual inspection, that the synthetic filter fabric was in contact with the sample. The top of the MB was then placed on top of the mold and set flush with the help of the rubber sleeve. The clamps were tightened using a nut driver. One clamp was used to tighten the sleeve on top of the mold while the other was used to tighten the sleeve on the bottom of the top of the MB (Figure 3.38).

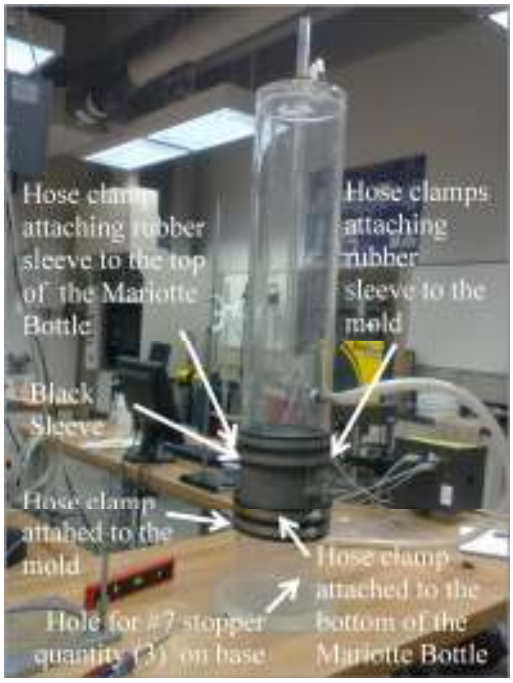

Figure 3.38. Constant head testing using the MB setup.

The second step in the testing process was testing. For each test, an empty five gallon plastic bucket was placed in a sink with a faucet. The bucket was filled with water until it was approximately two thirds full. The entire equipment assembly (shown previously in Figure 3.38) was placed in the bucket. The water level in the bucket was above the top of the mold after the bottom of the MB assembly was fully submerged in the bucket filled. The base of the MB was sealed using three number seven rubber stoppers. The stand pipe of the MB was adjusted such that the bottom of the standpipe was at 6.2 cm above the datum (the minimum *i* value), and the top of the stand pipe was sealed using a rubber stopper.

The MB was then filled with water from the faucet using the tubing attached to the top portion of the MB (Figure 3.39). While the MB was filled with water, the clip on the tubing on top of the device (controlling air flow in the equipment) remained open to prevent pressure build up in the equipment. When the bottle was almost completely filled, the faucet was turned off; the tubing was then removed from the faucet and sealed using a number three rubber stopper. The

clip on top of the MB was squeezed at the same time the faucet hose was plugged to close the vent valve. The three number seven stoppers were then removed from the base of the MB, and the test was initiated when the stopper was removed from the stand pipe. Removal of stopper from the stand pipe and the starting of the stopwatch (used to record time) were performed simultaneously.

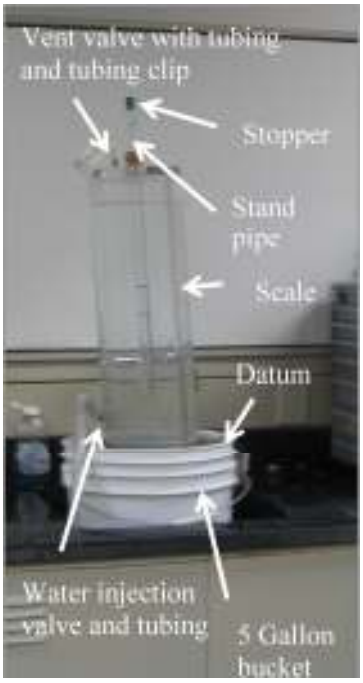

Figure 3.39. Mariotte bottle ready for testing.

The time required for every five centimeter drop in the water level, as measured using a scale on the side, was recorded. The test was conducted for *i* of values of 0.5, 1.0, and 2.0 by placing the bottom of the stand pipe at 6.2 cm, 12.2 cm and 23.8 cm above the datum (located at the top of the bucket), respectively. The hydraulic gradient, corrected area and hydraulic conductivity were calculated using Equations 3.11, 3.12, and 3.13, respectively.

$$i = \frac{h}{l}$$ **Equation 3.11**

$$A_{cb} = A_b - A_{sp}$$ **Equation 3.12**

$$k = \frac{A_{cb} \times l \times (wl_b - wl_a)}{(t_b - t_a) \times (h \times A_{cb})}$$ **Equation 3.13**

Where
i is the hydraulic gradient (unitless)
l is the length of the (six-inch diameter) proctor mold (in cm);
h is the position of the bottom of the stand pipe above the datum.
A_{cb} is the corrected area of the inside of the bottle (in cm^2);
A_b is the area of the inside of the bottle (in cm^2);
A_{sp} is the outside area of the standpipe (in cm^2);
wl_b is the water level at reading b (in cm);
wl_a is the water level at reading a (in cm);
t_b is the stop watch time at reading b (in seconds);
t_b is the stop watch time at reading a (in seconds);
h is the position of the bottom of the stand pipe above the datum.

The third step in the testing process was test completion. For each sample, water was drained from the equipment when the test was completed by loosening the hose clamps. The equipment was then completely disassembled by removing the hose clamps. The mold and each sample were then removed from the equipment. Each sample was manually extruded from the mold using a hammer. The sample was then split between two metal pans and oven dried at 105°C until the sample was dry. Sieve analyses were performed on each of the dried samples in accordance with Section 3.4.1.1. The results obtained from the hydraulic conductivity laboratory testing on base course samples are presented in Section 4.7, and all of the hydraulic conductivity results for base samples are presented in the Appendix, in Section A.10, for completeness.

The hydraulic conductivity of two recompacted base course samples (Sections 1A and 13W) was performed using a FWP device in accordance with ASTM D5084. The hydraulic conductivity for Sections 1A and 13W were obtained using a FWP for the reasons discussed in Section 3.4.1.6. The pressure in the cell water, head water, and tail water was fixed at 20 psi, 17 psi, and 16 psi, respectively which resulted in an effective stress of 4.0 psi (at the bottom of the sample). The calculated values of *i* for Sections 1A and 13W were 7.4 and 7.3, respectively. The

hydraulic conductivity values for the last five readings were averaged to obtain the average laboratory hydraulic conductivity values of the recompacted base course samples.

3.4.1.7 Moisture Content (ASTM D2216)

As mentioned in Sections 3.2.2 and 3.2.3, approximately 250 gram and 400 gram subgrade and base course samples, respectively, were obtained from each two inch thick lift placed in moisture content tins, and transported back to the U of A laboratory. The weight of the moist sample placed in moisture content tins was measured immediately on site before the samples were transported back to the laboratory. The 70 base course samples and 54 subgrade samples were oven dried at 105°C for 24 hours and the dry weights were recorded. The moisture content was calculated using Equation 3.14.

$$w = \frac{(M_1 - M_2)}{(M_2 - M_t)} \qquad \text{(ASTM D2216, 2005)} \qquad \textbf{Equation 3.14}$$

Where
w is the water content (%)
M_1 is the mass of container and moist sample (g);
M_2 is the mass of container and dried sample (g);
M_t is the mass of the tin (g).

A similar procedure was followed for the moisture content determination of the 54 proctor samples (described in Section 3.4.1.5). The moisture conditioned base course, remaining in the three foot by three foot pans after each sample was compacted, was collected and a moisture content test was performed following the above mentioned procedure on each respective sample. As a part of Atterberg limits testing (described in Section 3.4.1.3), the water content was obtained for 270 samples. Also, following the hydraulic conductivity testing conducted in the Mariotte bottle (Section 3.4.1.6) and flexible wall permeameter (Section 3.4.1.6), the water content was obtained for 16 and 2 samples, respectively.

3.4.1.8 Hydraulic Conductivity (empirical prediction)

The hydraulic conductivity of the base course was also estimated using the empirical equations presented by Hazen (1930), Moulton (1980), and Sherard et al. (1984) in a similar manner as discussed in Section 2.4.3. As discussed previously, the Hazen (1930) and Sherard et al.(1984) methods utilize only values obtained from grain size distribution (D_{10} or D_{15}, respectively) while the Moulton (1980) method utilizes both values obtained from the grain size distribution (D_{10} and P_{200}) and the porosity (n). The Hazen (1930) equation is provided in Equation 3.15 (previously presented as Equation 2.1) while the Sherard et al. (1984) equation is provided in Equation 3.16 (previously presented as Equation 2.2) and the Moulton (1980) equation is provided in Equation 3.17 (previously presented as Equation 2.3). The results based on these empirical predictions are presented in Section 4.9.

$$k = CD_{10}^{2} \qquad \text{(Hazen, 1930)} \qquad \textbf{Equation 3.15}$$

Where
k is hydraulic conductivity (cm/s);
D_{10} is size opening through which 10 percent by weight of dry sample will pass (mm);
C is empirical coefficient (for this study 1.0).

$$k = 0.35\,D_{15}^{2} \qquad \text{(Sherard et. al., 1984)} \qquad \textbf{Equation 3.16}$$

Where
k is hydraulic conductivity (cm/s);
D_{15} is size opening through which 15 percent by weight of dry sample will pass (mm).

$$k = \frac{6.214 * 10^{5} D_{10}^{1.478} n^{6.654}}{P_{200}^{0.597}} \qquad \text{(Moulton, 1980) and (Blanco, 2003)} \qquad \textbf{Equation 3.17}$$

Where
k is hydraulic conductivity (ft/day);
D_{10} is size opening through which 10 percent by weight of dry sample will pass (mm);
n is porosity of the material (unitless);

P_{200} is percent of material finer than the No. 200 sieve (75 μm).

Note**:** The dry sieving conducted in November, 2010 was used to obtain the D_{10}, D_{15}, P_{200} values. These values were then used in the previously listed empirical equations to obtain hydraulic conductivity estimates.

3.4.2. Transmissivity and Permittivity of Geosynthetic Separators [P&T]

Transmissivity testing and permittivity testing were performed to determine the in-plane flow and cross plane flow through a geosynthetic sample, respectively. A total of fifteen tests were performed for each testing technique, ten on exhumed geotextile samples and five on new geotextile samples. As mentioned in Section 3.2.2, the exhumed samples were previously obtained from the six-inch and ten-inch sections (5 samples per section thickness) in October 2010.

3.4.2.1 Transmissivity (ASTM D6574)

Transmissivity of a geotextile is the quantity of in-plane flow through a unit width. The transmissivity values of five geotextile samples in the six-inch sections, four geotextile samples in the ten-inch sections, and five new geotextile samples were obtained from laboratory measurements. The transmissivity testing was divided into individual steps including: sample preparation and placement, equipment setup, and testing.

The first step in the testing process was sample preparation and placement. The transmissivity device was placed on a table. A one foot by one foot geosynthetic sample was measured and carefully removed from each of the two foot by two foot exhumed sample. New samples sent from the fabrication plant measured one foot by one foot, as requested. Each geosynthetic sample was placed in the center of the device. It was ensured, by visual inspection, that the sample was placed in the area cutout for sample placement. Following placement of the geosynthetic sample, a one foot by one foot, half inch thick acrylic plate was placed on top of the

sample without moving the sample. A water tight cushion was then placed on top of the acrylic plate to prevent water from flowing over the sample to ensure the water only flows through the sample. Another one foot by one foot, half inch thick acrylic plate was then placed on top of the cushion to carry a load applied to simulate overburden stresses. A predetermined weight of approximately 172 pounds was placed on top of the acrylic sheet to simulate field conditions (vertical effective stress of 1.0 psi).

The second step in the testing process was equipment setup (Figures 3.40). The hose was connected to a faucet and turned on to fill up the device. The drain tube was placed in the laboratory catch basin to drain excess water. Another tube that discharged water passing through the geosynthetic sample was placed in an empty white bucket. The bucket was emptied out in a sink as needed. For each sample, the equipment was filled with water until a steady flow rate was observed. Head in the equipment was regulated using two adjustable stand pipes. One adjustable stand pipe was used to control the head water and one adjustable stand pipe was used to control the tail water. Two metallic rulers were used to measure heads (head water and tail water). One was used to read the head water level and one was attached to read the tail water level (Figure 3.40a).

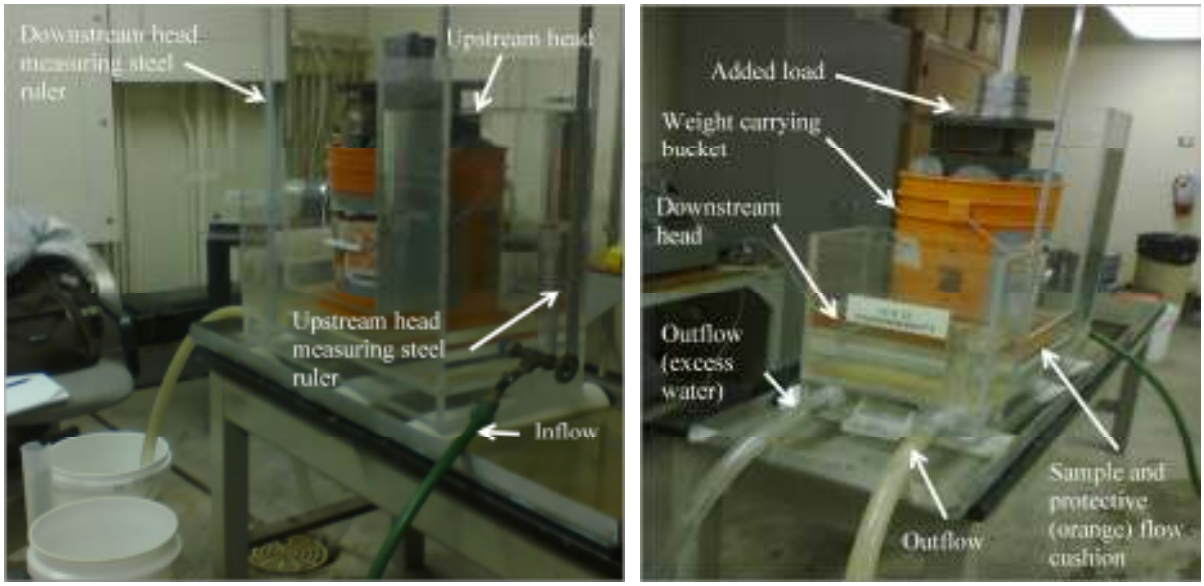

(a) **(b)**

Figure 3.40. Setup of transmissivity test a) upstream and b) downstream.

The third step in the testing process was testing. The tail water stand pipe was maintained at 14.8 cm (to achieve an effective stress of 1 psi) while the head water stand pipe was adjusted to obtain variable head difference for at least five measurements. The time required for a fixed volume of water to pass through the geosynthetic and discharge from the pipe was recorded using a stop watch. The fixed volumes used for testing of each sample were 100 mL, 250 mL, 500 mL, 1000 mL, 2000 mL and 5000 mL depending on the flow rate. A graduated cylinder was used for the 100 mL, 250 mL, 500 mL, and 1000 mL discharge while pre-determined volumes were marked in the bucket for the 2000 mL and 5000 mL discharge. Each measurement was performed twice, and an average flow was calculated for each volume of flow. The hydraulic gradient was calculated using Equation 3.18 and transmissivity values were obtained using Equation 3.19.

$$i = \frac{\Delta h}{l} \qquad \text{(ASTM D6574, 2005)} \qquad \textbf{Equation 3.18}$$

$$\theta = \frac{Q}{(i \times w)}$$ (ASTM D6574, 2005) **Equation 3.19**

Where
i is the hydraulic gradient (unitless)
Δh is the difference in upstream head and downstream head (in cm);
l is the length of the sample (in cm);
θ is the transmissivity of the geotextile (in m^2/s);
Q is the flow through the geotextile (in liter/sec);
w is the width of the geotextile sample (in cm);

A summary of the results obtained from the transmissivity testing conducted on all the geotextile samples are presented in Section 4.11.1, and all of the results that were obtained during the transmissivity testing are presented in the Appendix, in Section A.11, for completeness.

3.4.2.2 Permittivity (ASTM D4491)

The permittivity of a geotextile is a measure of the flow through an area in the transverse direction. The permittivity values of six geotextiles in the six-inch sections, four geotextiles in the ten-inch sections, and five new geotextile samples were obtained from laboratory measurement. The testing procedure for permittivity testing was divided into individual steps including sample preparation, equipment setup, and testing.

The first step in the testing procedure was sample preparation and sample placement. The permittivity device was placed on a table. A three inch diameter circle was marked (using a white Sharpie®) on each geotextile sample and removed using scissors. Samples were obtained from either the unused exhumed sample or the new sample. For the new sample, each sample was trimmed from the one foot by one foot sample received from the fabrication plant and previously tested, as described in Section 3.4.2.2.

The second step in the testing procedure was equipment setup. For each test, the top of the device was inverted and the circular sample was placed in the opening reserved for the

sample. A circular brass plate with openings for four screws, an outside diameter of three inches, and hollow diameter of 2.5 inches was placed on the top of each of the samples. Each sample was secured by clamping down the brass plate using the four screws inserted through the four openings in the brass plate (Figure 3.41).

Figure 3.41. Geotextile sample secured using brass plate in the permeability device.

Plumbers putty was applied on top of the base to avoid water leaks. The top assembly was then placed on the base of the device and pressed firmly. The top and base were secured using four 1/4 inch diameter bolts. A hose was connected to a water source on one end and to the permittivity device on the other. The device was then filled using water using the hose. A constant amount of water was supplied to the device to make water overflow through the weir on top of the device, creating a constant head. The permittivity device setup is presented in Figure 3.42.

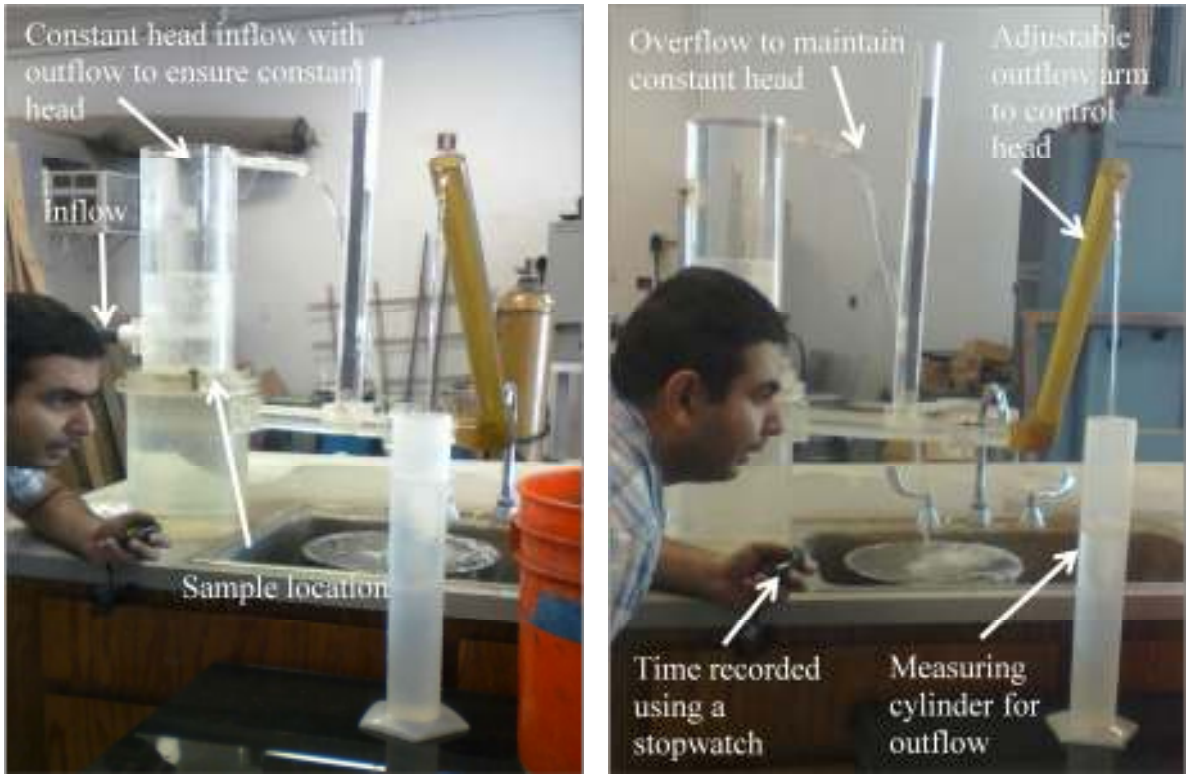

(a) **(b)**

Figure 3.42. Setup of permittivity device a) sample location and b) test reading.

The third step of the testing process was testing. The two standpipes (one is adjustable and the other is not adjustable) were kept vertical to obtain a steady state discharge. A head difference was created by rotating the adjustable stand pipe and collecting the discharge in a graduated cylinder. The volume of flow was recorded along with the time required to obtain this volume. The head in the non-adjustable standpipe was maintained at approximately 40 cm, and a variable head difference was created by inclining the adjustable outflow arm (Figure 3.42b). A summary of the results obtained from permittivity testing on the geotextile samples are presented in Section 4.11.2, and all the results for the permittivity testing on geotextiles samples are presented in the Appendix, in Section A.12, for completeness.

3.5. Pavement Conditions

Pavement conditions are an important indicator of the pavement performance. The vertical alignment of the top of the asphalt, the top of the base course, and the top of the subgrade were obtained during the site visit in October 2010 using surveying instruments (total station), as discussed in Section 3.5.1. Asphalt and base course depth measurements were also obtained using manual methods (tape measure) as discussed in Section 3.5.1. A pavement distress survey conducted by AHTD personnel and analyzed and reported by Goldman (2011) is presented in Section 3.5.2.

3.5.1. Pavement Profile (October 2010)

The top of the asphalt layer was measured, using a total station, at the four corners of each of the two foot by two foot test area: before the asphalt was removed, after the asphalt was removed, and after the base course was removed (Figure 3.43). The depth of the asphalt and the depth of the base course were obtained from these measurements by subtracting the top of the base course elevation from the top of the pavement elevation, and by subtracting the top of the subgrade elevation from the top of the base course elevation, respectively. The depth of the asphalt layer was also manually measured (using a tape measure) at the four corners of the two foot by two foot test area (after asphalt was removed) as presented in Figure 3.44a. Similarly the depth to the base course/subgrade interface was also measured using manual techniques as presented in Figure 3.44b. These values were used to determine the thickness of the asphalt and base course layers in all of the 18 test sections.

(a) (b)

Figure 3.43. Elevation recorded using survey equipment at a) top of asphalt and b) top of base course.

(a) (b)

Figure 3.44. Manual depth verification to a) top of asphalt and b) top of base course.

A summary of results of these elevation and pavement thickness measurements is presented in Section 4.13. These measurements were obtained to identify the actual thickness of the asphalt and base course layers. This data was obtained after the sections had been in service for five years. Some of the sections were demonstrating severe rutting at the time of data acquisition which may lead to discrepancies in results.

3.5.2. Pavement Distress Survey (modified from Goldman (2011))

Pavement distress survey data collected by AHTD personnel in June 2010 and April 2011 was analyzed and reported by Goldman et al. (2011). The data includes percentage of the lane with alligator cracking (based on area), total linear feet of longitudinal cracks, and average rut depth measurements. The data was used to analyze the pavement performance over its service life and compare the relative performance of six-inch thick sections to the ten-inch thick sections. The summary of results for this data is presented in Section 4.14.

3.6. Conclusion

Sample acquisition techniques for exhuming base course, subgrade, and geosynthetic samples were presented in this chapter. The procedures followed to perform the in-situ hydraulic conductivity testing on the base course (conducted using the TSB technique) in October 2010 and May 2011 was also presented in this chapter. In-situ testing using DCP and CBR, as conducted jointly with this project but as a part of TRC Project 0903, were briefly mentioned for completeness.

The methods and procedures utilized for laboratory testing in this research were presented in detail. The testing was performed in accordance with ASTM standards (any deviations from the ASTM were also reported). The laboratory testing for hydraulic conductivity of 16 base course were performed utilizing a constant head device (Mariotte Bottle) for which no

ASTM is present. The laboratory testing for hydraulic conductivity of two base course samples (with relatively low flow) was tested utilizing a Flexible Wall Permeameter which was conducted in accordance with ASTM D5084. Insufficient base course sample for modified proctor tests conducted on the samples from the base course/subgrade interface samples led to this sample being supplemented with certain grain sizes from other depths in the same section. The sieve sizes used to determine the base course particle size conformed to AHTD (2010) specifications.

The laboratory testing performed on exhumed subgrade samples included: wash sieve, hydrometer, Atterberg limits, and specific gravity testing. The laboratory testing performed on exhumed base course samples included: dry sieve, wet sieve, hydrometer, specific gravity, modified proctor, and hydraulic conductivity testing. Transmissivity and permittivity laboratory testing procedures were followed for testing the exhumed geotextile samples and newly acquired samples. The procedures followed to obtain field data to quantify pavement conditions (surface elevation, asphalt thickness, base course thickness, alligator cracking, longitudinal cracking, and rutting) were also presented in this chapter. The results obtained by following the testing procedures described in this chapter are discussed in Chapter 4 and presented for completeness in the Appendix.

Chapter 4. Results

4.1. Introduction

Results obtained from testing conducted in the laboratory and in the field are presented in this chapter. Discussion about the results is also presented within the chapter for each testing technique. Specifically, the results obtained from the: grain size analysis (sieve analysis and hydrometers), Atterberg limits, specific gravity, modified proctor, hydraulic conductivity, transmissivity, and permittivity testing are presented with discussion of the results also being presented.. Also, the results from the: in-situ hydraulic conductivity testing conducted on the base course, gravimetric moisture content testing conducted on the base course and subgrade, nuclear density testing conducted on the base course and subgrade, and pavement performance are presented and discussed.

The results obtained from grain size analysis testing conducted on the base course samples are presented in Section 4.2. The results obtained from subgrade Atterberg limits testing on the subgrade samples are presented in Sections 4.3. The results obtained from specific gravity, in-situ gravimetric moisture content, and unit weight testing is presented in Section 4.4. The results obtained from modified proctor testing conducted on the base course samples are presented in Section 4.5. Comparisons between the index properties obtained as a part of this research and the index properties obtained with past research are presented in Section 4.6. Hydraulic conductivity values, as obtained from laboratory and in-situ measurements, for the base course samples are presented in Sections 4.7 and 4.8, respectively. Comparisons between the laboratory and field obtained hydraulic conductivity results (for base course samples) and empirical predictions of hydraulic conductivity are presented in Section 4.9.

Geotextile design criteria, as applied to the geotextiles already in place at the Marked Tree Test Section, are presented and discussed in Section 4.10. Transmissivity and permittivity results obtained for new and exhumed geotextile samples are presented and discussed in Section 4.11.1 and 4.11.2. Observations made during the October 2010 during the geotechnical investigation and pavement profile measurement obtained during the October 2010 site visit are presented in Section 4.12 and 4.13, respectively. The pavement distress survey (as modified from Goldman, 2011) is presented and discussed in Sections 4.14.

4.2. Grain Size Analysis (dry sieve analysis, wet sieve analysis, and hydrometer analysis)

As discussed in Section 3.4.1.1, a grain size distribution was determined for each of the of the base course samples by performing sieve analysis (dry and wet) and by conducting hydrometer tests. A grain size distribution was determined for each of the subgrade samples by performing sieve analysis (wet) and by conducting hydrometer tests. The results of these grain size analyses are presented in Sections, 4.2.1, 4.2.2, and 4.2.3.

4.2.1. Sieve Analysis

A typical gradation of a base course sample, as obtained from Section 1B at a depth of 0-2 inches below the asphalt/base course interface, is presented in Figure 4.1. The sieve analyses were performed in accordance with the testing procedures presented in Section 3.4.1.1. The grain size results including D_{60}, D_{30}, D_{15}, D_{10}, C_u and C_g are also presented in Figure 4.1. The grain size distribution curves obtained for all the 70 base course sub-samples are presented in the Appendix, in Section A.1, for completeness.

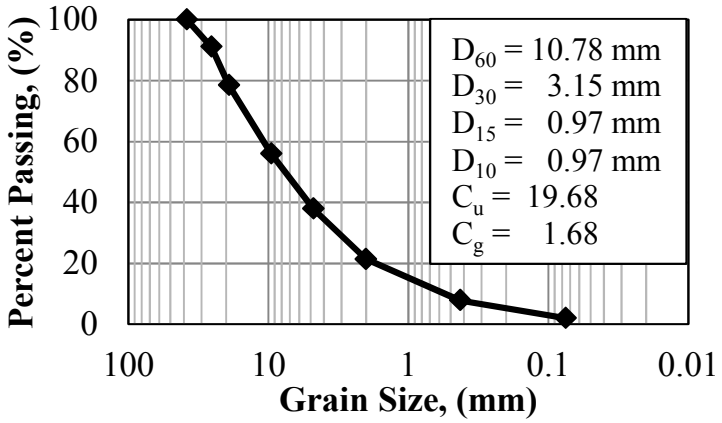

Figure 4.1. Gradation of base course sample obtained from Section 1B at a depth of 0-2 inches below the asphalt/base course interface.

Typical gradations of base course samples obtained from Section 1B at a depth of 8-10 inches below the asphalt/base course interface, as conducted: 1) after sampling (November 2010), 2) before proctor testing (July 2011), and 3) after hydraulic conductivity testing (October 2011) are presented in Figure 4.2.

The gradations obtained from the three dry sieving techniques are in close agreement. Minor changes in gradation are observed due to particle movement and breakage. The grain size results including D_{60}, D_{30}, D_{15}, D_{10}, C_u and C_g for the dry sieving conducted in November 2010, July 2011, and October 2011 on the Section 1B sample obtained from 8-10 inches below the asphalt/base course interface are also presented in Figure 4.2. All of the grain size distribution curves comparing the gradations obtained from the dry sieve analyses conducted in November 2010, July 2011, and October 2011 for the 18 base course samples obtained from the base course/subgrade interface (one from each section) are presented in the Appendix, in Section A.2, for completeness.

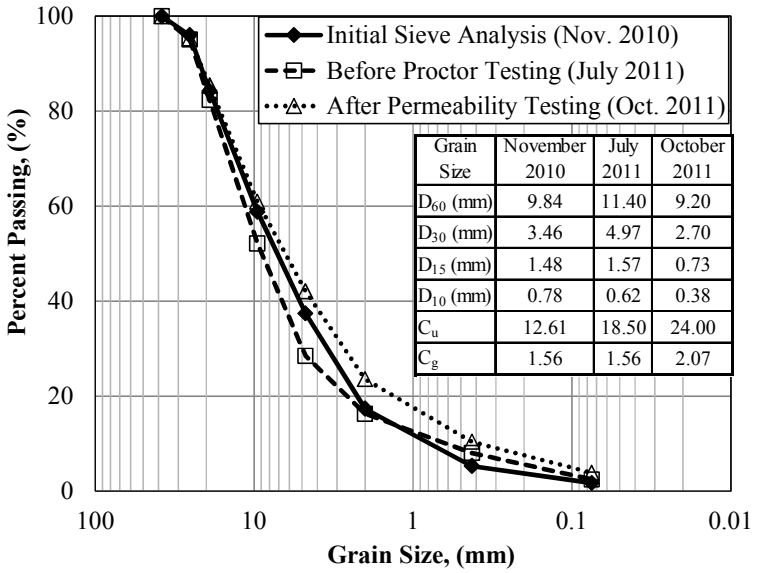

Figure 4.2. Gradation of base course sample from Section 1B at a depth of 8-10 inches below the asphalt/base course interface as conducted: 1) after sampling (November 2010), 2) before proctor testing (July 2011), and 3) after hydraulic conductivity testing (October 2011).

Wet sieve testing was also performed in March 2011 in accordance with the testing methods outlined in Section 3.4.1.1 to compare the fines content obtained using the two sieving methods (dry sieving and wet sieving). The fines content obtained for the base course at the base course/subgrade interface, within each of the 18 section, as obtained using the three dry sieving techniques and one wet sieving technique are tabulated in Table 4.1and presented graphically in Figure 4.3. The fines content values as obtained using the wet sieving technique for the 70 base course samples and 54 subgrade samples are presented in the Appendix, in Section A.3, for completeness.

Table 4.1. Fines content (in percent) for the base course at the base course/subgrade interface layer (4-6 inches below the asphalt/base course interface for the six-inch thick sections and 8-10 inches below the asphalt/base course interface for the ten-inch thick sections).

Location	Depth*	Dry Sieving			Wet Sieving March 2011	(Before Proctor Testing) - (3000g sample)	(After Permeability Testing) - (3000g sample)	(Wet Sieving) - (3000g sample)
		3000g oven dried sample November 2010	Before Proctor Testing July 2011	After Permeability Testing October 2011				
	(inch)	(percent)	(percent)	(percent)	(percent)	(percent)	(percent)	(percent)
Section 1B	8-10	1.71	2.44	3.85	9.88	0.73	2.13	8.16
Section 1A	8-10	1.68	1.78	4.27	8.13	0.10	***2.59***	6.45
Section 1	8-10	1.68	2.75	3.84	8.32	***1.07***	2.16	6.64
Section 2	8-10	2.39	2.86	4.33	7.52	0.47	1.94	5.13
Section 3	8-10	2.30	2.13	4.04	7.80	(0.17)	1.74	5.50
Section 4	8-10	1.50	2.11	3.57	7.60	0.61	2.07	6.10
Section 5	8-10	1.59	2.08	3.45	7.16	0.49	1.87	5.58
Section 6	8-10	1.52	1.59	3.25	10.71	0.07	1.73	***9.19***
Section 8	4-6	1.73	2.48	3.76	11.11	0.75	2.03	***9.38***
Section 9	4-6	1.38	1.46	3.42	10.27	0.08	2.04	8.90
Section 10	4-6	1.67	1.73	3.83	8.90	0.06	2.16	7.23
Section 11	4-6	1.53	2.01	3.70	7.57	0.48	***2.17***	6.04
Section 12	4-6	1.38	2.12	3.37	7.40	0.74	1.99	6.02
Section 13	4-6	1.49	2.14	3.14	10.49	0.65	1.65	9.01
Section 13W	4-6	3.10	2.65	4.04	5.14	(0.45)	0.94	2.04
Section 13A	4-6	1.76	1.90	3.30	7.58	0.14	1.54	5.83
Section 13B	4-6	1.30	2.02	2.69	8.77	0.72	1.40	7.47
Section 13BW	4-6	1.41	2.61	3.17	9.18	***1.20***	1.77	7.78

*Depth below asphalt/base course interface

Bold and *Italics* represent the maximum values for the six inch and ten inch thick sections. Negative values are presented in parenthesis.

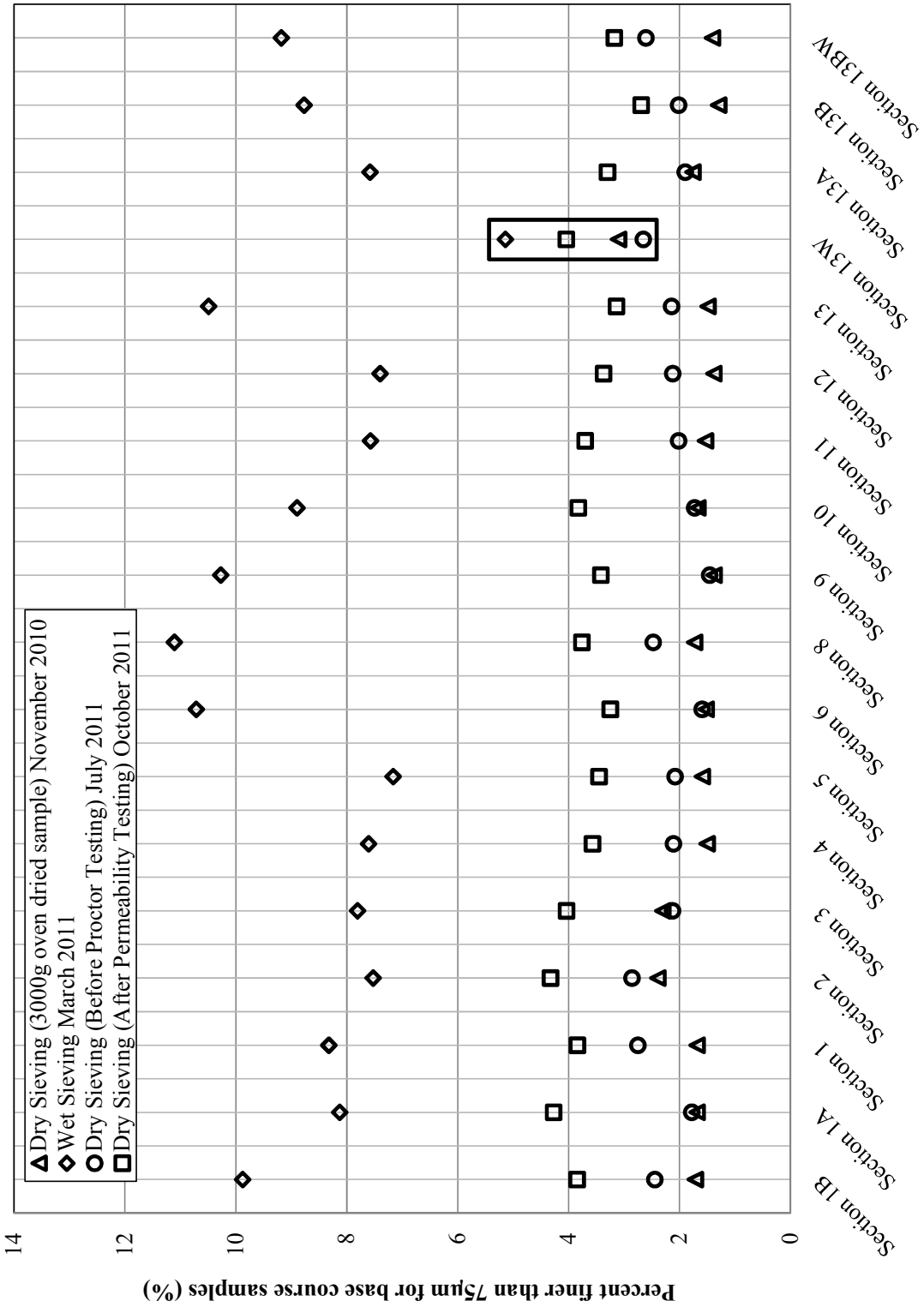

Figure 4.3. Fines content (in percent) for the samples as obtained from the base course/subgrade interface layer (4-6 inches for six-inch thick sections and 8-10 inches for the ten-inch thick sections, as measured below the asphalt/base course interface).

The fines content determined by dry sieving in July 2011 (on the remainder of the bucket sample before proctor testing) exhibited a higher fines content when compared to the initial dry sieving of the 3,000 gram samples in October 2010. However, for Section 3 and Section 13W the fines content decreased from 2.30 to 2.13 percent and from 3.10 percent to 2.65 percent, respectively, between the 3,000 gram sub-sample and the remainder sample. The typical increase in fines content may be attributed to the sample size. The base course samples remaining in the bucket as obtained from the base course/subgrade interface ranged in weight from 10,335 grams (Section 4) to 19,636 grams (Section 6) for the ten-inch thick sections and ranged in weight from 7,974 grams (Section 8) to 15,849 grams (Section 13A) for six-inch thick sections.

The fines content for the base course samples obtained from the base course/subgrade interface as determined by dry sieving (after hydraulic conductivity testing) on the recompacted base course samples exhibited higher fines content when compared to the initial dry sieving of a 3,000 gram sub-sample. A minimum increase of 1.73 percent (Section 6) and a maximum increase of 2.59 percent (Section 1A) were observed in the ten-inch thick sections. Similarly, a minimum increase of 0.94 percent (Section 13W) and a maximum increase of 2.17 percent (Section 11) were observed in the six-inch thick sections. The increase in fines may be attributed to sample size and particle breakage.

Each sample weighed approximately 5,500 grams before the proctor test as compared to the 3,000 gram sub-sample. Also, particle breakage occurred during the recompaction process (modified proctor testing) after which the hydraulic conductivity test was performed. The increase in fines content was attributable to these factors. Although hydraulic conductivity testing has been shown by other researchers (Blanco, 2003) to wash out fines it appears that

particle breakage had a larger influence than fines wash out as the fines contents were higher after hydraulic conductivity testing.

Higher fines contents were obtained by wet sieving than by dry sieving (when compared to the initial dry sieving of a 3,000 gram sub-sample) for base course samples obtained from the base course/subgrade interface. An average increase of 6.60 percent and 6.97 percent was observed for the ten-inch thick sections and six-inch thick sections, respectively. As observed previously in Figure 4.3, base course samples obtained from the base course/subgrade interface layer for Section 13W appear to be exception for all four of the sieving methods. The profile of fines content with depth as determined by wet sieving is presented for this section is presented in Figure 4.4.

Asphalt		
Base Course	0-2 inch	11.0 % fines content
	2-4 inch	10.2 % fines content
	4-6 inch	5.1 % fines content
Base Course	0-2 inch	61.3 % fines content
	2-4 inch	68.1 % fines content
	4-6 inch	82.2 % fines content

Figure 4.4. Profile of fines content (in percent) with depth for Section 13W as determined by wet sieving.

The fines content in the base course immediately above the base course/subgrade interface (as determined from the sample obtained at a nominal depth of 4-6 inches below the asphalt/base course interface) ranged from 2.65 to 5.14 percent in Section 13W, for the various sieving techniques. The measured fines content obtained by dry sieving were typically higher in Section 13W than the measured fines content in the adjacent sections. However, the lowest measured fines content in the base course, on samples obtained at the base course/subgrade interface, was obtained by wet sieving the sample from Section 13W. The loss in fines within the

base course may be caused by fines transport along the base course/subgrade interface layer, in the lateral direction, to another section. It was assumed that the as-placed fines content for the base course samples at this site was 10 percent (as obtained by wet sieving); this was the maximum value allowed (as per AHTD regulations) for fines content within base course when this test site was constructed. No values for fines content within the base course at the Marked Tree Test Section site were reported in Brooks (2009), Hall et al. (2007), or Howard (2006). Therefore, any deviation in fines content above or below 10 percent is of interest. As discussed in Chapter 2, and as will be discussed later in Section 4.7, the fines content within the base course is an important design parameter as it has been shown to correlate with permeability (Moulton, 1980, and to affect the permittivity and transmissivity of a geotextile placed within the pavement system (typically placed at the base course/subgrade interface (FHWA, 1998).

The fines contents as determined by wet sieving for the 18 interface base course samples, as obtained from the base course/subgrade interface layer (nominally 4-6 inches below the asphalt/base course interface for the six-inch thick sections and nominally 8-10 inches below the asphalt/base course interface for the ten-inch thick sections) are presented in Table 4.2, Likewise, the fines contents as determined by wet sieving for the 18 interface subgrade samples, as obtained from the subgrade/base course interface layer (0-2 inch below the base course/subgrade interface), are presented in Table 4.2. The differences in fines content (determined by wet sieving) between the subgrade and base course samples located below and above the base course/subgrade interface, are presented in Figure 4.5a along and the locations of the samples (for the different base course thicknesses) is identified with a schematic (Figure 4.5b).

Table 4.2. Fines content (in percent) determined by wet sieving for the base course samples obtained from the base course/subgrade interface layer and for the subgrade samples obtained from the subgrade/base course interface layer.

Location	Depth*	% Finer than 75μm (B)	Depth**	% Finer than 75μm (S)	(S)-(B)
	(inch)	(%)	(inch)	(%)	(%)
Section 1B	8-10	9.9	0-2	56.7	46.9
Section 1A	8-10	8.1	0-2	56.4	48.3
Section 1	8-10	8.3	0-2	70.7	62.4
Section 2	8-10	7.5	0-2	68.4	60.9
Section 3	8-10	7.8	0-2	69.0	61.2
Section 4	8-10	7.6	0-2	70.1	62.5
Section 5	8-10	7.2	0-2	62.2	55.0
Section 6	8-10	10.7	0-2	66.7	56.0
Mean	8-10	8.4	0-2	65.0	56.7
Section 8	4-6	11.1	0-2	64.7	53.6
Section 9	4-6	10.3	0-2	63.5	53.2
Section 10	4-6	8.9	0-2	59.9	51.0
Section 11	4-6	7.6	0-2	66.3	58.8
Section 12	4-6	7.4	0-2	45.9	38.5
Section 13	4-6	10.5	0-2	72.4	61.9
Section 13W	4-6	5.1	0-2	61.3	56.2
Section 13A	4-6	7.6	0-2	78.2	70.6
Section 13B	4-6	8.8	0-2	60.1	51.3
Section 13BW	4-6	9.2	0-2	75.4	66.2
Mean	4-6	8.6	0-2	64.8	56.1

*Depth below asphalt/base course interface

**Depth below base course/subgrade interface

S = Subgrade, B = Base Course

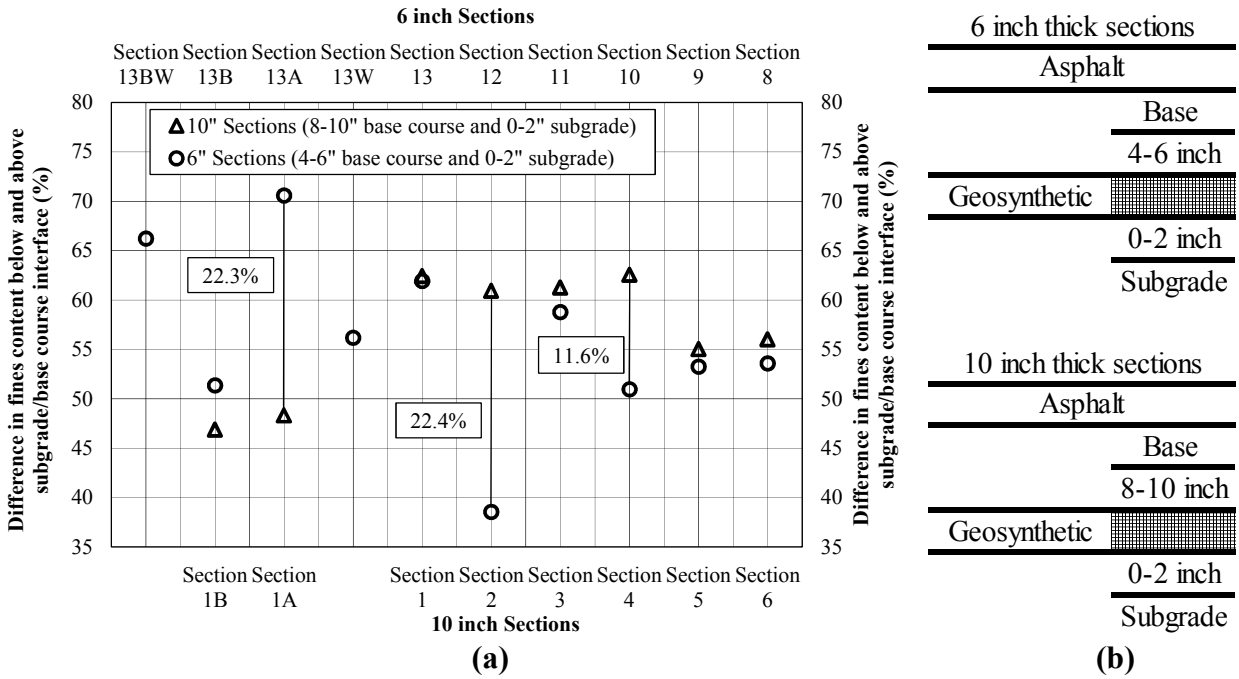

Figure 4.5. (a) Difference in fines content (in percent as determined by wet sieving) between the subgrade and the base course samples immediately above and below the base course/subgrade interface and (b) schematic identifying the locations of the samples within the depth profile.

Because the difference in the fines content (between the subgrade and base course samples immediately above and below the base course/subgrade interface) for the samples obtained in Sections 1 and 13 (the control sections) both have a difference of approximately 62 percent, this is treated as the standard and significant deviations away from this value are of interest.

The average difference in fines content (as obtained from wet sieving) was 56.7 percent and 56.1 percent for the ten-inch thick and six-inch thick sections, respectively. The comparison between the six-inch thick and the ten-inch thick sections reveal that the same difference in fines content between the base course and subgrade samples at the subgrade/base course interface for the same fabric in corresponding sections containing the same fabric but different base course thicknesses. The exceptions to this observation were Sections 1A and 13A, Sections 2 and 12

and, Sections 4 and 10. The difference in fines content between Sections 1A and 13A, Sections 2 and 12, Sections 4 and 10 is 22.3 percent, 22.4 percent, 11.6 percent, respectively. The difference in fines content might be an indication of fines retention or clogging in Section 1A, Section 10, and Section 12.

No comparison between the six-inch thick sections (13W and 13BW) and the corresponding ten-inch thick sections (1W and 1BW) was performed because no samples were obtained for the corresponding ten-inch thick sections (1W and 1BW). Sections 13W and 13BW were not initially within the scope of this research project (or previous research projects) but during the field visit in October, 2010 these sections were visually identified as failing. Hence samples were obtained from these sections to identify why these sections were failing. The fines content obtained by conducting wash sieve analyses on the 70 base course samples and the 54 subgrade samples are presented in the Appendix, in Section A.3, for completeness.

4.2.2. Hydrometer Analysis (Base Course)

Hydrometer testing was conducted on the base course samples in accordance with the procedures outlined in Section 3.4.1.2. Typical results from a hydrometer test conducted to determine the silt and clay content in a base course sample, normalized relative to percentage passing the No. 200 sieve and normalized by weight of the entire sample, are presented in Figures 4.6a and 4.6b, respectively. The typical sample results presented in Figure 4.6 were obtained for the sample from Section 1B at a depth of 0-2 inches below the asphalt/base course interface.

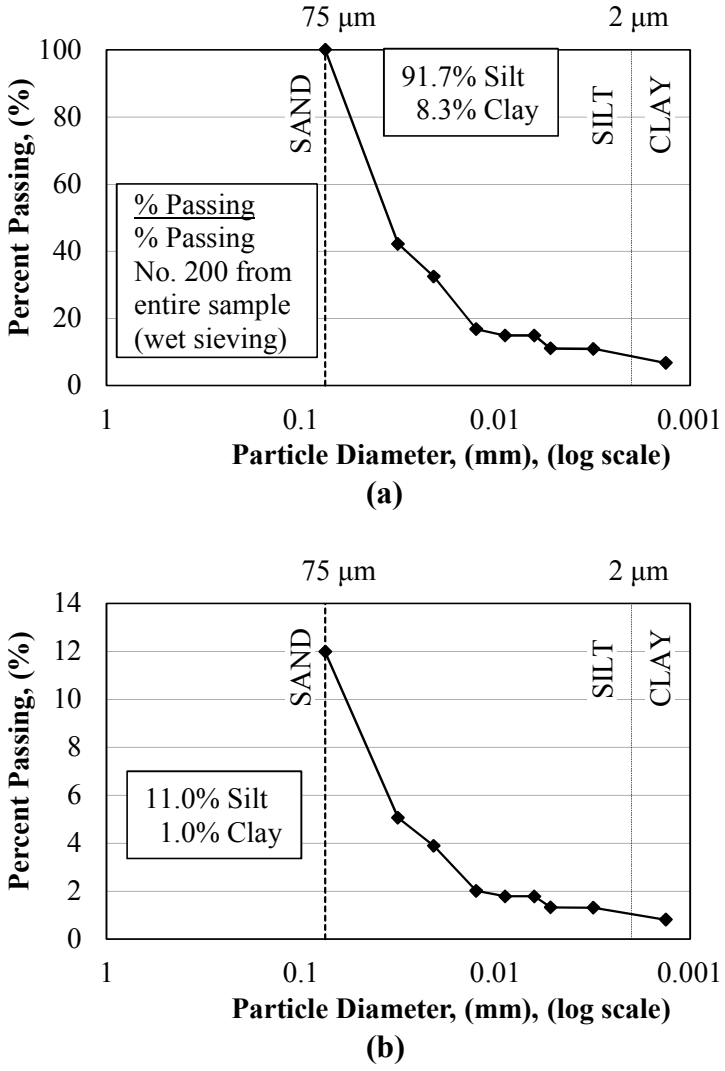

Figure 4.6. Result obtained from hydrometer testing conducted to determine the silt and clay contents a) normalized relative to percentage passing the No. 200 sieve and b) normalized by the weight of entire sample in the base course sample obtained from Section 1B at a depth of 0-2 inches below the asphalt/base course interface.

By normalizing the plots relative to the percent passing the No. 200, the percentage of fines that are silt or clay was determined. By normalizing the plots relative to the total weight of the sample, the percentage of the whole sample that is silt or clay was determined. For the example shown in Figure 4.6 (Section 1B 0-2 inches below the asphalt/base course interface), the fines are 91.7 percent silt and 8.3 percent clay, or the whole sample is 11.0 percent silt and 1.0

percent clay. The silt content of the fines in the base course at the base course/subgrade interface layers is presented in Figure 4.7.

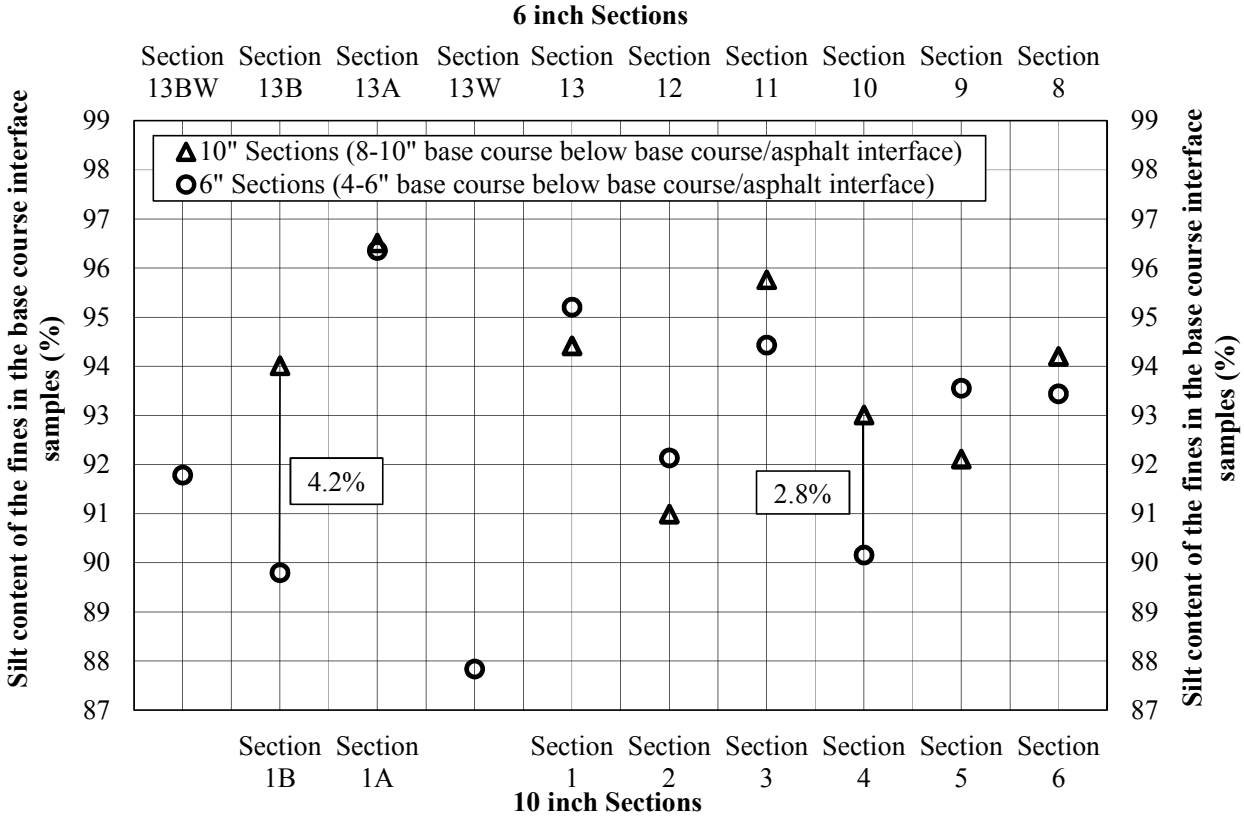

Figure 4.7. Silt content (in percent) of the fine particles for the base course samples obtained from the base course/subgrade interface layers for the six-inch thick sections and the ten-inch thick sections (as determined by hydrometer testing).

Comparing the silt content obtained from the corresponding six-inch thick and the ten-inch thick sections reveals that almost equal amounts of silt content is present in the base course at the base course/subgrade interface layers for both base course thicknesses. The differences between Sections 1B and 13B, and Sections 4 and 10 are more significant. The silt content in Section 1B is 4.2 percent higher than Section 13B, and the silt content in Section 4 is 2.8 percent higher than Section 10. Similarly, the clay content of the fines in the base course sample at the base course/subgrade interface layer for the six-inch thick sections and the ten-inch thick sections is presented in Figure 4.8. A summary of minimum and maximum silt content and clay

content of fine particles in the base course samples, at the base course/subgrade interface, for the six-inch thick and ten-inch thick sections is also presented in Table 4.3.

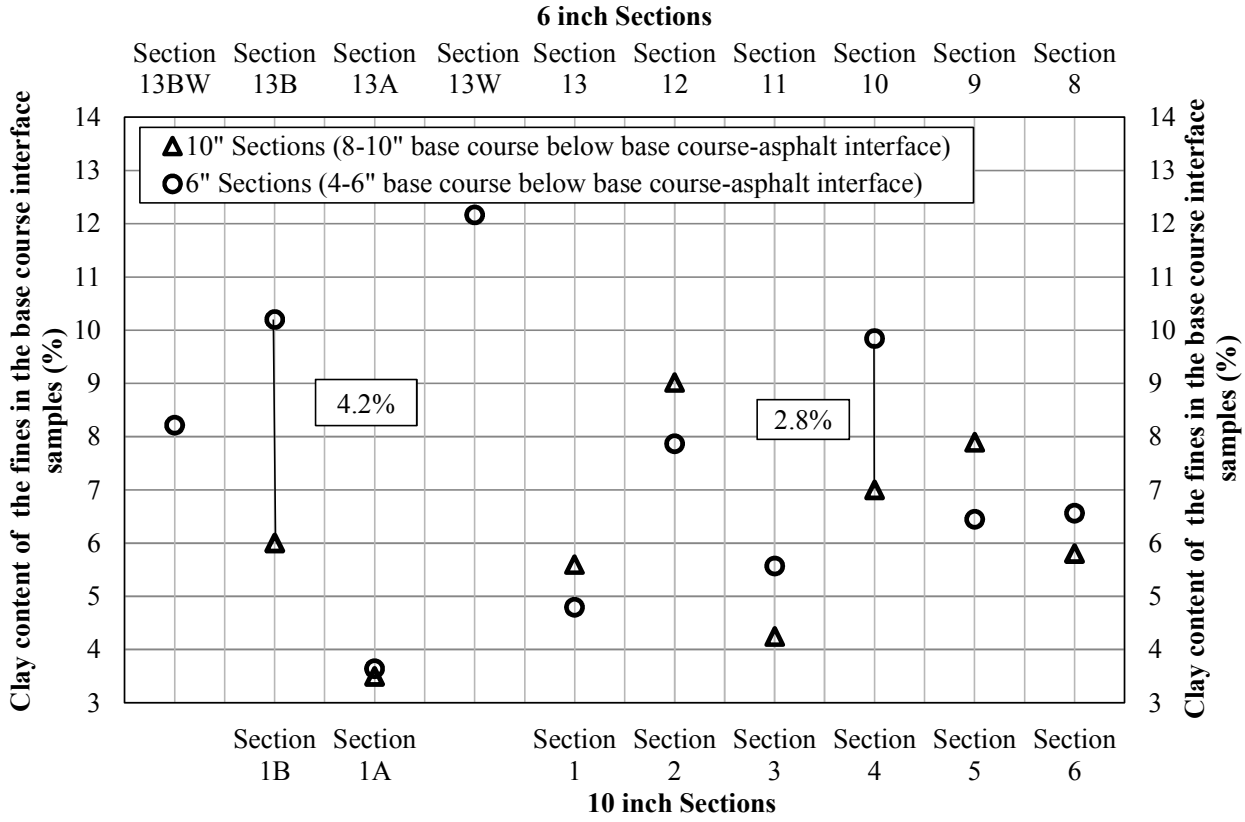

Figure 4.8. Clay content (in percent) for the base course samples obtained from the base course/subgrade interface layers for the six-inch thick sections and the ten-inch thick sections (as determined by hydrometer testing).

Table 4.3. Minimum and maximum silt and clay content of the fines in the base course samples for the six and ten-inch thick sections.

Silt Content (percent)						
Description	Min.	Section	Depth*	Max.	Section	Depth*
10 inch thick Section	87.76	Section 1B	2-4 inch	96.50	Section 1A	8-10 inch
6 inch thick Section	85.80	Section 13BW	2-4 inch	96.36	Section 13A	4-6 inch
Clay Content (percent)						
Description	Min.	Section	Depth*	Max.	Section	Depth*
10 inch thick Section	3.50	Section 1A	8-10 inch	12.24	Section 1B	2-4 inch
6 inch thick Section	3.64	Section 13A	4-6 inch	14.20	Section 13BW	2-4 inch

*Depth below asphalt/base course interface

The clay content in Section 13B is 4.2 percent higher than Section 1B, and the clay content in Section 10 is 2.84 percent higher than Section 4. As observed in Figure 4.8, the samples with the highest clay contents, within the fines in the base course, are found at the base course/subgrade interface in Sections 10, 13W, and 13B. The grain size distribution curves obtained for all 70 base course samples, as normalized relative to the fines content, and as normalized relative to the entire sample are presented in the Appendix, in Sections A.4 and A.5, respectively, for completeness.

4.2.3. Hydrometer Analysis (Subgrade)

The hydrometer testing conducted on the subgrade samples was performed in accordance with the procedures outlined in Section 3.4.1.2 to determine the silt and clay content of the entire sample. The fines content determined by wet sieving (following the procedures outlined in Section 3.4.1.1) provided the percentage of the soil sample that is classified as fines. Example results from a hydrometer test conducted on a subgrade sample obtained from Section 1B at depth of 0-2 inches below the base course/subgrade interface is presented in Figure 4.9.

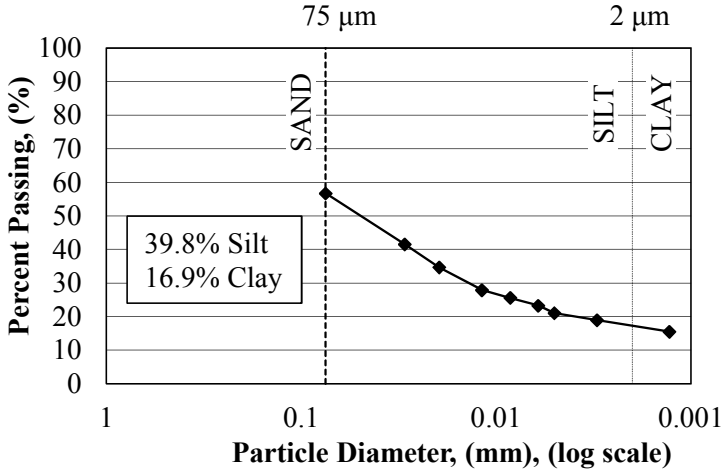

Figure 4.9. Result obtained from hydrometer testing conducted to determine the silt and clay content in the subgrade samples as obtained from Section 1B at a depth of 0-2 inches below the base course/subgrade interface.

As obtained from hydrometer testing, the silt content of the sample shown in Figure 4.9 is 39.8 percent while the clay content is 16.9 percent. Summaries of silt content and clay content of the subgrade samples from the six-inch thick and the ten-inch thick sections are presented in Tables 4.4a and 4.4b, respectively.

Table 4.4. Summary of silt and clay content for subgrade samples (normalized by weight of entire subgrade sample) for the a) six-inch thick sections and b) ten-inch thick sections.

(a)

Location	Depth* (inch)	Silt (%)	Clay (%)
Section 1B	0-2	39.8	16.9
Section 1B	2-4	37.6	15.2
Section 1B	4-6	39.0	17.5
Section 1A	0-2	37.9	18.5
Section 1A	2-4	**21.3**	**9.1**
Section 1A	4-6	36.2	17.8
Section 1	0-2	47.8	22.9
Section 1	2-4	44.2	20.3
Section 1	4-6	47.1	21.9
Section 2	0-2	44.7	23.7
Section 2	2-4	**50.2**	20.7
Section 2	4-6	45.1	23.8
Section 3	0-2	43.3	25.7
Section 3	2-4	42.0	25.7
Section 3	4-6	48.4	27.8
Section 4	0-2	44.4	25.7
Section 4	2-4	43.2	26.5
Section 4	4-6	42.2	21.7
Section 5	0-2	36.4	25.8
Section 5	2-4	33.5	25.1
Section 5	4-6	43.7	**32.0**
Section 6	0-2	41.1	25.6
Section 6	2-4	44.2	31.8
Section 6	4-6	43.0	31.6
Mean	-	41.9	24.0

*Depth below asphalt/base course interface
Bold represent the maximum and minimum values

(b)

Location	Depth* (inch)	Silt (%)	Clay (%)
Section 8	0-2	36.4	28.3
Section 8	2-4	40.5	31.1
Section 8	4-6	41.7	30.9
Section 9	0-2	39.1	24.4
Section 9	2-4	36.8	25.3
Section 9	4-6	43.7	26.0
Section 10	0-2	38.2	21.7
Section 10	2-4	47.1	24.5
Section 10	4-6	41.6	19.6
Section 11	0-2	39.7	26.6
Section 11	2-4	30.4	21.1
Section 11	4-6	45.2	33.9
Section 12	0-2	26.3	19.6
Section 12	2-4	**23.8**	17.6
Section 12	4-6	24.1	16.5
Section 13	0-2	39.0	33.4
Section 13	2-4	37.1	51.8
Section 13	4-6	36.0	51.2
Section 13W	0-2	36.0	25.3
Section 13W	2-4	37.2	30.9
Section 13W	4-6	40.7	41.5
Section 13A	0-2	**58.2**	20.0
Section 13A	2-4	28.3	**11.6**
Section 13A	4-6	35.2	**55.8**
Section 13B	0-2	32.8	27.4
Section 13B	2-4	30.8	22.8
Section 13B	4-6	29.5	19.0
Section 13BW	0-2	47.3	28.1
Section 13BW	2-4	48.2	28.7
Section 13BW	4-6	29.6	20.9
Mean	-	37.3	27.8

*Depth below base course/subgrade interface
Bold represent the maximum and minimum values

The silt content of the subgrade samples obtained from the ten-inch-thick sections and the six-inch thick sections ranged from 21.3 percent (Section 1A, 2-4 inches) to 50.2 percent (Section 2, 2-4 inches) and 23.8 percent (Section 12, 2-4 inches) to 58.2 percent (Section 13A, 0-

2 inches), respectively. The grain size distribution curves obtained for all 54 subgrade samples are presented in the Appendix, in Section A.6, for completeness.

The clay content for the ten-inch thick sections and the six-inch thick sections ranged from 9.1 percent (Section 1A, 2-4 inch) to 32.0 percent (Section 5, 4-6 inch) and 11.6 percent (Section 13A, 2-4 inch) to 55.8 percent (Section 13A, 4-6 inch), respectively. The average silt content for the ten-inch thick sections and the six-inch thick sections were 41.9 percent and 37.3 percent, respectively. The average clay content for the ten-inch thick sections and the six-inch thick sections were 24.0 percent and 27.8 percent, respectively.

The clay content as determined by hydrometer testing (normalized relative to percentage passing the No. 200 sieve - wet sieve basis) for the 18 base course samples obtained from the base course/subgrade interface layer (nominally 4-6 inches below the asphalt/base course interface for the six-inch thick sections and nominally 8-10 inches below the asphalt/base course interface for the ten-inch thick sections), and the clay content for the 18 subgrade samples as obtained from the subgrade/base course interface layer (0-2 inches below the base course/subgrade interface) are presented in Table 4.5. The differences in clay content (of the fine particles) between the subgrade and base course samples located above and below the geosynthetic at the base course/subgrade interface are presented in Figure 4.10.

Table 4.5. Clay content (in percent) determined by hydrometer testing (normalized relative to percentage passing the No. 200 sieve - wash sieve basis) for the base course samples as obtained from the base course/subgrade interface layer and clay content for the subgrade samples as obtained from the subgrade/base course interface layer.

Location	Depth*	Clay Content (B)	Depth**	Clay Content (S)	(S)-(B)
	(inch)	(%)	(inch)	(%)	(%)
Section 1B	8-10	6.00	0-2	16.91	10.91
Section 1A	8-10	3.50	0-2	18.50	15.01
Section 1	8-10	5.59	0-2	22.89	17.30
Section 2	8-10	9.02	0-2	23.68	14.67
Section 3	8-10	4.25	0-2	25.70	21.45
Section 4	8-10	7.00	0-2	25.74	18.74
Section 5	8-10	7.89	0-2	25.76	17.87
Section 6	8-10	5.80	0-2	25.60	19.80
Mean	8-10	6.13	0-2	23.10	16.97
Section 8	4-6	6.56	0-2	28.33	21.77
Section 9	4-6	6.45	0-2	24.38	17.93
Section 10	4-6	9.84	0-2	21.66	11.82
Section 11	4-6	5.57	0-2	26.64	21.07
Section 12	4-6	7.87	0-2	19.61	11.75
Section 13	4-6	4.80	0-2	33.44	28.64
Section 13W	4-6	12.16	0-2	25.29	13.13
Section 13A	4-6	3.64	0-2	19.98	16.33
Section 13B	4-6	10.20	0-2	27.36	17.16
Section 13BW	4-6	8.21	0-2	28.05	19.84
Mean	4-6	7.53	0-2	25.47	17.94

*Depth below asphalt-base course interface

**Depth below base course-subgrade interface

S = Subgrade, B = Base Course

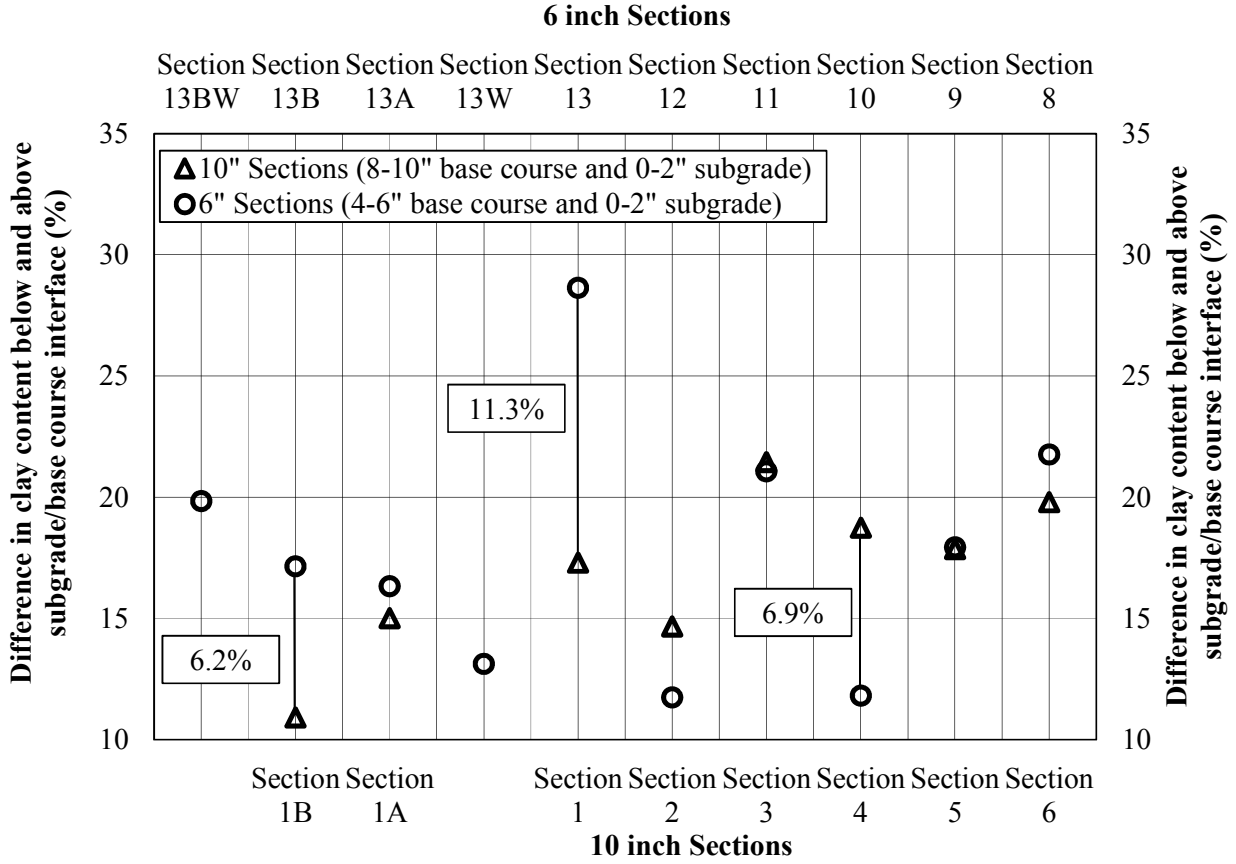

Figure 4.10. Difference in clay content of fines (in percent) between the base course and subgrade samples immediately below and above the geotextile at the base course/subgrade interface.

The comparison between six-inch thick and ten-inch thick sections reveal that the difference in the clay content (of the fine particles) is the same between the samples located above and below the subgrade/base course interface for the same geotextiles in corresponding sections containing the same fabric but different base course thicknesses. The exceptions to this observation were Sections 1B and 13B, Sections 1 and 13 and, Sections 4 and 10. The difference in clay content (of the fine particles) between Sections 1B and 13B, Sections 1 and 13, Sections 4 and 10 is 6.2 percent, 11.3 percent, 6.9 percent, respectively.

4.3. Atterberg Limits

Atterberg limits testing was performed on 54 subgrade samples in accordance with the procedures outlined in Section 3.4.1.3. The Liquid Limit (LL) and Plasticity Index (PI), as determined for all of subgrade samples by performing the Atterberg limits tests, are presented in Figure 4.11. Subgrade samples with PI and LL greater than 1.5 standard deviations from both the average PI and average LL are presented in Table 4.6.

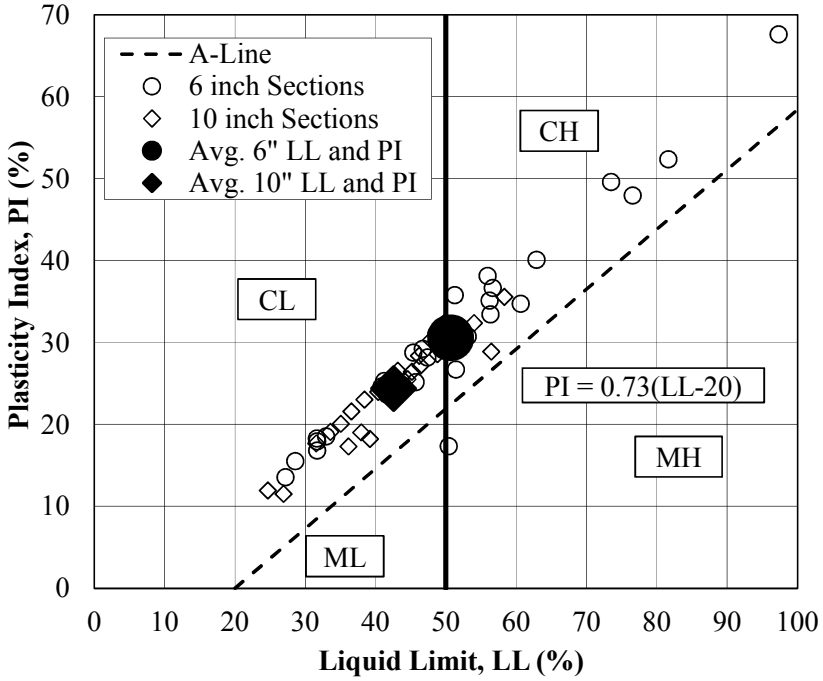

Figure 4.11. Classification of subgrade soil as per the United Soil Classification System (USCS).

Table 4.6. Subgrade samples with PI and LL greater than 1.5 standard deviations from both the average PI and average LL.

Location	Depth*	Liquid Limit, LL	Plascticity Index, PI	No. of Std. Deviations	
	(inch)	(%)	(%)	LL	PI
10 inch thick sections					
Section 6	2-4	57	36	1.8	1.7
6 inch thick sections					
Section 13	4-6	82	52	2.0	1.8
Section 13A	4-6	97	68	2.9	3.1

*Depth below base course/subgrade interface

The LL of 18 out of 54 subgrade samples obtained from the subgrade/base course interface was greater than 50, and hence the soil was classified as highly plastic clay (CH). One sample (Section 8, 0-2 inch) plotted below the A-line and has a LL greater than 50, so the sample was classified as highly plastic silt (MH). The remaining 35 subgrade samples were classified as low plasticity clay (CL) as the LL was lower than 50. The average LL in the ten-inch thick sections and six-inch thick sections were 43 and 51, respectively. The average PI in the ten-inch thick sections and six-inch thick sections were 24 and 31, respectively. The majority of the outlier samples were from the six-inch thick sections, namely Section 13 and its abutting sections. It may be deduced that the soil in these sections (surrounding Section 13) may not be the same as the rest of the six-inch thick sections or the ten-inch thick sections.

The clay content (or clay fraction, CF) obtained from hydrometer testing (as presented previously in Section 4.2.3) and the PI obtained from the Atterberg limits testing were used to calculate the activity of the subgrade samples and are presented in Figure 4.12. Subgrade samples with CF and PI values greater than 1.4 standard deviations from the mean CF and mean PI are presented in Table 4.7. The majority of the data lies between the Illite and Sodium Montmorillonite activity trend lines, bounding the Illite trend line.

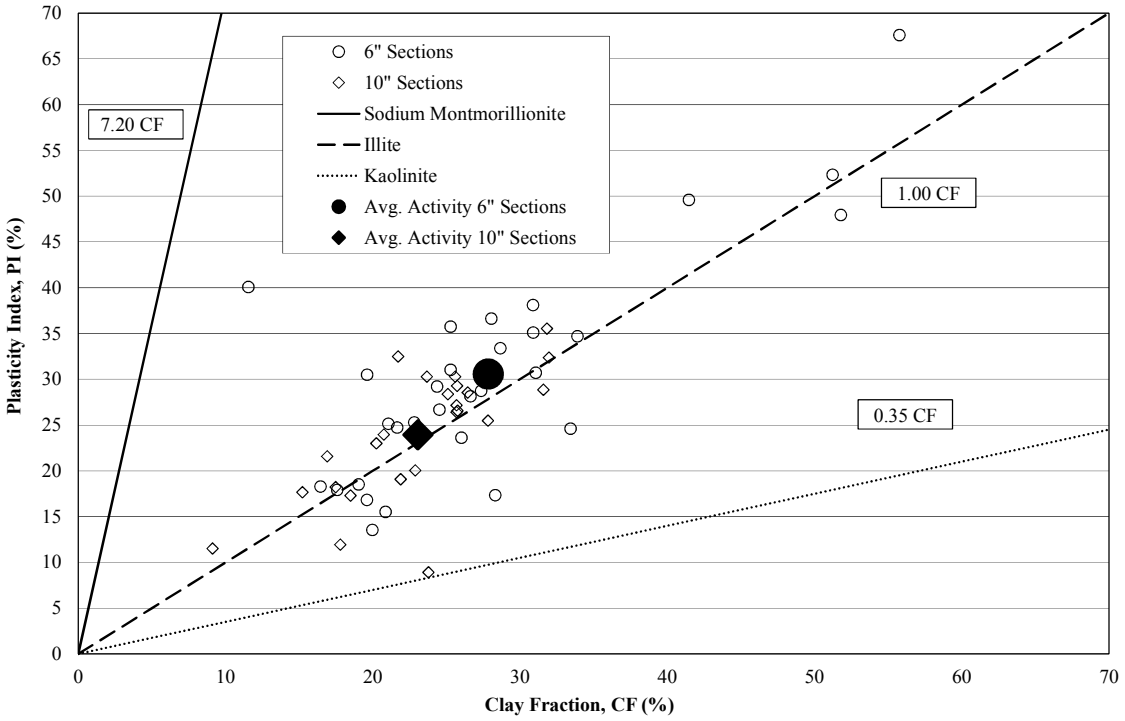

Figure 4.12. Subgrade soil mineralogy classification based on activity (Activity = Plasticity Index/Clay Content).

Table 4.7. Subgrade samples with CF and PI greater than 1.5 standard deviations from both the average CF and average PI.

Location	Depth*	Clay Fraction, CF	Plascticity Index, PI	No. of Std. Deviations	
	(inch)	(%)	(%)	CF	PI
Six inch thick sections					
Section 13A	4-6	55.78	67.60	2.68	3.04
Section 13	4-6	51.24	52.33	2.24	1.79
Ten inch thick sections					
Section 6	2-4	44.22	35.53	1.60	1.63

*Depth below base course/subgrade interface

The average CF in the ten-inch thick sections and six-inch thick sections are 23.1 percent and 27.8 percent, respectively. The average PI in the ten-inch thick sections and six-inch thick sections are 23.9 percent and 30.6 percent, respectively. More variation from the average CF and average PI was observed in samples obtained from the six-inch thick sections than from the samples obtained from the ten-inch thick sections. The samples that are 1.5 standard deviations greater than average PI and average CF are mostly from Section 13 and its abutting sections. The

only sample from the ten-inch thick sections that was 1.5 standard deviations greater than average was from Section 6 (2-4 inches). Subgrade Atterberg results for all samples are presented in the Appendix, in Section A.7, for completeness.

4.4. Specific Gravity, In-situ Gravimetric Moisture Content, and Unit Weight

A summary of the specific gravity, in-situ gravimetric moisture content, and dry unit weight values as determined for the 70 base course samples and 54 subgrade samples is presented in Table 4.8 on the next page. The specific gravity values, as obtained using ASTM D 854 (discussed previously in Section 3.4.1.4) for the subgrade and the base course samples for six-inch and ten- inch thick sections, respectively, are in close agreement (Table 4.8). The specific gravity of the base course was only measured on the fine particles and not on the whole sample. Specific gravity testing on a gradation of all particle sizes could not be completed because of the large particle sizes (requiring a very large pycnometer), and because of lack of sample. The specific gravity values, of the fines in the base course samples, ranged from 2.75 to 2.88 and from 2.73 to 2.84 for the ten-inch thick and six-inch thick sections, respectively. The specific gravity values, of subgrade samples, ranged from 2.61 to 2.80 and 2.58 to 2.73 for the ten-inch thick and six-inch thick sections, respectively. The specific gravity value obtained for the 70 base course samples and the 54 subgrade samples are presented in the Appendix, in Section A.8, for completeness.

The moisture content testing was performed in accordance with testing procedures presented in Section 3.4.1.7. The in-situ gravimetric moisture content values (dry weight basis) for the ten-inch thick sections and the six-inch thick sections ranged from 2.0 to 4.8 percent, and from 1.7 to 6.4 percent, respectively. The dry unit weight values reported in Table 4.8 (on the next page) were calculated using Equation 3.1 presented in Section 3.2.2). The total unit weight

values, as obtained by the nuclear density gauge, which were discarded due to non-rational results, are presented in Table 4.9 (on the next page). The dry unit weight values for the base course samples (as calculated using Equation 3.1) for the ten-inch thick sections and the six-inch thick sections ranged from 129 pcf to 150 pcf, and from 133 pcf to 150 pcf, respectively.

The in-situ gravimetric moisture content values (dry weight basis) for the ten-inch thick sections and the six-inch thick sections ranged from 14.2 to 25.1 percent, and from 17.2 to 41.5 percent, respectively. The dry unit weight for the subgrade samples (calculated based on Equation 3.1) for the ten-inch thick sections and the six-inch thick sections ranged from 93pcf to 113 pcf, and from 77 pcf to 104 pcf, respectively.

Table 4.8. Summary of specific gravity, moisture content, and dry unit weight for the six-inch thick and the ten-inch thick sections subgrade and base course samples.

BASE COURSE		
Property	Range of Values	Units
Specific Gravity at 20°C (six inch sections)	2.73 to 2.84	unitless
Specific Gravity at 20°C (ten inch sections)	2.75 to 2.88	unitless
Moisture Content (six inch sections)	1.7 to 6.4	percent
Moisture Content (ten inch sections)	2.0 to 4.8	percent
Dry Unit Weight (six inch sections) based on Equation 3.1	133 to 150	pcf
Dry Unit Weight (ten inch sections) based on Equation 3.1	129 to 150	pcf
SUBGRADE		
Specific Gravity at 20°C (six inch sections)	2.58 to 2.73	unitless
Specific Gravity at 20°C (ten inch sections)	2.61 to 2.80	unitless
Moisture Content (six inch sections)	17.2 to 41.5	percent
Moisture Content (ten inch sections)	14.2 to 25.1	percent
Dry Unit Weight (six inch sections) based on Equation 3.1	77 to 104	pcf
Dry Unit Weight (ten inch sections) based on Equation 3.1	93 to 113	pcf

Table 4.9. Summary of disregarded values obtained using nuclear gauge.

Sample	Location	Depth	Reason
Base Course	Section 13W	0-2 inch below asphalt/base course interface	Total density measured by nuclear gauge was 184.0 pcf which is exceptionally high for base course material.
Base Course	Section 1	0-2 inch below asphalt/base course interface	Total density measured by nuclear gauge was 189.4 pcf which is exceptionally high for base course material.
Subgrade	Section 13W	0-2 inch below base course/subgrade interface	Total density and dry density measured by nuclear gauge was 119.7 pcf and 148.3 pcf, respectively.
Subgrade	Section 13 BW	4-6 inch below base course/subgrade interface	Total density measured by nuclear gauge was 123.2 pcf which is exceptionally high for subgrade material.

The average moisture content is higher in the base course and subgrade samples of the six-inch thick sections (3.4 percent, 23.6 percent)as compared to the average moisture content of the base course and subgrade samples of ten-inch thick sections (3.2 percent, 20.3 percent), respectively. The in-situ gravimetric moisture content profiles, dry density profiles (based on the results obtained using Equation 3.1), and dry density profiles (based on results obtained using nuclear gauge) with depth for the six-inch thick sections are presented in Figures 4.13, 4.14, and 4.15, respectively. The individual gravimetric moisture content profiles, dry density profiles (based on the results obtained using Equation 3.1), and dry density profiles (based on results obtained using the nuclear gauge) with depth for each of the 18 sections are presented in the Appendix, in Sections B.1, B.2, and B.3, respectively, for completeness.

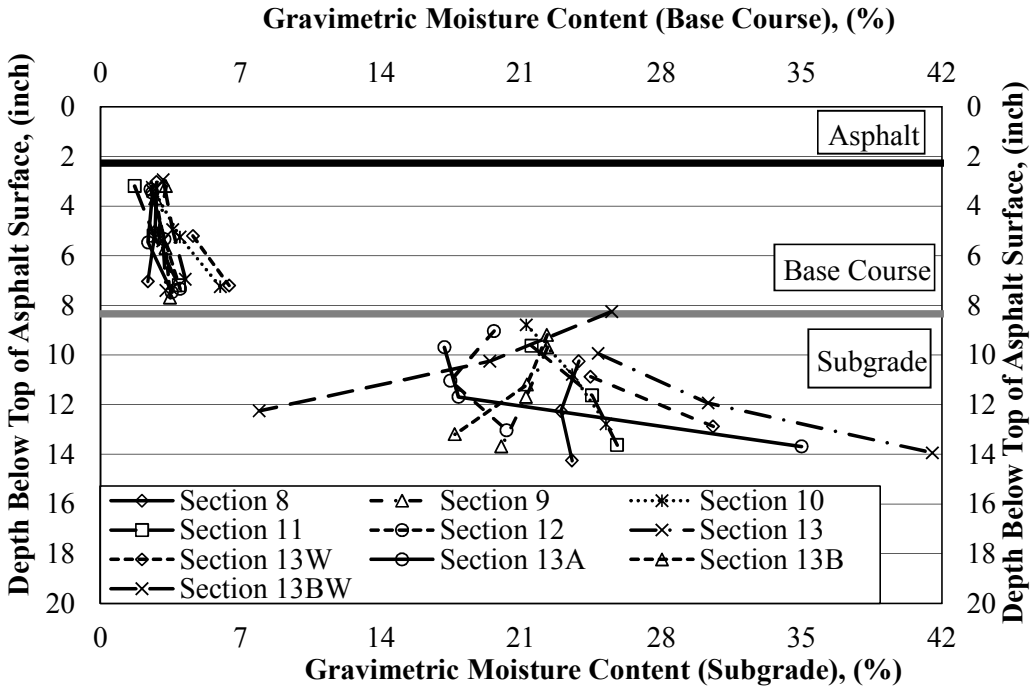

Figure 4.13. In-situ gravimetric moisture content profiles for six-inch thick sections.

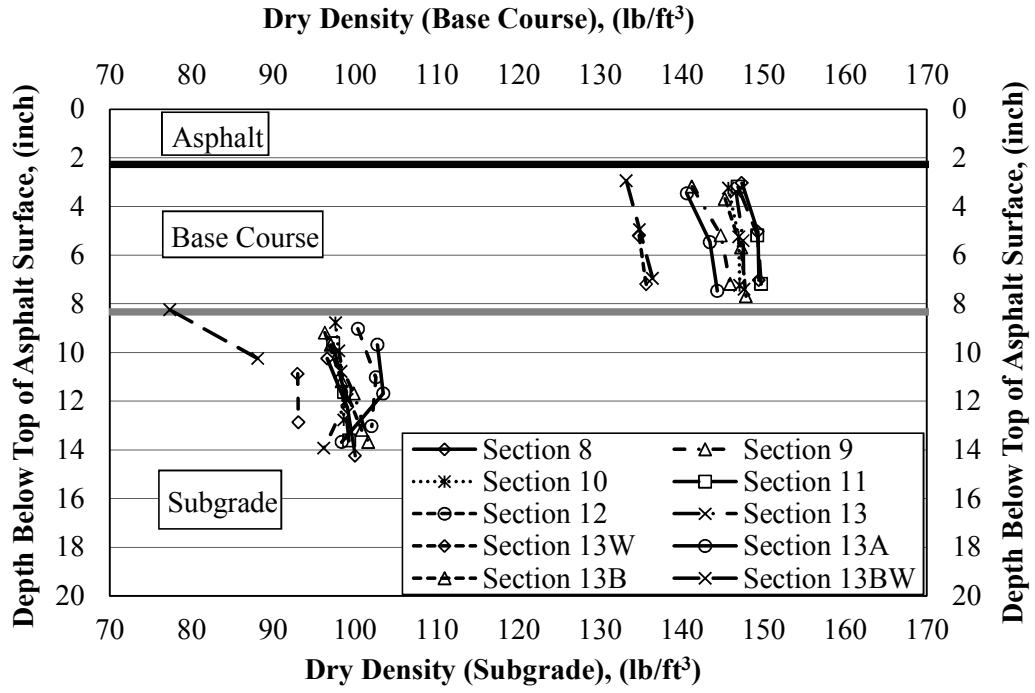

Figure 4.14. Dry density profiles (as calculated using Equation 3.1) for the six-inch thick sections.

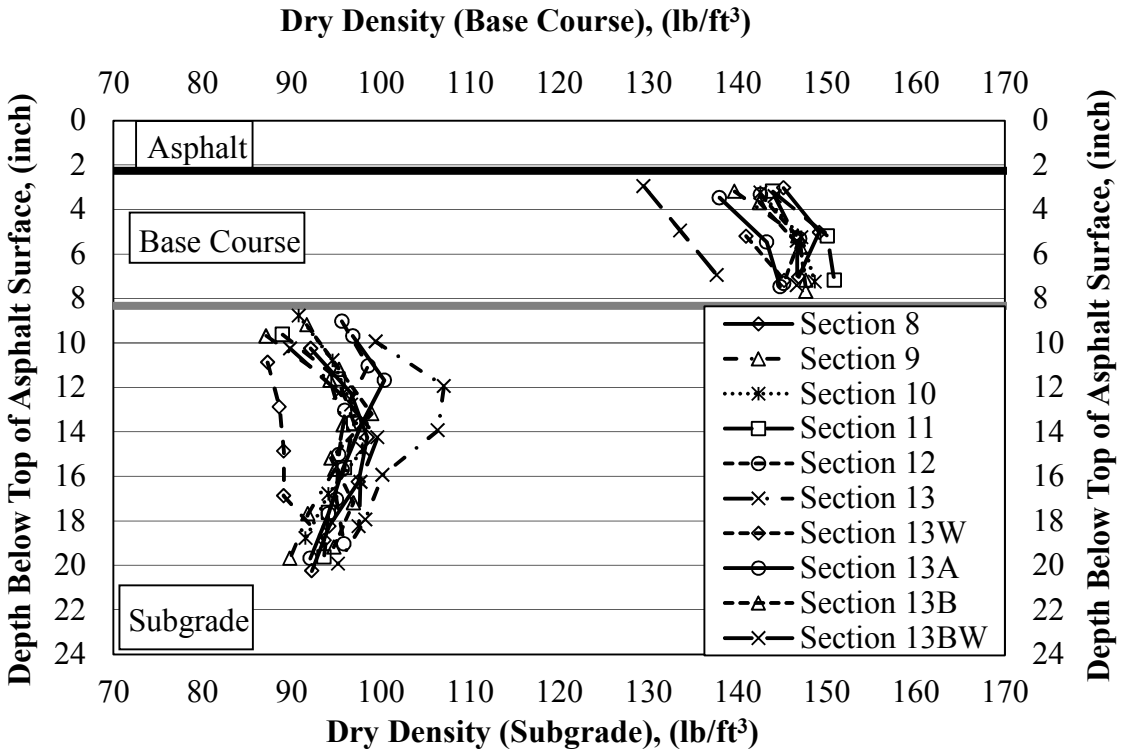

Figure 4.15. Dry density profiles (based on nuclear gauge) for the six-inch thick sections.

The base course gravimetric moisture content in the six-inch thick sections ranged from 1.7 percent (Section 11 0-2 inches) to 4.2 percent (Section 13BW 4-6 inches). Sections 10 (6.0 percent) and 13W (6.4 percent) at a depth of 4-6 inches below the asphalt/base course interface were outliers from the range presented in the previous sentence. During exhumation of Section 13W lateral seepage was observed at the base course/subgrade interface which might have led to the increased moisture content in the base course sample at the base course/subgrade interface within Section 13W. This lateral seepage is discussed in further detain in Section 4.12.

The subgrade moisture content values as determined for samples obtained from Section 13W were the highest as compared to the subgrade moisture content values for all other sections at comparable depths. The subgrade moisture content for Section 13BW reduced from 25.5 percent to 8.0 percent over a depth of six inches. The 8.0 percent moisture content value at the

depth of 4-6 inches below the base course/subgrade interface is in agreement with the field observations obtained by excavating a trench across the Westbound lane in Section 13BW. As discussed in Section 4.12, a change in visible subgrade properties at a depth of approximately six inches below the base course/subgrade interface was observed while excavating the trench. Based on visual-manual classification techniques, the soil also appeared to contain higher silt content at a depth of six inches below the base course/subgrade interface. The subgrade moisture content of Section 13A increased from 17.9 percent (at a depth of 2-4 inches below the base course/subgrade interface) to 35.0 percent (at a depth of 4-6 inches below the base course/subgrade interface). The rapid increase of moisture content with depth over a small sampling interval may not be an accurate representation of the actual in-situ moisture content.

The dry unit weight values for the base course in the six-inch thick sections ranges between 133pcf (Section 13BW, 0-2 inches) and 150pcf (Section 8, 4-6 inches), as calculated using Equation 3.1. The dry unit weight for Section 13BW (as calculated using Equation 3.1) ranged from 133pcf to 136pcf. The dry unit weight for Section 13BW was relatively lower than the other six-inch thick sections where the range was 141pcf to 150 pcf. These low unit weights may have contributed to failure within this section.

The dry unit weight of the subgrade (as calculated using Equation 3.1) as calculated for the six-inch thick sections ranged between 77pcf (Section 13BW 0-2 inches) to 104pcf (Section 13A 2-4 inches). The dry unit weight for Section 13BW increased from 77pcf to 88 pcf. The minimum dry unit weight for the subgrade samples (Section 13BW, 0-2 inch) was due to the in-situ gravimetric moisture content of 25.5 percent and a total unit weight (obtained using a nuclear gauge) of 97 pcf. The dry unit weights in Section 13BW was relatively lower than the

remaining six-inch thick sections that ranged between 96pcf and 103 pcf. These low unit weights may have contributed to failure of the pavement system in this section.

The dry unit weight of the base course (as directly obtained using a nuclear gauge) in the six-inch thick sections ranged between 138pcf (Section 13A 0-2 inches) to 154pcf (Section 13W 4-6 inches), except for Section 13BW. The dry unit weight values (as obtained directly using a nuclear gauge) for the base course in Section 13BW (130pcf to 138 lb/ft^3) were the lowest dry density values for all the six-inch thick sections. Although these dry unit weight values are incorrect, because of incorrect moisture contents, a trend of the dry unit weight values being the lowest in Section 13BW is observed. Again, these low dry unit weight values may have contributed to failure of the pavement system in Section 13BW (as discussed in Section 4.14).

The in-situ gravimetric moisture content profiles, dry density profiles (based on the results obtained using Equation 3.1), and dry density profiles (based on results obtained directly from the nuclear gauge) with depth, for the ten-inch thick sections are presented in Figures 4.16, 4.17, and 4.18, respectively.

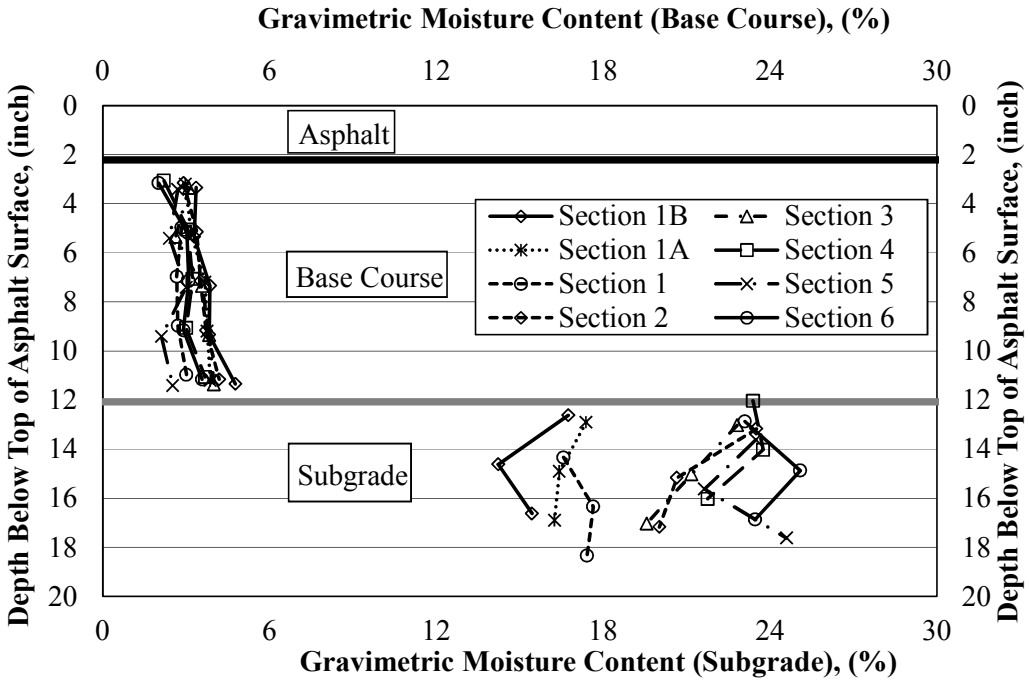

Figure 4.16. In-situ gravimetric moisture content profiles for the ten-inch thick sections.

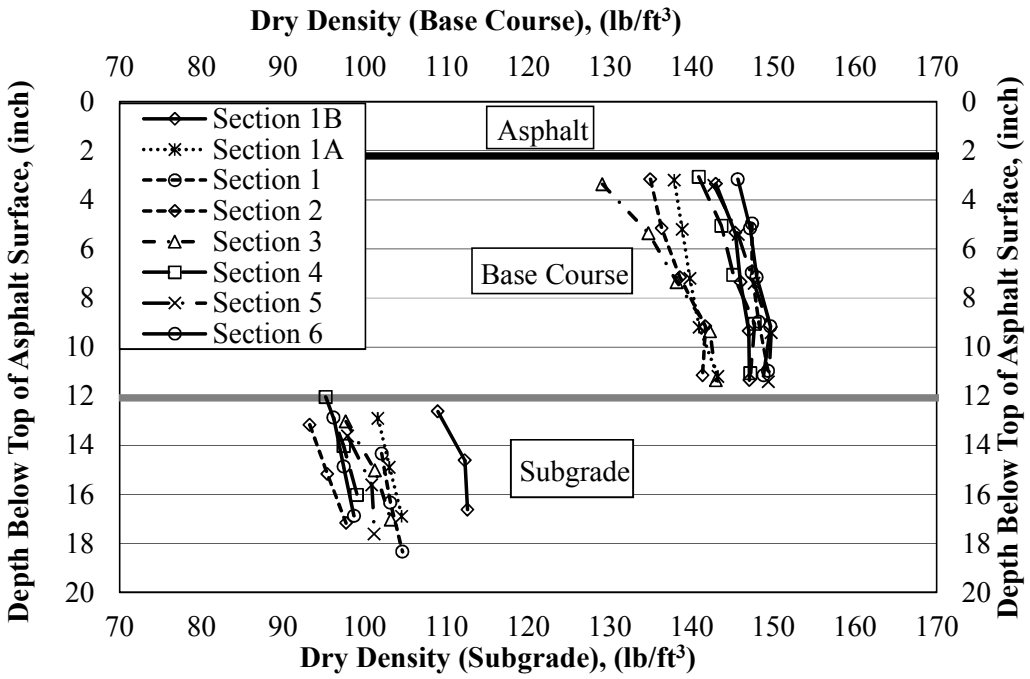

Figure 4.17. Dry density profile (as obtained using Equation 3.1) for the ten-inch thick sections.

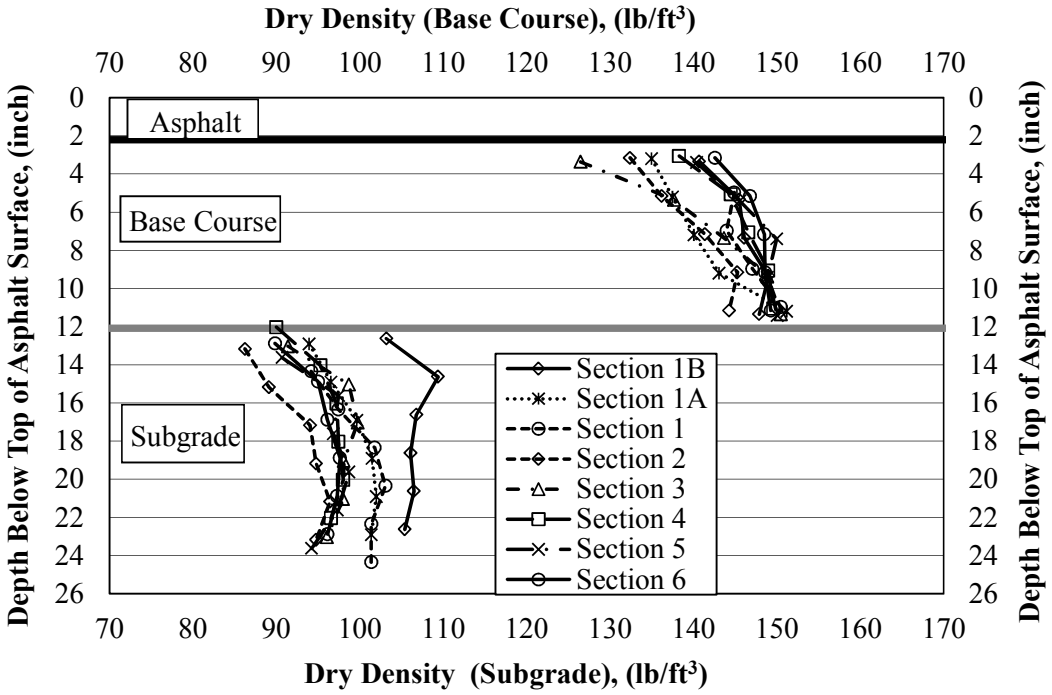

Figure 4.18. Dry density profile (based on nuclear gauge) for ten-inch thick sections.

The gravimetric moisture contents values of the base course samples in the ten-inch thick sections ranged between 2.0 percent (Section 6, 0-2 inches) and 4.8 percent (Section 1B, 8-10 inches). Consistent moisture content with depth was observed in each of the individual sections, and variations among the sections were not substantial. The subgrade gravimetric moisture content in the ten-inch thick sections ranged between 14.2 percent (Section 1B, 2-4 inches) to 25.1 percent (Section 6, 2-4 inches). Lower moisture content values were observed in Sections 1, 1A, and 1B. The reduction in moisture content may be attributed to the super elevation and higher vertical alignment in Frontage Road 3 at Section 1B) which provides gravity drainage for water to flow to the low spots (Section 6). The vertical alignment of the top of asphalt, top of base course and top of subgrade are presented in Section 4.13.

The dry unit weight values (as calculated using Equation 3.1) for the base course intervals in the ten-inch thick sections ranged between 129pcf (Section 3, 0-2 inches) to 150pcf

(Section 5, 6-8 inches). The dry unit weight (as calculated using Equation 3.1) for the subgrade in the ten-inch thick sections ranged between 93pcf (Section 2 0-2 inches) to 113pcf (Section 1B 4-6 inches). The dry unit weight (calculated based on Equation 3.1) of Section 1B ranged between 109pcf to 113pcf which was relatively higher than the remaining sections where the dry unit weight ranged from 93pcf to 105pcf.

The dry unit weight base course (as directly obtained using a nuclear gauge) in the ten-inch thick sections ranged between 132pcf (Section 2, 0-2 inches) to 151pcf (Section 1A, 8-10 inches). Section 3 from 0-2 inches below the asphalt/base course interface was an exception, as the dry unit weight (127pcf) was lower for this interval. The subgrade dry unit weight (as directly obtained using a nuclear gauge) in the ten-inch thick sections ranged between 86pcf (Section 2 0-2 inches) to 103pcf (Section 1 6-8 inches). An outlier was Section 1B, starting at 103pcf (0-2 inches),increasing to 109pcf (2-4 inches,) and decreased to 105pcf (8-10 inches). The higher dry unit weights values obtained in Section 1B (as directly obtained using a nuclear gauge)may have led to better performance this section (as discussed in Section 14.4).. Typically, an increase in dry unit weight (as directly obtained using a nuclear density gauge) with respect to depth was observed in base course and subgrade layers for the six-inch thick and the ten-inch thick sections.

4.5. Modified Proctor

As obtained from laboratory testing (as described previously in Section 3.4.1.5), the dry unit weights for the ten-inch thick sections ranged from 141pcf to 156pcf over a range in moisture content between 2.3 percent to 8.7 percent (gravimetric basis). The dry unit weight for the six-inch sections ranged from 144pcf to 155pcf over a range in moisture content between 1.7 percent and 8.4 percent (gravimetric basis). These laboratory obtained dry unit weights values

were within the ranges obtained in the field, for the respective ten-inch thick and six-inch thick sections, as obtained using the nuclear density gauge and gravimetric moisture content (Equation 3.1), assuming that the samples were compacted at 95 percent of maximum dry density (as obtained using modified energy). As discussed in the previous section, the dry unit weight (as calculated using Equation 3.1) for the ten-inch thick sections and the six-inch thick sections ranged from 129pcf to 150 lb/ft^3, and 133pcf to 150 lb/ft^3, respectively. The corresponding water contents obtaining in the field ranged from 2.0 to 4.8 percent for the ten-inch thick sections and from 1.7 percent to 6.4 percent for the six-inch thick sections. The maximum dry density and optimum moisture content obtained from the modified proctor testing ranged from 151pcf to 155pcf and 2.4 percent to 5.8 percent for the six-inch thick sections and from 146pcf to 156pcf and 2.8 percent to 6.7 percent for the ten-inch thick sections, respectively. A summary of maximum dry density and optimum moisture content values (obtained from the modified proctor testing), the previously reported dry unit weight values (as obtained in the field and calculated using Equation 3.1), and in-situ gravimetric moisture content values (from field obtained samples) are presented in Table 4.10 along with the relative compaction. The maximum dry unit weights (obtained from modified proctor testing) and the dry unit weights calculated using Equation 3.1 for the six-inch thick and ten-inch thick sections is presented in Figure 4.19 on page 153.

Table 4.10. Summary of maximum dry density and optimum moisture content (obtained from modified proctor testing), in-situ dry unit weight (calculated using Equation 3.1), and in-situ gravimetric moisture content.

Location	Depth*	Max. Dry Unit Weight	Optimum Moisture Content	Dry Unit Weight Based on Equation 3.1	Gravimetric Moisture Content	Relative Compaction
	(in)	(lb/ft^3)	(%)	(lb/ft^3)	(%)	(%)
Section 1B	8-10	152.5	5.25	147.1	4.77	96.44
Section 1A	8-10	148.2	5.77	143.2	3.87	96.68
Section 1	8-10	145.8	6.71	156.4	3.01	107.25
Section 2	8-10	147.7	6.35	141.4	4.19	95.71
Section 3[1]	8-10	155.6	2.84	143.0	4.00	91.92
Section 4[1]	8-10	156.5	2.97	147.2	3.68	94.08
Section 5	8-10	146.1	4.54	149.4	2.52	102.28
Section 6[1]	8-10	151.9	2.88	148.8	3.57	97.98
Section 8	4-6	153.1	4.82	149.5	2.37	97.64
Section 9[1]	4-6	154.1	2.36	146.0	3.75	94.70
Section 10	4-6	154.4	5.19	147.1	5.98	95.28
Section 11	4-6	152.8	5.80	149.7	3.91	98.02
Section 12[1]	4-6	154.7	2.95	146.6	3.97	94.81
Section 13	4-6	152.2	4.85	147.6	3.27	96.99
Section 13W	4-6	151.3	4.90	147.4	6.42	97.41
Section 13A	4-6	151.0	5.19	144.4	3.56	95.60
Section 13B	4-6	153.8	4.92	147.9	3.48	96.12
Section 13BW	4-6	153.0	5.82	136.4	4.24	89.17

*Depth below asphalt/base course interface

[1]Highest value used for max. dry unit weight

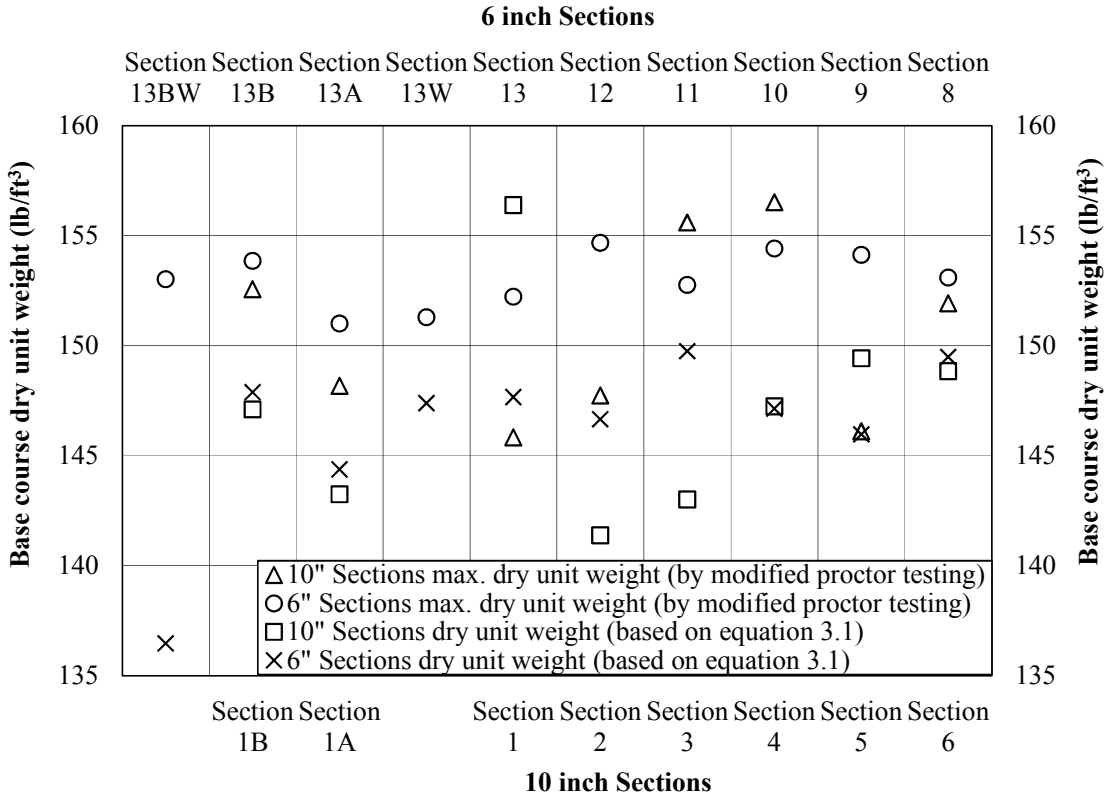

Figure 4.19. Maximum dry unit weight (based on modified proctor testing) and dry unit weight (calculated using Equation 3.1) for the six-inch thick and ten-inch thick sections.

Optimum moisture content values obtained from modified proctor testing and gravimetric moisture content values obtained from the geotechnical investigation are compared for the six-inch thick and the ten-inch thick sections in Figure 4.20. The optimum moisture content values, determined by proctor testing, for the base course samples in the ten-inch thick sections, as recovered from 8-10 inches below the asphalt/base course interface, were higher in five (out of eight sections) than the in-situ gravimetric moisture content values. Conversely, the optimum moisture content values, determined by proctor testing, for the base course samples in the six-inch thick sections, as recovered from 4-6 inches below the asphalt/base course interface, were lower in four (out of ten sections) than the in-situ gravimetric moisture content values.

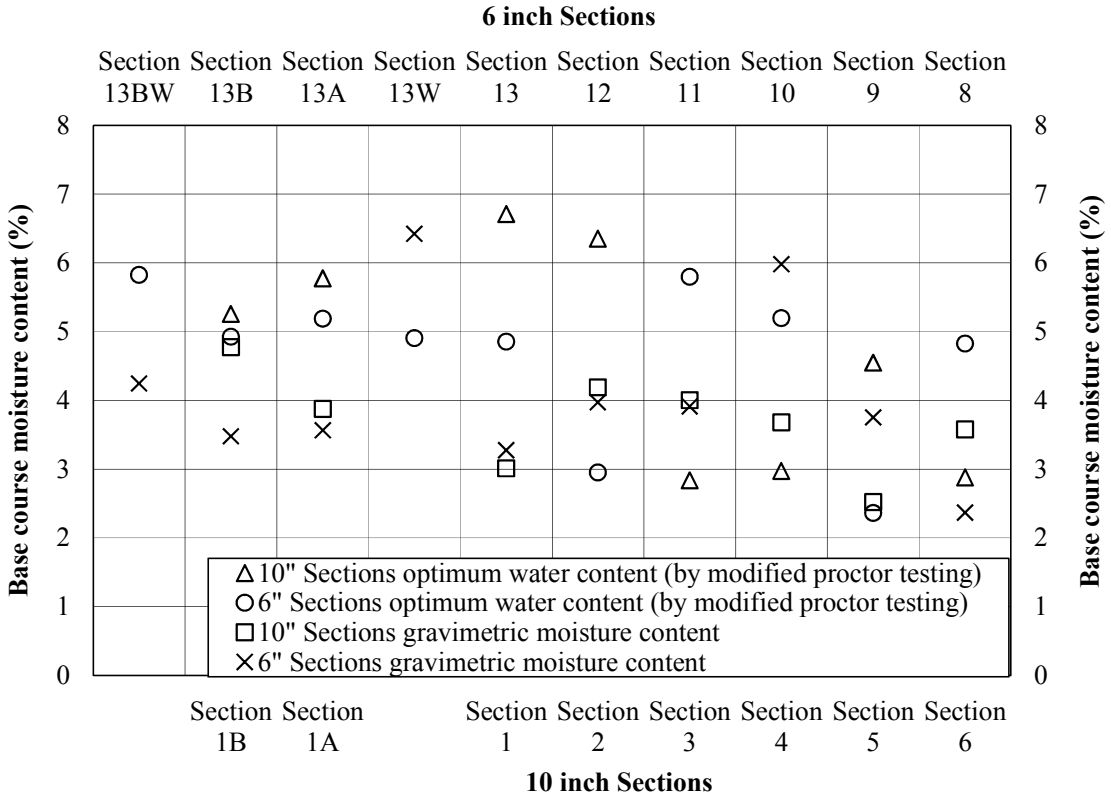

Figure 4.20. Optimum moisture content (based on modified proctor testing) and gravimetric moisture content for the six-inch thick and ten-inch thick sections.

Most of the proctor curves plotted above the zero air voids line because the zero air voids line was based on the measured specific gravity of the fines (as discussed in the previous section) rather than the specific gravity of the whole sample. Values of negative air volume were obtained from phase diagrams completed for samples (on which modified proctor testing was conducted). Negative air volume values are not possible, and were caused by using the specific gravity of the fines instead of the specific gravity of the whole sample.

Typical proctor curves obtained for a ten-inch thick section and six-inch thick section are presented in Figure 4.21. A traditional bell shaped curve was not observed for several of the proctor curves. For these curves there are small differences in the dry densities between each of the points, and the maximum dry density and optimum water content were selected as the highest

dry density value and the molding water content that corresponded with the dry density. A second order polynomial was used to determine the maximum dry density and optimum water content for the curves that did mimic a bell shaper curve. Although several of the curves were misshapen, the proctor testing was not recompleted because of lack of sample. The proctor curves obtained for the 18 base course samples obtained from the base course/subgrade interface are presented in the Appendix, in Section A.9, for completeness.

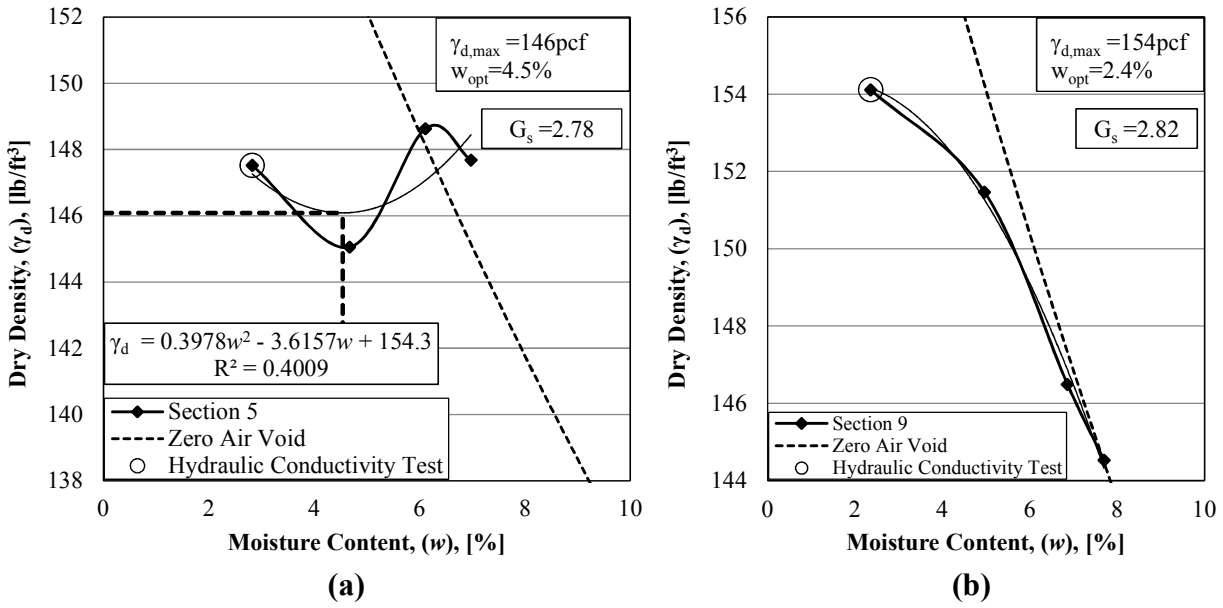

Figure 4.21. a) Proctor curve for Section 5 (ten-inch thick section), and b) Proctor curve for Section 9 (six-inch thick section).

4.6. Comparison of Index Properties with Past Research

The index properties of the base course and subgrade materials as obtained by Howard (2006), Brooks (2009), and the current research project are compared in this section. The maximum dry unit weight values for the base course, as reported by Howard (2006), ranged from 142pcf to 144pcf (as obtained from modified proctor testing) for an optimum water content of 6.5 percent to 8.2 percent, respectively. According to Howard (2006), the in-situ dry unit weight values obtained using a nuclear gauge ranged from 149pcf to 150pcf. It is uncommon for the in-

situ dry density values to be higher than the maximum dry density values as obtained in the field. The maximum dry unit weight for base course determined in conjunction with the MBTC-3020 project (hereinafter referred to as the current study) and reported in this report (as obtained from modified proctor testing) ranged from 145pcf to 155pcf for optimum water content values ranging from 4.5 percent to 6.9 percent, respectively. The in-situ dry unit weight values obtained in the current study ranged from 129 pcf to 150 pcf. The differences in the dry unit weight values and optimum moisture content values reported by Howard (2006) and current research are not significant even though the results reported in Howard (2006) are peculiar. However, the in-situ values reported in the current study are in fact lower than the values reported by Howard (2006). The specific gravity, Atterberg limits, and fines content for the subgrade soil obtained via laboratory testing associated with this project were compared with values reported by Brooks (2009), as presented in Table 4.11.

Table 4.11. Comparison of subgrade index properties obtained by laboratory testing with the values reported by Brooks (2009).

Property	Ten inch thick sections		Six inch thick sections		Units
	Range of Values		Range of Values		
	Brooks (2009)	Current Study	Brooks (2009)	Current Study	
Specific Gravity	2.68 to 2.72	2.61 to 2.80	2.67 to 2.71	2.58 to 2.73	unitless
Liquid Limits (LL)	63 to 67	25 to 58	49 to 73	27 to 97	percent
Plastic Limits (PL)	17 to 20	13 to 28	14 to 20	13 to 33	percent
Plasticity Index (PI)	41 to 47	11 to 36	35 to 54	14 to 68	percent
Passing No. 200	83 to 90	30 to 76	67 to 88	40 to 91	percent

Brooks (2009) reported conducting specific gravity test on bulk samples recovered from site (auger cuttings from unknown depths) while the current study had approximately 600 grams of exhumed samples out of which only the fines particle were utilized to conduct the specific gravity testing. As per Brooks (2009), the depth of sample acquisition was from 2.5 feet to deep to 12.5 feet deep and from 3.5 feet to 13.5 feet deep in the ten-inch thick and six-inch thick sections, respectively. The samples exhumed in the current study were obtained from the base

course/subgrade interface to a depth of six-inches. These factors may have caused the discrepancy in specific gravity values in the subgrade samples. Similarly the Atterberg testing was conducted using the dry method of preparation, on bulk samples acquired from the depths mentioned above (Brooks, 2009). The current research had limited sample which was acquired from shallow depths of subgrade and the testing was conducted utilizing the wet method of preparation. These factors may be responsible for the discrepancy in fines content and Atterberg limits.

4.7. Hydraulic Conductivity (Laboratory)

The hydraulic conductivity of the 18 base course samples was obtained from the base course/subgrade interface was measured using a Mariotte Bottle (MB), for 16 samples, or a Flexible Wall Permeameter (FWP), for 2 samples, (in accordance with the procedures outlined in Section 3.4.1.6). A summary of average hydraulic conductivity (as obtained from laboratory measurements) of the base course samples obtained from the base course/subgrade interface for the ten-inch thick sections is presented in Table 4.12. A graphical representations of the data provided in Table 4.12 is presented in Figure 4.22.

Table 4.12. Summary of average hydraulic conductivity (ft/day) of base course samples at the base course/subgrade interface for the ten-inch thick sections as obtained from laboratory measurements (MB and FWP*).

Section	Depth**	Hydraulic Gradient	Avg. Hydraulic Conductivity	Hydraulic Gradient	Avg. Hydraulic Conductivity	Hydraulic Gradient	Avg. Hydraulic Conductivity	Dry Density	Measured Molding Moisture Content	Gravimetric Moisture Content	Fines Content (after permeability testing)
		(i)	(k_{avg})	(i)	(k_{avg})	(i)	(k_{avg})	(γ_d)	(w)	(w)	(P_{200})
	(inch)	(unitless)	(ft/day)	(unitless)	(ft/day)	(unitless)	(ft/day)	(lb/ft^3)	(%)	(%)	(%)
Section 1B	8-10	0.5	229.69	1.0	71.24	2.1	123.53	154	4.9	4.8	3.9
Section 1A*	8-10	7.5*	0.01	7.5*	0.01	7.5*	0.01	145	3.0	3.9	4.3
Section 1	8-10	0.5	129.49	1.0	136.88	2.1	117.08	150	2.3	3.0	3.8
Section 2	8-10	0.5	506.12	1.0	302.81	2.1	138.17	146	5.1	4.2	4.3
Section 3	8-10	0.5	7.52	1.0	16.63	2.1	15.11	156	2.8	4.0	4.0
Section 4	8-10	0.5	56.98	1.0	48.64	2.1	49.09	156	3.0	3.7	3.6
Section 5	8-10	0.5	93.28	1.0	101.30	2.1	88.41	148	2.8	2.5	3.5
Section 6	8-10	0.5	35.72	1.0	30.19	2.1	24.28	152	2.9	3.6	3.3

*Hydraulic Conductivity obtained using flexible wall permeameter, therefore gradients are higher than obtained using the Mariotte Bottle
** Depth below asphalt/base course interface

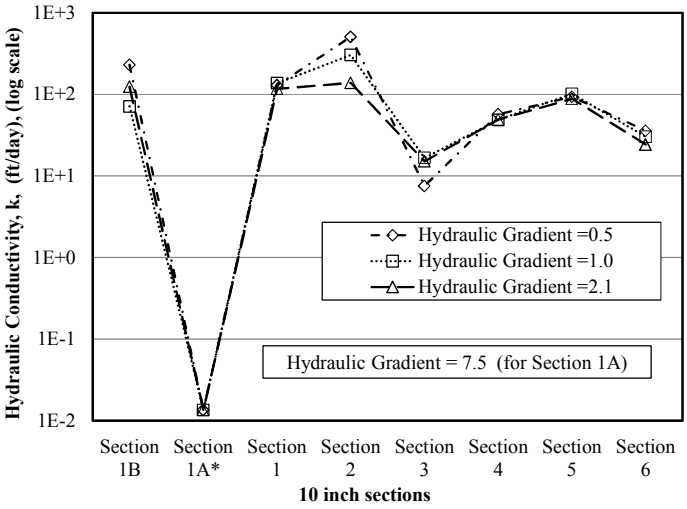

Figure 4.22. The average hydraulic conductivity (ft/day) of base course samples at the base course/subgrade interface for the ten-inch thick sections as obtained from laboratory measurements (MB and FWP*).

The effective stress at half height of the sample in the MB ranged from 0.3 psi to 0.9 psi for hydraulic gradients of 0.5 to 4.3, respectively, compared to the 3.5 psi effective stress (at half height of the sample) in FWP. The fines in Section 1A may have clogged the porous stone in the FWP which may have caused low flow and resulted in the lower measured average hydraulic conductivity value of 0.01 ft/day. Also the applied effective stress in the FWP (3.6 psi) was higher than the applied effective stress in the MB (0.3 psi to 0.9 psi) which may have resulted in lower hydraulic conductivity values for the base course sample obtained from Section 1A. The average base course hydraulic conductivity (averaged over three hydraulic gradients) obtained using MB for the ten-inch thick sections range from 13.1 ft/day (Section 3) to 315.7 ft/day (Section 2). The difference in in-situ gravimetric moisture content as compared to measured molding water content ranged from 0.1 percent (Section 1B) to 1.2 percent (Section 3). The difference can be attributed to sample size and material preparation procedures. The sample size for gravimetric moisture content was approximately 400 grams compared to approximately 100 grams of sample utilized to determine the molding water content.

A summary of average hydraulic conductivity (as obtained from laboratory measurements) of the base course samples obtained from the base course/subgrade interface for the six-inch thick sections is presented in Table 4.13. A graphical representations of the data provided in Table 4.10 is presented in Figure 4.23.

Table 4.13. Summary of average hydraulic conductivity (ft/day) of base course samples at the base course/subgrade interface for the six-inch thick sections as obtained from laboratory measurements (MB and FWP*).

Section	Depth**	Hydraulic Gradient	Avg. Hydraulic Conductivity	Hydraulic Gradient	Avg. Hydraulic Conductivity	Hydraulic Gradient	Avg. Hydraulic Conductivity	Dry Density	Measured Molding Moisture Content	Gravimetric Moisture Content	Fines Content (after permeability testing)
		(i)	(k_{avg})	(i)	(k_{avg})	(i)	(k_{avg})	(γ_d)	(w)	(w)	(P_{200})
	(inch)	(unitless)	(ft/day)	(unitless)	(ft/day)	(unitless)	(ft/day)	(lb/ft^3)	(%)	(%)	(%)
Section 8	4-6	0.5	69.01	1.0	59.09	2.1	54.11	151	3.3	2.4	3.8
Section 9	4-6	0.5	13.61	1.0	21.19	2.1	21.17	154	2.4	3.7	3.4
Section 10	4-6	3.1*	0.30	3.6*	0.25	4.3*	0.82	155	4.5	6.0	3.8
Section 11	4-6	0.5	23.45	1.0	16.49	2.1	15.84	153	5.7	3.9	3.7
Section 12	4-6	3.1*	0.83	3.6*	0.74	4.3*	1.38	155	2.9	4.0	3.4
Section 13	4-6	0.5	46.90	1.0	54.17	2.1	54.70	146	1.7	3.3	3.1
Section 13W*	4-6	7.3*	0.10	7.3*	0.10	7.3*	0.10	153	5.5	6.4	4.0
Section 13A	4-6	0.5	12.51	1.0	22.15	2.1	54.70	146	3.3	3.6	3.3
Section 13B	4-6	0.5	1.91	1.0	5.41	2.1	11.40	151	3.2	3.5	2.7
Section 13BW	4-6	0.5	84.02	1.0	156.32	2.1	111.56	150	4.3	4.2	3.2

*Hydraulic Conductivity obtained using flexible wall permeameter, therefore gradients are higher than obtained using the Mariotte Bottle

** Depth below asphalt/base course interface

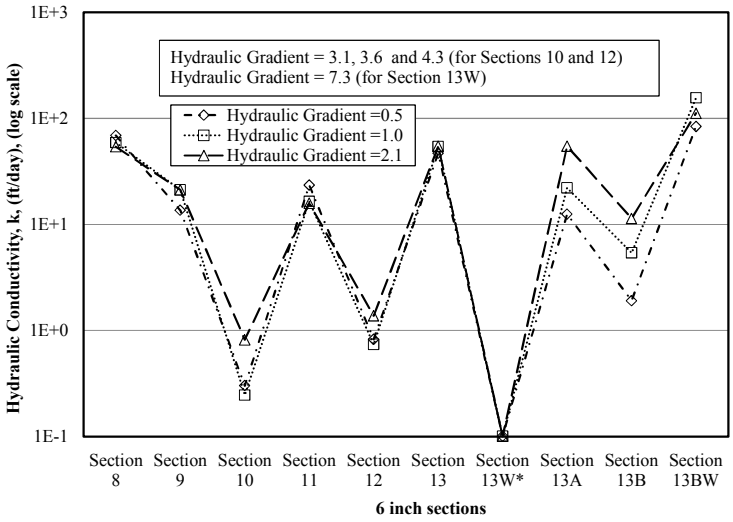

Figure 4.23. The average hydraulic conductivity (ft/day) of base course samples at the base course/subgrade interface for the six-inch thick sections as obtained from laboratory measurements (MB and FWP*).

The average base course hydraulic conductivity (averaged over three hydraulic gradients) obtained using MB for the six-inch thick sections range from 0.5 ft/day (Section 10) to 117.3 ft/day (Section 13BW). The difference in gravimetric moisture content as compared to measured molding water content ranged from 0.1 percent (Section 13BW) to 1.8 percent (Section 11). The difference can be attributed to sample size and material preparation procedures. The sample size for gravimetric moisture content was approximately 400 grams compared to approximately 100 grams of sample utilized to determine the molding water content.

The laboratory measured hydraulic conductivity and the fines content (obtained by dry sieving after permeability testing) are presented in Figures 4.24 and 4.25, for the ten-inch thick and six-inch thick sections, respectively. No correlation was observed between the laboratory measured hydraulic conductivity and the fines content (obtained by dry sieving after permeability testing). Lawrence (2006) reported hydraulic conductivity decreased by one order of magnitude for one percent increase in fines content between six percent and ten percent.

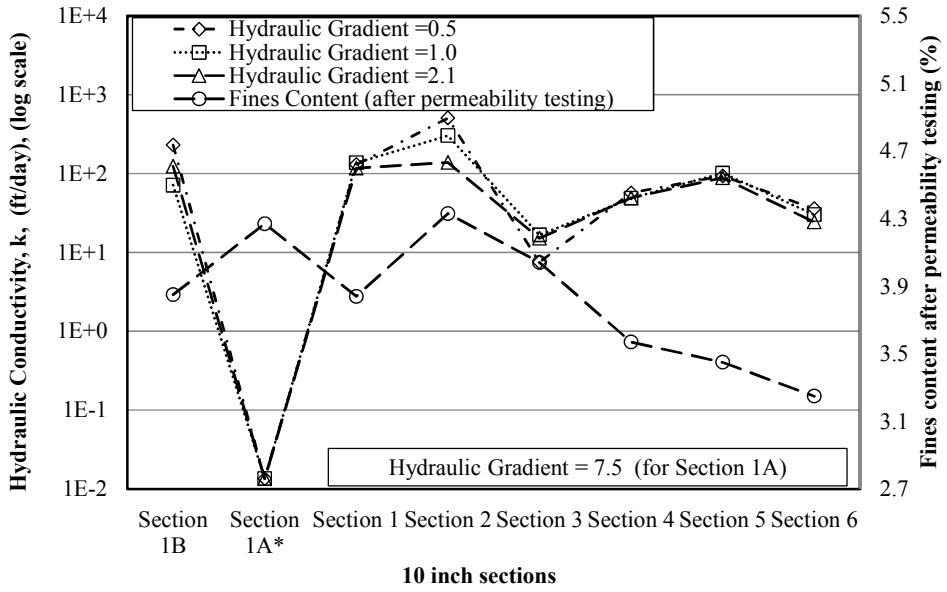

Figure 4.24. Comparison between the average hydraulic conductivity (ft/day) and fines content (percent) after permeability testing of base course samples at the base course/subgrade interface for the ten-inch thick sections.

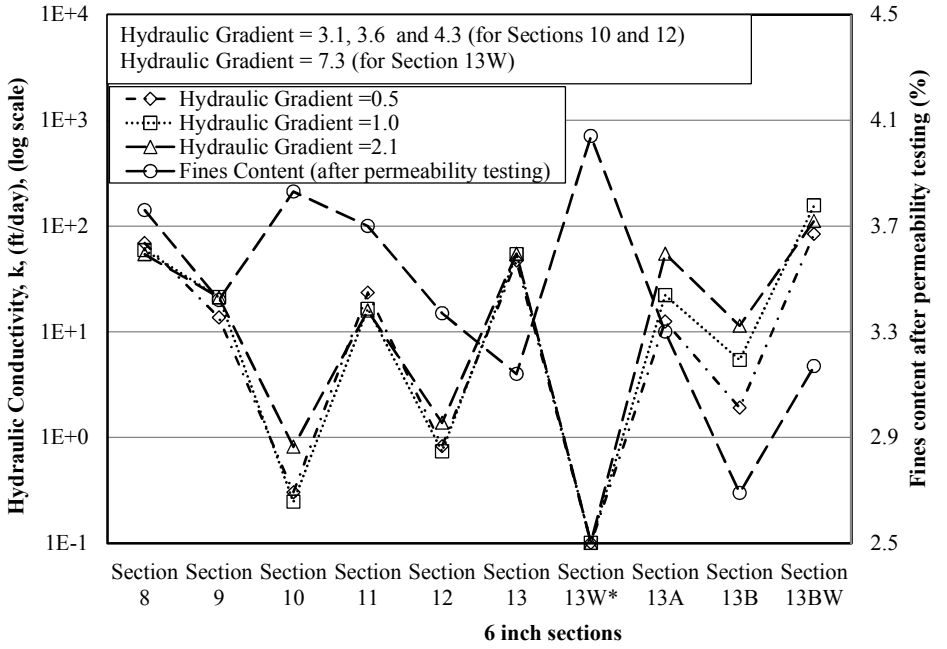

Figure 4.25. Comparison between the average hydraulic conductivity (ft/day) and fines content (percent) after permeability testing of base course samples at the base course/subgrade interface for the six-inch thick sections.

As reported by Cedergren (1994), for base course (in the pavement system) to be freely draining a minimum hydraulic conductivity of 10,000 ft/day (3.5 cm/sec) is required. The laboratory measured hydraulic conductivity did not satisfy the requirement to be classified as freely draining base course. The laboratory measured hydraulic conductivity is two to four orders of magnitude lower than the criteria reported by Cedergren (1994). The laboratory measured hydraulic conductivity results for the base course samples are presented in the Appendix, in Section A.10, for completeness.

4.8. Hydraulic Conductivity (In-situ)

A summary of average apparent hydraulic conductivity is presented in Table 4.14. The average in-situ apparent hydraulic conductivity obtained in October for the ten-inch thick sections ranged between 2.76E-03 ft/day (Section 1B) and 1.50E-01 ft/day (Section 4). The average in-situ apparent hydraulic conductivity obtained in May for the ten-inch thick sections ranged between 1 ft/day (Section 2) and 8.17 E-02 ft/day (Section 4). As reported by Cedergren (1994), for base course (in pavement systems) to be freely draining a minimum hydraulic conductivity of 10,000 ft/day is required. Based on this requirement, and based on the values measured in the field, the base course cannot be categorized as a freely draining base course. The hydraulic conductivity results, as measured in the field, for the base course samples are presented in the Appendix, in Section B.4, for completeness.

Table 4.14. Summary of average apparent hydraulic conductivity (ft/day) obtained using the Two Stage Borehole method (ASTM D6391) in October 2010 and May 2011.

LOCATION	October 2010		May 2011
	Test 1	Test 2	
	(ft/day)	(ft/day)	(ft/day)
Section 1B	2.76E-03	2.75E-03	2.11E-01
Section 1	2.23E-02	2.14E-02	1.84E-01
Section 2	3.47E-02	1.92E-02	1.00E+00
Section 3	2.34E-02	2.44E-02	1.38E-01
Section 4	2.07E-01	1.50E-01	8.17E-02
Section 10	1.49E-01	-	8.47E-02
Section 11	1.11E-01	-	1.25E-01
Section 12	1.81E-01	-	2.53E-01
Section 13	4.98E-03	-	1.72E-02
Section 13B	1.06E-01	-	6.13E-04

4.9. Hydraulic Conductivity (empirical prediction and comparison)

Summary tables containing the estimated hydraulic conductivity based on the Hazen (1930), Sherard et al. (1984), and Moulton (1980) equations (previously presented in Section 3.4.1.8) for the ten-inch thick sections and the six-inch sections are presented in Tables 4.15 and 4.16, respectively. The graphical representations of the data provided in Tables 4.15 and 4.16 along with the laboratory obtained hydraulic conductivity and in-situ measured apparent hydraulic conductivity are presented for comparison purposes in Figures 4.26 and 4.27, respectively.

Table 4.15. Summary of estimated hydraulic conductivity of the ten-inch thick sections using Hazen (1930), Sherard et al. (1984) and Moulton (1980) equations.

Location	Depth*	Hazen (k)	Hazen (k)	Sherard (k)	Sherard (k)	Moulton (k)
	(inch)	(cm/s)	(ft/day)	(cm/s)	(ft/day)	(ft/day)
Section 1B	8-10	0.61	1726	0.77	2183	0.08
Section 1A	8-10	0.37	1047	0.34	966	1.48
Section 1	8-10	0.71	2000	0.97	2752	0.56
Section 2	8-10	1.20	3406	2.01	5710	2.14
Section 3	8-10	0.43	1210	0.55	1556	0.06
Section 4	8-10	0.96	2729	1.50	4257	0.10
Section 5	8-10	0.98	2782	1.53	4325	1.47
Section 6	8-10	1.32	3749	2.00	5660	0.84

* Depth below asphalt/base course interface

Table 4.16. Summary of estimated hydraulic conductivity of the six-inch thick sections using Hazen (1930), Sherard et al. (1984) and Moulton (1980) equations.

Section	Depth*	Hazen (k)	Hazen (k)	Sherard (k)	Sherard (k)	Moulton (k)
	(inch)	(cm/s)	(ft/day)	(cm/s)	(ft/day)	(ft/day)
Section 8	4-6	0.65	1830	0.88	2485	0.55
Section 9	4-6	1.18	3348	1.59	4504	0.53
Section 10	4-6	1.57	4441	1.96	5555	0.28
Section 11	4-6	0.71	1999	1.05	2986	0.20
Section 12	4-6	1.23	3486	1.82	5162	0.26
Section 13	4-6	0.56	1590	0.97	2753	2.14
Section 13W	4-6	0.31	891	0.86	2433	0.20
Section 13A	4-6	0.51	1447	0.69	1963	2.27
Section 13B	4-6	1.14	3219	1.56	4422	0.84
Section 13BW	4-6	5.26	14904	3.68	10428	1.39

* Depth below asphalt/base course interface

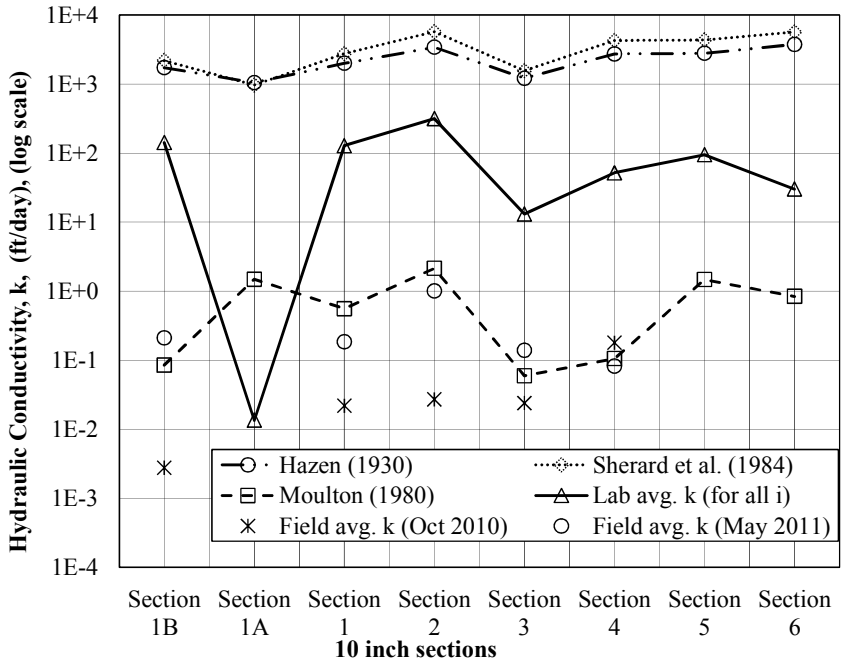

Figure 4.26. Estimated hydraulic conductivity, laboratory obtained average hydraulic conductivity (k) for interface base course sample, and in-situ average apparent hydraulic conductivity (Stage 1) for the ten-inch thick sections.

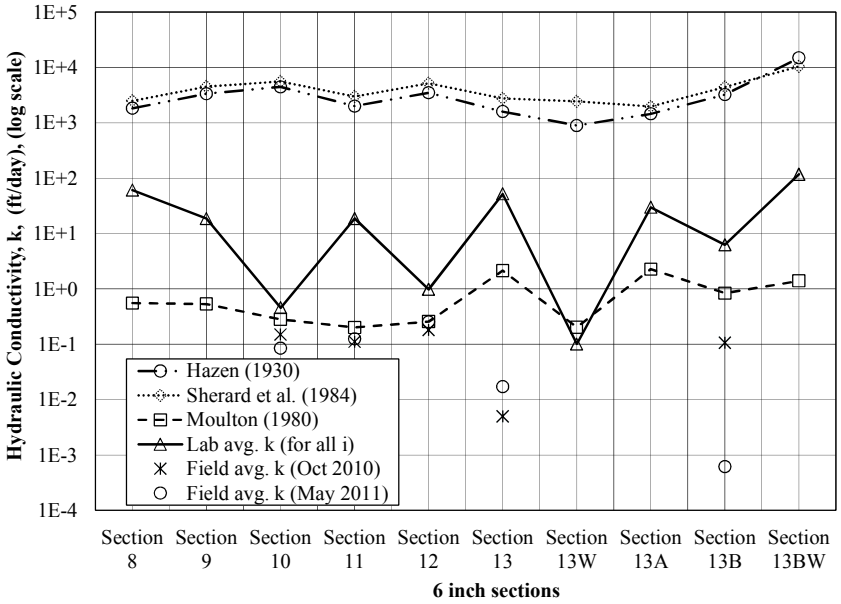

Figure 4.27. Estimated hydraulic conductivity, laboratory obtained average hydraulic conductivity (k) for interface base course sample, and in-situ average apparent hydraulic conductivity (Stage 1) for the six-inch thick sections.

It was observed that hydraulic conductivity predicted based on the Moulton (1980) equation was three to four orders of magnitude lower than the hydraulic conductivity predicted based on the Sherard et al. (1984) and Hazen (1930) equations even though all of the equations are correlated to grain size data. The laboratory obtained average hydraulic conductivity (k) values for all hydraulic gradients (i) does not align with any of the estimated values except for Sections 10, 12, and 13W; sections in which distress was observed (as discussed in Section 4.14). The hydraulic conductivity values for these sections are in close agreement with the estimates obtained using the Moulton (1980) prediction.

On average, the hydraulic conductivity measured in the laboratory was two and three orders of magnitude higher than the values obtained using the Moulton (1980) estimation for the six-inch thick and the ten-inch thick sections, respectively, except for Section 1A which was two orders of magnitude lower than Moulton (1980) prediction. The average laboratory hydraulic conductivity was one to three orders of magnitude lower than values obtained using the Sherard et al. (1984) and Hazen (1930) equation. This was expected as the values obtained from Hazen (1930) and Sherard et al. (1984) are intended to be used for clean sand and are not applicable for this application. The equation presented by Moulton (1980) has been shown to work for base course (Blanco, 2003), so the comparable results between the values obtained from the Moulton (1980) equation and the laboratory measured data were expected.

The measured in-situ apparent hydraulic conductivity in May 2011 was observed to be higher than the hydraulic conductivity measured in October 2010 except for Sections 4, 10, and 13B, which are all sections in which distress was observed (Section 4.14). The hydraulic conductivity measured in these sections in October 2010 was insignificantly higher than the hydraulic conductivity measured in May 2011 (0.065 to 0.105 ft/day). The lower in-situ

hydraulic conductivity in October 2010 may be attributed to unsaturated subgrade conditions. The measured in-situ hydraulic conductivity in May 2011 was in close agreement with the values obtained from the Moulton (1980) estimation except for Sections 13 and 13B, both of which are sections in which distress was observed (Section 4.14).

The hydraulic conductivity values determined in field are validated by the estimation obtained using the Moulton (1980) equation. The control sections (without geotextiles) exhibited similar in-situ hydraulic conductivity when compared to sections with geotextiles. The addition of geotextiles in these sections does not appear to impact the hydraulic conductivity of the base course. Based on the vertical hydraulic conductivity values obtained at the Marked Tree Test Section, the addition of geotextiles did not increase or decrease the hydraulic conductivity of the base course (as compared with the control sections).

4.10. Transmissivity and Permittivity of Geotextiles

The transmissivity and permittivity testing for new and exhumed geotextile sample were performed in accordance with the procedures outlined in Section 3.4.2.1 and 3.4.2.2, respectively. The results obtained from the transmissivity and permittivity testing as performed on exhumed geotextile samples and new geotextile samples are presented in Sections 4.10.1 and 4.10.2, respectively. The results obtained from permittivity testing (as discussed in Section 4.10.2) are utilized in Section 4.11 when reviewing the geotextile design criteria.

4.10.1. Transmissivity of Geotextiles

A summary table with the laboratory obtained transmissivity values is presented (Table 4.17). A graphical representation of the data tabulated in Table 4.17 is also presented graphically in Figure 4.28.

Table 4.17. Summary of geotextiles transmissivity values obtained from laboratory measurement and fines content obtained by dry sieving conducted in November 2010.

Section	Description of exhumed samples	New Description	Transmissivity (θ)	Fines Content (Dry Sieving November 2010)
			(m^2/s)	(percent)
Six inch sections				
Section 10	Amoco Propex 4553	Propex Geotex 801	4.48E-05	1.67
Section 11	Amoco Propex 2006	Propex Geotex 315ST	3.43E-05	1.53
Section 12	Amoco Propex 2044	Propex 4x4	1.30E-04	1.38
Section 13B	Mirafi HP 570	Mirafi HP 570	1.25E-04	1.30
Section 13W	Carthage Mill FX 66	Carthage Mill FX 66	8.02E-05	3.10
Section 13BW	Carthage Mill FX 66	Carthage Mill FX 66	9.43E-05	1.41
Ten inch sections				
Section 1B	Mirafi HP 570	Mirafi HP 570	2.00E-04	1.71
Section 2	Amoco Propex 2044	Propex 4x4	7.53E-05	2.39
Section 3	Amoco Propex 2006	Propex Geotex 315ST	3.47E-05	2.30
Section 4	Amoco Propex 4553	Propex Geotex 801	5.33E-05	1.50
Tested in University of Arkansas Laboratory				
New Samples	Amoco Propex 4553	Propex Geotex 801	2.95E-05	-
	Amoco Propex 2006	Propex Geotex 315ST	4.63E-05	-
	Amoco Propex 2044	Propex 4x4	7.30E-05	-
	Mirafi HP 570	Mirafi HP 570	1.37E-04	-
	Carthage Mill FX 66	Carthage Mill FX 66	1.41E-04	-

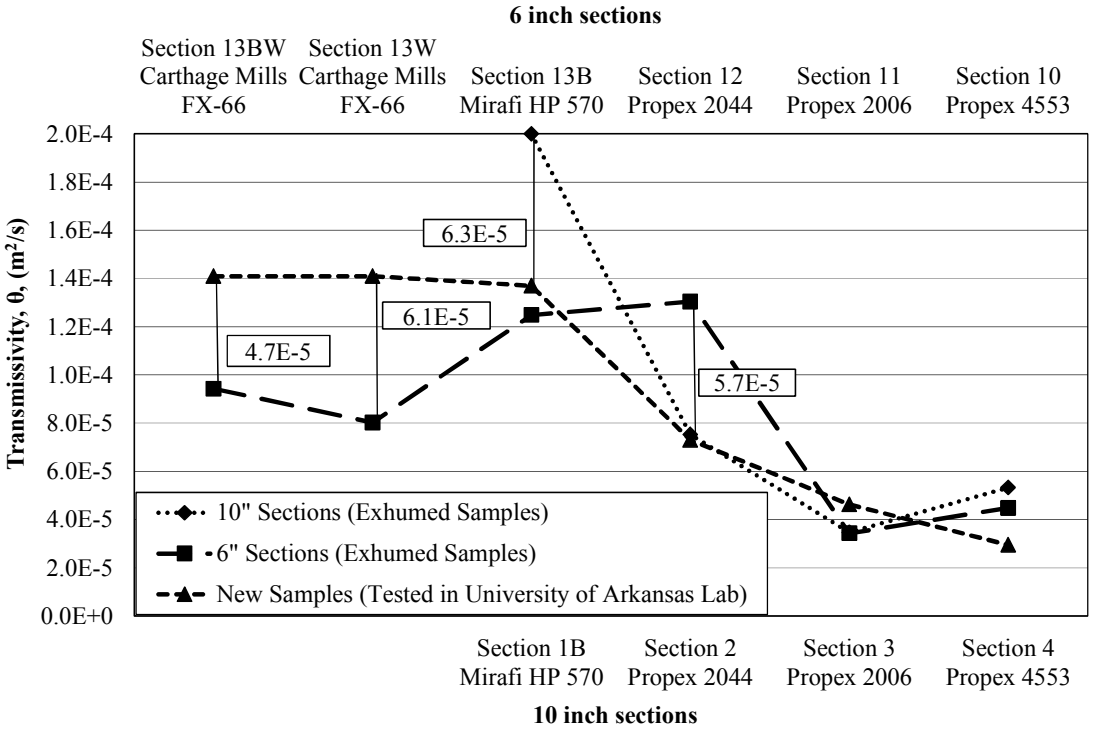

Figure 4.28. Transmissivity values of exhumed and new geotextile samples obtained from laboratory measurement.

The transmissivity values of exhumed samples for the six-inch thick sections as compared to the ten-inch thick sections are in close agreement except for Mirafi HP570 and Propex 2044. The transmissivity of exhumed samples ranged from 3.4E-5 m^2/s in Section 11 (Propex 2006) to 2.0E-4 m^2/s in Section 1B (Mirafi HP 570). The transmissivity value measured for the Propex 2044 sample obtained from Section 12 is 5.7E-5 m^2/s higher than the new sample and higher than the transmissivity values obtained for the same type of geosynthetic obtained from the corresponding ten-inch thick section (Section 2). The transmissivity value for Mirafi HP 570 (Section 1B) was 6.3E-5 5 m^2/s higher than the new sample. The higher transmissivity value in the exhumed samples as compared to the new samples may indicate that the exhumed sample was damaged during exhumation or may be due to larger aperture opening size (AOS) from being in service for 5 years. The transmissivity value of Mirafi HP 570 (Section 13B) and the new sample are in close agreement. As discussed in Section 4.11 the geotextiles utilized in this study did not meet the AOS requirement (AOS $\leq$0.3mm) except for Propex 4553. The transmissivity value of new Carthage Mills FX-66 sample were 4.7E-5 m^2/s and 6.1 E-05 m^2/s higher than the exhumed (Carthage Mills FX-66) samples in Sections 13W and 13BW, respectively. As will be discussed in Section 4.11, the Carthage Mills FX-66 geotextile does not meet the AOS criteria, soil retention criteria, and permittivity requirement and hence lower transmissivity values are expected, and were observed for exhumed samples (Sections 13W and 13BW), as compared to new samples. Graphs of transmissivity values for the ten exhumed geotextile samples and five new geotextile samples (as tested in UofA laboratory) are presented in the Appendix, in Section A.11, for completeness.

4.10.2. Permittivity of Geotextiles

A summary of permittivity values obtained in the laboratory is presented in Table 4.18. A graphical representation of the data tabulated in Table 4.18 is also presented in Figure 4.29 for clarity.

Table 4.18. Summary of geotextiles permittivity values obtained from laboratory measurement and fines content obtained by dry sieving conducted in November 2010.

Section	Description of exhumed samples	New Description	Permittivity (ψ)	Fines Content (Dry Sieving November 2010)
			(s^{-1})	(percent)
Six inch Sections				
Section 10	Amoco Propex 4553	Propex Geotex 801	0.18	1.67
Section 11	Amoco Propex 2006	Propex Geotex 315ST	0.07	1.53
Section 12	Amoco Propex 2044	Propex 4x4	0.16	1.38
Section 13B	Mirafi HP 570	Mirafi HP 570	0.31	1.30
Section 13W	Carthage Mills FX 66	Carthage Mills FX 66	0.07	3.10
Section 13BW	Carthage Mills FX 66	Carthage Mills FX 66	0.12	1.41
Ten inch Sections				
Section 1B	Mirafi HP 570	Mirafi HP 570	0.20	1.71
Section 2	Amoco Propex 2044	Propex 4x4	0.08	2.39
Section 3	Amoco Propex 2006	Propex Geotex 315ST	0.05	2.30
Section 4	Amoco Propex 4553	Propex Geotex 801	0.32	1.50
Tested at University of Arkansas Laboratory				
New Samples	Amoco Propex 4553	Propex Geotex 801	0.32	-
	Amoco Propex 2006	Propex Geotex 315ST	0.12	-
	Amoco Propex 2044	Propex 4x4	0.13	-
	Mirafi HP 570	Mirafi HP 570	0.27	-
	Carthage Mills FX 66	Carthage Mills FX 66	0.05	-
Manufacturer's Data	Amoco Propex 2006	Propex Geotex 315ST	0.05	-
	Amoco Propex 2044	Propex 4x4	0.15	-
	Amoco Propex 4553	Propex Geotex 801	1.50	-
	Mirafi HP 570	Mirafi HP 570	0.40	-
	Carthage Mills FX 66	Carthage Mills FX 66	0.05	-

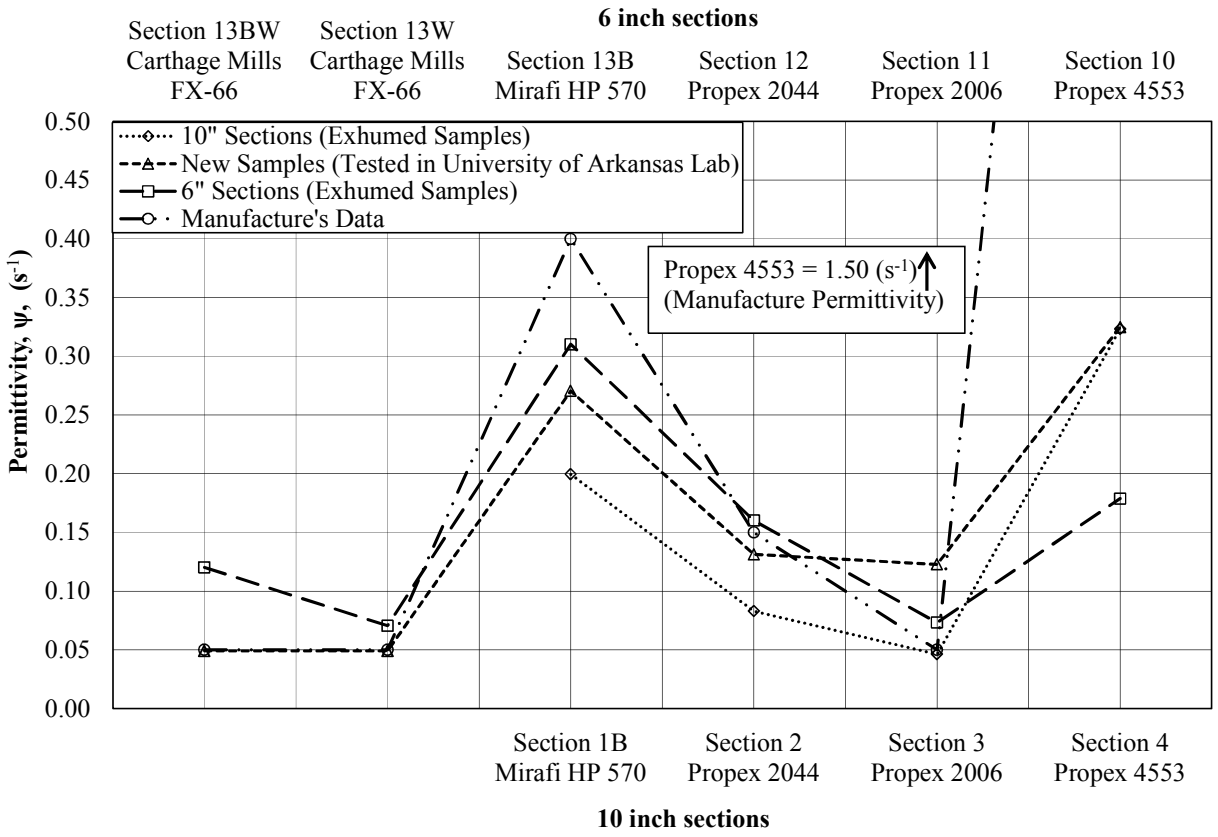

Figure 4.29. Permittivity values of exhumed and new geotextile samples obtained from laboratory measurement.

The permittivity values for the exhumed samples measured in laboratory ranged from 0.07 s^{-1} (Section 11, Propex 2006) to 0.31 s^{-1} (Section 13B, Mirafi HP 570) for the six-inch thick sections, and ranged from 0.05 s^{-1} (Section 3, Propex 2006) to 0.32 s^{-1} (Section 4, Propex 4553) for the ten-inch thick sections. The permittivity values obtained in the laboratory for the exhumed and new samples are in close agreement. As discussed in the next section, the permittivity and the clogging requirement were fulfilled for all of the geotextile products installed in the ten-inch thick and six-inch thick sections, but the sections did not meet the Aperture Opening Size (AOS $\leq$0.3mm) criteria, except for the Propex 4553 product.

The permittivity of the exhumed geotextile samples in the ten-inch thick sections was lower than the permittivity of exhumed geotextile samples in the six-inch thick section except in

Section 4 (Propex 4553). The permittivity of the Propex 4553 geotextile (Section 4) was higher than the corresponding exhumed sample in Section 10 by 0.14 s^{-1} but was in close agreement with the new sample. The permittivity values published by the manufacture were in accordance with the new samples tested in the laboratory except for the Propex 4553 sample. The permittivity value (for Propex 4553) published by the manufacturer was 4.62 times higher than the permittivity value for a new sample as obtained in the UofA laboratory. The sample tested in the laboratory may not be a representative sample and hence additional testing may be required to ascertain the cause of the discrepancy. Graphs of permittivity values for the ten exhumed geotextile samples and five new geotextile samples (tested in U of A laboratory) are presented in the Appendix, in Section A.12, for completeness.

4.11. Review of Geotextile Design Criteria

The geotextile design guidelines presented in FHWA (1998) were utilized to evaluate the geotextiles installed in the Marked Tree, AR site. Each geotextile was evaluated to determine if the product met the soil retention, permittivity/permeability (filtration), and clogging criterias for the application. The evaluation was performed for the ten-inch thick and the six-inch thick sections. The calculated parameters for subgrade soil and geotextiles along with the criteria fulfillment for the aforementioned three criteria are presented in the Appendix, in Section A.13, for completeness.

Summaries of the criteria satisfaction matrices for various geotextiles in the ten-inch thick sections and the six-inch thick sections are presented in Tables 4.19 and 4.20, respectively. All of the previously installed geotextiles at the Marked Tree Test Section fulfilled the permittivity criteria and the clogging requirement in the ten-inch and the six-inch thick sections; all products did not fulfill the permittivity requirement. The permittivity value (for the Propex

4553 Non-Woven geotextile) published by the manufacturer was 4.62 times higher than the permittivity value for a new sample obtained in the laboratory. As a result of discrepancy, for the permittivity requirement each geotextile product was evaluated using both the manufacturer published permittivity value and the laboratory obtained permittivity value measured during the course of this research project.

The Propex 4553 non-woven product met all criteria in both the ten-inch thick and the six-inch thick sections. Conversely, the Carthage Mills FX-66 slit film product did not satisfy four out of six criteria. The Aperture Opening Size (AOS $\leq$0.3mm) criterion was not met for any of the products except for Propex 4553 product. The retention criterion was not met for any of the products except for the products except for the Propex 4553 product.

Table 4.19. Summary of criteria satisfaction for the various geotextiles in the ten-inch thick sections.

Geotextile	For non dispersive cohesive soils with PI>7 (AOS or $O_{95} \leq 0.3$ mm)	Permittivity Criteria ($k_{GT} \geq k_{soil}$)	Clogging Criteria ($O_{95} \geq 3D_{15}$)	Retention Criteria ($AOS \leq B*D_{85}$)	Permittivity Requirement ($\psi_{lab} > \psi$)	Permittivity Requirement ($\psi_{mfg} > \psi$)
Propex 4553 Non-Woven	✓	✓	✓	✓	✓*	✓
Propex 2006 Woven	x	✓	✓	x	✓	x
Propex 2044Woven	x	✓	✓	x	✓	✓
Mirafi Geolon HP 570 Woven	x	✓	✓	x	✓	✓

x - criteria or requirement not met

✓- criteria or requirement met

* Discrepancy between manufacture published and laboratory obtained permittivity values

Table 4.20. Summary of criteria satisfaction for the various geotextiles in the six-inch thick sections.

Geotextile	For non dispersive cohesive soils with PI>7 (AOS or $O_{95} \leq 0.3$ mm)	Permittivity Criteria ($k_{GT} \geq k_{soil}$)	Clogging Criteria ($O_{95} \geq 3D_{15}$)	Retention Criteria ($AOS \leq B*D_{85}$)	Permittivity Requirement ($\psi_{lab} > \psi$)	Permittivity Requirement ($\psi_{mfg} > \psi$)
Propex 4553 Non-Woven	✓	✓	✓	✓	✓*	✓
Propex 2006 Woven	x	✓	✓	x	✓	x
Propex 2044Woven	x	✓	✓	✓	x	x
Carthage Mills FX-66 Slit Film	x	✓	✓	x	x	x
Mirafi Geolon HP 570 Woven	x	✓	✓	x	✓	✓

x - criteria or requirement not met

✓- criteria or requirement met

* Discrepancy between manufacture published and laboratory obtained permittivity values

Based on the review of the geotextile design criteria which utilized information as previously discussed in this document including: grain size, Atterberg limits, apparent opening size of the geotextile, geotextile permittivity, and subgrade permeability, only the Propex 4553 Non-Woven product would have bettered the performance of the roadway system and should have been installed at the Marked Tree Test Section . Although the Carthage Mills FX-66 Slit Film was not intended to be included in the study, because of the roadway failure discussed in Section 4.14, the product was investigated. If proper design protocols were followed, and all design criteria were met, this product should not have been installed in the adjacent lane.

4.12. Site Observation (October 2010)

During the site visit conducted in October, 2010 Sections 13W and 13BW were visually identified as failing. Therefore, although these sections were not initially instrumented and constructed with the other 16 sections, base course, subgrade, and the geotextile samples were exhumed from Sections 13W and 13BW. As discussed previously in Chapters 3 and 4, the samples obtained from these sections were sent to the laboratory and tested with the samples obtained from the other 16 sections. The pavement in Section 13BW had an undulating surface in the transverse direction of traffic flow and hence a trench (the width of the westbound lane) was excavated to perform a forensic analysis (Figure 4.30).

(a) (b)

Figure 4.30. Section 13BW a) trench excavation performed by AHTD personnel using a backhoe, b) after asphalt removal (undulating pavement surface).

The asphalt was first removed to determine if the undulation in the roadway was transferred to the base course. After determine the undulation was transferred to the base course, the base course was also excavated. After the base course was removed, the geosynthetic was also removed, and moist subgrade was observed (Figure 4.31). As observed during the exhumation of the geosynthetic in Section 13W, the base course did not puncture the geosynthetic, the base course did not indent into the subgrade, and water infiltrated the trench from the geosynthetic at the edges of the trench. For all of the excavations, no puncture in the geosynthetic or indention into the base course was observed, even for the control sections and the sections containing only geogrids. Therefore, the geosynthetics served their purpose for separation, but may not have been required as the base course and subgrade particles within the control sections were separated even though no geotextile was present.

A void space underneath the geotextile was also observed as presented in Figure 4.32. This void space may be attributed to the excavation process, or may be attributed to flow along the geosynthetic interface creating a drainage channel. Up to three layers of overlapped geotextile and discoloration in the subgrade soil were observed as presented in Figure 4.33. The

discoloration on the east side of the trench was different than the discoloration on the west side of the trench (Figure 4.33). This discoloration is believed to be caused spatial variability in the material properties (as previously discussed in Section 4.4).

(a) **(b)**

Figure 4.31. Section 13BW subgrade a) after the geotextile removed and b) the zoomed in view after geotextile removal.

Figure 4.32. Void space observed (Section 13BW) underneath the geotextile.

(a) **(b)**

Figure 4.33. Discoloration in subgrade soil in Section 13BW after trench excavation on the a) east side and b) west side of the trench.

Excessive alligator cracking was observed in the outer wheel path of Section 13W as presented in Figure 4.34 and discussed further in Section 4.14. Lateral seepage was also observed from the geotextile at the base course/subgrade interface of Section 13W during and after nuclear gauge testing on the subgrade, DCP testing on the subgrade, and CBR testing on the subgrade (Figure 4.35).

Figure 4.34. Alligator cracking in the outer wheel path of Section 13W.

(a) **(b)**

Figure 4.35. Lateral seepage observed in subgrade of Section 13W a) after DCP testing and b) after completion of CBR testing.

4.13. Pavement Profile (October 2010)

The elevations measured for top of pavement, top of base, and top of subgrade which were obtained in accordance with Section 3.5.1 and are graphically presented in Figure 4.36. These measurements were obtained to identify the actual asphalt and base course thickness. These elevations are based on an arbitrary site-specific benchmark elevation (elevation=100 feet) rather than a standardized datum. Because the goal was to determine base course and pavement thicknesses and the relative changes in elevation of the roadway surface between sections, the selection of the site specific benchmark was insignificant.

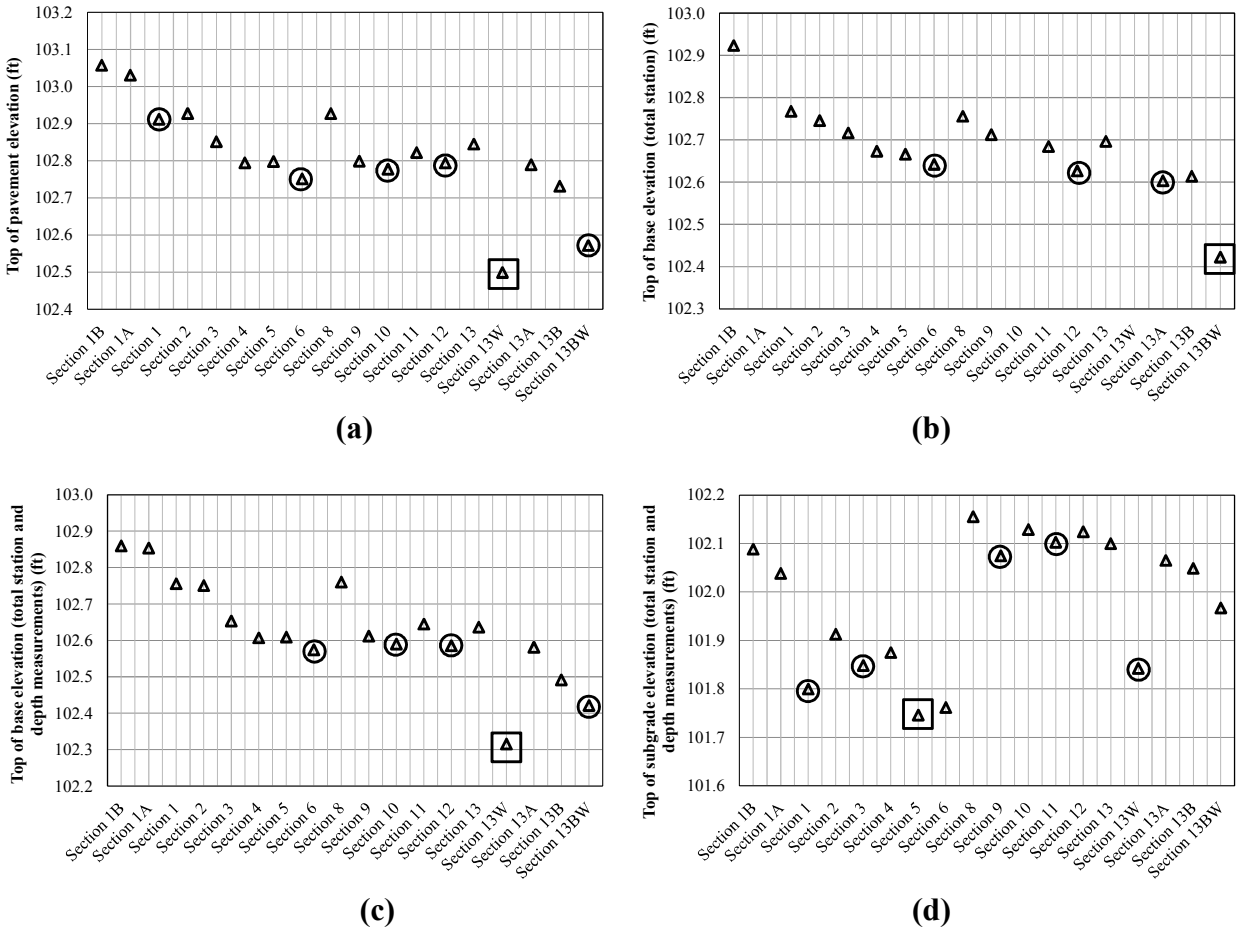

Figure 4.36. Pavement profile a) top of pavement elevation, b) top of base elevation (total station), c) top of base elevation (total station and depth measurements) and d) top of subgrade elevation (total station and depth measurements).

Sections 1, 6, 10, 12, 13W, and 13BW were the local low points for top of asphalt elevations with respect to their abutting sections. Similarly, Sections 6, 10, 12, 13W, and 13BW were the local low points for top of base elevation (determined by total station and manual measurements) with respect to their abutting sections. Section 13W has the lowest top of pavement elevation measured at the lowest top of course base elevation which is an indication of a low spot in the roadway alignment and indication of rutting. Ponding of water may occur in this low spot, and was observed in Section 13W, and in other six inch sections, during the site visit in May 2011 as presented in Figure 4.37.

Figure 4.37. Ponding in six-inch thick sections in May, 2011 (from Goldman, 2011) [view from Section 13W looking East].

The average pavement thickness ranges between 1.97 inches (Section 1) to 2.41 inches (Section 5) in the ten-inch thick sections and 1.95 inches (Section 13BW) to 2.69 inches (Section 13B) in the six-inch thick sections, respectively. The average base course layer thickness ranges between 8.97 inches (Section 4) to 11.38 inches (Section 1) in the ten-inch thick sections and 5.30 inches (Section 13BW) to 7.22 inches (Section 8) in the six-inch thick sections. Section 13BW has the smallest base course thickness in the six-inch thick sections and Section 1 has the largest base course thickness in the ten-inch thick sections. Also for the combined thickness of asphalt and base course Section 13BW had the lowest thickness in the six-inch sections and Section 1 had the highest thickness in the ten-inch thick sections.

The asphalt and base course thickness obtained in October 2010 were compared with thickness values reported by Howard (2006) and AHTD (2002). The thicknesses were subtracted from the top of pavement elevation obtained from AHTD (2002). Section 6 was selected as a fixed reference point and the elevations obtained in October 2010 were adjusted to align with the elevations reported by AHTD (2002). Section 6 had the least amount of rutting and the lowest percent area of lane with alligator cracking (as described in Section 4.14) and hence was selected

as the fixed reference point. The obtained elevations were then plotted to compare the differences in top of pavement and top of base course elevations. The elevations for top of pavement, top of base, and top of subgrade for October 2010 site data and values reported by Howard (2006) and AHTD (2002) are graphically represented in Figure 4.38.

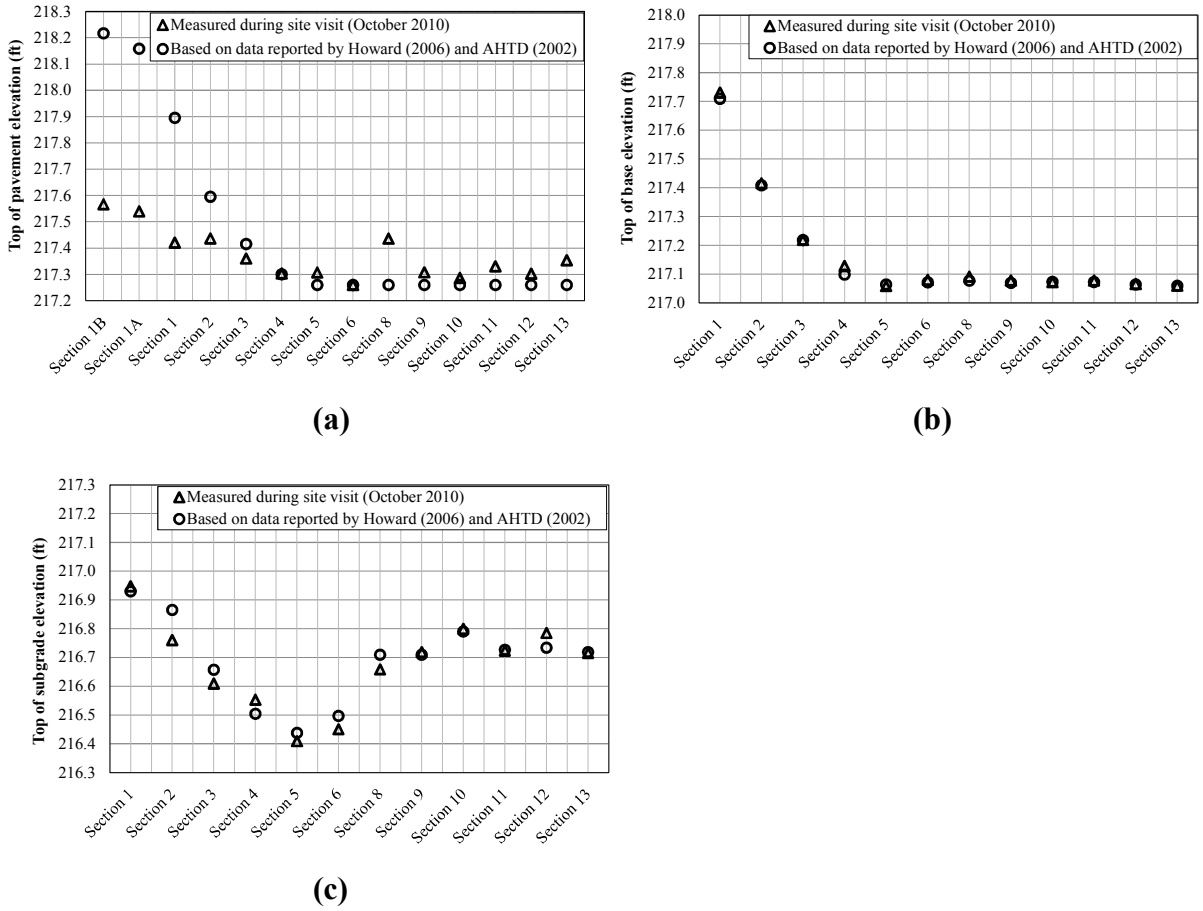

Figure 4.38. Comparison of pavement profile a) top of pavement elevation, b) top of base elevation, and c) top of subgrade elevation reported by AHTD (2002) and Howard (2006) and measured during site visit in October 2010.

No apparent difference in top of pavement and top of base course elevations were observed between the data obtained in October 2010 and values reported by Howard (2006) and AHTD (2002) except for Sections 1B, 1A, 1, and 8. The differences in top of pavement elevations for Sections 1B, 1A and 1are not accurate as the elevations utilized were obtained from AHTD design drawings for the centerline of the roadway and these sections contain super-

elevation. No as-built drawings were available to obtain the actual elevations. Pavement elevations as reported in AHTD (2002) for Section 8 did not match the onsite pavement elevations, as the driveway connecting to the nursing home to Frontage Road 3 was constructed after the design of Frontage Road 3. The actual top of pavement elevation of Section 8 was lower than the elevation reported by AHTD (2002). For these reasons the discrepancy in top of pavement elevation, as obtained from the October 2011 measurements and from AHTD (2002) in Sections 1B, 1A, 1, and 8 were not real. These discrepancies are attributed to variation from the design during construction.

4.14. Pavement Distress Survey (Modified from Goldman (2011))

Pavement distress survey data was obtained from Goldman (2011) and was used to quantify the distress in the pavement system (as previously discussed in Section 3.5.2). The alligator cracking, longitudinal cracking, and rut depth measurements are presented in Sections 4.11.1, 4.11.2, and 4.11.3, respectively.

4.14.1. Alligator Cracking

The percentage of the lane with alligator cracking (based on the area of the lane) for all the 18 sections is presented in Figure 4.39. As observed in Figure 4.39, the maximum percentages of the lane with alligator cracking are 3.58 percent (Section 4) and 83.3 percent (Section 13BW) in the ten-inch thick and six-inch thick sections, respectively. Section 13BW was deemed to be failing during the October, 2010 site visit. A trench (previously discussed in Section 4.12) was excavated to determine the extent of the rutting in Section 13BW. Although the trench and damaged portions of Section 13BW were patched by AHTD personnel during the October 2010 site visit, however, in April, 2011 83.3 percent of the lane had alligator cracking.

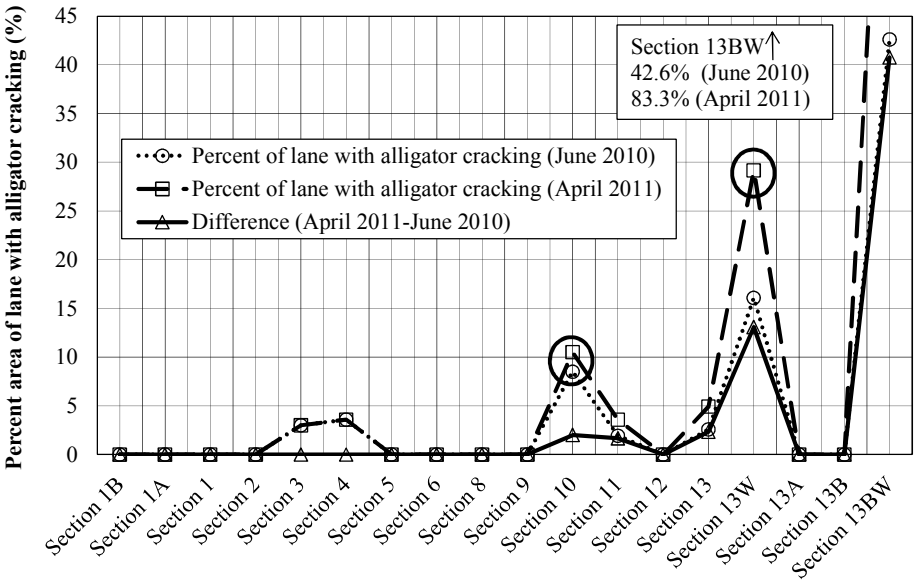

Figure 4.39. Percent area of lane with alligator cracking for June 2010 and April 2011 (modified from Goldman, 2011).

More alligator cracking was observed in April 2011 as compared to June 2010 in all of the 18 sections. Several sections, specifically (Sections 3, 4,10,11,13, 13W, and 13BW) show elevated levels of alligator cracking as compared to the other sections. Section 10 had relatively more alligator cracking as compared to abutting sections and as compared to the alligator cracking observed in the corresponding ten-inch thick section with the same geosynthetic type (Section 4). Section 11 which had less alligator cracking than Section 10, but slightly more alligator cracking as compared to the corresponding ten-inch thick section (Section 3). Section 13 has similar alligator cracking as compared to Section 11. The alligator cracking observed in Section 1 was insignificant. The average area of lane with alligator cracking for Sections 13W and 13BW was 22.6 percent and 63.0 percent, respectively. These two sections both contain the same geosynthetic type. Based on alligator cracking measurements, Sections 13W, 13BW, and 10 are the worst performing sections.

4.14.2. Longitudinal Cracking

The total linear feet of longitudinal cracks for all 18 sections is presented in Figure 4.40. Again due to continued use more longitudinal cracks were observed in April 2011 as compared to June 2010.

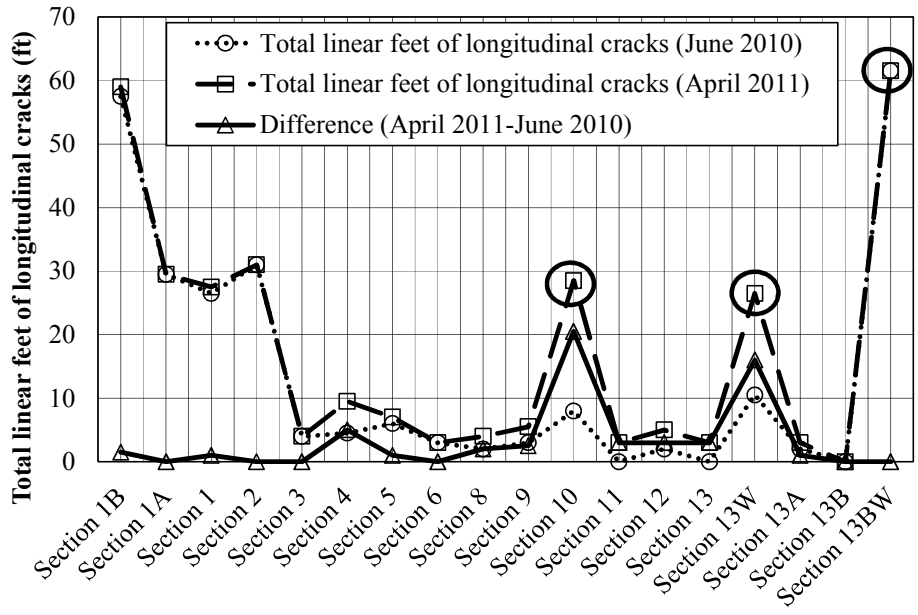

Figure 4.40. Total linear feet of longitudinal cracks observed in June 2010 and April 2011 (modified from Goldman, 2011).

The maximum total linear feet of longitudinal cracks was 58.3 feet (Section 1B) and 61.5 feet (Section 13BW) in the ten-inch thick and the six-inch thick sections, respectively. Section 10 has more longitudinal cracks as compared to abutting sections and compared to the longitudinal cracks observed in the corresponding ten-inch thick section with the same geosynthetic type (Section 4). Section 13W and Section 10 each contain similar quantities of longitudinal cracks. The longitudinal cracking values (as presented in Figure 4.40) for Sections 10 and 13W are local maxima, while Section 13BW is the global maximum. The differences (between June 2010 and April 2011) in longitudinal cracking values for the local and global

maxima are higher as compared to the rest of the sections. Based on longitudinal cracking, Sections 13W, 13BW, and 10 are the worst performing sections.

4.14.3. Rut depth

The average rut depth measurements for the 18 sections are presented in Figure 4.41. As per Figure 4.41, more rutting was observed in Section 10 as compared to abutting sections and compared to the rutting observed in the corresponding ten-inch thick section with the same geosynthetic type (Section 4). The maximum average rut depth measurement was 0.3 inches (Section 1) for the ten-inch thick sections and 1.5 inches (Section 13BW) for the six-inch thick sections. The rut depths measured in Sections 13W and 13BW are significantly greater than the rut depths measured in abutting sections. Based on rut depth measurements Sections 13W, 13BW, and 10 are the worst performing sections.

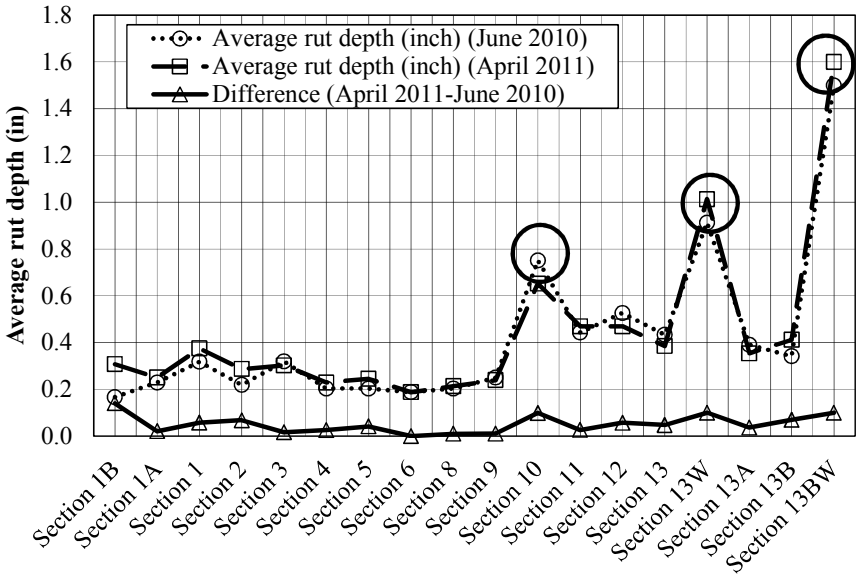

Figure 4.41. Average rut depth (inch) observed in June 2010 and April 2011 (modified from Goldman (2011)).

4.15. Conclusion

Based on the results of this research (as obtained from the field and laboratory testing), in combination with the performance data (rutting and cracking) data presented by Goldman (2011), and field observations made during the October 2010 and May 2011 site visits, the following conclusions are obtained.

- The sections which have average rut depths measurements near or in excess of 20 mm (defined as failure based on Al-Qadi et al., 1999), include Sections 10 (19 mm), 13W (25.6 mm), and 13BW (40.64 mm).
- These sections are the three sections in which the sum of the base course and asphalt thicknesses are the smallest. The sum is less than eight inches for each section.
- Specific instances in which Sections 10, 13W, and 13BW are the worst performers (based on the laboratory, field testing, and field observation conducted as a part of this research project) are listed below.
    - The water content values within the base course at the base course/subgrade interface are the highest for Sections 13BW, 10, and 13W (4.2, 6.0, and 6.4 percent, respectively).
    - The lowest top of pavement and top of base course elevation were observed in Sections 13BW and 13W (based on pavement profile). The low spots caused ponding in these sections.
    - Water infiltration from the base course/subgrade interface was observed in the field during the forensic investigation of Sections 4, 10, 13W, and 13BW (within the two foot by two foot excavation and within the trench excavation). The infiltration appeared during the nuclear density testing

of the subgrade and during the California Bearing Ratio (CBR) testing on the subgrade (the CBR testing is discussed in Goldman, 2011). It is important to note that these sections were exhumed following a rain storm in which ponding of water was observed in the wheel paths in these sections. Water may have infiltrated into the cracks in the pavement, traveled through the base course, and ponded at the interface between the base course and subgrade due to the low permeability of the subgrade preventing infiltration into the subgrade. The effective stress and total head were reduced within the excavations, causing water to flow into the excavation during testing.

- As observed in the trench that was excavated across the worst performing section (Section 13BW), the surface deformation (rutting) was transferred from the asphalt through the base course and into the subgrade. Intimate contact was observed between the geosynthetic and the subgrade. It was discovered that up to three layers of geotextile were overlapped at various locations across the lane. This overlapping may have contributed to failure.
- From the results obtained from the base course sieve analysis testing (dry sieve, wet sieve, hydrometer analysis) conducted on samples located directly below and above the base course/subgrade interface, the difference in fines content for the control sections (13/1) was the same (62 percent). The difference in clay and silt content for comparable six-inch thick and ten-inch thick sections for Section 13B/1B and 10/4 was

the greatest, with differences of 4.2 percent and 2.8 percent, respectively. The difference in silt and clay content the control sections (13/1) was similar (approximately 95 percent and 5 percent, respectively). Section 13BW, 13B, 13W, and 10 contained the highest clay contents, at approximately 8 percent, 10 percent, 12 percent and 10 percent, respectively.

- From the results obtained from the gravimetric moisture content testing, the moisture content in the base course of the six-inch thick and ten-inch thick sections ranged from 1.7 to 6.4 percent and 2.0 to 4.8 percent, respectively. The moisture contents in the base course at the base course/subgrade interface are considerably higher for Sections 10 and 13W than for the other sections.
- From the results obtained from the gravimetric moisture content testing, the moisture content in the subgrade of the six-inch thick and ten-inch thick sections ranged from 17.2 to 41.5 percent and 14.2 to 25.1 percent, respectively. The moisture contents in the subgrade at the subgrade/base course interface are considerably higher for Sections 10 and 13W than for the other sections.
- From the results obtained for the base course dry unit weight values (calculated based on Equation 3.1) ranged from 133pcf to 150pcf and from 129pcf to 150pcf for the six-inch thick and ten inch thick sections, respectively. The base course dry unit weight for Section 13BW was the lowest in the six-inch sections.

- From the results obtained for the subgrade dry unit weight values (calculated based on Equation 3.1) ranged from 77pcf to 104pcf and from 93pcf to 113pcf for the six-inch thick and ten inch thick sections, respectively. The lowest subgrade dry unit weight values obtained were found in Section 13BW. The highest subgrade dry unit weight values obtained were found in Section 1B.
- From the results obtained from the geotextile design criteria review, only the Propex 4553 met all of the design criteria. The Carthage Mills FX-66 product failed the most criteria (four of six criteria); the Carthage Mills FX-66 product was installed in sections 13W and 13BW.

- From the results obtained from the sieve analysis testing (dry sieve, wet sieve, hydrometer analysis) conducted on samples located directly below and above the base course/subgrade interface, the difference in fines content for comparable six-inch thick and ten-inch thick sections for Section 13A/1A, 12/2, and 10/4 was the greatest, with deviations of 22.3, 22.4 and 11.6 percent, respectively, between the respective sections.
- From the results obtained from the Atterberg Limits testing, in combination with the results obtained from the wet sieving, the subgrade in the six-inch thick sections were more plastic and more active as compared to the subgrade in the ten-inch thick sections, even though almost all of the samples plotted along the Illite activity line.
- From the results obtained from the specific gravity testing, the specific gravity of the fines in the base course specific gravity ranged from 2.73 to 2.84 and 2.75 to

2.88 for the six-inch thick and ten-inch thick sections, respectively. The subgrade specific gravity ranged from 2.58 to 2.73 and 2.61 to 2.80 for the six-inch thick and ten-inch thick sections, respectively.

- From the results obtained from the modified proctor testing, the base course maximum dry unit weight and optimum moisture content ranged from 148pcf to 155pcf and 4.5 percent to 6.4 percent for the six-inch thick sections and from 145pcf to 154pcf and 4.7 percent to 6.9 percent for the ten-inch thick sections, respectively.
- From the results obtained from in-situ hydraulic conductivity testing, laboratory hydraulic conductivity testing, and correlations between grain size and hydraulic conductivity, the in-situ hydraulic conductivity values were the lowest. The correlation proposed by Moulton (1980) provides the best comparison to the measured values. Typically, the values estimated using the Moulton (1980) equation were between the laboratory measured values and the in-situ measured values. Based on the values obtained for vertical hydraulic conductivity, the addition of geotextiles did not increase or decrease the hydraulic conductivity of the base course (as compared with the control sections). Also the minimum criteria for free draining base ($\geq$10,000 ft/day) was not met for the base course samples investigated from all of the sections.
- From the results obtained from the geotextile design criteria review, all of the geotextile products fulfilled the permittivity criteria and the clogging requirement but did not satisfy the soil retention criteria.

- From the results obtained from transmissivity and permittivity testing, the transmissivity and permittivity of the exhumed geotextiles from the six-inch thick and ten-inch thick sections ranged from 3.4E-5 m^2/s to 2.0E-4 m^2/s and from 0.05 s^{-1} to 0.32 s^{-1}, respectively.
- More rutting and alligator cracking was observed in the six-inch thick sections as compared to the ten-inch thick sections.
- The combined thickness of asphalt and base course was highest in Section 1 and lowest in Section 13BW.

Chapter 5. Conclusions and Recommendations

Drainage is a crucial element in pavement performance. Historical applications and benefits in utilizing geotextiles as evidenced through field studies were presented in Chapter 2. More specifically, the past field studies (located in various states) which were examined utilized geotextiles to stabilize roadways, equestrian trails, and hike and bike trails. The studies were able to identify and enumerate the benefits of geotextiles. In addition to the field studies, laboratory studies that explored new techniques to predict base course and geotextile performance in the field were also presented. The laboratory methods explored were able to identify the problem (reduced permeability of base course or geotextiles) but could not accurately predict field performance. The laboratory testing method (long term flow test) which identified the geotextile clogging issue and accurately predicted the problem was very time consuming.

Sample acquisition techniques utilized in this research project were presented in detail in Chapter 3. Specifically, the in-situ testing procedures, the laboratory testing schedule, and laboratory testing procedures used to conduct this research were identified. The field testing program consisted of performing in-situ density and moisture content measurements, collecting samples (of the base course, geotextiles, and subgrade samples for the purpose of additional laboratory testing), and performing in-situ hydraulic conductivity measurements. The testing was performed to identify and characterize the base course and the subgrade samples (based on in-situ density, moisture content, grain size analysis, specific gravity of fines, Atterberg limits, maximum dry density, and optimum water content), to obtain values of laboratory and field hydraulic conductivity of the base course material, and to measure the transmissivity and permittivity of the geotextiles. Conclusions drawn from the results obtained from the aforementioned field and laboratory testing (as discussed in Chapter 4) are presented in Section

5.1. Recommendations, for the correct implementation of geotextile products for filtration and separation in roadway applications, based on the results (as discussed in Chapter 4), are presented in Section 5.2. This chapter is concluded with recommendations for future work, as presented in Section 5.3.

5.1. Conclusions Drawn from Results of Field and Laboratory Testing

Based on the results of this research (as obtained from the field and laboratory testing), in combination with the performance data (rutting and cracking) data presented by Goldman (2011), and field observations, the following conclusions were obtained.

- The installed base course at the Marked Tree Test Section does not meet the freely draining base course requirement ($k \geq 10{,}000$ ft/day),
- No increase or decrease in in-situ vertical hydraulic conductivity was observed by the addition of geotextiles,
- The thickness of base course in the pavement system directly affects pavement performance especially on clayey subgrades,
- Only one of the geotextile products (Propex 4553) installed in the Marked Tree Test Section meet all of the design requirements (retention, permittivity, clogging) established by the FHWA (1998).
- The Carthage Mills FX-66 product installed in the Marked Tree Test Section failed to meet four of the six design requirements. This product was installed in Sections 13W and 13BW, the two sections which failed.
- The base course permeability can be estimated using the Moulton (1980) equation.

- The Two Stage Borehole testing method produced in-situ hydraulic conductivity values which were reasonable (as compared with laboratory data, Moutlon (1980), and Blanco (2003).
- Sections 13W and 13BW had the smallest pavement thicknesses (combined asphalt and base course thicknesses). The highest moisture content was also observed for the base course and subgrade samples at the base course/subgrade interface within these sections.

5.2. Recommendations Based on Results of Laboratory and Field Testing

Based on the results of this research, in combination with the performance data (rutting and cracking) data presented by Goldman (2011), the following recommendations are suggested.

- Base course thicknesses in excess of six-inches to be used for secondary roads constructed over marginal subgrade in the state of Arkansas.
- The geosynthetic products investigated in this study NOT to be used at the base course/subgrade interface for secondary roads constructed over marginal subgrade in the state of Arkansas. As no observations of increased pavement performance were observed for the sections containing geosynthetics as compared with sections containing no geosynthetics.
- If geotextile products are used at the base course/subgrade interface in secondary roads in the state of Arkansas, detailed construction inspection of the vertical alignment of the roadway should be conducted to prevent localized low spots where the geosynthetic may deposit water transferred from other locations, causing decreased performance.

- If geotextile products are used at the base course/subgrade interface in secondary roads in the state of Arkansas, the geotextile products should be day-lighted or connected to edge drain to drain water collected at the base course/subgrade interface.
- If geotextile products are used at the base course/subgrade interface in secondary roads in the state of Arkansas, the geotextile products should be designed to meet the FHWA (1998) geotextile design criteria.

5.3. Recommendations for Future Work

Recommendations for future work, based on the results obtained from this research project include:

- Atterberg limits testing on the fines in the base course samples,
- day-lighting of the geosynthetics to prevent the geotextiles from carrying water to the low spots in the pavement system,
- reconstruction of the Marked Tree Test Section utilizing geosynthetics that meet the FHWA (1998) design criteria, and utilizing construction quality control/quality assurance practices,
- and a cost-benefit study investigating the contribution of geosynthetics to a pavement system as compared to the contribution of additional base course thickness to a pavement system.

5.3.1. Atterberg Limits on Base Course Samples

Atterberg limits testing were conducted on all of the "disturbed" subgrade samples collected in the bags. To determine if highly plastic fines are migrating from the subgrade to the base course, Atterberg limits testing must be conducted on the base course samples located at the

base course/subgrade interface. Atterberg limits testing were scheduled to be conducted on the fines from these base course samples, and the samples were prepared. However, the samples were deemed to be non-plastic after being unable to roll threads (and therefore obtain the plastic limit) for two of the samples, and additional testing on the remaining samples was aborted. A more trained laboratory technician may have been able to determine if the base course samples did contain some plasticity.

5.3.2. Day-lighting of Geosynthetics at Marked Tree Test Site

Based on the survey data reported in Section 4.13, local low spots within the pavement alignment may lead to locations where water can pond. More specifically, the geosynthetics may wick water to the low spots at the base course/subgrade interface, creating ponding which may be detrimental to the performance of the pavement system. The geosynthetics at the Marked Tree Test Site should be day-lighted to prevent the opportunity for ponding. After the geosynthetics have been day lighted, further investigation should be conducted to determine the effects of day lighting.

5.3.3. Reconstruction of Marked Tree Test Section

Although no benefit in pavement performance was by observed utilizing geosynthetic products at the Marked Tree Test Site, this may be caused by incorrect placement of the geosynthetics and incorrect types of geosynthetics. Because of the excessive rutting (Section 13BW) and the damage incurred as the result of the forensic geotechnical field investigation (Section 13BW), it is recommended that the Marked Tree Test Site be reconstructed. During the reconstruction, the following inherent difficulties of the current site (listed below) may be addressed:

- Location of the geosynthetics,

- uniform traffic count and loading,
- uniform subgrade soils,
- well documented construction,
- and care for the in-situ sensors.

5.3.3.1 Location of Geosynthetics

All of the geosynthetics installed at the Marked Tree Test Site were installed at the base course/subgrade interface. Whereas, this location is the most beneficial for geotextile separators and geotextile filters, this location may not be the best location for geogrid reinforcement. It is suggested that in sections containing geogrid, the geogrid specimens be placed at the middle of the base course layer instead of at the base course/subgrade interface.

All but one of the geotextiles installed at the Marked Tree Test Site did not meet all of the FHWA (1998) design criteria for geotextile fabrics. Additional fabrics that meet FHWA criteria should be installed at the Marked Tree Test Site.

5.3.3.2 Uniform Traffic Count and Loading

Although not discussed in the report, the traffic count data (as presented in Goldman, 2011) obtained from the Marked Tree Test Site is non-uniform. This non-uniformity was caused by the construction of the nursing home with the driveway spanning Sections 7 and 8. The location of the nursing home, resulted in more traffic on the ten-inch thick sections as opposed to the six-inch thick sections. Following construction of the nursing home, continuous traffic count data should have been obtained for both the Eastbound and Westbound lanes in Section 13 and in Section 1. By investigating the data the exact amount of traffic that traveled over each section could have been determined.

Because of construction at the technical school located just West of Section 13B, the traffic that traveled over the Westbound lane was also more heavily loaded. The trucks traveling in the Westbound lane carried building materials and supplies and unloaded the materials and supplies at the school prior to traveling back to the Interstate in the Eastbound lane. This additional loading may have been an additional cause of the failure in Sections 13B and 13BW. Weigh stations may have supplied needed information about the loading of the pavement system by these material suppliers.

5.3.3.3 Uniform Subgrade Soils

Based on the results presented in Sections 4.1 and 4.3, the subgrade soils within the six-inch thick sections and the ten-inch thick sections are not the same. The soils below the six-inch thick section are more active than the soils below the ten-inch thick sections. This variation in subgrade soils may have been an additional cause in the poor performance of the six-inch thick sections as compared with the ten-inch thick sections. To investigate only the components of the geosynthetics or base course thickness, the subgrade soils should be the same in all sections.

5.3.3.4 Well Documented Construction

Upon initiation of the research project associated with this report, it was believed that the westbound lane contained no geosynthetics. However, after obtaining unpublished photos of the site during construction of the site, it was determined that the Westbound lane was reinforced with geosynthetics (up to three layers thick in some locations). Additionally, onsite density measurements during placement of the subgrade and base course, elevations of the alignment, and saved unused samples of the geosynthetics used in the pavement system would have proven very beneficial to this project.

5.3.3.5 Care for the In-situ Sensors

Upon initiation of the research project associated with this report, the in-situ sensors including the asphalt strain gauges, earth pressure cells, geotextile strain gauges, geogrid strain gauges, moisture content probes, piezometers, and thermocouples installed when the site was constructed were not working. Proper care for these sensors would have enabled additional data that may have provided more insight into the performance of the geosynthetics and the overall performance of the flexible pavement system.

5.3.4. Cost Benefit Analysis

To truly determine if geosynthetic products should be used in pavement systems to reduce the cost associated with additional thickness of base course, the contribution of the geosynthetics must be known. Following the reconstruction of the Marked Tree Test Site (implementing strategies to prevent: poor performance of the in-situ devices, poor selection of the location of the geosynthetics within the pavement system, and poor construction practices), a cost benefit analysis may be conducted to determine the savings or loss in savings of using geosynthetics.

5.3.5. Recommended Changes in Testing Schedule

While extensive testing was conducted as previously described in Chapter 3, the results (previously described in Chapter 4) do not provide a sufficiently complete understanding of geotextile performance in pavement drainage application. Therefore, as a result of the findings of this research project, the following areas have been identified for improvement to the field and laboratory testing program:

- Measure the AOS of geotextiles to determine the change in AOS after being in service for five years,

- weigh the geotextile after exhumation to determine the weight of fines trapped in the geotextiles which is a good indicator of geotextile clogging,
- more samples from each sections should had been exhumed so more test could have been performed (especially a five point modified proctor test instead of a four point proctor test),
- conduct specific gravity tests on large particles to obtain a more representative laboratory obtained specific gravity,
- conduct forensic investigation on Sections 1W and 1BW (ten-inch thick sections) to compare the performance with the failing Sections 13W and 13BW (six-inch thick sections),
- conduct transmissivity and permittivity testing on additional new geotextile samples,
- and conduct TSB on Sections 1W, 1BW, 13W and 13BW to obtain vertical hydraulic conductivity of base course materials.

References

Al-Qadi, I. L., Loulizi A, Flintsch G.W., Bhutta, S. A., (1999), "Evaluation of geosynthetics used as separators," Transportation Research Record 1687, TRB, National Research Council, Washington, D. C., pp. 104-110.

American Society for Testing and Materials (2005), "Standard Test Method for Sieve Analysis of Fine and Course Aggregate," Annual Book of ASTM Standards, Designation C 136, Vol. 4.08, ASTM, West Conshohocken, PA.

American Society for Testing and Materials (2005), "Standard Test Method for Particle Size Analysis of Soils," Annual Book of ASTM Standards, Designation D 422, Vol. 4.08, ASTM, West Conshohocken, PA.

American Society for Testing and Materials (2005), "Standard Test Methods for Specific Gravity of Soil Solids by Water Pycnometer," Annual Book of ASTM Standards, Designation D 854, Vol. 4.08, ASTM, West Conshohocken, PA.

American Society for Testing and Materials (2005), "Standard Test Method for Amounts of Material in Soils Finer than the No 200 (75μm) sieve," Annual Book of ASTM Standards, Designation D 1140, Vol. 4.08, ASTM, West Conshohocken, PA.

American Society for Testing and Materials (2005), "Standard Test Methods for Laboratory Compaction Characteristics of Soil Using Modified Effort (56,000 ft-lbf/ft3 (2,700 kN-m/m3))," Annual Book of ASTM Standards, Designation D 1557, Vol. 4.08, ASTM, West Conshohocken, PA.

American Society for Testing and Materials (2005), "Standard Practice for Thin-walled Tube Sampling of Soils for Geotechnical Purposes," Annual Book of ASTM Standards, Designation D 1587, Vol. 4.08, ASTM, West Conshohocken, PA.

American Society for Testing and Materials (2005), "Standard Test Methods for Laboratory Determination of Water (Moisture) Content of Soil and Rock by Mass," Annual Book of ASTM Standards, Designation D 2216, Vol. 4.08, ASTM, West Conshohocken, PA.

American Society for Testing and Materials (2008), "Standard Test Methods for Infiltration Rate of Soils in Field Using Double-Ring Infiltrometer," Annual Book of ASTM Standards, Designation D 3385, Vol. 4.08, ASTM, West Conshohocken, PA.

American Society for Testing and Materials (2005), "Standard Test Methods for Liquid Limit, Plastic Limit, and Plasticity Index of Soils," Annual Book of ASTM Standards, Designation D 4318, Vol. 4.08, ASTM, West Conshohocken, PA.

American Society for Testing and Materials (2005), "Standard Terminology for Geosynthetics," Annual Book of ASTM Standards, Designation D 4439, Vol. 4.08, ASTM, West Conshohocken, PA.

American Society for Testing and Materials (2005), "Standard Test Methods for Water Permeability of Geotextiles by Permittivity," Annual Book of ASTM Standards, Designation D 4491, Vol. 4.08, ASTM, West Conshohocken, PA.

American Society for Testing and Materials (2005), "Standard Test Methods for Measurement of Hydraulic Conductivity of Saturated Porous Materials using a Flexible Wall Permeameter," Annual Book of ASTM Standards, Designation D 5084, Vol. 4.08, ASTM, West Conshohocken, PA.

American Society for Testing and Materials (2005), "Standard Test Method for Field Measurement of Hydraulic Conductivity Limits of Porous Materials using Two Stages of Infiltration from a Borehole," Annual Book of ASTM Standards, Designation D 6391, Vol. 4.09, ASTM, West Conshohocken, PA.

American Society for Testing and Materials (2005), "Standard Test Method for Determining the (In-plane) Hydraulic Transmissivity of a Geosynthetic by Radial Flow," Annual Book of ASTM Standards, Designation D 6574, Vol. 4.13, ASTM, West Conshohocken, PA.

American Society for Testing and Materials (2005), "Standard test method for in-place density and water content of soil and soil-aggregate by nuclear methods (shallow depth)," Annual Book of ASTM Standards, Designation D 6938, Vol. 4.09, ASTM, West Conshohocken, PA.

Appea, Alexander K., (1997), "In-situ Behavior of Geosynthetically Stabilized Flexible Pavement," Master Thesis, Virginia Polytechnic Institute and State University, June.

Arkansas State Highway and Transportation Department (2002), Hwy. 149 Interchange Drawings (Marked Tree), Poinsett County, Route 63, Section 9, Job 1005422.

Arkansas State Highway and Transportation Department (2010), Table 303-1: Aggregate Base Course Gradation. pg. 190. <http://www.arkansashighways.com/standard_spec/2003/final300.pdf>. Accessed November 22, 2010.

Asphalt Institute, (1982), "Research and development of the asphalt institutes thickness design manual" Research Report No. 82-2, ed. 9.

Benson, C. H., Kucukkirca, I.E. and Scalia, J. (2010), "Properties of geosynthetics exhumed from a final cover at a solid waste landfill," Journal of Geotextiles and Geomembranes, Vol. 28, pp.536-546.

Bhutta, S. A., (1998), "Mechanistic-Empirical Pavement Design Procedure for Geosynthetically Stabilized Flexible Pavements," PhD Dissertation, Virginia Polytechnic Institute and State University, April.

Blanco, A.W., (2003), "Drainage Performance Analysis of Missouri Roadway Bases," Master Thesis, University of Missouri-Columbia, May.

Boga, A.A.R., (2012), "Efficacy of Geosynthetic Separators and Filters: An Evaluation of Test Sections in Marked Tree, Arkansas," Master Thesis, University of Arkansas, May.

Brooks, J. A., (2009), "Strain Gage Installation and Survivability on Geosynthetics used in Flexible Pavements," Master Thesis, University of Arkansas, December.

Cedergren, H. R., (1994), "America's Pavements: World's Longest Bathtubs", Civil Engineering, ASCE, New York, Vol. 64, No. 9, pp. 56-58.

Coffman, Richard A., (2010), "Performance of flexible pavement systems containing geosynthetic separators," Proposal to Mack-Blackwell Rural Transportation Center, University of Arkansas, April.

FHWA (1998), "Geosynthetics design and construction guidelines," Pub. No. FHWA HI-95-038, NHI Course No. 13213.

Freeman, E., Loehr, J.E., and Bowders, J.J., (2000), "Geotextile Separators for Hike and Bike Trail," Geo-Institute/ASCE Specialty Conference Proceedings, pp. 377-387, University of Massachusetts, April.

Goldman, T. M., (2011), "The Marked Tree Site: Evaluation of Basal Reinforcement of Flexible Pavements with Geosynthetics," Master Thesis, University of Arkansas, December.

Google Maps (2010), <http//:www.googlemaps.com>. Accessed December 21, 2010.

Google Maps (2011), <http//:www.googlemaps.com>. Accessed November 25, 2011.

Hall, K. D., Warren, A.K, Howard, I.L., (2007), "Low volume flexible pavement roads reinforced with geosynthetics," Report prepared for Arkansas State Highway and Transportation Department and Transportation Research Program (Report No. TRC 0406).

Hazen, A., (1930), "Water Supply", American Society of Civil Engineers Handbook, John Wiley and Sons, New York, pp. 1444-1518.

Holtz, R. D., Christopher, B.R., and Berg, R.R., (1998), "Geosynthetics Engineering, Chapter 5: Geosynthetics in Roadways," BiTech Publishers Limited, Richmond, Canada, pp. 127 to 168.

Howard, I.L., (2006), "Full Scale Field Study and Finite Element Modeling of a Flexible Pavement Containing Geosynthetics," PhD Dissertation, University of Arkansas

Indiana Department of Transportation (2011), Chapter 12 Nuclear Gauge Testing pp.12-4. <http://www.in.gov/indot/2590.htm>. Accessed November 15, 2011.

Lawrence, J. H., (2006), "Investigation of the Affect of Fines on the Performance of Aggregate Base Course," Master Thesis, University of Arkansas, December.

Koerner, R.M., (2005), "Designing with Geosynthetics," Pearson Education Inc., Upper Saddle River, NJ, 5th ed. pp. 1 -15.

Koerner, R.M., Koerner, G.R., Fahim, A.K. and Wilson-Fahmy, R.F., (1994), "Long-Term performance of geosynthetics in drainage applications," NCHRP Report 367, Drexel University, Philadelphia.

Marked Tree, Arkansas, website (2011), <http://www.markedtreearkansas.org/>. Accessed August 1, 2011.

Missouri Department of Transportation (2011), Section 1007.2.2, < http://www.modot.org/business/standards_and_specs/Sec1007.pdf>. Accessed November 25, 2011.

Moulton, L.K., (1980), "Highway subdrainage manual", FHWA report no. FHWA-TS-80-224.

NOAA (2011), Vol. 115, No. 13 <http//:www.noaa.gov>. Accessed August 1, 2011.

Sherard J.L., Dunnigan, L.P., and Talbot, J.R., (1984) "Basic properties of sand and gravel filters," Journal of Geotechnique, vol. 110, no. 6. Pp. 684-700.

Tabor, N.K., (2007) "Development of solution techniques and design guidelines for equestrian trails on public lands," Master Thesis, University of Missouri-Columbia, May.

Tingle, J.S. and Jersey, S.R. (1989), "Empirical design methods for geosynthetic-reinforced low-volume roads," Transportation Research Board, vol. 2, pp. 91-101.

VWR International (2011), < https://www.vwrsp.com/catalog/product/index.cgi?product_id=4550248>. Accessed July 15, 2011.

Appendix A

The results of the laboratory testing performed on base course, subgrade, and geotextile samples during the research project are presented in this Appendix. Grain size distribution (sieve analysis and hydrometer), specific gravity, and wet sieving tests were performed on exhumed base course samples. Atterberg limits, hydrometer, specific gravity, and fines content (by wet sieving method) tests were performed on exhumed subgrade samples. Transmissivity and permittivity tests were performed on exhumed and new geotextile samples. All testing was performed in accordance to the testing procedures outlined in Chapter 3. The results are summarized in Chapter 4. This Appendix contains the collected data for completeness.

A.1. Sieve Analysis

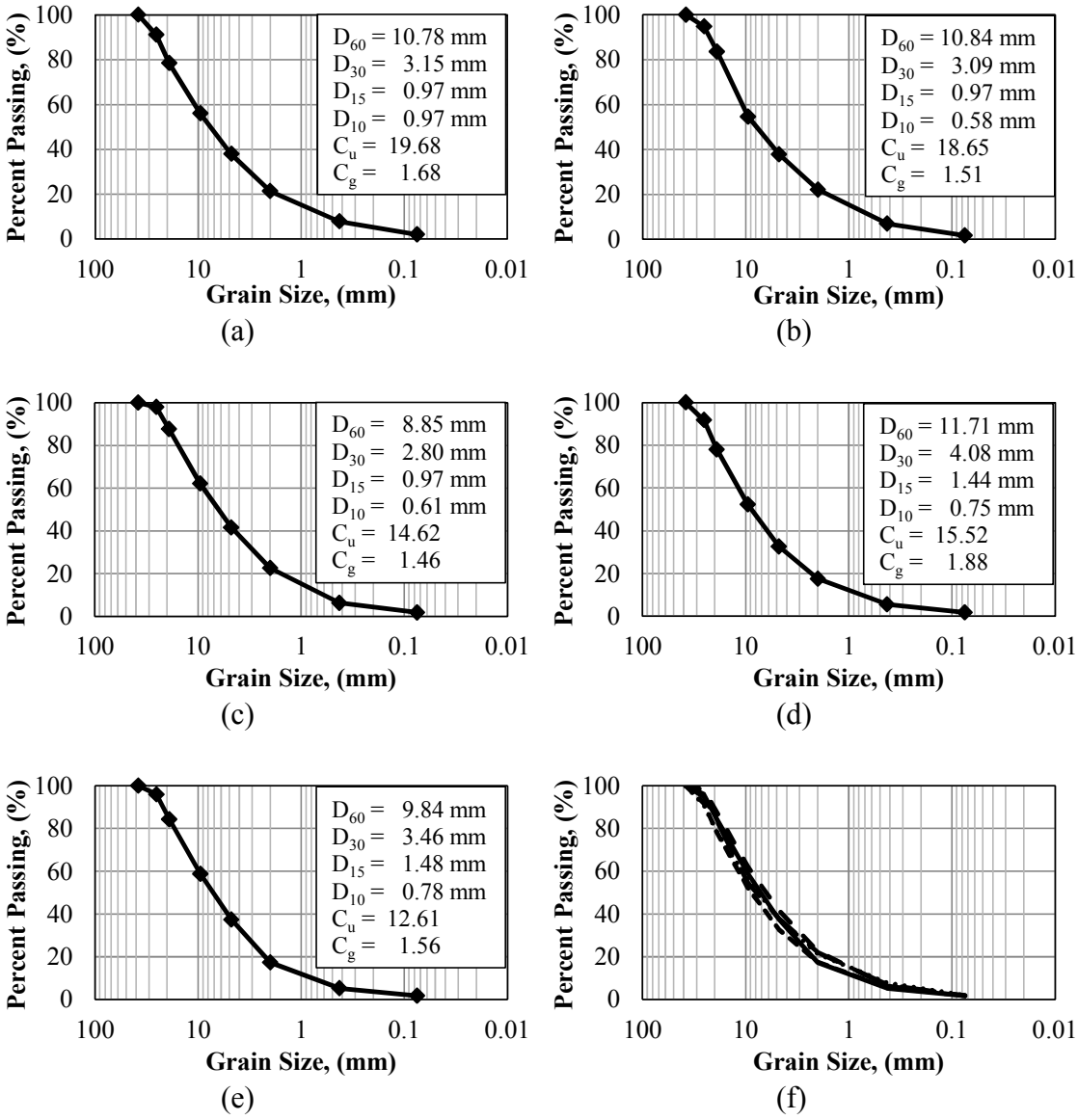

Figure A.1.1. Gradation of base course samples obtained from Section 1B taken from depths of: a) 0-2 inches, b) 2-4 inches, c) 4-6 inches, d) 6-8 inches, e) 8-10 inches, and f) all depths below the asphalt/base course interface.

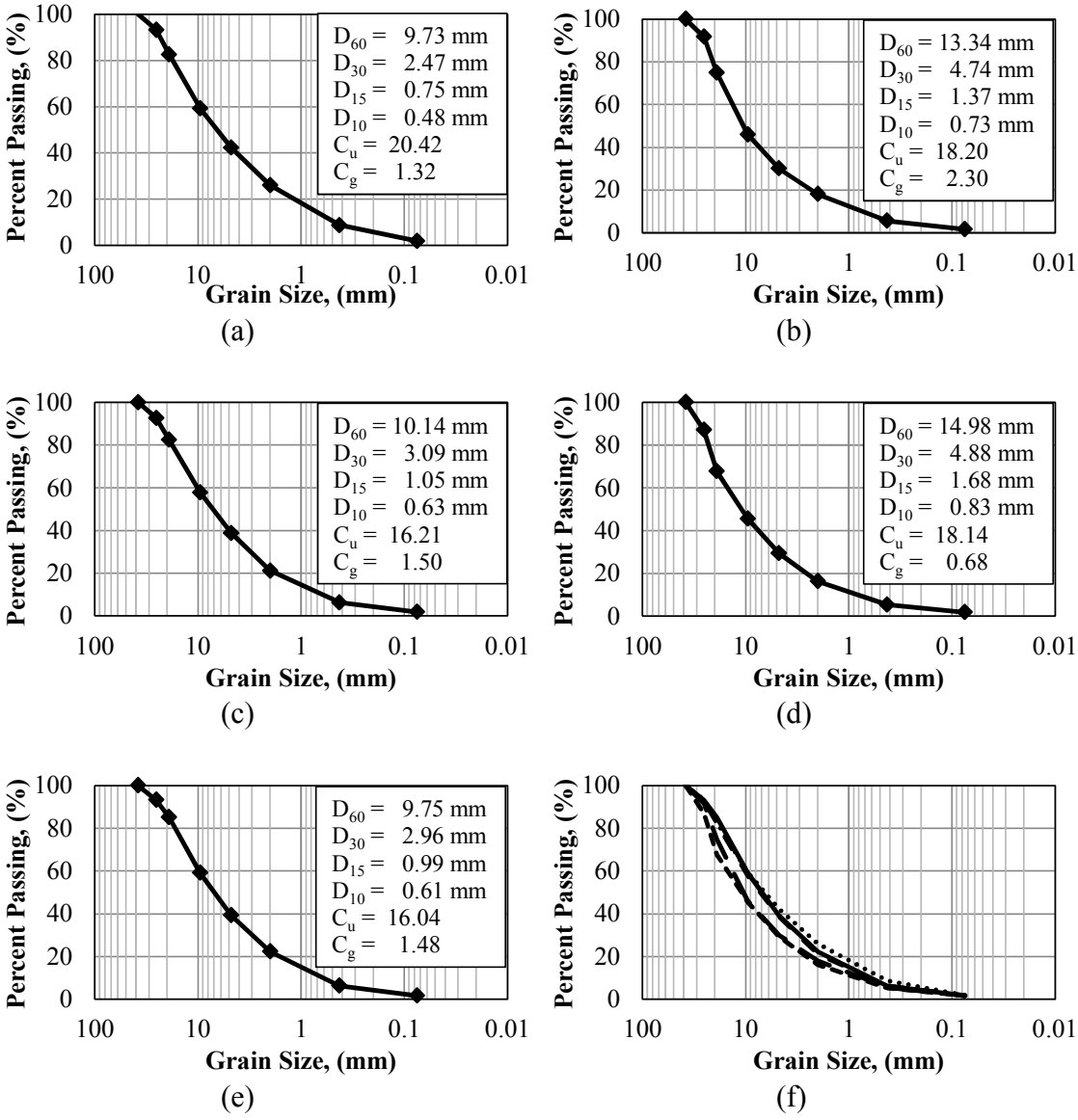

Figure A.1.2. Gradation of base course samples obtained from Section 1A taken from depths of: a) 0-2 inches, b) 2-4 inches, c) 4-6 inches, d) 6-8 inches, e) 8-10 inches, and f) all depths below the asphalt/base course interface.

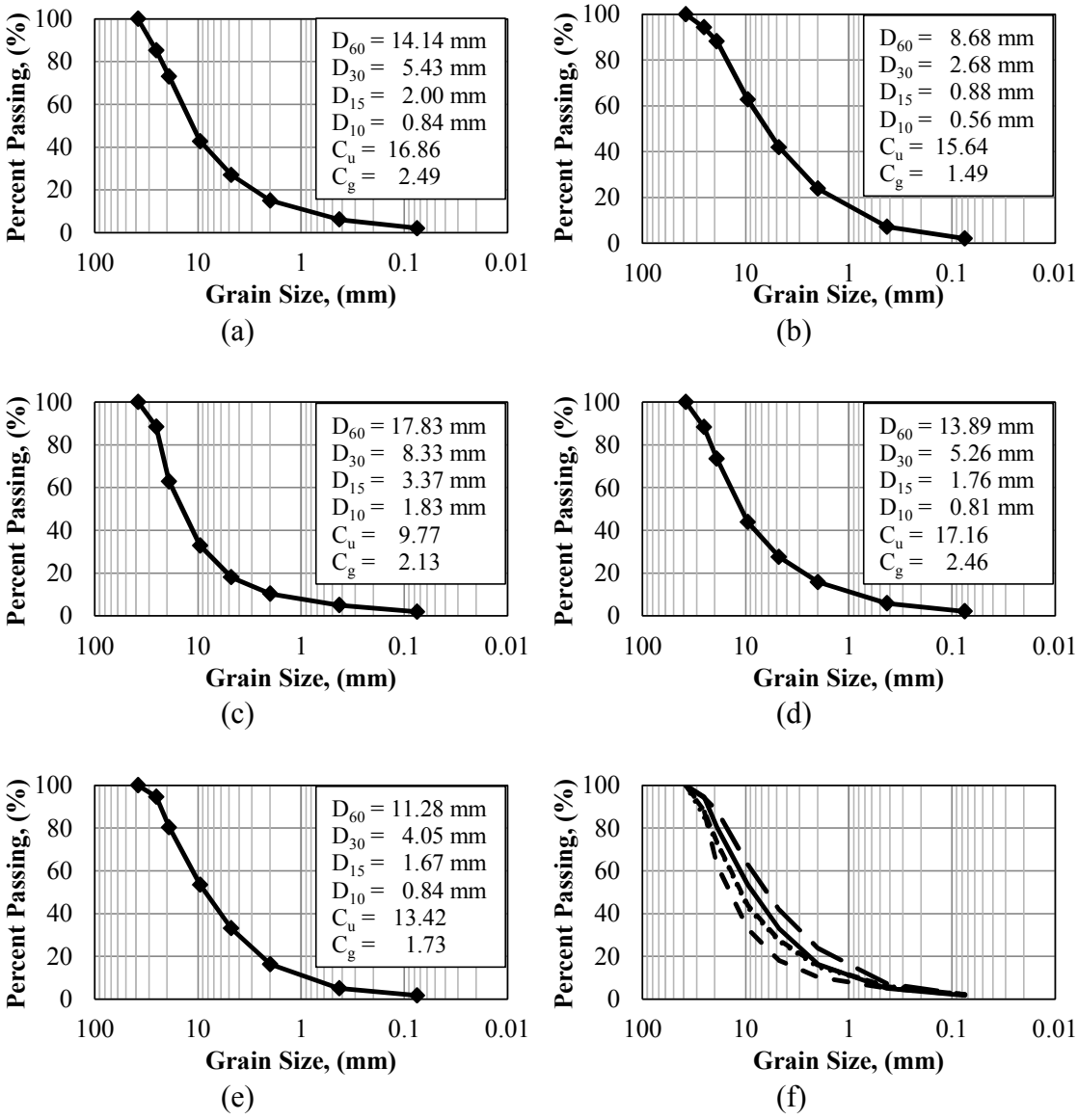

Figure A.1.3. Gradation of base course samples obtained from Section 1 taken from depths of: a) 0-2 inches, b) 2-4 inches, c) 4-6 inches, d) 6-8 inches, e) 8-10 inches, and f) all depths below the asphalt/base course interface.

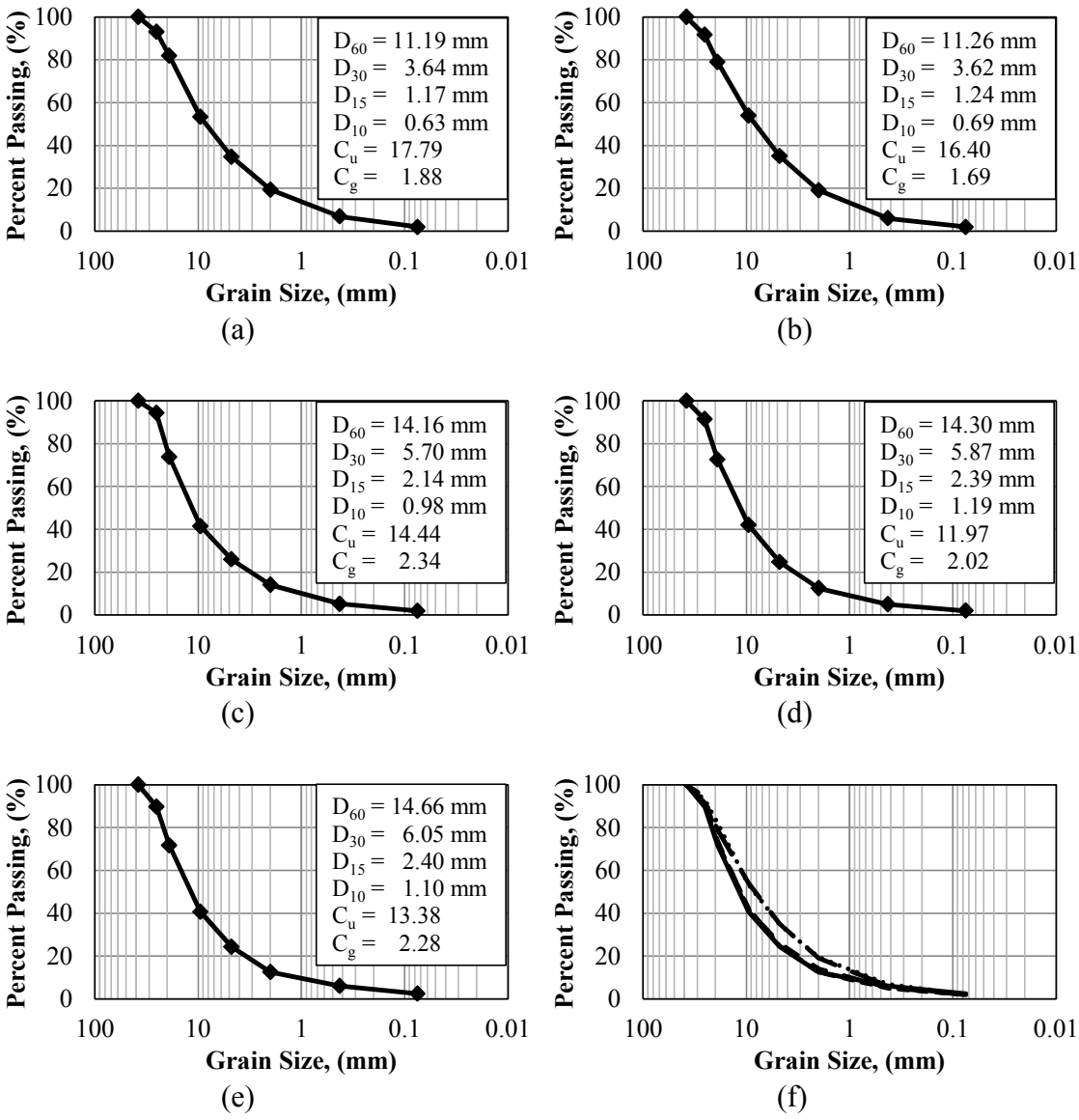

Figure A.1.4. Gradation of base course samples obtained from Section 2 taken from depths of: a) 0-2 inches, b) 2-4 inches, c) 4-6 inches, d) 6-8 inches, e) 8-10 inches, and f) all depths below the asphalt/base course interface.

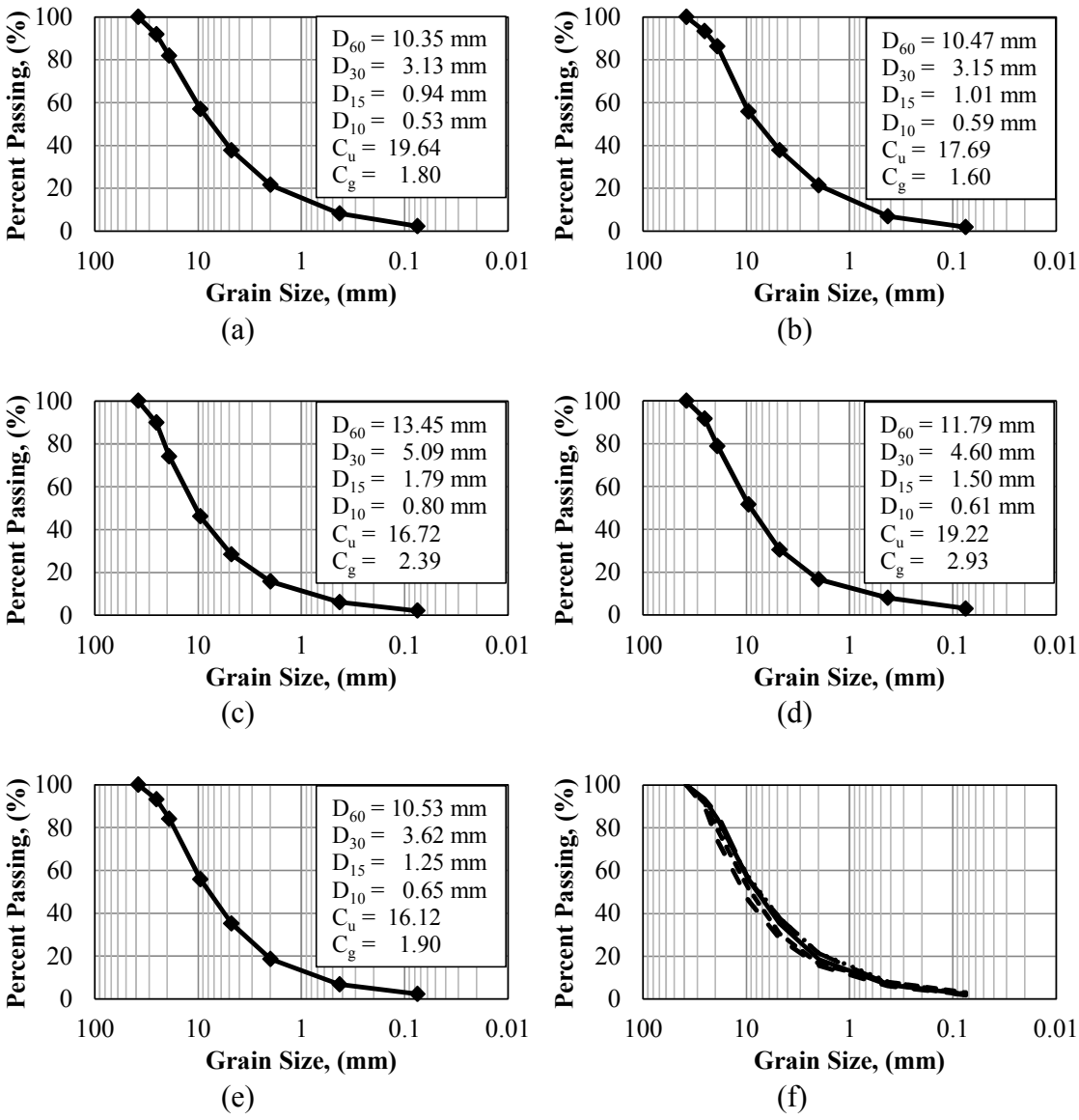

Figure A.1.5. Gradation of base course samples obtained from Section 3 taken from depths of: a) 0-2 inches, b) 2-4 inches, c) 4-6 inches, d) 6-8 inches, e) 8-10 inches, and f) all depths below the asphalt/base course interface.

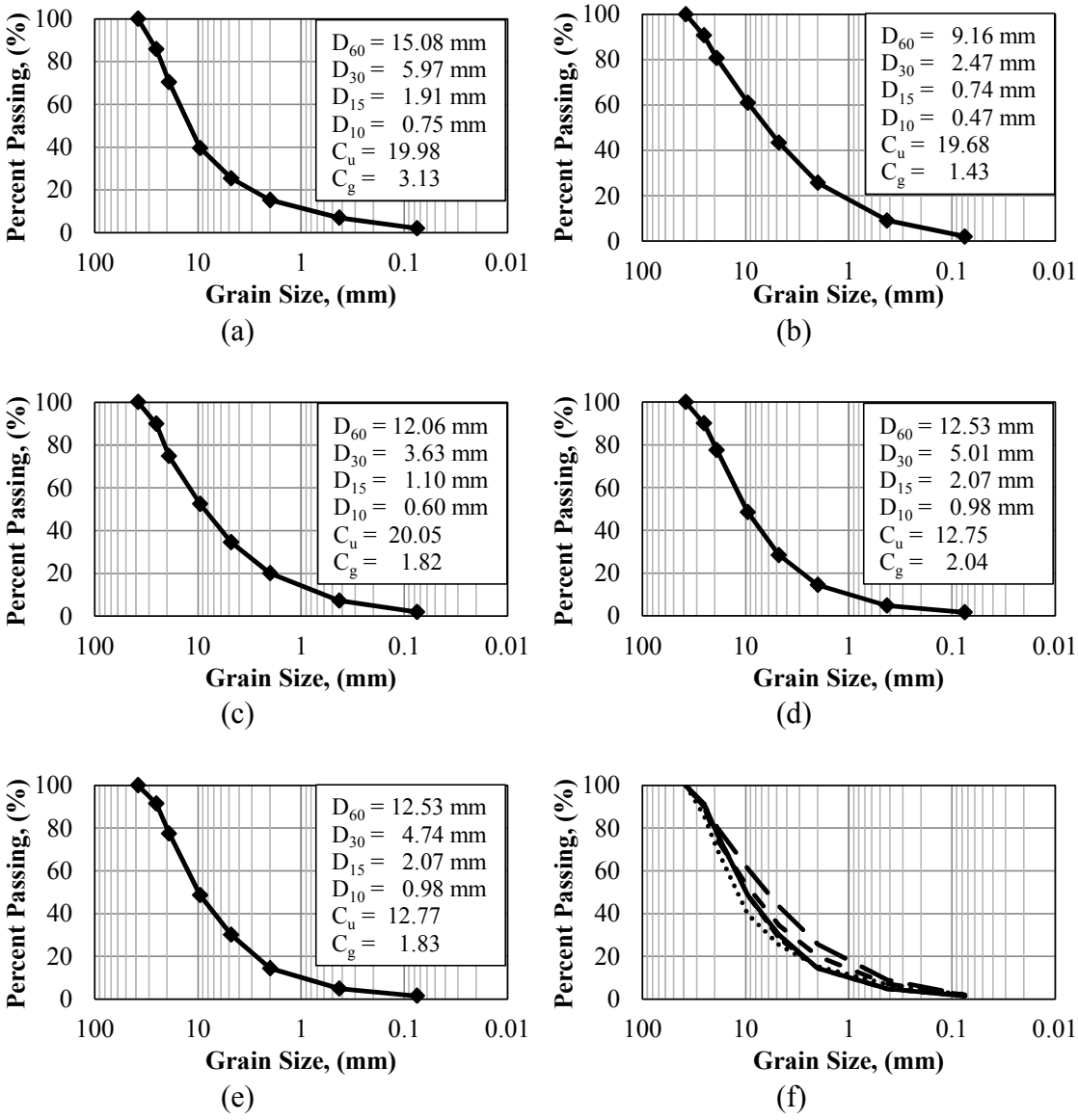

Figure A.1.6. Gradation of base course samples obtained from Section 4 taken from depths of: a) 0-2 inches, b) 2-4 inches, c) 4-6 inches, d) 6-8 inches, e) 8-10 inches, and f) all depths below the asphalt/base course interface.

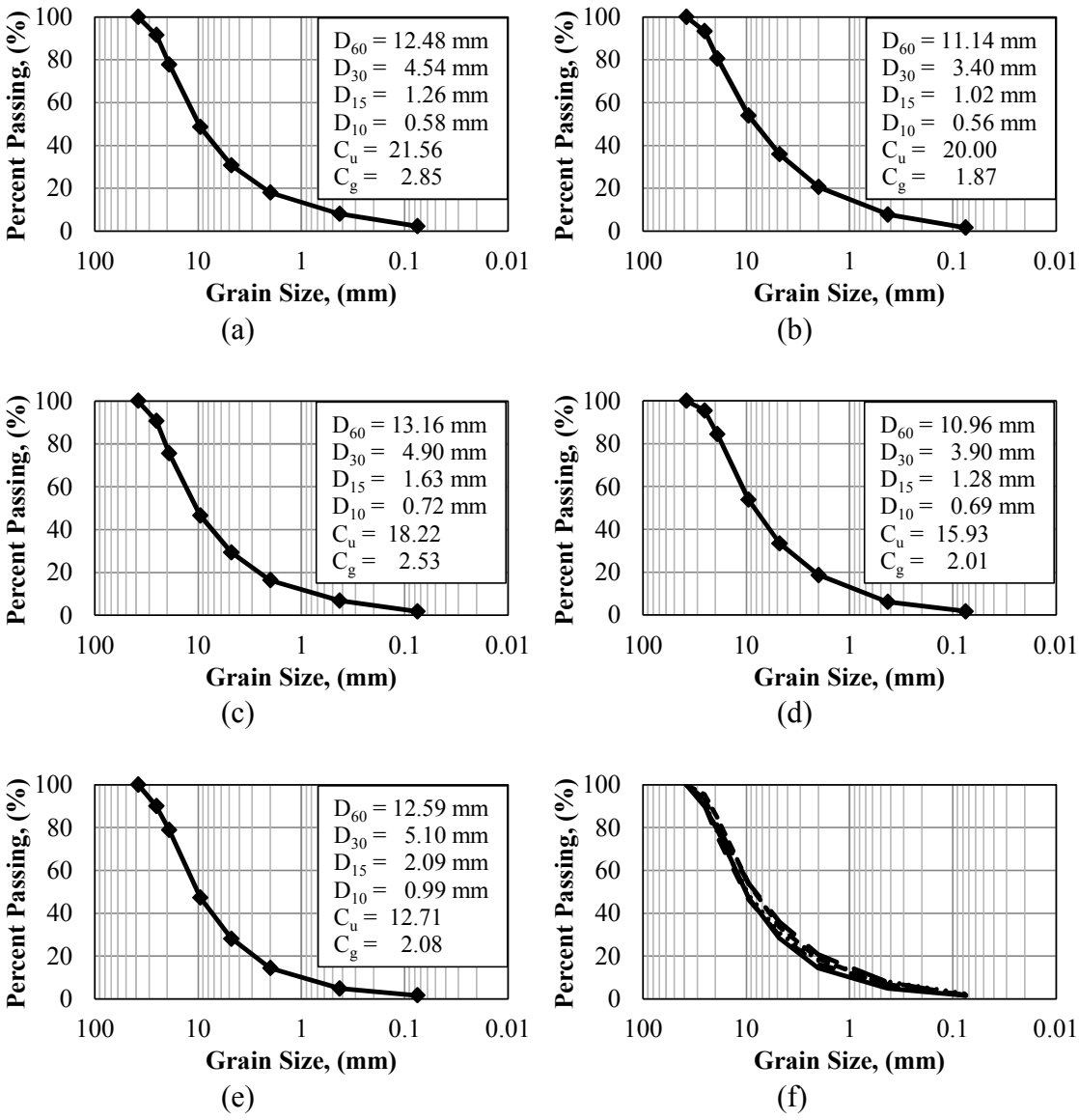

Figure A.1.7. Gradation of base course samples obtained from Section 5 taken from depths of: a) 0-2 inches, b) 2-4 inches, c) 4-6 inches, d) 6-8 inches, e) 8-10 inches, and f) all depths below the asphalt/base course interface.

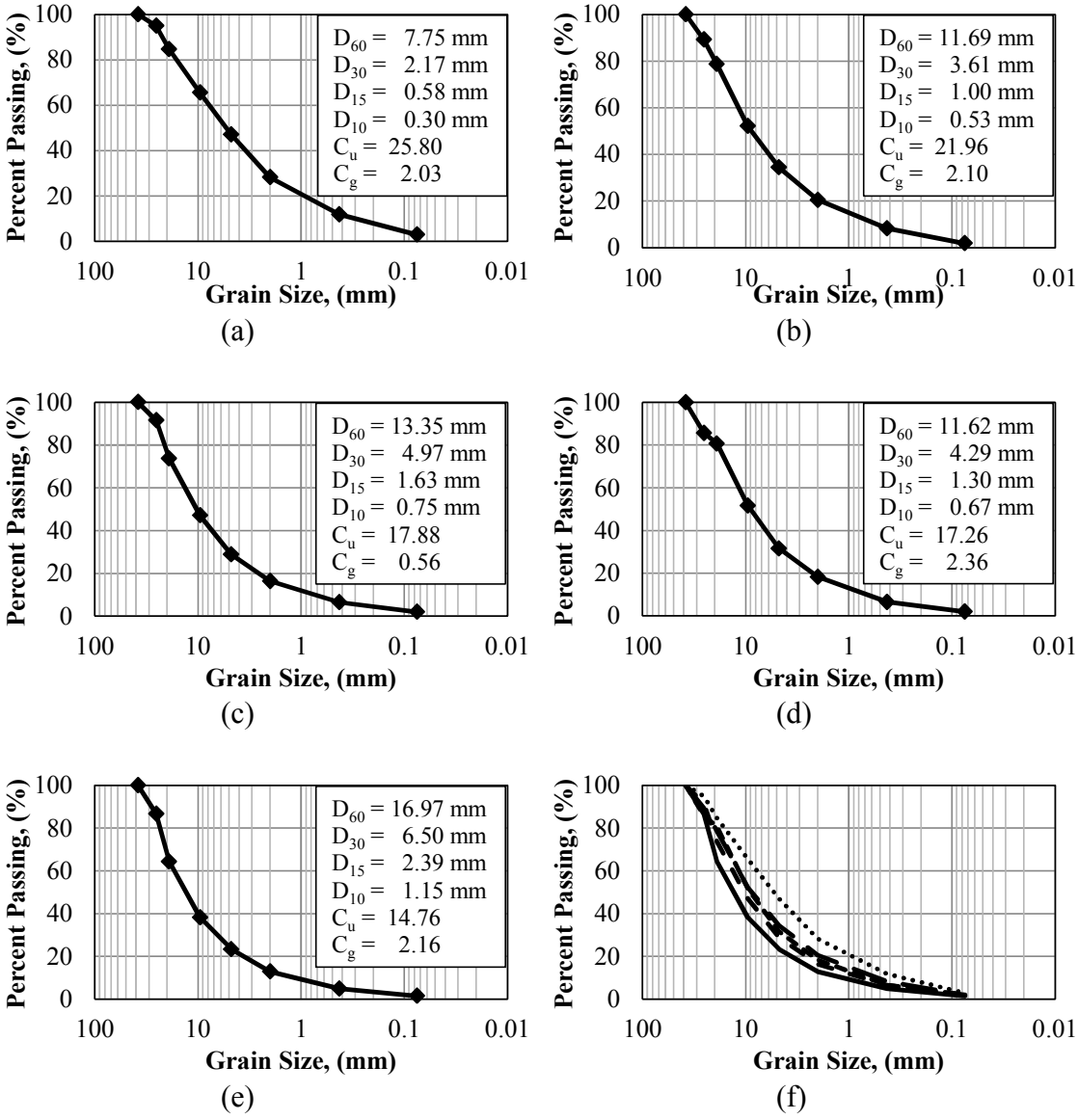

Figure A.1.8. Gradation of base course samples obtained from Section 6 taken from depths of: a) 0-2 inches, b) 2-4 inches, c) 4-6 inches, d) 6-8 inches, e) 8-10 inches, and f) all depths below the asphalt/base course interface.

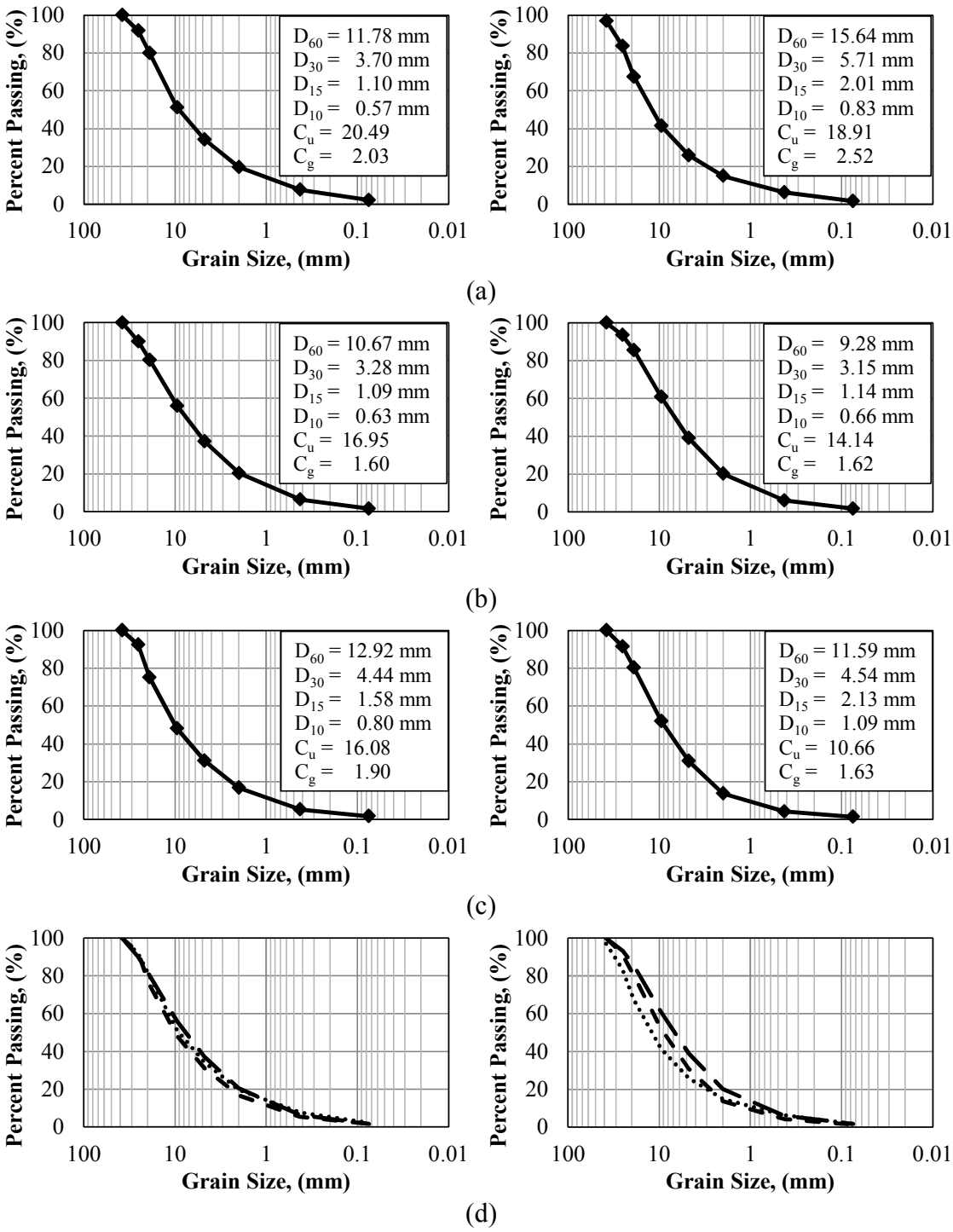

Figure A.1.9. Gradation of base course samples obtained from Section 8 (left) and Section 9 (right) taken from depths of: a) 0-2 inches, b) 2-4 inches, c) 4-6 inches, and d) all depths below the asphalt/base course interface.

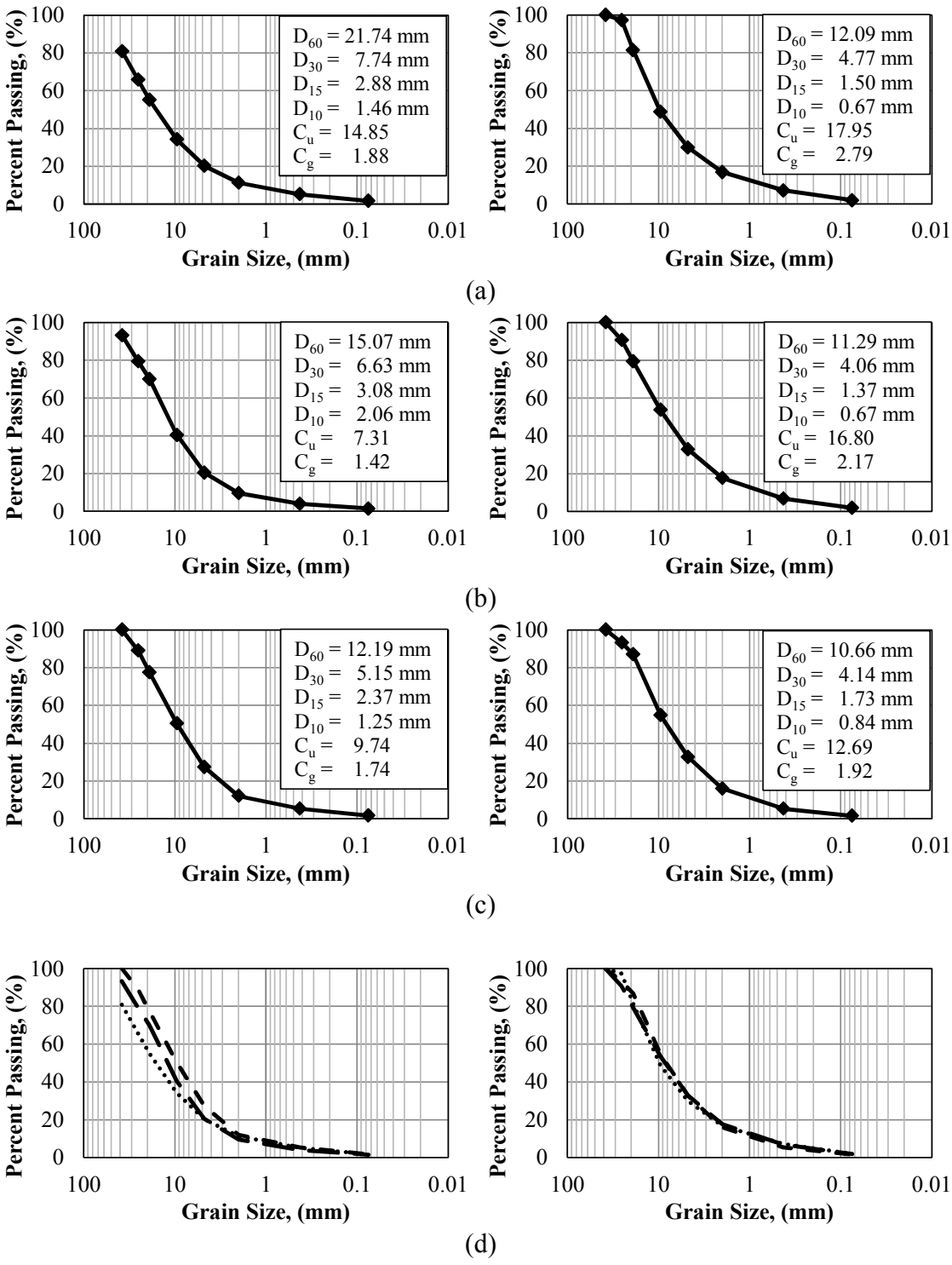

Figure A.1.10. Gradation of base course samples obtained from Section 10 (left) and Section 11 (right) taken from depths of: a) 0-2 inches, b) 2-4 inches, c) 4-6 inches, and d) all depths below the asphalt/base course interface.

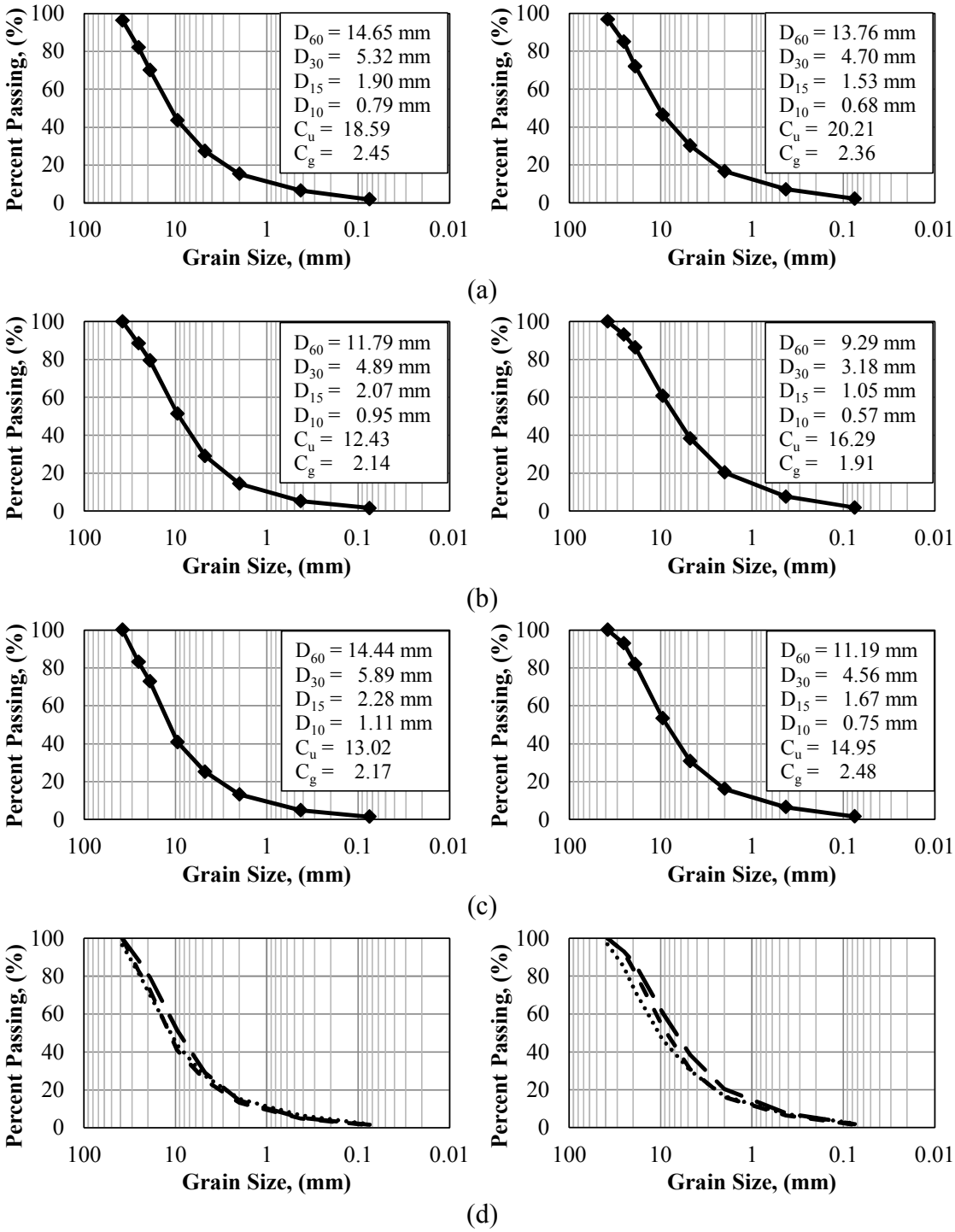

Figure A.1.11. Gradation of base course samples obtained from Section 12 (left) and Section 13 (right) taken from depths of: a) 0-2 inches, b) 2-4 inches, c) 4-6 inches, and d) all depths below the asphalt/base course interface.

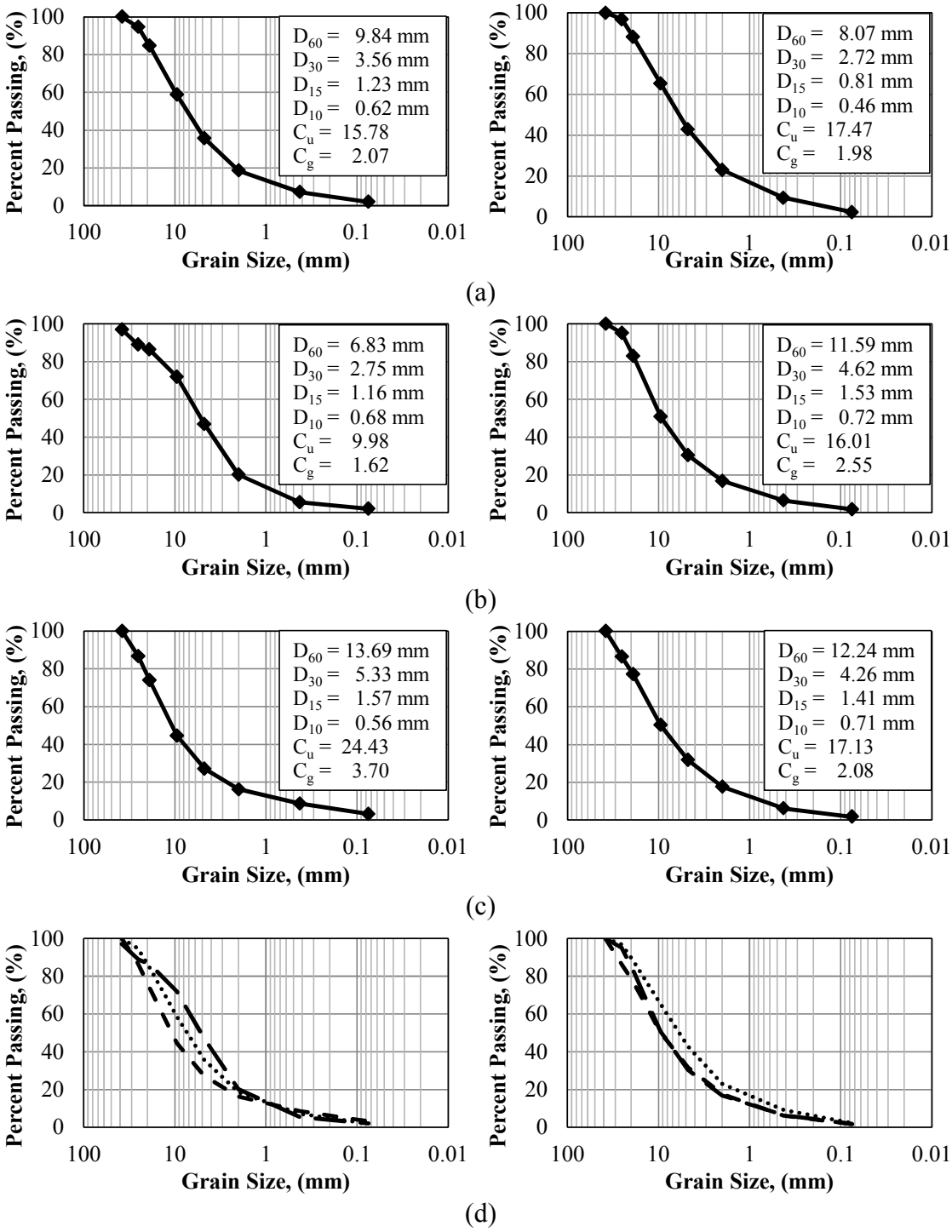

Figure A.1.12. Gradation of base course samples obtained from Section 13W (left) and Section 13A (right) taken from depths of: a) 0-2 inches, b) 2-4 inches, c) 4-6 inches, and d) all depths below the asphalt/base course interface.

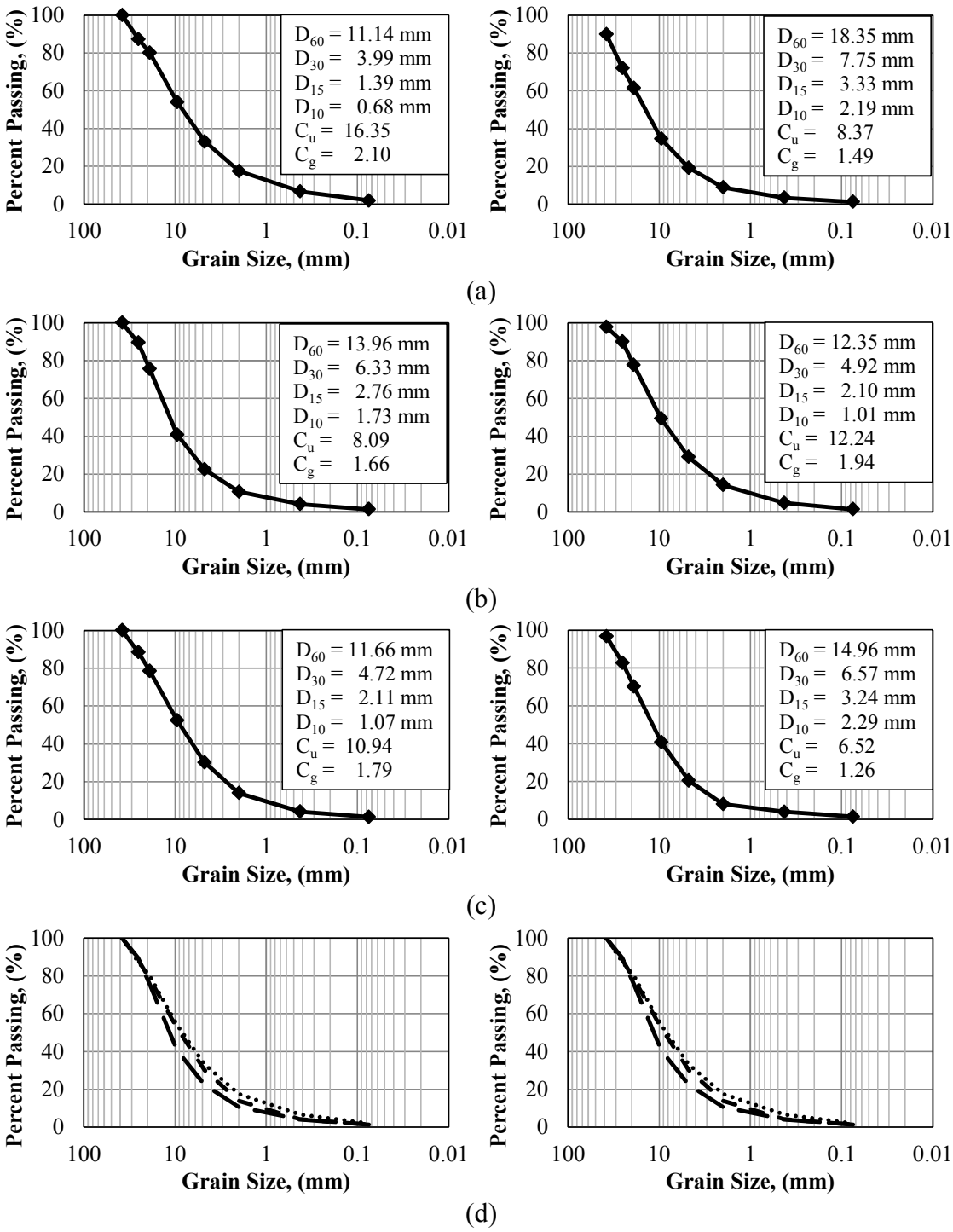

Figure A.1.13. Gradation of base course samples obtained from Section 13B (left) and Section 13BW (right) taken from depths of: a) 0-2 inches, b) 2-4 inches, c) 4-6 inches, and d) all depths below the asphalt/base course interface.

Table A.1.1. Tabulated grain size results for the ten inch thick sections.

Location	Depth*	Passing 200	D_{60}	D_{30}	D_{15}	D_{10}	C_u	C_g
	(inch)	(%)	(mm)	(mm)	(mm)	(mm)	(unitless)	(unitless)
Section 1B	0-2	1.96	10.78	3.15	0.97	0.55	19.68	1.68
Section 1B	2-4	1.69	10.84	3.09	0.97	0.58	18.65	1.51
Section 1B	4-6	1.78	8.85	2.80	0.97	0.61	14.62	1.46
Section 1B	6-8	1.80	11.71	4.08	1.44	0.75	15.52	1.88
Section 1B	8-10	1.71	9.84	3.46	1.48	0.78	12.61	1.56
Section 1A	0-2	1.84	9.73	2.47	0.75	0.48	20.42	1.32
Section 1A	2-4	1.69	13.34	4.74	1.37	0.73	18.20	2.30
Section 1A	4-6	1.87	10.14	3.09	1.05	0.63	16.21	1.50
Section 1A	6-8	1.74	14.98	4.88	1.68	0.83	18.14	1.93
Section 1A	8-10	1.68	9.75	2.96	0.99	0.61	16.04	1.48
Section 1	0-2	2.03	14.14	5.43	2.00	0.84	16.86	2.49
Section 1	2-4	2.05	8.68	2.68	0.88	0.56	15.64	1.49
Section 1	4-6	1.95	17.83	8.33	3.37	1.83	9.77	2.13
Section 1	6-8	2.07	13.89	5.26	1.76	0.81	17.16	2.46
Section 1	8-10	1.68	11.28	4.05	1.67	0.84	13.42	1.73
Section 2	0-2	1.89	11.19	3.64	1.17	0.63	17.79	1.88
Section 2	2-4	1.94	11.26	3.62	1.24	0.69	16.40	1.69
Section 2	4-6	1.89	14.16	5.70	2.39	0.98	14.44	2.34
Section 2	6-8	1.97	14.30	5.87	2.40	1.19	11.97	2.02
Section 2	8-10	2.39	14.66	6.05	2.40	1.10	13.38	2.28
Section 3	0-2	2.30	10.35	3.13	0.94	0.53	19.64	1.80
Section 3	2-4	1.83	17.69	1.60	1.01	0.35	17.69	1.60
Section 3	4-6	2.02	13.45	5.09	1.79	0.80	16.72	2.39
Section 3	6-8	2.99	11.79	4.60	1.50	0.61	19.22	2.93
Section 3	8-10	2.30	10.53	3.62	1.25	0.65	16.12	1.90
Section 4	0-2	1.97	15.08	5.97	1.91	0.75	19.98	3.13
Section 4	2-4	1.95	9.16	2.47	0.74	0.47	19.68	1.43
Section 4	4-6	1.80	12.06	3.63	1.10	0.60	20.05	1.82
Section 4	6-8	1.62	12.53	5.01	2.07	0.98	12.75	2.04
Section 4	8-10	1.50	12.53	4.74	2.07	0.98	12.77	1.83
Section 5	0-2	2.30	12.48	4.54	1.26	0.58	21.56	2.85
Section 5	2-4	1.64	11.14	3.40	1.02	0.56	20.00	1.87
Section 5	4-6	1.70	13.16	4.90	1.63	0.72	18.22	2.53
Section 5	6-8	1.67	10.96	3.90	1.28	0.69	15.93	2.01
Section 5	8-10	1.59	12.59	5.10	2.09	0.99	12.71	2.08
Section 6	0-2	2.84	7.75	2.17	0.58	0.30	25.80	2.03
Section 6	2-4	1.89	11.69	3.61	1.00	0.53	21.96	2.10
Section 6	4-6	1.87	13.35	4.97	1.63	0.75	17.88	2.48
Section 6	6-8	1.96	11.62	4.29	1.30	0.67	17.26	2.36
Section 6	8-10	1.52	16.97	6.50	2.39	1.15	14.76	2.16

*Depth below asphalt/base course interface

Table A.1.2. Tabulated grain size results for the six inch thick sections.

Location	Depth*	Passing 200	D_{60}	D_{30}	D_{15}	D_{10}	C_u	C_g
	(inch)	(%)	(mm)	(mm)	(mm)	(mm)	(unitless)	(unitless)
Section 8	0-2	2.13	11.78	3.70	1.10	0.57	20.49	2.03
Section 8	2-4	1.62	10.67	3.28	1.09	0.63	16.95	1.60
Section 8	4-6	1.73	12.92	4.44	1.58	0.80	16.08	1.90
Section 9	0-2	1.69	15.64	5.71	2.01	0.83	18.91	2.52
Section 9	2-4	1.68	9.28	3.15	1.14	0.66	14.14	1.62
Section 9	4-6	1.38	11.59	4.54	2.13	1.09	10.66	1.63
Section 10	0-2	1.69	21.74	7.74	2.88	1.46	14.85	1.88
Section 10	2-4	1.43	15.07	6.63	3.08	2.06	7.31	1.42
Section 10	4-6	1.67	12.19	5.15	2.37	1.25	9.74	1.74
Section 11	0-2	1.90	12.09	4.77	1.50	0.67	17.95	2.79
Section 11	2-4	1.82	11.29	4.06	1.37	0.67	16.80	2.17
Section 11	4-6	1.53	10.66	4.14	1.73	0.84	12.69	1.92
Section 12	0-2	1.87	14.65	5.32	1.90	0.79	18.59	2.45
Section 12	2-4	1.57	11.79	4.89	2.07	0.95	12.43	2.14
Section 12	4-6	1.38	14.44	5.89	2.28	1.11	13.02	2.17
Section 13	0-2	2.16	13.76	4.70	1.53	0.68	20.21	2.36
Section 13	2-4	1.77	9.29	3.18	1.05	0.57	16.29	1.91
Section 13	4-6	1.49	11.19	4.56	1.67	0.75	14.95	2.48
Section 13W	0-2	1.99	9.84	3.56	1.23	0.62	15.78	2.07
Section 13W	2-4	2.08	6.83	2.75	1.16	0.68	9.98	1.62
Section 13W	4-6	3.10	13.69	5.33	1.57	0.56	24.43	3.70
Section 13A	0-2	2.24	8.07	2.72	0.81	0.46	17.47	1.98
Section 13A	2-4	1.71	11.59	4.62	1.53	0.72	16.01	2.55
Section 13A	4-6	1.76	12.24	4.26	1.41	0.71	17.13	2.08
Section 13B	0-2	1.90	11.14	3.99	1.39	0.68	16.35	2.10
Section 13B	2-4	1.35	13.96	6.33	2.76	1.73	8.09	1.66
Section 13B	4-6	1.49	11.66	4.72	2.11	1.07	10.94	1.79
Section 13BW	0-2	1.25	18.35	7.75	3.33	2.19	8.37	1.49
Section 13BW	2-4	1.36	12.35	4.92	2.10	1.01	12.24	1.94
Section 13BW	4-6	1.41	14.96	6.57	3.24	2.29	6.52	1.26

*Depth below asphalt/base course interface

A.2. Sieve Analysis Comparison

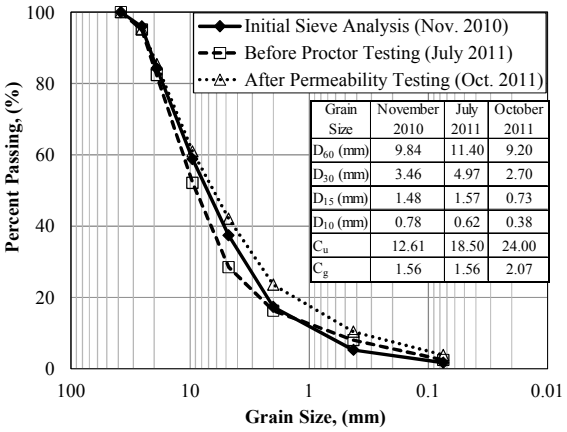

Grain Size	November 2010	July 2011	October 2011
D_{60} (mm)	9.84	11.40	9.20
D_{30} (mm)	3.46	4.97	2.70
D_{15} (mm)	1.48	1.57	0.73
D_{10} (mm)	0.78	0.62	0.38
C_u	12.61	18.50	24.00
C_g	1.56	1.56	2.07

(a)

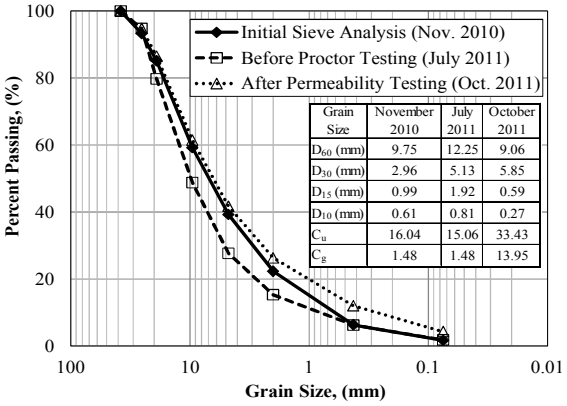

Grain Size	November 2010	July 2011	October 2011
D_{60} (mm)	9.75	12.25	9.06
D_{30} (mm)	2.96	5.13	5.85
D_{15} (mm)	0.99	1.92	0.59
D_{10} (mm)	0.61	0.81	0.27
C_u	16.04	15.06	33.43
C_g	1.48	1.48	13.95

(b)

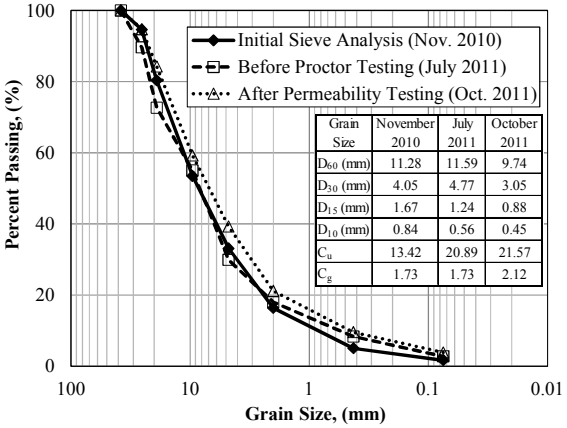

Grain Size	November 2010	July 2011	October 2011
D_{60} (mm)	11.28	11.59	9.74
D_{30} (mm)	4.05	4.77	3.05
D_{15} (mm)	1.67	1.24	0.88
D_{10} (mm)	0.84	0.56	0.45
C_u	13.42	20.89	21.57
C_g	1.73	1.73	2.12

(c)

Figure A.2.1. Gradation of base course sample from Sections a) 1B 8-10 inches, b) 1A 8-10 inches, and c) 1 8-10 inches below the asphalt/base course interface conducted after sampling (November 2010), conducted before proctor testing (July 2011) and conducted after hydraulic conductivity testing (October 2011).

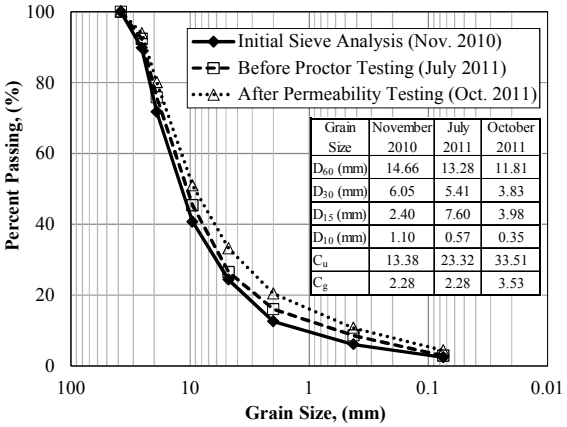

Grain Size	November 2010	July 2011	October 2011
D_{60} (mm)	14.66	13.28	11.81
D_{30} (mm)	6.05	5.41	3.83
D_{15} (mm)	2.40	7.60	3.98
D_{10} (mm)	1.10	0.57	0.35
C_u	13.38	23.32	33.51
C_g	2.28	2.28	3.53

(a)

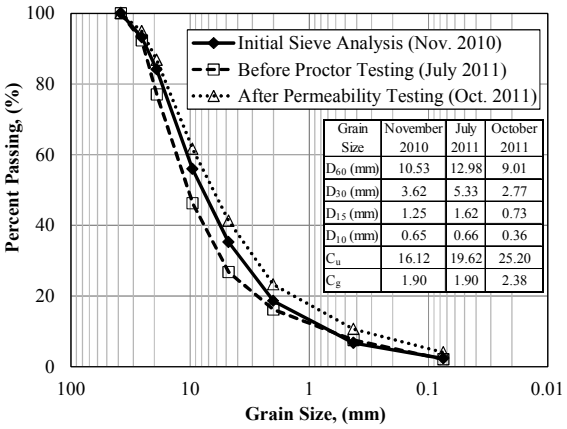

Grain Size	November 2010	July 2011	October 2011
D_{60} (mm)	10.53	12.98	9.01
D_{30} (mm)	3.62	5.33	2.77
D_{15} (mm)	1.25	1.62	0.73
D_{10} (mm)	0.65	0.66	0.36
C_u	16.12	19.62	25.20
C_g	1.90	1.90	2.38

(b)

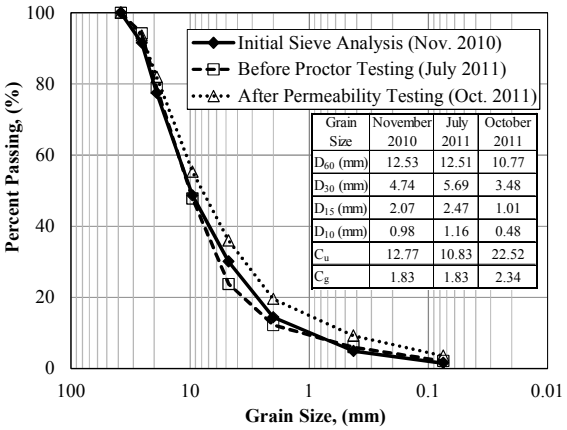

Grain Size	November 2010	July 2011	October 2011
D_{60} (mm)	12.53	12.51	10.77
D_{30} (mm)	4.74	5.69	3.48
D_{15} (mm)	2.07	2.47	1.01
D_{10} (mm)	0.98	1.16	0.48
C_u	12.77	10.83	22.52
C_g	1.83	1.83	2.34

(c)

Figure A.2.2. Gradation of base course sample from Sections a) 2 8-10 inches, b) 3 8-10 inches, and c) 4 8-10 inches below the asphalt/base course interface conducted after sampling (November 2010), conducted before proctor testing (July 2011) and conducted after hydraulic conductivity testing (October 2011).

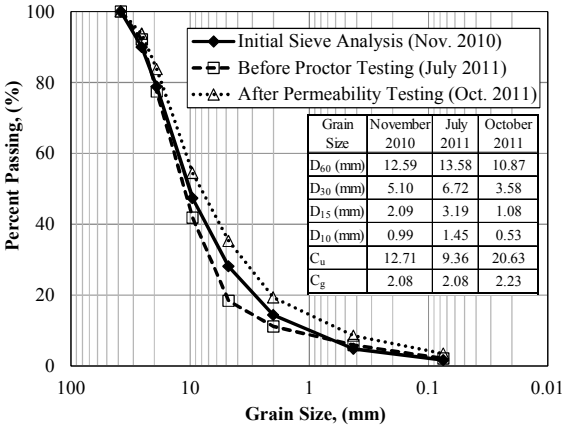

Grain Size	November 2010	July 2011	October 2011
D_{60} (mm)	12.59	13.58	10.87
D_{30} (mm)	5.10	6.72	3.58
D_{15} (mm)	2.09	3.19	1.08
D_{10} (mm)	0.99	1.45	0.53
C_u	12.71	9.36	20.63
C_g	2.08	2.08	2.23

(a)

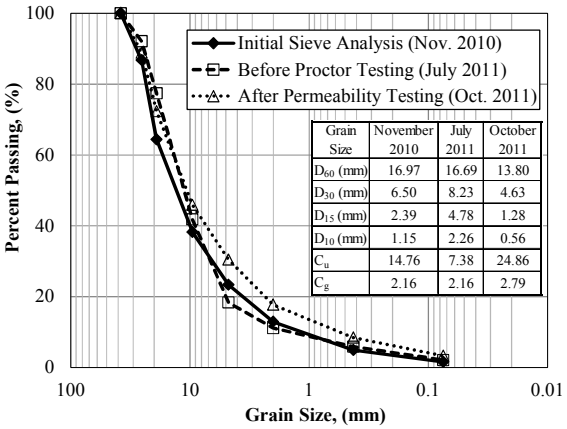

Grain Size	November 2010	July 2011	October 2011
D_{60} (mm)	16.97	16.69	13.80
D_{30} (mm)	6.50	8.23	4.63
D_{15} (mm)	2.39	4.78	1.28
D_{10} (mm)	1.15	2.26	0.56
C_u	14.76	7.38	24.86
C_g	2.16	2.16	2.79

(b)

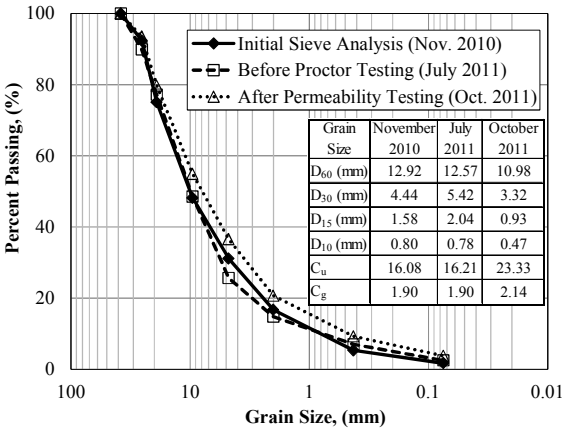

Grain Size	November 2010	July 2011	October 2011
D_{60} (mm)	12.92	12.57	10.98
D_{30} (mm)	4.44	5.42	3.32
D_{15} (mm)	1.58	2.04	0.93
D_{10} (mm)	0.80	0.78	0.47
C_u	16.08	16.21	23.33
C_g	1.90	1.90	2.14

(c)

Figure A.2.3. Gradation of base course sample from Sections a) 5 8-10 inches, b) 6 8-10 inches, and c) 8 4-6 inches below the asphalt/base course interface conducted after sampling (November 2010), conducted before proctor testing (July 2011) and conducted after hydraulic conductivity testing (October 2011).

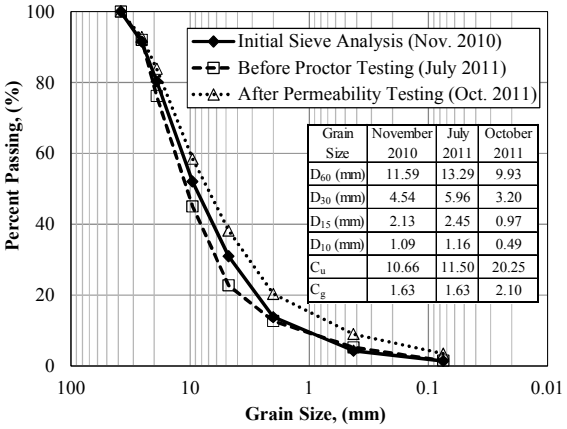

Grain Size	November 2010	July 2011	October 2011
D_{60} (mm)	11.59	13.29	9.93
D_{30} (mm)	4.54	5.96	3.20
D_{15} (mm)	2.13	2.45	0.97
D_{10} (mm)	1.09	1.16	0.49
C_u	10.66	11.50	20.25
C_g	1.63	1.63	2.10

(a)

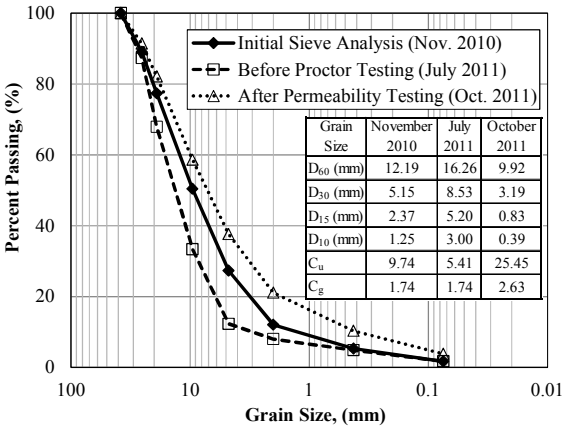

Grain Size	November 2010	July 2011	October 2011
D_{60} (mm)	12.19	16.26	9.92
D_{30} (mm)	5.15	8.53	3.19
D_{15} (mm)	2.37	5.20	0.83
D_{10} (mm)	1.25	3.00	0.39
C_u	9.74	5.41	25.45
C_g	1.74	1.74	2.63

(b)

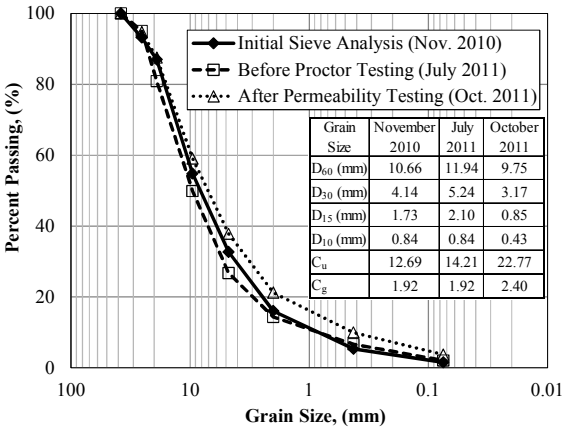

Grain Size	November 2010	July 2011	October 2011
D_{60} (mm)	10.66	11.94	9.75
D_{30} (mm)	4.14	5.24	3.17
D_{15} (mm)	1.73	2.10	0.85
D_{10} (mm)	0.84	0.84	0.43
C_u	12.69	14.21	22.77
C_g	1.92	1.92	2.40

(c)

Figure A.2.4. Gradation of base course sample from Sections a) 9 4-6 inches, b) 10 4-6 inches, and c) 11 4-6 inches below the asphalt/base course interface conducted after sampling (November 2010), conducted before proctor testing (July 2011) and conducted after hydraulic conductivity testing (October 2011).

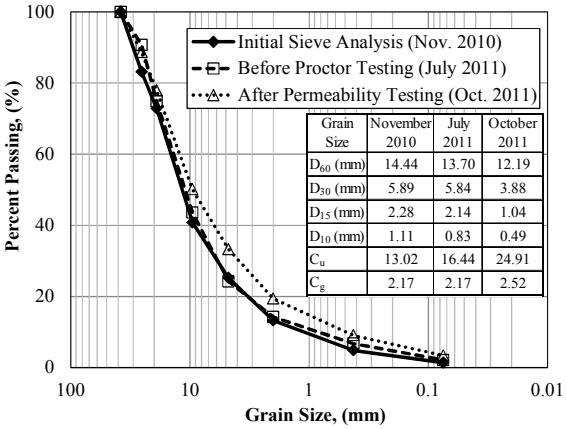

Grain Size	November 2010	July 2011	October 2011
D_{60} (mm)	14.44	13.70	12.19
D_{30} (mm)	5.89	5.84	3.88
D_{15} (mm)	2.28	2.14	1.04
D_{10} (mm)	1.11	0.83	0.49
C_u	13.02	16.44	24.91
C_g	2.17	2.17	2.52

(a)

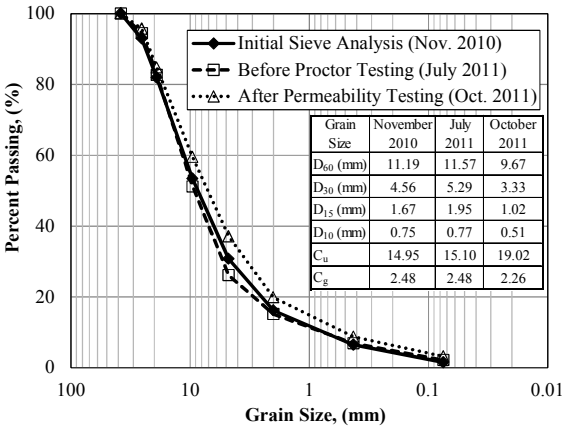

Grain Size	November 2010	July 2011	October 2011
D_{60} (mm)	11.19	11.57	9.67
D_{30} (mm)	4.56	5.29	3.33
D_{15} (mm)	1.67	1.95	1.02
D_{10} (mm)	0.75	0.77	0.51
C_u	14.95	15.10	19.02
C_g	2.48	2.48	2.26

(b)

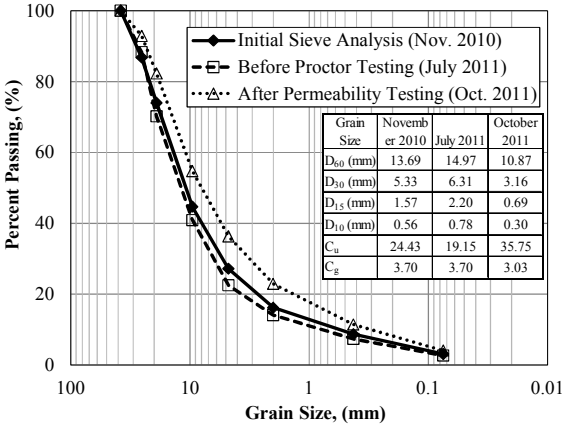

Grain Size	Novemb er 2010	July 2011	October 2011
D_{60} (mm)	13.69	14.97	10.87
D_{30} (mm)	5.33	6.31	3.16
D_{15} (mm)	1.57	2.20	0.69
D_{10} (mm)	0.56	0.78	0.30
C_u	24.43	19.15	35.75
C_g	3.70	3.70	3.03

(c)

Figure A.2.5. Gradation of base course sample from Sections a) 12 4-6 inches, b) 13 4-6 inches, and c) 13W 4-6 inches below the asphalt/base course interface conducted after sampling (November 2010), conducted before proctor testing (July 2011) and conducted after hydraulic conductivity testing (October 2011).

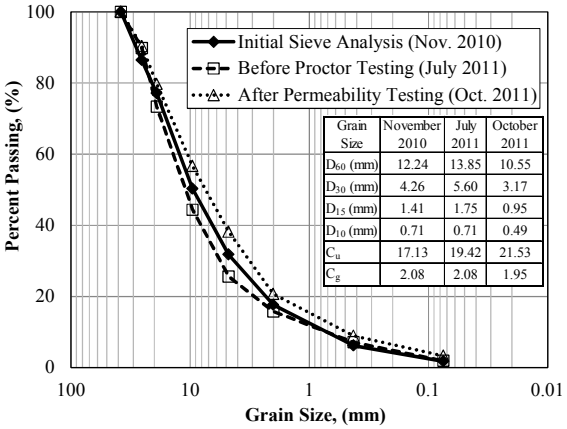

Grain Size	November 2010	July 2011	October 2011
D_{60} (mm)	12.24	13.85	10.55
D_{30} (mm)	4.26	5.60	3.17
D_{15} (mm)	1.41	1.75	0.95
D_{10} (mm)	0.71	0.71	0.49
C_u	17.13	19.42	21.53
C_g	2.08	2.08	1.95

(a)

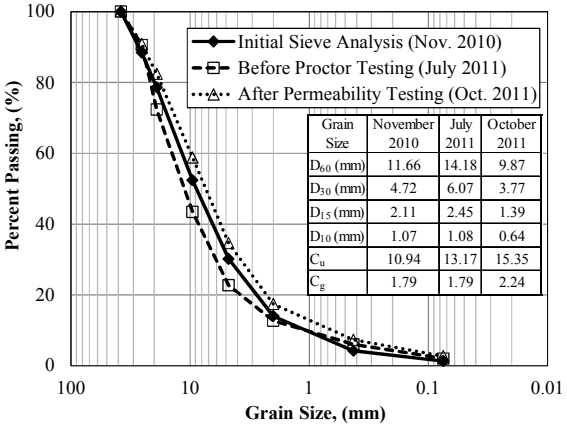

Grain Size	November 2010	July 2011	October 2011
D_{60} (mm)	11.66	14.18	9.87
D_{30} (mm)	4.72	6.07	3.77
D_{15} (mm)	2.11	2.45	1.39
D_{10} (mm)	1.07	1.08	0.64
C_u	10.94	13.17	15.35
C_g	1.79	1.79	2.24

(b)

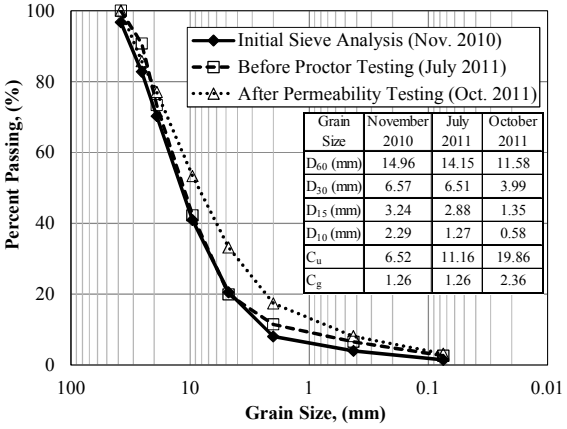

Grain Size	November 2010	July 2011	October 2011
D_{60} (mm)	14.96	14.15	11.58
D_{30} (mm)	6.57	6.51	3.99
D_{15} (mm)	3.24	2.88	1.35
D_{10} (mm)	2.29	1.27	0.58
C_u	6.52	11.16	19.86
C_g	1.26	1.26	2.36

(c)

Figure A.2.6. Gradation of base course sample from Sections a) 13A 4-6 inches, b) 13B 4-6 inches, and c) 13BW 4-6 inches below the asphalt/base course interface conducted after sampling (November 2010), conducted before proctor testing (July 2011) and conducted after hydraulic conductivity testing (October 2011).

A.3. Fines Content (Wash Sieve Method)

Table A.3.1. Fines content results for base course samples obtained from the ten inch thick sections.

Location	Depth*	Pan Wt.	Pan + Dry Wt.	Dry Wt.	Pan + Dry Wt. After Wet Sieving	Dry Wt. After Wet Sieving	% Finer than 75μm
	(inch)	(g)	(g)	(g)	(g)	(g)	(%)
Base Section 1B	0-2	234.09	1693.0	1458.9	1518.3	1284.2	12.0
Base Section 1B	2-4	235.36	1860.2	1624.8	1723.5	1488.1	8.4
Base Section 1B	4-6	240.44	1825.6	1585.2	1677.4	1437.0	9.3
Base Section 1B	6-8	233.32	1672.3	1439.0	1529.6	1296.3	9.9
Base Section 1B	8-10	297.47	1533.9	1236.4	1411.8	1114.3	9.9
Base Section 1A	0-2	297.78	1675.7	1377.9	1550.5	1252.7	9.1
Base Section 1A	2-4	238.88	1855.6	1616.7	1746.3	1507.4	6.8
Base Section 1A	4-6	301.82	1793.4	1491.6	1636.0	1334.2	10.6
Base Section 1A	6-8	301.44	2114.5	1813.1	1969.1	1667.7	8.0
Base Section 1A	8-10	298.87	1938.6	1639.7	1805.3	1506.4	8.1
Base Section 1	0-2	235.24	1672.1	1436.9	1539.6	1304.4	9.2
Base Section 1	2-4	296.29	1750.0	1453.7	1610.5	1314.2	9.6
Base Section 1	4-6	297.05	1766.1	1469.1	1675.8	1378.8	6.1
Base Section 1	6-8	298.66	2074.1	1775.4	1913.3	1614.6	9.1
Base Section 1	8-10	234.50	1664.5	1430.0	1545.5	1311.0	8.3
Base Section 2	0-2	302.35	1758.7	1456.4	1624.6	1322.3	9.2
Base Section 2	2-4	300.63	1750.7	1450.1	1586.1	1285.5	11.4
Base Section 2	4-6	297.70	1730.5	1432.8	1612.5	1314.8	8.2
Base Section 2	6-8	239.19	1863.7	1624.5	1707.9	1468.7	9.6
Base Section 2	8-10	235.25	1876.5	1641.3	1753.0	1517.8	7.5
Base Section 3	0-2	301.32	1890.4	1589.1	1729.3	1428.0	10.1
Base Section 3	2-4	299.62	1753.7	1454.1	1633.0	1333.4	8.3
Base Section 3	4-6	239.42	1636.5	1397.1	1493.0	1253.6	10.3
Base Section 3	6-8	236.98	1900.6	1663.6	1773.5	1536.5	7.6
Base Section 3	8-10	240.80	1848.8	1608.0	1723.3	1482.5	7.8
Base Section 4	0-2	297.50	1732.9	1435.4	1628.0	1330.5	7.3
Base Section 4	2-4	300.15	1675.5	1375.4	1518.6	1218.5	11.4
Base Section 4	4-6	238.92	1757.6	1518.7	1634.7	1395.8	8.1
Base Section 4	6-8	235.81	1805.5	1569.7	1621.6	1385.8	11.7
Base Section 4	8-10	233.49	1906.2	1672.7	1779.0	1545.5	7.6
Base Section 5	0-2	296.17	1384.7	1088.5	1273.6	977.4	10.2
Base Section 5	2-4	297.74	1547.0	1249.3	1440.0	1142.3	8.6
Base Section 5	4-6	300.88	1731.0	1430.1	1571.0	1270.1	11.2
Base Section 5	6-8	234.28	1664.6	1430.3	1533.9	1299.6	9.1
Base Section 5	8-10	298.11	2085.1	1787.0	1957.1	1659.0	7.2
Base Section 6	0-2	297.70	2180.2	1882.5	1945.0	1647.3	12.5
Base Section 6	2-4	239.14	1699.1	1460.0	1562.9	1323.8	9.3
Base Section 6	4-6	235.21	1843.4	1608.2	1703.4	1468.2	8.7
Base Section 6	6-8	296.95	1597.3	1300.4	1482.3	1185.4	8.8
Base Section 6	8-10	297.53	1970.0	1672.5	1790.8	1493.3	10.7

*Depth below asphalt/base course interface

Table A.3.2. Fines content results for base course samples obtained from the six inch thick sections.

Location	Depth*	Pan Wt.	Pan + Dry Wt.	Dry Wt.	Pan + Dry Wt. After Wet Sieving	Dry Wt. After Wet Sieving	% Finer than 75μm
	(inch)	(g)	(g)	(g)	(g)	(g)	(%)
Base Section 8	0-2	302.34	1842.1	1539.8	1688.0	1385.7	10.0
Base Section 8	2-4	300.63	2081.5	1780.9	1934.8	1634.2	8.2
Base Section 8	4-6	300.79	1918.8	1618.0	1739.1	1438.3	11.1
Base Section 9	0-2	239.26	1700.6	1461.3	1545.5	1306.2	10.6
Base Section 9	2-4	237.01	1751.6	1514.6	1592.0	1355.0	10.5
Base Section 9	4-6	234.29	1852.0	1617.7	1685.8	1451.5	10.3
Base Section 10	0-2	301.32	1840.6	1539.3	1659.6	1358.3	11.8
Base Section 10	2-4	299.60	1584.9	1285.3	1450.7	1151.1	10.4
Base Section 10	4-6	300.14	2305.7	2005.6	2127.3	1827.2	8.9
Base Section 11	0-2	301.82	1636.3	1334.5	1528.0	1226.2	8.1
Base Section 11	2-4	235.88	1545.4	1309.5	1410.3	1174.4	10.3
Base Section 11	4-6	238.97	1993.9	1754.9	1861.0	1622.0	7.6
Base Section 12	0-2	234.28	1579.7	1345.4	1458.8	1224.5	9.0
Base Section 12	2-4	297.50	2051.4	1753.9	1897.4	1599.9	8.8
Base Section 12	4-6	297.35	1953.2	1655.9	1830.7	1533.4	7.4
Base Section 13	0-2	300.15	2082.9	1782.8	1887.0	1586.9	11.0
Base Section 13	2-4	238.93	1515.7	1276.8	1396.9	1158.0	9.3
Base Section 13	4-6	299.01	2169.0	1870.0	1972.8	1673.8	10.5
Base Section 13W	0-2	234.02	1657.6	1423.6	1501.7	1267.7	10.95
Base Section 13W	2-4	235.19	1637.5	1402.3	1494.9	1259.7	10.17
Base Section 13W	4-6	234.72	1604.2	1369.5	1533.8	1299.1	5.14
Base Section 13A	0-2	300.88	1859.1	1558.2	1710.1	1409.2	9.6
Base Section 13A	2-4	297.74	1902.4	1604.7	1758.1	1460.4	9.0
Base Section 13A	4-6	234.43	1987.3	1752.9	1854.4	1620.0	7.6
Base Section 13B	0-2	240.47	1616.5	1376.0	1483.8	1243.3	9.6
Base Section 13B	2-4	233.26	2050.7	1817.4	1840.3	1607.0	11.6
Base Section 13B	4-6	233.80	1896.1	1662.3	1750.3	1516.5	8.8
Base Section 13BW	0-2	298.60	1706.1	1407.5	1523.1	1224.5	13.0
Base Section 13BW	2-4	297.02	1580.5	1283.5	1424.6	1127.6	12.1
Base Section 13BW	4-6	235.65	1776.7	1541.1	1635.2	1399.6	9.2

*Depth below asphalt/base course interface

Table A.3.3. Fines content results for subgrade samples obtained from the ten inch thick sections.

Location	Depth*	Can + Dry Wt.	Dry Wt. Before Wet Sieving	Bowl Wt.	Bowl+ Dry Wt.	Dry Wt. After Wet Sieving	% Finer than 75µm
	(inch)	(g)	(g)	(g)	(g)	(g)	(%)
Subgrade Section 1B	0-2	114.16	85.32	204.05	240.97	36.92	56.73
Subgrade Section 1B	2-4	114.76	87.46	203.00	244.28	41.28	52.80
Subgrade Section 1B	4-6	116.86	89.30	204.94	243.80	38.86	56.48
Subgrade Section 1A	0-2	117.01	89.59	227.61	266.65	39.04	56.42
Subgrade Section 1A	2-4	125.16	92.87	204.07	268.66	64.59	30.45
Subgrade Section 1A	4-6	114.16	86.85	206.34	246.26	39.92	54.04
Subgrade Section 1	0-2	123.54	95.71	195.99	224.00	28.01	70.73
Subgrade Section 1	2-4	122.60	94.76	176.71	210.35	33.64	64.50
Subgrade Section 1	4-6	125.91	93.01	206.59	235.45	28.86	68.97
Subgrade Section 2	0-2	112.32	85.13	277.39	304.27	26.88	68.42
Subgrade Section 2	2-4	122.00	89.73	277.94	304.02	26.08	70.94
Subgrade Section 2	4-6	107.49	78.63	269.95	294.45	24.50	68.84
Subgrade Section 3	0-2	119.70	87.62	274.65	301.78	27.13	69.04
Subgrade Section 3	2-4	118.21	86.41	276.48	304.39	27.91	67.70
Subgrade Section 3	4-6	118.36	89.29	274.60	295.78	21.18	76.28
Subgrade Section 4	0-2	115.67	87.27	277.37	303.43	26.06	70.14
Subgrade Section 4	2-4	117.08	84.44	274.62	300.26	25.64	69.64
Subgrade Section 4	4-6	114.96	82.94	277.95	307.87	29.92	63.93
Subgrade Section 5	0-2	117.48	85.21	271.21	303.45	32.24	62.16
Subgrade Section 5	2-4	117.19	88.18	279.41	315.95	36.54	58.56
Subgrade Section 5	4-6	113.31	81.53	282.51	302.35	19.84	75.67
Subgrade Section 6	0-2	116.98	84.92	277.38	305.65	28.27	66.71
Subgrade Section 6	2-4	117.81	85.32	271.92	292.35	20.43	76.05
Subgrade Section 6	4-6	112.40	83.64	272.74	294.02	21.28	74.56

*Depth below base course/subgrade interface

Table A.3.4. Fines content results for subgrade samples obtained from the six inch thick sections.

Location	Depth*	Can + Dry Wt.	Dry Wt. Before Wet Sieving	Bowl Wt.	Bowl+ Dry Wt.	Dry Wt. After Wet Sieving	% Finer than 75µm
	(inch)	(g)	(g)	(g)	(g)	(g)	(%)
Subgrade Section 8	0-2	112.58	85.04	279.64	309.67	30.03	64.69
Subgrade Section 8	2-4	119.59	92.09	277.94	304.15	26.21	71.54
Subgrade Section 8	4-6	123.49	91.41	277.30	302.32	25.02	72.63
Subgrade Section 9	0-2	114.63	87.23	278.92	310.74	31.82	63.52
Subgrade Section 9	2-4	112.16	85.02	275.02	307.23	32.21	62.11
Subgrade Section 9	4-6	113.65	86.30	273.65	299.80	26.15	69.70
Subgrade Section 10	0-2	121.41	88.92	227.58	263.28	35.70	59.85
Subgrade Section 10	2-4	133.66	101.14	206.32	234.99	28.67	71.65
Subgrade Section 10	4-6	113.81	86.38	195.98	229.49	33.51	61.21
Subgrade Section 11	0-2	123.54	91.52	176.71	207.51	30.80	66.35
Subgrade Section 11	2-4	116.71	88.03	206.58	249.30	42.72	51.47
Subgrade Section 11	4-6	109.96	81.23	204.02	221.00	16.98	79.10
Subgrade Section 12	0-2	127.58	98.95	202.98	256.48	53.50	45.93
Subgrade Section 12	2-4	123.27	96.02	269.96	326.25	56.29	41.38
Subgrade Section 12	4-6	117.52	89.65	279.39	332.70	53.31	40.54
Subgrade Section 13	0-2	115.01	87.56	204.93	229.08	24.15	72.42
Subgrade Section 13	2-4	112.93	80.36	204.07	212.97	8.90	88.92
Subgrade Section 13	4-6	116.58	88.07	277.39	288.64	11.25	87.23
Subgrade Section 13W	0-2	112.53	85.25	277.94	310.91	32.97	61.33
Subgrade Section 13W	2-4	116.61	84.34	274.60	301.52	26.92	68.08
Subgrade Section 13W	4-6	112.50	83.98	276.46	291.40	14.94	82.21
Subgrade Section 13A	0-2	118.26	86.20	274.58	293.40	18.82	78.17
Subgrade Section 13A	2-4	111.45	83.01	277.36	327.30	49.94	39.84
Subgrade Section 13A	4-6	105.21	77.73	277.92	284.96	7.04	90.94
Subgrade Section 13B	0-2	121.00	89.19	272.73	308.30	35.57	60.12
Subgrade Section 13B	2-4	109.93	82.64	279.65	317.98	38.33	53.62
Subgrade Section 13B	4-6	121.38	93.71	277.95	326.21	48.26	48.50
Subgrade Section 13BW	0-2	111.37	82.42	277.30	297.58	20.28	75.39
Subgrade Section 13BW	2-4	118.58	90.96	278.92	300.00	21.08	76.82
Subgrade Section 13BW	4-6	124.99	97.32	275.05	323.27	48.22	50.45

*Depth below base course/subgrade interface

A.4. Base Course Hydrometer (percentages normalized by percent passing No. 200 sieve from entire sample)

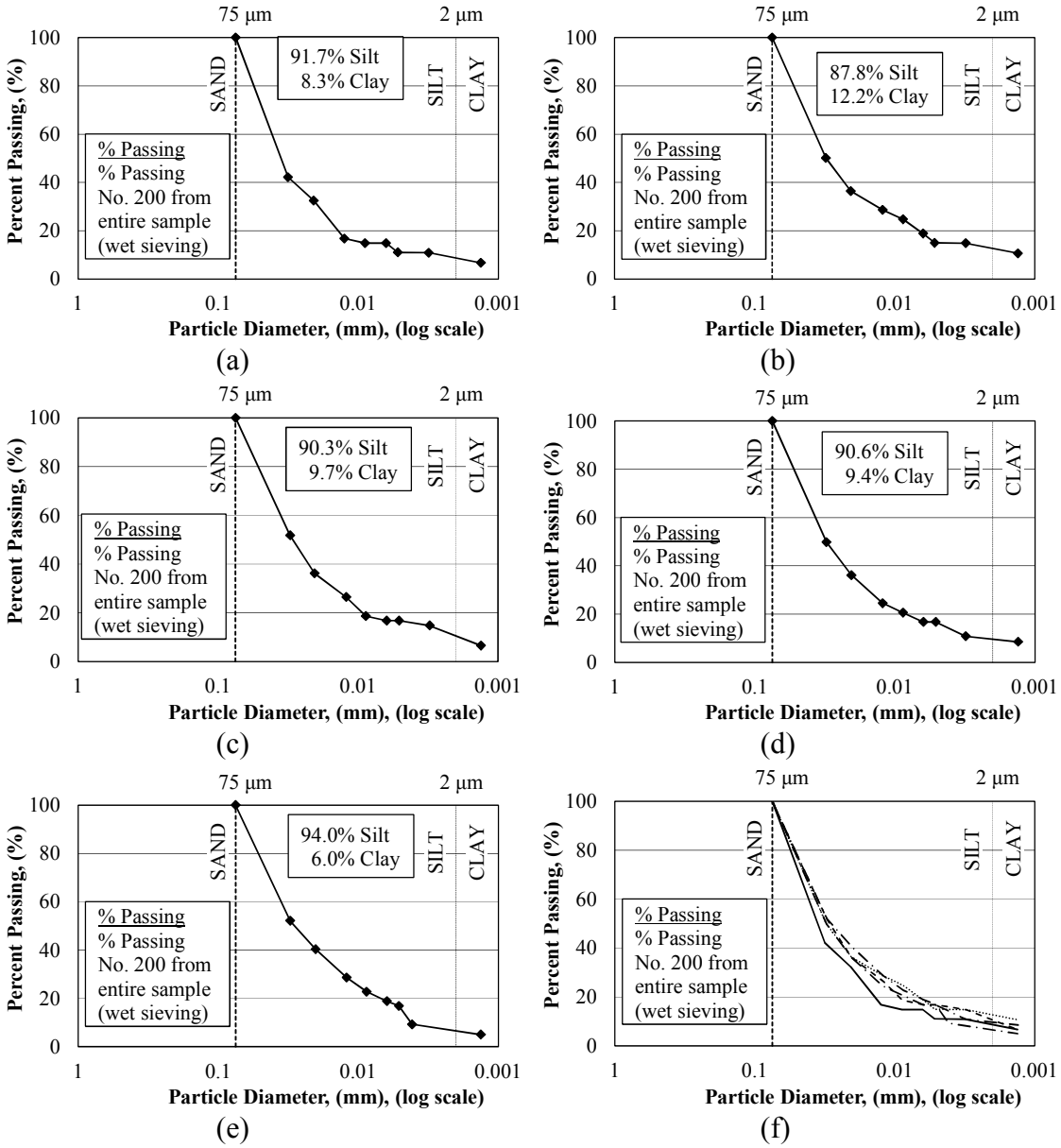

Figure A.4.1. Results obtained from hydrometer testing conducted to determine silt and clay contents (of the fine particles) in the base course samples obtained from Section 1B at depths of: a) 0-2 inches, b) 2-4 inches, c) 4-6 inches, d) 6-8 inches, and e) 8-10 inches, and f) all depths below the asphalt/base course interface.

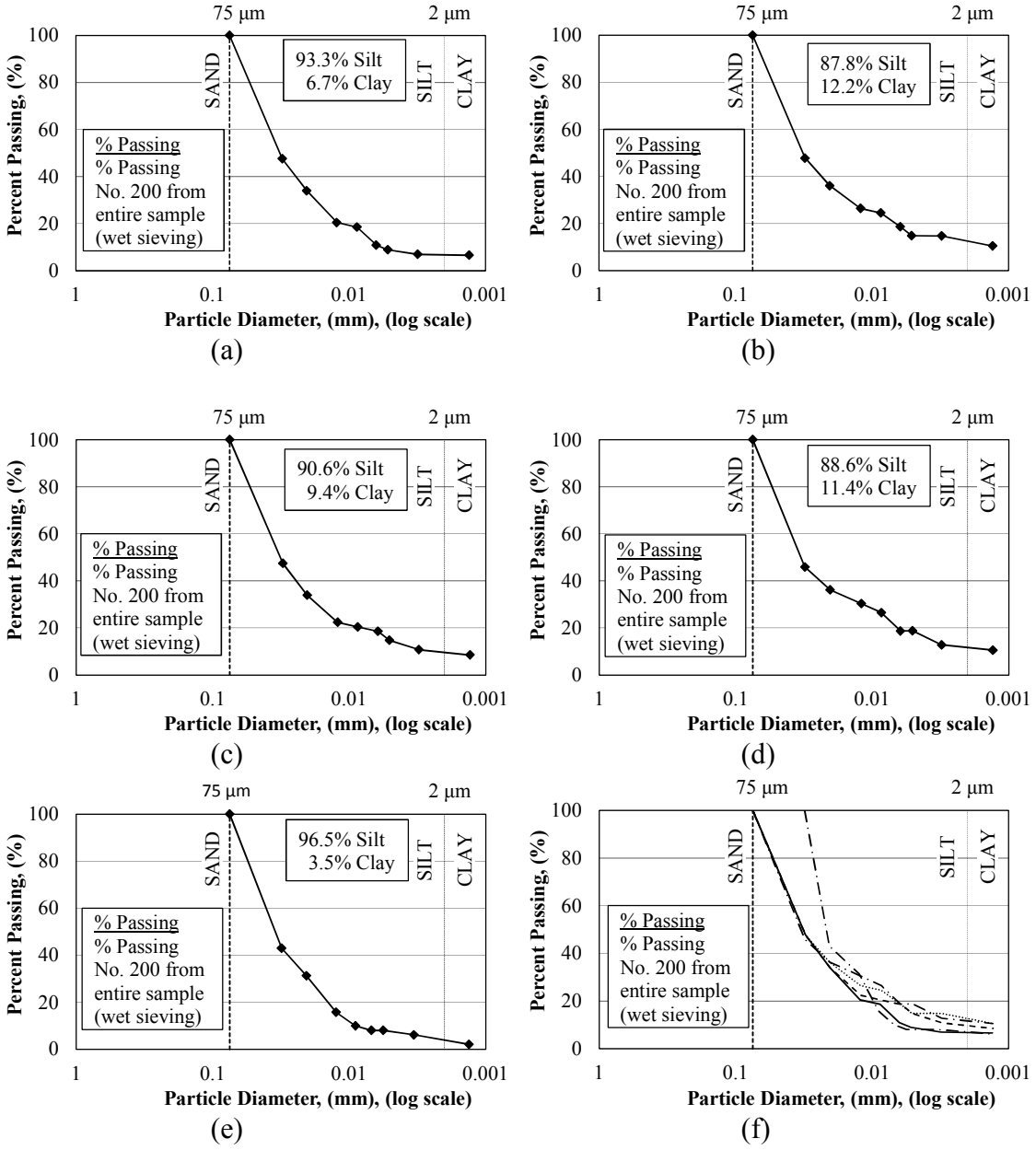

Figure A.4.2. Results obtained from hydrometer testing conducted to determine silt and clay contents (of the fine particles) in the base course samples obtained from Section 1A at depths of: a) 0-2 inches, b) 2-4 inches, c) 4-6 inches, d) 6-8 inches, and e) 8-10 inches, and f) all depths below the asphalt/base course interface.

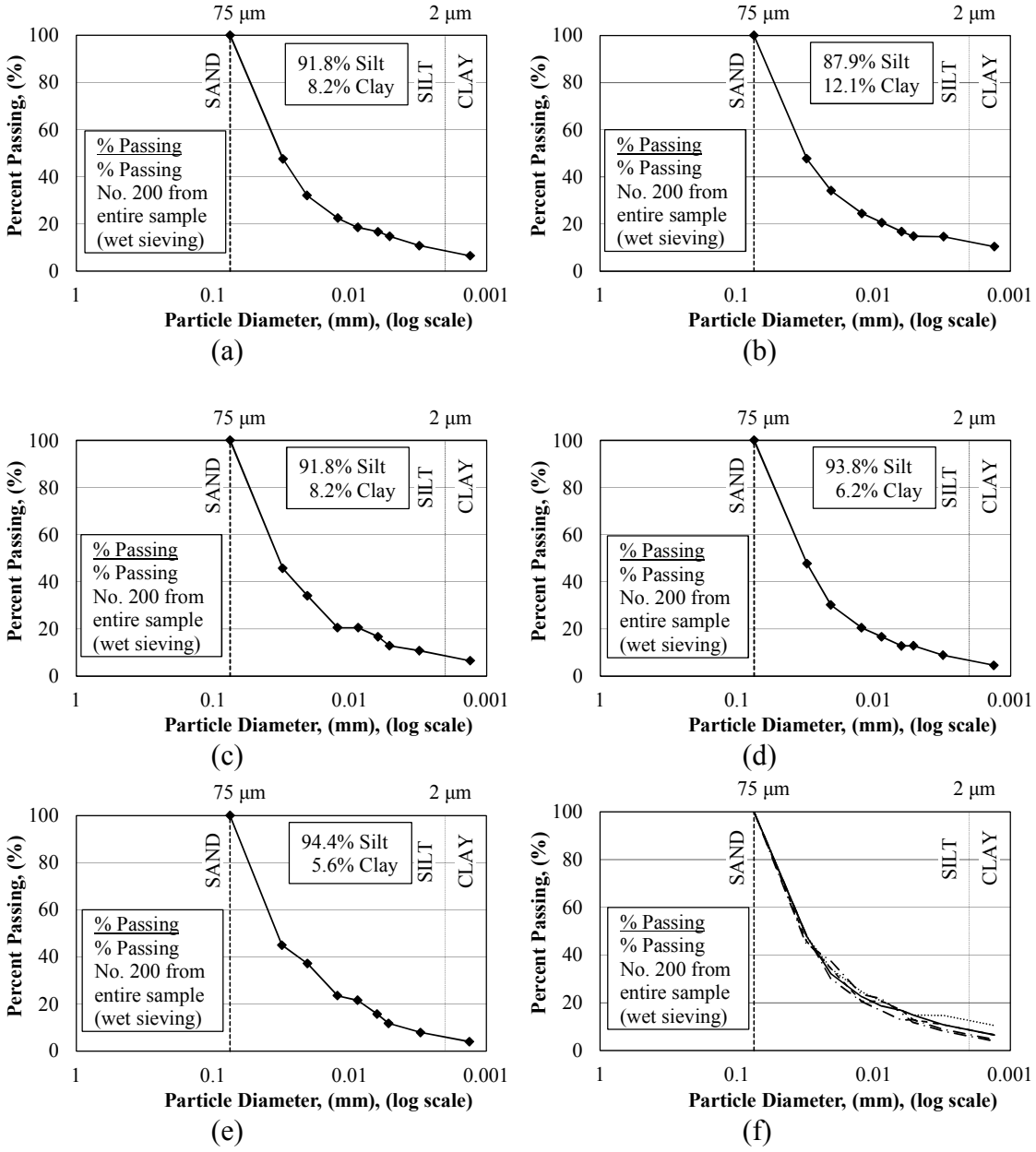

Figure A.4.3. Results obtained from hydrometer testing conducted to determine silt and clay contents (of the fine particles) in the base course samples obtained from Section 1 at depths of: a) 0-2 inches, b) 2-4 inches, c) 4-6 inches, d) 6-8 inches, and e) 8-10 inches, and f) all depths below the asphalt/base course interface.

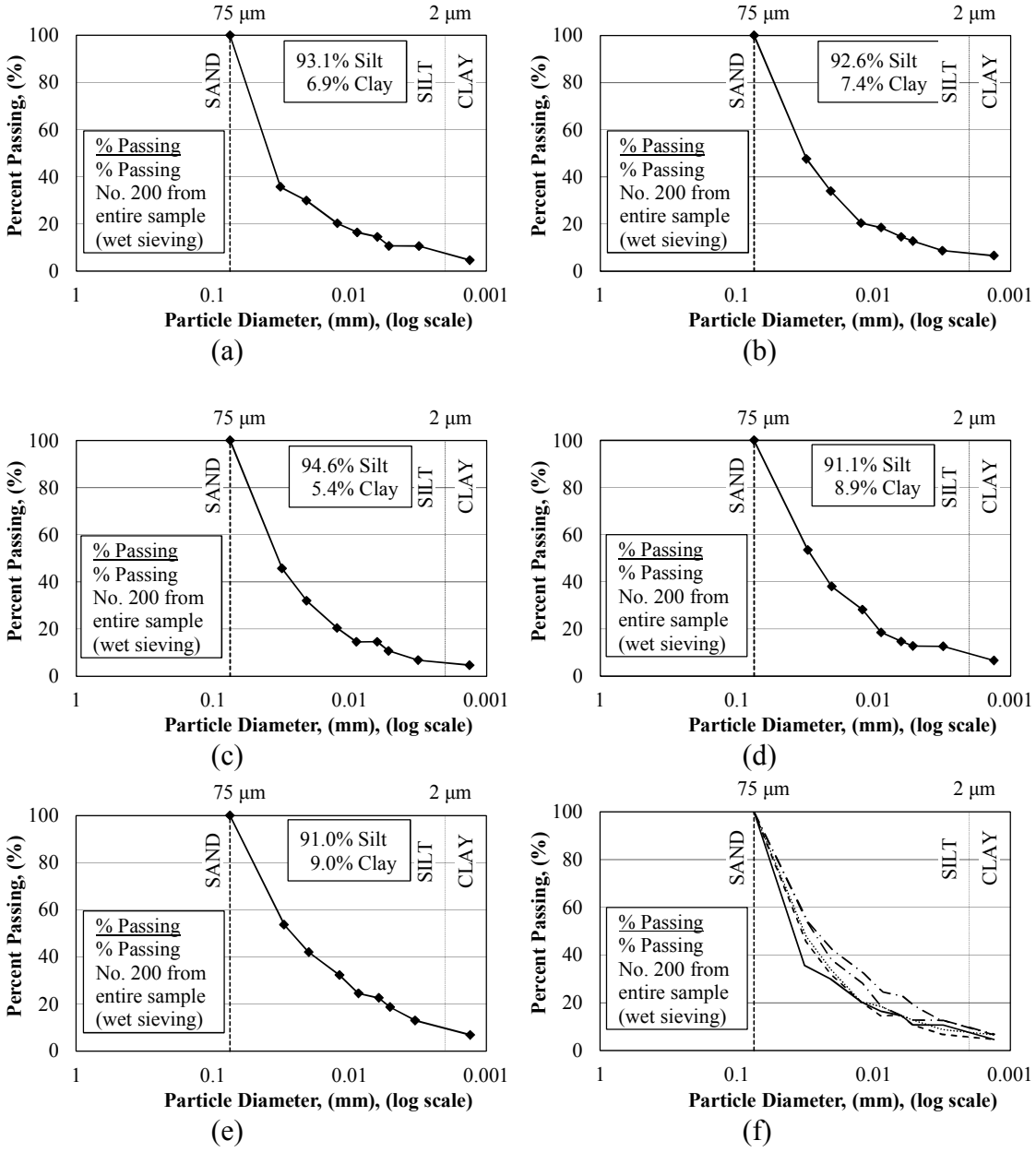

Figure A.4.4. Results obtained from hydrometer testing conducted to determine silt and clay contents (of the fine particles) in the base course samples obtained from Section 2 at depths of: a) 0-2 inches, b) 2-4 inches, c) 4-6 inches, d) 6-8 inches, and e) 8-10 inches, and f) all depths below the asphalt/base course interface.

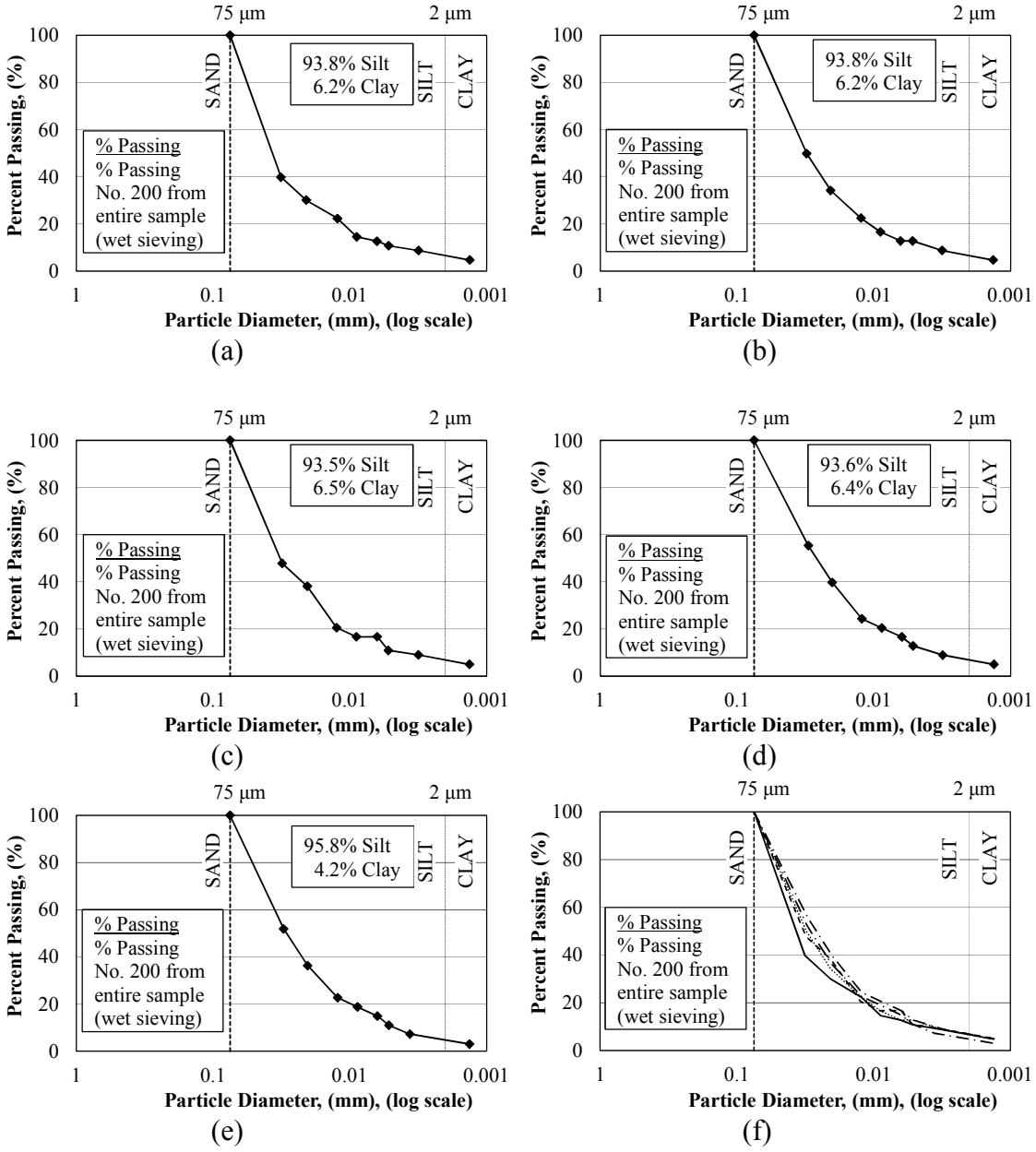

Figure A.4.5. Results obtained from hydrometer testing conducted to determine silt and clay contents (of the fine particles) in the base course samples obtained from Section 3 at depths of: a) 0-2 inches, b) 2-4 inches, c) 4-6 inches, d) 6-8 inches, and e) 8-10 inches, and f) all depths below the asphalt/base course interface.

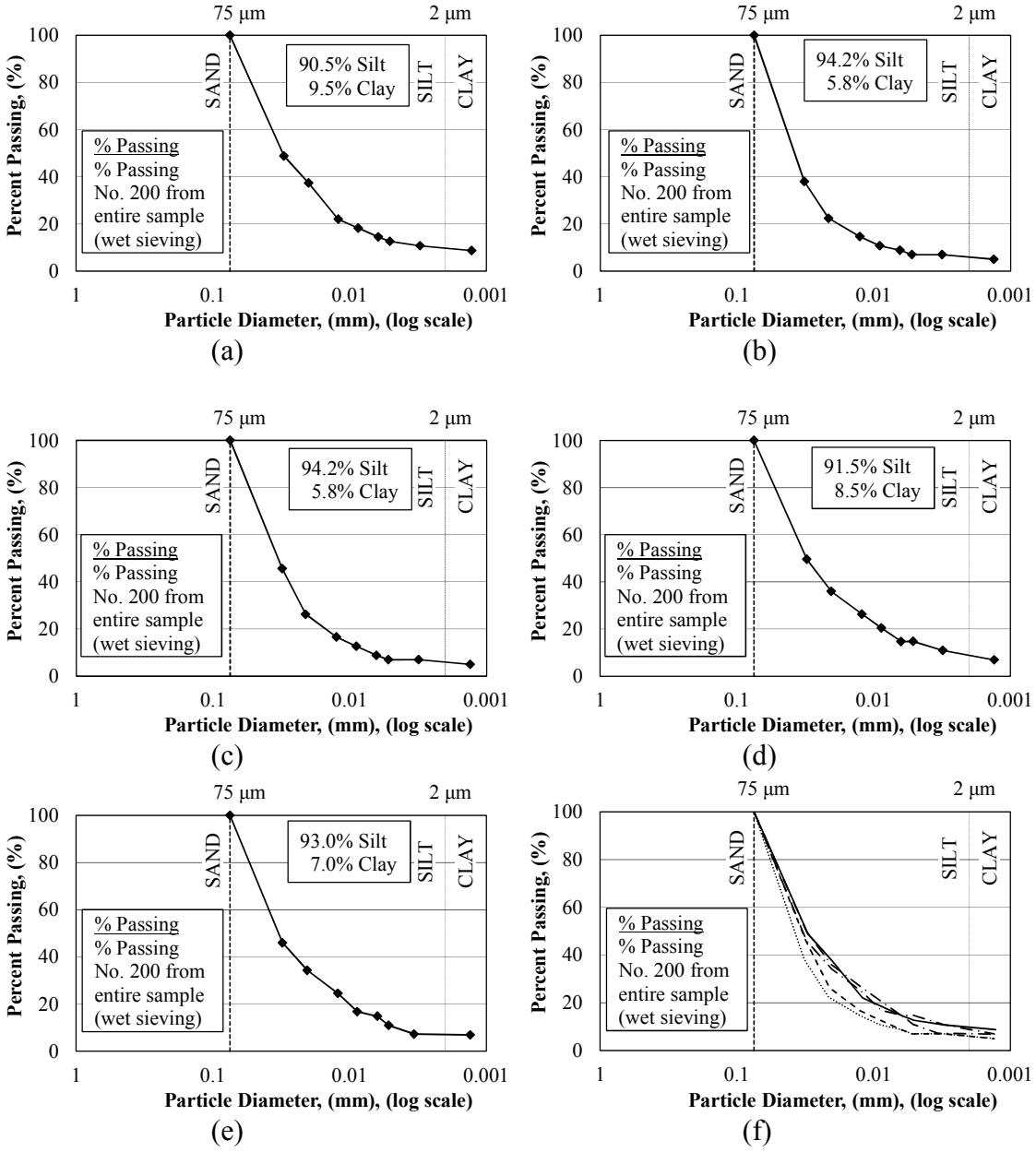

Figure A.4.6. Results obtained from hydrometer testing conducted to determine silt and clay contents (of the fine particles) in the base course samples obtained from Section 4 at depths of: a) 0-2 inches, b) 2-4 inches, c) 4-6 inches, d) 6-8 inches, and e) 8-10 inches, and f) all depths below the asphalt/base course interface.

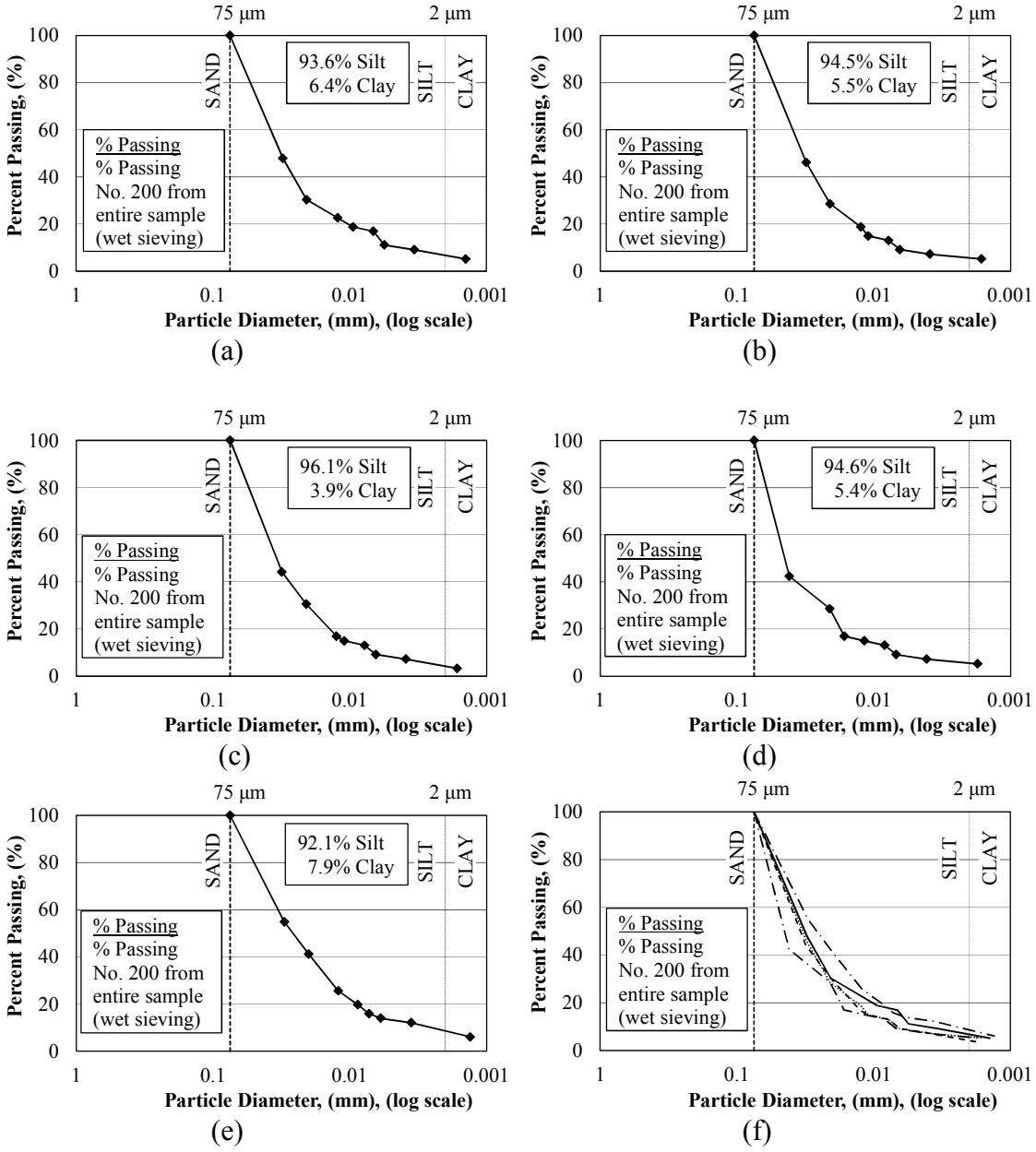

Figure A.4.7. Results obtained from hydrometer testing conducted to determine silt and clay contents (of the fine particles) in the base course samples obtained from Section 5 at depths of: a) 0-2 inches, b) 2-4 inches, c) 4-6 inches, d) 6-8 inches, and e) 8-10 inches, and f) all depths below the asphalt/base course interface.

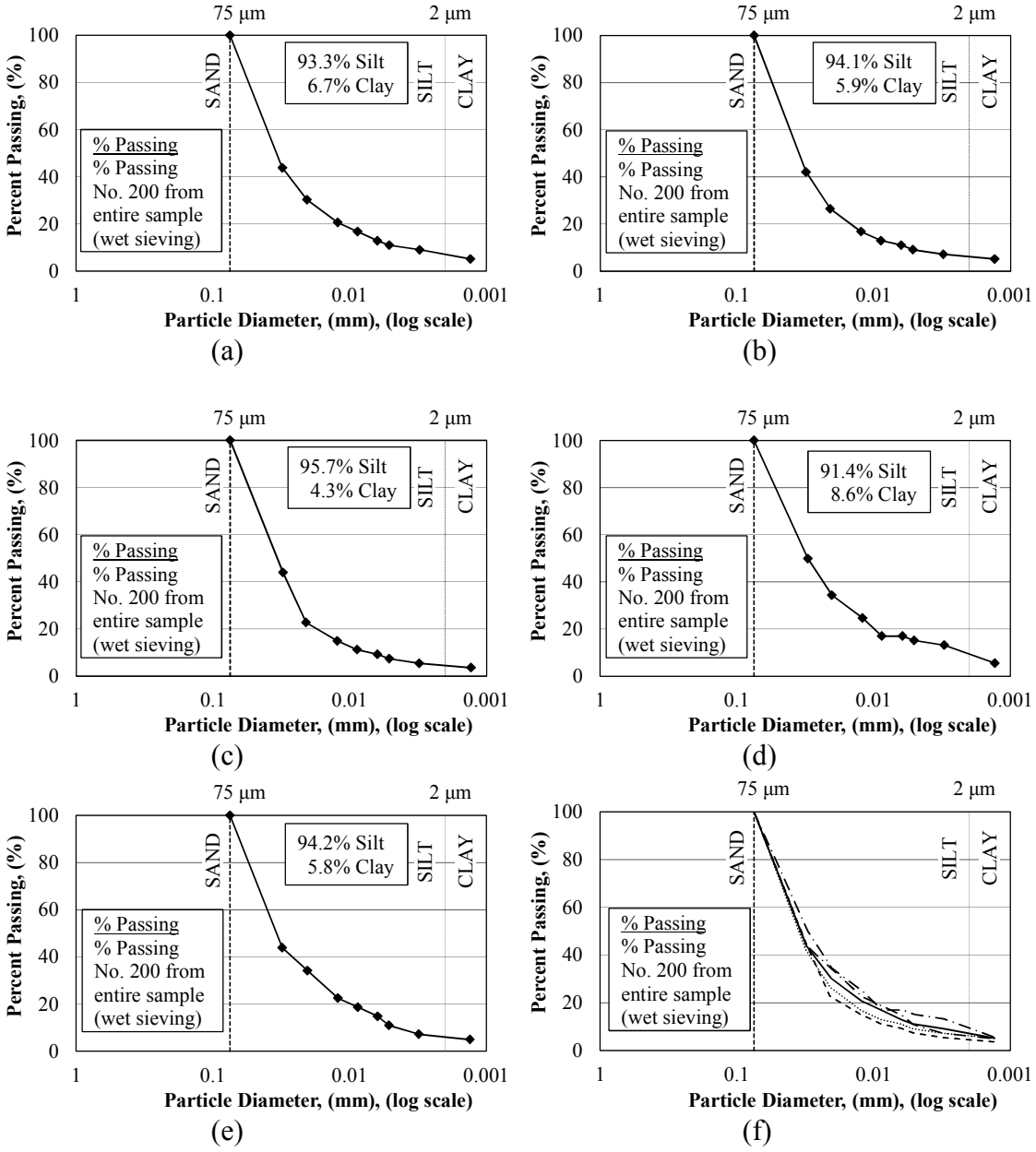

Figure A.4.8. Results obtained from hydrometer testing conducted to determine silt and clay contents (of the fine particles) in the base course samples obtained from Section 6 at depths of: a) 0-2 inches, b) 2-4 inches, c) 4-6 inches, d) 6-8 inches, and e) 8-10 inches, and f) all depths below the asphalt/base course interface.

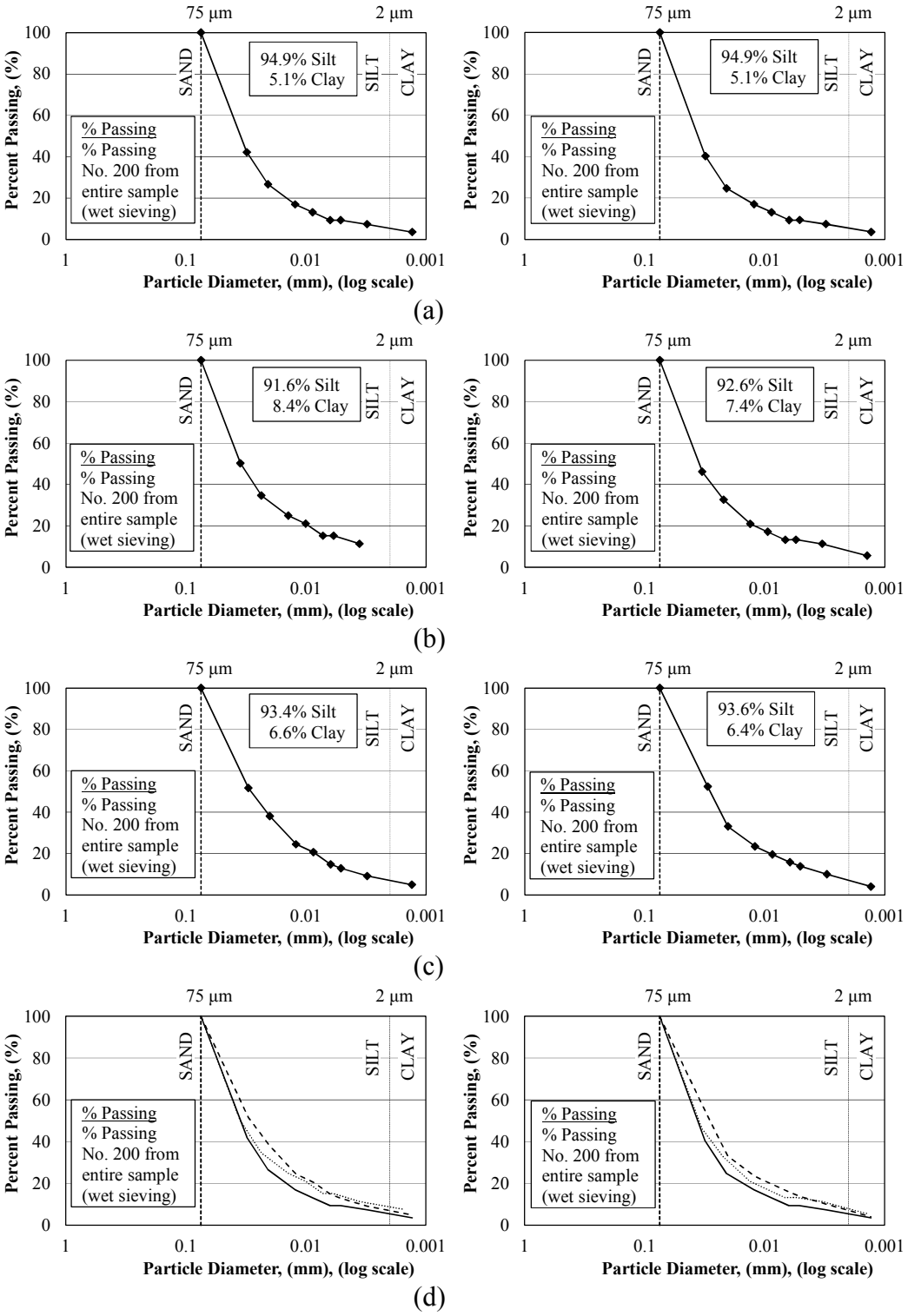

Figure A.4.9. Results obtained from hydrometer testing conducted to determine silt and clay contents (of the fine particles) in the base course samples obtained from Section 8 (left) and 9 (right) from depths of: a) 0-2 inches, b) 2-4 inches, c) 4-6 inches, and d) all depths below the asphalt/base course interface.

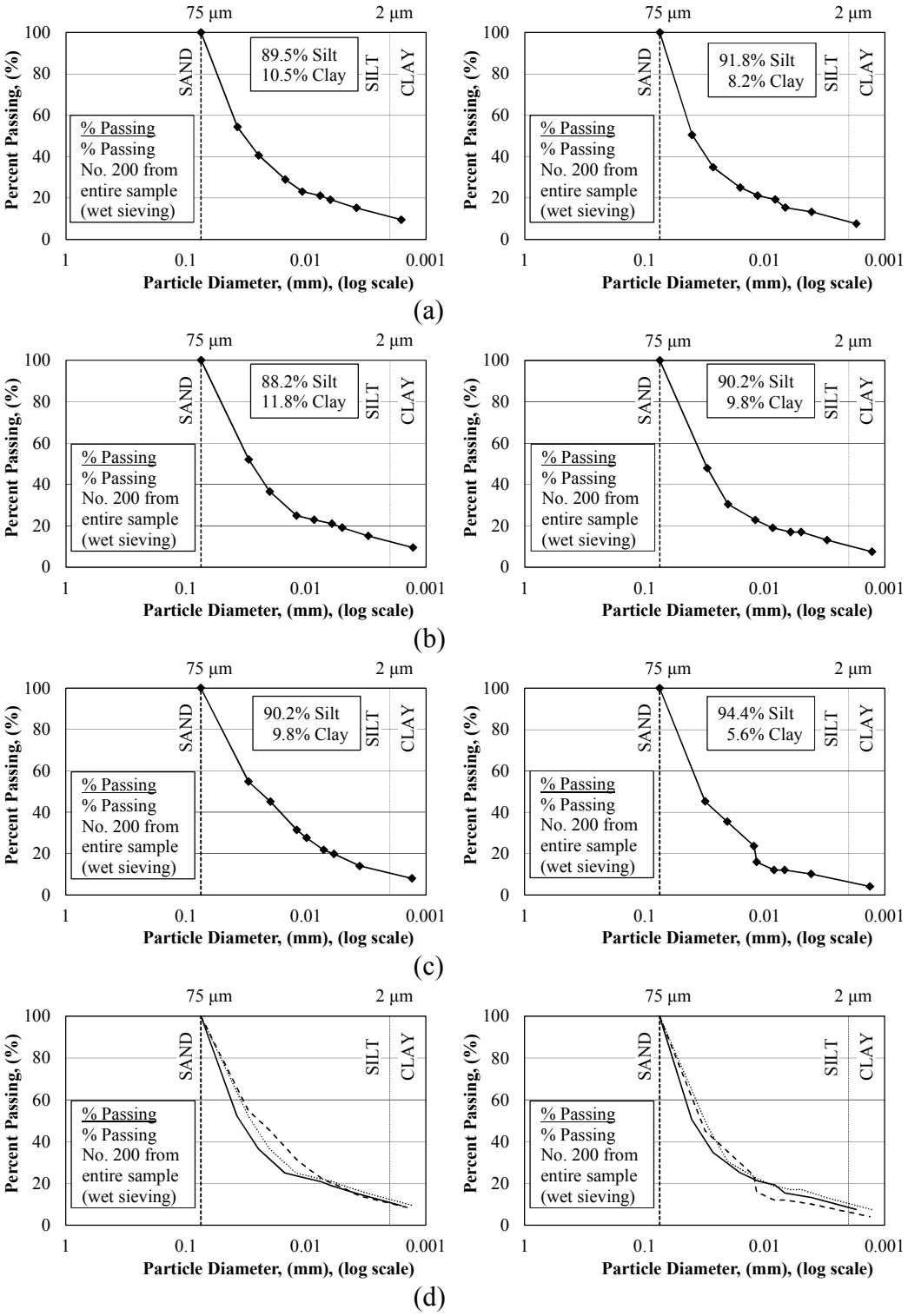

Figure A.4.10. Results obtained from hydrometer testing conducted to determine silt and clay contents (of the fine particles) in the base course samples obtained from Section 10 (left) and 11 (right) from depths of: a) 0-2 inches, b) 2-4 inches, c) 4-6 inches, and d) all depths below the asphalt/base course interface.

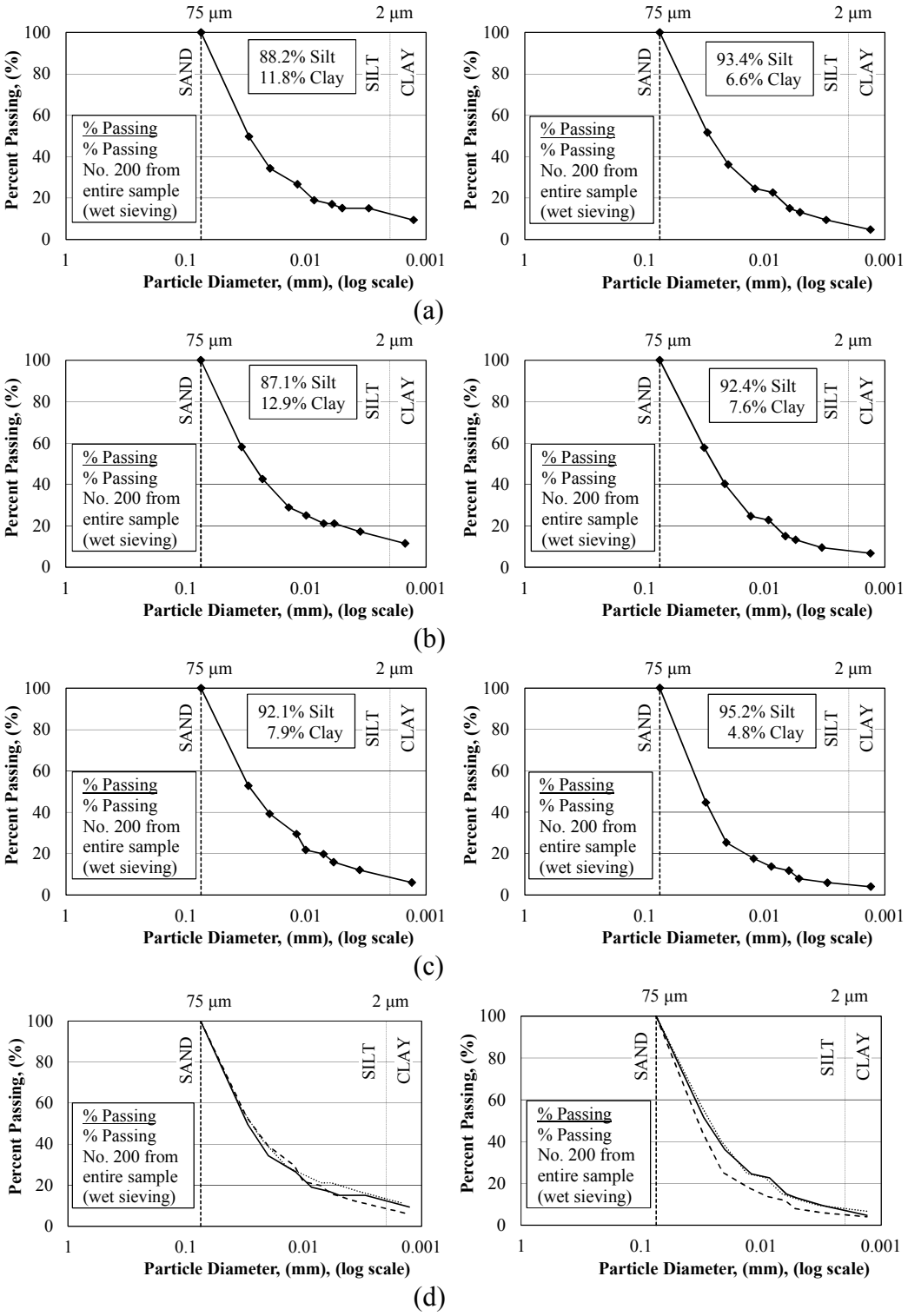

Figure A.4.11. Results obtained from hydrometer testing conducted to determine silt and clay contents (of the fine particles) in the base course samples obtained from Section 12 (left) and 13 (right) from depths of: a) 0-2 inches, b) 2-4 inches, c) 4-6 inches, and d) all depths below the asphalt/base course interface.

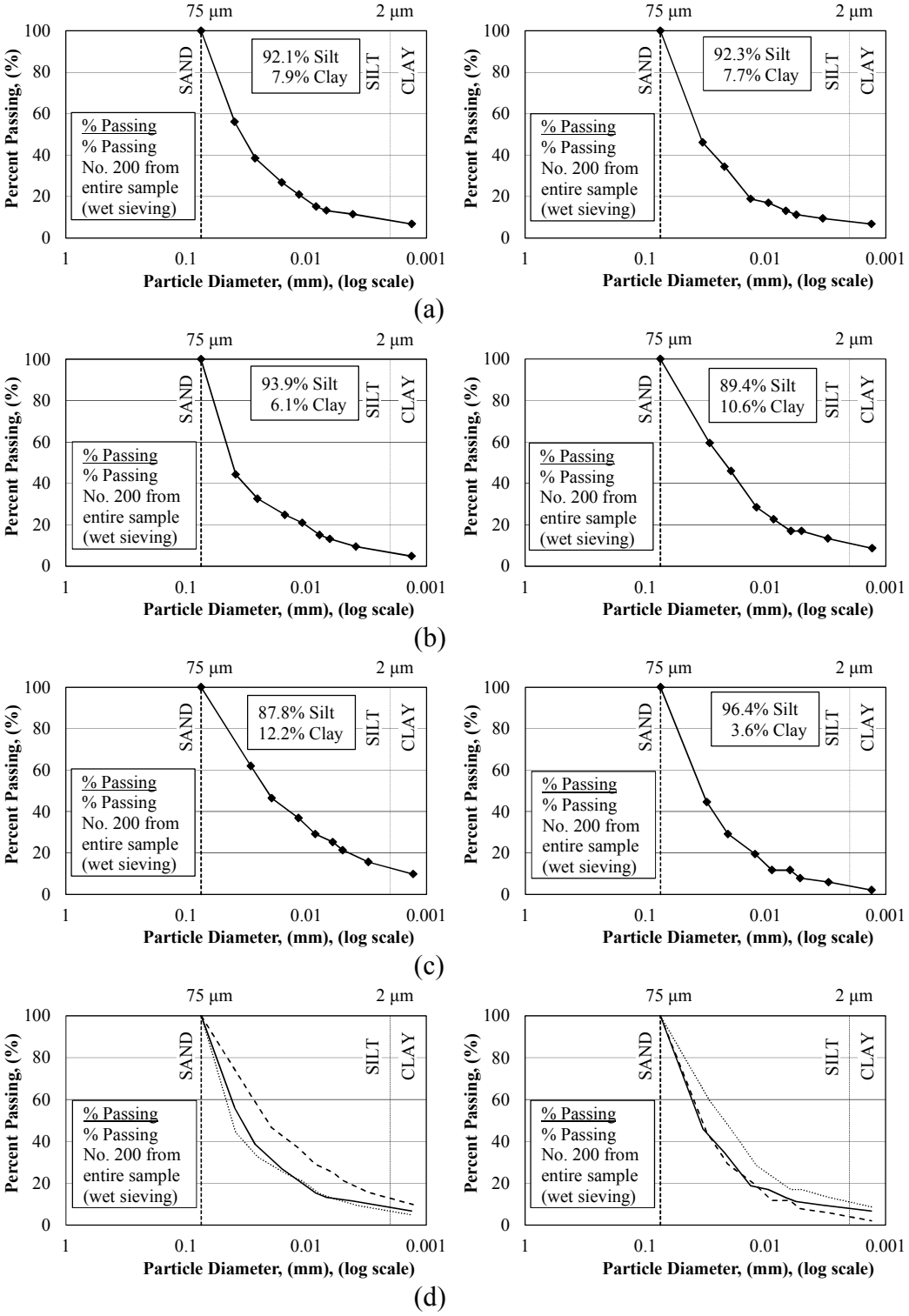

Figure A.4.12. Results obtained from hydrometer testing conducted to determine silt and clay contents (of the fine particles) in the base course samples obtained from Section 13W (left) and 13A (right) from depths of: a) 0-2 inches, b) 2-4 inches, c) 4-6 inches, and d) all depths below the asphalt/base course interface.

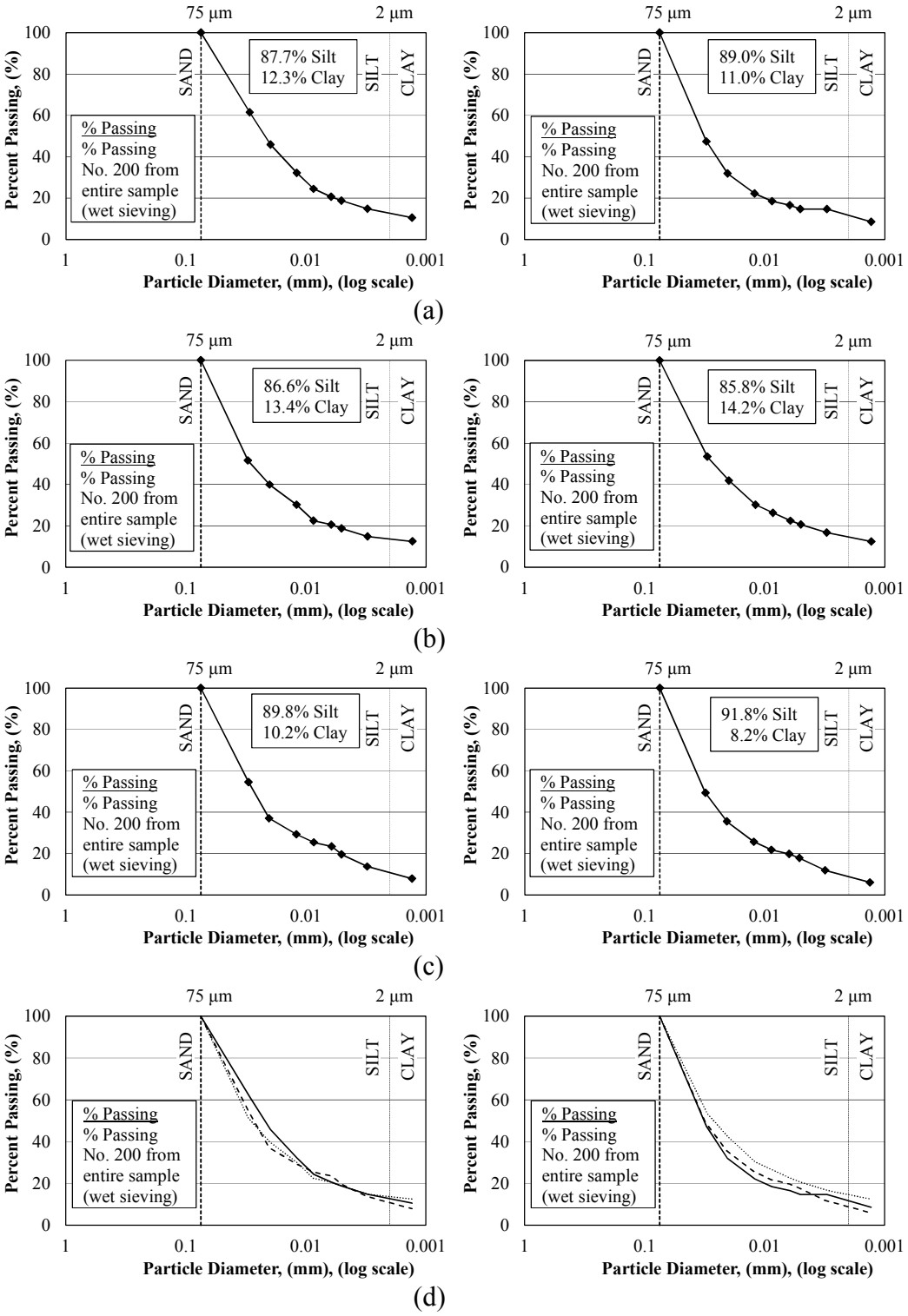

Figure A.4.13. Results obtained from hydrometer testing conducted to determine silt and clay contents (of the fine particles) in the base course samples obtained from Section 13B (left) and 13BW (right) from depths of: a) 0-2 inches, b) 2-4 inches, c) 4-6 inches, and d) all depths below the asphalt/base course interface.

A.5. Base Course Hydrometer (normalized by weight of entire sample)

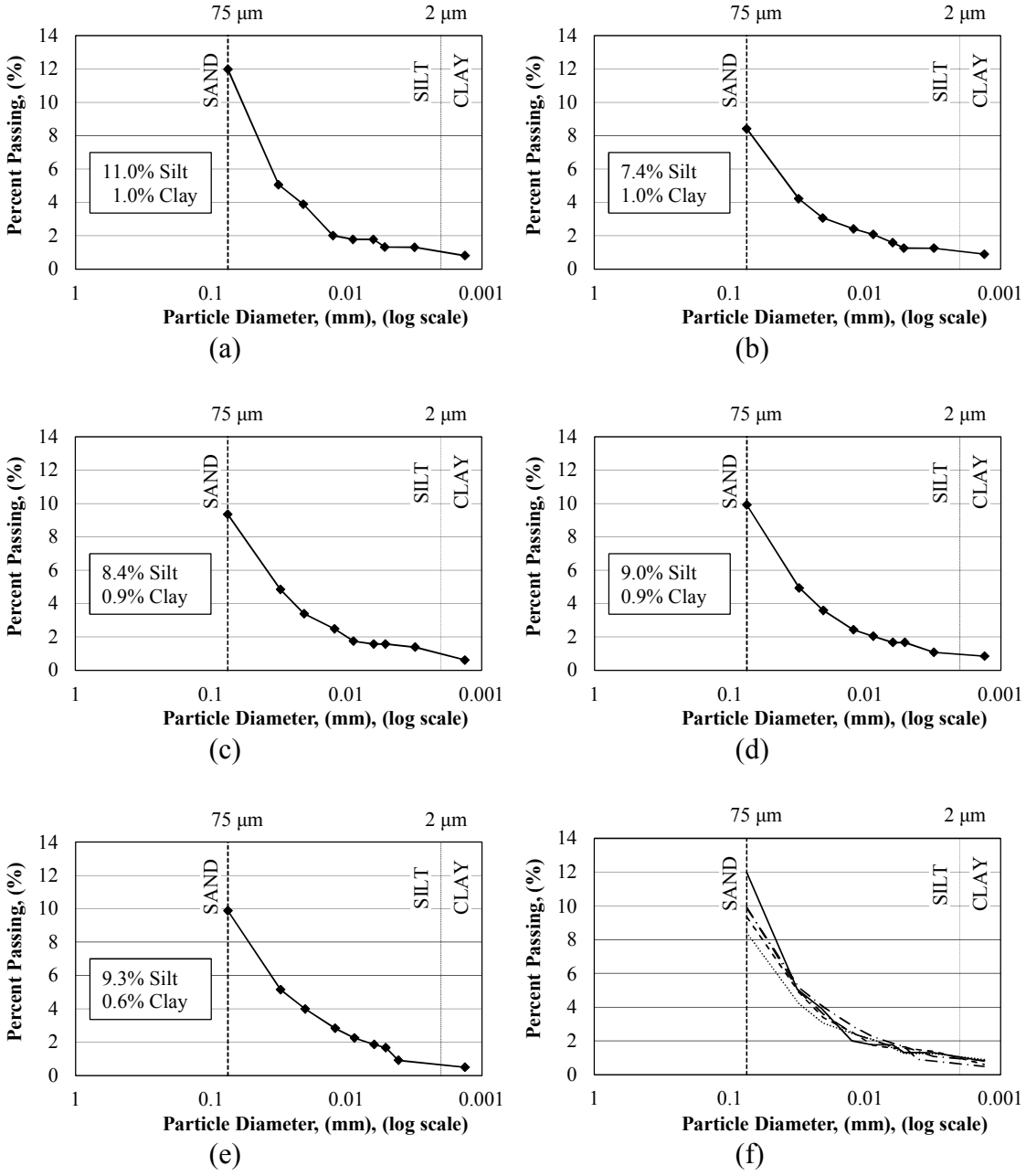

Figure A.5.1. Results from hydrometer tests conducted to determine silt and clay content of entire base course samples obtained from Section 1B from depths of: a) 0-2 inches, b) 2-4 inches, c) 4-6 inches, d) 6-8 inches, and e) 8-10 inches, and f) all depths below the asphalt/base course interface.

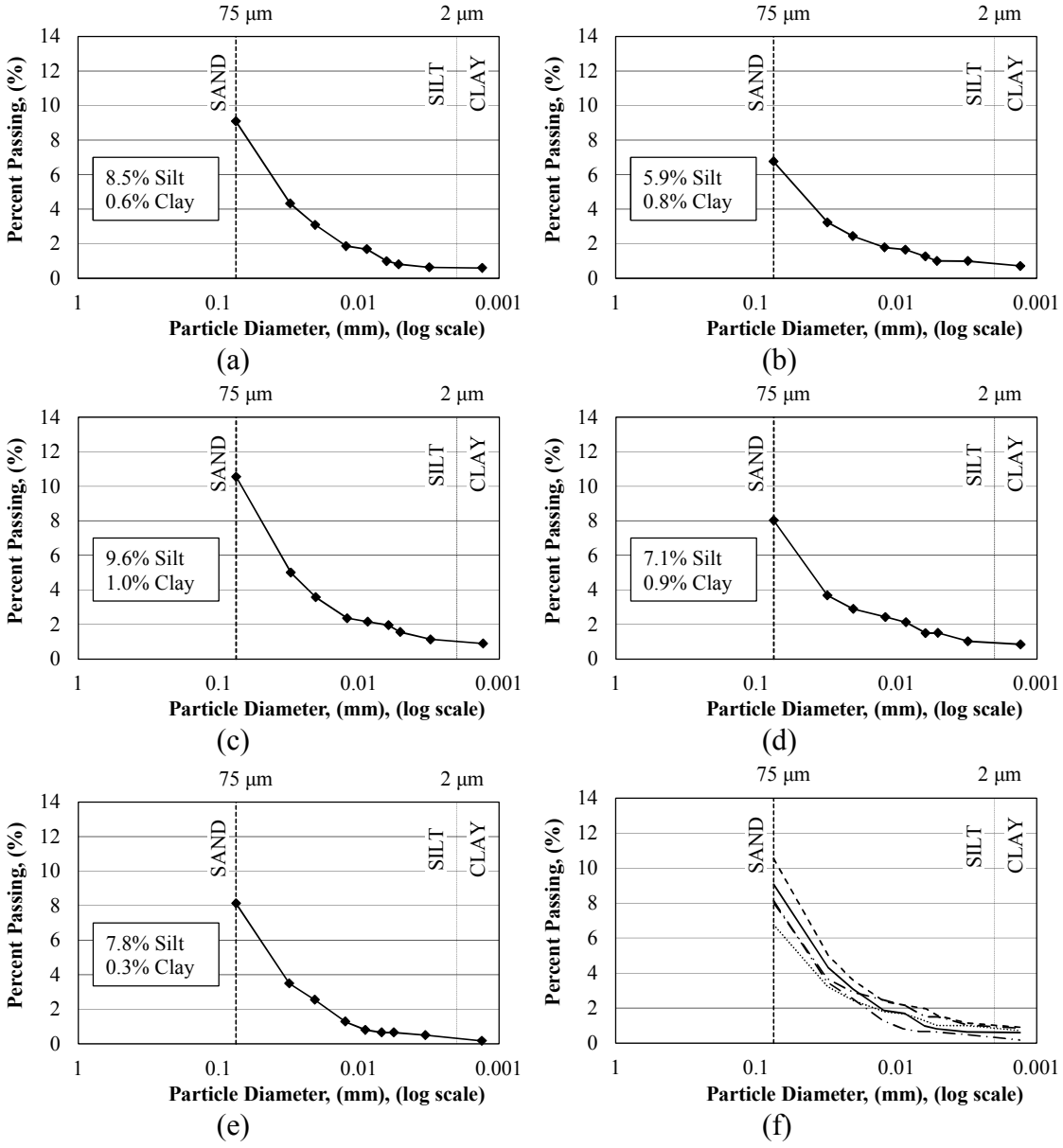

Figure A.5.2. Results from hydrometer tests conducted to determine silt and clay content of entire base course samples obtained from Section 1A from depths of: a) 0-2 inches, b) 2-4 inches, c) 4-6 inches, d) 6-8 inches, and e) 8-10 inches, and f) all depths below the asphalt/base course interface.

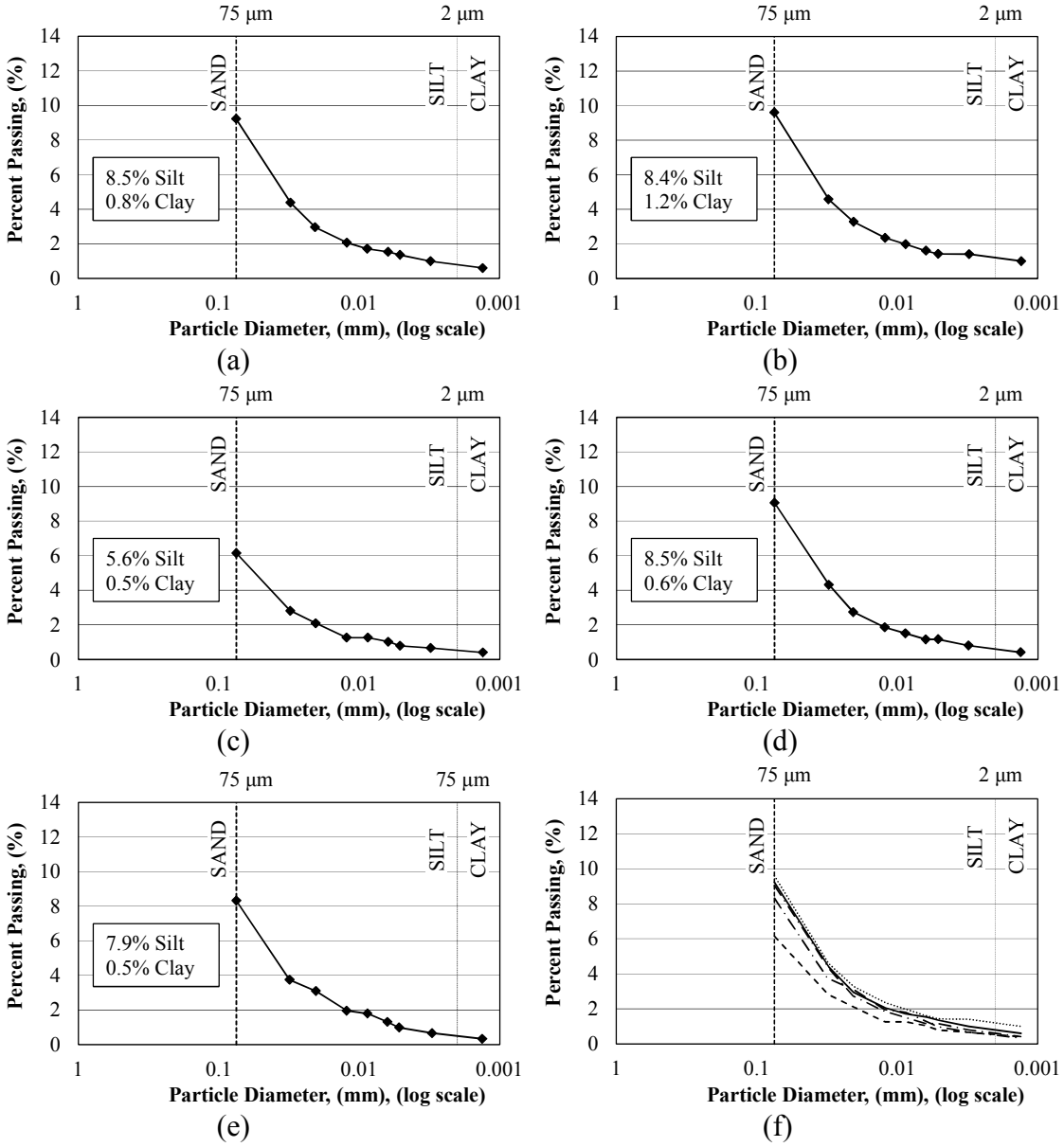

Figure A.5.3. Results from hydrometer tests conducted to determine silt and clay content of entire base course samples obtained from Section 1 from depths of: a) 0-2 inches, b) 2-4 inches, c) 4-6 inches, d) 6-8 inches, and e) 8-10 inches, and f) all depths below the asphalt/base course interface.

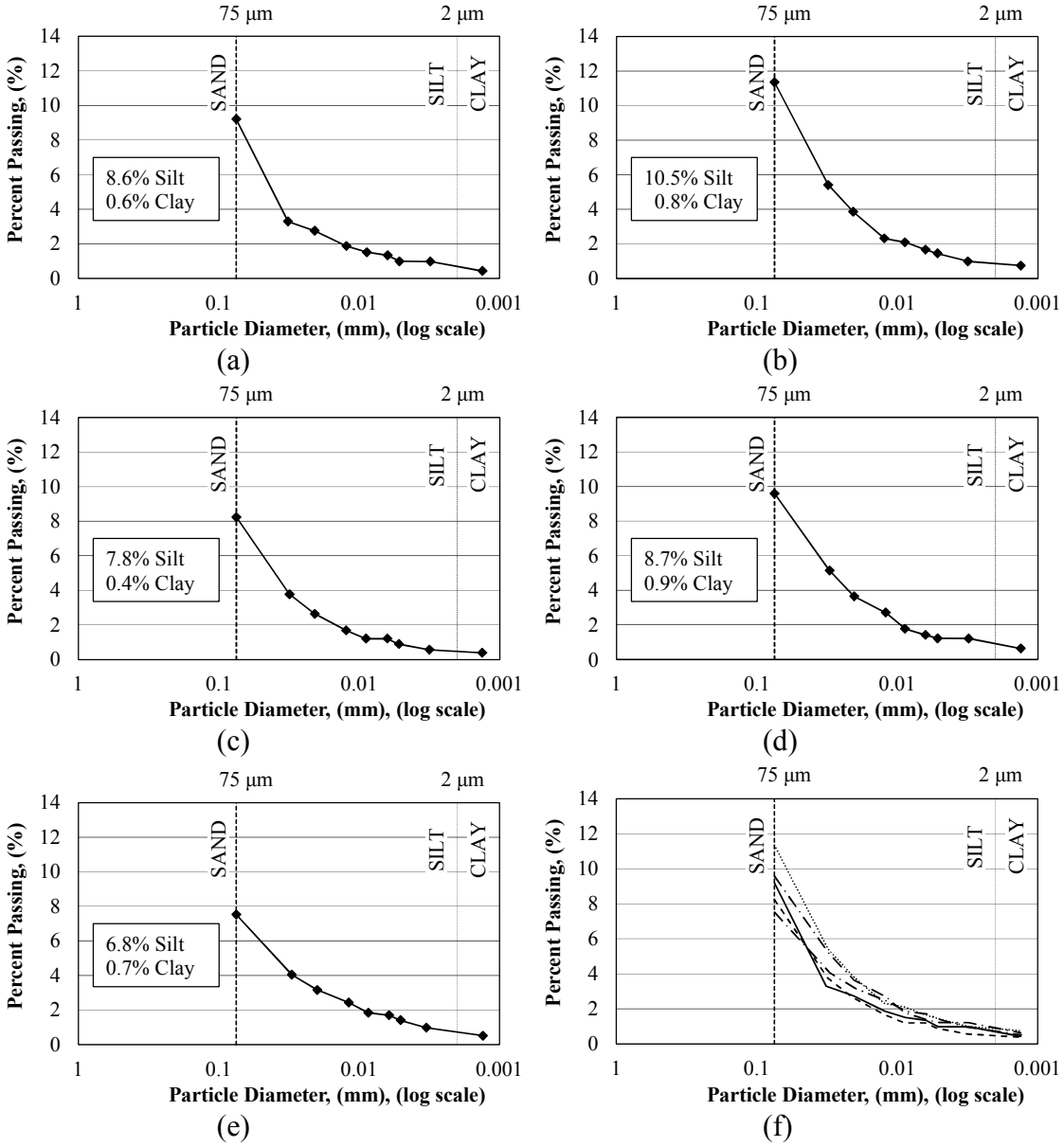

Figure A.5.4. Results from hydrometer tests conducted to determine silt and clay content of entire base course samples obtained from Section 2 from depths of: a) 0-2 inches, b) 2-4 inches, c) 4-6 inches, d) 6-8 inches, and e) 8-10 inches, and f) all depths below the asphalt/base course interface.

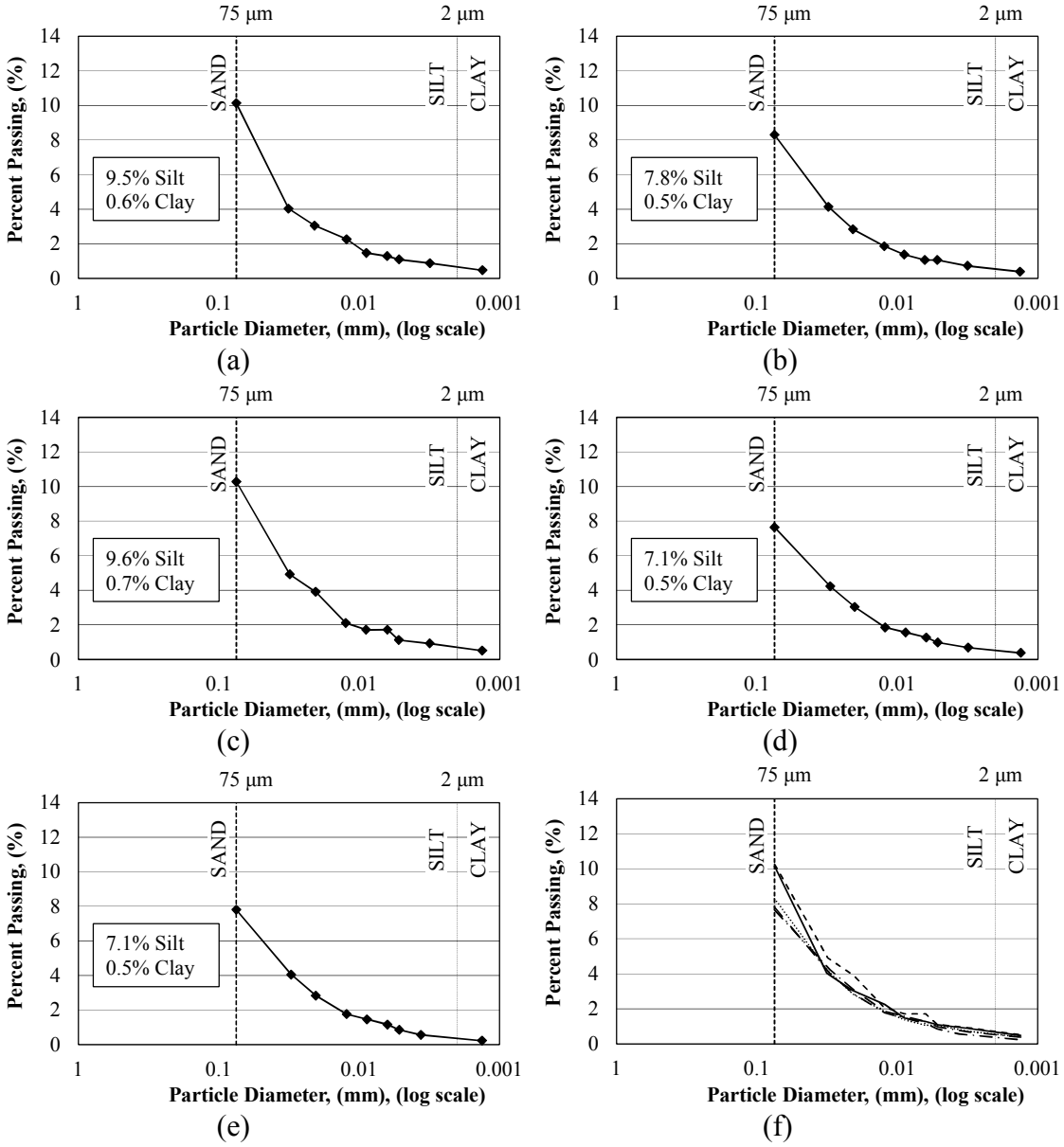

Figure A.5.5. Results from hydrometer tests conducted to determine silt and clay content of entire base course samples obtained from Section 3 from depths of: a) 0-2 inches, b) 2-4 inches, c) 4-6 inches, d) 6-8 inches, and e) 8-10 inches, and f) all depths below the asphalt/base course interface.

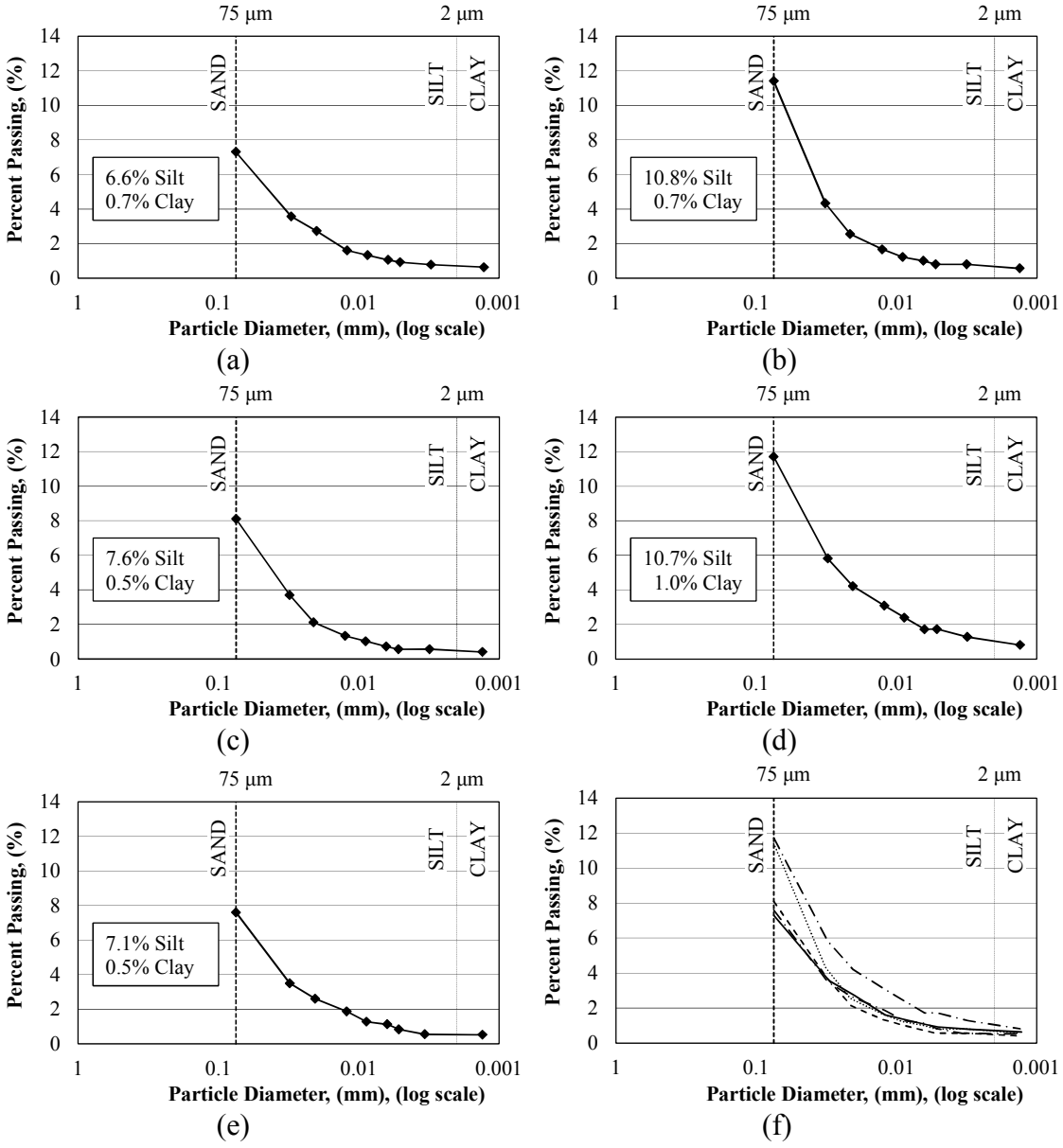

Figure A.5.6. Results from hydrometer tests conducted to determine silt and clay content of entire base course samples obtained from Section 4 from depths of: a) 0-2 inches, b) 2-4 inches, c) 4-6 inches, d) 6-8 inches, and e) 8-10 inches, and f) all depths below the asphalt/base course interface.

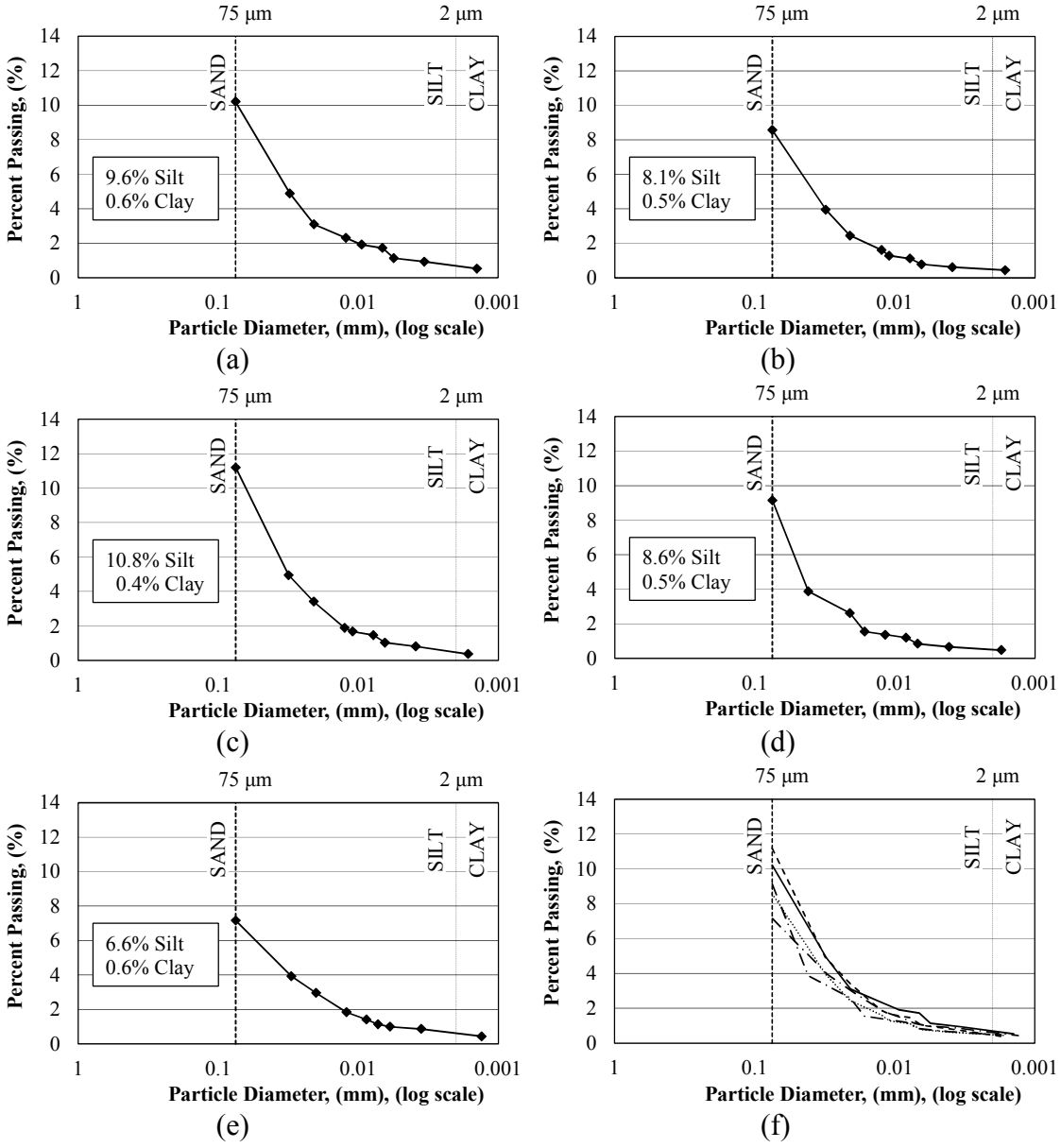

Figure A.5.7. Results from hydrometer tests conducted to determine silt and clay content of entire base course samples obtained from Section 5 from depths of: a) 0-2 inches, b) 2-4 inches, c) 4-6 inches, d) 6-8 inches, and e) 8-10 inches, and f) all depths below the asphalt/base course interface.

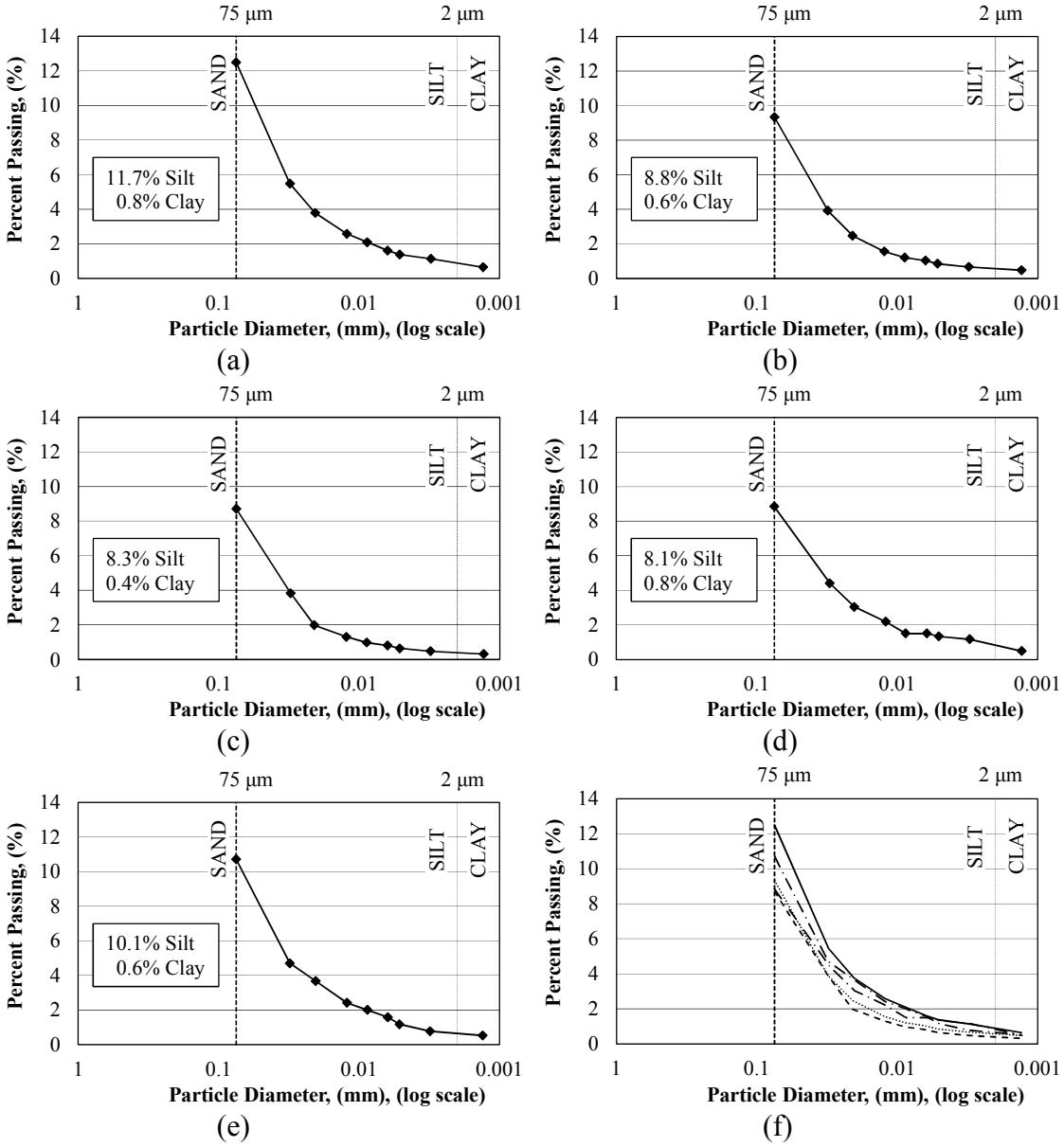

Figure A.5.8. Results from hydrometer tests conducted to determine silt and clay content of entire base course samples obtained from Section 6 from depths of: a) 0-2 inches, b) 2-4 inches, c) 4-6 inches, d) 6-8 inches, and e) 8-10 inches, and f) all depths below the asphalt/base course interface.

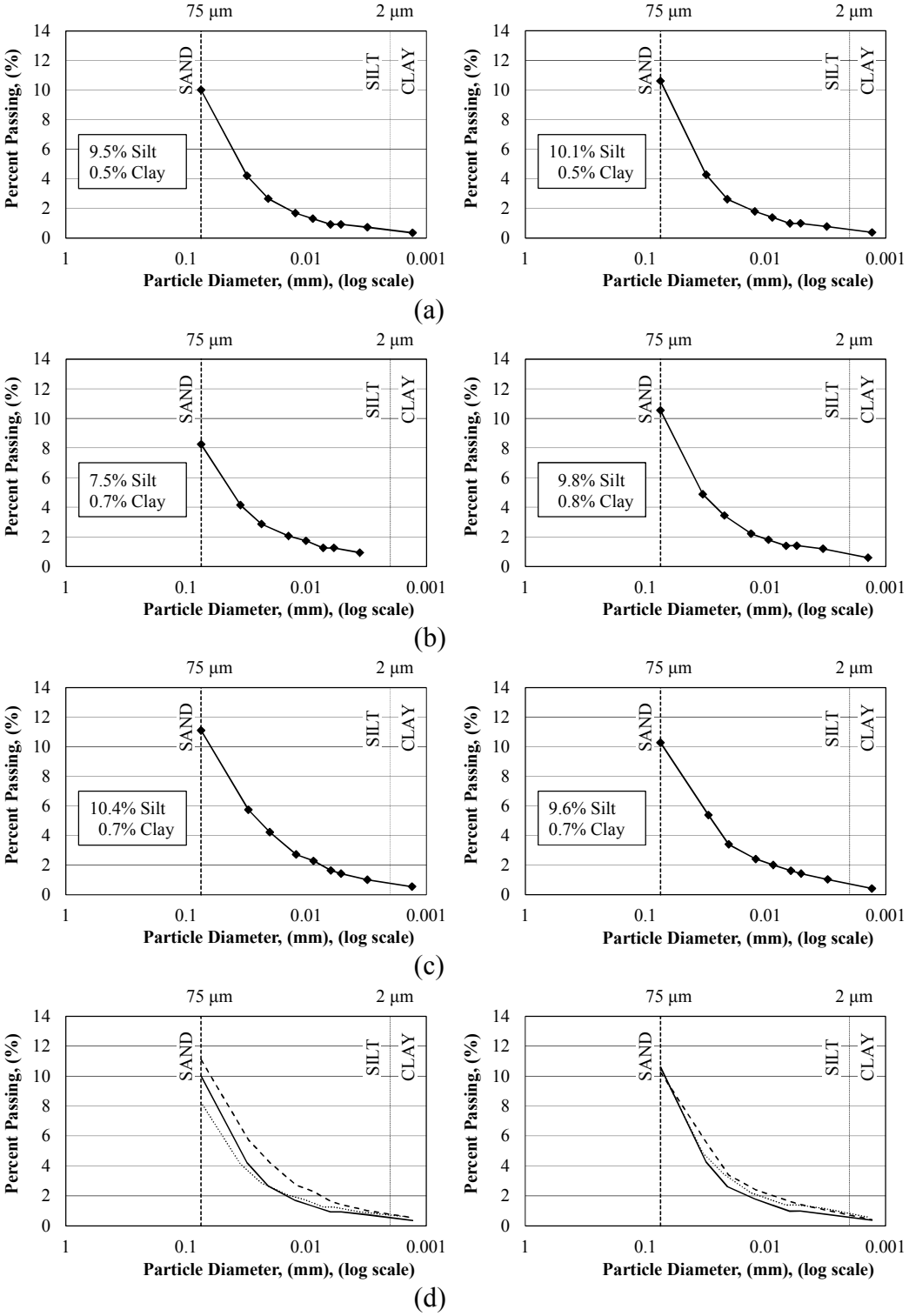

Figure A.5.9. Results obtained from hydrometer testing conducted to determine silt and clay content of entire base course samples obtained from Section 8 (left) and 9 (right) from depths of: a) 0-2 inches, b) 2-4 inches, c) 4-6 inches, and d) all depths below the asphalt/base course interface.

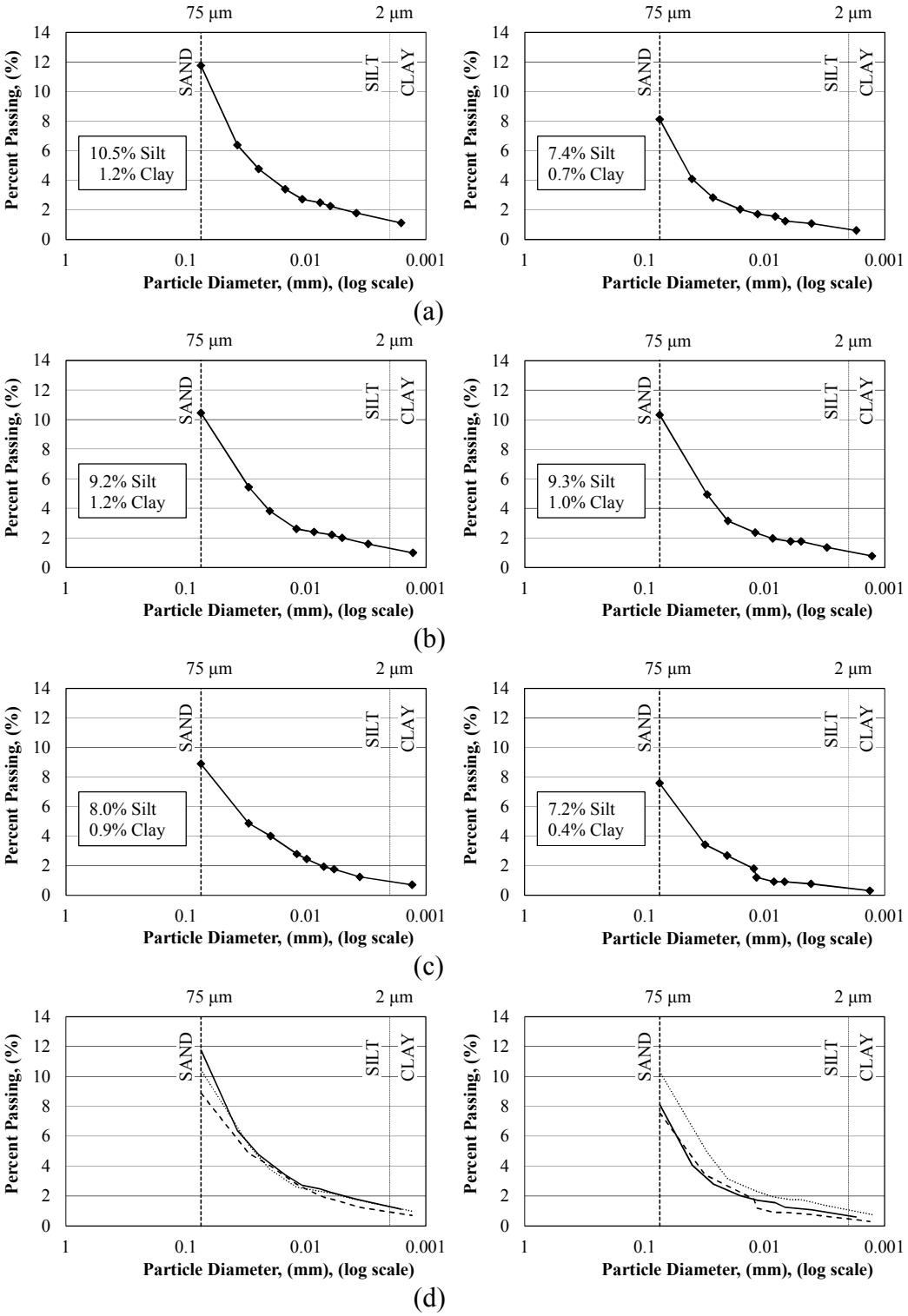

Figure A.5.10. Results obtained from hydrometer testing conducted to determine silt and clay contents of entire base course samples obtained from Section 10 (left) and 11 (right) from depths of: a) 0-2 inches, b) 2-4 inches, c) 4-6 inches, and d) all depths below the asphalt/base course interface.

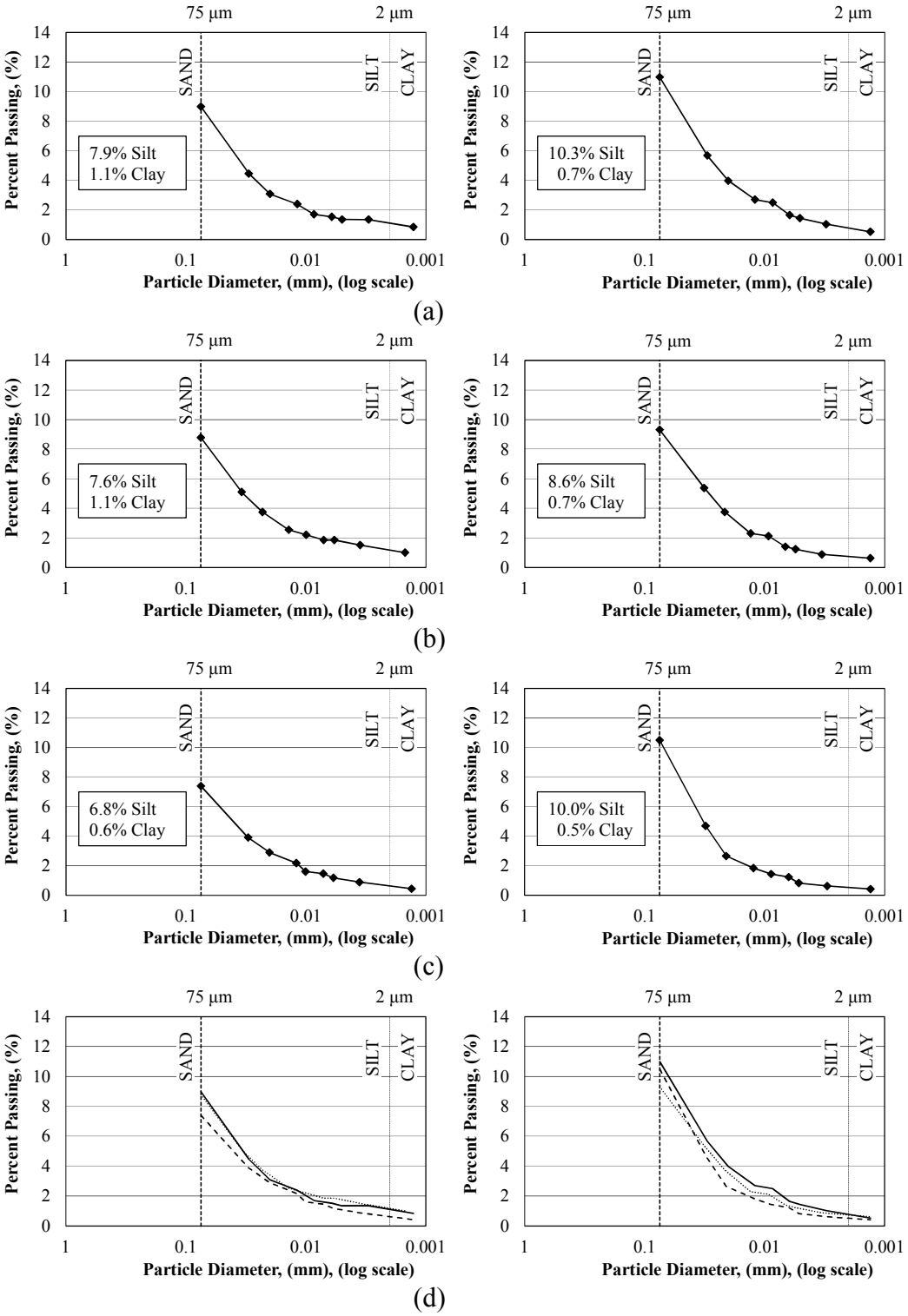

Figure A.5.11. Results obtained from hydrometer testing conducted to determine silt and clay contents of entire base course samples obtained from Section 12 (left) and 13 (right) from depths of: a) 0-2 inches, b) 2-4 inches, c) 4-6 inches, and d) all depths below the asphalt/base course interface.

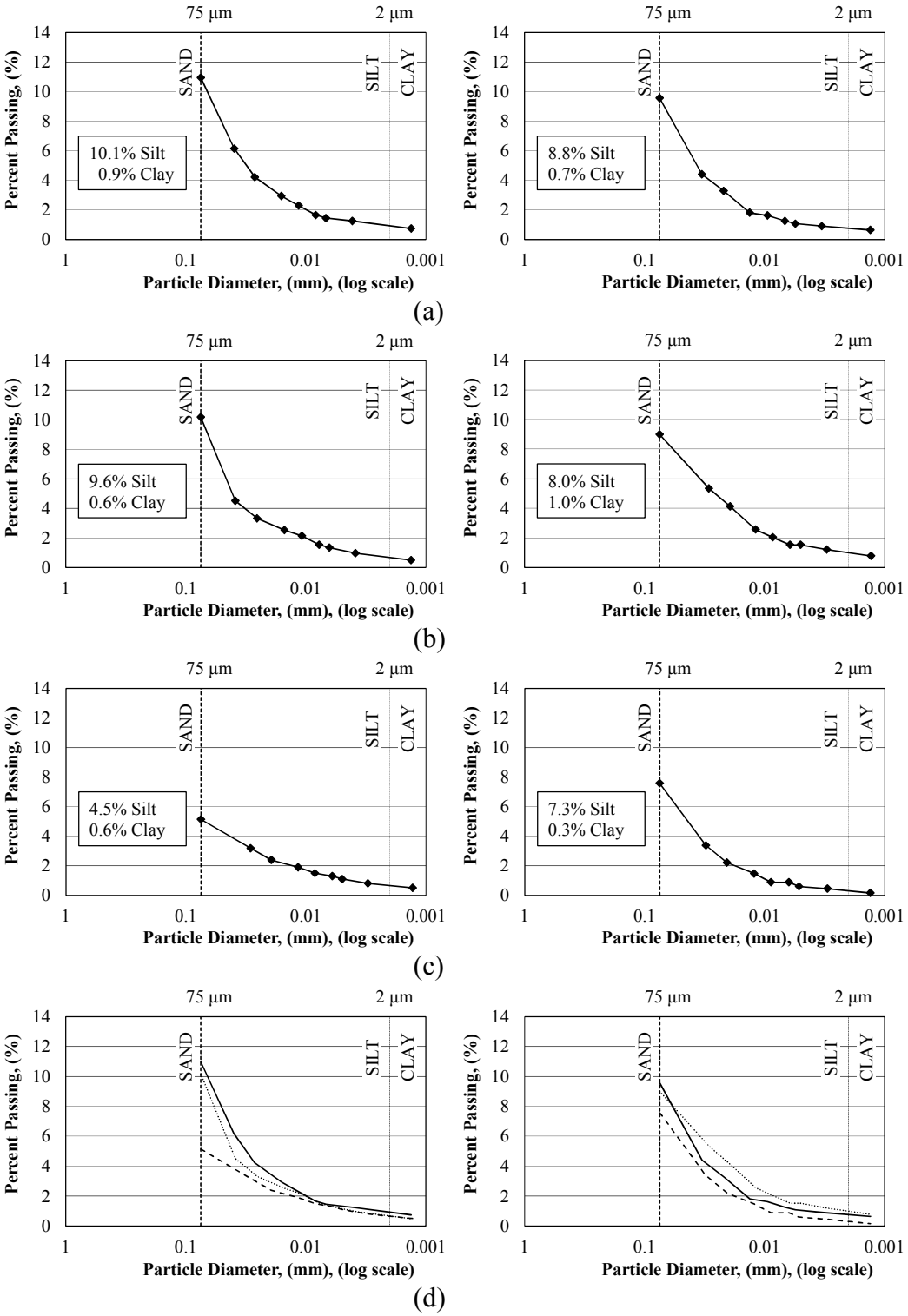

Figure A.5.12. Results obtained from hydrometer testing conducted to determine silt and clay contents of entire base course samples obtained from Section 13W (left) and 13A (right) from depths of: a) 0-2 inches, b) 2-4 inches, c) 4-6 inches, and d) all depths below the asphalt/base course interface.

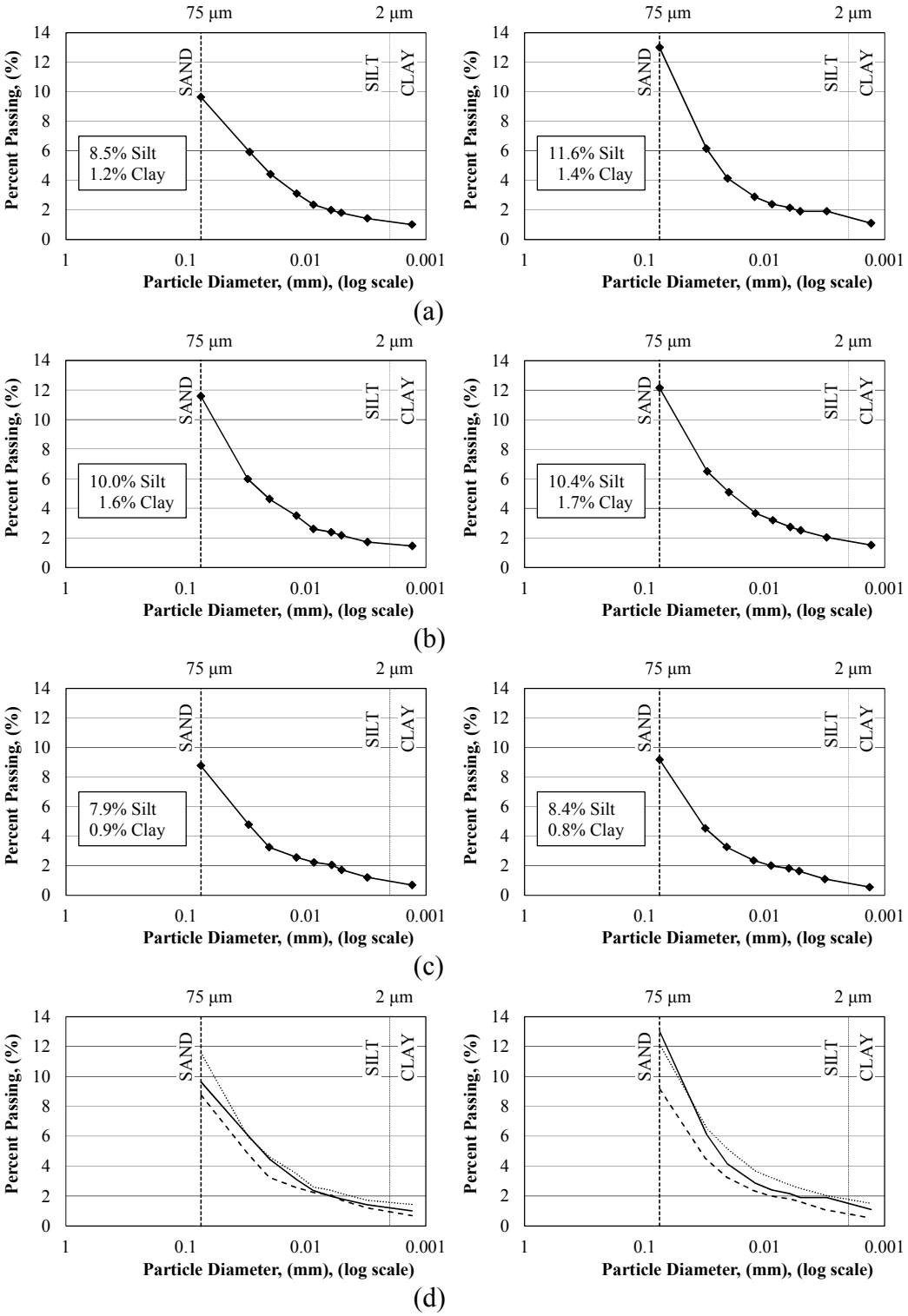

Figure A.5.13. Results obtained from hydrometer testing conducted to determine silt and clay contents of entire base course samples obtained from Section 13B (left) and 13BW (right) from depths of: a) 0-2 inches, b) 2-4 inches, c) 4-6 inches, and d) all depths below the asphalt/base course interface.

A.6. Subgrade Hydrometer

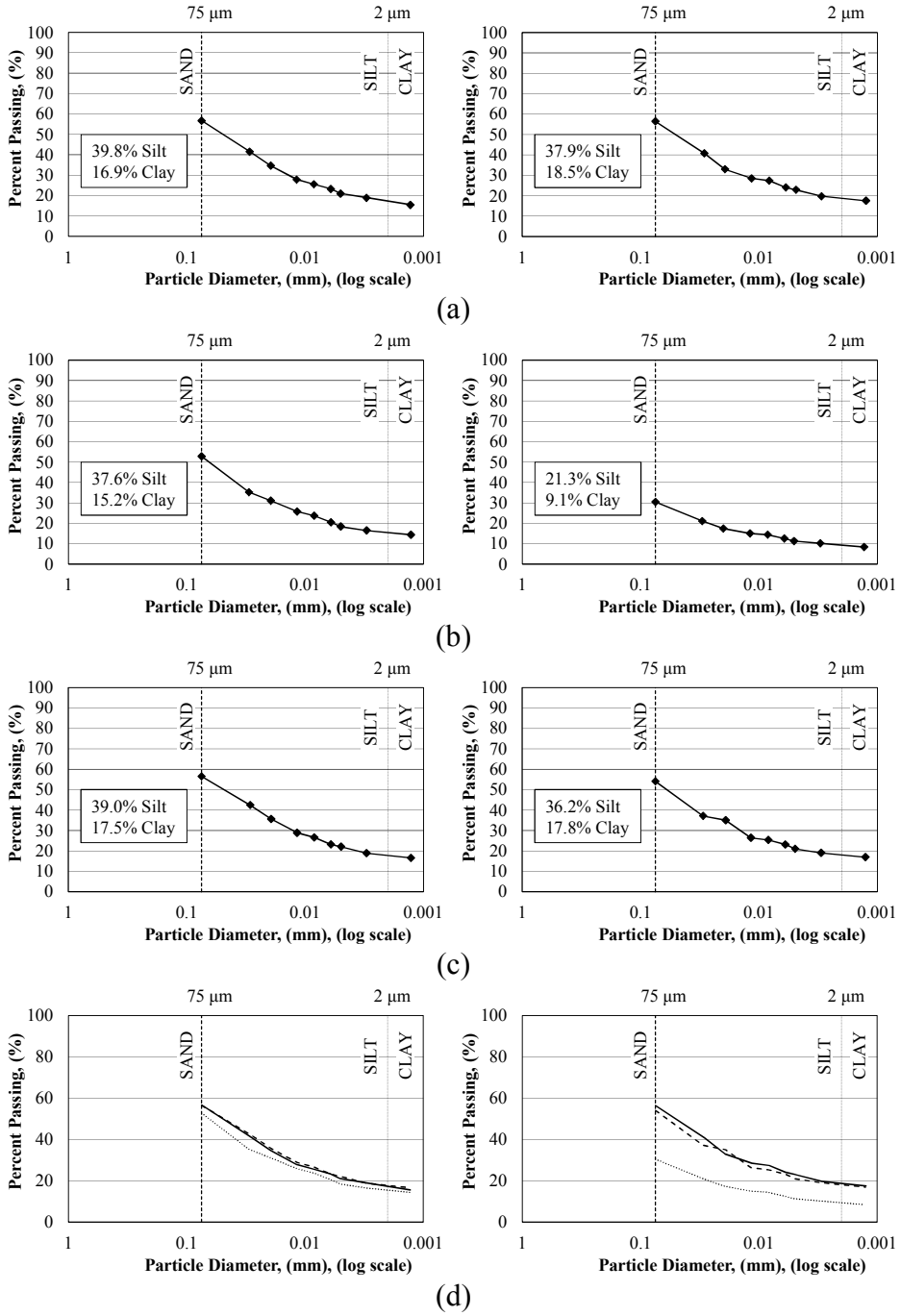

Figure A.6.1.Results from hydrometer testing conducted to determine silt and clay content in the subgrade samples obtained from Section 1B (left) and Section 1A (right) from depths of: a) 0-2 inches, b) 2-4 inches, and c) 4-6 inches, and d) all depths below the base course/subgrade interface.

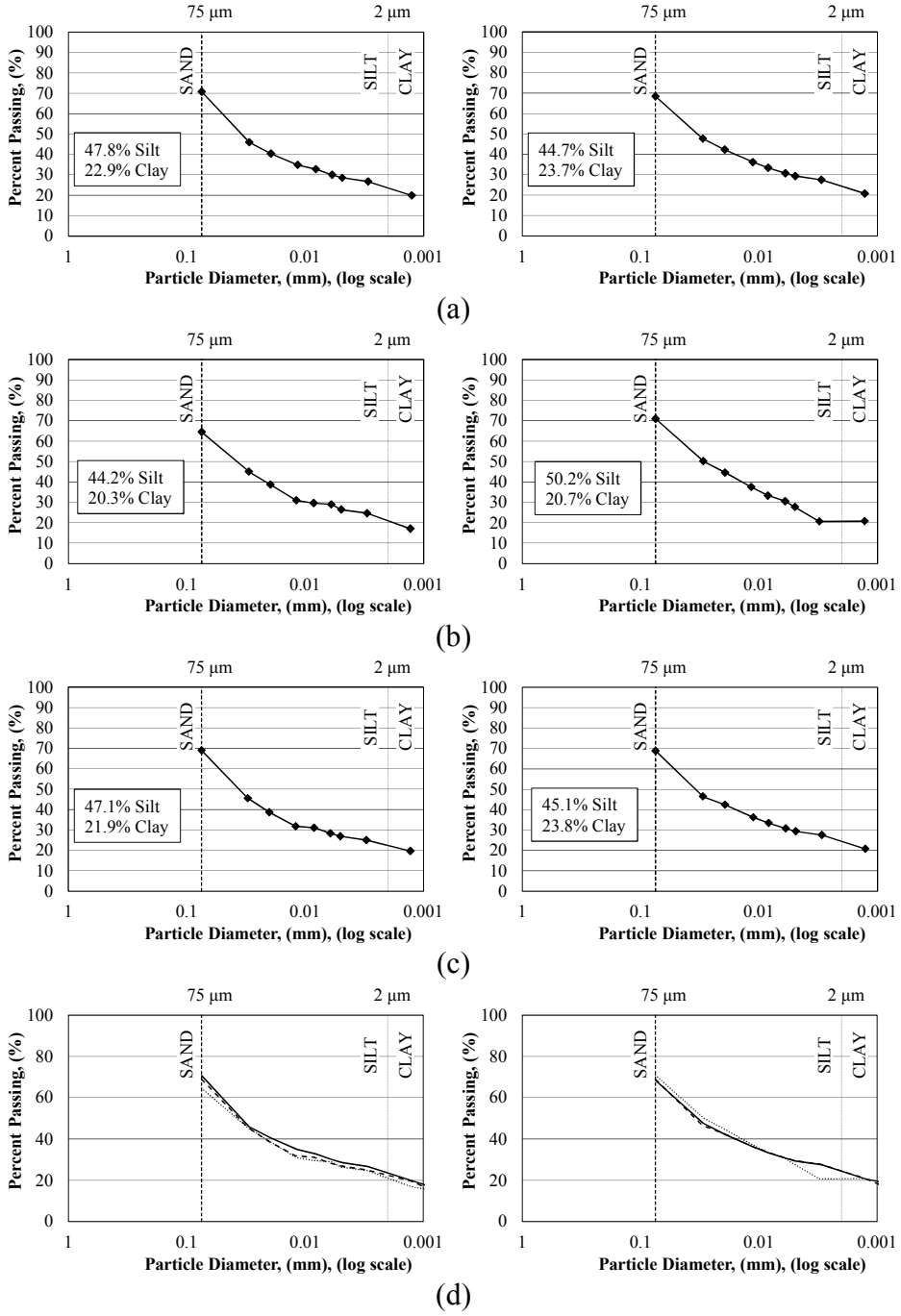

Figure A.6.2.Results from hydrometer testing conducted to determine silt and clay content in the subgrade samples obtained from Section 1 (left) and Section 2 (right) from depths of: a) 0-2 inches, b) 2-4 inches, and c) 4-6 inches, and d) all depths below the base course/subgrade interface.

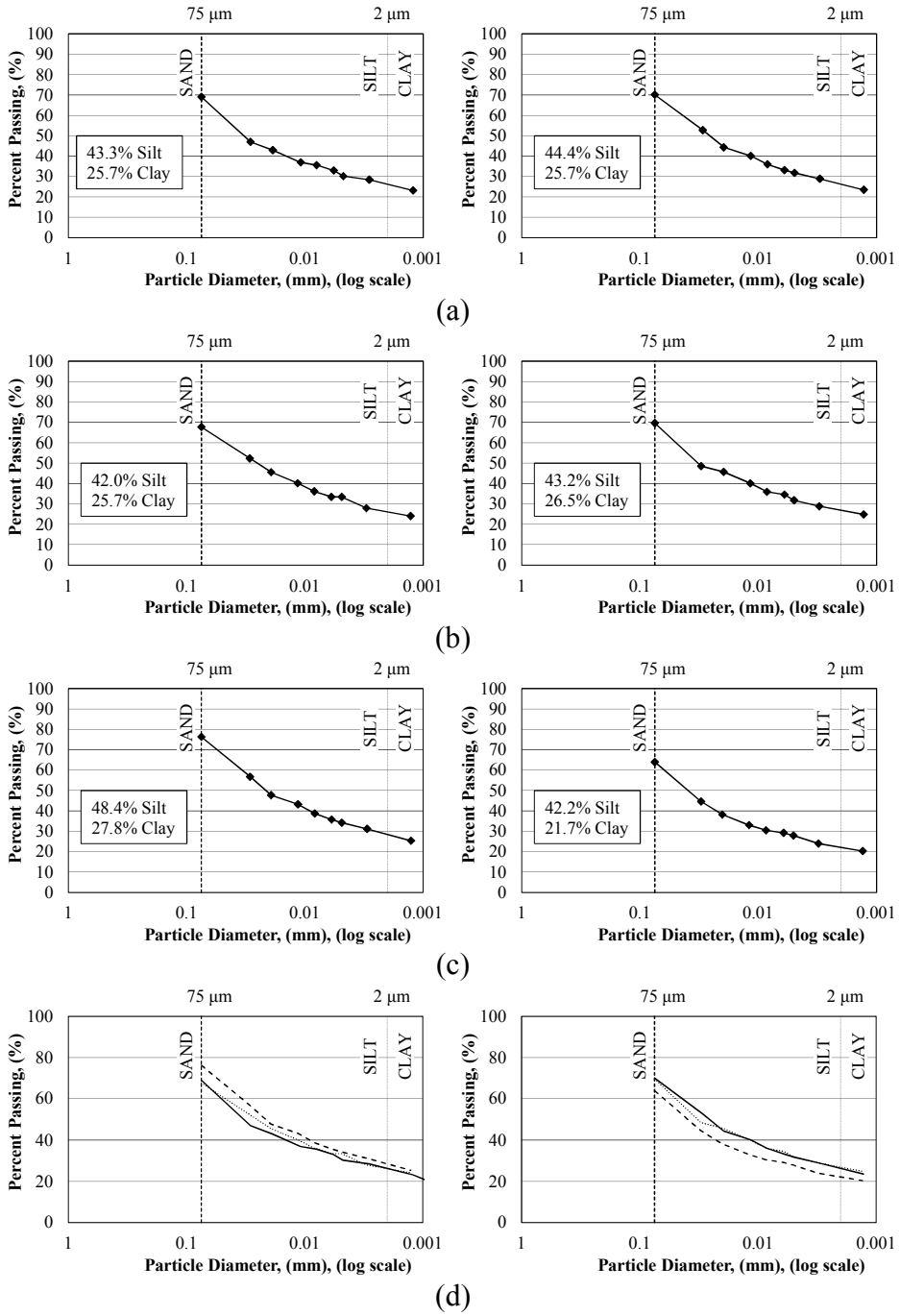

Figure A.6.3.Results from hydrometer testing conducted to determine silt and clay content in the subgrade samples obtained from Section 3 (left) and Section 4 (right) from depths of: a) 0-2 inches, b) 2-4 inches, and c) 4-6 inches, and d) all depths below the base course/subgrade interface.

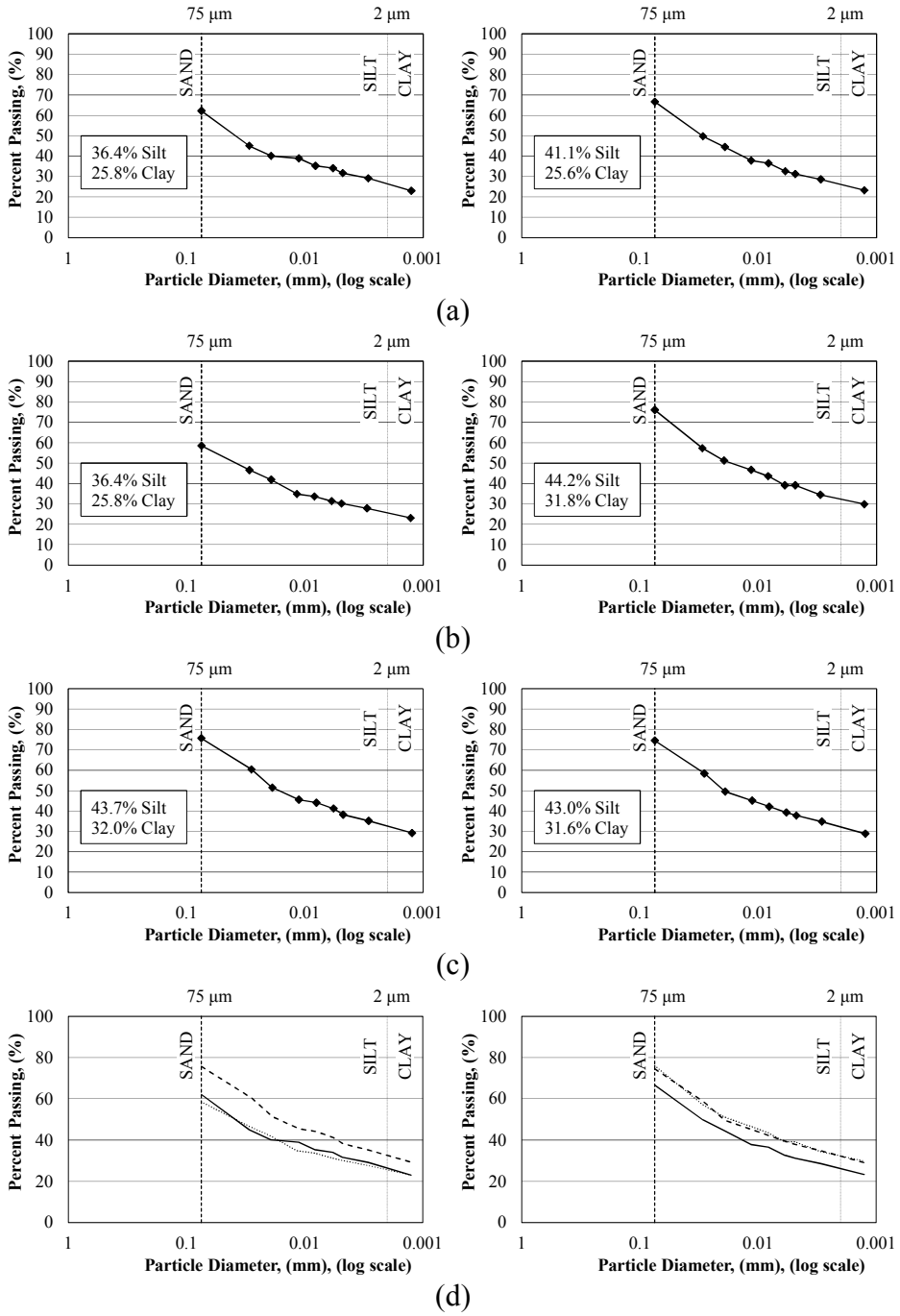

Figure A.6.4.Results from hydrometer testing conducted to determine silt and clay content in the subgrade samples obtained from Section 5 (left) and Section 6 (right) from depths of: a) 0-2 inches, b) 2-4 inches, and c) 4-6 inches, and d) all depths below the base course/subgrade interface.

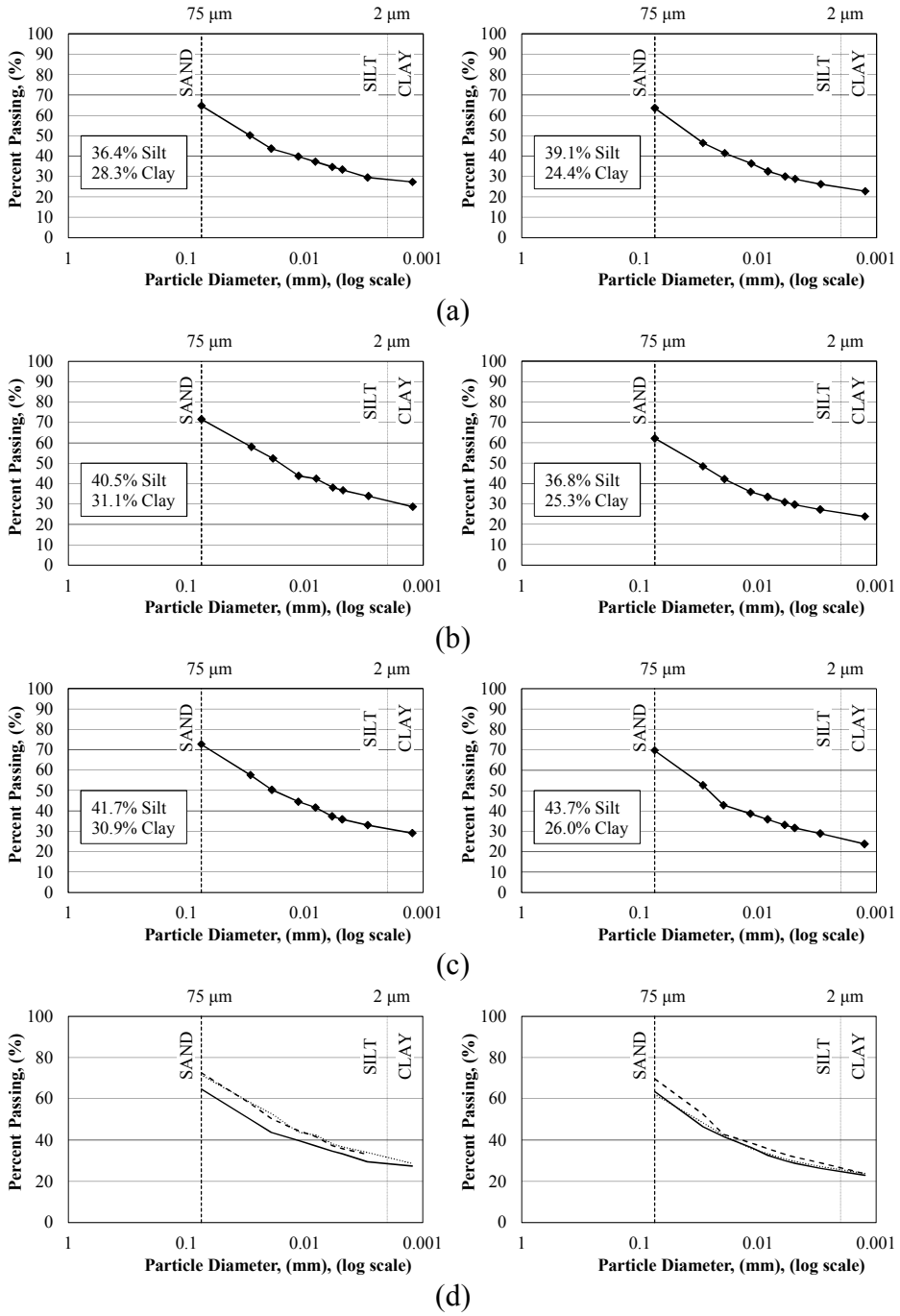

Figure A.6.5.Results from hydrometer testing conducted to determine silt and clay content in the subgrade samples obtained from Section 8 (left) and Section 9 (right) from depths of: a) 0-2 inches, b) 2-4 inches, and c) 4-6 inches, and d) all depths below the base course/subgrade interface.

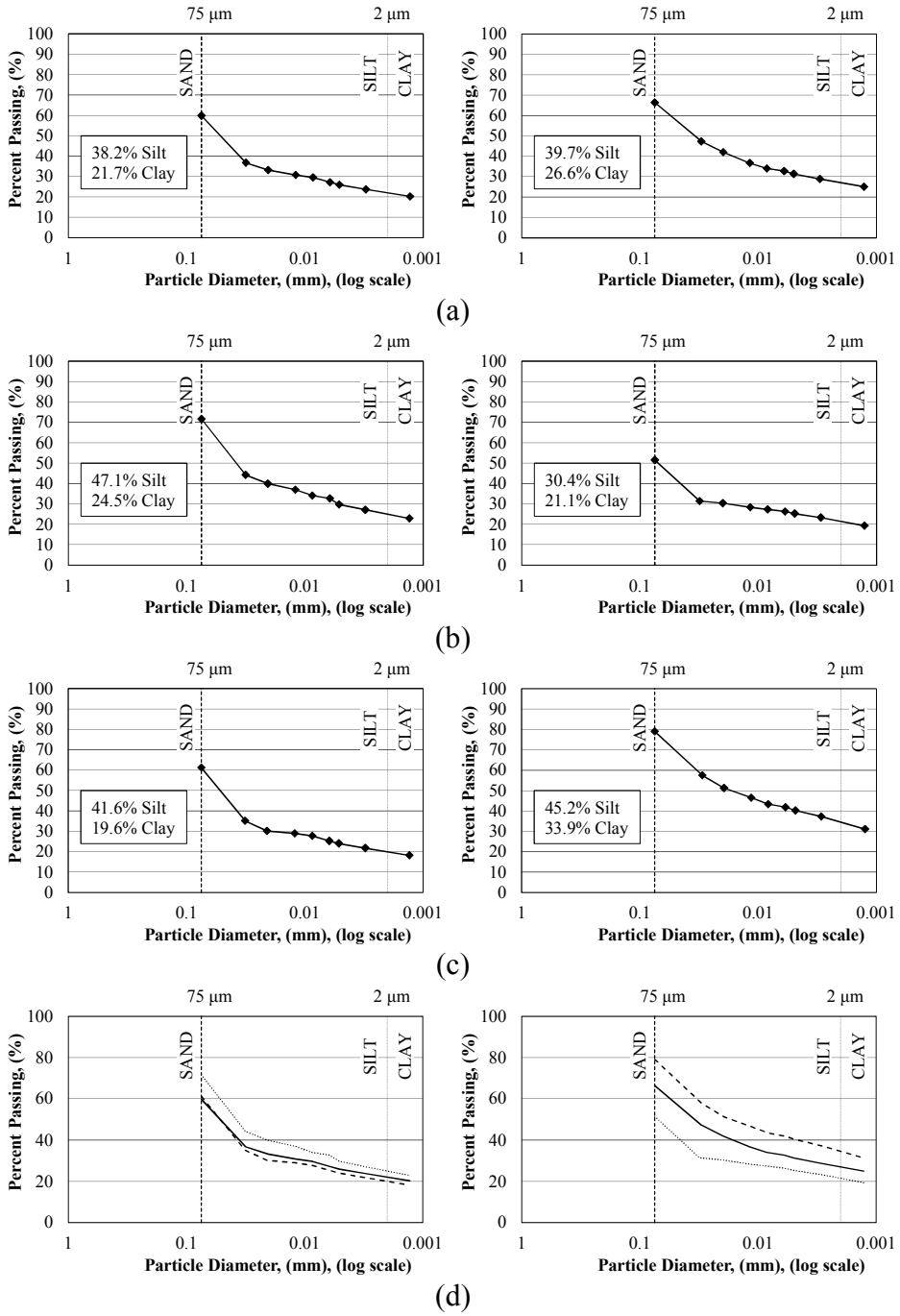

Figure A.6.6.Results from hydrometer testing conducted to determine silt and clay content in the subgrade samples obtained from Section 10 (left) and Section 11 (right) from depths of: a) 0-2 inches, b) 2-4 inches, and c) 4-6 inches, and d) all depths below the base course/subgrade interface.

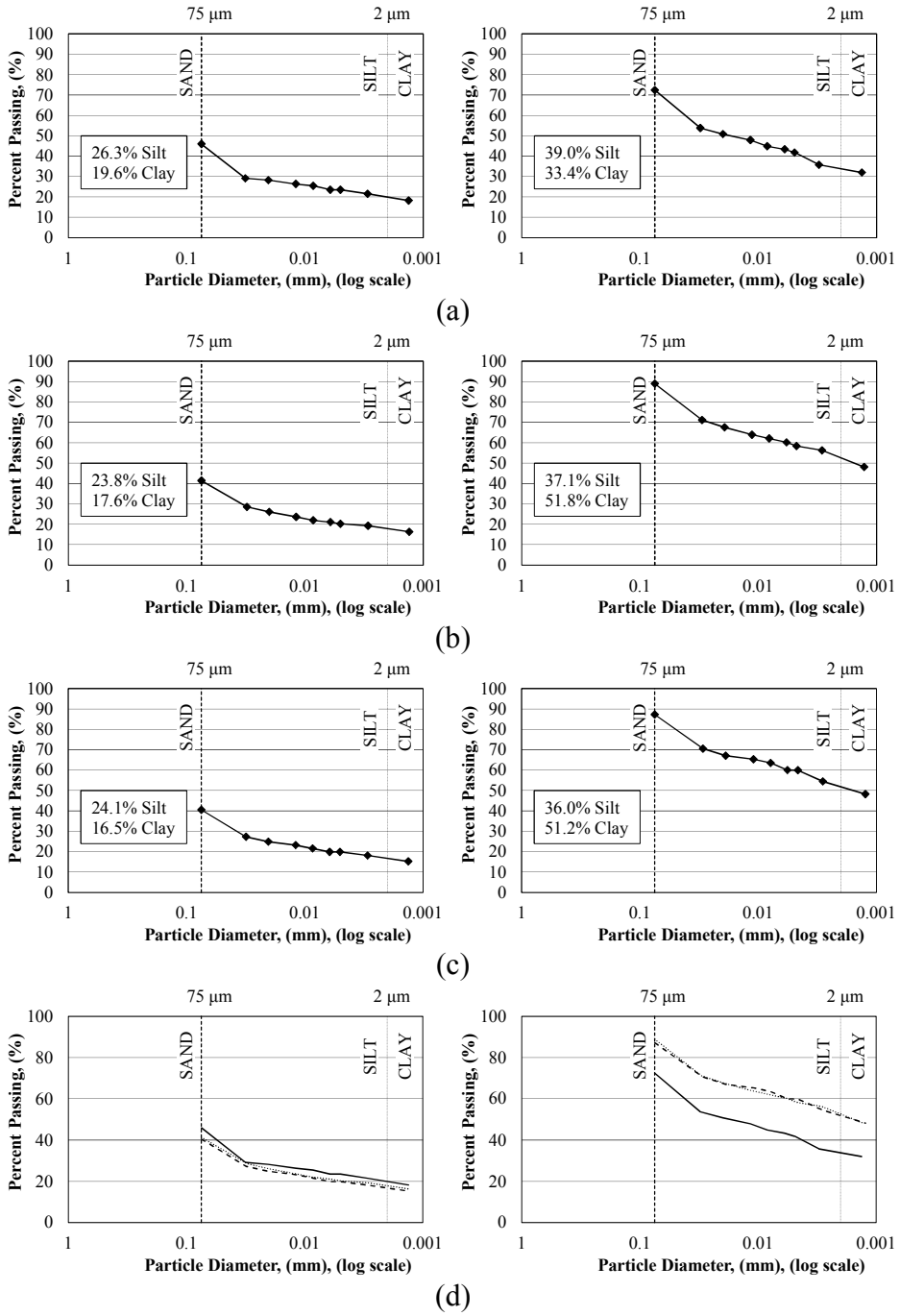

Figure A.6.7.Results from hydrometer testing conducted to determine silt and clay content in the subgrade samples obtained from Section 12 (left) and Section 13 (right) from depths of: a) 0-2 inches, b) 2-4 inches, and c) 4-6 inches, and d) all depths below the base course/subgrade interface.

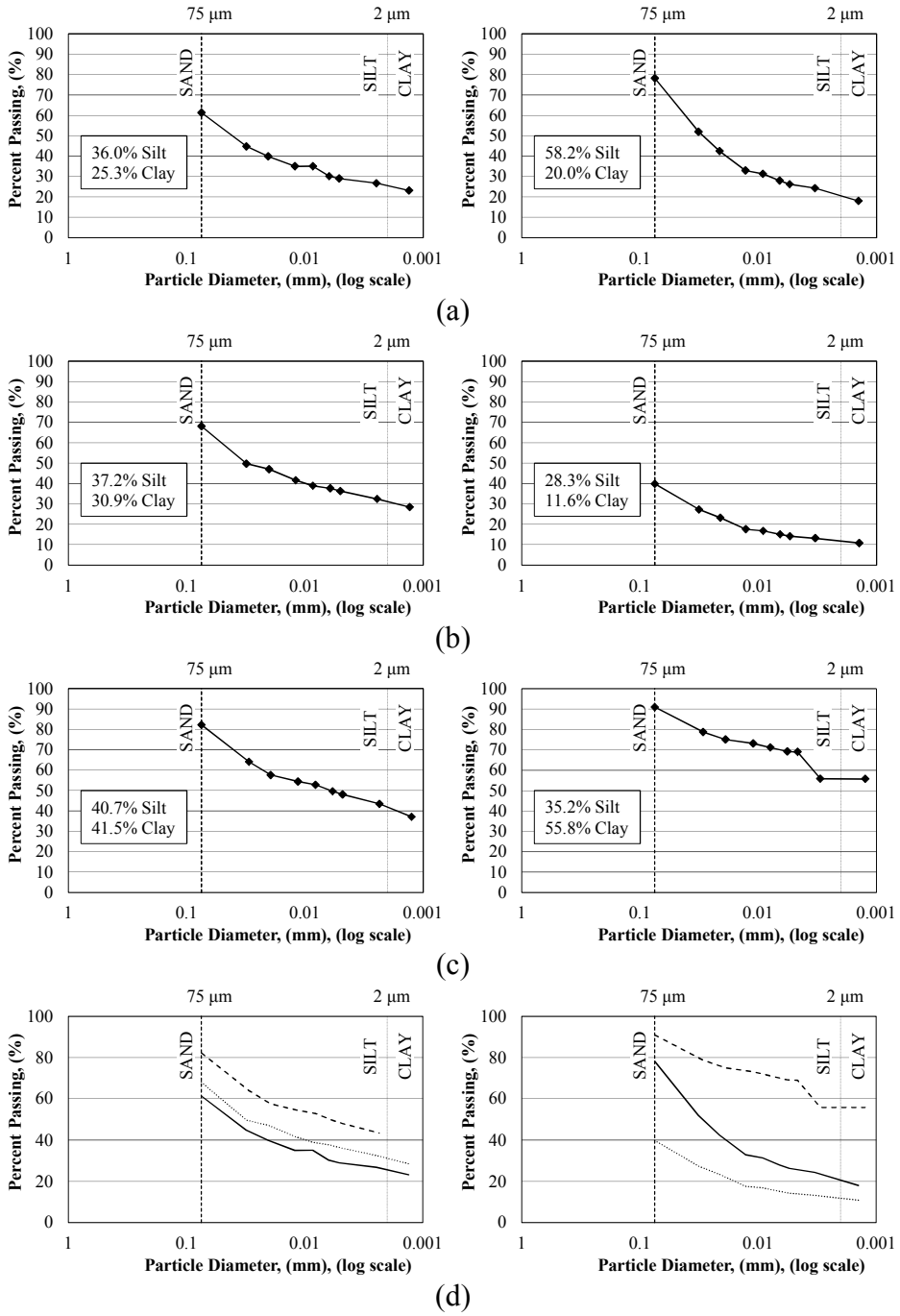

Figure A.6.8.Results from hydrometer testing conducted to determine silt and clay content in the subgrade samples obtained from Section 13W (left) and Section 13A (right) from depths of: a) 0-2 inches, b) 2-4 inches, and c) 4-6 inches, and d) all depths below the base course/subgrade interface.

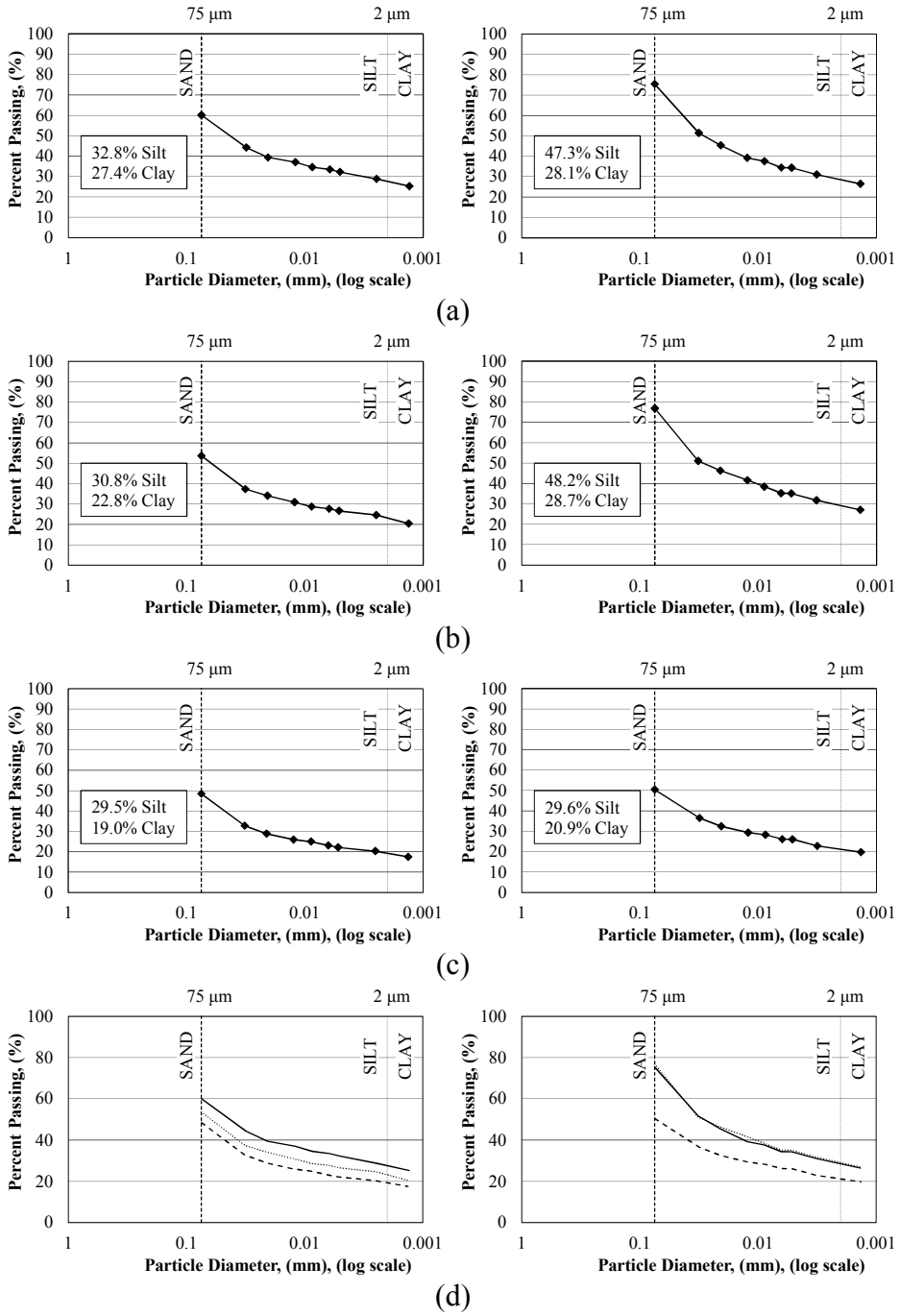

Figure A.6.9.Results from hydrometer testing conducted to determine silt and clay content in the subgrade samples obtained from Section 13B (left) and Section 13BW (right) from depths of: a) 0-2 inches, b) 2-4 inches, and c) 4-6 inches, and d) all depths below the base course/subgrade interface.

A.7. Atterberg Limits

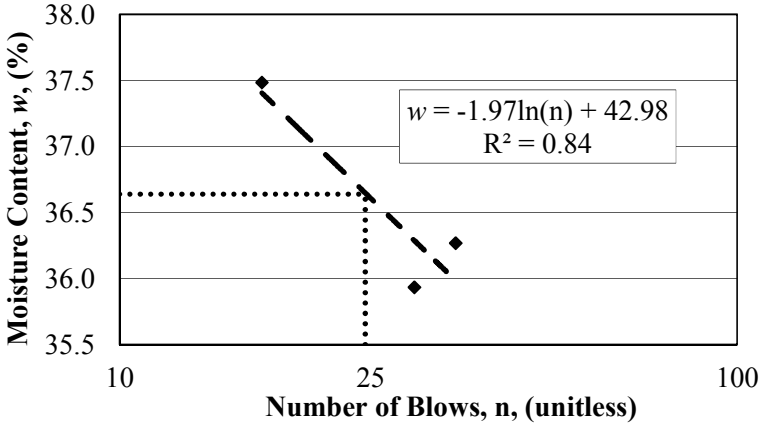

(a)

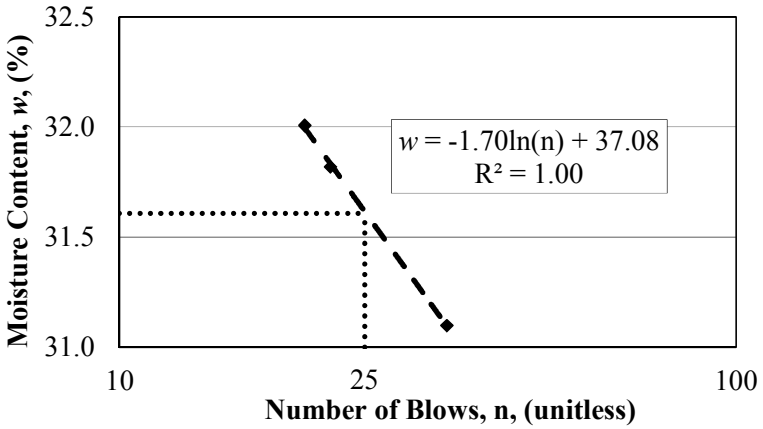

(b)

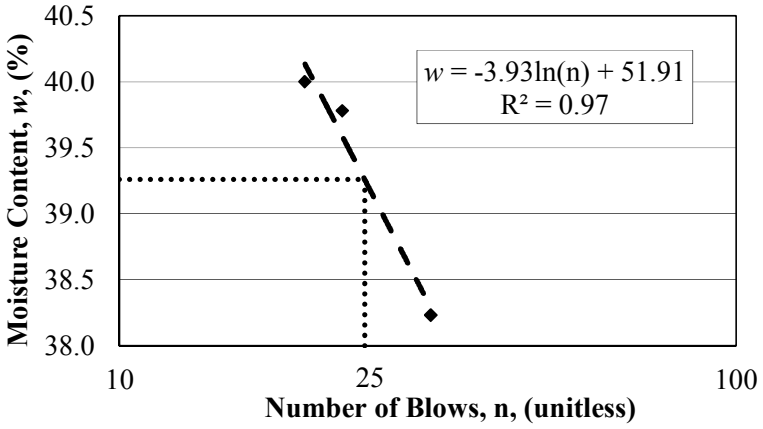

(c)

Figure A.7.1. Subgrade Liquid Limit plots for samples obtained from Section 1B at depths of: a) 0-2 inches, b) 2-4 inches, and c) 4-6 inches below the base course/subgrade interface.

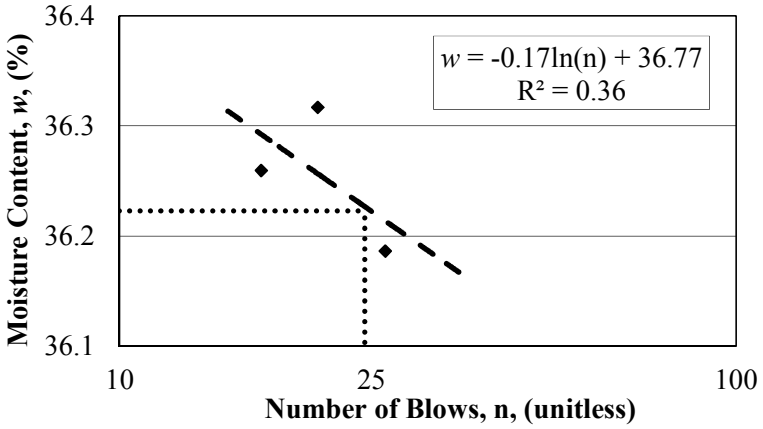

(a)

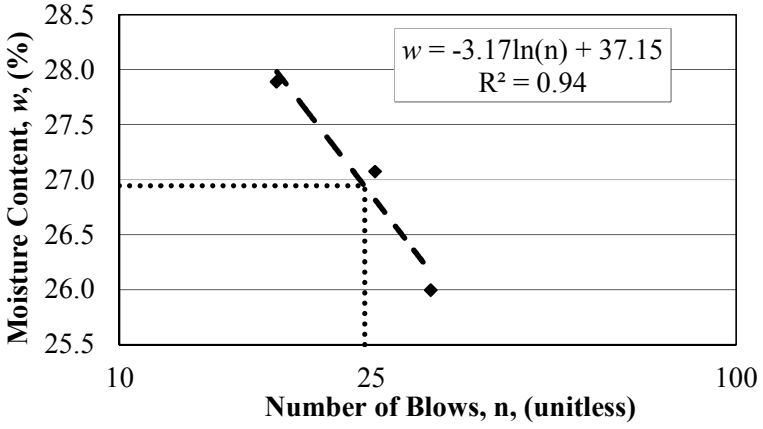

(b)

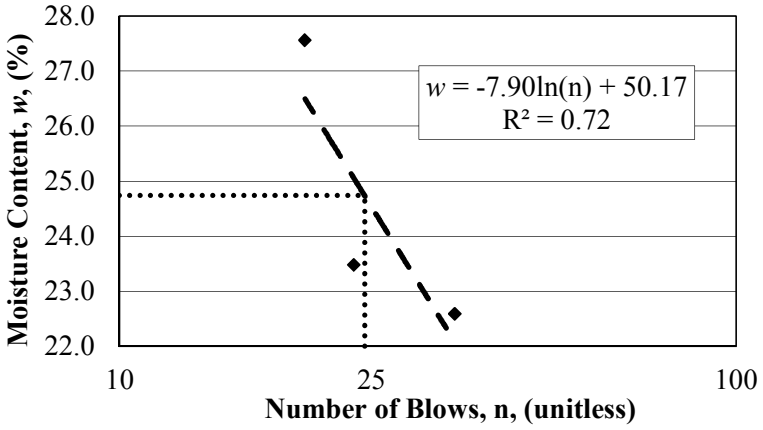

(c)

Figure A.7.2. Subgrade Liquid Limit plots for samples obtained from Section 1A at depths of: a) 0-2 inches, b) 2-4 inches, and c) 4-6 inches below the base course/subgrade interface.

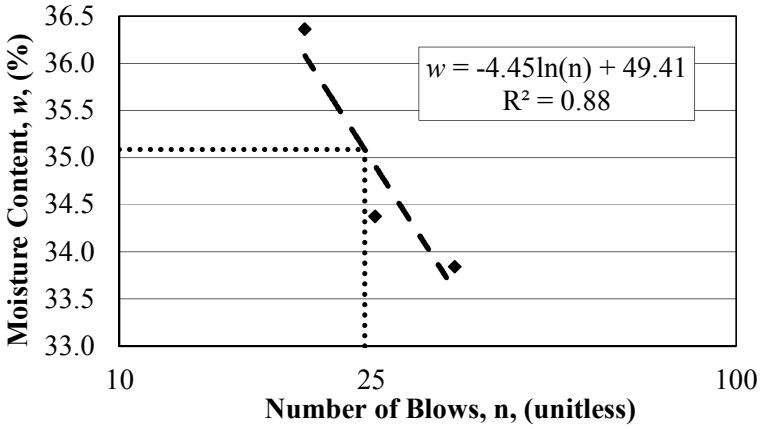

(a)

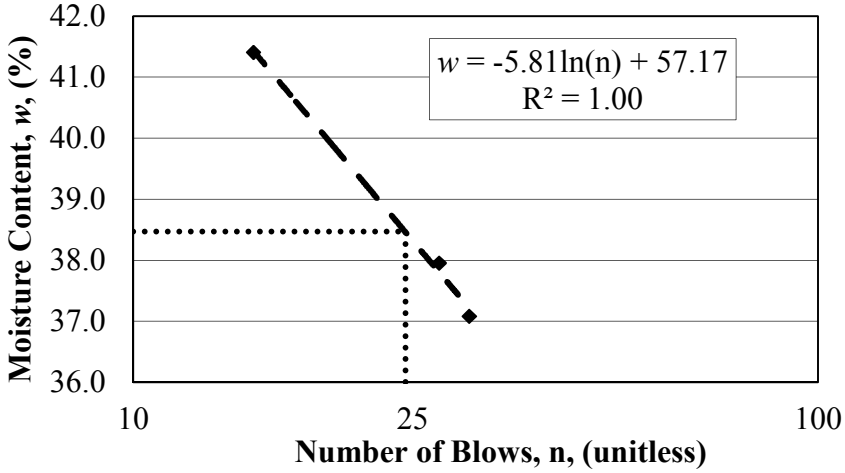

(b)

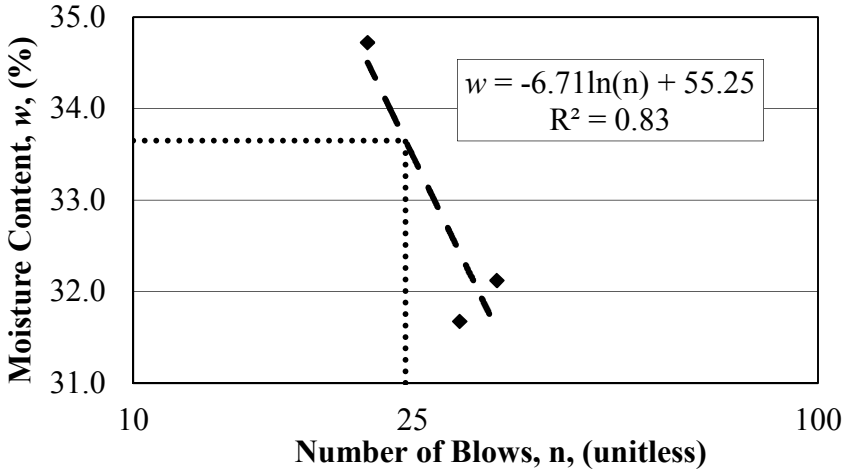

(c)

Figure A.7.3. Subgrade Liquid Limit plots for samples obtained from Section 1 at depths of: a) 0-2 inches, b) 2-4 inches, and c) 4-6 inches below the base course/subgrade interface.

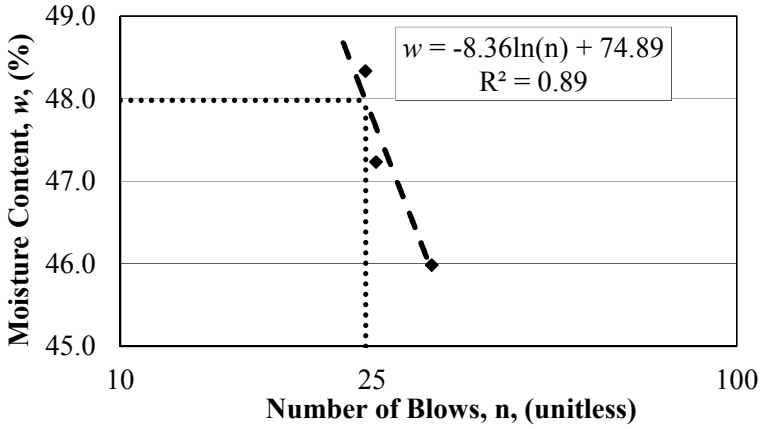

(a)

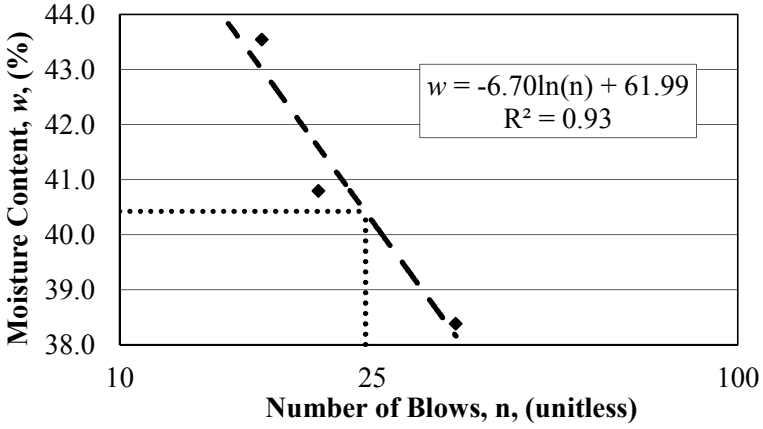

(b)

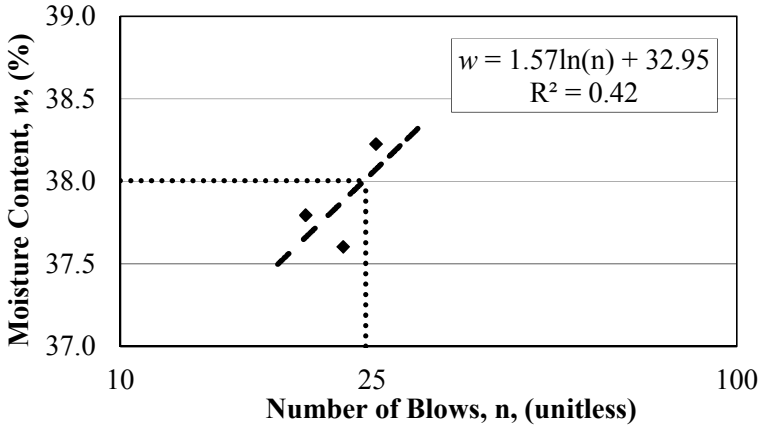

(c)

Figure A.7.4. Subgrade Liquid Limit plots for samples obtained from Section 2 at depths of: a) 0-2 inches, b) 2-4 inches, and c) 4-6 inches below the base course/subgrade interface.

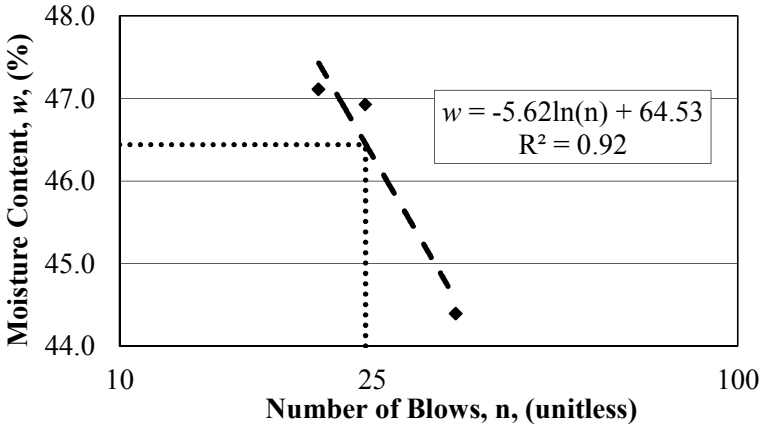

(a)

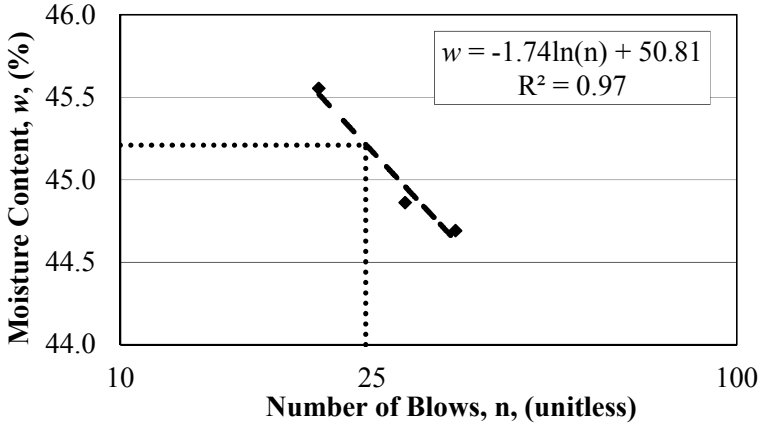

(b)

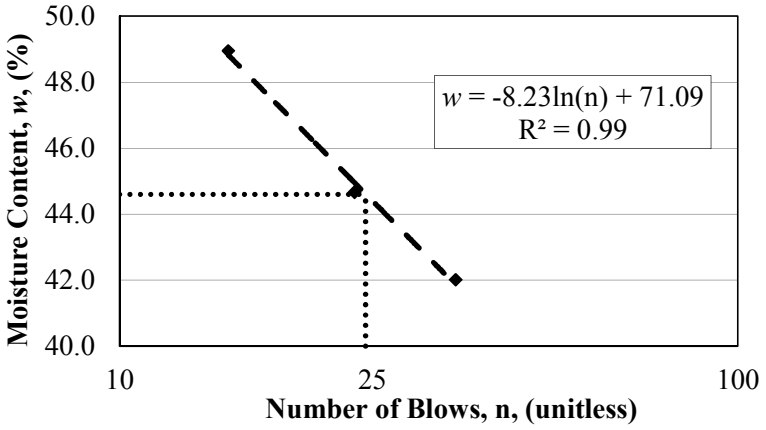

(c)

Figure A.7.5. Subgrade Liquid Limit plots for samples obtained from Section 3 at depths of: a) 0-2 inches, b) 2-4 inches, and c) 4-6 inches below the base course/subgrade interface.

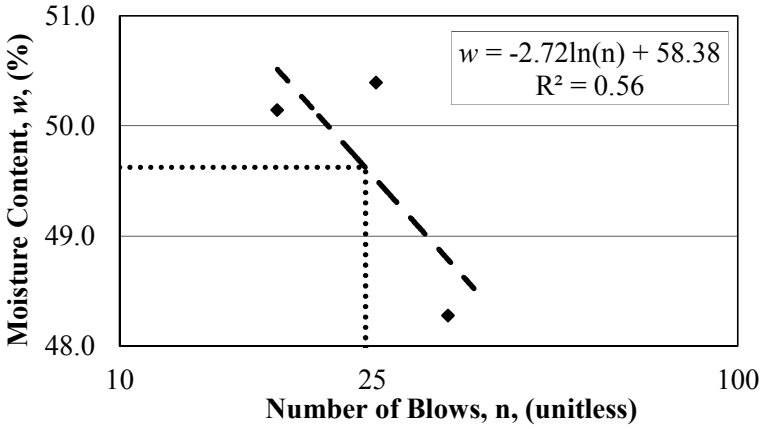

(a)

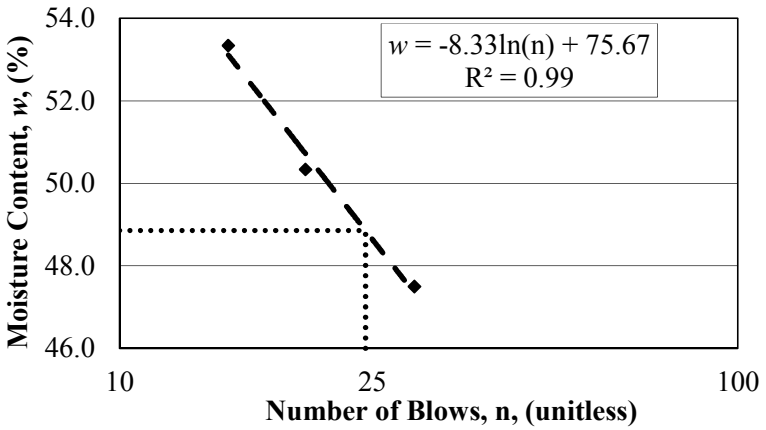

(b)

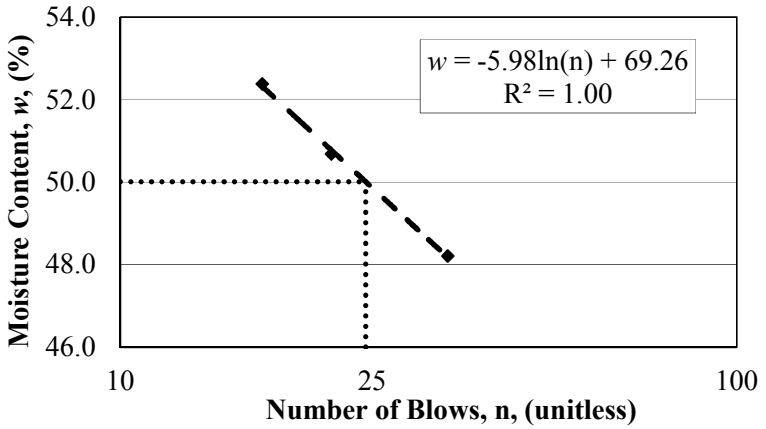

(c)

Figure A.7.6. Subgrade Liquid Limit plots for samples obtained from Section 4 at depths of: a) 0-2 inches, b) 2-4 inches, and c) 4-6 inches below the base course/subgrade interface.

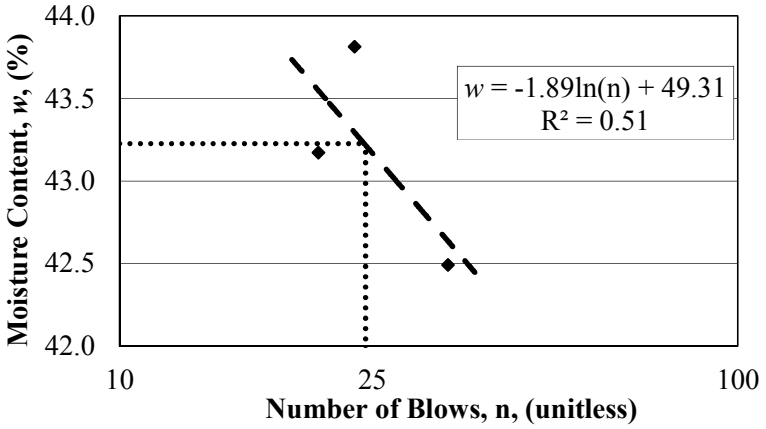

(a)

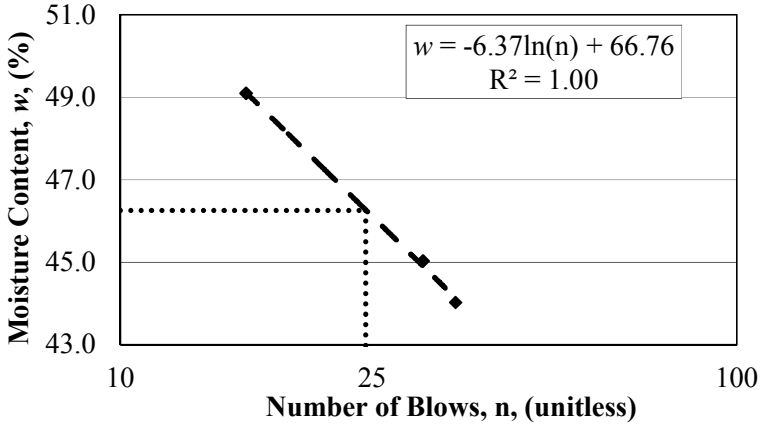

(b)

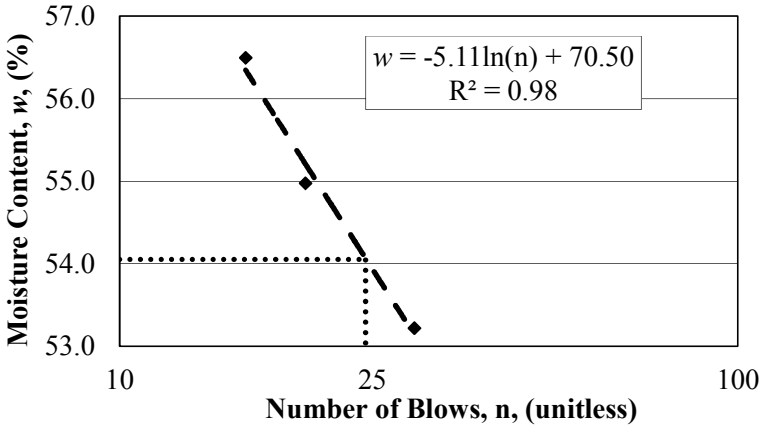

(c)

Figure A.7.7. Subgrade Liquid Limit plots for samples obtained from Section 5 at depths of: a) 0-2 inches, b) 2-4 inches, and c) 4-6 inches below the base course/subgrade interface.

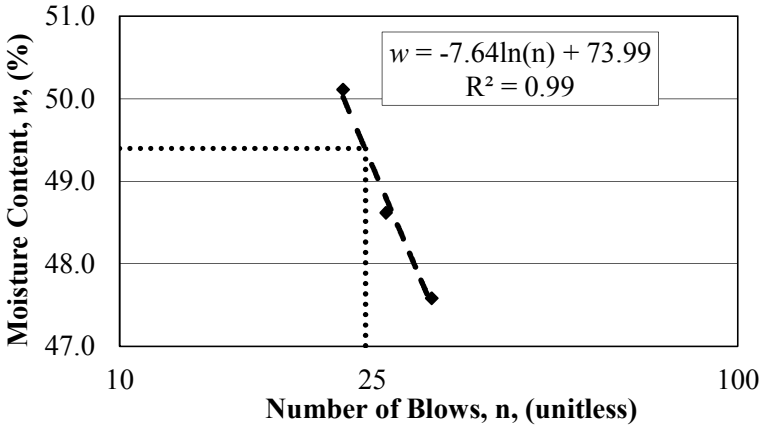

(a)

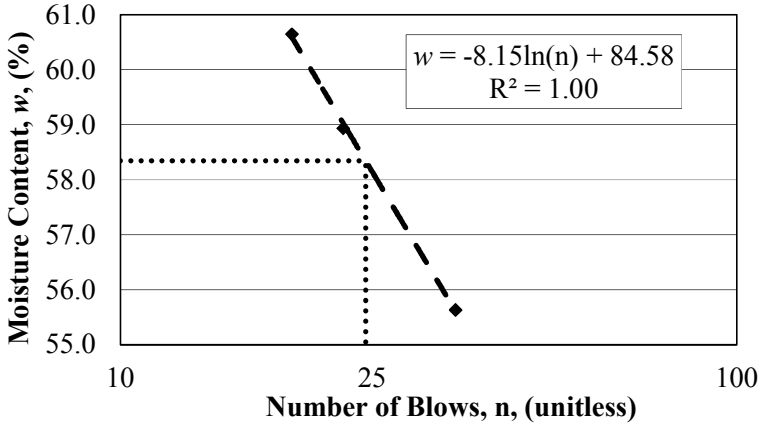

(b)

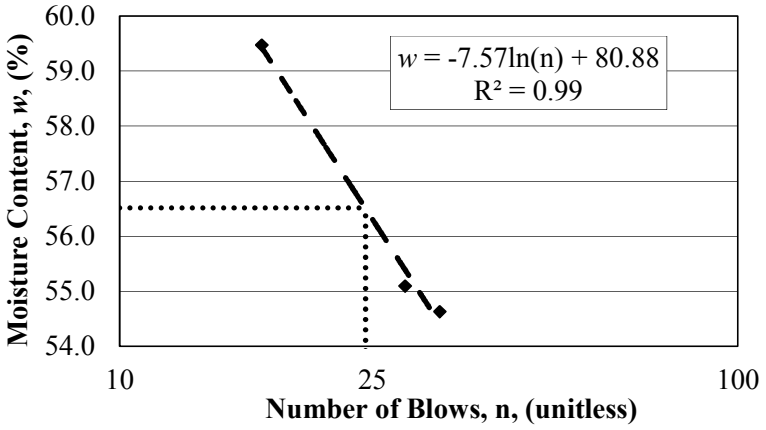

(c)

Figure A.7.8. Subgrade Liquid Limit plots for samples obtained from Section 6 at depths of: a) 0-2 inches, b) 2-4 inches, and c) 4-6 inches below the base course/subgrade interface.

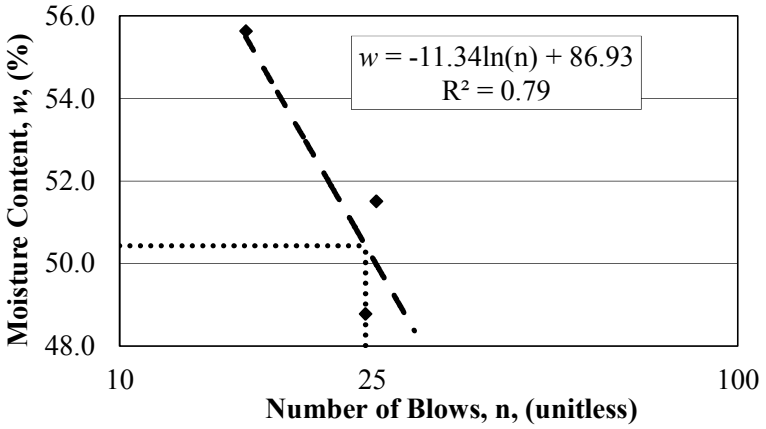

(a)

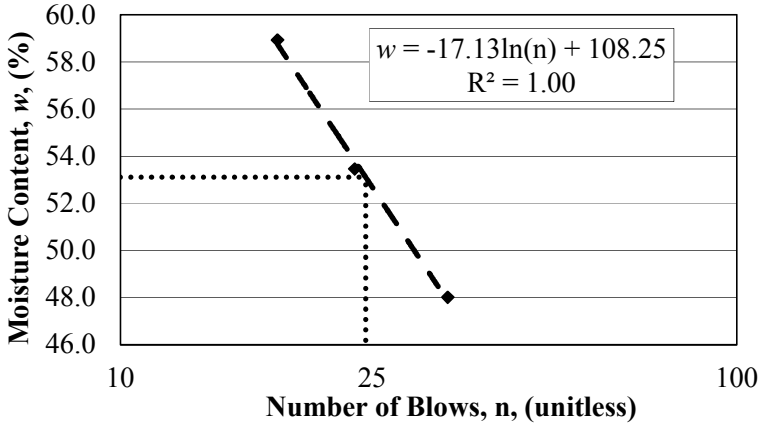

(b)

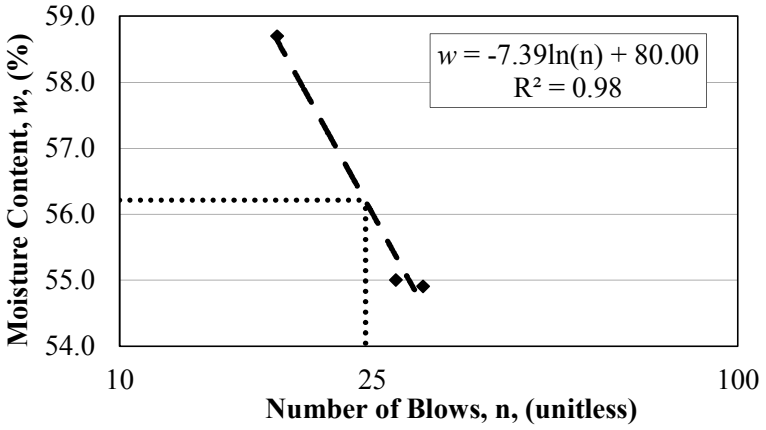

(c)

Figure A.7.9. Subgrade Liquid Limit plots for samples obtained from Section 8 at depths of: a) 0-2 inches, b) 2-4 inches, and c) 4-6 inches below the base course/subgrade interface.

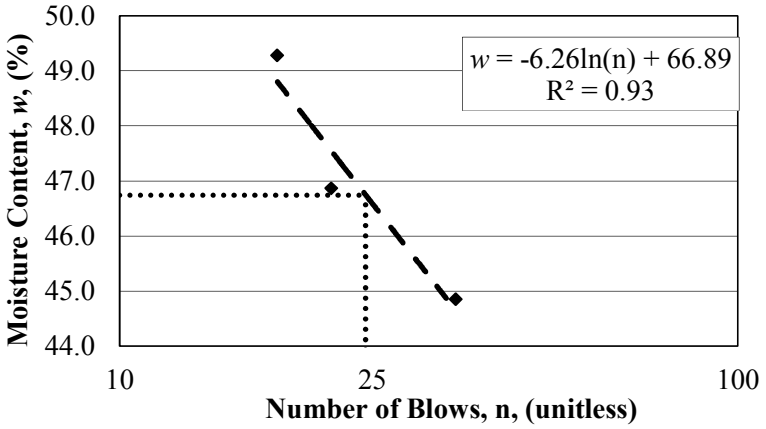

(a)

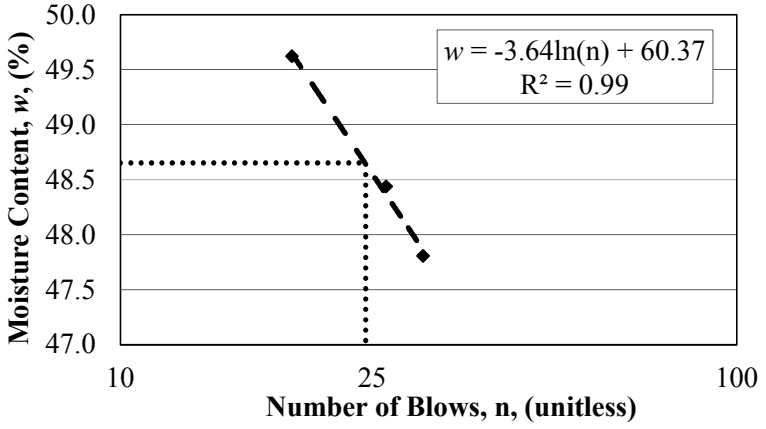

(b)

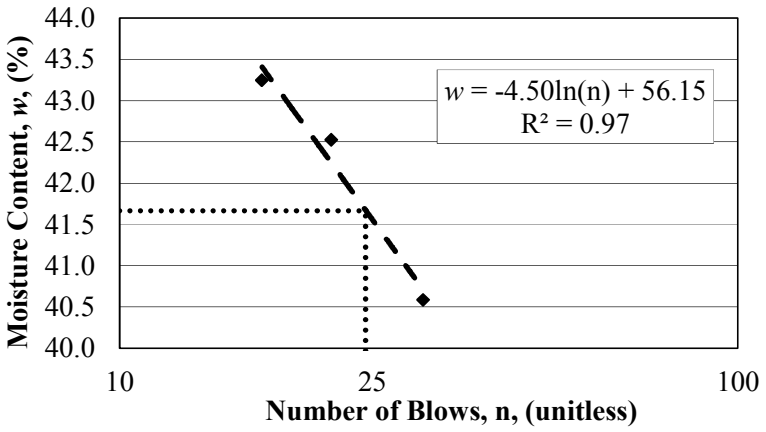

(c)

Figure A.7.10. Subgrade Liquid Limit plots for samples obtained from Section 9 at depths of: a) 0-2 inches, b) 2-4 inches, and c) 4-6 inches below the base course/subgrade interface.

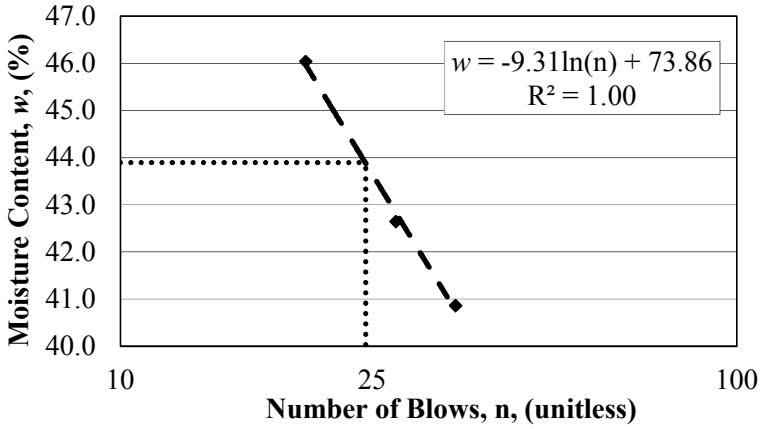

(a)

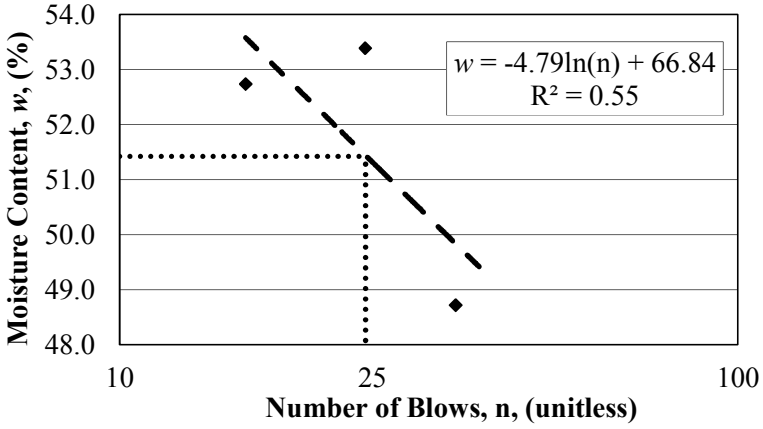

(b)

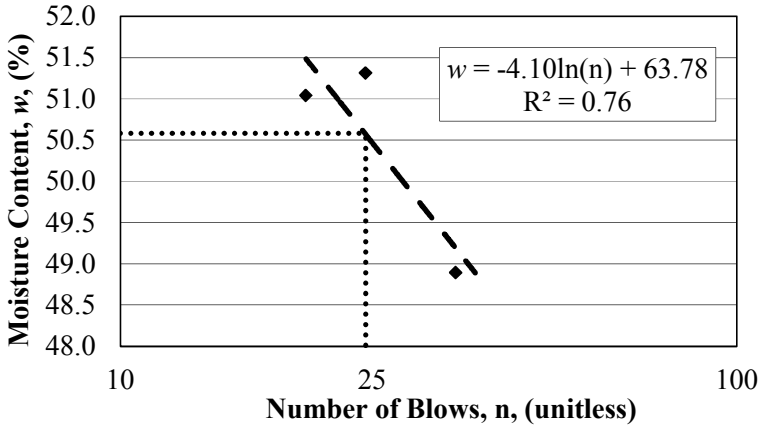

(c)

Figure A.7.11. Subgrade Liquid Limit plots for samples obtained from Section 10 at depths of: a) 0-2 inches, b) 2-4 inches, and c) 4-6 inches below the base course/subgrade interface.

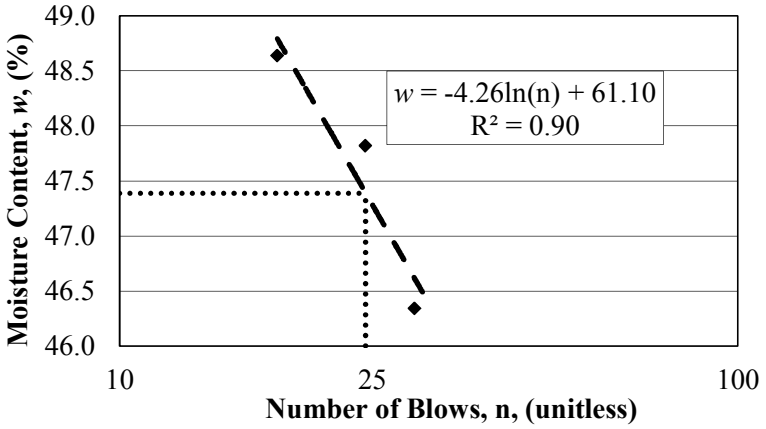

(a)

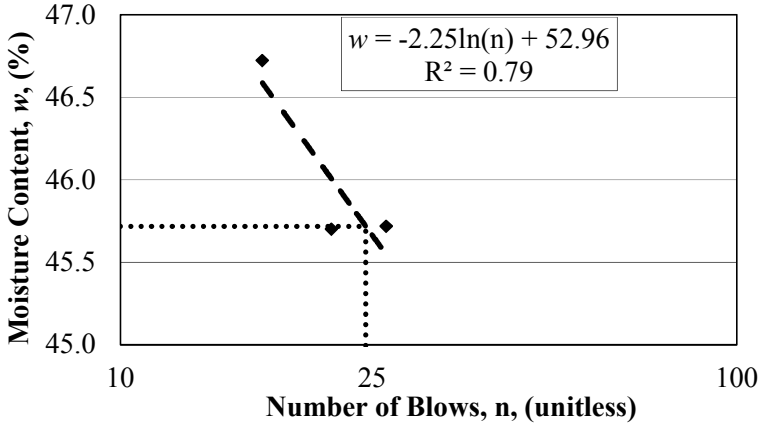

(b)

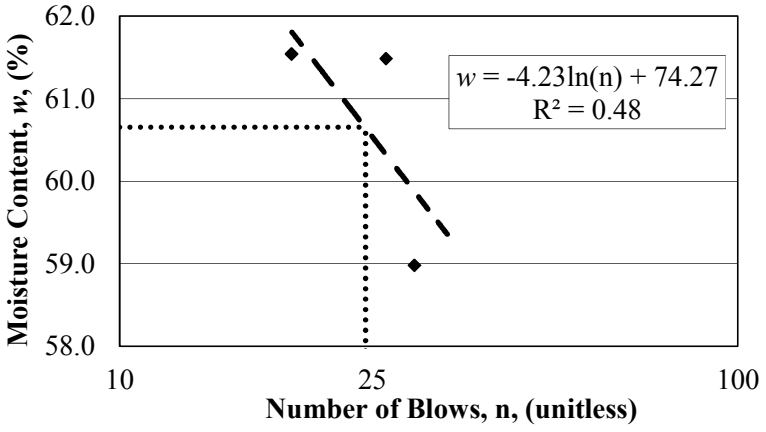

(c)

Figure A.7.12. Subgrade Liquid Limit plots for samples obtained from Section 11 at depths of: a) 0-2 inches, b) 2-4 inches, and c) 4-6 inches below the base course/subgrade interface.

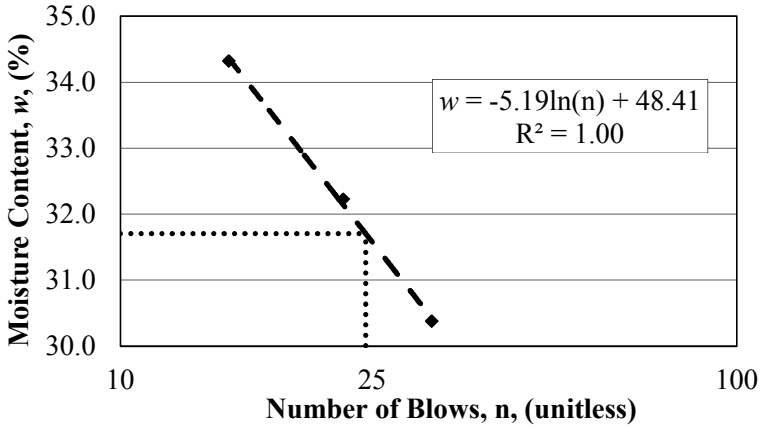

(a)

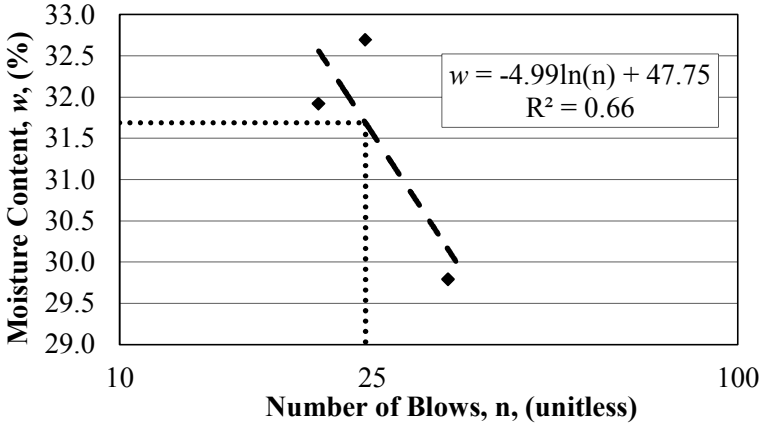

(b)

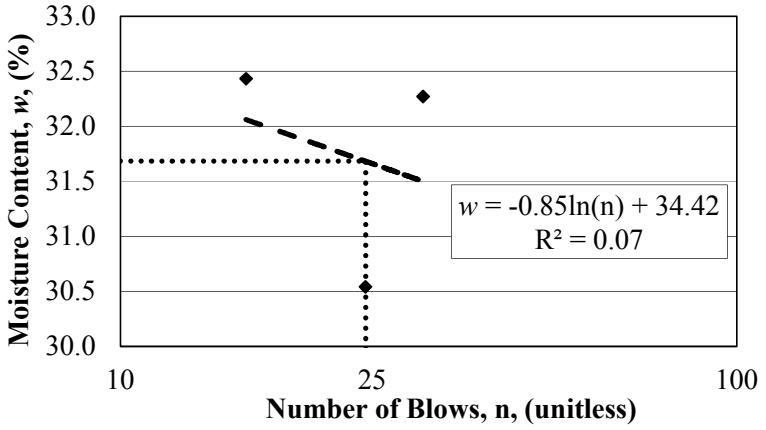

(c)

Figure A.7.13. Subgrade Liquid Limit plots for samples obtained from Section 12 at depths of: a) 0-2 inches, b) 2-4 inches, and c) 4-6 inches below the base course/subgrade interface.

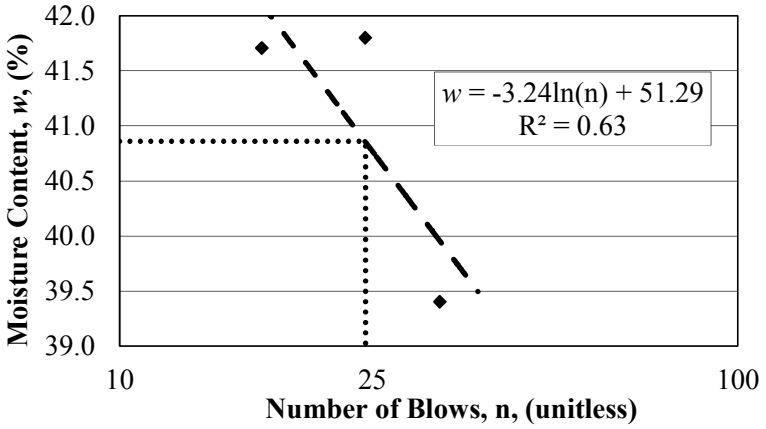

(a)

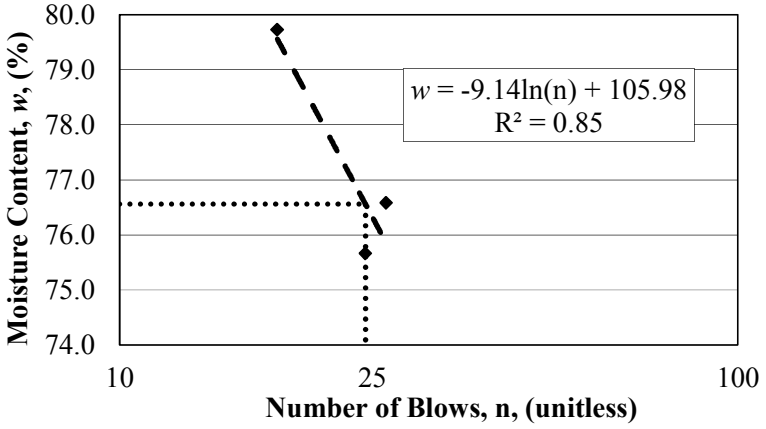

(b)

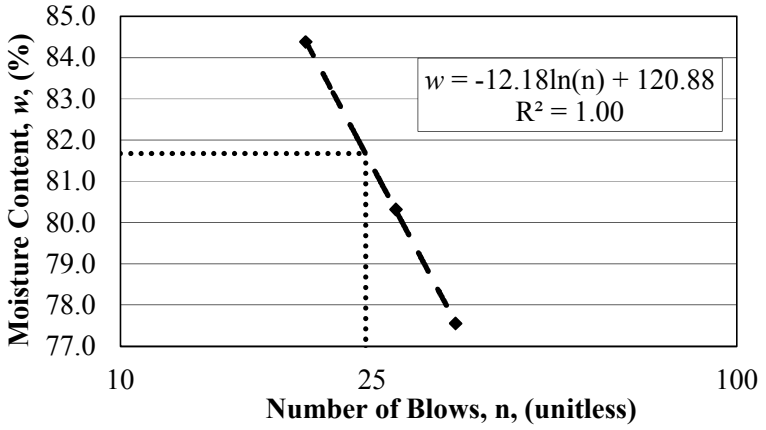

(c)

Figure A.7.14. Subgrade Liquid Limit plots for samples obtained from Section 13 at depths of: a) 0-2 inches, b) 2-4 inches, and c) 4-6 inches below the base course/subgrade interface.

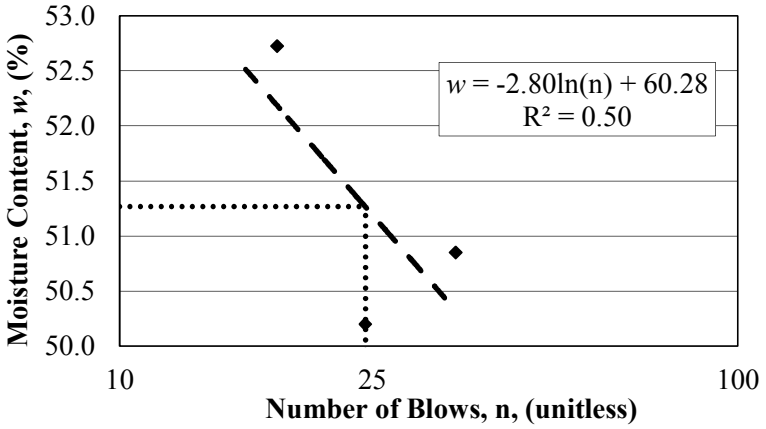

(a)

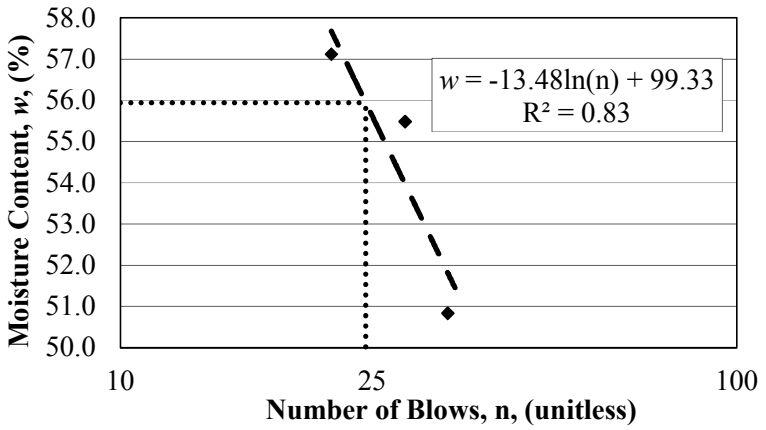

(b)

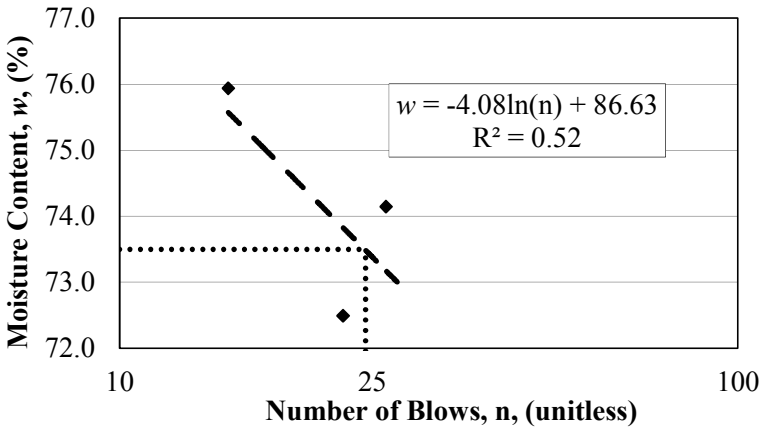

(c)

Figure A.7.15. Subgrade Liquid Limit plots for samples obtained from Section 13W at depths of: a) 0-2 inches, b) 2-4 inches, and c) 4-6 inches below the base course/subgrade interface.

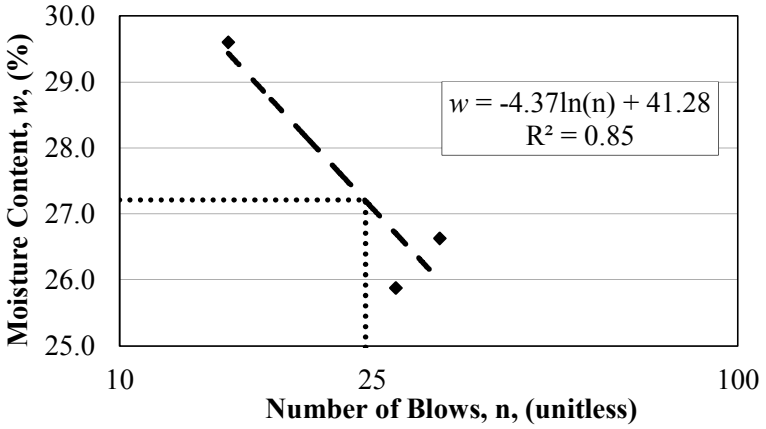

(a)

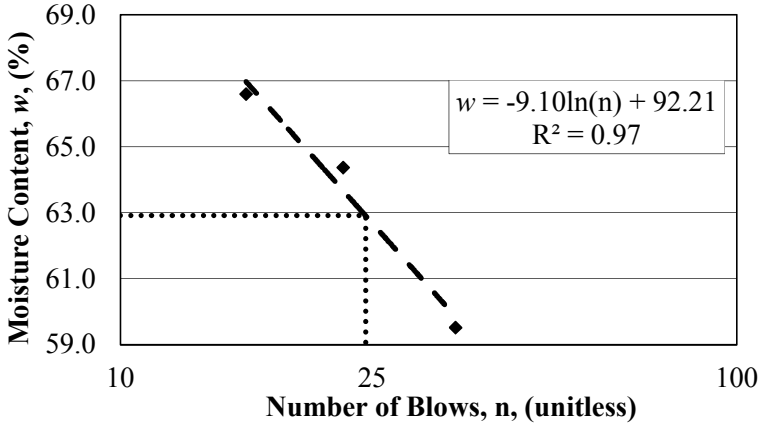

(b)

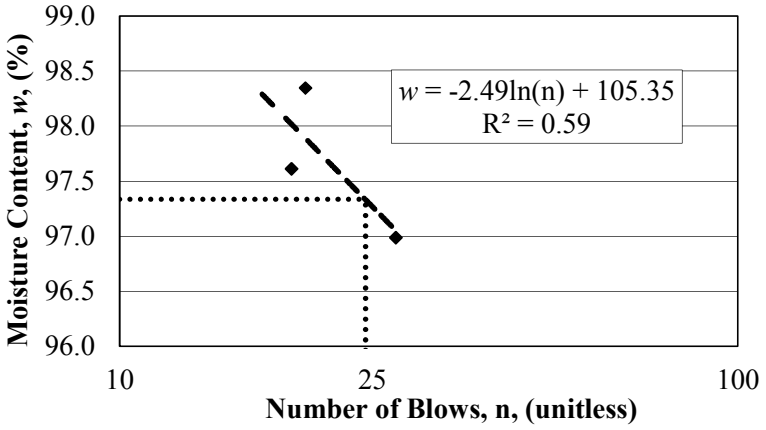

(c)

Figure A.7.16. Subgrade Liquid Limit plots for samples obtained from Section 13A at depths of: a) 0-2 inches, b) 2-4 inches, and c) 4-6 inches below the base course/subgrade interface.

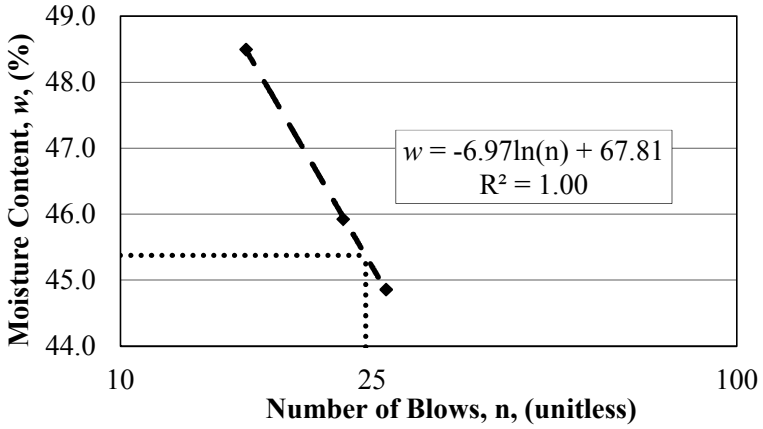

(a)

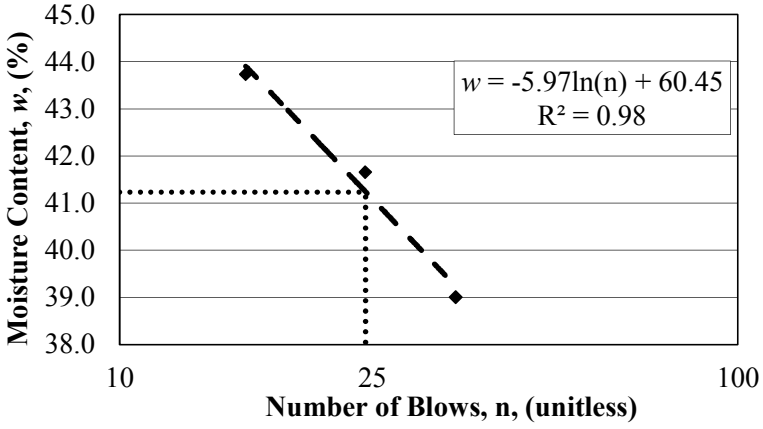

(b)

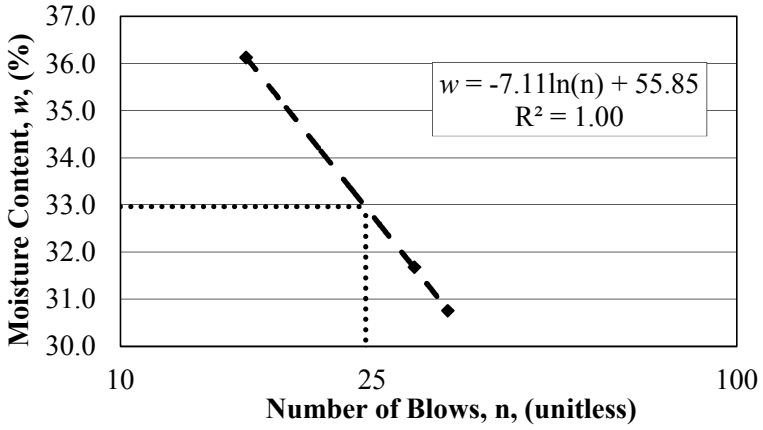

(c)

Figure A.7.17. Subgrade Liquid Limit plots for samples obtained from Section 13B at depths of: a) 0-2 inches, b) 2-4 inches, and c) 4-6 inches below the base course/subgrade interface.

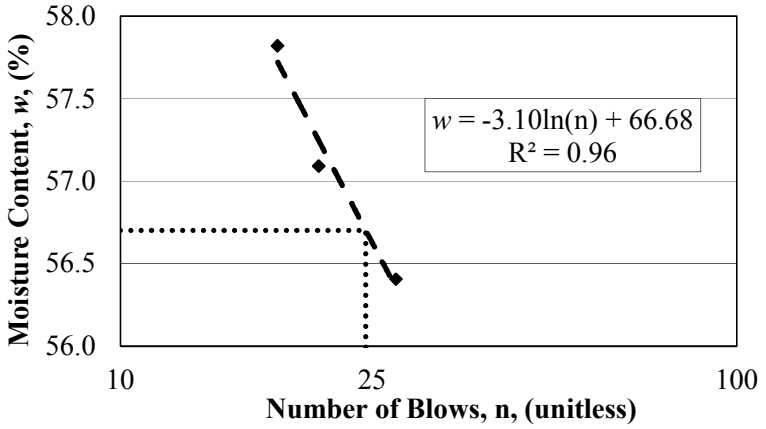

(a)

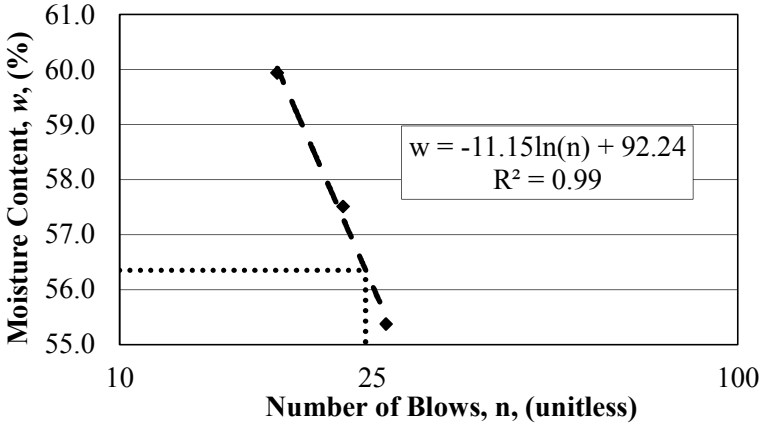

(b)

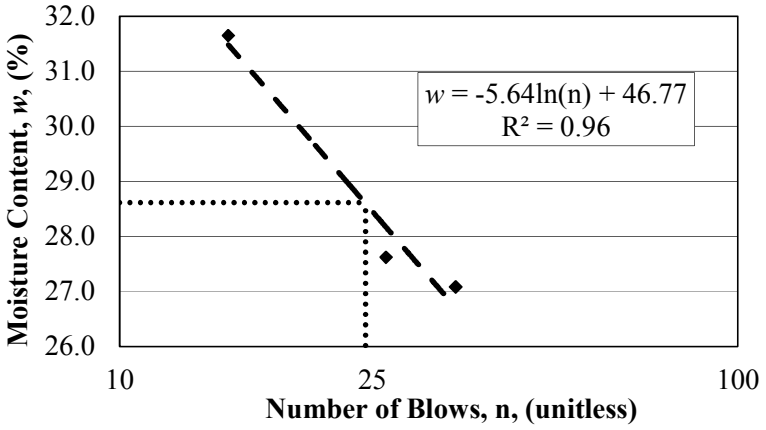

(c)

Figure A.7.18. Subgrade Liquid Limit plots for samples obtained from Section 13BW at depths of: a) 0-2 inches, b) 2-4 inches, and c) 4-6 inches below the base course/subgrade interface.

Table A.7.1. Liquid Limit (LL), Plastic Limit (PL), and Plasticity Index (PI) for the subgrade samples in the ten inch thick sections.

Location	Depth*	LL	PL	PI
	(inch)	(%)	(%)	(%)
Section 1B	0-2	37	15	22
Section 1B	2-4	32	14	18
Section 1B	4-6	39	21	18
Section 1A	0-2	36	19	17
Section 1A	2-4	27	15	11
Section 1A	4-6	25	13	12
Section 1	0-2	35	15	20
Section 1	2-4	38	15	23
Section 1	4-6	34	15	19
Section 2	0-2	48	18	30
Section 2	2-4	40	16	24
Section 2	4-6	38	19	19
Section 3	0-2	46	19	27
Section 3	2-4	45	19	26
Section 3	4-6	45	19	25
Section 4	0-2	50	20	29
Section 4	2-4	49	20	29
Section 4	4-6	50	18	32
Section 5	0-2	43	17	27
Section 5	2-4	46	18	28
Section 5	4-6	54	22	32
Section 6	0-2	49	19	30
Section 6	2-4	58	23	36
Section 6	4-6	57	28	29

* Depth below base course/subgrade interface

Table A.7.2. Liquid Limit (LL), Plastic Limit (PL), and Plasticity Index (PI) for the subgrade samples in the six inch thick sections.

Location	Depth*	LL	PL	PI
	(inch)	(%)	(%)	(%)
Section 8	0-2	50	33	17
Section 8	2-4	53	22	31
Section 8	4-6	56	21	35
Section 9	0-2	47	18	29
Section 9	2-4	49	18	31
Section 9	4-6	42	18	24
Section 10	0-2	44	19	25
Section 10	2-4	51	25	27
Section 10	4-6	51	20	30
Section 11	0-2	47	19	28
Section 11	2-4	46	21	25
Section 11	4-6	61	26	35
Section 12	0-2	32	15	17
Section 12	2-4	32	14	18
Section 12	4-6	32	13	18
Section 13	0-2	41	16	25
Section 13	2-4	77	29	48
Section 13	4-6	82	29	52
Section 13A	0-2	27	14	14
Section 13A	2-4	63	23	40
Section 13A	4-6	97	30	68
Section 13B	0-2	45	17	29
Section 13B	2-4	41	16	25
Section 13B	4-6	33	14	19
Section 13W	0-2	51	16	36
Section 13W	2-4	56	18	38
Section 13W	4-6	73	24	50
Section 13BW	0-2	57	20	37
Section 13BW	2-4	56	23	33
Section 13BW	4-6	29	13	16

* Depth below base course/subgrade interface

A.8. Specific Gravity

Table A.8.1. Specific gravity results for the fines from base course samples obtained from the ten inch thick sections.

Location	Depth*	Test Temp.	Mass of dry pycnometer	Calibrated volume of pycnometer	Mass of pycnometer and water	Mass of pycnometer with water and soil	Specific Gravity	Correction Factor (K)	Specific Gravity at 20°C
	(in)	(°C)	(g)	(mL)	(g)	(g)	(unitless)		
Base Section 1B	0-2	23.1	103.29	249.42	352.09	383.99	2.76	0.99931	2.76
Base Section 1B	2-4	23.1	102.02	249.46	350.87	382.70	2.75	0.99931	2.75
Base Section 1B	4-6	23.2	102.02	249.46	350.86	382.82	2.77	0.99929	2.77
Base Section 1B	6-8	22.7	99.55	249.30	348.26	380.31	2.79	0.99941	2.78
Base Section 1B	8-10	23.3	103.29	249.42	352.08	383.95	2.76	0.99926	2.76
Base Section 1A	0-2	23.1	99.55	249.30	348.24	380.38	2.80	0.99931	2.80
Base Section 1A	2-4	23.4	103.29	249.42	352.07	384.10	2.78	0.99924	2.78
Base Section 1A	4-6	23.4	102.02	249.46	350.85	383.15	2.83	0.99924	2.82
Base Section 1A	6-8	23.0	99.55	249.30	348.24	380.26	2.78	0.99934	2.78
Base Section 1A	8-10	23.2	103.29	249.42	352.09	384.17	2.79	0.99929	2.79
Base Section 1	0-2	23.0	99.55	249.30	348.24	380.38	2.80	0.99934	2.80
Base Section 1	2-4	23.0	102.02	249.46	350.87	382.98	2.79	0.99934	2.79
Base Section 1	4-6	23.3	103.29	249.42	352.08	384.23	2.80	0.99926	2.80
Base Section 1	6-8	23.1	102.02	249.46	350.87	383.04	2.80	0.99931	2.80
Base Section 1	8-10	23.0	99.55	249.30	348.24	380.23	2.78	0.99934	2.77
Base Section 2	0-2	23.2	102.02	249.46	350.86	383.10	2.82	0.99929	2.81
Base Section 2	2-4	22.9	99.55	249.30	348.25	380.27	2.78	0.99936	2.78
Base Section 2	4-6	23.1	103.29	249.42	352.09	384.10	2.78	0.99931	2.78
Base Section 2	6-8	22.4	99.55	249.30	348.28	380.33	2.79	0.99948	2.78
Base Section 2	8-10	22.4	102.02	249.46	350.91	383.00	2.79	0.99948	2.79
Base Section 3	0-2	22.7	99.55	249.30	348.26	380.38	2.80	0.99941	2.79
Base Section 3	2-4	22.7	103.29	249.42	352.12	384.01	2.76	0.99941	2.76
Base Section 3	4-6	23.4	103.29	249.42	352.07	383.94	2.76	0.99924	2.76
Base Section 3	6-8	22.7	102.02	249.46	350.89	382.96	2.79	0.99941	2.79
Base Section 3	8-10	22.7	99.55	249.30	348.26	380.30	2.78	0.99941	2.78
Base Section 4	0-2	22.9	99.55	249.30	348.25	380.90	2.88	0.99936	2.88
Base Section 4	2-4	22.7	102.02	249.46	350.89	382.88	2.78	0.99941	2.77
Base Section 4	4-6	22.7	103.29	249.42	352.12	384.18	2.79	0.99941	2.79
Base Section 4	6-8	22.6	99.55	249.30	348.26	380.26	2.78	0.99943	2.78
Base Section 4	8-10	22.1	102.02	249.46	350.92	382.98	2.79	0.99954	2.79
Base Section 5	0-2	22.7	102.02	249.46	350.89	383.01	2.80	0.99941	2.79
Base Section 5	2-4	22.8	103.29	249.42	352.11	384.06	2.77	0.99938	2.77
Base Section 5	4-6	22.3	103.29	249.42	352.14	384.09	2.77	0.99950	2.77
Base Section 5	6-8	22.3	102.02	249.46	350.91	382.83	2.77	0.99950	2.76
Base Section 5	8-10	22.4	99.55	249.30	348.28	380.28	2.78	0.99948	2.78
Base Section 6	0-2	22.2	103.29	249.42	352.14	384.36	2.81	0.99952	2.81
Base Section 6	2-4	22.6	99.55	249.30	348.26	380.42	2.80	0.99943	2.80
Base Section 6	4-6	22.3	102.02	249.46	350.91	383.16	2.82	0.99950	2.82
Base Section 6	6-8	22.4	103.29	249.42	352.13	384.36	2.81	0.99948	2.81
Base Section 6	8-10	22.6	99.55	249.30	348.26	380.44	2.81	0.99943	2.80

*Depth below asphalt/base course interface

Table A.8.2. Specific gravity results for the fines from base course samples obtained from the six inch thick sections.

Location	Depth*	Test Temp.	Mass of dry pycnometer	Calibrated volume of pycnometer	Mass of pycnometer and water	Mass of pycnometer with water and soil	Specific Gravity	Correction Factor (K)	Specific Gravity at 20°C
	(in)	(°C)	(g)	(mL)	(g)	(g)	(unitless)		
Base Section 8	0-2	22.6	102.02	249.46	350.89	383.11	2.81	0.99943	2.81
Base Section 8	2-4	22.4	103.29	249.42	352.13	384.18	2.79	0.99948	2.78
Base Section 8	4-6	22.7	99.55	249.30	348.26	380.44	2.81	0.99941	2.80
Base Section 9	0-2	22.8	102.02	249.46	350.88	383.10	2.81	0.99938	2.81
Base Section 9	2-4	22.4	102.02	249.46	350.91	383.00	2.79	0.99948	2.79
Base Section 9	4-6	22.5	103.29	249.42	352.13	384.39	2.82	0.99945	2.82
Base Section 10	0-2	22.4	103.29	249.42	352.13	384.12	2.78	0.99948	2.77
Base Section 10	2-4	22.3	99.55	249.30	348.28	380.41	2.80	0.99950	2.80
Base Section 10	4-6	22.4	99.55	249.30	348.28	380.33	2.79	0.99948	2.78
Base Section 11	0-2	22.8	102.02	249.46	350.88	382.81	2.77	0.99938	2.76
Base Section 11	2-4	22.7	102.02	249.46	350.89	383.22	2.83	0.99941	2.83
Base Section 11	4-6	23.5	99.55	249.30	348.21	380.12	2.76	0.99922	2.76
Base Section 12	0-2	22.7	103.29	249.42	352.12	384.51	2.84	0.99941	2.84
Base Section 12	2-4	22.6	103.29	249.42	352.12	384.14	2.78	0.99943	2.78
Base Section 12	4-6	23.0	99.55	249.30	348.24	380.30	2.79	0.99934	2.78
Base Section 13	0-2	22.6	99.55	249.30	348.26	380.50	2.81	0.99943	2.81
Base Section 13	2-4	22.9	103.29	249.42	352.10	384.20	2.79	0.99936	2.79
Base Section 13	4-6	22.8	99.55	249.30	348.25	380.50	2.82	0.99938	2.81
Base Section 13W	0-2	23.0	102.02	249.46	350.87	382.76	2.76	0.99934	2.76
Base Section 13W	2-4	22.6	103.29	249.42	352.12	384.10	2.77	0.99943	2.77
Base Section 13W	4-6	22.4	99.55	249.30	348.28	380.57	2.82	0.99948	2.82
Base Section 13A	0-2	22.8	103.29	249.42	352.11	384.20	2.79	0.99938	2.79
Base Section 13A	2-4	23.0	102.02	249.46	350.87	383.06	2.81	0.99934	2.81
Base Section 13A	4-6	22.7	102.02	249.46	350.89	383.14	2.82	0.99941	2.82
Base Section 13B	0-2	22.9	103.29	249.42	352.10	384.14	2.78	0.99936	2.78
Base Section 13B	2-4	22.4	99.55	249.30	348.28	380.37	2.79	0.99948	2.79
Base Section 13B	4-6	22.6	102.02	249.46	350.89	382.97	2.79	0.99943	2.79
Base Section 13BW	0-2	23.0	99.55	249.30	348.24	380.61	2.84	0.99934	2.83
Base Section 13BW	2-4	22.4	102.02	249.46	350.91	383.04	2.80	0.99948	2.80
Base Section 13BW	4-6	22.7	103.29	249.42	352.12	383.84	2.74	0.99941	2.73

*Depth below asphalt/base course interface

Table A.8.3. Specific gravity results for subgrade samples obtained from the ten inch sections.

Location	Depth*	Test Temp.	Mass of dry pycnometer	Calibrated volume of pycnometer	Mass of pycnometer and water	Mass of pycnometer with water and soil	Specific Gravity	Correction Factor (K)	Specific Gravity at 20°C
	(in)	(°C)	(g)	(mL)	(g)	(g)	(unitless)		
Subgrade Section 1B	0-2	23.0	103.29	249.42	352.10	383.18	2.64	0.99934	2.64
Subgrade Section 1B	2-4	21.8	102.02	249.46	350.94	382.20	2.67	0.99961	2.67
Subgrade Section 1B	4-6	22.2	103.29	249.42	352.14	383.28	2.65	0.99952	2.65
Subgrade Section 1A	0-2	21.6	102.02	249.46	350.95	382.42	2.70	0.99966	2.70
Subgrade Section 1A	2-4	22.1	99.55	249.30	348.29	379.20	2.62	0.99954	2.62
Subgrade Section 1A	4-6	21.6	99.55	249.30	348.32	379.60	2.67	0.99966	2.67
Subgrade Section 1	0-2	22.3	102.02	249.46	350.91	382.66	2.74	0.99950	2.74
Subgrade Section 1	2-4	23.2	103.29	249.42	352.09	383.35	2.67	0.99929	2.67
Subgrade Section 1	4-6	21.7	99.55	249.30	348.32	379.50	2.66	0.99963	2.66
Subgrade Section 2	0-2	22.6	103.29	249.42	352.12	383.50	2.69	0.99943	2.68
Subgrade Section 2	2-4	23.3	103.29	249.42	352.08	383.65	2.71	0.99926	2.71
Subgrade Section 2	4-6	No Sample							
Subgrade Section 3	0-2	25.1	102.02	249.46	350.74	382.88	2.80	0.99882	2.80
Subgrade Section 3	2-4	22.7	99.55	249.30	348.26	379.57	2.68	0.99941	2.67
Subgrade Section 3	4-6	22.9	102.02	249.46	350.88	382.60	2.74	0.99936	2.73
Subgrade Section 4	0-2	23.0	102.02	249.46	350.87	382.25	2.69	0.99934	2.68
Subgrade Section 4	2-4	22.9	99.55	249.30	348.25	379.40	2.65	0.99936	2.65
Subgrade Section 4	4-6	23.2	102.02	249.46	350.86	381.93	2.64	0.99929	2.64
Subgrade Section 5	0-2	22.7	99.55	249.30	348.26	379.60	2.68	0.99941	2.68
Subgrade Section 5	2-4	24.0	103.29	249.42	352.04	382.93	2.62	0.99909	2.61
Subgrade Section 5	4-6	23.8	103.29	249.42	352.05	383.67	2.72	0.99914	2.72
Subgrade Section 6	0-2	23.6	102.02	249.46	350.84	382.20	2.68	0.99919	2.68
Subgrade Section 6	2-4	22.6	99.55	249.30	348.26	379.27	2.63	0.99943	2.63
Subgrade Section 6	4-6	23.0	99.55	249.30	348.24	379.71	2.70	0.99934	2.70

*Depth below base course/subgrade interface

Table A.8.4. Specific gravity results for subgrade samples obtained from the six inch thick sections.

Location	Depth*	Test Temp.	Mass of dry pycnometer	Calibrated volume of pycnometer	Mass of pycnometer and water	Mass of pycnometer with water and soil	Specific Gravity	Correction Factor (K)	Specific Gravity at 20°C
	(in)	(°C)	(g)	(mL)	(g)	(g)	(unitless)		
Subgrade Section 8	0-2	23.3	103.29	249.42	352.08	383.15	2.64	0.99926	2.64
Subgrade Section 8	2-4	22.8	102.02	249.46	350.88	382.18	2.67	0.99938	2.67
Subgrade Section 8	4-6	23.3	103.29	249.42	352.08	383.31	2.66	0.99926	2.66
Subgrade Section 9	0-2	23.1	102.02	249.46	350.87	382.18	2.68	0.99931	2.67
Subgrade Section 9	2-4	22.9	99.55	249.30	348.25	379.20	2.63	0.99936	2.62
Subgrade Section 9	4-6	22.9	102.02	249.46	350.88	382.04	2.65	0.99936	2.65
Subgrade Section 10	0-2	22.7	99.55	249.30	348.26	379.40	2.65	0.99941	2.65
Subgrade Section 10	2-4	23.3	103.29	249.42	352.08	383.07	2.63	0.99926	2.63
Subgrade Section 10	4-6	23.1	103.29	249.42	352.09	383.29	2.66	0.99931	2.66
Subgrade Section 11	0-2	23.3	103.29	249.42	352.08	383.29	2.66	0.99926	2.66
Subgrade Section 11	2-4	22.8	102.02	249.46	350.88	382.22	2.68	0.99938	2.68
Subgrade Section 11	4-6	23.7	103.29	249.42	352.06	383.52	2.70	0.99917	2.70
Subgrade Section 12	0-2	22.6	99.55	249.30	348.26	379.30	2.64	0.99943	2.63
Subgrade Section 12	2-4	23.0	102.02	249.46	350.87	382.10	2.66	0.99934	2.66
Subgrade Section 12	4-6	23.0	99.55	249.30	348.24	379.30	2.64	0.99934	2.64
Subgrade Section 13	0-2	22.6	99.55	249.30	348.26	378.89	2.58	0.99943	2.58
Subgrade Section 13	2-4	22.9	102.02	249.46	350.88	381.66	2.60	0.99936	2.60
Subgrade Section 13	4-6	23.7	103.29	249.42	352.06	383.32	2.67	0.99917	2.67
Subgrade Section 13W	0-2	22.6	99.55	249.30	348.26	379.51	2.67	0.99943	2.66
Subgrade Section 13W	2-4	22.9	99.55	249.30	348.25	379.44	2.66	0.99936	2.66
Subgrade Section 13W	4-6	23.0	102.02	249.46	350.87	382.54	2.73	0.99934	2.73
Subgrade Section 13A	0-2	23.5	103.29	249.42	352.07	382.98	2.62	0.99922	2.62
Subgrade Section 13A	2-4	23.9	99.55	249.30	348.19	379.09	2.62	0.99912	2.62
Subgrade Section 13A	4-6	23.6	99.55	249.30	348.21	379.12	2.62	0.99919	2.62
Subgrade Section 13B	0-2	24.5	103.29	249.42	352.01	382.99	2.63	0.99897	2.63
Subgrade Section 13B	2-4	24.2	99.55	249.30	348.17	379.14	2.63	0.99905	2.63
Subgrade Section 13B	4-6	23.7	103.29	249.42	352.06	383.06	2.63	0.99917	2.63
Subgrade Section 13BW	0-2	23.1	99.55	249.30	348.24	379.25	2.63	0.99931	2.63
Subgrade Section 13BW	2-4	23.5	103.29	249.42	352.07	382.93	2.61	0.99922	2.61
Subgrade Section 13BW	4-6	23.7	103.29	249.42	352.06	382.98	2.62	0.99917	2.62

*Depth below base course/subgrade interface

A.9. Modified Proctor

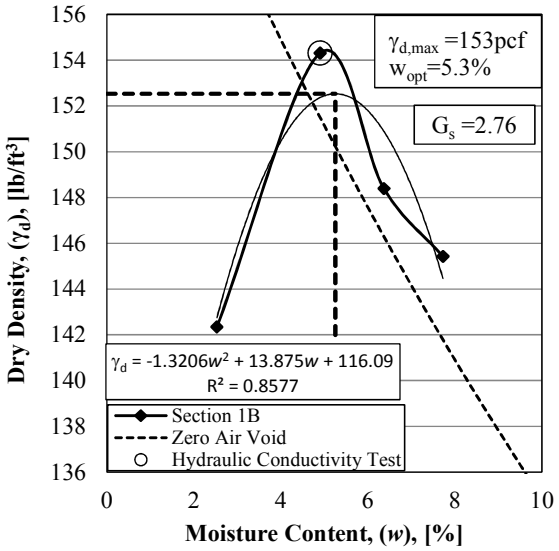

Figure A.9.1. Proctor curve for Section 1B base course sample obtained from 8-10 inches below the asphalt/base course interface.

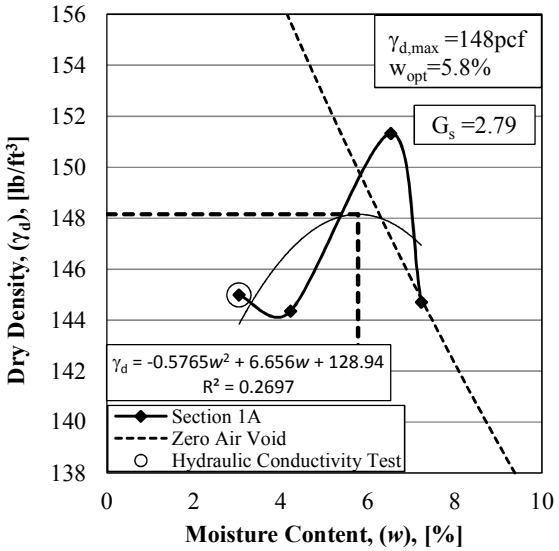

Figure A.9.2. Proctor curve for Section 1A base course sample obtained from 8-10 inches below the asphalt/base course interface.

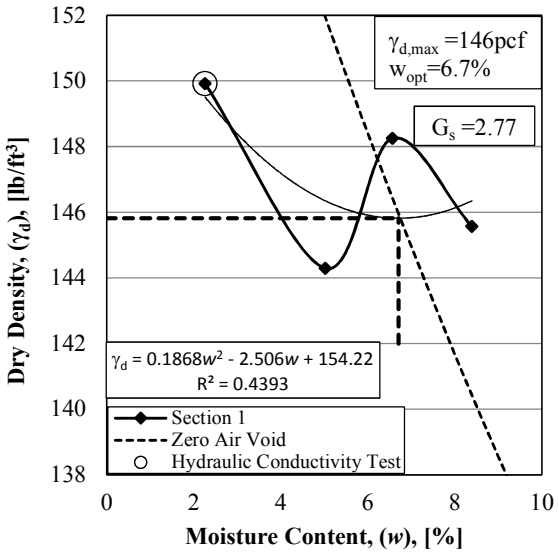

Figure A.9.3. Proctor curve for Section 1 base course sample obtained from 8-10 inches below the asphalt/base course interface.

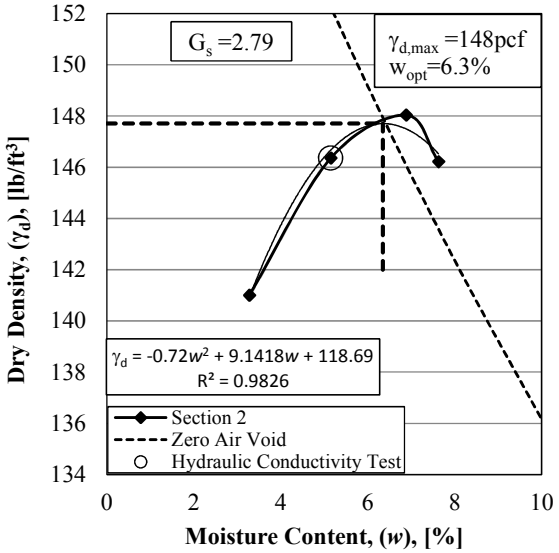

Figure A.9.4. Proctor curve for Section 2 base course sample obtained from 8-10 inches below the asphalt/base course interface.

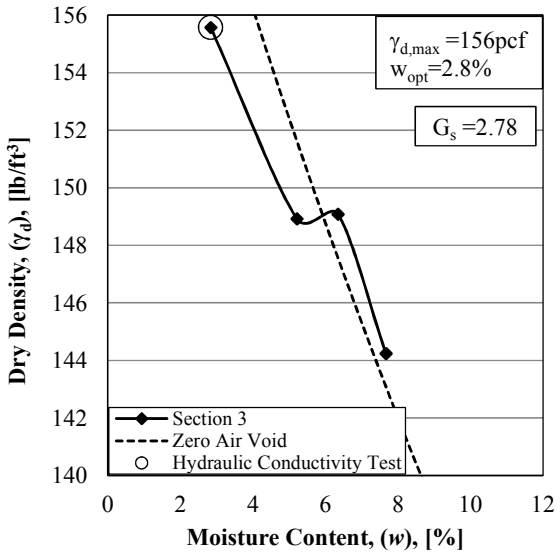

Figure A.9.5. Proctor curve for Section 3 base course sample obtained from 8-10 inches below the asphalt/base course interface.

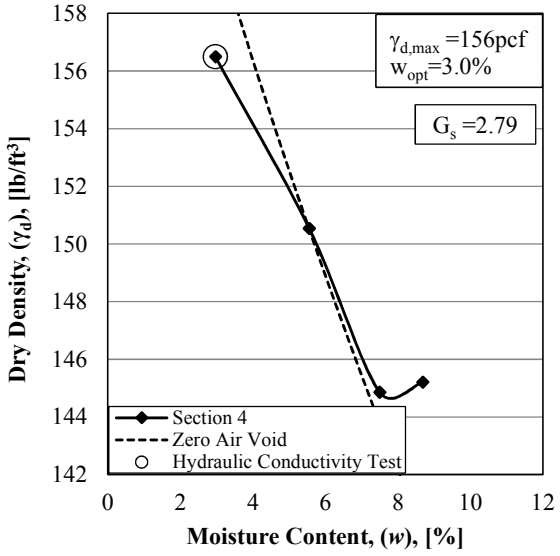

Figure A.9.6. Proctor curve for Section 4 base course sample obtained from 8-10 inches below the asphalt/base course interface.

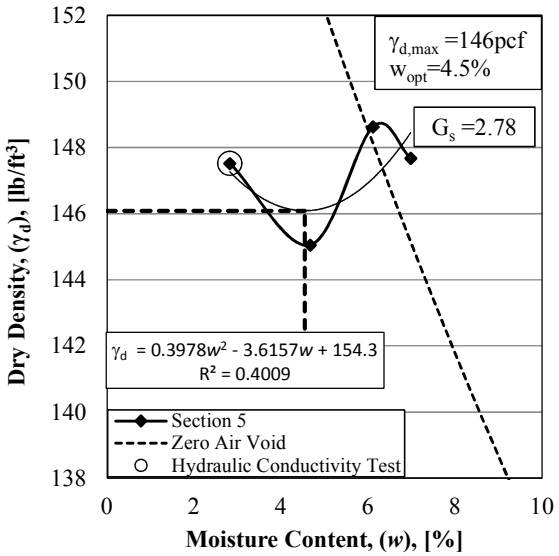

Figure A.9.7. Proctor curve for Section 5 base course sample obtained from 8-10 inches below the asphalt/base course interface.

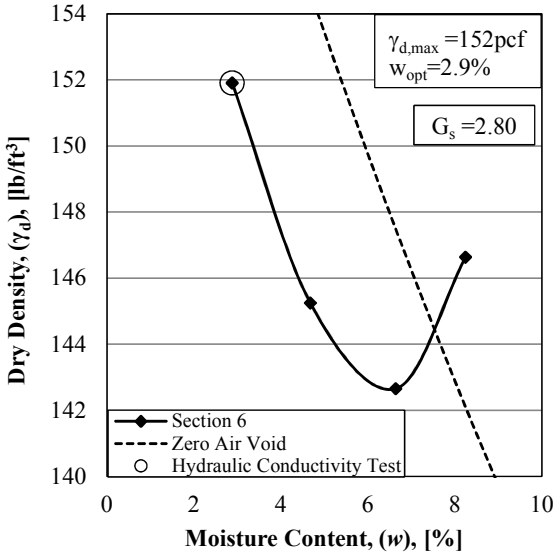

Figure A.9.8. Proctor curve for Section 6 base course sample obtained from 8-10 inches below the asphalt/base course interface.

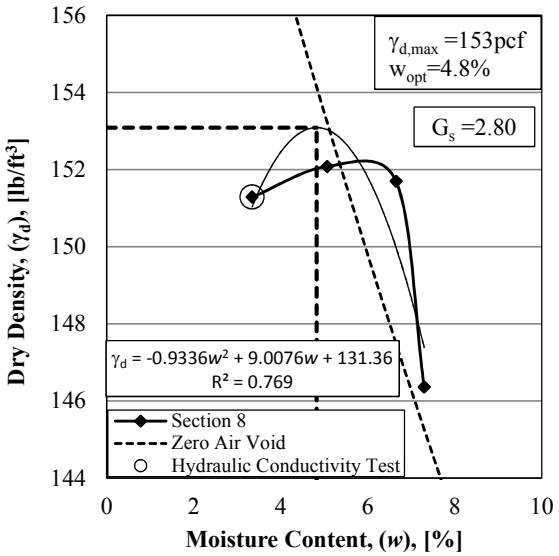

Figure A.9.9. Proctor curve for Section 8 base course sample obtained from 4-6 inches below the asphalt/base course interface.

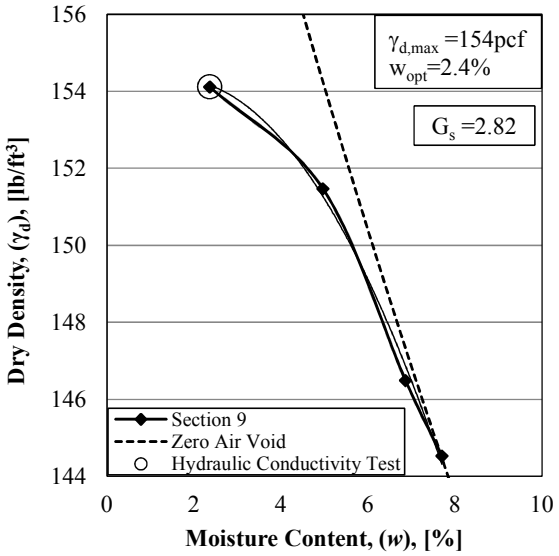

Figure A.9.10. Proctor curve for Section 9 base course sample obtained from 4-6 inches below the asphalt/base course interface.

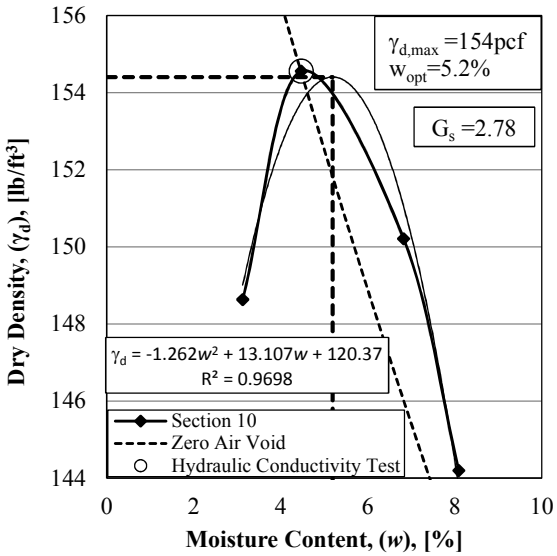

Figure A.9.11. Proctor curve for Section 10 base course sample obtained from 4-6 inches below the asphalt/base course interface.

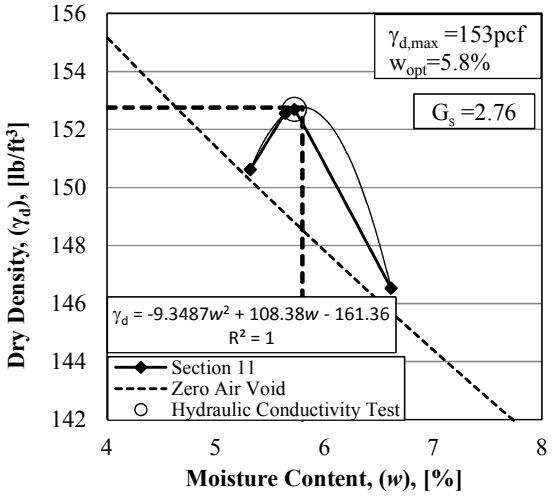

Figure A.9.12. Proctor curve for Section 11 base course sample obtained from 4-6 inches below the asphalt/base course interface.

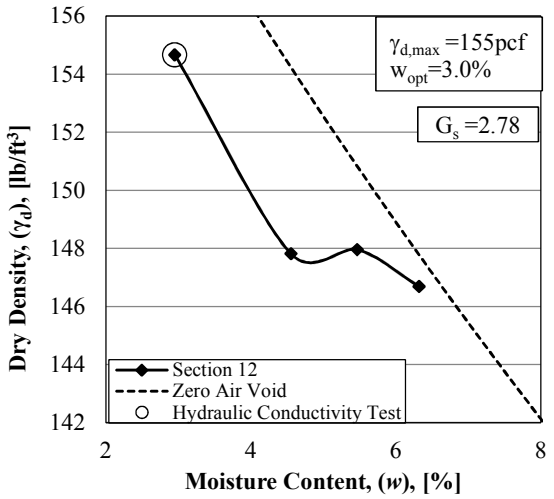

Figure A.9.13. Proctor curve for Section 12 base course sample obtained from 4-6 inches below the asphalt/base course interface.

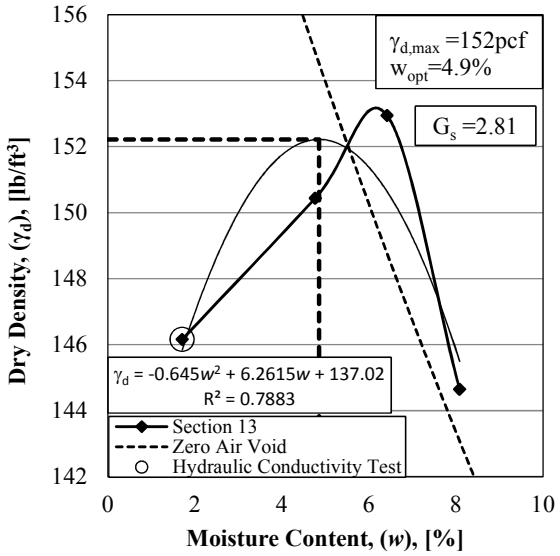

Figure A.9.14. Proctor curve for Section 13 base course sample obtained from 4-6 inches below the asphalt/base course interface.

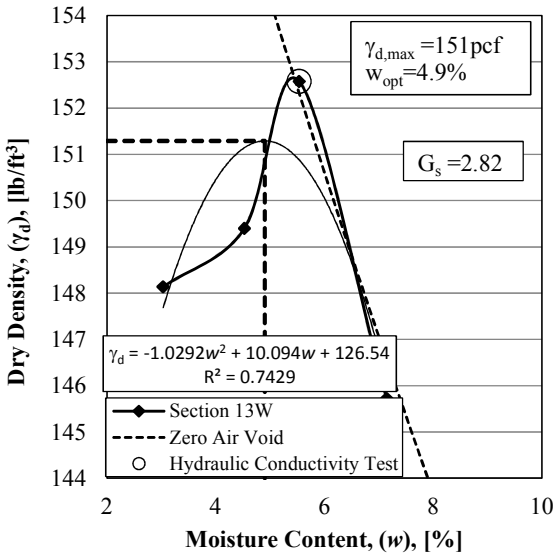

Figure A.9.15. Proctor curve for Section 13W base course sample obtained from 4-6 inches below the asphalt/base course interface.

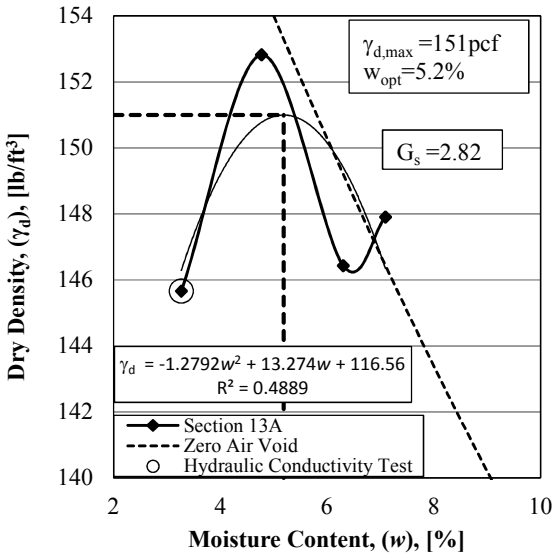

Figure A.9.16. Proctor curve for Section 13A base course sample obtained from 4-6 inches below the asphalt/base course interface.

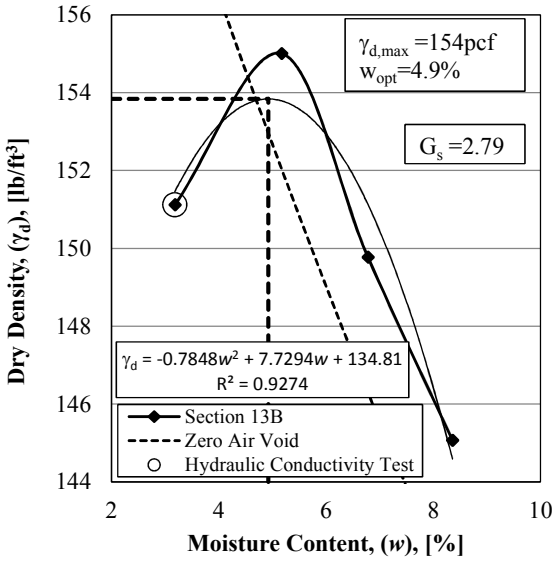

Figure A.9.17. Proctor curve for Section 13B base course sample obtained from 4-6 inches below the asphalt/base course interface.

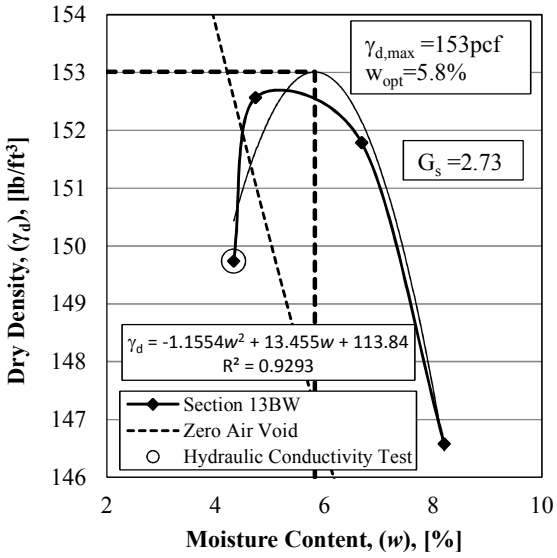

Figure A.9.18. Proctor curve for Section 13BW base course sample obtained from 4-6 inches below the asphalt/base course interface.

A.10. Hydraulic Conductivity (Laboratory)

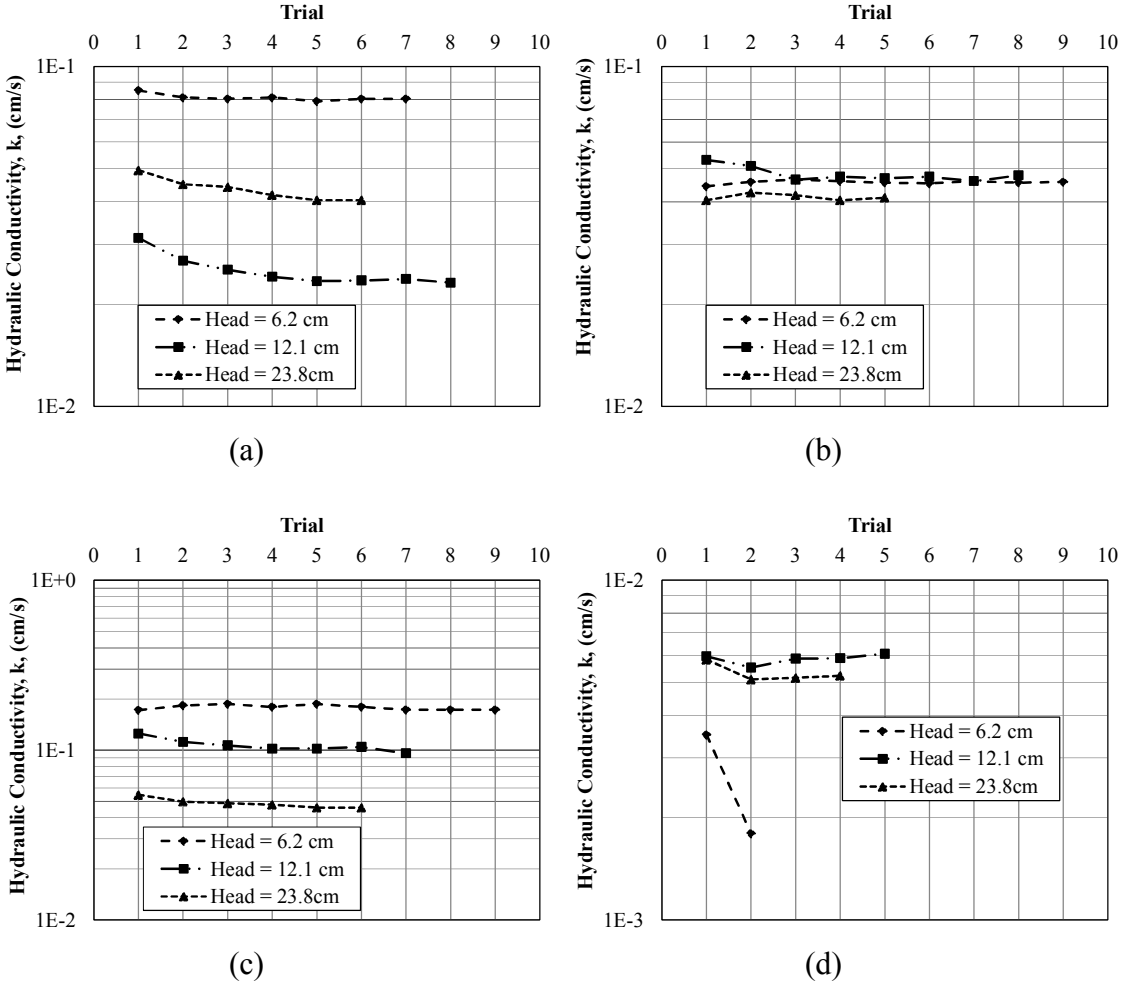

Figure A.10.1. Results from hydraulic conductivity tests using constant head test (Marriotte Bottle): a) Section 1B (8-10 inch below the asphalt/base course interface), b) Section 1 (8-10 inch below the asphalt-base course interface), c) Section 2 (8-10 inch below the asphalt/base course interface), and d) Section 3 (8-10 inch below the asphalt/base course interface).

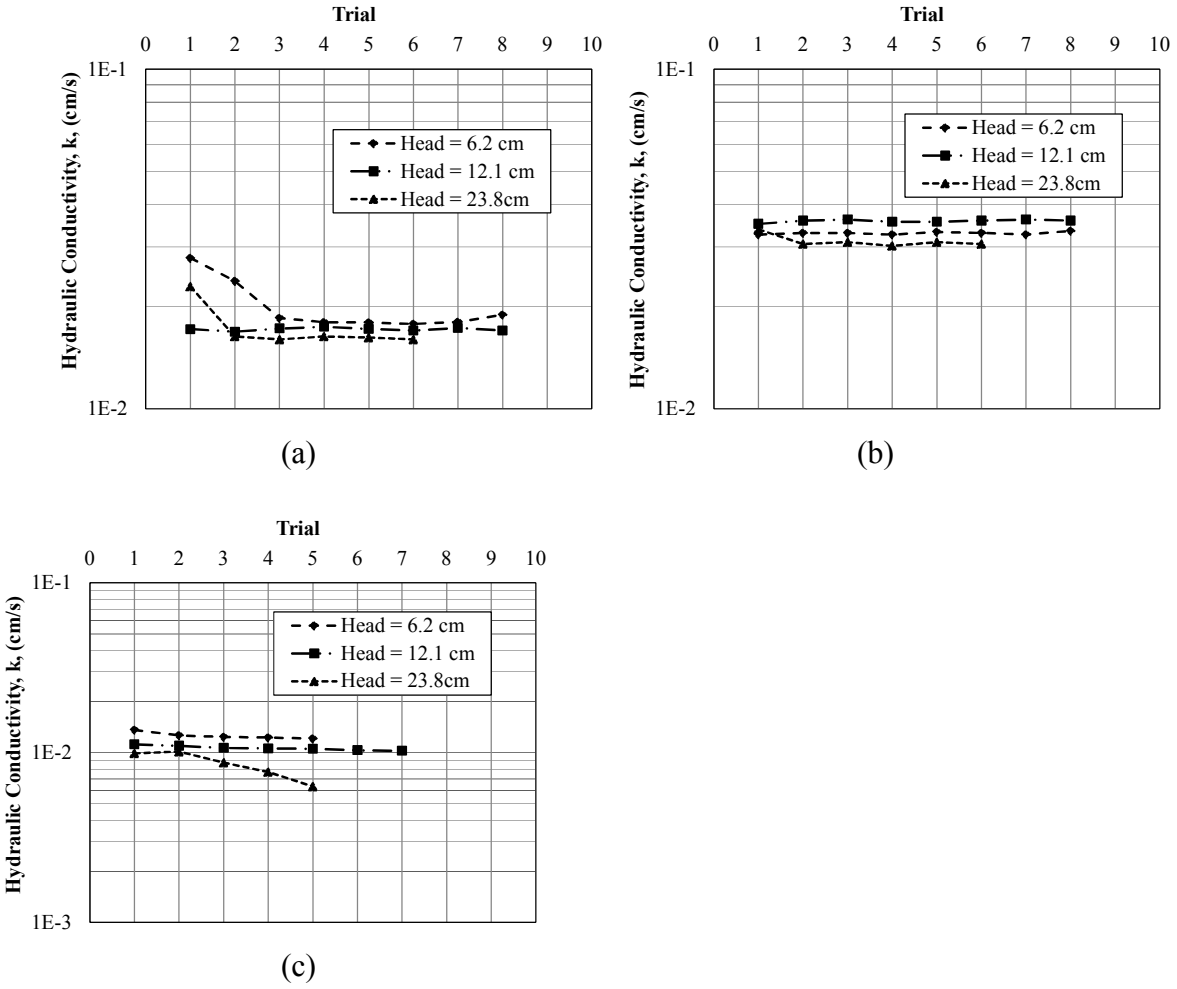

Figure A.10.2. Results from hydraulic conductivity tests using constant head test (Marriotte Bottle): a) Section 4 (8-10 inch below the asphalt/base course interface), b) Section 5 (8-10 inch below the asphalt/base course interface), and c) Section 6 (8-10 inch below the asphalt/base course interface)

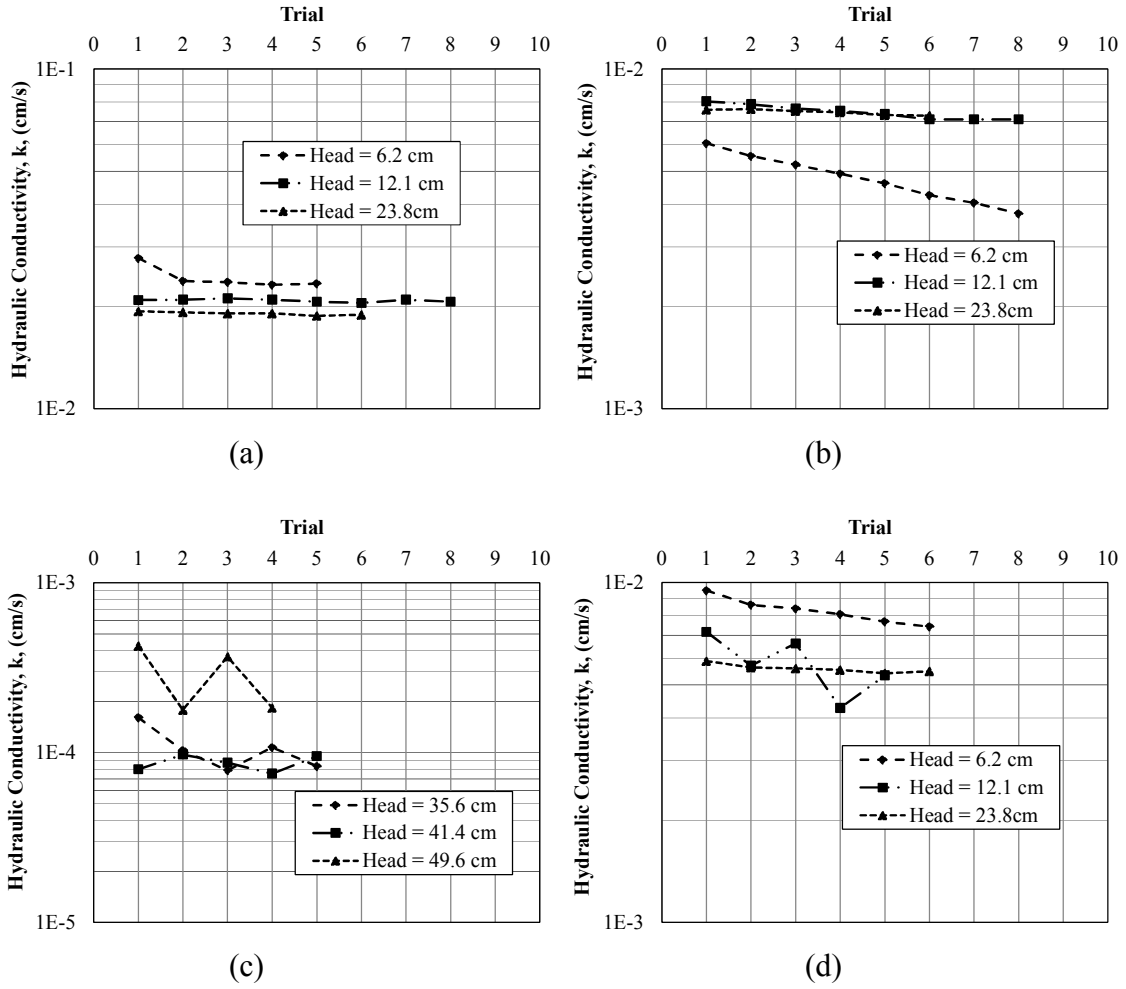

Figure A.10.3. Results from hydraulic conductivity tests using constant head test (Marriotte Bottle): a) Section 8 (4-6 inch below the asphalt/base course interface), b) Section 9 (4-6 inch below the asphalt/base course interface), c) Section 10 (4-6 inch below the asphalt/base course interface), and d) Section 11 (4-6 inch below the asphalt/base course interface).

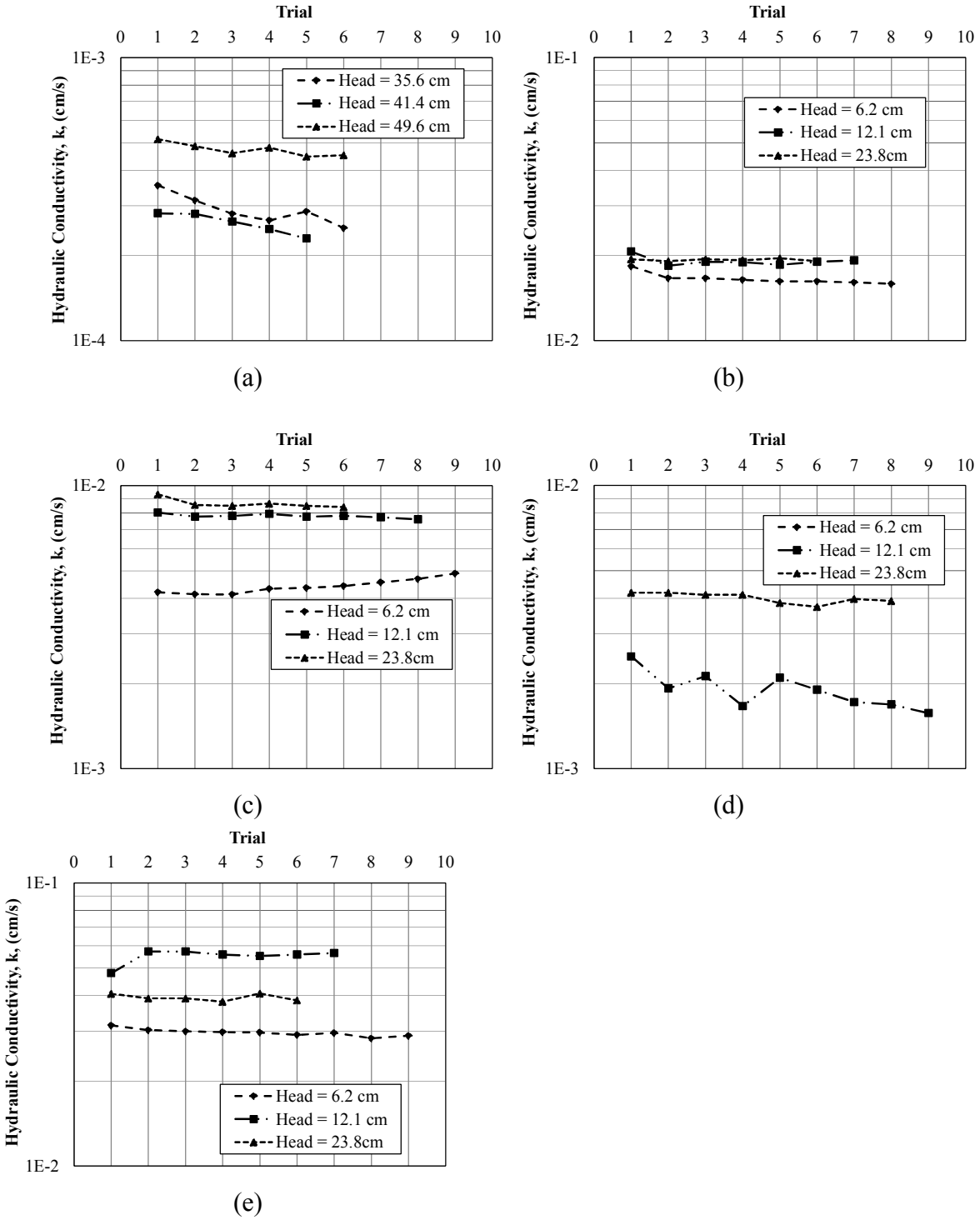

Figure A.10.4. Results from hydraulic conductivity tests using constant head test (Marriotte Bottle): a) Section 12 (4-6 inch below the asphalt/base course interface), b) Section 13 (4-6 inch below the asphalt/base course interface), c) Section 13A (4-6 inch below the asphalt/base course interface), d) Section 13B (4-6 inch below the asphalt/base course interface), and e) Section 13BW (4-6 inch below the asphalt/base course interface).

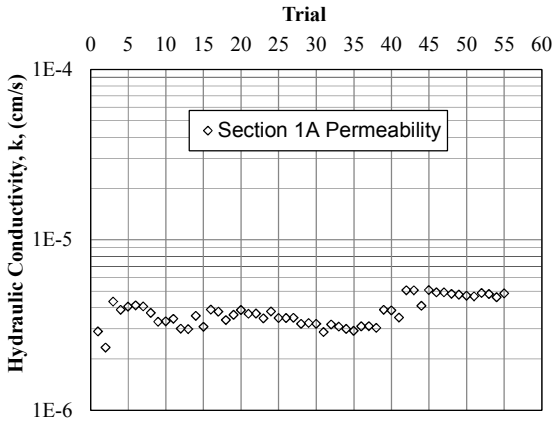

Figure A.10.5. Result from hydraulic conductivity test using flexible wall permeameter for Section 1A (8-10 inch below the asphalt/base course interface).

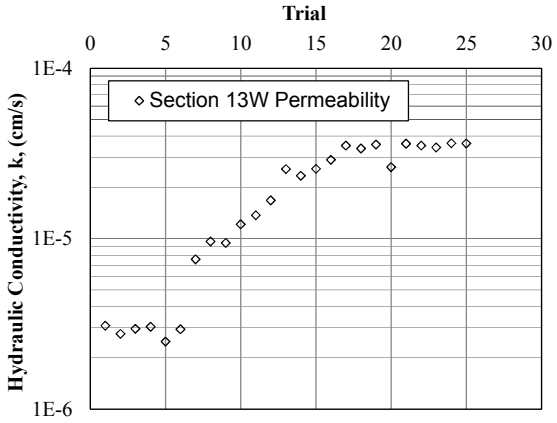

Figure A.10.6. Result from hydraulic conductivity test using flexible wall permeameter for Section 13W (4-6 inch below the asphalt/base course interface).

A.11. Transmissivity

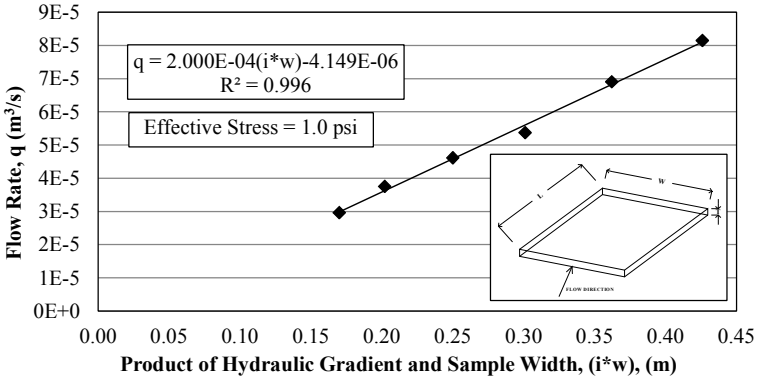

Figure A.11.1. Transmissivity of geotextile from Section 1B (Mirafi HP 570) at a constant effective stress of 1.0 psi.

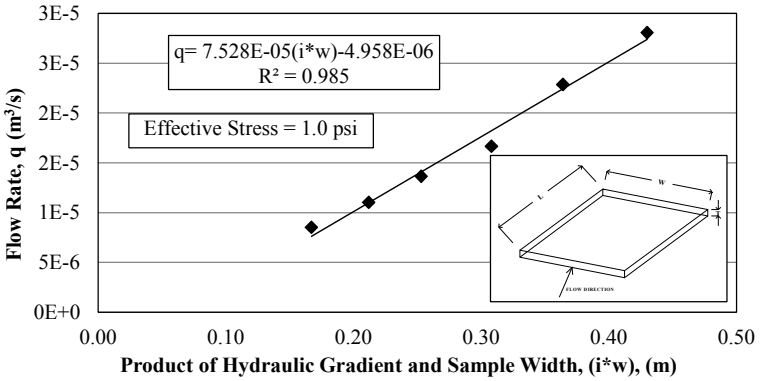

Figure A.11.2. Transmissivity of geotextile from Section 2 (Propex 2044) at a constant effective stress of 1.0 psi.

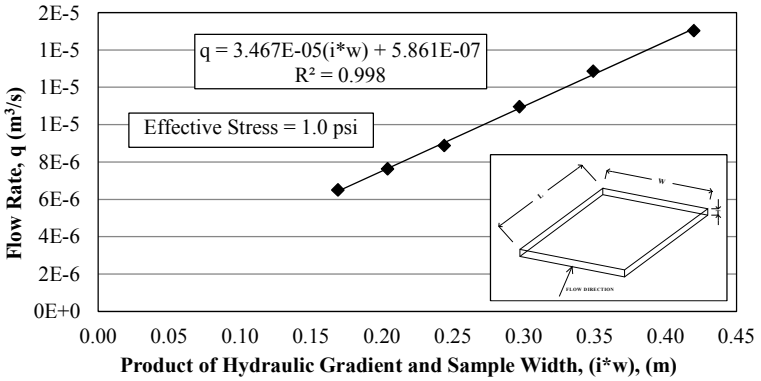

Figure A.11.3. Transmissivity of geotextile from Section 3 (Propex 2006) at a constant effective stress of 1.0 psi.

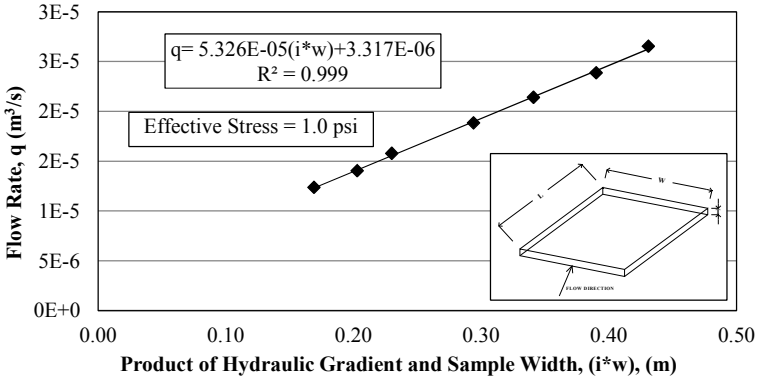

Figure A.11.4. Transmissivity of geotextile from Section 4 (Propex 4553) at a constant effective stress of 1.0 psi.

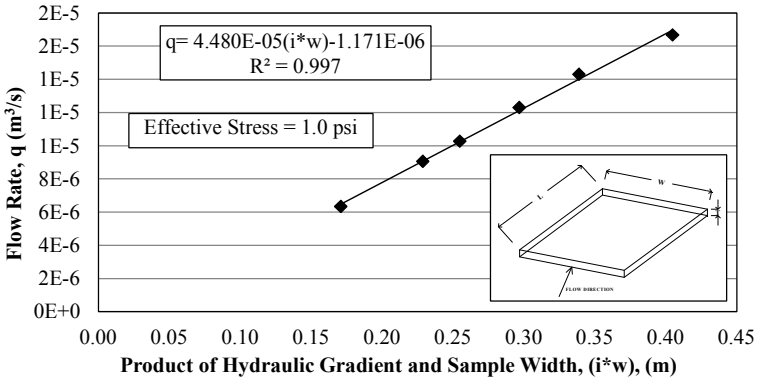

Figure A.11.5. Transmissivity of geotextile from Section 10 (Propex 4553) at a constant effective stress of 1.0 psi.

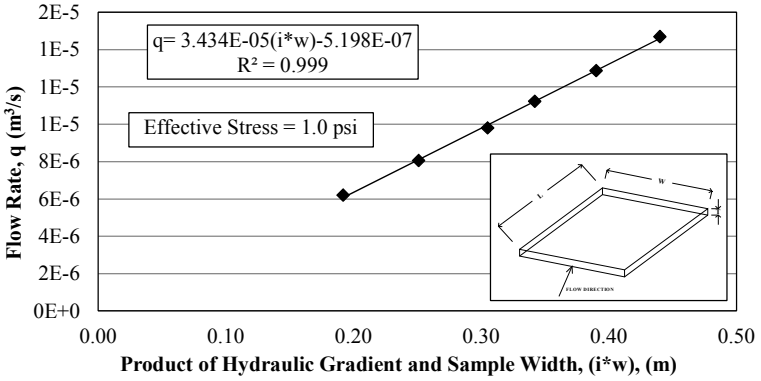

Figure A.11.6. Transmissivity of geotextile from Section 11 (Propex 2006) at a constant effective stress of 1.0 psi.

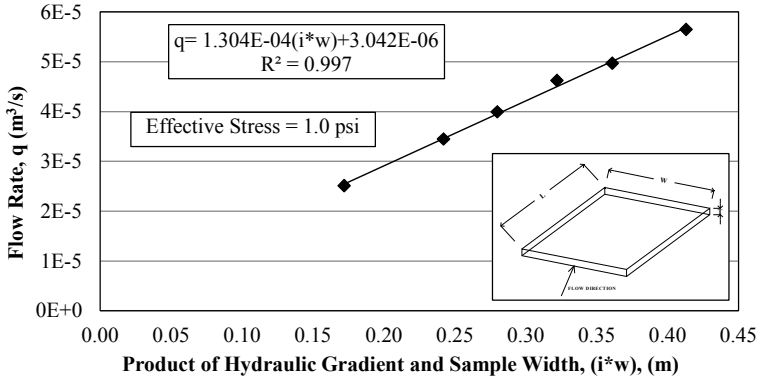

Figure A.11.7. Transmissivity of geotextile from Section 12 (Propex 2044) at a constant effective stress of 1.0 psi.

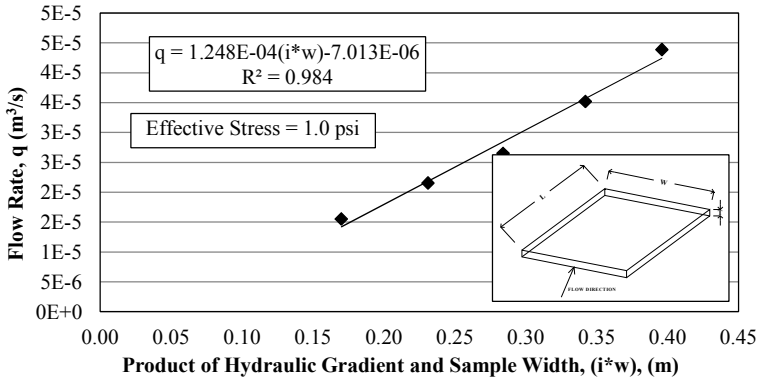

Figure A.11.8. Transmissivity of geotextile from Section 13B (Mirafi HP 570) at a constant effective stress of 1.0 psi.

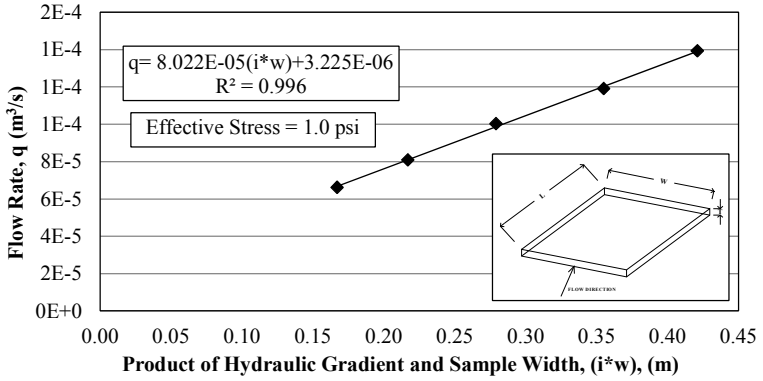

Figure A.11.9. Transmissivity of geotextile from Section 13W (Carthage Mills FX-66) at a constant effective stress of 1.0 psi.

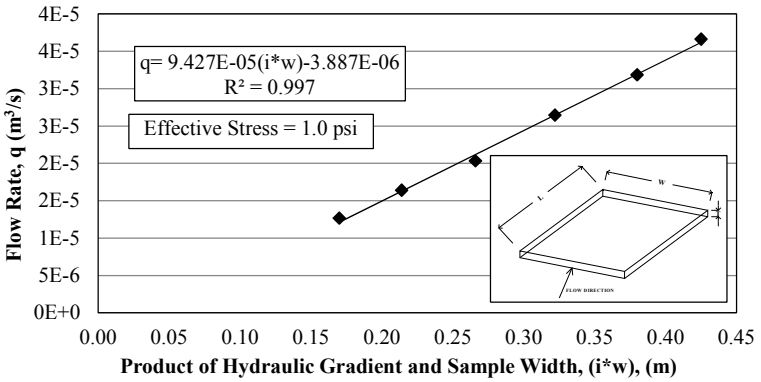

Figure A.11.10. Transmissivity of geotextile from Section 13BW (Carthage Mills FX-66) at a constant effective stress of 1.0 psi.

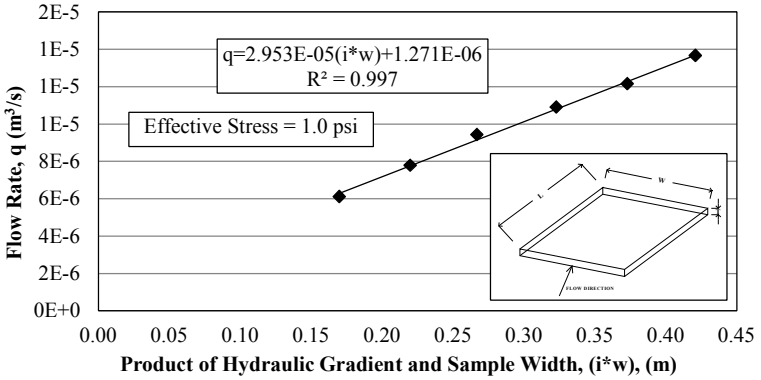

Figure A.11.11. Transmissivity of new geotextile (Propex 4553) at a constant effective stress of 1.0 psi.

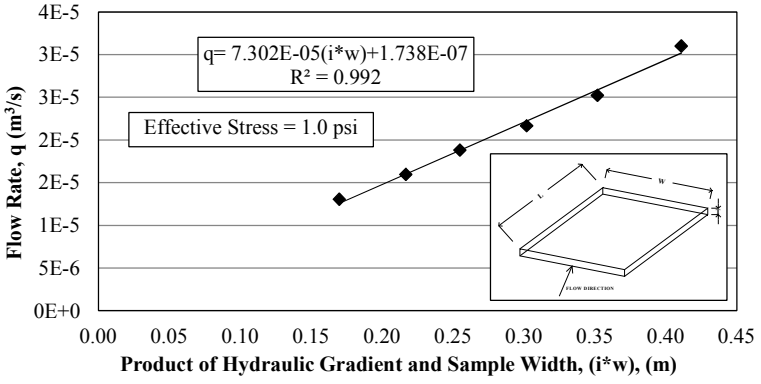

Figure A.11.12. Transmissivity of new geotextile (Propex 2044) at a constant effective stress of 1.0 psi.

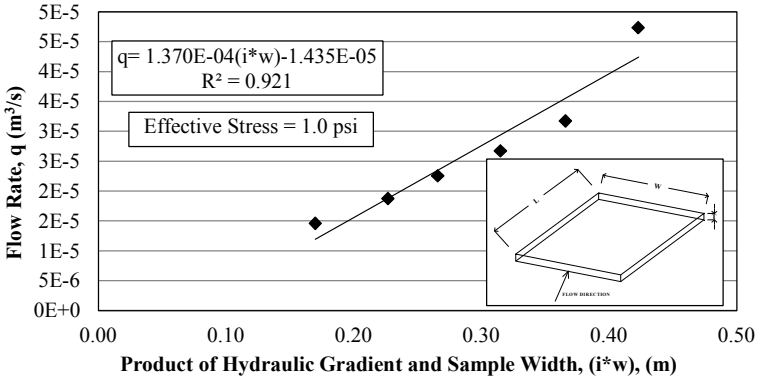

Figure A.11.13. Transmissivity of new geotextile (Mirafi HP 570) at a constant effective stress of 1.0 psi.

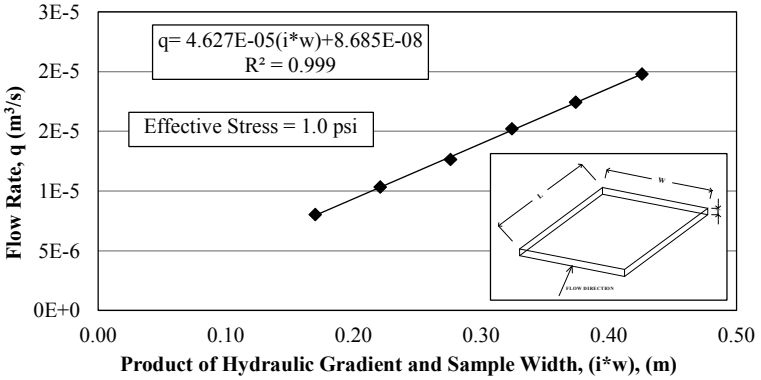

Figure A.11.14. Transmissivity of new geotextile (Propex 2006) at a constant effective stress of 1.0 psi.

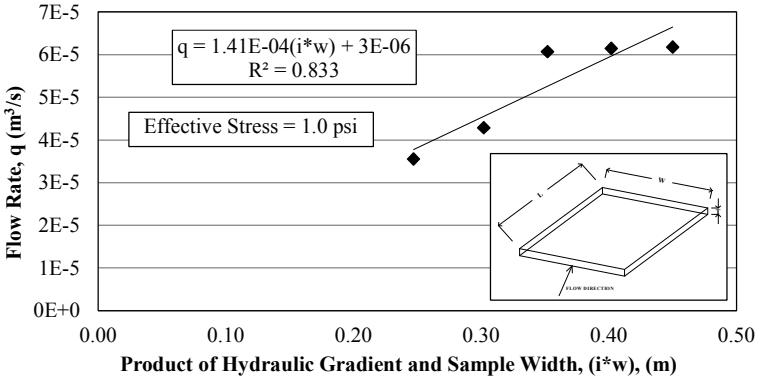

Figure A.11.15. Transmissivity of new geotextile (Carthage Mills FX-66) at a constant effective stress of 1.0 psi.

A.12. Permittivity

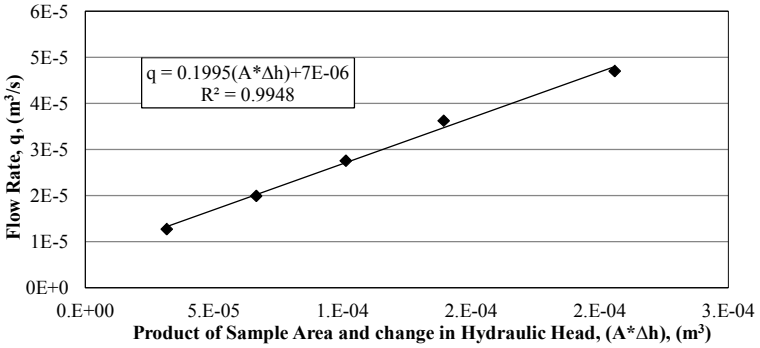

Figure A.12.1. Permittivity of geotextile from Section 1B (Mirafi HP 570) by a falling head test.

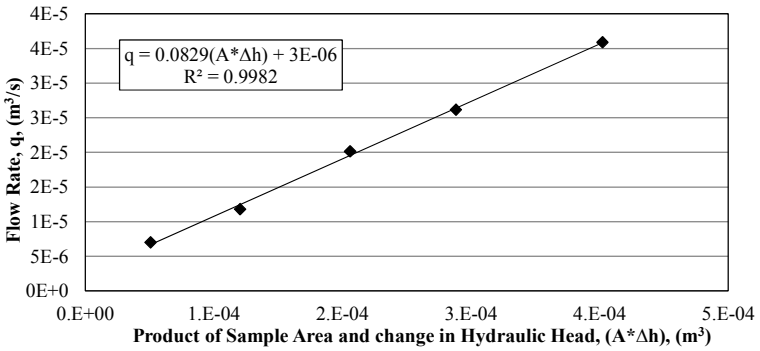

Figure A.12.2. Permittivity of geotextile from Section 2 (Propex 2044) by a falling head test.

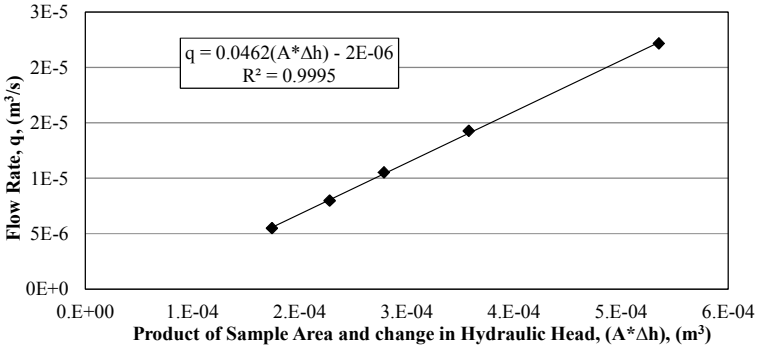

Figure A.12.3. Permittivity of geotextile from Section 3 (Propex 2006) by a falling head test.

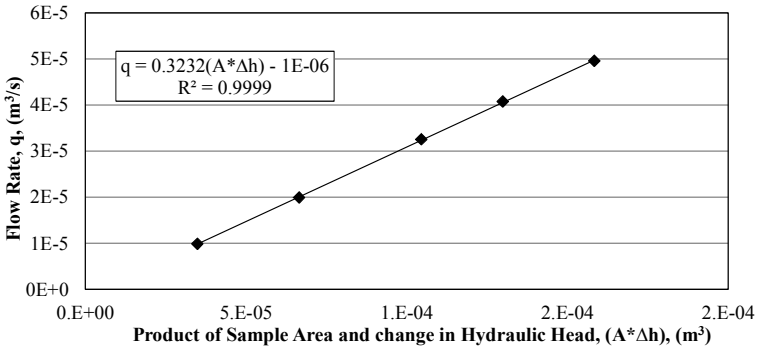

Figure A.12.4. Permittivity of geotextile from Section 4 (Propex 4553) by a falling head test.

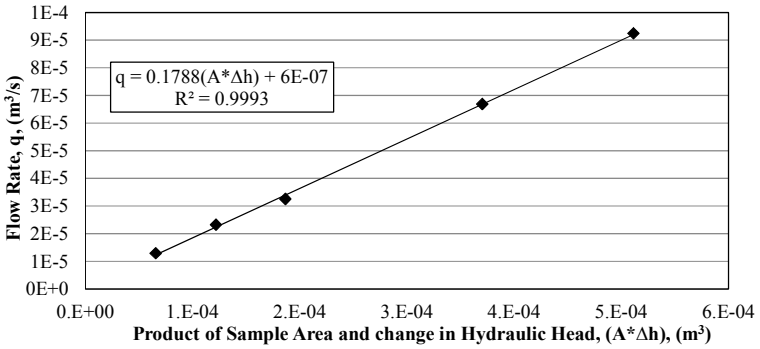

Figure A.12.5. Permittivity of geotextile from Section 10 (Propex 4553) by a falling head test.

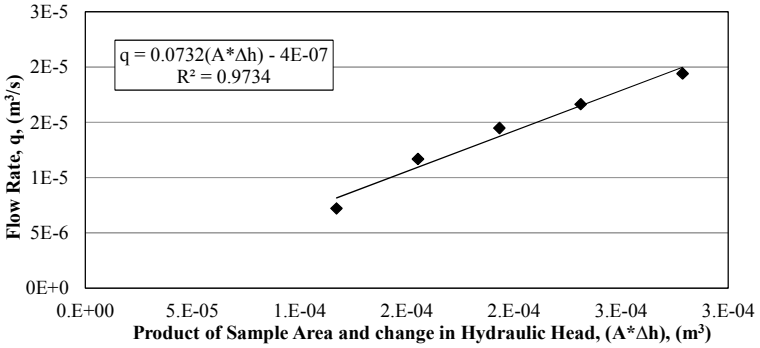

Figure A.12.6. Permittivity of geotextile from Section 11 (Propex 2006) by a falling head test.

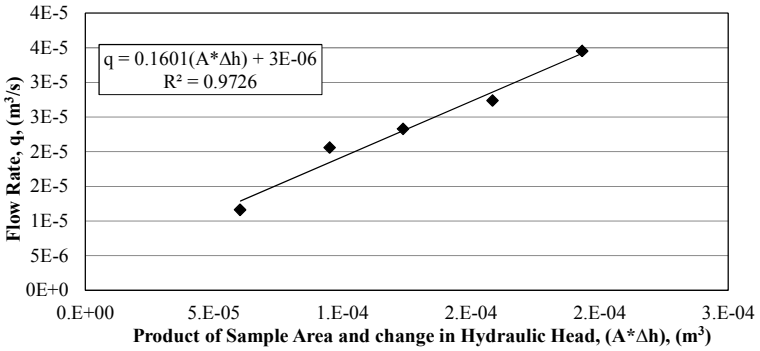

Figure A.12.7. Permittivity of geotextile from Section 12 (Propex 2044) by a falling head test.

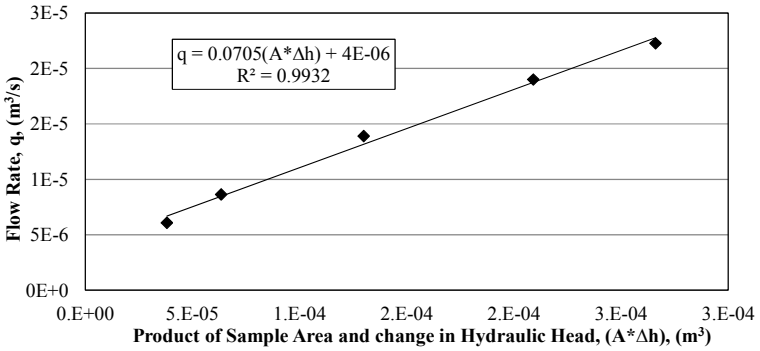

Figure A.12.8. Permittivity of geotextile from Section 13W (Carthage Mills FX-66) by a falling head test.

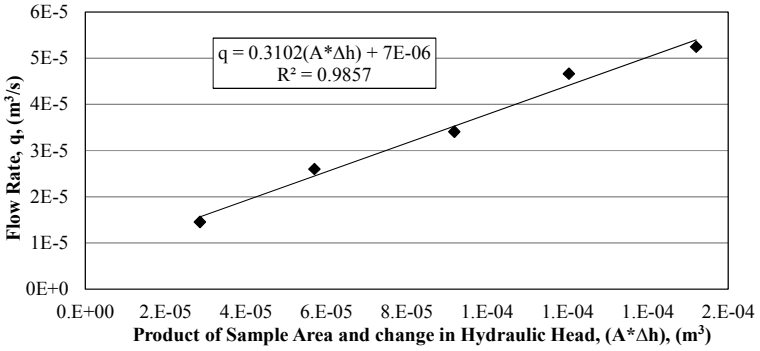

Figure A.12.9. Permittivity of geotextile from Section 13B (Mirafi HP 570) by a falling head test.

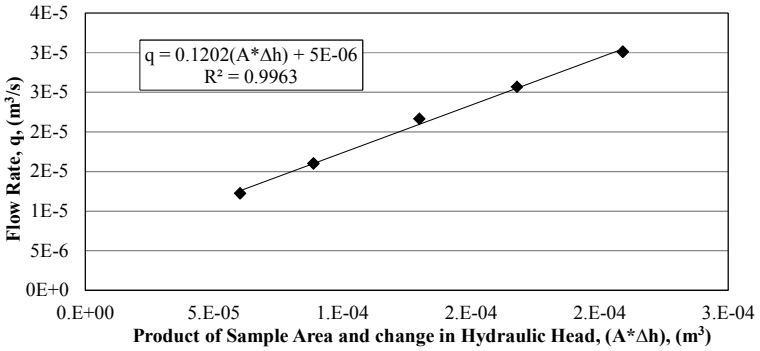

Figure A.12.10. Permittivity of geotextile from Section 13BW (Carthage Mills FX-66) by a falling head test.

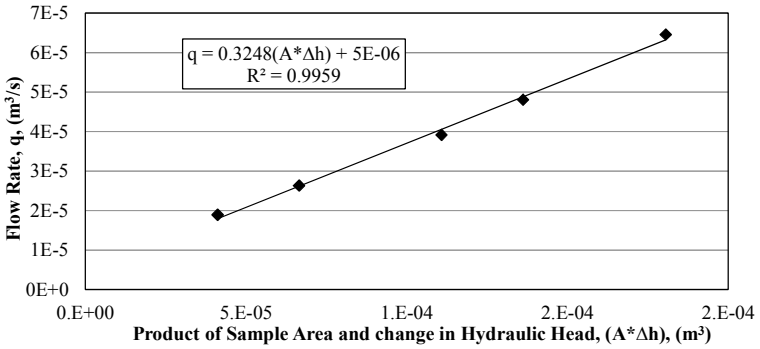

Figure A.12.11. Permittivity of new geotextile (Propex 4553) by a falling head test.

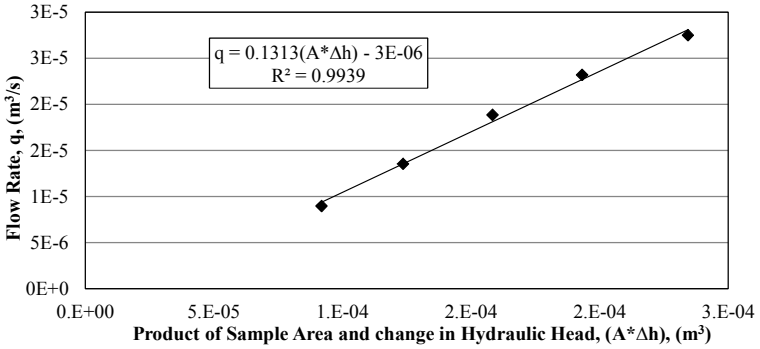

Figure A.12.12. Permittivity of new geotextile (Propex 2044) by a falling head test.

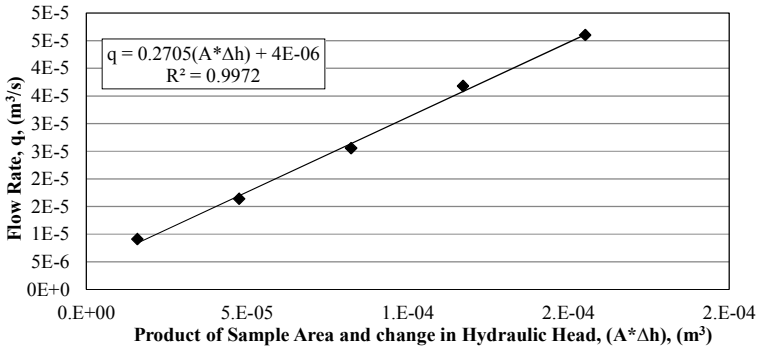

Figure A.12.13. Permittivity of new geotextile (Mirafi HP 570) by a falling head test.

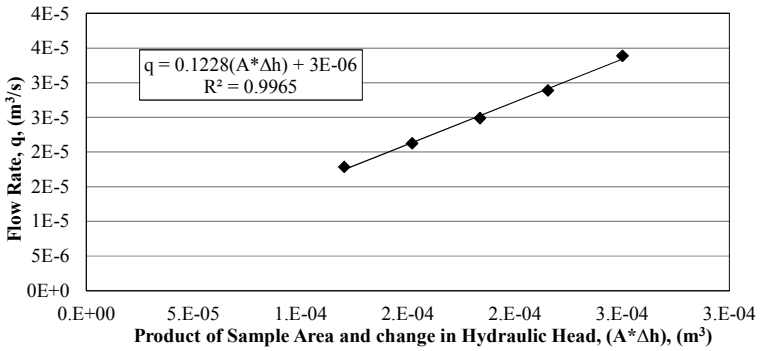

Figure A.12.14. Permittivity of new geotextile (Propex 2006) by a falling head test.

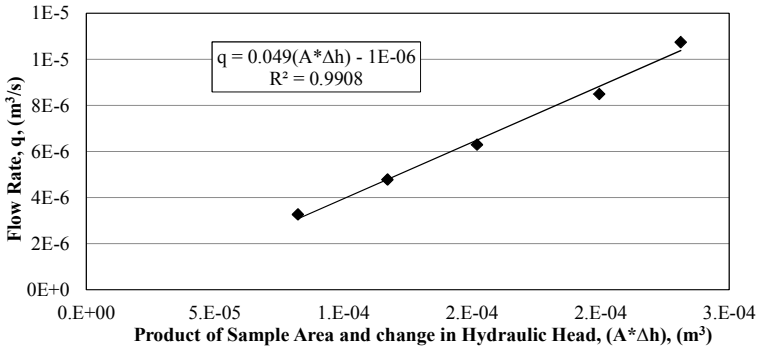

Figure A.12.15. Permittivity of new geotextile (Carthage Mills FX-66) by a falling head test.

A.13. Geotextile Design Review

Table A.13.1. Evaluation of the geotextiles based on the subgrade soil retention, filtration, and clogging criteria for the ten inch thick sections (criteria obtained from FHWA, 1998).

Location	[1]Depth	Geotextile	Percent Passing 75µm	Percent Passing 75µm >50%	B	AOS or O_{95}	PI	PI>7	AOS or O_{95} ≤0.3mm (PI>7)	D_{85}	B*D_{85}	**AOS≤ B*D_{85}**	[2]ψ	[3]ψ_{lab}	[4]ψ_{mfg}	ψ_{lab}> ψ	ψ_{mfg}> ψ	[5]t	[6]t	k_{GT} = ψ_{lab}*t	k_{GT} = ψ_{mfg}*t	D_{10}	k_{soil}= CD_{10}^2	**k_{GT}≥ k_{soil}**	AOS or O_{95}	D_{15}	3*D_{15}	**O_{95}≥ 3D_{15}**
	(inch)		(%)		(unitless)	(mm)	(%)			(mm)	(mm)		(s^{-1})	(s^{-1})	(s^{-1})			(cm)	(cm)	(cm/s)	(cm/s)	(mm)	(cm/s)		(mm)	(mm)	(mm)	
Section 1B	0-2	Mirafi Geolon HP 570	57	Yes	1.00	0.600	22	Yes	No	0.43	0.43	No	0.10	0.27	0.40	Yes	Yes	0.16	0.17	4.3E-2	6.6E-2	3.4E-4	1.1E-7	Yes	0.600	1.1E-3	3.4E-3	Yes
	2-4		53	Yes	1.00	0.600	18	Yes	No	0.41	0.41	No	0.10	0.27	0.40	Yes	Yes	0.16	0.17	4.3E-2	6.6E-2	3.0E-4	9.3E-8	Yes	0.600	1.7E-3	5.0E-3	Yes
	4-6		56	Yes	1.00	0.600	18	Yes	No	0.51	0.51	No	0.10	0.27	0.40	Yes	Yes	0.16	0.17	4.3E-2	6.6E-2	3.5E-4	1.2E-7	Yes	0.600	7.2E-4	2.2E-3	Yes
Section 2	0-2	Propex 2044 Woven	68	Yes	1.00	0.600	30	Yes	No	0.16	0.16	No	0.10	0.13	0.15	Yes	Yes	0.13	0.13	1.8E-2	2.0E-2	4.7E-4	2.2E-7	Yes	0.600	4.1E-4	1.2E-3	Yes
	2-4		71	Yes	1.00	0.600	24	Yes	No	0.14	0.14	No	0.10	0.13	0.15	Yes	Yes	0.13	0.13	1.8E-2	2.0E-2	4.1E-4	1.7E-7	Yes	0.600	2.1E-3	6.4E-3	Yes
	4-6		69	Yes	1.00	0.600	19	Yes	No	0.15	0.15	No	0.10	0.13	0.15	Yes	Yes	0.13	0.13	1.8E-2	2.0E-2	4.8E-4	2.3E-7	Yes	0.600	7.2E-4	2.1E-3	Yes
Section 3	0-2	Propex 2006 Woven	69	Yes	1.00	0.425	27	Yes	No	0.15	0.15	No	0.10	0.12	0.05	Yes	No	0.06	0.07	7.8E-3	3.4E-3	5.1E-4	2.6E-7	Yes	0.425	5.4E-4	1.6E-3	Yes
	2-4		68	Yes	1.00	0.425	26	Yes	No	0.22	0.22	No	0.10	0.12	0.05	Yes	No	0.06	0.07	7.8E-3	3.4E-3	5.1E-4	2.6E-7	Yes	0.425	1.7E-4	5.1E-4	Yes
	4-6		76	Yes	1.00	0.425	25	Yes	No	0.11	0.11	No	0.10	0.12	0.05	Yes	No	0.06	0.07	7.8E-3	3.4E-3	5.6E-4	3.1E-7	Yes	0.425	2.8E-4	8.4E-4	Yes
Section 4	0-2	Propex 4553 Non-Woven	70	Yes	1.85	0.150	29	Yes	Yes	0.17	0.31	Yes	0.10	0.32	1.50	Yes	Yes	0.19	0.13	6.1E-2	2.0E-1	5.1E-4	2.6E-7	Yes	0.150	3.3E-4	9.9E-4	Yes
	2-4		70	Yes	1.85	0.150	29	Yes	Yes	0.14	0.27	Yes	0.10	0.32	1.50	Yes	Yes	0.19	0.13	6.1E-2	2.0E-1	5.3E-4	2.8E-7	Yes	0.150	1.6E-4	4.7E-4	Yes
	4-6		64	Yes	1.85	0.150	32	Yes	Yes	0.20	0.37	Yes	0.10	0.32	1.50	Yes	Yes	0.19	0.13	6.1E-2	2.0E-1	4.3E-4	1.9E-7	Yes	0.150	3.7E-4	1.1E-3	Yes

Bold represents evaluation criteria

[1]Depth below base course/subgrade interface

[2]Required permittivity (ψ) (based on % passing 75µm)

[3]Laboratory permittivity (ψ_{lab}) for new geotextile samples

[4]Manufacture permittivity (ψ_{mfg})

[5]Geotextile thickness (t) for the exhumed samples

[6]Geotextile thickness (t) for the new samples

Table A.13.2. Evaluation of the geotextiles based on the subgrade soil retention, filtration, and clogging criteria for the six inch thick sections (criteria obtained from FHWA, 1998).

Location	[1]Depth	Geotextile	Percent Passing 75µm	Percent Passing 75µm >50%	B	AOS or O_{95}	PI	PI>7	**AOS or O_{95} ≤0.3mm (PI>7)**	D_{85}	$B*D_{85}$	**AOS≤ B*D_{85}**	[2]ψ	[3]ψ_{lab}	[4]ψ_{mfg}	**ψ_{lab} >ψ**	**ψ_{mfg} >ψ**	[5]t	[6]t	k_{GT} = ψ_{lab}*t	k_{GT} = ψ_{mfg}*t	D_{10}	k_{soil}= CD_{10}^2	**$k_{GT} \geq k_{soil}$**	AOS or O_{95}	D_{15}	$3*D_{15}$	**$O_{95} \geq 3D_{15}$**
	(inch)		(%)		(unitless)	(mm)	(%)			(mm)	(mm)		(s^{-1})	(s^{-1})	(s^{-1})			(cm)	(cm)	(cm/s)	(cm/s)	(mm)	(cm/s)		(mm)	(mm)	(mm)	
Section 10	0-2	Propex 4553 Non-Woven	60	Yes	1.85	0.150	25	Yes	Yes	0.19	0.36	Yes	0.10	0.32	1.50	Yes	Yes	0.16	0.13	5.3E-2	2.0E-1	4.3E-4	1.9E-7	Yes	0.150	3.5E-4	1.1E-3	Yes
	2-4		72	Yes	1.85	0.150	27	Yes	Yes	0.11	0.21	Yes	0.10	0.32	1.50	Yes	Yes	0.16	0.13	5.3E-2	2.0E-1	4.9E-4	2.4E-7	Yes	0.150	2.6E-4	7.7E-4	Yes
	4-6		61	Yes	1.85	0.150	30	Yes	Yes	0.16	0.30	Yes	0.10	0.32	1.50	Yes	Yes	0.16	0.13	5.3E-2	2.0E-1	3.9E-4	1.5E-7	Yes	0.150	6.0E-4	1.8E-3	Yes
Section 11	0-2	Propex 2006 Woven	66	Yes	1.00	0.425	28	Yes	No	0.18	0.18	No	0.10	0.12	0.05	Yes	No	0.06	0.07	7.2E-3	3.4E-3	5.3E-4	2.8E-7	Yes	0.425	1.4E-4	4.1E-4	Yes
	2-4		51	Yes	1.00	0.425	25	Yes	No	0.32	0.32	No	0.10	0.12	0.05	Yes	No	0.06	0.07	7.2E-3	3.4E-3	4.2E-4	1.8E-7	Yes	0.425	5.0E-4	1.5E-3	Yes
	4-6		79	Yes	1.00	0.425	35	Yes	No	0.10	0.10	No	0.10	0.12	0.05	Yes	No	0.06	0.07	7.2E-3	3.4E-3	6.8E-4	4.6E-7	Yes	0.425	1.3E-4	4.0E-4	Yes
Section 12	0-2	Propex 2044Woven	46	No	1.00	0.600	17	Yes	No	0.55	0.55	No	0.20	0.13	0.15	No	No	0.14	0.13	1.9E-2	2.0E-2	3.9E-4	1.5E-7	Yes	0.600	6.0E-4	1.8E-3	Yes
	2-4		41	No	1.00	0.600	18	Yes	No	1.55	1.55	Yes	0.20	0.13	0.15	No	No	0.14	0.13	1.9E-2	2.0E-2	3.5E-4	1.2E-7	Yes	0.600	9.1E-4	2.7E-3	Yes
	4-6		41	No	1.00	0.600	18	Yes	No	1.41	1.41	Yes	0.20	0.13	0.15	No	No	0.14	0.13	1.9E-2	2.0E-2	3.3E-4	1.1E-7	Yes	0.600	1.2E-3	3.7E-3	Yes
Section 13W	0-2	Carthage Mills FX-66 Slit Film	61	Yes	1.00	0.425	36	Yes	No	0.26	0.26	No	0.10	0.05	0.05	No	No	0.07	0.06	3.4E-3	2.8E-3	5.1E-4	2.6E-7	Yes	0.425	3.1E-4	9.3E-4	Yes
	2-4		68	Yes	1.00	0.425	38	Yes	No	0.17	0.17	No	0.10	0.05	0.05	No	No	0.07	0.06	3.4E-3	2.8E-3	6.2E-4	3.8E-7	Yes	0.425	1.5E-4	4.6E-4	Yes
	4-6		82	Yes	1.00	0.425	50	Yes	No	0.09	0.09	No	0.10	0.05	0.05	No	No	0.07	0.06	3.4E-3	2.8E-3	8.3E-4	6.9E-7	Yes	0.425	1.4E-4	4.3E-4	Yes
Section 13B	0-2	Mirafi Geolon HP 570 Woven	60	Yes	1.00	0.600	29	Yes	No	0.29	0.29	No	0.10	0.27	0.40	Yes	Yes	0.14	0.17	3.8E-2	6.6E-2	5.5E-4	3.0E-7	Yes	0.600	2.0E-4	6.1E-4	Yes
	2-4		54	Yes	1.00	0.600	25	Yes	No	0.39	0.39	No	0.10	0.27	0.40	Yes	Yes	0.14	0.17	3.8E-2	6.6E-2	4.6E-4	2.1E-7	Yes	0.600	5.9E-4	1.8E-3	Yes
	4-6		49	No	1.00	0.600	19	Yes	No	0.54	0.54	No	0.20	0.27	0.40	Yes	Yes	0.14	0.17	3.8E-2	6.6E-2	3.8E-4	1.5E-7	Yes	0.600	7.7E-4	2.3E-3	Yes
Section 13BW	0-2	Carthage Mills FX-66 Slit Film	75	Yes	1.00	0.425	37	Yes	No	0.11	0.11	No	0.10	0.05	0.05	No	No	0.07	0.06	3.2E-3	2.8E-3	5.6E-4	3.1E-7	Yes	0.425	1.6E-4	4.8E-4	Yes
	2-4		77	Yes	1.00	0.425	33	Yes	No	0.10	0.10	No	0.10	0.05	0.05	No	No	0.07	0.06	3.2E-3	2.8E-3	5.7E-4	3.3E-7	Yes	0.425	1.5E-4	4.6E-4	Yes
	4-6		50	Yes	1.00	0.425	16	Yes	No	0.65	0.65	Yes	0.10	0.05	0.05	No	No	0.07	0.06	3.2E-3	2.8E-3	4.2E-4	1.7E-7	Yes	0.425	3.6E-4	1.1E-3	Yes

Bold represents evaluation criteria

[1]Depth below base course/subgrade interface

[2]Required permittivity (ψ) (based on % passing 75µm)

[3]Laboratory permittivity (ψ_{lab}) for new geotextile samples

[4]Manufacture permittivity (ψ_{mfg})

[5]Geotextile thickness (t) for the exhumed samples

[6]Geotextile thickness (t) for the new samples

Appendix B

The results of field testing specifically the in-situ moisture content profile measured in October 2010 and the in-situ hydraulic conductivity measured in October 2010 and May 2011 are presented in this Appendix. The in-situ hydraulic conductivity was measured using a Two Stage Borehole technique (Stage 1 only). The testing was performed in accordance to testing procedure outlined in Chapter 3. The results are summarized in Chapter 4.

B.1. In-situ Gravimetric Moisture Content (October 2010)

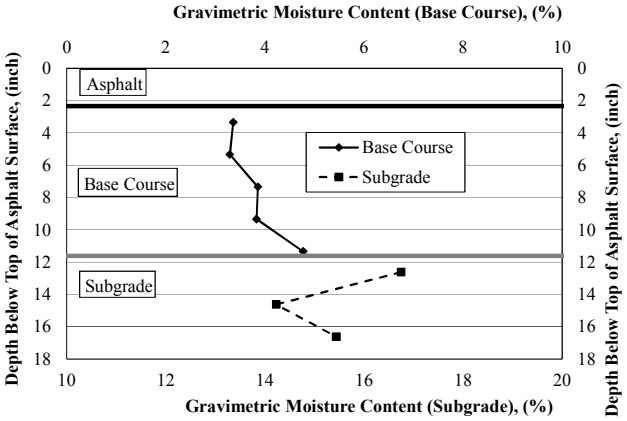

Figure B.1.1. In-situ gravimetric moisture content profile for Section 1B.

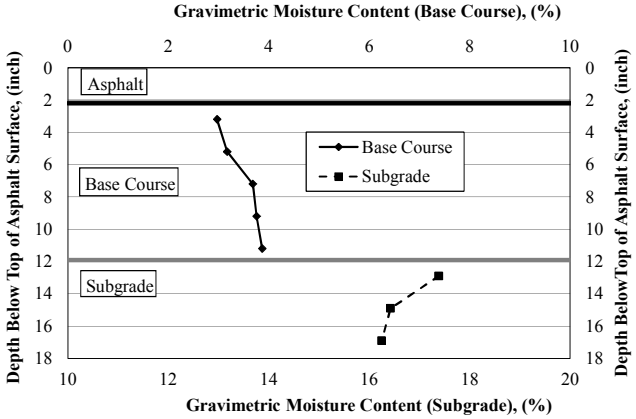

Figure B.1.2. In-situ gravimetric moisture content profile for Section 1A.

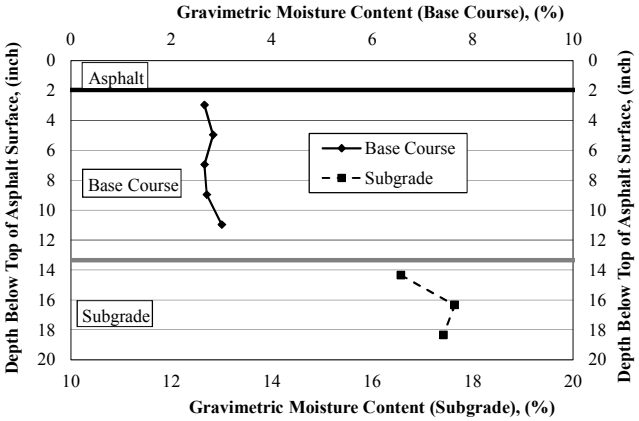

Figure B.1.3. In-situ gravimetric moisture content profile for Section 1.

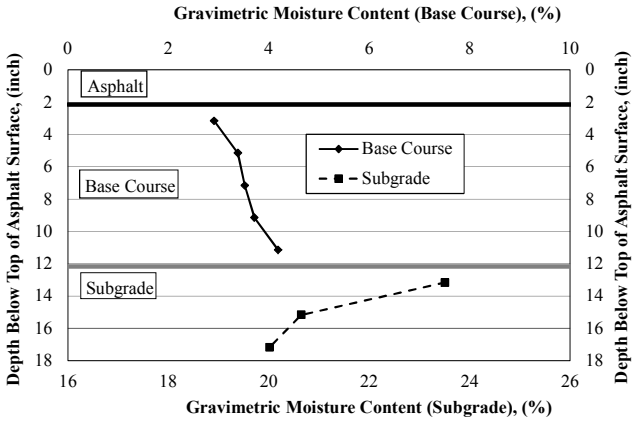

Figure B.1.4. In-situ gravimetric moisture content profile for Section 2.

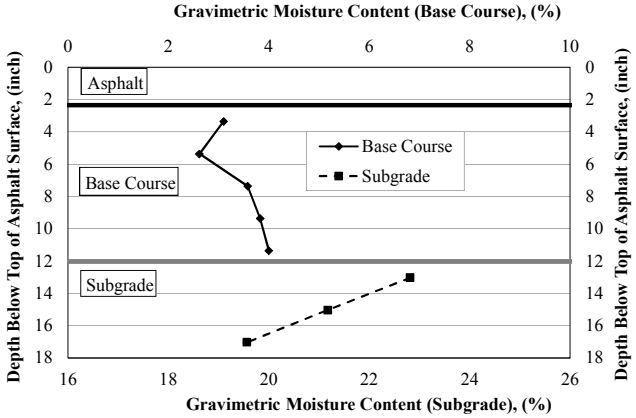

Figure B.1.5. In-situ gravimetric moisture content profile for Section 3.

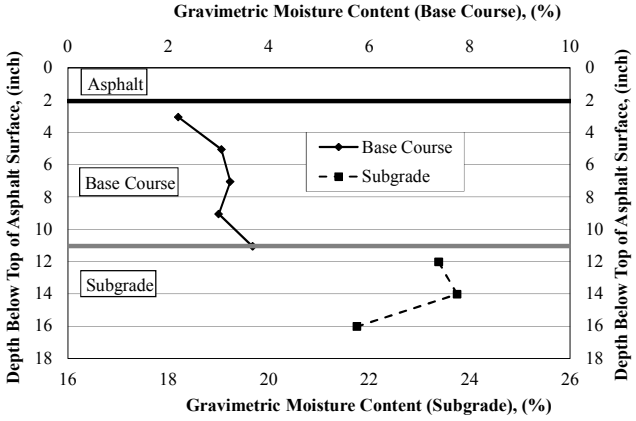

Figure B.1.6. In-situ gravimetric moisture content profile for Section 4.

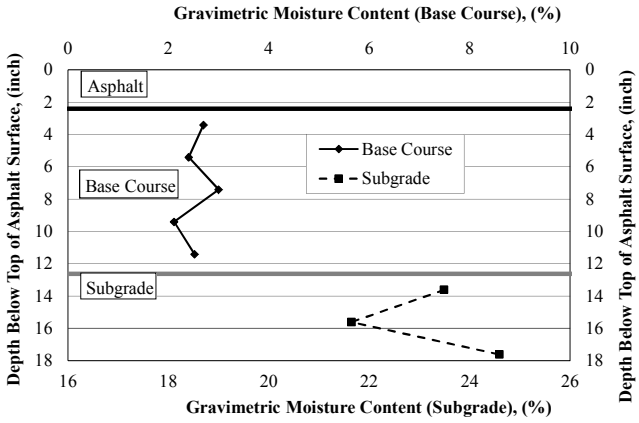

Figure B.1.7. In-situ gravimetric moisture content profile for Section 5.

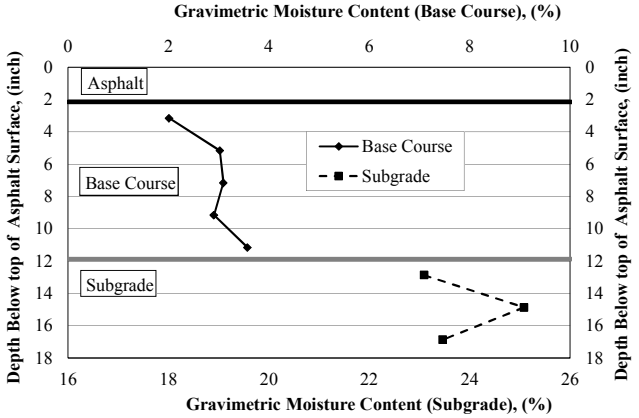

Figure B.1.8. In-situ gravimetric moisture content profile for Section 6.

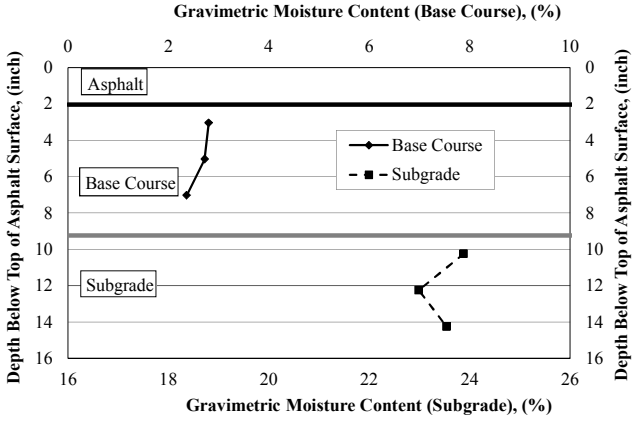

Figure B.1.9. In-situ gravimetric moisture content profile for Section 8.

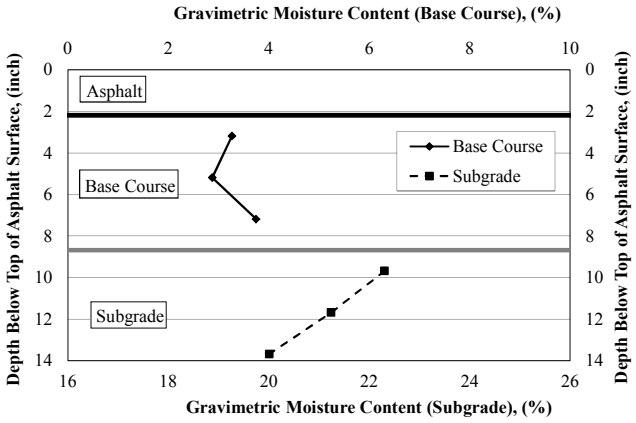

Figure B.1.10. In-situ gravimetric moisture content profile for Section 9.

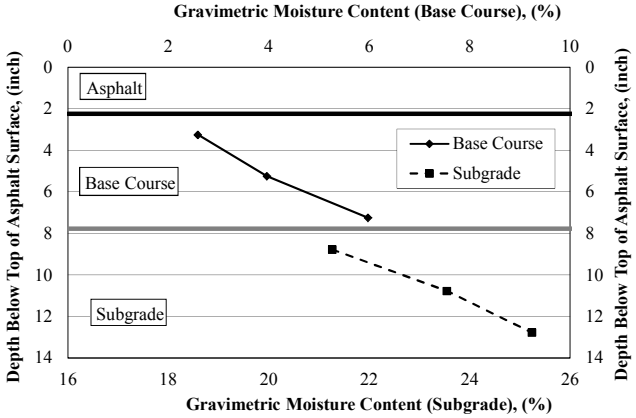

Figure B.1.11. In-situ gravimetric moisture content profile for Section 10.

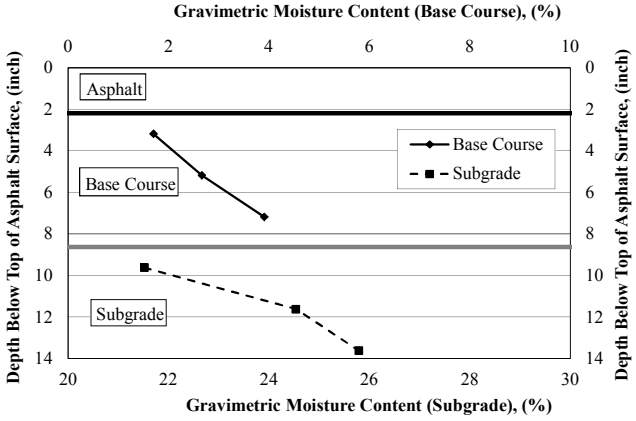

Figure B.1.12. In-situ gravimetric moisture content profile for Section 11.

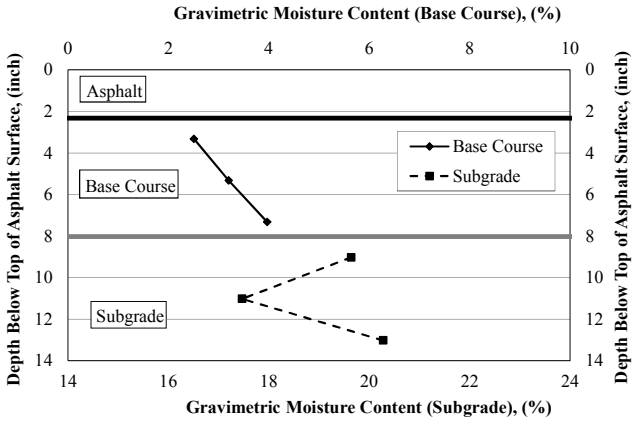

Figure B.1.13. In-situ gravimetric moisture content profile for Section 12.

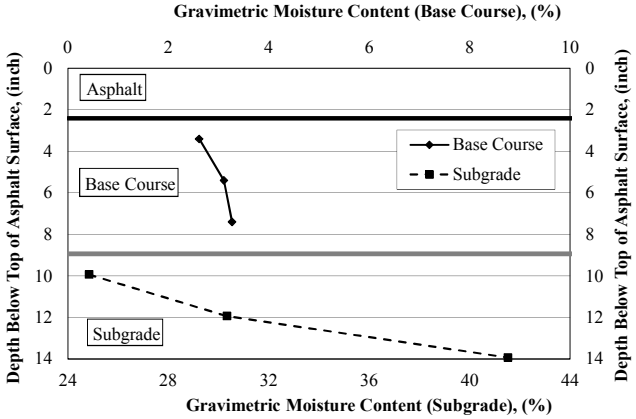

Figure B.1.14. In-situ gravimetric moisture content profile for Section 13.

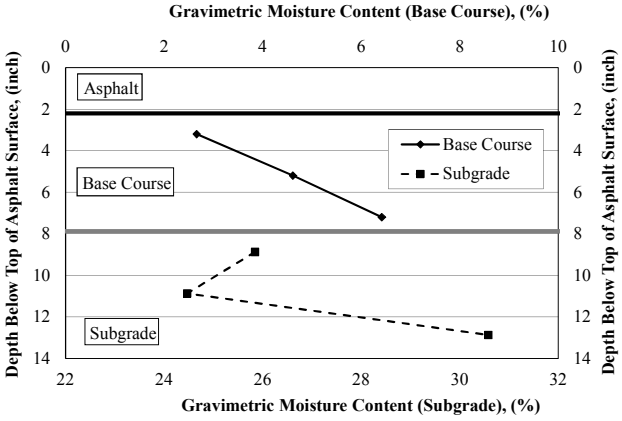

Figure B.1.15. In-situ gravimetric moisture content profile for Section 13W.

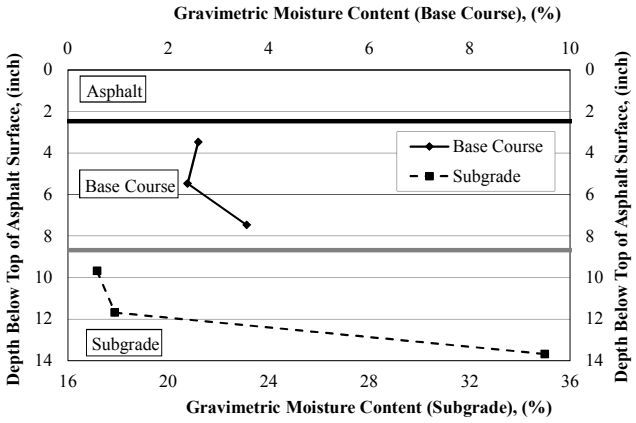

Figure B.1.16. In-situ gravimetric moisture content profile for Section 13A.

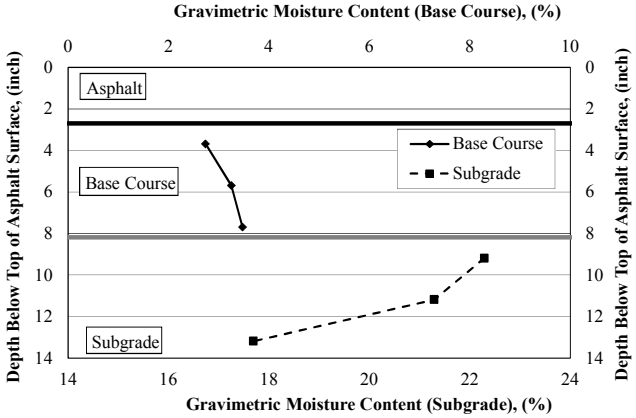

Figure B.1.17. In-situ gravimetric moisture content profile for Section 13B.

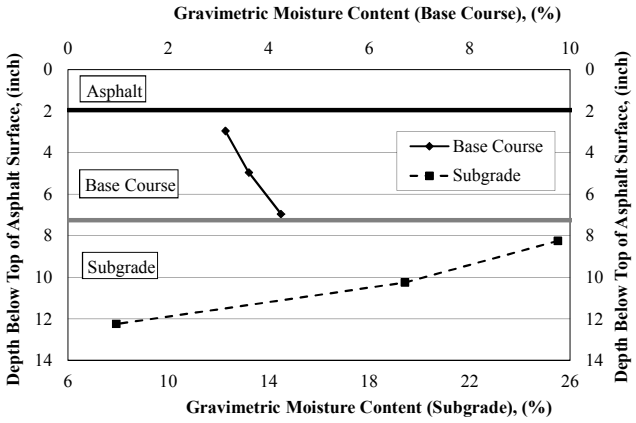

Figure B.1.18. In-situ gravimetric moisture content profile for Section 13BW.

B.2. Dry Unit Weight (Based on Equation 3.1)

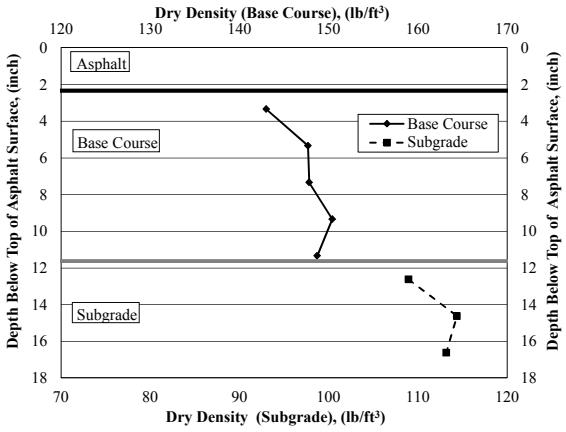

Figure B.2.1. Dry unit weight profile (based on Equation 4.1) for Section 1B.

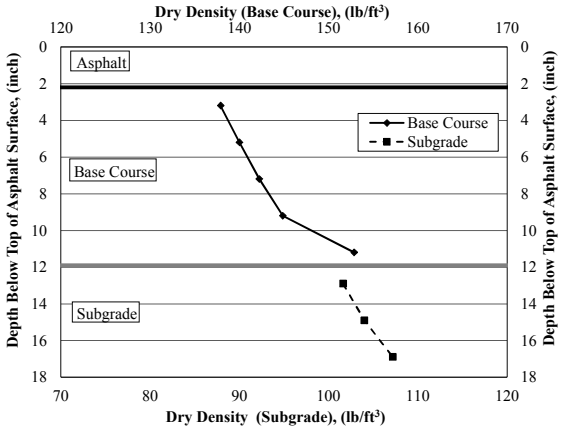

Figure B.2.2. Dry unit weight profile (based on Equation 4.1) for Section 1A.

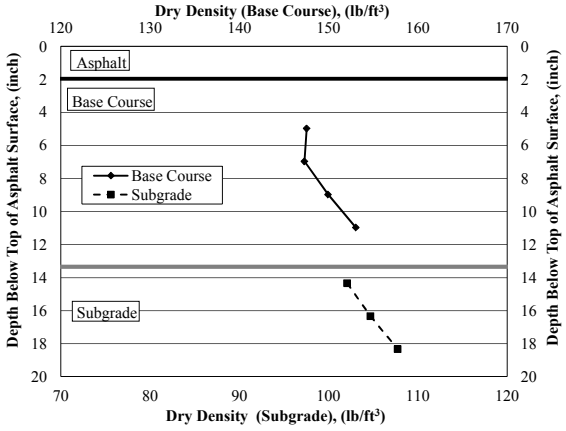

Figure B.2.3. Dry unit weight profile (based on Equation 4.1) for Section 1.

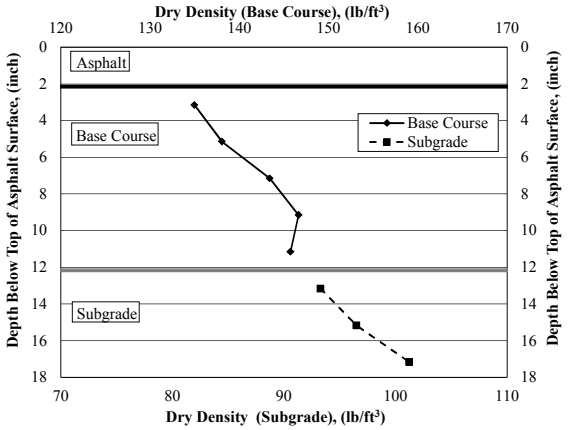

Figure B.2.4. Dry unit weight profile (based on Equation 4.1) for Section 2.

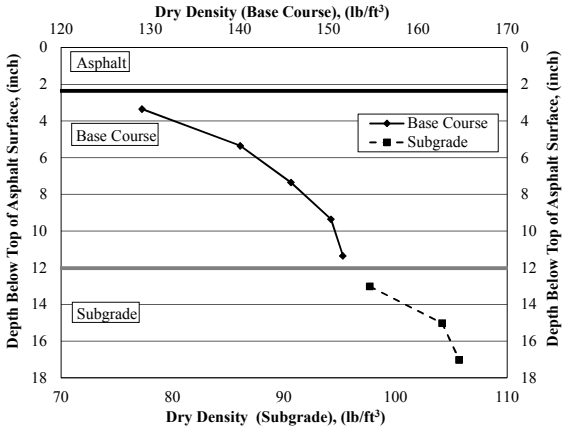

Figure B.2.5. Dry unit weight profile (based on Equation 4.1) for Section 3.

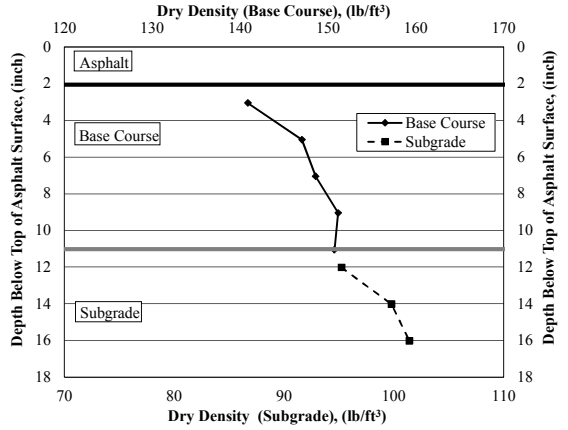

Figure B.2.6. Dry unit weight profile (based on Equation 4.1) for Section 4.

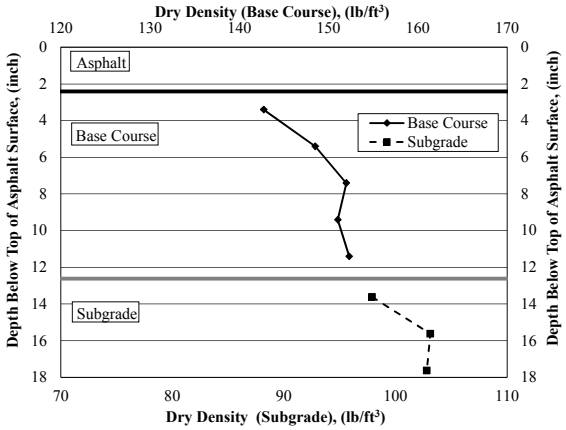

Figure B.2.7. Dry unit weight profile (based on Equation 4.1) for Section 5.

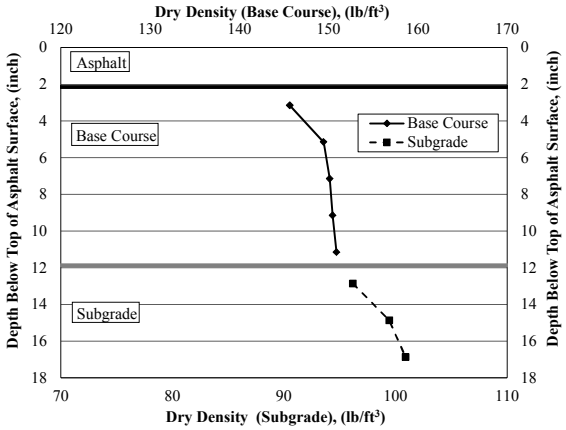

Figure B.2.8. Dry unit weight profile (based on Equation 4.1) for Section 6.

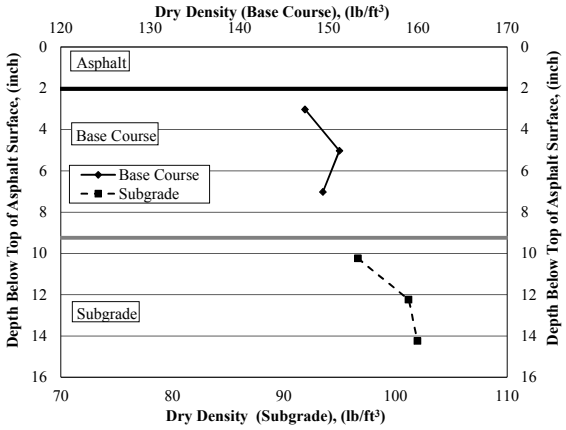

Figure B.2.9. Dry unit weight profile (based on Equation 4.1) for Section 8.

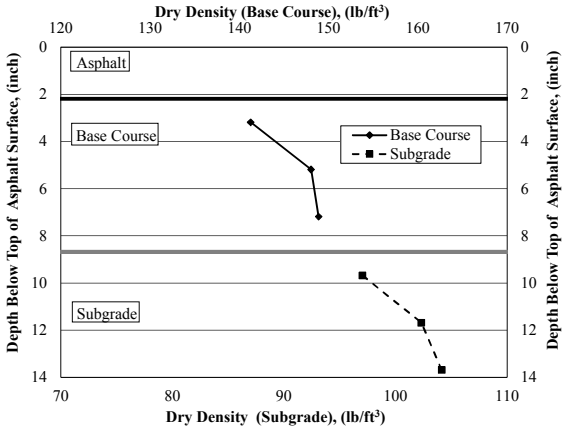

Figure B.2.10. Dry unit weight profile (based on Equation 4.1) for Section 9.

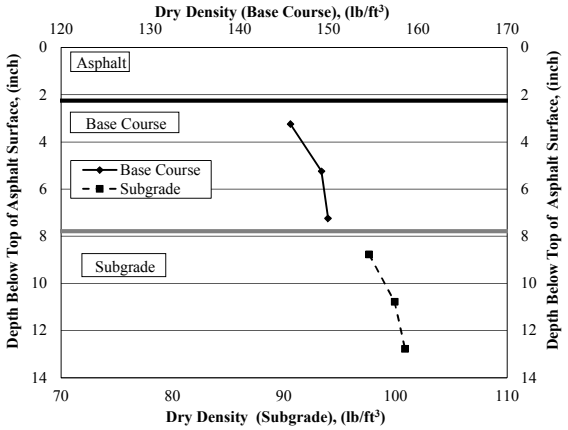

Figure B.2.11. Dry unit weight profile (based on Equation 4.1) for Section 10.

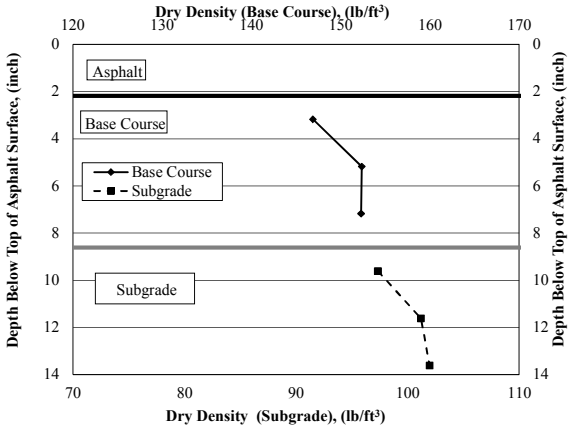

Figure B.2.12. Dry unit weight profile (based on Equation 4.1) for Section 11.

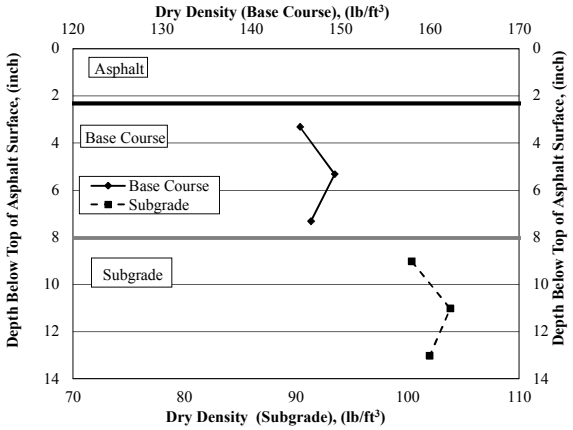

Figure B.2.13. Dry unit weight profile (based on Equation 4.1) for Section 12.

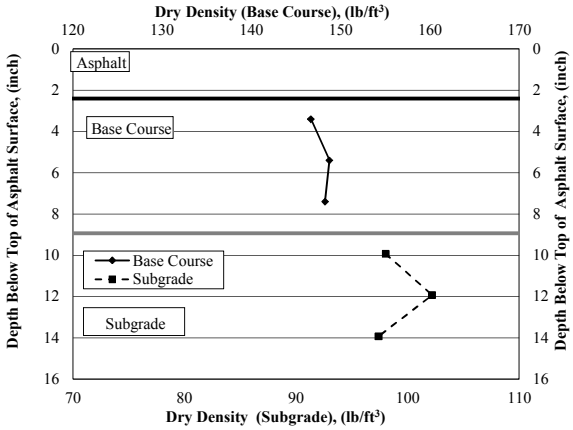

Figure B.2.14. Dry unit weight profile (based on Equation 4.1) for Section 13.

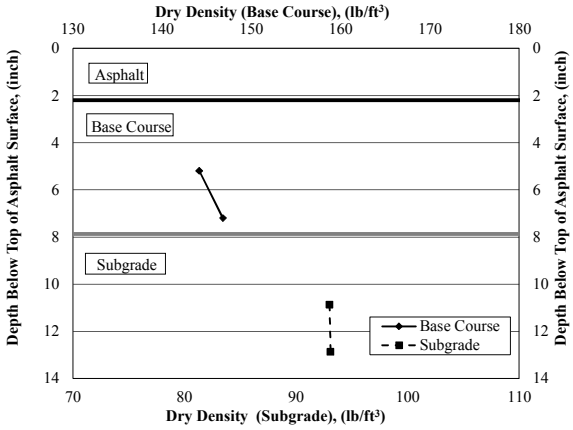

Figure B.2.15. Dry unit weight profile (based on Equation 4.1) for Section 13W.

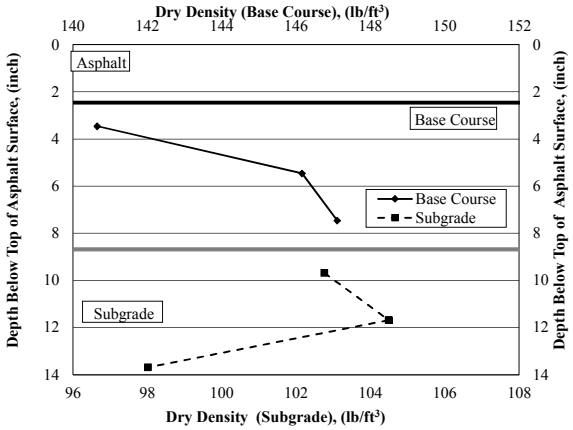

Figure B.2.16. Dry unit weight profile (based on Equation 4.1) for Section 13A.

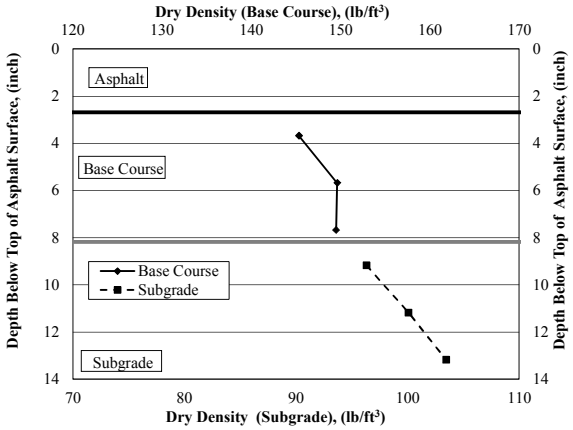

Figure B.2.17. Dry unit weight profile (based on Equation 4.1) for Section 13B.

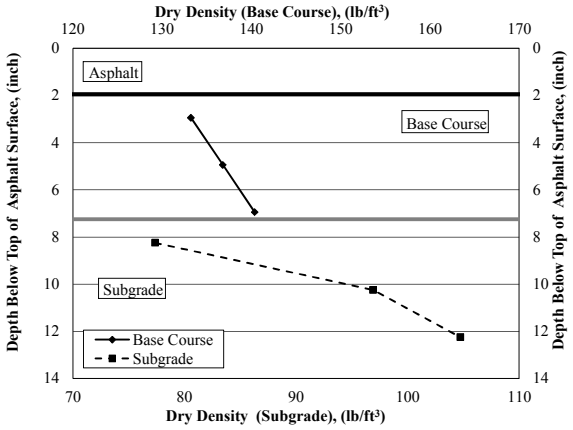

Figure B.2.18. Dry unit weight profile (based on Equation 4.1) for Section 13BW.

B.3. Dry Unit Weight (Based on Nuclear Density Gauge)

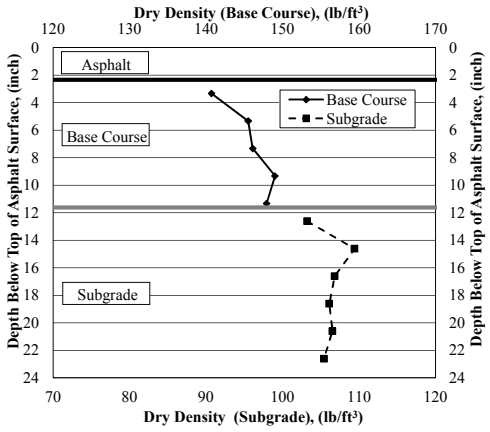

Figure B.3.1. Dry unit weight profile (based on nuclear density gauge) for Section 1B.

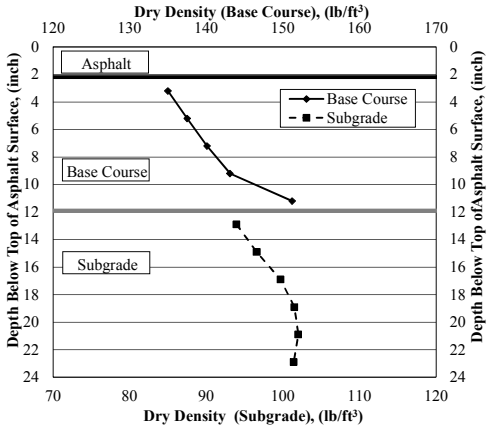

Figure B.3.2. Dry unit weight profile (based on nuclear density gauge) for Section 1A.

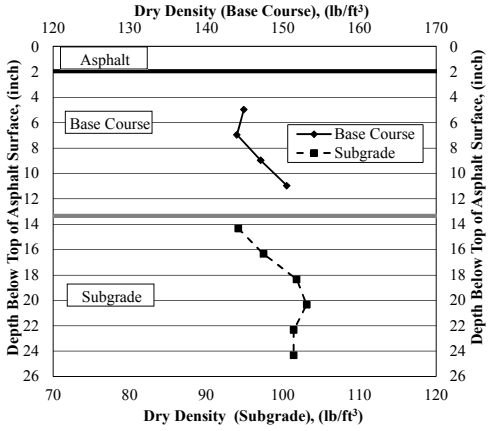

Figure B.3.3. Dry unit weight profile (based on nuclear density gauge) for Section 1.

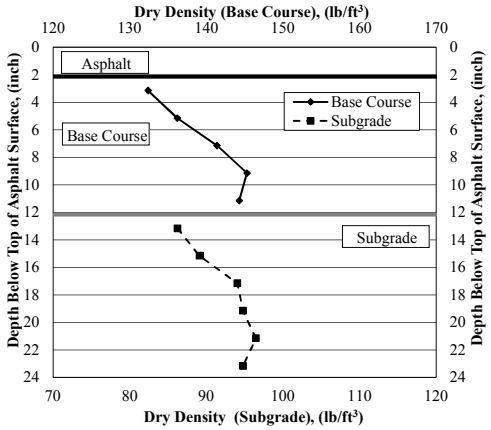

Figure B.3.4. Dry unit weight profile (based on nuclear density gauge) for Section 2.

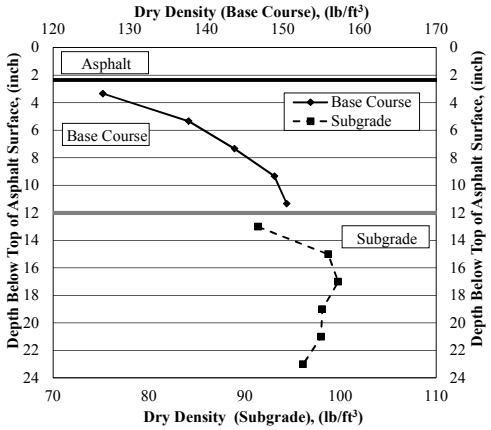

Figure B.3.5. Dry unit weight profile (based on nuclear density gauge) for Section 3.

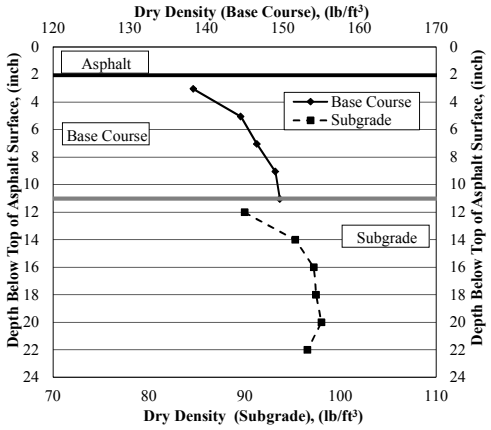

Figure B.3.6. Dry unit weight profile (based on nuclear density gauge) for Section 4.

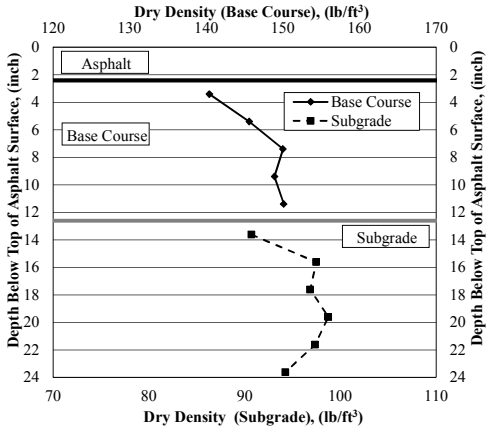

Figure B.3.7. Dry unit weight profile (based on nuclear density gauge) for Section 5.

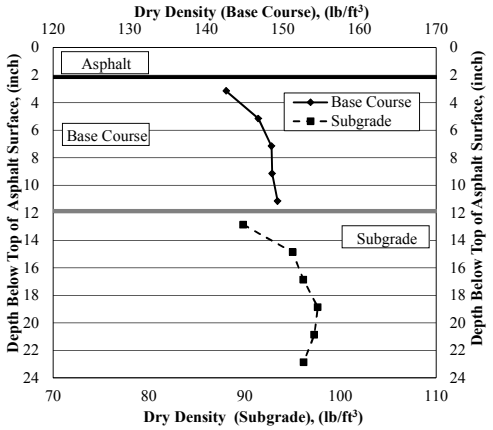

Figure B.3.8. Dry unit weight profile (based on nuclear density gauge) for Section 6.

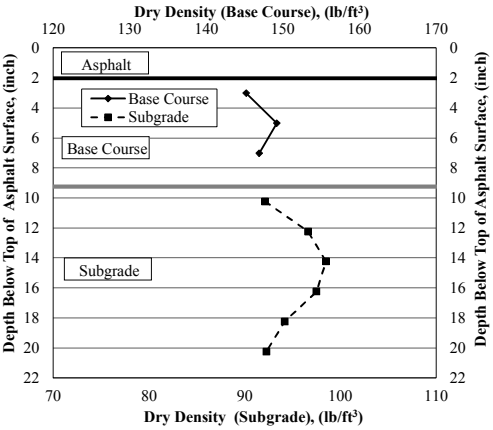

Figure B.3.9. Dry unit weight profile (based on nuclear density gauge) for Section 8.

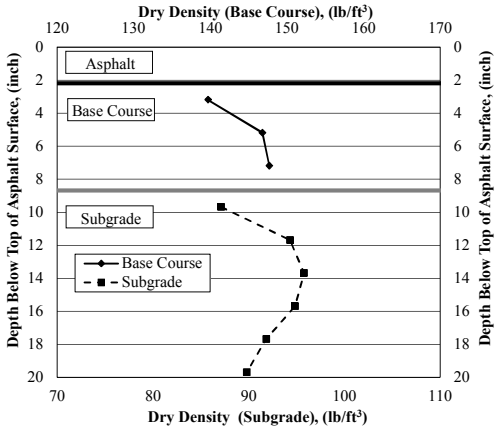

Figure B.3.10. Dry unit weight profile (based on nuclear density gauge) for Section 9.

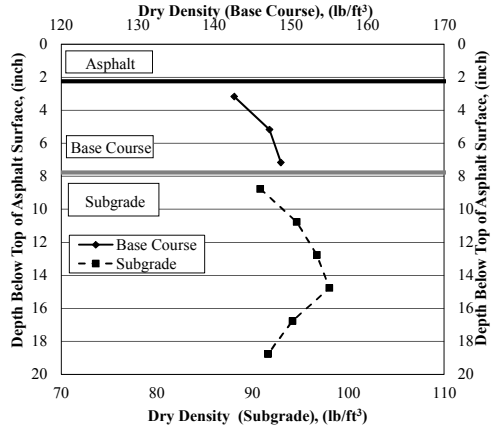

Figure B.3.11. Dry unit weight profile (based on nuclear density gauge) for Section 10.

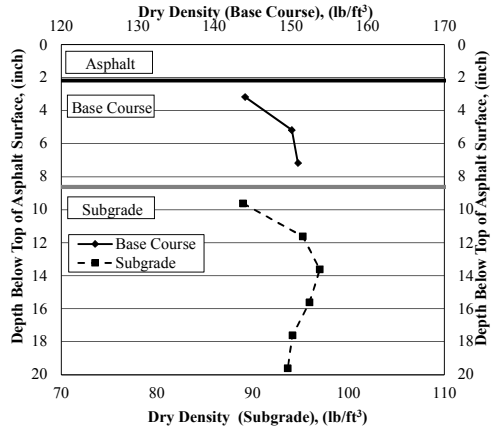

Figure B.3.12. Dry unit weight profile (based on nuclear density gauge) for Section 11.

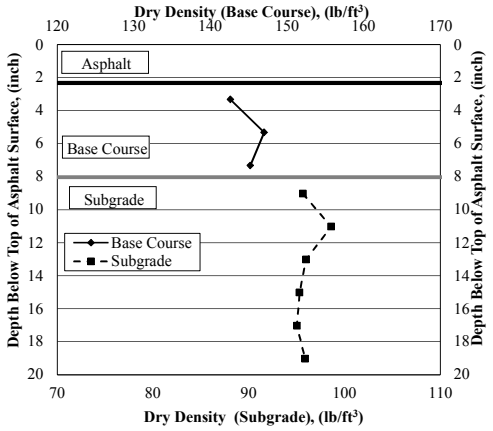

Figure B.3.13. Dry unit weight profile (based on nuclear density gauge) for Section 12.

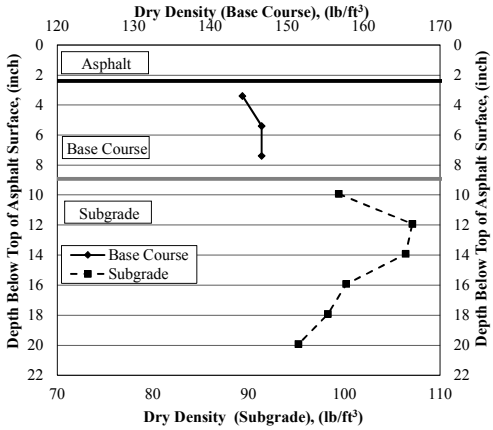

Figure B.3.14. Dry unit weight profile (based on nuclear density gauge) for Section 13.

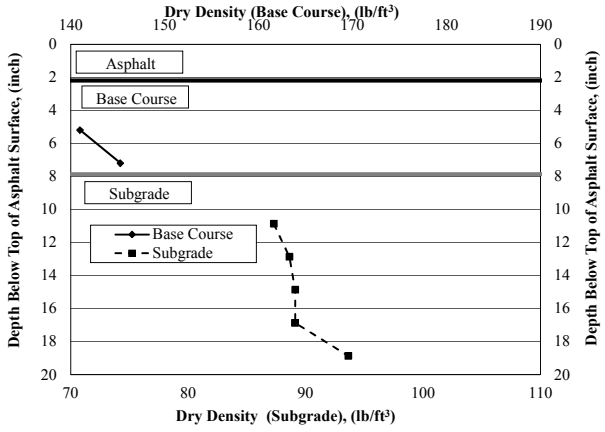

Figure B.3.15. Dry unit weight profile (based on nuclear density gauge) for Section 13W.

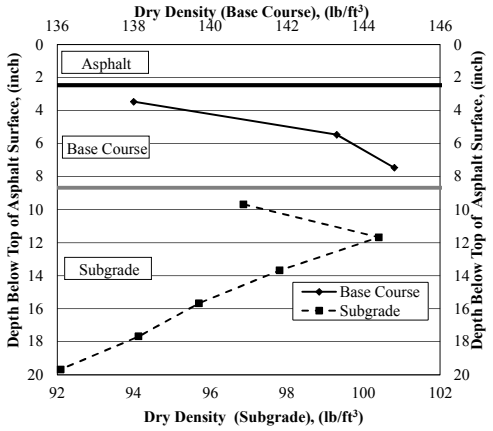

Figure B.3.16. Dry unit weight profile (based on nuclear density gauge) for Section 13A.

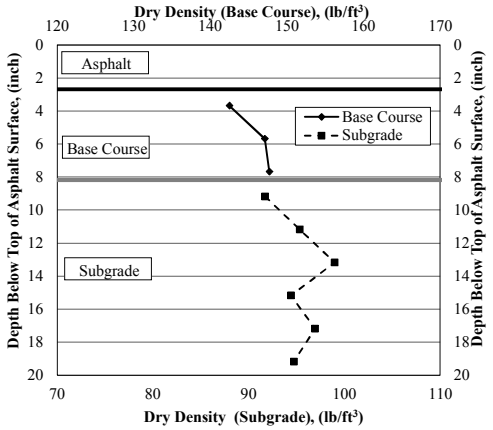

Figure B.3.17. Dry unit weight profile (based on nuclear density gauge) for Section 13B.

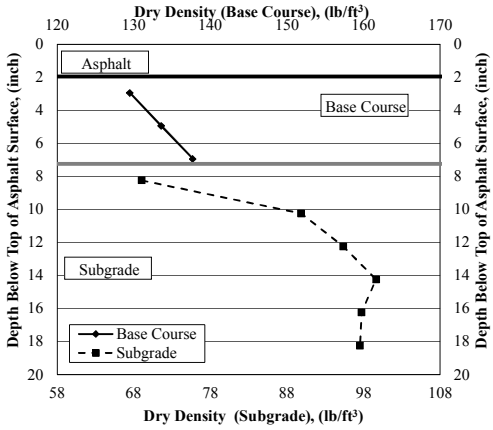

Figure B.3.18. Dry unit weight profile (based on nuclear density gauge) for Section 13BW.

B.4. Field Hydraulic Conductivity

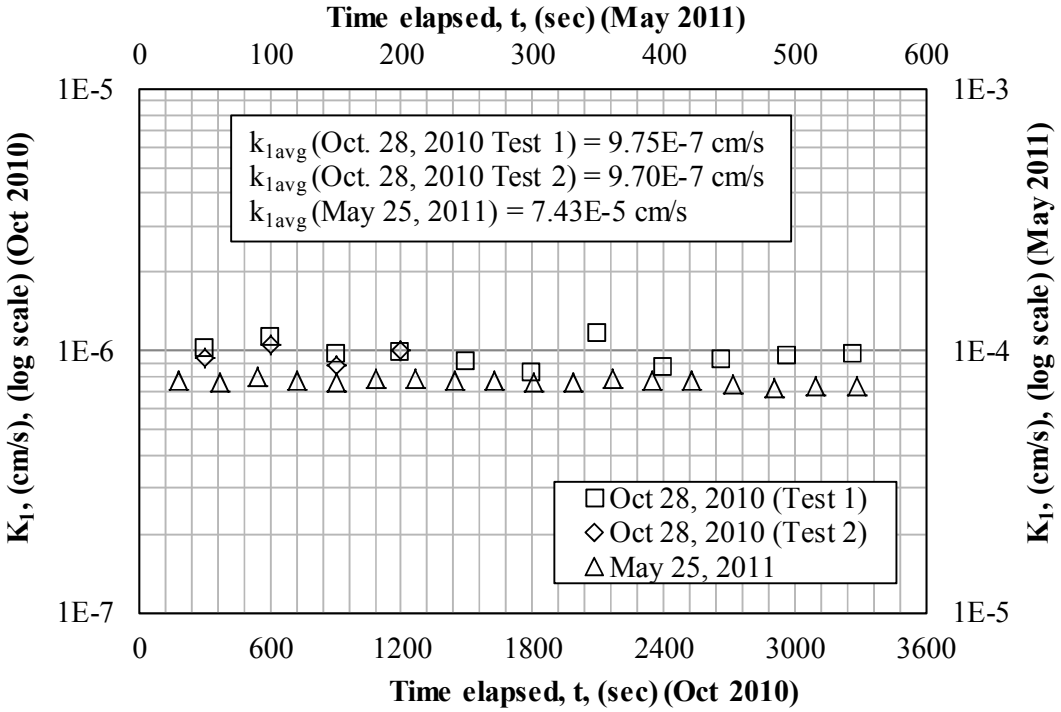

Figure B.4.1. Apparent hydraulic conductivity values (stage 1 only) for Section 1B obtained using two stage borehole in October 2010 and May 2011.

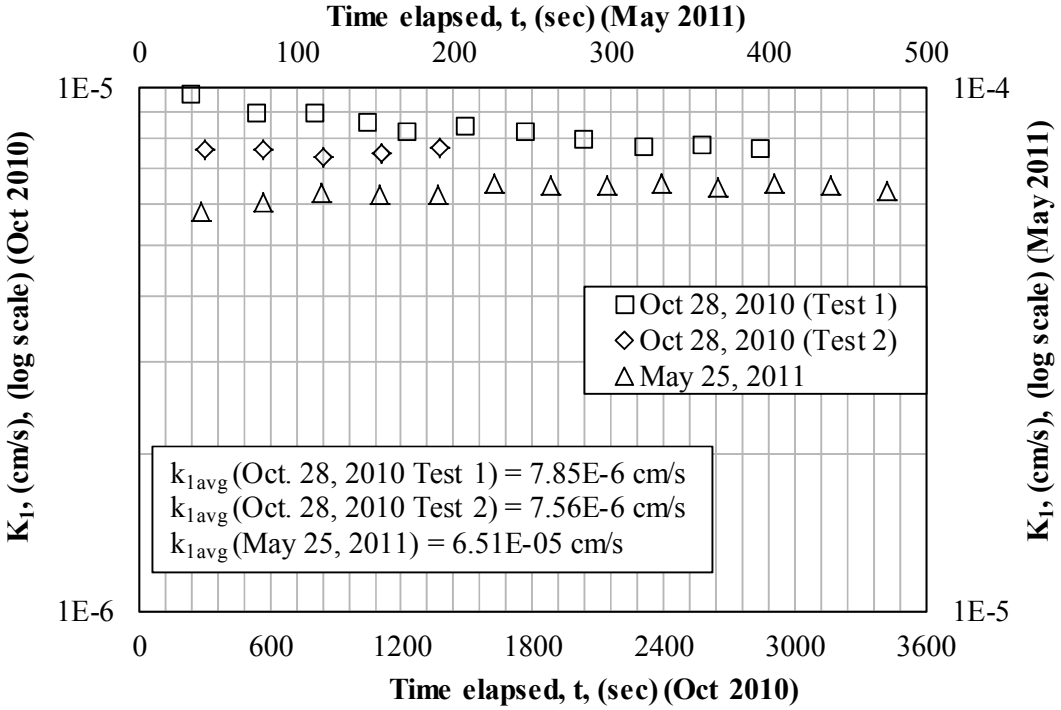

Figure B.4.2. Apparent hydraulic conductivity values (stage 1 only) for Section 1 obtained using two stage borehole in October 2010 and May 2011.

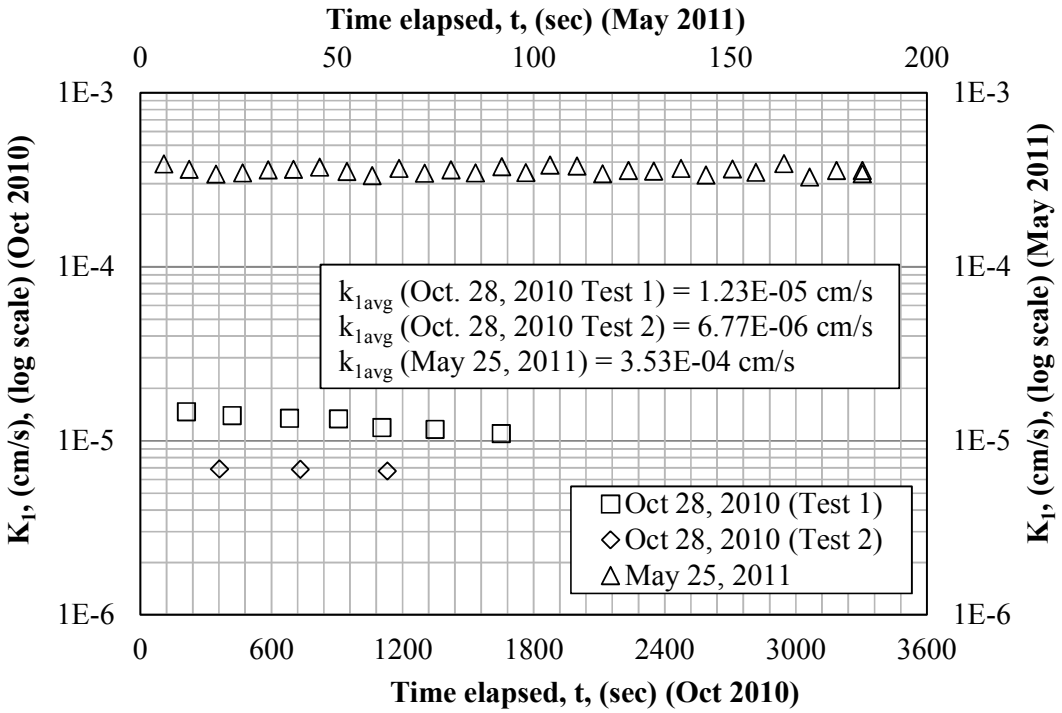

Figure B.4.3. Apparent hydraulic conductivity values (stage 1 only) for Section 2 obtained using two stage borehole in October 2010 and May 2011.

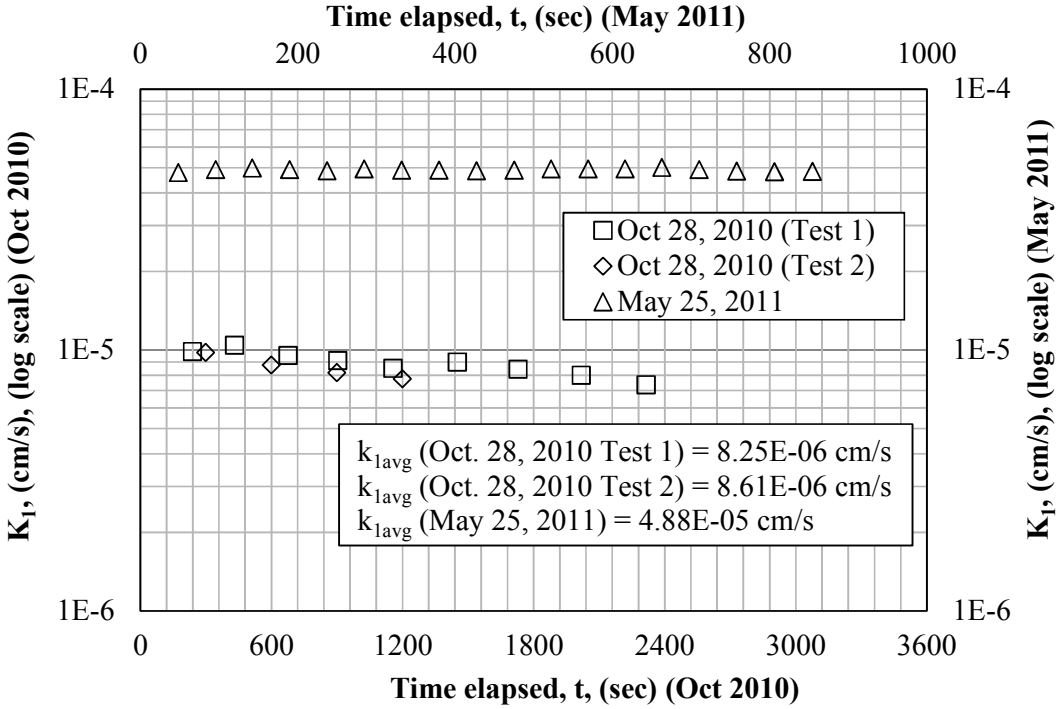

Figure B.4.4. Apparent hydraulic conductivity values (stage 1 only) for Section 3 obtained using two stage borehole in October 2010 and May 2011.

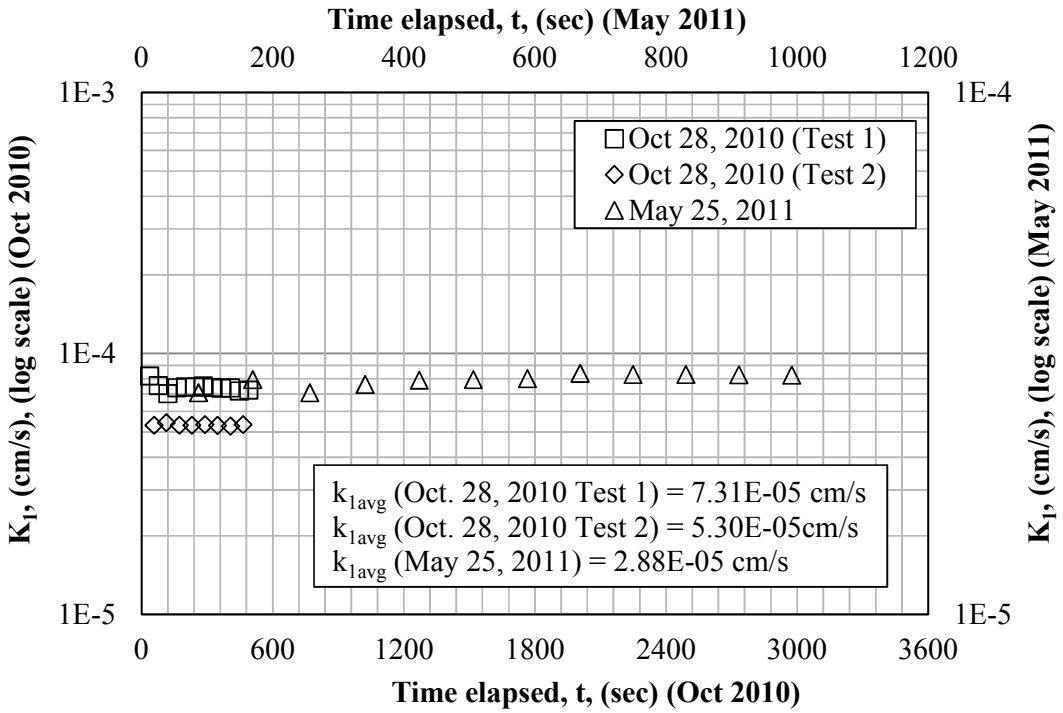

Figure B.4.5. Apparent hydraulic conductivity values (stage 1 only) for Section 4 obtained using two stage borehole in October 2010 and May 2011.

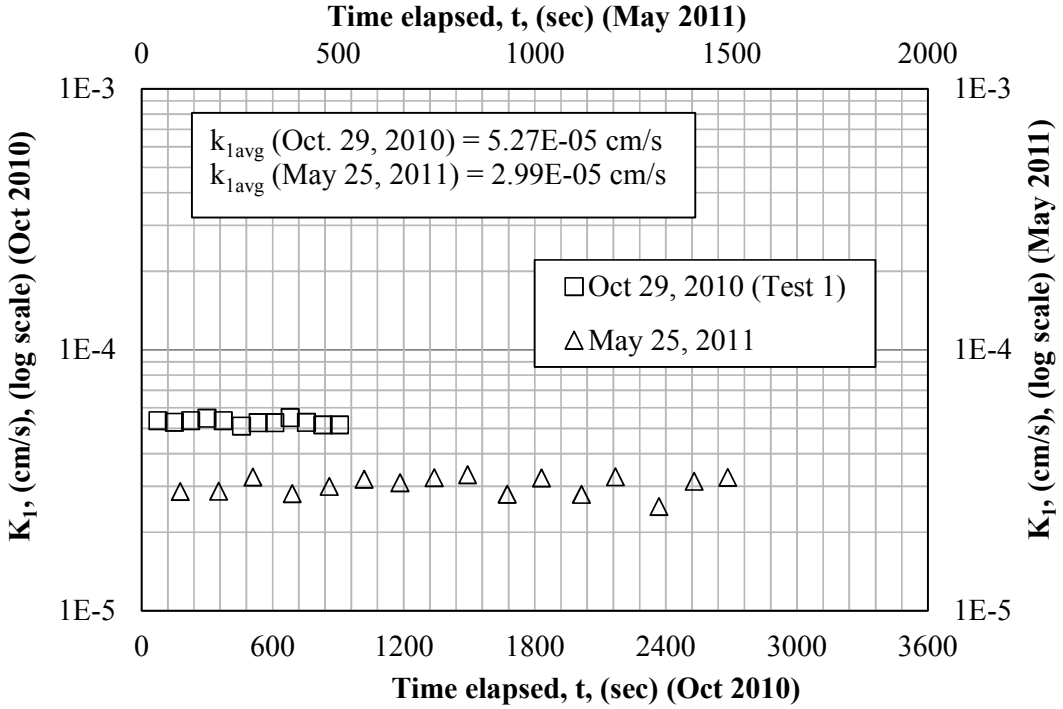

Figure B.4.6. Apparent hydraulic conductivity values (stage 1 only) for Section 10 obtained using two stage borehole in October 2010 and May 2011.

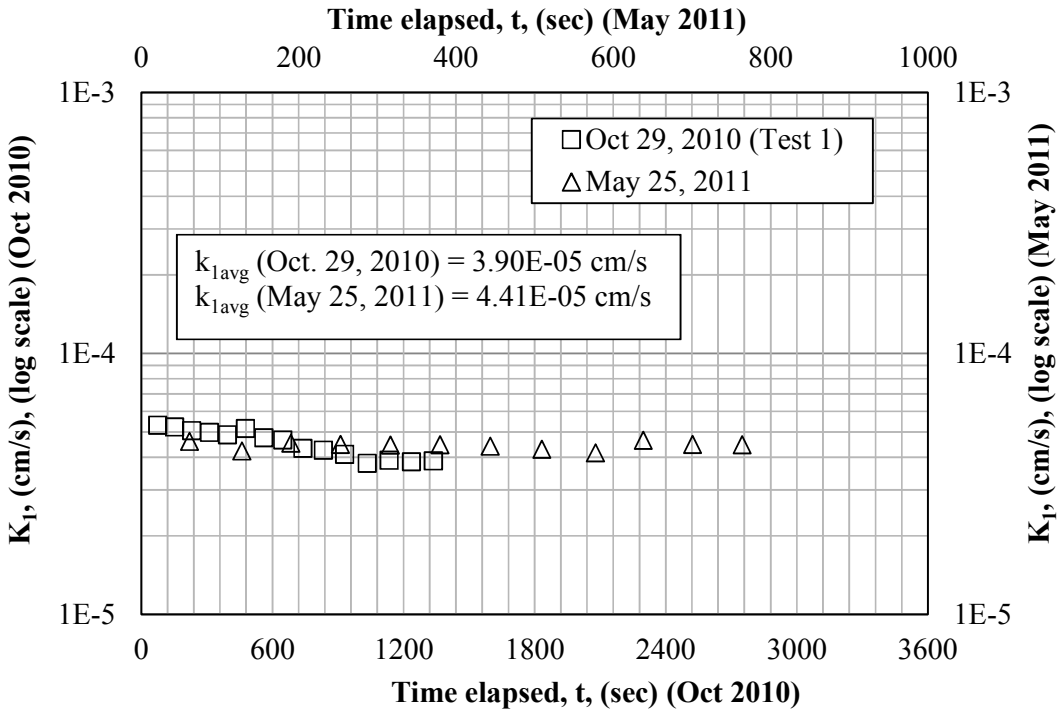

Figure B.4.7. Apparent hydraulic conductivity values (stage 1 only) for Section 11 obtained using two stage borehole in October 2010 and May 2011.

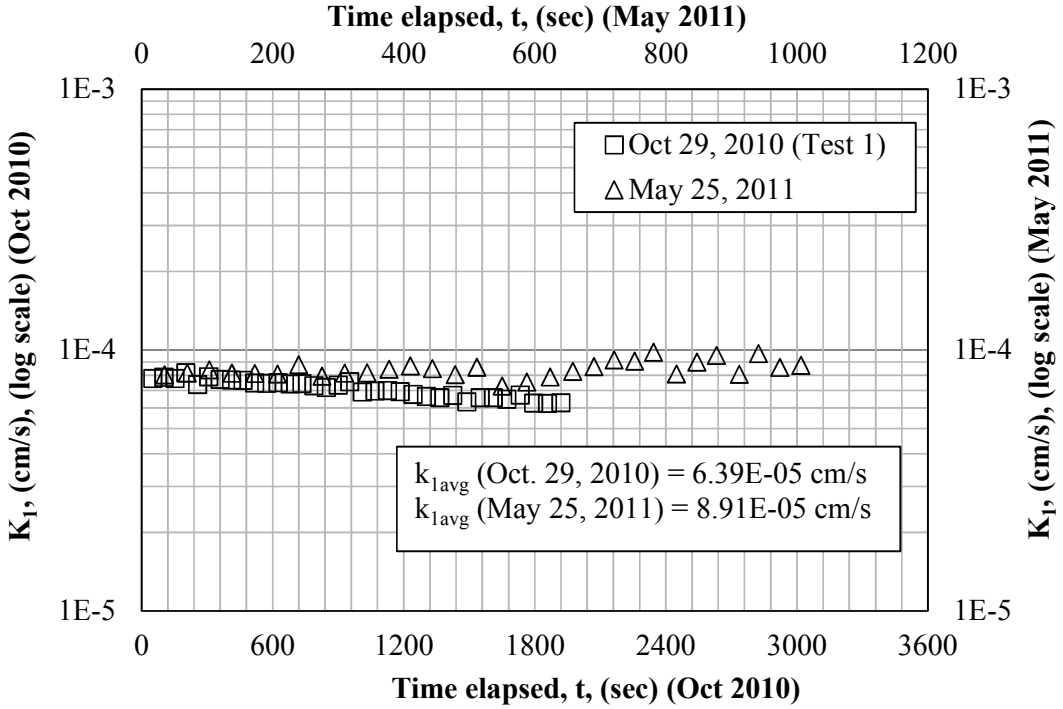

Figure B.4.8. Apparent hydraulic conductivity values (stage 1 only) for Section 12 obtained using two stage borehole in October 2010 and May 2011.

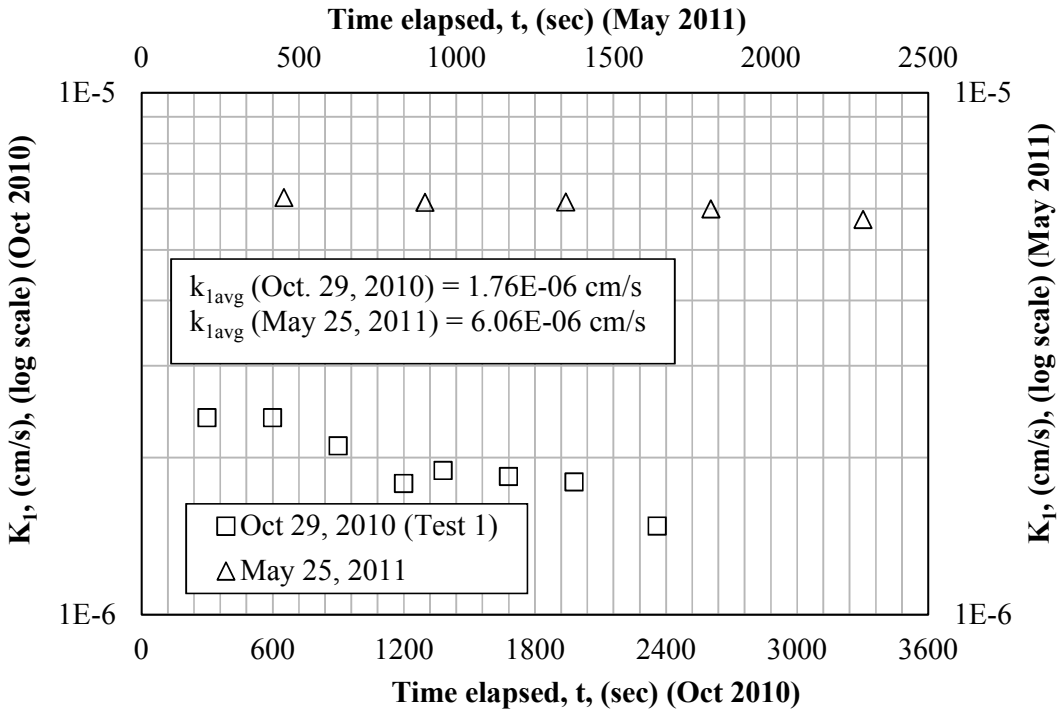

Figure B.4.9. Apparent hydraulic conductivity values (stage 1 only) for Section 13 obtained using two stage borehole in October 2010 and May 2011.

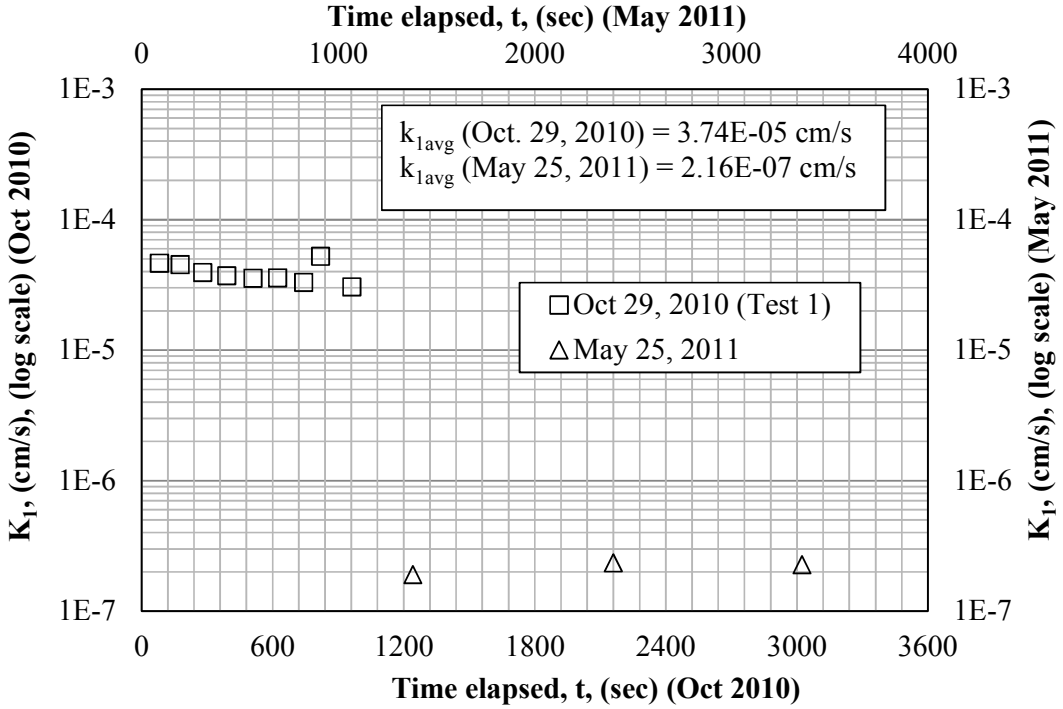

Figure B.4.10. Apparent hydraulic conductivity values (stage 1 only) for Section 13B obtained using two stage borehole in October 2010 and May 2011.